Morphology and ecology during the course of teleost adaptive radiations

Inauguraldissertation

zur

Erlangung der Würde eines Doktors der Philosophie

vorgelegt der

Philosophisch-Naturwissenschaftlichen Fakultät

der Universität Basel

von

Marco Colombo

aus Stabio (TI)

Basel, 2017

Genehmigt von der Philosophisch-Naturwissenschaftlichen Fakultät auf Antrag von

Prof. Dr. Walter Salzburger, Prof. Dr. Marcelo Sánchez

(Mitglieder des Dissertationskomitees: Fakultätsverantwortliche/r, Dissleiter/in, Korreferent/in)

Basel, den 21.04.2015

(Datum der Genehmigung durch die Fakultät)

Unterschrift des Fakultätsverantwortlichen

Prof. Dr. Jörg Schibler

Dekanin/Dekan

Morphology and ecology during the course of teleost adaptive radiations

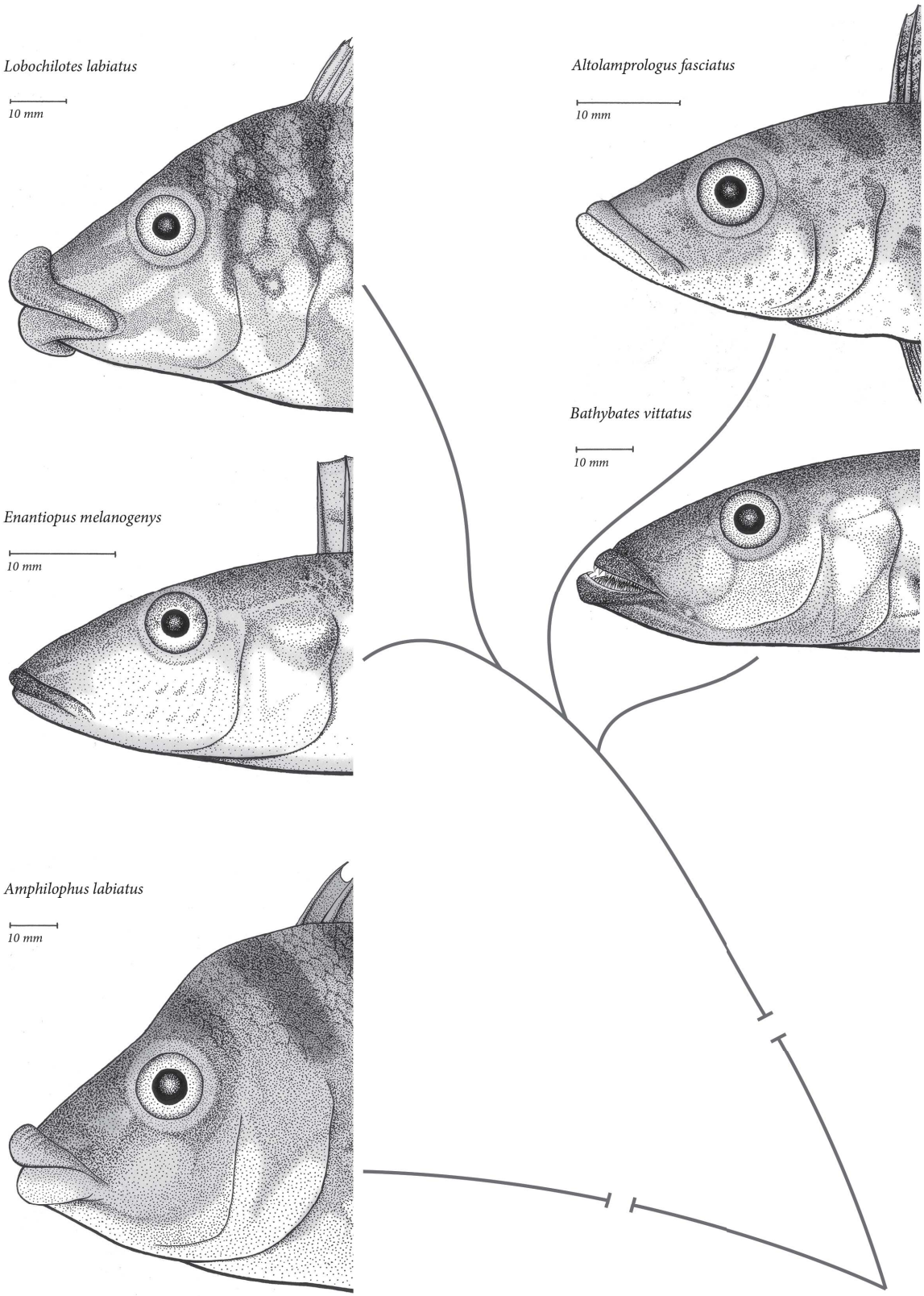

Inauguraldissertation zur
Erlangung der Würde eines Doktors der Philosophie
Philosophisch-Naturwissenschaftliche Fakultät der Universität Basel

von
Marco Colombo
aus Stabio (TI)

For the ones I love - to hell and back

Contents

Introduction

Most people with an evolutionary thinking that had the opportunity to dive in one of the East African Great Lakes Malawi, Victoria or Tanganyika must have inevitably wondered how a species richness such as found in these lakes could have arisen. How could one or a few ancestral cichlid species evolve to generate species flocks that today consist of hundreds to close to a thousand species (Turner et al. 2001)? And how can they coexist? Most people that then took a closer look at the fish must have also asked themselves what processes may have lead to those species being morphologically and ecologically highly diverse although all of them are phylogenetically closely related? And what was the course of this evident divergence?
Those are also the broad questions that I was engaged with during my Ph.D. and that I hope I can help to answer with this thesis.

The East African cichlid flocks that were briefly introduced above are the results of adaptive radiations. We speak of an adaptive radiation if a multitude of ecologically and morphologically distinct species rapidly emerges from a common ancestor due to the adaptation to distinct ecological niches (Schluter 2000, Gavrilets and Losos 2009). Typically, this happens after an ancestral species colonizes a new, more or less empty habitat and thus comes across a variety of empty ecological niches. We then speak of 'ecological opportunity'. Such an opportunity may also arise after the extinction of antagonists (like discussed for notothenioids, see part two of this thesis), or after the evolution of 'key innovations', i.e. novel traits that facilitate the exploitation of previously unoccupied niches (Schluter 2000, Yoder et al. 2010, Gavrilets and Vose 2005). Four main criteria are used to define an 'adaptive radiation' (Schluter 2000): common ancestry, rapid diversification, trait utility and phenotype-environment correlation. There are several well-established cases of adaptive radiations that fulfill those criteria, occurring in a diverse set of vertebrate and invertebrate species: lizards of the genus *Anolis* on the Caribbean islands representing reptiles

(e.g. Losos 1990, Irschick and Losos 1999, Mattingly and Jayne 2004, Vanhooydonck, Herrel and Irschick 2006, Losos et al. 1998, Mahler et al. 2013), Darwin's finches on the Galapagos archipelago representing birds (e.g. Schluter 2000, Grant 1999, Herrel et al. 2005, Grant 2001) or Hawaiian web-building spiders as an example for invertebrates (e.g. Blackledge and Gillespie 2004, Gillespie 2004), to name only a few.

However, the most astonishing examples of extant adaptive radiations are found in cichlid fish, the teleost family that the first part of my thesis deals with. The bulk of cichlid diversity is concentrated in the beforehand mentioned East African Great Lakes: collectively, the cichlid species flocks of Lakes Malawi, Victoria and Tanganyika reach a degree of species richness that is unparalleled in vertebrates, with about 2000 ecologically and morphologically diverse species (Kocher 2004, Salzburger, Van Bocxlaer and Cohen 2014, Santos and Salzburger 2012). In contrast to this diversity, recurrent examples of ecologically and morphologically convergent species can be found between the East African Great Lakes (Kocher et al. 1993) and, more recently, also within Lake Tanganyika (Muschick, Indermaur and Salzburger 2012, Rueber and Adams 2001). In **chapter 1.1**, I went in the opposite direction and investigated a case of intercontinental convergent evolution between a species from Lake Tanganyika and a Central American cichlid species with regards to ecology, morphology and the genetic basis of a pronounced lip-hypertrophism.

Taking up one of the four criteria outlined by Schluter (2000), namely the occurrence of phenotype-environment correlations, I investigated, in **chapter 1.2**, how the composition of the vertebral column relates to ecology in Lake Tanganyikan cichlids. Furthermore, I tried to answer more general questions concerning the vertebral column i.e. if the vertebral column consists of distinct developmental modules and how vertebrae number and morphology relate to body elongation in teleost fish.

Other than the monophyletic and relatively young species flocks of Lakes Malawi and Victoria, Lake Tanganyika exhibits a genetically more diverse cichlid fauna (Koblmüller, Sefc and Sturmbauer 2008, Salzburger et al. 2002) enabling the computation of increasingly reliable phylogenetic hypotheses using molecular

markers (e.g. Sturmbauer and Meyer 1993, Kocher et al. 1995, Salzburger et al. 2002, Clabaut, Salzburger and Meyer 2005, Muschick et al. 2012, Meyer, Matschiner and Salzburger 2015). The availability of reliable phylogenies allows the study of trait divergence through time and makes the Lake Tanganyikan cichlid flock, amongst other things, an ideal system to test hypotheses about the course of vertebrate adaptive radiations.

I made use of this to investigate the course of evolution regarding trophic morphology, namely head shape and oral jaw shape and, inferred from that, relative bite force in **chapter 1.3**. **Chapter 1.4** then again deals with phenotype-environment correlations, this time regarding locomotory morphology. Furthermore, the course of niche partitioning according to macro-habitats is investigated over a large sample of Lake Tanganyikan cichlids. **Chapter 1.5** deals again with a trophic-related trait: the opercular bone. Correlations between operculum shape and feeding mode and preference are established and opercular shape divergence during the course of the Lake Tanganyikan cichlid radiation is discussed. The operculum is one of only a few features that can be compared in extant as well a extinct taxa due to its good preservation and frequent occurrence in the fossil record. This enabled a comparison with an extinct species flock, the nearly globally distributed *Saurichthys* that roamed both marine and freshwater habitats between the Late Permian and Early Jurassic (Romano et al. 2012). Closing the cichlid subsection, **chapter 1.6** picks up a topic already approached in chapter 1: the Central American Midas cichlid species complex (*Amphilophus* spp.). The focus of this study lies on the basic ecological parameters of multiple convergent species pairs in two Nicaraguan crater lakes.

The second part of my thesis deals with a radiation that, in terms of environmental influence, could hardly be more different from the cichlid flocks that emerged in warm freshwater environments: the adaptive radiation of Notothenioid fish in the freezing seawaters around Antarctica. **Chapter 2.1** reviews, in the form of a book chapter, this radiation and discusses various aspects of Notothenioid evolution and ecology. In **Chapter 2.2** I investigate, similarly to my work on cichlids mentioned above, the course of evolution in

respect to trophic morphology and other factors in Antarctic Notothenioids. Finally, **chapter 2.3** deals again with opercular bone shape in notothenioids, and its implications on ecology.

References

Blackledge, T. A. & R. G. Gillespie (2004) Convergent evolution of behavior in an adaptive radiation of Hawaiian web-building spiders. *Proc Natl Acad Sci U S A,* 101**,** 16228-33.

Clabaut, C., W. Salzburger & A. Meyer (2005) Comparative phylogenetic analyses of the adaptive radiation of Lake Tanganyika cichlid fish: nuclear sequences are less homoplasious but also less informative than mitochondrial DNA. *J Mol Evol,* 61**,** 666-81.

Gavrilets, S. & J. B. Losos (2009) Adaptive radiation: contrasting theory with data. *Science,* 323**,** 732-7.

Gavrilets, S. & A. Vose (2005) Dynamic patterns of adaptive radiation. *Proc Natl Acad Sci U S A,* 102**,** 18040-5.

Gillespie, R. (2004) Community assembly through adaptive radiation in Hawaiian spiders. *Science,* 303**,** 356-9.

Grant, P. 1999. *The ecology and evolution of Darwin's finches*.

Grant, P. R. (2001) Reconstructing the evolution of birds on islands: 100 years of research. *Oikos,* 92**,** 385-403.

Herrel, A., J. Podos, S. K. Huber & A. P. Hendry (2005) Bite performance and morphology in a population of Darwin's finches: implications for the evolution of beak shape. *Functional Ecology,* 19**,** 43-48.

Irschick, D. J. & J. B. Losos (1999) Do Lizards Avoid Habitats in Which Performance Is Submaximal? The Relationship between Sprinting Capabilities and Structural Habitat Use in Caribbean Anoles. *Am Nat,* 154**,** 293-305.

Koblmüller, S., K. M. Sefc & C. Sturmbauer (2008) The Lake Tanganyika cichlid species assemblage: recent advances in molecular phylogenetics. *Patterns and Processes of ...*, 5-20.

Kocher, T. D. (2004) Adaptive evolution and explosive speciation: the cichlid fish model. *Nat Rev Genet,* 5**,** 288-98.

Kocher, T. D., J. A. Conroy, K. R. McKaye & J. R. Stauffer (1993) Similar morphologies of cichlid fish in Lakes Tanganyika and Malawi are due to convergence. *Mol Phylogenet Evol,* 2**,** 158-65.

Kocher, T. D., J. A. Conroy, K. R. McKaye, J. R. Stauffer & S. F. Lockwood (1995) Evolution of NADH dehydrogenase subunit 2 in east African cichlid fish. *Mol Phylogenet Evol,* 4**,** 420-32.

Losos, J. B. (1990) Concordant evolution of locomotor behaviour, display rate and morphology in< i> Anolis</i> lizards. *Animal Behaviour*.

Losos, J. B., T. R. Jackman, A. Larson, K. Queiroz & L. Rodriguez-Schettino (1998) Contingency and determinism in replicated adaptive radiations of island lizards. *Science,* 279**,** 2115-8.

Mahler, D. L., T. Ingram, L. J. Revell & J. B. Losos (2013) Exceptional convergence on the macroevolutionary landscape in island lizard radiations. *Science,* 341**,** 292-5.

Mattingly, W. B. & B. C. Jayne (2004) Resource use in arboreal habitats: Structure affects locomotion of four ecomorphs of Anolis lizards. *Ecology,* 85**,** 1111-1124.

Meyer, B. S., M. Matschiner & W. Salzburger (2015) A tribal level phylogeny of Lake Tanganyika cichlid fishes based on a genomic multi-marker approach. *Mol Phylogenet Evol,* 83**,** 56-71.
Muschick, M., A. Indermaur & W. Salzburger (2012) Convergent evolution within an adaptive radiation of cichlid fishes. *Curr Biol,* 22**,** 2362-8.
Romano, C., I. Kogan, J. Jenks, I. Jerjen & W. Brinkmann (2012) Saurichthys and other fossil fishes from the late Smithian (Early Triassic) of Bear Lake County (Idaho, USA), with a discussion of saurichthyid palaeogeography and evolution. *Bulletin of Geosciences,* 87**,** 543-570.
Rueber, L. & D. C. Adams (2001) Evolutionary convergence of body shape and trophic morphology in cichlids from Lake Tanganyika. *Journal of Evolutionary Biology,* 14**,** 325-332.
Salzburger, W., A. Meyer, S. Baric, E. Verheyen & C. Sturmbauer (2002) Phylogeny of the Lake Tanganyika cichlid species flock and its relationship to the Central and East African haplochromine cichlid fish faunas. *Syst Biol,* 51**,** 113-35.
Salzburger, W., B. Van Bocxlaer & A. S. Cohen (2014) Ecology and Evolution of the African Great Lakes and Their Faunas. *Annual Review of Ecology, Evolution, and Systematics, Vol 45,* 45**,** 519-+.
Santos, M. E. & W. Salzburger (2012) How cichlids diversify. *Science,* 338**,** 619-21.
Schluter, D. 2000. *The ecology of adaptive radiation*. Oxford University Press.
Sturmbauer, C. & A. Meyer (1993) Mitochondrial phylogeny of the endemic mouthbrooding lineages of cichlid fishes from Lake Tanganyika in eastern Africa. *Mol Biol Evol,* 10**,** 751-68.
Turner, G. F., O. Seehausen, M. E. Knight, C. J. Allender & R. L. Robinson (2001) How many species of cichlid fishes are there in African lakes? *Molecular Ecology,* 10**,** 793-806.
Vanhooydonck, B., A. Herrel & D. J. Irschick (2006) Out on a limb: The differential effect of substrate diameter on acceleration capacity in Anolis lizards. *J Exp Biol,* 209**,** 4515-23.
Yoder, J. B., E. Clancey, S. Des Roches, J. M. Eastman, L. Gentry, W. Godsoe, T. J. Hagey, D. Jochimsen, B. P. Oswald, J. Robertson, B. A. Sarver, J. J. Schenk, S. F. Spear & L. J. Harmon (2010) Ecological opportunity and the origin of adaptive radiations. *J Evol Biol,* 23**,** 1581-96.

Part 1
The adaptive radiations of cichlids

1.1
The ecological and genetic basis of convergent thick-lipped phenotypes in cichlid fishes

Molecular Ecology

This work was done during my master thesis and the first year of my Ph.D. I helped collecting the specimens and collected and analysed the morphological, ecological and classical genetic data. ED, NB and myself did the gene expression and real-time PCR analyses. I drafted the first version of the manuscript; all authors then participated in discussing and drafting the final manuscript.

MOLECULAR ECOLOGY

Molecular Ecology (2012) doi: 10.1111/mec.12029

The ecological and genetic basis of convergent thick-lipped phenotypes in cichlid fishes

MARCO COLOMBO,*[1] EVELINE T. DIEPEVEEN,*[1] MORITZ MUSCHICK,*‡ M. EMILIA SANTOS,* ADRIAN INDERMAUR,* NICOLAS BOILEAU,* MARTA BARLUENGA† and WALTER SALZBURGER*

Zoological Institute, University of Basel, Vesalgasse 1, 4051, Basel, Switzerland, †Museo Nacional de Ciencias Naturales, CSIC, José Gutierrez Abascal 2, 28006, Madrid, Spain

Abstract

The evolution of convergent phenotypes is one of the most interesting outcomes of replicate adaptive radiations. Remarkable cases of convergence involve the thick-lipped phenotype found across cichlid species flocks in the East African Great Lakes. Unlike most other convergent forms in cichlids, which are restricted to East Africa, the thick-lipped phenotype also occurs elsewhere, for example in the Central American Midas Cichlid assemblage. Here, we use an ecological genomic approach to study the function, the evolution and the genetic basis of this phenotype in two independent cichlid adaptive radiations on two continents. We applied phylogenetic, demographic, geometric morphometric and stomach content analyses to an African (*Lobochilotes labiatus*) and a Central American (*Amphilophus labiatus*) thick-lipped species. We found that similar morphological adaptations occur in both thick-lipped species and that the 'fleshy' lips are associated with hard-shelled prey in the form of molluscs and invertebrates. We then used comparative Illumina RNA sequencing of thick vs. normal lip tissue in East African cichlids and identified a set of 141 candidate genes that appear to be involved in the morphogenesis of this trait. A more detailed analysis of six of these genes led to three strong candidates: *Actb*, *Cldn7* and *Copb*. The function of these genes can be linked to the loose connective tissue constituting the fleshy lips. Similar trends in gene expression between African and Central American thick-lipped species appear to indicate that an overlapping set of genes was independently recruited to build this particular phenotype in both lineages.

Keywords: adaptive radiation, cichlid species flocks, convergent evolution, East Africa, ecological genomics, RNAseq

Received 9 March 2012; revision received 4 July 2012; accepted 15 July 2012

Introduction

Adaptive radiation is the rapid evolution of an array of species from a common ancestor as a consequence of the emerging species' adaptations to distinct ecological niches (Simpson 1953; Schluter 2000; Gavrilets & Losos 2009). It is typically triggered by ecological opportunity in form of underutilized resources—just as being provided after the colonization of a new habitat, the extinction of antagonists and/or the evolution of a novel trait, which is then termed an evolutionary 'key innovation' (Gavrilets & Vose 2005; Gavrilets & Losos 2009; Losos & Ricklefs 2009; Losos 2010; Yoder *et al.* 2010; Matschiner *et al.* 2011). Whatever the circumstances were that initiated an adaptive radiation, there is always a strong link between adaptively relevant traits and the habitat and/or foraging niche (a 'phenotype–environment correlation'; Schluter 2000). In the most illustrative examples of adaptive radiation, the Darwin's finches on the Galapagos archipelago, the *Anolis* lizards on the

Correspondence: Walter Salzburger, Fax: +41 61 267 0301; E-mail: walter.salzburger@unibas.ch
‡ Present address: Department of Animal and Plant Sciences, The University of Sheffield, Sheffield, S10 2TN, UK.
[1]These authors contributed equally to this work.

Caribbean islands and the cichlid fishes of the East African Great Lakes, this correlation exists between beak-shape and food source (finches), limb morphology and twig diameter (anoles), and the architecture of the mouth and jaw apparatus and foraging mode (cichlids) (Schluter 2000; Butler *et al.* 2007; Grant & Grant 2008; Losos 2009; Salzburger 2009).

An interesting aspect of many adaptive radiations is the frequent occurrence of convergent (or parallel) evolution (Schluter & Nagel 1995; Harmon *et al.* 2005; Arendt & Reznick 2008; Losos 2011; Wake *et al.* 2011). For example, similar ecotype morphs of anoles lizards have evolved independently on different Caribbean islands (Losos *et al.* 1998; Harmon *et al.* 2005; Losos & Ricklefs 2009), benthic–limnetic and lake–stream species pairs of threespine sticklebacks emerged repeatedly in and around postglacial lakes (Rundle *et al.* 2000; Berner *et al.* 2010; Roesti *et al.* 2012), and a whole array of convergent forms of cichlid fish emerged between the lakes of East Africa (Kocher *et al.* 1993; Salzburger 2009). Such instances of convergent evolution are generally interpreted as the result of the action of similar selection regimes in isolated settings (Schluter & Nagel 1995; Rundle *et al.* 2000; Nosil *et al.* 2002; Harmon *et al.* 2005; Losos 2011). It has further been suggested that if radiations are truly replicated (i.e. driven by adaptive processes), convergence in morphology should tightly be associated with convergence in ecology and behaviour (Johnson *et al.* 2009).

The species flocks of cichlid fishes in the East African Great Lakes Victoria, Malawi and Tanganyika represent the most species-rich extant adaptive radiations in vertebrates (Kocher 2004; Seehausen 2006; Salzburger 2009). Several hundreds of endemic cichlid species have emerged in each lake within a period of several millions of years (as is the case for Lake Tanganyika; Salzburger *et al.* 2002; Genner *et al.* 2007) to <150 000 years (as in Lake Victoria; Verheyen *et al.* 2003). The various endemic cichlid species differ greatly in the morphology of the trophic apparatus (mouth form and shape, jaw structure and dentition) as well as in coloration and pigmentation, suggesting that both natural and sexual selection are jointly responsible for adaptive radiation and explosive speciation in cichlids (Salzburger 2009). Interestingly, convergent forms that emerged in independent cichlid adaptive radiations often show very similar coloration patterns in addition to matching body shapes and mouth morphologies (Kocher *et al.* 1993; Stiassny & Meyer 1999; Salzburger 2009). This has led to speculations whether selection alone is sufficient to explain convergence, or whether genetic or developmental constraints have contributed to the morphogenesis of these matching phenotypes (Brakefield 2006).

The present study focuses on the morphology, ecology and the genetic basis of a peculiar mouth trait in cichlid fishes, which has evolved multiple times: hypertrophied ('fleshy') lips (see Box 1 in Salzburger 2009). The exact function of the thick lips in cichlids is unknown, although this feature is generally implicated in a specific foraging mode (Fryer 1959; Fryer & Iles 1972; Arnegard *et al.* 2001). Fleshy lips are often interpreted as an adaptation for feeding on invertebrates and crustaceans hidden in crannies, with the lips being used to seal cracks and grooves to facilitate the sucking of prey (Barlow & Munsey 1976; Ribbink *et al.* 1983; Seehausen 1996; Konings 1998). Alternatively, it has been suggested that hypertrophied lips protect from mechanical shocks (Greenwood 1974; Yamaoka 1997), and that they function as taste receptors (Arnegard *et al.* 2001) or as mechanoreceptors (Fryer 1959; Fryer & Iles 1972). [Note, however, that there is no increase in sensory cells in lip tissue (Greenwood 1974).]

It is remarkable that thick-lipped species appear to be a common outcome of cichlid adaptive radiations. For example, the large cichlid assemblages in East Africa all contain at least one such taxon (Lake Victoria: *Haplochromis chilotes*; Lake Malawi: *Chilotilapia euchilus, Abactochromis labrosus*, *Otopharynx pachycheilus, Placidochromis milomo*, *Protomelas ornatus*; Lake Tanganyika: *Lobochilotes labiatus*). In addition, cichlids featuring hypertrophied lips are known from, for example, the Midas Cichlid (*Amphilophus* spp.) assemblage in the large lakes of Nicaragua, where a thick-lipped species (*A. labiatus*) is common in rocky habitats (Fig. 1). Occasionally, hypertrophied lips are also observed in other related cichlids in Nicaragua, such as in the riverine species *Tomacichla tuba* (Villa 1982) or in *Astatheros rostratus* (pers. obs.). Additional riverine representatives with hypertrophied lips are also found in South America (*Crenicichla tendybaguassu*) and Western Africa (*Thoracochromis albolabris*). Hypertrophied lips are not unique to cichlids, though. For example, the adaptive radiation of the sailfin silverside fish (Telmatherinidae) in the Malili lakes of Sulawesi (Herder *et al.* 2006) and the barbs of Lake Tana in Ethiopia (Sibbing *et al.* 1998; de Graaf *et al.* 2008) also produced thick-lipped species.

Members of the family Cichlidae are distributed in the Southern hemisphere, with a few ancestral lineages in India, Sri Lanka and Madagascar and two exceptionally species-rich clades, one in Central and South America and one in Africa (Salzburger & Meyer 2004). This biogeographical pattern is consistent with a Gondwanan origin of the Cichlidae, dating the split between American and African representatives to ~100 Ma (Salzburger & Meyer 2004; Sereno *et al.* 2004; Genner *et al.* 2007). This set-up opens the possibility to study the ecological and genetic basis of a convergent trait across one of the

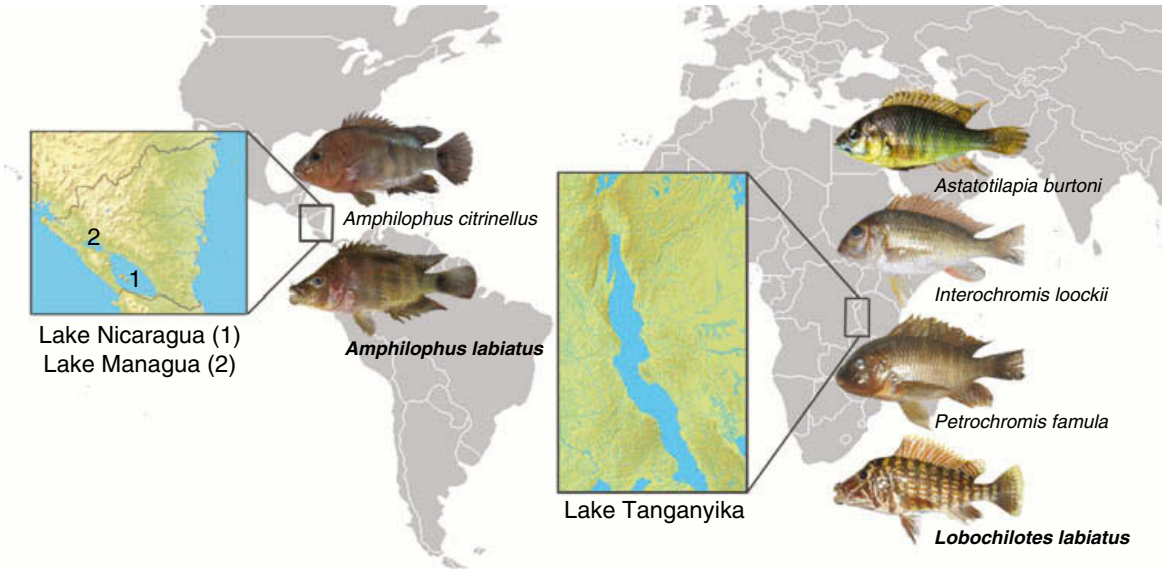

Fig. 1 Map of the Southern hemisphere showing the two study systems, the Midas Cichlid (*Amphilophus* sp.) species complex in Nicaragua, Central America, and the Tropheini in Lake Tanganyika, East Africa.

largest possible phylogenetic and geographical distances in cichlids and, hence, in the complete absence of gene flow and outside the influence of ancestral polymorphism and/or standing genetic variation.

Here, we applied an integrative approach in two cichlid fish radiations, the one of the Tropheini in East African Lake Tanganyika and the Midas Cichlid assemblage in Nicaragua, to uncover the ecological and genetic basis of the thick-lipped phenotype. More specifically, we compared the two '*labiatus*' species to one another and to their sister species by means of geometric morphometric and stomach content analyses; we placed them in their respective radiations by phylogenetic and demographic analyses; and we provide field observations on foraging strategies for one of them (*L. labiatus*). To study the genetic basis of hypertrophied lips, we first applied comparative transcriptome analyses (RNA-seq) on the basis of Illumina next-generation sequencing of juvenile and adult individuals of the African species *L. labiatus* (in comparison with a closely related species for which a genome sequence is available). In a second step, we tested candidate genes identified by RNAseq in representatives of both radiations in a quantitative real-time PCR environment.

Materials and methods

Study species

This study focuses on two thick-lipped species, *Lobochilotes labiatus* from East African Lake Tanganyika and *Amphilophus labiatus* from Nicaragua. *Lobochilotes labiatus* is a member of the rock-dwelling Tanganyikan cichlid tribe Tropheini and therefore part of the most species-rich group of cichlids, the haplochromines, which include the Tanganyikan Tropheini, many riverine species and the species flocks of Lakes Victoria and Malawi (Salzburger *et al.* 2002, 2005). The Tropheini themselves underwent a subradiation within Lake Tanganyika (see e.g. Sturmbauer *et al.* 2003). *Amphilophus labiatus* is part of the Midas Cichlid assemblage in Nicaragua and occurs in the large Central American lakes Managua and Nicaragua, where it co-occurs with the most common species in the area, *A. citrinellus* (Barlow 1976; Barluenga & Meyer 2010). For this study, we sampled a total of 84 and 74 specimens of the Central American species *Amphilophus citrinellus* and *A. labiatus*, respectively, and 143 specimens of *L. labiatus* plus 14 additional Haplochromini/Tropheini specimens from Lake Tanganyika. Exact sampling locations and dates for specimens used for the genetic analysis and GenBank accession numbers are provided in Appendix S1.

Sampling, DNA and RNA extraction

Sampling of *L. labiatus* and other Tropheini species was performed between 2007 and 2011 in the Southern part of Lake Tanganyika, East Africa; *A. labiatus* and its congeners were collected in September 2009 in the two large Nicaraguan lakes Managua and Nicaragua (see Appendix S1 for details). Fishes were processed in the field following our standard operating procedure: fishes were individually labelled, measured (total and standard length) and weighted and a photograph was taken from the left side

of each specimen using a Nikon P5000 or a Nikon D5000 digital camera (fins were spread out using clips); then, a piece of muscle tissue and a fin-clip were taken as DNA sample and preserved in ethanol; fishes were then dissected and RNA samples from lip and other tissues were preserved in RNAlater (Ambion); the whole intestinal tract was removed and stored in ethanol.

For DNA extraction, we either applied a high-salt extraction method (Bruford *et al.* 1998) or used a MagnaPure extraction robot (Roche, Switzerland) following the manufacturer's protocol. RNA was extracted according to the Trizol method with either Trizol (Invitrogen) or TRI reagent (Sigma). Lip tissue was homogenized with a PRO200 Homogenizer (PRO Scientific Inc.) or with a BeadBeater (FastPrep-24; MP Biomedicals). DNase treatment following the DNA Free protocol (Ambion) was performed to remove any genomic DNA from the samples. Subsequent reverse transcription was achieved by using the High Capacity RNA-to-cDNA kit (Applied Biosystems). For the *A. burtoni* samples, up to two individuals (adults) or up to eight individuals (juveniles) were used per sample, due to a diminutive amount of lip tissue extracted from these fishes. All other samples were taken from a single specimen.

Phylogenetic and demographic analyses

We first wanted to phylogenetically place the thick-lipped species into the respective clade of East African and Nicaraguan cichlids. We thus performed a phylogenetic analysis of the Tanganyikan cichlid tribe Tropheini (see also Sturmbauer *et al.* 2003) and used haplotype genealogies to reconstruct the evolutionary history in the much younger *Amphilophus* species assemblage in Nicaragua, where phylogenetic analyses are not expedient due to the lack of phylogenetic signal (see also Barluenga *et al.* 2006; Barluenga & Meyer 2010). We also performed mismatch analyses within *A. citrinellus*, *A. labiatus* and *L. labiatus* to compare their demographic histories.

We amplified three gene segments for each of the three focal species and additional Tropheini/Haplochromini species: the first segment of the noncoding mtDNA control region and two nuclear loci containing coding and noncoding DNA (a segment each of the *endothelin receptor 1*, *ednrb1* and the *phosphatidin phosphatase 1*, *phpt1*). We used previously published primers L-Pro-F (Meyer *et al.* 1994) and TDK-D (Lee *et al.* 1995) for the control region and ednrb1F and ednrb1R (Lang *et al.* 2006) for *ednrb1*, and so far unpublished primers 38a_F (5′-AGC AGG GTT GAC CTT CTC AA-3′) and 38a_R (5′-TGG CTA AAA TCC CCG ATG TA-3′) for *phpt1*. Polymerase chain reaction (PCR) amplification, purification and cycle sequencing were performed as described elsewhere (Diepeveen & Salzburger 2011); an ABI 3130*xl* capillary genetic analyzer (Applied Biosystems) was used for DNA sequencing.

The resulting sequences were complemented with already available sequences. In the case of the Tropheini, we also included available sequences of the mitochondrial NADH dehydrogenase subunit 2 gene (ND2) (see Appendix S1 for GenBank accession numbers). Sequences were aligned with MAFFT (Katoh & Toh 2008) resulting in a total length of 2345 bp for the Tropheini (control region: 371 bp; ND2: 1047 bp; ednrb1: 538 bp; *phpt1:* 389 bp) and 1620 bp for *Amphilophus* (control region: 371 bp; ednrb1: 743 bp; *phpt1:* 469 bp). Maximum-likelihood and Bayesian inference phylogenetic analyses of the Tropheini were performed for each gene segment separately (not shown) and for a concatenated alignment with PAUP* (Swofford 2003) and MRBAYES (Ronquist & Huelsenbeck 2003), respectively. The appropriate model of sequence evolution was detected with JMODELTEST (Posada 2008) applying the Akaike Information Criterion (AIC). A maximum-likelihood bootstrap analysis with 100 pseudoreplicates was performed in PAUP*, and MR. BAYES was run for eight million generations with a sample frequency of 100 and a burn-in of 10%. We then used MESQUITE (www.mesquiteproject.org) to map feeding specializations on the resulting maximum-likelihood topology and to reconstruct ancestral character states with parsimony. Data on feeding mode from the Haplochromini/Tropheini species other than *L. labiatus* are based on Brichard (1989), Nori (1997), Yamaoka (1997) and Konings (1998).

Haplotype genealogies for the *Amphilophus* data set were constructed following the method described in the study by Salzburger *et al.* (2011) on the basis of a maximum-likelihood tree and sequences of the mitochondrial control region and the nuclear *ednrb1* gene (*phpt1* was not used here due to the limited number of haplotypes found). Mismatch analyses were performed on the basis of mtDNA sequences with ARLEQUIN 3.0 (Excoffier *et al.* 2005).

Geometric morphometric analyses

In order to test for similarities in overall body shape between the thick-lipped forms from Central America and East Africa, we performed geometric morphometric analyses on the basis of digital images. Body shape was quantified in a set of 58 *A. citrinellus*, 27 *A. labiatus* and 27 *L. labiatus* using 17 homologous landmarks (see Appendix S2; note that lip shape was not assessed to prevent a bias). Data acquisition was carried out using TPSDIG (Rohlf 2006), and data were analysed with MORPHOJ (Klingenberg 2011). For all shape comparisons, we used the residuals of a within-species regression of shape on centroid size to reduce allometric effects within species, in

order to retain shape differences between differently sized species. For the same reason, we only included *L. labiatus* individuals with a body size larger than 12 cm total length. We then performed a discriminant function analysis between all pairs of species and a principal component analysis (PCA). To identify morphological changes associated with the enlarged lip phenotype, we compared *A. labiatus* to its closest relative, *A. citrinellus*. In the case of *L. labiatus*, we made use of our new phylogeny of the Tropheini (Fig. 2a) and body shape data of *L. labiatus* and its nine closest relatives [*Petrochromis macrognathus*, *P. polyodon*, *P. ephippium*, *Lobochilotes labiatus*, *Simochromis diagramma*, *S. babaulti*, *Gnathochromis pfefferi*, *Pseudosimochromis curvifrons*, *Limnotilapia dardenni* and *Ctenochromis horei* (M. Muschick, A. Indermaur & W. Salzburger, unpublished data)] to reconstruct the landmark configuration of the direct ancestor to *L. labiatus*. This was carried out in MorphoJ using branch length-weighted squared-change parsimony. The changes in landmark configurations along a discriminant function (Nicaraguan species) or along the shape-change vector from the estimated ancestral shape to *L. labiatus* were increased threefold to produce Fig. 3. The shape differences between species shown in Fig. 3 accurately reflect the shape-change vectors for landmark positions. Outlines were interpolated and added to Fig. 3 to help the reader envision these shape differences in the context of fish body shape.

Stomach and gut content analyses

To assess trophic specialization of the thick-lipped cichlid species, we performed comparative stomach and gut content analyses. To this end, stomachs and guts were opened step-by-step. First, the stomach was opened and emptied under a binocular followed by the remaining parts of the intestine. All items were grouped into seven food categories: hard-shelled (crustaceans, snails, mussels), small arthropods (insects and zooplankton), fish scales, fish remains, plant seeds and plant material other than seeds. For each specimen, the wet weight of each food category was measured on a Kern ALS 120-4 scale (Kern, Germany) and was then used to calculate Schoener's index of proportional diet overlap (Schoener 1970). We analysed stomach and gut contents in a total of 159 specimens: *A. citrinellus* ($N = 58$; of which 25 had contents), *A. labiatus* ($N = 62$; 34) and *L. labiatus* ($N = 39$; 29). We note that such an analysis has the drawback that it only covers food uptake in the last few hours or days before sampling.

Field observations in Lobochilotes labiatus

The feeding behaviour of *L. labiatus* was observed at our field site near Mpulungu, Zambia, in concrete ponds ($1.5 \times 1.5 \times 1$ m). The purpose of these observations under semi-natural conditions and with wild specimens was to document if and how the lips are used in processing the main prey item identified in the stomach content analyses. The ponds were equipped with stones of ~20–30 cm diameters that covered the ground and formed caves as they occur naturally in the habitat of *L. labiatus*. Each pond was stocked with five to six freshly caught and unharmed adult individuals of *L. labiatus*. After an acclimatization period of at least 4 days, fish were offered snails of different sizes and their feeding behaviour was recorded with two underwater cameras (Canon Ixus 65 with WP-DC3 underwater case; Olympus μ tough-6000) for a period of 1 h each.

Comparative gene expression assays using RNAseq

For the identification of differentially expressed genes in thick-lipped species, we performed RNA sequencing (RNAseq) comparing lip tissue from a thick-lipped species to lip tissue from a reference species. We decided to perform these experiments in the African species *L. labiatus* and to use the closely related species *Astatotilapia burtoni* as reference taxon for several reasons such as the availability of laboratory strains and of sufficient RNA samples from adult and juvenile individuals. Most importantly, we chose this set-up because of the availability of various genomic resources for *A. burtoni*, such as a whole-genome sequence and a set of ~50 000 partly annotated expressed sequence tags (ESTs) (Salzburger *et al.* 2008; Baldo *et al.* 2011), which is crucial for the analysis and interpretation for RNAseq data. Such resources are currently not publicly available for *Amphilophus*.

In a first step, RNA was extracted from adult and juvenile individuals of *L. labiatus* and *A. burtoni* (see above for the RNA extraction protocol). RNA quality and quantity were determined on a NanoDrop 1000 spectrophotometer (Thermo Scientific) and by gel electrophoresis. RNA samples were pooled to create four samples subjected to RNA sequencing (RNAseq): (i) *A. burtoni* adult ($N = 3$); (ii) *A. burtoni* juvenile ($N = 1$); (iii) *L. labiatus* adult ($N = 2$); and (iv) *L. labiatus* juvenile ($N = 3$). Five micrograms of RNA per RNAseq sample was sent for Illumina sequencing at the Department of Biosystems Science and Engineering (D-BSSE), University of Basel and ETH Zurich. For library construction and sequencing, standard protocols were applied. Poly-A mRNA was selected using poly-T oligo-attached magnetic beads. The recovered mRNA was fragmented into smaller pieces using divalent cations under increased temperature. cDNA was produced using reverse transcriptase and random primers, followed by second-strand cDNA synthesis using DNA polymerase

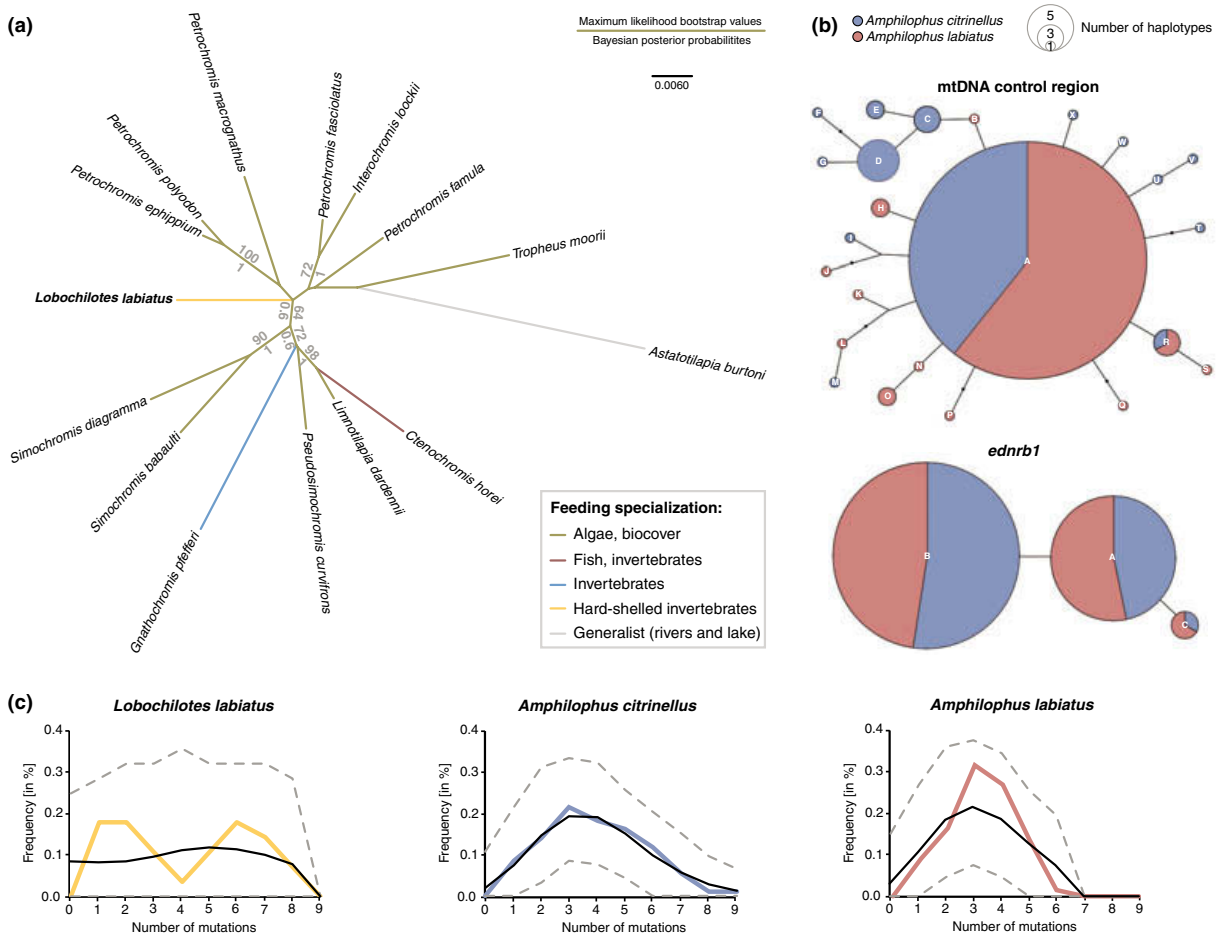

Fig. 2 Evolutionary origin of the thick-lipped species in East African Lake Tanganyika and in the Great Lakes of Nicaragua. (a) Maximum-likelihood tree of the Tropheini from Lake Tanganyika based on two mitochondrial (control region and ND2) and two nuclear (*ednrb1* and *phpt1*) gene segments (2345 bp in total) and the GTR+G+I model of molecular evolution. Numbers above the branches refer to maximum-likelihood bootstrap values, and numbers below are Bayesian posterior probabilities (note that support values are only shown for branches with bootstrap values >60). Branches are colour-coded according to feeding specializations; the trait values for internal branches have been reconstructed with MESQUITE. (b) Haplotype genealogies of the two *Amphilophus* species based on the mitochondrial control region and the nuclear *endrb1* gene. A large fraction of the haplotypes is shared between *A. citrinellus* and *A. labiatus*. (c) Results from the mismatch analysis on the basis of the mitochondrial control region showing the inferred demographic histories for *L. labiatus*, *A. citrinellus* and *A. labiatus*. Coloured lines represent the observed data, the black line indicates the best-fit model, and the dashed lines in grey indicate the upper and lower boundaries from the simulations in ARLEQUIN.

I and RNaseH. cDNA went through an end-repair process, the addition of a single 'A' base and ligation of the adapters. It was then purified and enriched with PCR to create the final cDNA library. Each library was sequenced in one lane on an Illumina Genome Analyzer IIx (read length was 76 bp). Illumina reads are available from the Sequence Read Archive (SRA) at NCBI under the accession number SRA052992.

The Illumina reads were assembled into three different data sets for further analyses: (i) a quality-filtered data set (Data set 1), where the quality of the reads was assessed with the FASTX toolkit tools implemented in GALAXY [version September/October 2011; available at http://main.g2.bx.psu.edu/ (Giardine *et al.* 2005; Blankenberg *et al.* 2010; Goecks *et al.* 2010)]; low-quality reads were discarded applying quality filter cut-off values of 22–33. (ii) a quality-filtered plus trimmed data set (Data set 2), in which all the reads were trimmed to a length of 42 bp to evaluate the effects of read length (iii) as a control for the effect of trimming and filtering, a nonquality-filtered, nontrimmed data set (Data set 3).

The reads of the three data sets were then aligned to a reference cichlid assembly (Baldo *et al.* 2011) with NOVOALIGN 2.07.06 (http://www.novocraft.com/) after indexing the reference sequences with NOVOINDEX (http://www.novocraft.com/) using default parame-

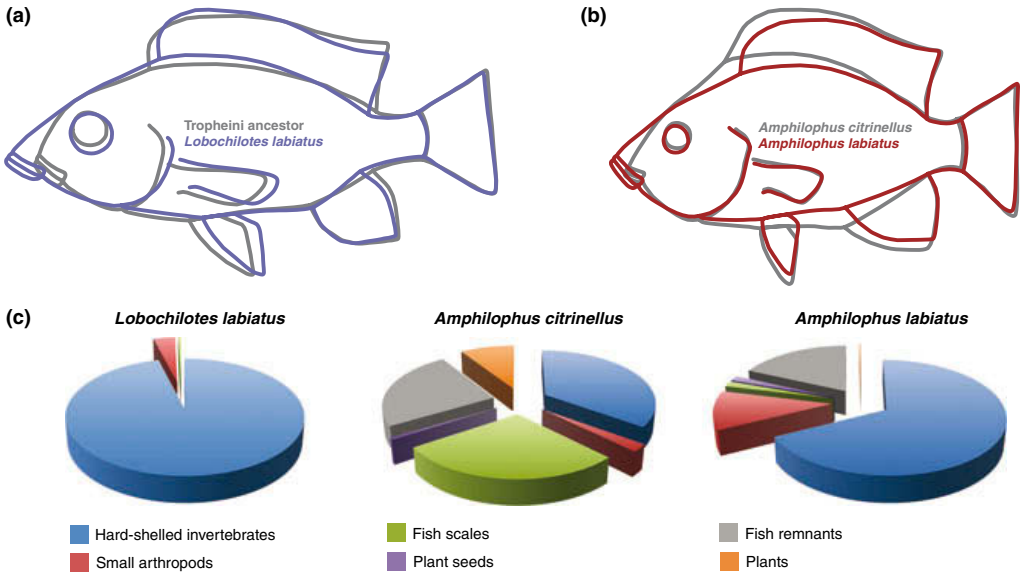

Fig. 3 Ecomorphology of the thick-lipped cichlid species in Central America and in Lake Tanganyika. (a) Body shape of *L. labiatus* in comparison with a reconstruction of the ancestor of *L. labiatus* and nine closely related Tropheini species. (b) Differences in body shape between *A. citrinellus* and *A. labiatus* along a discriminate function. In both plots, changes in landmark positions were increased threefold and interpolated outlines added for illustration purposes. Landmark locations are indicated in black on the reconstructed outlines in plot (a). (c) Analysis of stomach and gut content in the focal species. The fraction of each food category is shown.

ters. The alignment was performed using default settings with a maximum alignment score (t) of 180 and a maximum number of alignments for a single read (e) of 100; reads with multiple alignment locations were discarded. Next SAMTOOLS version 0.1.18 (Li *et al.* 2009) was used to sort and index the files and to generate count files, which were subsequently transformed into count tables and analysed in the R package DESEQ version 1.0.5 (Anders & Huber 2010). Differentially expressed genes between the four experimental groups were detected using a model based on a negative binomial distribution implemented in DESEQ. Differentially expressed genes with *P*-values (adjusted for multiple testing) >0.05 and/or a quotient of variance >1.00 were discarded to reduce the number of false positives. The remaining differentially expressed genes of all pairwise comparisons were tested for multiple hits. Next the hits of the three data sets were compared with each other to create a candidate gene list, consisting of genes that were found in multiple analyses in all three data sets. Lastly, these hits were compared to the annotated *A. burtoni* ESTs of Baldo *et al.* (2011).

Comparative gene expression assays using quantitative real-time PCR

Based on their function according to gene ontology terms (GO terms; http://www.geneontology.org/) and their putative involvement in lip formation and/or hypertrophy in other organisms, six candidate genes were selected out of the list of differentially expressed genes for further characterization by means of quantitative real-time PCR (qPCR). These candidate genes are the *Bcl2 adenovirus e1b 19-kda protein-interacting protein 3* (*BNIP3*), *long-chain-fatty-acid(CoA)-ligase 4* (*ACSL4*), *histone 3.3* (*His3*), *beta actin* (*Actb*), *coatomer subunit beta* (*Copb*) and *claudin 7* (*Cldn7*; see Table 1 for primer details). qPCR experiments were performed in total of 36 cichlid specimens: *L. labiatus* (six adults, six juveniles), *A. burtoni* (six adults, six juveniles), *A. labiatus* (six adults) and *A. citrinellus* (six adults). By performing two pairwise comparisons between a thick-lipped and a normal-lipped species (a species pair each from Africa and Nicaragua), we effectively control for species-specific expression differences, as genes specific to thick-lip tissue should be upregulated in both comparisons.

The experiments were conducted on a StepOnePlus Real-Time PCR system (Applied Biosystems) as described elsewhere (Diepeveen & Salzburger 2011) using the *elongation factor 1* (*EF1*) and the *ribosomal protein SA3* (*RpSA3*) as endogenous controls. Average relative quantifications (RQ) were calculated for the six experimental groups and subsequently analysed with a two-tailed unpaired t-test using GRAPHPAD PRISM version 5.0a for Mac OS X (www.graphpad.com). We compared the expression levels between the two thick-lipped species and a closely related normally lipped species (i.e. *L. labiatus* vs. *A. burtoni* and *A. labiatus* vs. *A. citrinellus*). We also compared adults vs.

Table 1 Primers used for the quantitative real-time PCR experiments

Locus	Forward (5′–3′)	Reverse (5′–3′)
Actb	CAGGCATCAGGGTGTAATGGTT	CAGGCATCAGGGTGTAATGGTT
Copb	GAGGCTACCTTGGCTGTCAAAG	GTGCTGGATGGTTTGAGGGTAA
His3	CATCTACTGGTGGAGTGAAGAAACC	GGATCTCACGCAGAGCAACA
ACSL4	TGGTTCTGCACCGGAGATG	TCTTGCGGTCAACAATTTGTAGA
BNIP3	AACAGTCCACCAAAGGAGTTCCT	CCTGATGCTGAGAGAGGTTGTG
Cldn7	GACATCATCCGGGCCTTCT	CACCGAACTCATACTTAGTGTTGACA
EF1	GCCCCTGCAGGACGTCTA	CGGCCGACGGGTACAGT
RpSA3	AGACCAATGACCTGAAGGAAGTG	TCTCGATGTCCTTGCCAACA

juveniles in the African species, as hypertrophy in lips is much less pronounced at juvenile stages, so that this experiment also captures ontogenetic changes in lip formation. As primer efficiency was lower in the Nicaraguan samples, no direct comparisons between African and Nicaraguan tissues were possible.

Results

Phylogenetic and demographic analyses

Our phylogenetic analysis of members of the Tanganyikan cichlid tribe Tropheini based on two mitochondrial and two nuclear DNA gene segments reveals only limited phylogenetic resolution between the main lineages of the tribe (Fig. 2a). This confirms an earlier analysis based on mitochondrial DNA only, which attributed the star-like phylogeny of the Tropheini to the rapidity of lineage formation in the early stages of the adaptive radiation of this clade (Sturmbauer *et al.* 2003). Just as in the previous study, the thick-lipped species *L. labiatus* represents a separate lineage (without a closely related sister-taxon) that branches off relatively early in the phylogeny, but shows affinities to the algae-eating genera *Petrochromis* and *Simochromis*.

The haplotype genealogies of the *Amphilophus* samples based on the mitochondrial control region and the nuclear *ednrb1* gene (Fig. 2b) revealed haplotype sharing between *A. citrinellus* and *A. labiatus* (see also Barluenga & Meyer 2010). While all *Amphilophus* sequences were identical in *phpt1*, we detected three shared haplotypes in ednrb1 and 24 haplotypes in the mitochondrial control region (two shared, ten unique to *A. labiatus* and twelve unique to *A. citrinellus*).

The mismatch analyses based on the mitochondrial control region sequences revealed unimodal distributions for the two sympatrically occurring *Amphilophus* species and a bimodal distribution for *L. labiatus* (Fig. 2c). According to this analysis, the demographic expansion of the two *Amphilophus* species happened at similar times, with the one of *A. citrinellus* being slightly older than that of *A. labiatus* (mean number of differences: 3.9 vs. 3.2; τ: 3.9 vs. 3.5; see also Barluenga & Meyer 2010, who provide a relative time frame for the evolution of the Midas Cichlid species complex); the mean number of differences in *L. labiatus* was 6.4 (τ: 6.5).

Geometric morphometric analyses

The PCA of overall body shape revealed substantial overlap between the two Nicaraguan species *A. citrinellus* and *A. labiatus* (Appendix S3). The African thick-lipped species *L. labiatus* is separated from these mainly by principal component 1 (accounting for 20.2% of the variance), whereas principal component 2 (covering 16.0% of the variance) did not discriminate much between species. The discriminant function analysis, in which we compared species in a pairwise manner, revealed the main morphological differences between species. Of the two Nicaraguan species, *A. labiatus* had a more acute head, less deep body and a larger mouth than *A. citrinellus* (Fig. 3) (see also Klingenberg *et al.* 2003). These characters were even more pronounced in *L. labiatus*, when compared to either of the *Amphilophus* species. However, the distance in morphospace between the two species with fleshy lips was somewhat smaller than between *A. citrinellus* and *L. labiatus* (procrustes distance 0.08 and 0.1, respectively). We also estimated the body shape of the ancestor of *L. labiatus* and the 9 most closely related Tropheini species. A comparison of this reconstructed shape and the mean shape of our *L. labiatus* samples highlighted similar morphological differences as the comparison of the Nicaraguan species (Fig. 3), especially in the mouth region.

Stomach and gut content analyses

The fractions of food categories in guts and stomachs differed between *A. citrinellus*, *A. labiatus* and *L. labiatus* (Fig. 3c). While the diet of *A. citrinellus* did not overlap with that of *A. labiatus* (Schoener's index: 0.58) or *L. labiatus* (Schoener's index: 0.38), we found significant overlap between the two thick-lipped species *A. labiatus* and *L. labiatus* (Schoener's index: 0.71) (note that any value >0.6 is considered 'biologically significant'; see Wallace 1981). The stomach and gut contents of both

thick-lipped species consisted of a substantial fraction of hard-shelled prey (*Lobochilotes labiatus* 96%, *Amphilophus labiatus* 67.6%, *Amphilophus citrinellus* 35%).

Field observations in Lobochilotes labiatus

A careful inspection of the video material confirmed the findings from the stomach and gut content analyses that *L. labiatus* regularly feeds on snails (more than 90% of the stomach and gut content of *L. labiatus* consisted of snail shells). Small snails were engulfed using suction feeding without the lips touching the prey item or the surface (rocks) on which the items were placed. When feeding on larger snails, however, *L. labiatus* exhibited a different feeding strategy and snails were no longer taken up using suction feeding. Instead, *L. labiatus* used their lips to snatch the snails and they turned the snails a few times before they either swallowed the snails or spat them out (see Appendix S4).

Comparative gene expression assays using RNAseq

On average, ca. 42 million total reads were retrieved for each of the four RNAseq samples (*A. burtoni* adult, *A. burtoni* juvenile, *L. labiatus* adult and *L. labiatus* juvenile). Quality filtering and trimming reduced this number so that on average 21.9 (Data set 1), 24.6 (Data set 2) and 23.5 (Data set 3) million reads were aligned to the reference cichlid assembly. Five different pairwise comparisons were made to obtain genes that are differentially expressed between thick lips and normal lips (see Table 2 for the three comparisons with the highest number of genes being different). The largest number of differentially expressed genes between *L. labiatus* and *A. burtoni* was detected in adult lip tissue, with the majority of the genes being upregulated in *L. labiatus*. The total number of differentially expressed genes ranged from 9050 (Data set 3; three pairwise comparisons) to 15230 (Data set 2; five pairwise comparisons). A substantial fraction of these differentially expressed genes appeared in at least two comparisons in each data set (Data set 1: 2085 [22.1% of all hits]; Data set 2: 8078 [53.0%]; Data set 3: 1693 [18.7%]). Of these 'multiple hits', 1463 were detected in all three data sets and 560 of those could be unequivocally annotated.

A more stringent analysis, in which only loci that appeared in at least three of five comparisons were included, resulted in 231 differentially expressed genes. A functional annotation of these 231 hits with Blast2GO resulted in a total of 141 annotations (122 upregulated and 19 downregulated in *L. labiatus*; see Appendix S3). Based on their annotations, known functions and/or exceptional fold change (>1000) between *A. burtoni* and *L. labiatus*, thirteen genes were identified as good candidates for being involved in the morphogenesis of fleshy lips (Table 3).

Comparative gene expression assays using quantitative real-time PCR

The results of the comparative gene expression assays between the thick-lipped species and the normal-lipped species are depicted in Fig. 4 and Appendix S5. Overall, the qPCR experiments largely validate differential gene expression in normal and hypertrophied lip tissue as indicated by RNAseq. In the African species pair *L. labiatus* and *A. burtoni*, which were the two species used for RNAseq, differences were highly significant in four of the six genes tested: *Actb* ($P = 0.0099$), *Cldn7* ($P = 0.004$), *ACSL4* ($P = 0.0005$) and *His3* ($P = 0.0003$). However, we would like to point out one inconsistency between RNAseq and qPCR. *Actb* was actually found to be downregulated in hypertrophied lips by RNAseq, while it shows significantly higher expression levels in lip tissue in the qPCR experiments (Fig. 4).

The comparison between lip tissue in adult and juvenile *L. labiatus* and *A. burtoni* further revealed a trend towards higher expression in lip tissue of adult *L. labiatus* in *Actb*, *BNIP3*, *Cldn7* and *Copb* (Appendix S5), whereas, generally, an opposite trend is observed in *A. burtoni*, although statistical support was only found in two cases [*Cldn7* ($P = 0.0063$) and *ACSL4* ($P = 0.0328$)]. This again suggests that these genes are involved in the formation of fleshy lips. In the Nicaraguan species pair, a similar trend was observed as in the African species pair, with four of the five genes tested appearing to be upregulated in lip tissue

Table 2 Pairwise comparisons of differentially expressed genes and total number of unique differentially expressed genes in the three data sets compiled in this study

Comparison	Data set 1	Data set 2	Data set 3
AB vs. LL	7120 (4606; 2514)	7080 (4689; 2391)	7285 (4665; 2620)
AB vs. LLjuv	3611 (3395; 216)	13747 (10683; 3064)	2618 (2514; 104)
ABjuv vs. LLjuv	1116 (792; 324)	3971 (2710; 1261)	986 (687; 298)
Total	9407	15225	9050

AB, *Astatotilapia burtoni;* LL, *Lobochilotes labiatus*; juv, juvenile; numbers in brackets denote the number of upregulated and downregulated genes in *L. labiatus*.

Table 3 Thirteen candidate loci for the genetic basis of lip development in the East African cichlid *Lobochilotes labiatus*, based on RNAseq and qPCR in comparison with *Astatotilapia burtoni*, in combination with information on gene functions (in alphabetical order)

Locus	Abbreviation
ATPase mitochondrial precursor	*ATPmp*
Bcl2 adenovirus e1b 19-kda protein-interacting protein 3	*BNIP3*
Beta actin	*Actb*
Caspase-8	*Casp8*
Claudin 7	*Cldn7*
Coatomer subunit beta	*Copb*
Grainyhead-like protein 1 homolog	*Grhl1*
Heat-shock 70-kda protein 12a-like	*Hspa12al*
Histone 3.3	*His3*
Laminin subunit gamma-2	*Lamc2*
Long-chain-fatty-acid(CoA)-ligase 4	*ACSL4*
Sodium-dependent phosphate transporter 1	*Slc17a1*
Transcription factor ap-2 gamma	*Tfap2*

of *A. labiatus* as compared to *A. citrinellus* (Fig. 4; we could not amplify *BNIP3* here). We would like to note, however, that qPCR efficiency was less good in the *Amphilophus* samples, most likely because we used primers designed for the African species pair based on the available genomic resources, which also explains the limited statistical support for these comparisons. Interestingly, it seems that several loci (i.e. *Actb*, *Cldn7*, *Copb*, *His3*) are upregulated in both thick-lipped species when compared to their normally lipped relatives.

Discussion

The species flocks of cichlid fishes in the East African Great Lakes Victoria, Malawi and Tanganyika, counting hundreds of endemic species each, are prime examples of adaptive radiation and explosive speciation (see e.g. Kocher 2004; Seehausen 2006; Salzburger 2009). Interestingly, the cichlid adaptive radiations in East Africa have independently produced ecomorphs with highly similar colour patterns and (mouth) morphologies (Kocher *et al.* 1993). Here, we explore the ecological and genetic basis of one of the particular trophic structures of cichlids, which has evolved convergently in various cichlid assemblages: fleshy lips. Instead of focusing on species with hypertrophied lips between the radiations in the East African lakes, we compare the thick-lipped phenotype between a cichlid assemblage in East African (Lake Tanganyika) and in Central American (the lake Nicaragua/Managua system), where thick-lipped species have evolved in parallel (see Fig. 1).

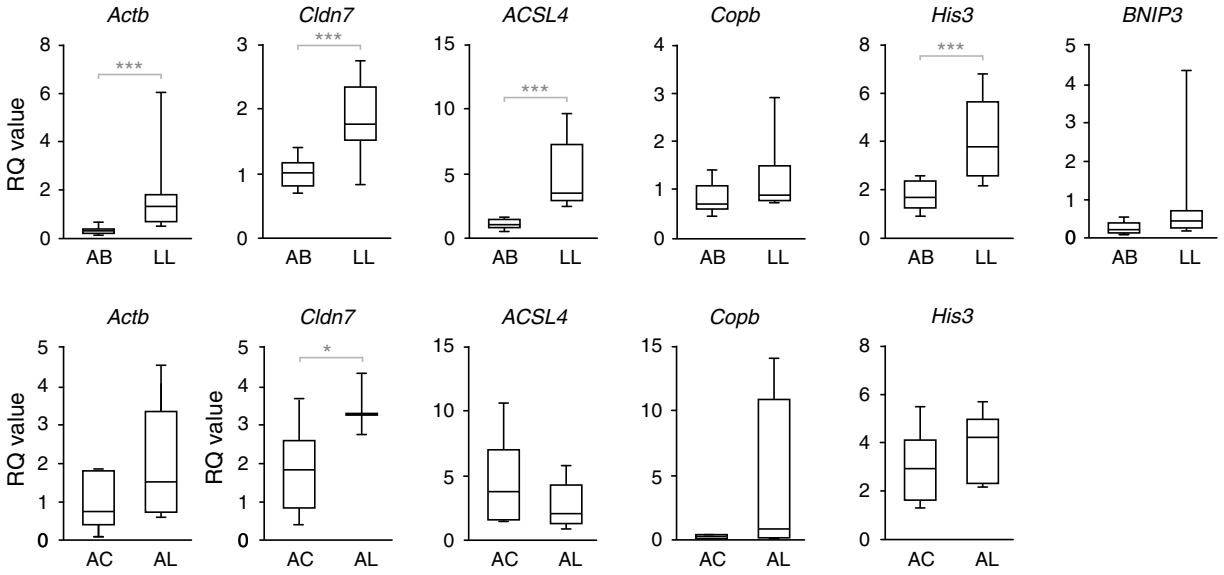

Fig. 4 Results from the comparative gene expression experiments via quantitative real-time PCR. The six genes tested in this experiment were selected on the basis of comparative RNA sequencing. All genes tested show a higher expression level in lip tissue of the Tanganyikan thick-lipped species *L. labiatus* as compared to *A. burtoni* (top panel; note that we used both juvenile and adult samples in these analyses to increase statistical power). A similar trend was found when comparing the Nicaraguan thick-lipped species *A. labiatus* to its sister species *A. citrinellus* (with the exception of *ACSL4*; lower panel). Note that *BNIP3* could not amplified in the *Amphilophus* species. *Astatotilapia burtoni* (AB); *Lobochilotes labiatus* (LL); *Amphilophus citrinellus* (AC); *Amphilophus labiatus* (AL); **P* < 0.05; ****P* < 0.01.

The evolution of hypertrophied lips in cichlid adaptive radiations

Our phylogenetic and demographic analyses in the Tanganyikan Tropheini and the Nicaragua Midas Cichlid species complex reveal that the thick-lipped species are nested within their respective clade. The molecular phylogeny of 14 Tropheini species (Fig. 2a) shows a footprint characteristic for adaptive radiations: a 'bottom heavy' topology with only limited phylogenetic resolution at the deeper nodes due to rapid lineage formation (Gavrilets & Vose 2005). Our new analysis thus confirms previous results based on mtDNA only (Sturmbauer *et al.* 2003) or a combination of mtDNA and AFLPs (Koblmuller *et al.* 2010). In all analyses thus far, the thick-lipped species *L. labiatus* forms an independent evolutionary lineage that branches off deep in the Tropheini. Its exact position remains unclear, though. In the AFLP phylogeny of Koblmuller *et al.* (2010), *L. labiatus* appears as sister group to all Tropheini except for the genus *Tropheus*, which is sister to all other representatives of that clade (the topology has very little support, though). In our new phylogeny and the previous mtDNA trees of Sturmbauer *et al.* (2003), *L. labiatus* shows affinities to *Simochromis* and *Petrochromis* (with moderate support). In all phylogenies, however, *L. labiatus* is nested within a clade formed by various species that feed on algae and biocover (see our character state reconstruction in Fig. 2a).

In the Midas Cichlid species complex from Central America, a phylogenetic approach is not applicable with the available molecular markers. There is simply too little genetic variation, even in the rapidly evolving mitochondrial control region, as a consequence of the young age of the assemblage (see Barluenga & Meyer 2004, 2010; Barluenga *et al.* 2006). The structures of our haplotype genealogies, which now also include the analysis of a nuclear gene (Fig. 2b), confirm this scenario. In combination with the mismatch analyses (Fig. 2c), these data suggest that *A. labiatus* underwent its main demographic expansion soon after the expansion of the sympatric *A. citrinellus* populations (see Barluenga & Meyer 2010 for a large-scale analysis of the Midas Cichlid species complex).

In both species assemblages, the evolution of the thick-lipped phenotype was associated with similar modifications of overall body shape (Fig. 3a,b). Reduced body depth, a more acute head shape and a larger mouth, along with the prominently enlarged lips, can be hypothesized to be adaptations to the species' microhabitat and trophic niche. If individuals search for food in narrow rock crevices, these modifications appear advantageous. Klingenberg *et al.* (2003) already suggested that the elongation of the head, as observed in both '*labiatus*' species, increases suction power. Other morphological differences between the two thick-lipped species, such as eye size or the length of anal fin insertion, might be either due to adaptations to the specific environments or due to phylogenetic effects. Inclusion of other thick-lipped species in future studies focusing on the ecology and morphological evolution of this trait might answer this question.

The function of hypertrophied lips in cichlids

Hypertrophied lips in cichlids have been implicated in several functions. For example, it has been suggested that fleshy lips are used to seal cracks and grooves to facilitate sucking of invertebrates (Barlow & Munsey 1976; Ribbink *et al.* 1983; Seehausen 1996; Konings 1998), that they act as bumpers to protect from mechanical shock (Greenwood 1974; Yamaoka 1997) or that they function as taste (Arnegard *et al.* 2001) or mechanoreceptors (Fryer 1959; Fryer & Iles 1972). Previous food web analyses on *L. labiatus* identified this species as mollusc eater (Nori 1997).

Our ecomorphological analysis of the thick-lipped species *L. labiatus* from Lake Tanganyika and *A. labiatus* from the large lakes in Nicaragua suggests that this phenotype is indeed associated with feeding on hard-shelled prey such as snails, mussels and crustaceans in rocky habitats (Fig. 3c). We cannot, however, conclusively answer the question whether the lips are used to seal rock crevices or whether they serve as bumpers or receptors. In the underwater observations at our field site at Lake Tanganyika, small snails were usually engulfed by *L. labiatus* via suction feeding, whereas larger snails were turned around several times before being swallowed or spit out (see Appendix S4). This would classify the lips as instrument to handle hard-shelled invertebrate food (mostly molluscs). Note, however, that our observations were made in semi-natural conditions only, in the form of concrete ponds equipped with stones from the lake and filled with lake water.

Our experimental set-up could not address the possibility that phenotypic plasticity plays a role in the formation of fleshy lips, as has previously been shown in certain foraging traits in cichlid fishes (oral jaws: Meyer 1987; pharyngeal jaws: e.g. Greenwood 1965; Huysseune 1995; Muschick *et al.* 2011). Interestingly, it has been reported that thick-lipped cichlid species lose their fleshy lips under unnatural conditions in captivity (when fed with standard food; Barlow & Munsey 1976; Barlow 1976; Loiselle 1998). So far, there is no evidence for the opposite process, the plastic development of fleshy lips due to environmental or feeding properties. In the common garden experiment of Muschick *et al.*

(2011), one group of normally lipped *A. citrinellus* individuals was fed with whole snails over a period of several months, and—although not formally assessed—no increase in lip size was apparent (compared to the other two treatment groups peeled snails and crushed snails). Another study on a snail crusher (Huysseune 1995) did not report such changes either, which seems to suggest that phenotypic plasticity in the lips, if at all present, is specific to thick-lipped species only. Future common garden and feeding experiments should thus expand on this question. Such experiments, combined with molecular analyses, should focus on the plastic component of this trait and its genomic basis.

Insights into the genetic basis of hypertrophied lips in cichlids

Our comparative gene expression assays with RNA sequencing between tissue from thick and normal lips identified a set of 141 candidate genes that might be responsible for the morphogenesis or the maintenance of fleshy lips in (East African) cichlid fish (Appendix S3). Six genes were tested further by means of quantitative real-time PCR, and these experiments largely confirm the results obtained from RNAseq (Fig. 4). While there is no obvious functional connection to fleshy lips for three of these differentially expressed genes (*ACSL4*, *His3* and *BNIP3*), the observed upregulation of the remaining three (*Actb*, *Cldn7* and *Copb*) makes sense in the light of the structure of hypertrophied lips. These three genes (together with *BNIP3*) also show a higher expression in lip tissue from adult vs. juvenile *L. labiatus* (Appendix S5).

It has previously been shown that the 'fleshy' lips of the Lake Malawi cichlid *Otopharynx pachycheilus* mainly consist of loose connective tissue covered by dermis and a layer of epithelial cells (Arnegard *et al.* 2001). Interestingly, the known functions of *Actb*, *Cldn7* and *Copb* can be directly implicated in cell and/or intercell or membrane structure. The cytoplasmic *Actb* is found in high abundance in nonmuscle cells, where it promotes cell surface and cell thickness (Schevzov *et al.* 1992), which is also consistent with its upregulation in the more massive adult compared to juvenile *L. labiatus* lips (Appendix S5). The integral membrane protein *Cldn7* (among other *claudin* gene family members) constitutes the backbone of tide junctions between epithelial cells (Tsukita *et al.* 2001). The coatomer coat proteins (such as *Copb*) are involved in protein and membrane trafficking via vesicle secreting between the endoplasmic reticulum and the Golgi apparatus, plus the intra-Golgi transport (Duden 2003). In addition, they mediate lipid homoeostasis and lipid storage for energy use and membrane assembly (Soni *et al.* 2009). *Copb* might thus be involved in cellular (membrane) development but possibly also in the formation of fat cells that compose adipose tissue, a specific subtype of connective tissue. Clearly, much more work will be necessary to unravel the development and genetic basis of hypertrophied lips in cichlids, for which we herewith established a valuable starting ground.

Our results, especially the comparison of gene expression levels between the thick-lipped species in East Africa and Central America (Fig. 4), allow us to touch on ongoing discussions related to the genetic basis of convergent morphologies (reviewed in Brakefield 2006; Arendt & Reznick 2008; Elmer & Meyer 2011). Although our qPCR results in Midas Cichlid (*Amphilophus* spp.) species must be taken with caution (efficiency was lower as a consequence of using molecular tools developed for the African species leading to a lack of statistical power), we find rather similar trends in gene expression. Our results seem to indicate that a largely overlapping set of genes was recruited to develop the hypertrophied lips in Nicaraguan and African species, which are—according to most authors—separated by ~ 100 million years of evolution. This important question about the basis of convergent phenotypes should be addressed in future studies, and thick-lipped fish species, including those outside the family Cichlidae, appear as an excellent model system.

Conclusion

Our integrative evolutionary, ecological, morphological, observational and genomic analysis of thick-lipped species in East Africa and in Nicaragua reveals stunning similarities between these convergent morphs. Both thick-lipped species appear to have evolved early in the respective clade, they seem to have adapted to the same habitat (rocks) and food source (hard-shelled prey), and their evolution was associated with comparable morphological trajectories, especially in the mouth and head region. Importantly, we also show that the expression patterns of at least some genes are similar, too. We thus provide valuable resource for future studies focusing on the development of this trait and genetic basis of convergence.

Acknowledgements

We would like to thank our helpers in the field, V. Campos, C. Heule, B. Meyer, M. Roesti; E. P. van den Berghe and G. Tembo and his crew for their logistic support in Nicaragua and Africa, respectively; the Ministerio del Ambiente y los Recursos Naturales Nicaragua (MARENA) and the Lake Tanganyika Research Unit, Department of Fisheries, Republic of Zambia,

for research permits; and three anonymous referees and the Subject Editor, C. Eizaguirre, for valuable comments. This study was supported by grants from the Fundacao para Ciencia e a Tecnologia (FCT, Portugal) to M. E. S., the Swiss Academy of Sciences to A. I., the Spanish Minsiterio de Economía y Competitividad to M. B., and the European Research Council (ERC, Starting Grant 'INTERGENADAPT'), the University of Basel and the Swiss National Science Foundation (SNF, grants 3100A0_122458 and CRSII3_136293) to W. S.

References

Anders S, Huber W (2010) Differential expression analysis for sequence count data. *Genome Biology*, **11**, R106.

Arendt J, Reznick D (2008) Convergence and parallelism reconsidered: what have we learned about the genetics of adaptation? *Trends in Ecology and Evolution*, **23**, 26–32.

Arnegard ME, Snoeks J, Schaefer SA (2001) New three-spotted cichlid species with hypertrophied lips (Teleostei: Cichlidae) from the deep waters of Lake Malaŵi/Nyasa, Africa. *Copeia*, **2001**, 705–717.

Baldo L, Santos ME, Salzburger W (2011) Comparative transcriptomics of Eastern African cichlid fishes shows signs of positive selection and a large contribution of untranslated regions to genetic diversity. *Genome Biology and Evolution*, **3**, 443–455.

Barlow GW (1976) The Midas cichlid in Nicaragua. In: *Investigations of the Ichthyofauna of Nicaraguan lakes* (ed. Thorson TB), pp. 333–358. School of Life Sciences, University of Nebraska, Lincoln, Nebraska.

Barlow GW, Munsey JW (1976) The Red Devil Midas Cichlid species complex in Nicaragua. In: *Investigations of the Ichthyofauna of Nicaraguan Lakes* (ed. Thorson TB), pp. 359–370. School of Life Sciences, University of Nebraska, Lincoln, Nebraska.

Barluenga M, Meyer A (2004) The Midas cichlid species complex: incipient sympatric speciation in Nicaraguan cichlid fishes? *Molecular Ecology*, **13**, 2061–2076.

Barluenga M, Meyer A (2010) Phylogeography, colonization and population history of the Midas cichlid species complex (*Amphilophus* spp.) in the Nicaraguan crater lakes. *BMC Evolutionary Biology*, **10**, 326.

Barluenga M, Stolting KN, Salzburger W, Muschick M, Meyer A (2006) Sympatric speciation in Nicaraguan crater lake cichlid fish. *Nature*, **439**, 719–723.

Berner D, Roesti M, Hendry AP, Salzburger W (2010) Constraints on speciation suggested by comparing lake-stream stickleback divergence across two continents. *Molecular Ecology*, **19**, 4963–4978.

Blankenberg D, Von Kuster G, Coraor N (2010) Galaxy: a web-based genome analysis tool for experimentalists. *Current protocols in molecular biology/edited by Frederick M. Ausubel et al.* Chapter 19, Unit 19 10 11-21.

Brakefield PM (2006) Evo-devo and constraints on selection. *Trends in Ecology and Evolution*, **21**, 362–368.

Brichard P (1989) Cichlids and all Other Fishes of Lake Tanganyika, T.H.F. Publications, Neptune City, New Jersey.

Bruford MW, Hanotte O, Brookfield JFY, Burke T (1998) Multilocus and single-locus DNA fingerprinting. In: *Molecular Analysis of Populations* (ed. Hoelzel AR), pp. 283–336. Oxford University Press, New York.

Butler MA, Sawyer SA, Losos JB (2007) Sexual dimorphism and adaptive radiation in Anolis lizards. *Nature*, **447**, 202–205.

Diepeveen ET, Salzburger W (2011) Molecular characterization of two endothelin pathways in East African cichlid fishes. *Journal of Molecular Evolution*, **73**, 355–368.

Duden R (2003) ER-to-Golgi transport: COP I and COP II function (Review). *Molecular Membrane Biology*, **20**, 197–207.

Elmer KR, Meyer A (2011) Adaptation in the age of ecological genomics: insights from parallelism and convergence. *Trends in Ecology and Evolution*, **26**, 298–306.

Excoffier L, Laval G, Schneider S (2005) Arlequin (version 3.0): an integrated software package for population genetics data analysis. *Evolutionary Bioinformatics Online*, **1**, 47–50.

Fryer G (1959) The trophic interrelationships and ecology of some littoral communities of Lake Nyasa with a special reference to the fishes, and a discussion on the evolution of a group of rock-frequenting Cichlidae. *Proceedings of the Zoological Society of London*, **132**, 153–281.

Fryer G, Iles TD (1972) The Cichlid Fishes of the Great Lakes of Africa: Their Biology and Evolution. Oliver & Boyd, Edinburgh.

Gavrilets S, Losos JB (2009) Adaptive radiation: contrasting theory with data. *Science*, **323**, 732–737.

Gavrilets S, Vose A (2005) Dynamic patterns of adaptive radiation. *Proceeding of the National Academy of Sciences U S A*, **102**, 18040–18045.

Genner MJ, Seehausen O, Lunt DH *et al.* (2007) Age of cichlids: new dates for ancient lake fish radiations. *Molecular Biology and Evolution*, **24**, 1269–1282.

Giardine B, Riemer C, Hardison RC *et al.* (2005) Galaxy: a platform for interactive large-scale genome analysis. *Genome Research*, **15**, 1451–1455.

Goecks J, Nekrutenko A, Taylor J (2010) Galaxy: a comprehensive approach for supporting accessible, reproducible, and transparent computational research in the life sciences. *Genome Biology*, **11**, R86.

de Graaf M, Dejen E, Osse JWM, Sibbing FA (2008) Adaptive radiation of Lake Tana's (Ethiopia) *Labeobarbus* species flock (Pisces, Cyprinidae). *Marine and Freshwater Research*, **59**, 391–407.

Grant PR, Grant BR (2008) How and Why Species Multiply: The Radiations of Darwin's Finches. Princeton University Press, Princeton, USA.

Greenwood PH (1965) Environmental effects on the pharyngeal mill of a cichlid fish, *Astatoreochromis alluaudi*, and their taxonomic implications. *Proceedings of the Linnean Society London*, **176**, 1–10.

Greenwood PH (1974) The cichlid fishes of Lake Victoria East Africa: the biology and evolution of a species flock. *Bulletin of the British Museum for Natural History (Zool.) Supplementary*, **6**, 1–134.

Harmon LJ, Kolbe JJ, Cheverud JM, Losos JB (2005) Convergence and the multidimensional niche. *Evolution*, **59**, 409–421.

Herder F, Schwarzer J, Pfaender J, Hadiaty RK, Schliewen UK (2006) Preliminary checklist of sailfin silversides (Teleostei: Telmatherinidae) in the Malili Lakes of Sulawesi (Indonesia), with a synopsis of systematics and threats. *Verhandlungen der Gesellschaft für Ichthyologie*, **5**, 139–163.

Huysseune A (1995) Phenotypic plasticity in the lower pharyngeal jaw dentition of *Astatoreochromis alluaudi* (Teleostei: Cichlidae). *Archives in Oral Biology*, **40**, 1005–1014.

Johnson MA, Revell LJ, Losos JB (2009) Behavioral convergence and adaptive radiation: effects of habitat use on territorial behavior in Anolis lizards. *Evolution*, **64**, 1151–1159.

Katoh K, Toh H (2008) Recent developments in the MAFFT multiple sequence alignment program. *Briefings in Bioinformatics*, **9**, 286–298.

Klingenberg CP (2011) MorphoJ: an integrated software package for geometric morphometrics. *Molecular Ecology Resources*, **11**, 353–357.

Klingenberg CP, Barluenga M, Meyer A (2003) Body shape variation in cichlid fishes of the *Amphilophus citrinellus* species complex. *Biological Journal of the Linnean Society*, **80**, 397–408.

Koblmuller S, Egger B, Sturmbauer C, Sefc KM (2010) Rapid radiation, ancient incomplete lineage sorting and ancient hybridization in the endemic Lake Tanganyika cichlid tribe Tropheini. *Molecular Phylogenetics and Evolution*, **55**, 318–334.

Kocher TD (2004) Adaptive evolution and explosive speciation: the cichlid fish model. *Nature Reviews Genetics*, **5**, 288–298.

Kocher TD, Conroy JA, McKaye KR, Stauffer JR (1993) Similar morphologies of cichlid fish in lakes Tanganyika and Malawi are due to convergence. *Molecular Phylogenetics and Evolution*, **2**, 158–165.

Konings A (1998) Tanganyikan Cichlids in their Natural Habitat. Cichlid Press, El Paso.

Lang M, Miyake T, Braasch I *et al.* (2006) A BAC library of the East African haplochromine cichlid fish *Astatotilapia burtoni*. *Journal of Experimental Zoology. Part B, Molecular and Developmental Evolution*, **306B**, 35–44.

Lee WJ, Conroy J, Howell WH, Kocher TD (1995) Structure and evolution of teleost mitochondrial control regions. *Journal of Molecular Evolution*, **41**, 54–66.

Li H, Handsaker B, Wysoker A *et al.* (2009) The sequence alignment/map format and SAMtools. *Bioinformatics*, **25**, 2078–2079.

Loiselle PV (1998) The *Amphilophus labiatus* Species Complex. The Cichlid Room Companion. Retrieved on June 05, 2012, from: http://www.cichlidae.com/article.php?id=106.

Losos JB (2009) Lizards in an Evolutionary Tree: Ecology and Adaptive Radiation of Anoles. University of California Press, Berkeley.

Losos JB (2010) Adaptive radiation, ecological opportunity, and evolutionary determinism. American Society of Naturalists E. O. Wilson award address. *American Naturalist*, **175**, 623–639.

Losos JB (2011) Convergence, adaptation and constraint. *Evolution*, **65**, 1827–1840.

Losos JB, Ricklefs RE (2009) Adaptation and diversification on islands. *Nature*, **457**, 830–836.

Losos JB, Jackmann TR, Larson A, De Queiroz K, Rodrigues-Schettino L (1998) Contingency and determinism in replicated adaptive radiations of island lizards. *Science*, **279**, 2115–2118.

Matschiner M, Hanel R, Salzburger W (2011) On the origin and trigger of the notothenioid adaptive radiation. *PLoS One*, **6**, e18911.

Meyer A (1987) Phenotypic plasticity and heterochrony in *Cichlasoma managuense* (Pisces, Cichlidae) and their implications for speciation in cichlid fishes. *Evolution*, **41**, 1357–1369.

Meyer A, Morrissey JM, Schartl M (1994) Recurrent origin of a sexually selected trait in *Xiphophorus* fishes inferred from a molecular phylogeny. *Nature*, **368**, 539–542.

Muschick M, Barluenga M, Salzburger W, Meyer A (2011) Adaptive phenotypic plasticity in the Midas cichlid fish pharyngeal jaw and its relevance in adaptive radiation. *BMC Evolutionary Biology*, **11**, 116.

Nori M (1997) Structure of littoral fish communities. In: *Fish Communities in Lake Tanganyika* (eds Kawanabe H, Hori M, Nagoshi M), pp. 277–298. Kyoto University Press, Kyoto.

Nosil P, Crespi BJ, Sandoval DP (2002) Host-plant adaptation drives the parallel evolution of reproductive isolation. *Nature*, **417**, 440–443.

Posada D (2008) jModelTest: phylogenetic model averaging. *Molecular Biology and Evolution*, **25**, 1253–1256.

Ribbink AJ, Marsch BA, Marsch AC, Ribbink AC, Sharp BJ (1983) A preliminary survey of the cichlid fishes of rocky habitats in Lake Malawi. *South African Journal of Zoology*, **18**, 149–310.

Roesti M, Hendry AP, Salzburger W, Berner D (2012) Genome divergence during evolutionary diversification as revealed in replicate lake–stream stickleback population pairs. *Molecular Ecology*, **21**, 2852–2862.

Rohlf FJ (2006) DIG, Version 2.10.0. Department of Ecology and Evolution. State University of New York, Stony Brook, NY.

Ronquist F, Huelsenbeck JP (2003) MrBayes 3: Bayesian phylogenetic inference under mixed models. *Bioinformatics*, **19**, 1572–1574.

Rundle HD, Nagel L, Wenrick Boughman J, Schluter D (2000) Natural selection and parallel speciation in sympatric sticklebacks. *Science*, **287**, 306–308.

Salzburger W (2009) The interaction of sexually and naturally selected traits in the adaptive radiations of cichlid fishes. *Molecular Ecology*, **18**, 169–185.

Salzburger W, Meyer A (2004) The species flocks of East African cichlid fishes: recent advances in molecular phylogenetics and population genetics. *Naturwissenschaften*, **91**, 277–290.

Salzburger W, Meyer A, Baric S, Verheyen E, Sturmbauer C (2002) Phylogeny of the Lake Tanganyika cichlid species flock and its relationship to the Central and East African haplochromine cichlid fish faunas. *Systematic Biology*, **51**, 113–135.

Salzburger W, Mack T, Verheyen E, Meyer A (2005) Out of Tanganyika: Genesis, explosive speciation, key-innovations and phylogeography of the haplochromine cichlid fishes. *BMC Evolutionary Biology*, **5**, 17.

Salzburger W, Renn SC, Steinke D, Braasch I, Hofmann HA, Meyer A (2008) Annotation of expressed sequence tags for the East African cichlid fish *Astatotilapia burtoni* and evolutionary analyses of cichlid ORFs. *BMC Genomics*, **9**, 96.

Salzburger W, Ewing GB, Von Haeseler A (2011) The performance of phylogenetic algorithms in estimating haplotype genealogies with migration. *Molecular Ecology*, **20**, 1952–1963.

Schevzov G, Lloyd C, Gunning P (1992) High level expression of transfected beta- and gamma-actin genes differentially impacts on myoblast cytoarchitecture. *The Journal of Cell Biology*, **117**, 775–785.

Schluter D (2000) The Ecology of Adaptive Radiation. Oxford University Press, New York.

Schluter D, Nagel LM (1995) Parallel speciation by natural selection. *American Naturalist*, **146**, 292–301.

Schoener TW (1970) Nonsynchronous spatial overlap of lizards in patchy habitats. *Ecology*, **51**, 408–418.

Seehausen O (1996) Lake Victoria Rock Cichlids, Verdujin Cichlids, Zevenhuizen, The Netherlands.
Seehausen O (2006) African cichlid fish: a model system in adaptive radiation research. *Proceeding of the Royal Society London B*, **273**, 1987–1998.
Sereno PC, Wilson JA, Conrad JL (2004) New dinosaurs link southern landmasses in the Mid-Cretaceous. *Proceeding of the Royal Society London B*, **271**, 1325–1330.
Sibbing FA, Nagelkerke LAJ, Stet RJM, Osse JWM (1998) Speciation of endemic Lake Tana barbs (*Cyprinidae*, Ethiopia) driven by trophic resource partitioning: a molecular and ecomorphological approach. *Aquatic Ecology*, **32**, 217–227.
Simpson GG (1953) The Major Features of Evolution, Columbia University Press, New York.
Soni KG, Mardones GA, Sougrat R, Smirnova E, Jackson CL, Bonifacino JS (2009) Coatomer-dependent protein delivery to lipid droplets. *Journal of Cell Science*, **122**, 1834–1841.
Stiassny MLJ, Meyer A (1999) Cichlids of the Rift Lakes. *Scientific American*, **280**, 64–69.
Sturmbauer C, Hainz U, Baric S, Verheyen E, Salzburger W (2003) Evolution of the tribe Tropheini from Lake Tanganyika: synchronized explosive speciation producing multiple evolutionary parallelism. *Hydrobiologia*, **500**, 51–64.
Swofford DL (2003) PAUP*—Phylogenetic Analyses Using Parsimony and Other Methods, Version 4.0, Sinauer, Sunderland, Massachusetts.
Tsukita S, Furuse M, Itoh M (2001) Multifunctional strands in tight junctions. *Nature Reviews in Molecular Cell Biology*, **2**, 285–293.
Verheyen E, Salzburger W, Snoeks J, Meyer A (2003) Origin of the superflock of cichlid fishes from Lake Victoria, East Africa. *Science*, **300**, 325–329.
Villa J (1982) Peces Nicaragüenses de Agua Dulce, Fondo de Promoción Cultural, Banco de América, Managua.
Wake DB, Wake MH, Specht CD (2011) Homoplasy: from detecting pattern to determining process and mechanism of evolution. *Science*, **331**, 1032–1035.
Wallace RK (1981) An assessment of diet-overlap indexes. *Transactions of the American Fisheries Society*, **110**, 72–76.
Yamaoka K (1997) Trophic ecomorphology of Tanganyikan cichlids. In: *Fish Communities in Lake Tanganyika* (eds Kawanabe H, Hori M, Nagoshi M), pp. 27–56. Kyoto University Press, Kyoto.
Yoder JB, Clancey E, Des Roches S *et al*. (2010) Ecological opportunity and the origin of adaptive radiations. *Journal of Evolutionary Biology*, **23**, 1581–1596.

M.C., E.T.D., M.E.S. and A.I. are PhD students in the group of W.S. M.C. is interested in parallel evolution events as natural replicates to test hypotheses about trait evolution and the different (or similar) genetic bases that underlie these phenotypes. E.T.D. is interested in the genetic basis of adaptive traits and the selective forces acting upon these genes. M.E.S. is interested in the ecological and developmental mechanisms underlying the emergence and diversification of novel adaptive traits. A.I. is interested in ecomorphological adaptations, phylogeography and taxonomy in cichlid fishes. M.M. recently finished his PhD in the group of W.S. and is now postdoctoral fellow with Patrik Nosil in Sheffied. His research is concerned with morphological and genomic evolution in adaptive radiations. N.B. is a technical assistant who is involved in several projects of the SalzburgerLab. M.B. is a group leader at the Natural History Museum in Madrid. Her research focuses on understanding incipient stages of speciation and the sequence of adaptations and specializations that organisms undergo after the colonization of new habitats. W.S. is Professor of Zoology and Evolutionary Biology at the University of Basel. The research of his team focuses on the genetic basis of adaptation, evolutionary innovation and animal diversification. The main model systems in the laboratory are threespine stickleback fish, Antarctic notothenioids and the exceptionally diverse assemblages of cichlid fishes. The laboratory's homepage at http://www.evolution.unibas.ch/salzburger/ provides further details on the group's (research) activities.

Data accessibility

Newly generated DNA sequences for phylogenetic and haplotype analyses have been deposited in GenBank under accession numbers JX402217–JX402407 (see Appendix S1 for details). Illumina reads from the RNA-seq experiments are available from the Sequence Read Archive (SRA) at NCBI under the accession number SRA052992. Data from the stomach and gut content analyses, the MORPHOJ input files and the quantitative real-time PCR experiments have been deposited at Dryad (doi:10.5061/dryad.vf1ms).

Supporting information

Additional Supporting Information may be found in the online version of this article.

Appendix S1 List of specimens used in this study including sampling date and location and GenBank accession numbers.

Appendix S2 PCA of overall body shape of the African cichlid *Lobochilotes labiatus* and the Nicaraguan species *Amphilophus labiatus* and *A. citrinellus* (a) and distribution of landmarks for morphometric analyses (b).

Appendix S3 Blast2GO annotations of genes with differential expression between lip tissue from thick-lipped and normal-lipped cichlid species.

Appendix S4 Underwater video showing snail feeding in *Lobochilotes labiatus*.

Appendix S5 Results of the quantitative real-time PCR experiments comparing adult and juvenile lip tissue of the African cichlid species *Lobochilotes labiatus* and *Astatotilapia burtoni*.

Please note: Wiley-Blackwell are not responsible for the content or functionality of any supporting materials supplied by the authors. Any queries (other than missing material) should be directed to the corresponding author for the article.

1.1.2
Supporting information

Appendix S1 List of specimens used in this study including sampling date and location and GenBank accession numbers

Sample ID		Species	Sampling	Location	DNA/RNA sequencing/GenBank accession numbers				qPCR					
DNA	RNA		Date		mtControl	ednrb1	phpt1	RNA sequencing	BNIP3	Actb	Cldn7	Copb	His3	ACSL4
23H8		*Amphilophus citrinellus*	9/5/09	Isletas		JX402280	JX402217							
23H9		*Amphilophus citrinellus*	9/5/09	Isletas		JX402281	JX402218							
23I1		*Amphilophus citrinellus*	9/5/09	Isletas		JX402282	JX402219							
23I2		*Amphilophus citrinellus*	9/5/09	Isletas			JX402220							
24A2		*Amphilophus citrinellus*	9/5/09	Isletas		JX402283	JX402221							
24A3		*Amphilophus citrinellus*	9/5/09	Isletas		JX402284	JX402222							
24A4		*Amphilophus citrinellus*	9/5/09	Isletas		JX402285	JX402223							
24A5		*Amphilophus citrinellus*	9/5/09	Isletas		JX402286	JX402224							
25D1	31I8	*Amphilophus citrinellus*	9/9/09	Isletas		JX402288	JX402225							
25D2	30D7	*Amphilophus citrinellus*	9/9/09	Isletas		JX402289	JX402226							
25D6	30F1	*Amphilophus citrinellus*	9/9/09	Isletas			JX402227		y	y	y	y	y	y
25D7	30F3	*Amphilophus citrinellus*	9/9/09	Isletas		JX402298	JX402228							
25D8	30F9	*Amphilophus citrinellus*	9/9/09	Isletas		JX402299	JX402229							
25E1	30F6	*Amphilophus citrinellus*	9/9/09	Isletas			JX402230							
25E2	30G2	*Amphilophus citrinellus*	9/9/09	Isletas		JX402292	JX402231							
25E3	30G4	*Amphilophus citrinellus*	9/9/09	Isletas		JX402287	JX402232		y	y	y	y	y	y
25E4	30G6	*Amphilophus citrinellus*	9/9/09	Isletas		JX402293	JX402233							
25E6	30H3	*Amphilophus citrinellus*	9/9/09	Isletas			JX402234							
25E8	30H6	*Amphilophus citrinellus*	9/9/09	Isletas		JX402296	JX402235							
25E9	30H7	*Amphilophus citrinellus*	9/9/09	Isletas		JX402297	JX402236							
25D3	30E2	*Amphilophus citrinellus*	9/9/09	Isletas		JX402290								
25D4	30E7	*Amphilophus citrinellus*	9/9/09	Isletas					y	y	y	y	y	y
25E5	30G8	*Amphilophus citrinellus*	9/9/09	Isletas		JX402294			y	y	y	y	y	y
25E7	30H5	*Amphilophus citrinellus*	9/9/09	Isletas		JX402295								
25F1	30H9	*Amphilophus citrinellus*	9/9/09	Isletas		JX402298								
26I3	32A7	*Amphilophus citrinellus*	9/14/09	Managua Miraflores					y	y	y	y	y	y
26I4	32B1	*Amphilophus citrinellus*	9/14/09	Managua Miraflores					y	y	y	y	y	y
23F9		*Amphilophus labiatus*	9/5/09	Isletas	JX402360	JX402301	JX402237							
23G1		*Amphilophus labiatus*	9/5/09	Isletas	JX402354	JX402302	JX402238							
23G3		*Amphilophus labiatus*	9/5/09	Isletas			JX402239							
23G6		*Amphilophus labiatus*	9/5/09	Isletas	JX402367		JX402240							
23G9		*Amphilophus labiatus*	9/5/09	Isletas	JX402361	JX402305	JX402241							
23H3		*Amphilophus labiatus*	9/5/09	Isletas	JX402365	JX402306	JX402242							
23H6		*Amphilophus labiatus*	9/5/09	Isletas	JX402368		JX402243							
23H7		*Amphilophus labiatus*	9/5/09	Isletas	JX402375	JX402308	JX402244							
25A1	31C3	*Amphilophus labiatus*	9/9/09	Isletas	JX402371	JX402310	JX402245							
25A5	31D6	*Amphilophus labiatus*	9/9/09	Isletas	JX402364	JX402311	JX402246							
25A6	31D9	*Amphilophus labiatus*	9/9/09	Isletas	JX402369		JX402247							
25A7	31E2	*Amphilophus labiatus*	9/9/09	Isletas	JX402378	JX402312	JX402248							
25A8	31E3	*Amphilophus labiatus*	9/9/09	Isletas	JX402376	JX402313	JX402249							
25B1	31E7	*Amphilophus labiatus*	9/9/09	Isletas	JX402363	JX402314	JX402250		y	y	y	y	y	y
25B3	31F2	*Amphilophus labiatus*	9/9/09	Isletas	JX402366	JX402316	JX402251							
25B4	31F4	*Amphilophus labiatus*	9/9/09	Isletas	JX402351	JX402309	JX402252							
25B5	31F5	*Amphilophus labiatus*	9/9/09	Isletas	JX402372		JX402253							
25B6	31F7	*Amphilophus labiatus*	9/9/09	Isletas	JX402359	JX402317	JX402254							
25B7	31F9	*Amphilophus labiatus*	9/9/09	Isletas	JX402377	JX402318	JX402255							
25B9	31G3	*Amphilophus labiatus*	9/9/09	Isletas	JX402349	JX402320	JX402256							
23F8		*Amphilophus labiatus*	9/5/09	Isletas	JX402353	JX402300								
23G2		*Amphilophus labiatus*	9/5/09	Isletas	JX402374	JX402303								
23H5		*Amphilophus labiatus*	9/5/09	Isletas	JX402350	JX402307								
25B2	31E9	*Amphilophus labiatus*	9/9/09	Isletas	JX402358	JX402315								
25B8	31G2	*Amphilophus labiatus*	9/9/09	Isletas	JX402370	JX402319								
23G5		*Amphilophus labiatus*	9/5/09	Isletas	JX402373									
23G7		*Amphilophus labiatus*	9/5/09	Isletas	JX402355									
23G8		*Amphilophus labiatus*	9/5/09	Isletas	JX402356	JX402304								
23H1		*Amphilophus labiatus*	9/5/09	Isletas	JX402357									
25A3	31C9	*Amphilophus labiatus*	9/9/09	Isletas	JX402352									
25A4	31D4	*Amphilophus labiatus*	9/9/09	Isletas	JX402348									
25A9	31E5	*Amphilophus labiatus*	9/9/09	Isletas	JX402362				y	y	y	y	y	y
25C1	31G6	*Amphilophus labiatus*	9/9/09	Isletas					y	y	y	y	y	y
25C6	31H7	*Amphilophus labiatus*	9/9/09	Isletas					y	y	y	y	y	y
28A3	32G6	*Amphilophus labiatus*	9/18/09	Managua Miraflores					y	y	y	y	y	y
28C6	32H7	*Amphilophus labiatus*	9/20/09	Ometepe, San Ramon	J				y	y	y	y	y	y
35A1		*Lobochilotes labiatus*	2/21/10	Mbita Island W	JX402388	JX402321	JX402257							
35A2		*Lobochilotes labiatus*	2/21/10	Mbita Island W	JX402383	JX402322	JX402278							
35A3		*Lobochilotes labiatus*	2/21/10	Mbita Island W	JX402398	JX402323	JX402263							
35A4		*Lobochilotes labiatus*	2/21/10	Mbita Island W	JX402399	JX402324	JX402266							
35A5		*Lobochilotes labiatus*	2/21/10	Mbita Island W	JX402400	JX402325	JX402268							
35A6		*Lobochilotes labiatus*	2/21/10	Mbita Island W	JX402405	JX402326	JX402262							
35A7		*Lobochilotes labiatus*	2/21/10	Mbita Island W	JX402391	JX402327	JX402279							
35A8		*Lobochilotes labiatus*	2/21/10	Mbita Island W	JX402392	JX402328	JX402259							
35B6		*Lobochilotes labiatus*	2/21/10	Mbita Island W	JX402401	JX402329	JX402258							
36B3		*Lobochilotes labiatus*	2/22/10	Mpulungu area	JX402404	JX402330	JX402267							
36B4		*Lobochilotes labiatus*	2/22/10	Mpulungu area	JX402406	JX402331	JX402275							
36H7		*Lobochilotes labiatus*	2/23/10	Kasakalawe Lodge	JX402403	JX402333	JX402277							
43D7	81A2	*Lobochilotes labiatus*	2/28/10	Toby's Place	JX402379	JX402334	JX402261	y	y	y	y	y	y	y
43D8	81A5	*Lobochilotes labiatus*	2/28/10	Toby's Place	JX402407	JX402335	JX402260	y	y	y	y	y	y	y
43E4	81B9	*Lobochilotes labiatus*	2/28/10	Toby's Place	JX402390	JX402340	JX402264		y	y	y	y	y	y
43E5	81B4	*Lobochilotes labiatus*	2/28/10	Toby's Place	JX402381	JX402341	JX402273	y	y	y	y	y	y	y
43E6		*Lobochilotes labiatus*	2/28/10	Toby's Place	JX402382	JX402342	JX402265							
44G8		*Lobochilotes labiatus*	3/1/10	Toby's Place	JX402395	JX402343	JX402270							
44G9		*Lobochilotes labiatus*	3/1/10	Toby's Place	JX402386	JX402344	JX402271							
44H1		*Lobochilotes labiatus*	3/1/10	Toby's Place	JX402380	JX402345	JX402269							
44H3		*Lobochilotes labiatus*	3/1/10	Toby's Place	JX402396		JX402276							

44H5		*Lobochilotes labiatus*	3/1/10	Toby's Place	JX402387	JX402346	JX402272							
44H6		*Lobochilotes labiatus*	3/1/10	Toby's Place	JX402402	JX402347	JX402274							
36H8		*Lobochilotes labiatus*	2/23/10	Kasakalawe Lodge	JX402389	JX402332								
43D9	81A7	*Lobochilotes labiatus*	2/28/10	Toby's Place	JX402384	JX402336								
43E1	81B1	*Lobochilotes labiatus*	2/28/10	Toby's Place	JX402385	JX402337								
43E2	81B3	*Lobochilotes labiatus*	2/28/10	Toby's Place	JX402393	JX402338								
43E3	81B7	*Lobochilotes labiatus*	2/28/10	Toby's Place	JX402394	JX402339								
44H4		*Lobochilotes labiatus*	3/1/10	Toby's Place	JX402397									
43D6	81A3	*Lobochilotes labiatus*	2/28/10	Toby's Place				y	y	y	y	y	y	y
55D1	81H9	*Lobochilotes labiatus*	3/11/10	Mpulungu area					y	y	y	y	y	y
55D2	81I2	*Lobochilotes labiatus*	3/11/10	Mpulungu area					y	y	y	y	y	y
55D8	79A5	*Lobochilotes labiatus*	3/11/10	Mukaka					y	y	y	y	y	y
55D9	79A9	*Lobochilotes labiatus*	3/11/10	Mukaka				y	y	y	y	y	y	y
BIB4	BMB4	*Lobochilotes labiatus*	7/20/11	Toby`s place					y	y	y	y	y	y
BIC4	BMC4	*Lobochilotes labiatus*	7/20/11	Toby`s place					y	y	y	y	y	y
BIC6	BMC6	*Lobochilotes labiatus*	7/20/11	Toby`s place					y	y	y	y	y	y
BIC7	BMC7	*Lobochilotes labiatus*	7/20/11	Toby`s place					y	y	y	y	y	y
BIC9	BMC9	*Lobochilotes labiatus*	7/20/11	Toby`s place					y	y	y	y	y	y

additional Tropheini species for phylogenetic analyses:

Species	**mtControl**	**ednrb1**	**phpt1**	**ND2**
Astatotilapia burtoni	AY930000	JF900252	JF900181	JF900319
Ctenochromis horei	AY301952	JF900262	JF900191	EU753935
Gnathochromis pfefferi	AY301954	JF900269	JF900198	U07248
Interochromis loockii	GQ995855	JF900304	JF900232	JF900322
Limnotilapia dardennii	AY301956	JF900285	JF900214	GQ995724
Lobochilotes labiatus	AY301958	JF900286	JF900215	U07254
Petrochromis ephippium	AY301959	JF900300	JF900229	JF900323
Petrochromis famula	AY301960	JF900301	JF900230	JF900324
Petrochromis fasciolatus	GQ995911	JF900325	JF900231	JF900325
Petrochromis macrognathus	AY929963	JF900304	JF900233	AY930068
Petrochromis polyodon	AY301967	JF900305	JF900234	JF900326
Pseudosimochromis curvifrons	AY301973	JF900307	JF900236	GQ995777
Simochromis babaulti	AY301975	JF900309	JF900238	GQ995782
Simochromis diagramma	AY301977	JF900310	JF900239	AY930087
Tropheus moorii	AY930020	JF900314	JF900243	AY930093

additional *Amphilophus citrniellus* mitochondrial control region sequences:

ampcit1	AY567011
ampcit2	AY567018
ampcit3	AY567012
ampcit4	AY567013
ampcit5	AY567014
ampcit6	AY567015
ampcit7	AY567016
ampcit8	AY567017
ampcit9	EF219270
ampcit10	EF219269
ampcit11	EF219268
ampcit12	EF219252
ampcit13	EF219251
ampcit14	EF219250
ampcit15	EF219249
ampcit16	EF219248
ampcit17	EF219247
ampcit18	AY567470
ampcit19	AY567469
ampcit20	AY567468
ampcit21	AY567467
ampcit22	AY567466
ampcit23	AY567465
ampcit24	AY567464
ampcit25	AY567463
ampcit26	AY567462
ampcit27	AY567461
ampcit28	AY567460
ampcit29	AY567459
ampcit30	AY567458
ampcit31	AY567457

(a)

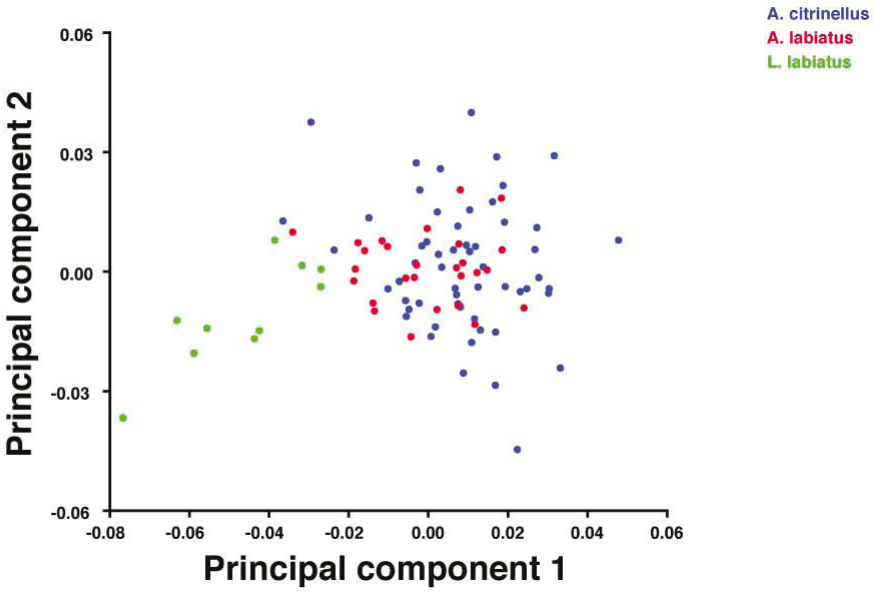

(b)

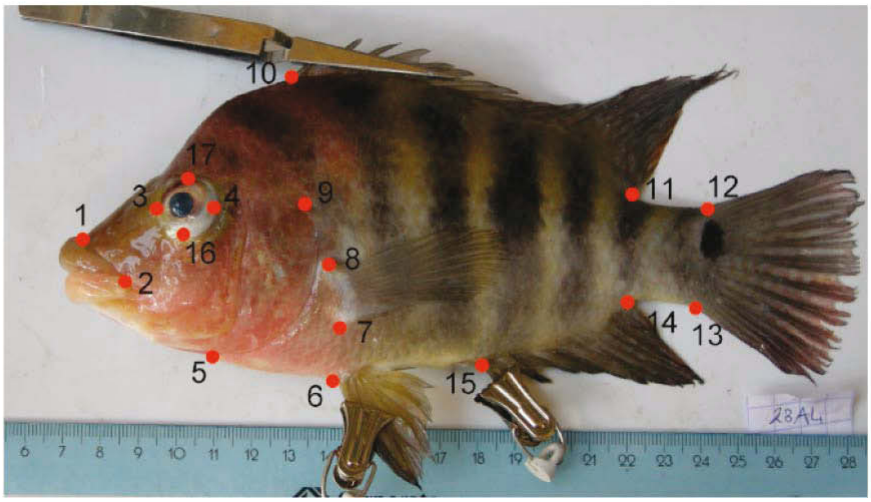

Appendix S2
PCA of overall body shape of the African cichlid *Lobochilotes labiatus* and the Nicaraguan species *Amphilophus labiatus* and *A. citrinellus* (a) and distribution of landmarks for morphometric analyses (b).

Appendix S3
Blast2GO annotations of genes with differential expression between lip tissue from thick-lipped and normal- lipped cichlid species.

Blast2GO annotations of genes with differential expression between lip-tissue from thick-lipped and normal-lipped cichlid species

26s protease regulatory subunit 8
3-hydroxyanthranilate -dioxygenase
60s acidic ribosomal protein p2
actin-related protein 2-a
actin-related protein 3
activating transcription factor 4
acyl carrier mitochondrial precursor
acyl- -binding protein
adaptor-related protein complex mu 1 isoform cra_a
adaptor-related protein complex mu 1 subunit
adp-dependent glucokinase-like
adp-ribose mitochondrial-like
atp synthase subunit mitochondrial precursor
atpase mitochondrial precursor
baculoviral iap repeat-containing protein 4
bcl2 adenovirus e1b 19 kda protein-interacting protein 3
bcl2 adenovirus e1b 19 kda protein-interacting protein 3-like
beta actin
calpastatin
carboxypeptidase z-like
caspase-8
chaperonin containing subunit 6a (zeta 1)
chromobox protein homolog 3
claudin 7
cmp-n-acetylneuraminate-beta-galactosamide-alpha- -sialyltransferase 1-like
coatomer subunit beta
comm domain-containing protein 9
complement c1q tumor necrosis factor-related protein 3-like
cop9 signalosome complex subunit 8
coproporphyrinogen oxidase
cystathionine gamma-lyase
cystatin precursor
cysteine and glycine-rich protein 1
cytochrome c oxidase polypeptide viia-liver mitochondrial precursor
dcn1-like protein 1
dihydrolipoyllysine-residue succinyltransferase component of 2-oxoglutarate dehydrogenase mitochondrial
dnaj homolog subfamily c member 9-like
dynactin subunit 5
ectonucleoside triphosphate diphosphohydrolase 3
estradiol 17-beta-dehydrogenase 12-b
eukaryotic translation initiation factor 3 subunit i
eukaryotic translation initiation factor 3 subunit k
eukaryotic translation initiation factor 3 subunit l
eukaryotic translation initiation factor 3 subunit m
eukaryotic translation initiation factor 4 gamma 2-like
eukaryotic translation initiation factor 4h
excitatory amino acid transporter 1 isoform 1
fk506-binding protein 2 precursor
forkhead box q1

glutamate dehydrogenase
glyoxalase domain-containing protein 4-like
grainyhead-like protein 1 homolog
granulins precursor
gtpase imap family member 4-like
gtpase imap family member 7-like
gtpase imap family member 8-like
gtpase imap family member 8-like
h1 histone
heat shock 70 kda protein 12a-like
histone
iars protein
importin-7
integrin beta-4-like
interferon-induced protein 35
isocitrate dehydrogenase
l _3
lamin b1
laminin subunit gamma-2
loc100127300 protein
long-chain-fatty-acid-- ligase 4
low quality protein: coronin-1c-like
lrr and pyd domains-containing protein 3-like
magnesium transporter 1
major vault protein
membrane magnesium transporter 1-like
methylmalonyl epimerase
microfibril-associated glycoprotein 4-like
mortality factor 4 like 1
myosin regulatory light chain smooth muscle isoform
nadh dehydrogenase
nadh dehydrogenase 1 alpha subcomplex subunit 11
nedd4 family-interacting protein 1
nedd4 family-interacting protein 1
nuclear factor erythroid 2-related factor 1-like
ornithine decarboxylase
pancreatic progenitor cell differentiation and proliferation factor
peptidylprolyl isomerase b (cyclophilin b)
phosphoglycerate kinase 1
piggybac transposable element-derived protein 4-like
pre-mrna splicing factor
PREDICTED: galectin-3-like [Oreochromis niloticus]
PREDICTED: hypothetical protein LOC100704514 [Oreochromis niloticus]
prefoldin subunit 4
probable glutathione peroxidase 8-like
programmed cell death 6-interacting protein
proteasome subunit alpha type-1
proteasome subunit alpha type-6
protein disulfide isomerase family member 4
protein fam100a-like
protein fam176b-like
protein kiaa0664-like
protein rer1

rab acceptor 1
ras-related protein rab-11b
regulator of g-protein signaling 2
renin receptor isoform 3
ribosomal l1 domain-containing protein 1-like
rilp-like protein 1
scinderin like a
scinderin like a
secretory carrier-associated membrane protein 2-like
septin 10
signal peptidase complex catalytic subunit sec11a
signal peptide peptidase-like 2a-like
small 1
sodium-dependent phosphate transporter 1
solute carrier family facilitated glucose transporter member 11-like
solute carrier family member 30
splicing factor 3b subunit 1
subfamily member 11
syntaxin 12
t-cell receptor type 1
t-complex protein 1 subunit alpha-like
t-complex protein 1 subunit theta
tbc1 domain member 15
thioredoxin domain containing 4 (endoplasmic reticulum)
threonyl-trna cytoplasmic
transaldolase
transcription factor ap-2 gamma (activating enhancer binding protein 2 gamma)
transmembrane protein 214
transmembrane protein 59 precursor
transmembrane protein 79
transposon tx1 uncharacterized 149 kda
tumor protein 63
tumor-associated calcium signal transducer 2 precursor
u6 snrna-associated sm-like protein lsm8
uap56-interacting factor-like
uncharacterized protein c22orf25-like
upf0510 protein inm02 precursor
v-type proton atpase catalytic subunit a
v-type proton atpase subunit d 1

Appendix S4*
Underwater video showing snail feeding in *Lobochilotes labiatus*.
* a still-frame of the video is shown here

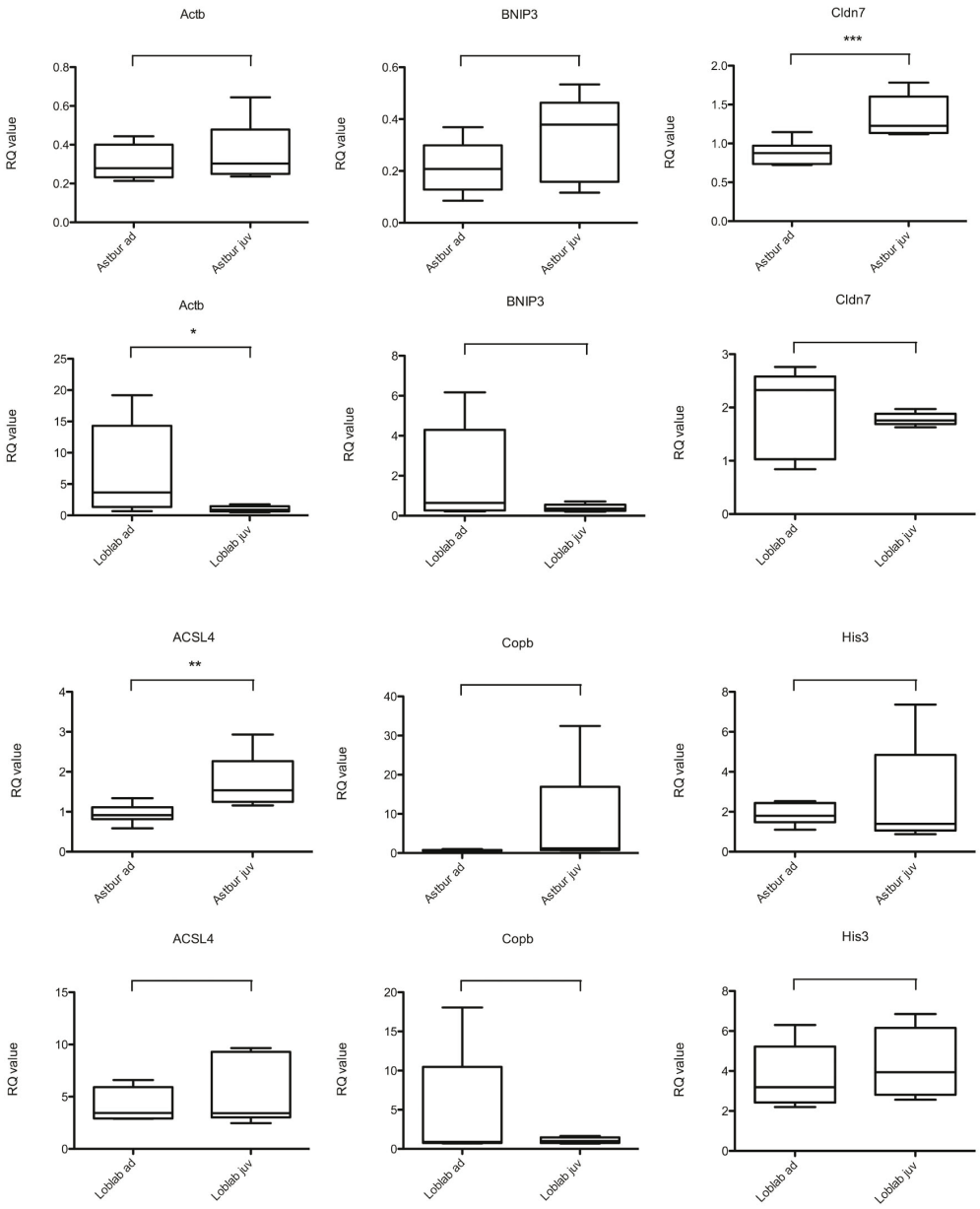

Appendix S5
Results of the quantitative real-time PCR experiments comparing adult and juvenile lip tissue of the African cichlid species Lobochilotes labiatus and Astatotilapia burtoni.

1.2
The evolution of the vertebral column and its interrelation with elongation and ecology in a massive adaptive radiation

To be submitted to Nature Ecology & Evolution

HB sampled the specimens and conducted the x-rays. FM and me collected the data. I analysed the data and drafted the manuscript. All authors participated in discussing the manuscript and drafting the final version.

The evolution of the vertebral column and its interrelation with elongation and ecology in a massive adaptive radiation

Marco Colombo[1], Florian Meury[1], Heinz H. Büscher[1], Marcelo Sanchez[2], and Walter Salzburger[1]

1. Zoological Institute, University of Basel, Vesalgasse 1, CH 4051, Basel, Switzerland

2. Paläontologisches Institut und Museum, Karl-Schmid Strasse 4, CH 8006, Zürich, Switzerland

Abstract

The form and composition of the vertebral column influences many morphological aspects in vertebrates, e.g. the length of the vertebral column defines maximal axial elongation and hence influences a diverse set of aspects of vertebrate life. However, the vertebral column is subdivided and different subregions might evolve independently. We here use the adaptive radiation of Lake Tanganyikan cichlids to investigate how the different subregions of the vertebral column relate to body elongation, if elongation was facilitated due to a increase in vertebral number or the prolongation of individual vertebrae, how the composition of the vertebral column is influenced by ecological pressures and how the vertebral column evolved throughout the course of the adaptive radiation. We find that the caudal part of the vertebral column correlates much stronger with elongation than the abdominal part and that elongation depends on both the addition and prolongation of vertebrae. The abdominal and caudal part of the vertebral column may evolve independently, without affecting each other and developmental abnormalities show to be more common in the caudal part. The two main parts of the teleost vertebral column depict independent developmental modules that correlate differently with ecological factors, e.g. the number of abdominal vertebrae shows to correlate negatively with a species' position within the food web whereas we find no such pattern for the number of caudal vertebrae. Furthermore, we discuss patterns of trait evolution through time, the occurrence of burst of morphological divergence and if the Lake Tanganyikan cichlid radiation might have proceeded in defined stages.

Introduction

The diversification of the animal body plan is tightly linked with variation in axial patterning, which in turn is regulated by a conserved set of genes including, most notably, *Hox* genes (Burke [1]; Carroll [2]). In vertebrates, the body axis is primarily determined by the number and identity of vertebrae in the vertebral column, both of which correlate with embryonic *Hox* gene expression patterns as well (Kessel&Gruss [3]; Burke [1, 4, 5]).

The total number of vertebrae differs substantially between vertebrates and ranges from six in some frogs to several hundreds in highly elongated forms such as snakes and eels (Gomez [6]). The different classes of vertebrates also differ with respect to the degree of axial regionalization of the vertebral column. While mammals possess five types of vertebrae (cervical, thoracic, lumbar, sacral and caudal (Gaunt [7], Burke [1])), actinopterygian fish generally feature only two (abdominal and caudal), which can, however, show a certain degree of 'subregionalization' (Ford [8],Theodore [9]).

Depending on the vertebrate class, the number of vertebrae within a certain vertebrae type can be highly variable or constraint. Perhaps the most famous example of such a constraint is the number of cervical vertebrae in mammals, which is almost exclusively fixed at seven, with only two known exceptions, manatees (*Trichechus*) having six and sloths having eight to ten (*Bradypus tridactylus) or five to six (Choloepus hoffmanni)* (Owen [10], Galis [11], Hautier [12], Buchholtz [13]). Another example of a constraint involves the number of trunk vertebrae (thoracic plus lumbar vertebrae), which is more or less constant in mammals, while there is great variation in the number of trunk vertebrae in reptiles and birds and in the number of the corresponding abdominal vertebrae in fish ([14]Owen [15], Ward [16], Müller [17]).

Owing to the functional and morphological distinctiveness of the different vertebrae types and the varying degrees of constraints between them, it has been suggested that the vertebral column is organized in a modular way, where different developmental modules (i.e. different parts of the vertebral column) evolve independently (Polly [18], Ward [16], Müller [17]). Such a modular organization is particularly evident in elongated forms within reptiles ([4]Polly [18]) and fishes (Ward [16]).

Elongated forms have evolved repeatedly in all vertebrate classes, most dramatically in fish, amphibians and reptiles (Ward [19], Parra-Olea [20], Wiens [21]). Longer bodies are typically associated with adaptations to particular life-styles and feeding modes, greater body flexibility, and/or different locomotion strategies (Ward [19], Brainerd [22], Breder [23]). In general, body elongation in vertebrates can be achieved through an increase in the number of vertebrae, by making the individual vertebrae longer, or via a combination of both (Ward [16] [19], Johnson [24], Wake [25], Parra-Olea [20], Polly [18]). While elongated bodies in amphibians and reptiles mainly coincide with an increase in both vertebral number and length (Johnson [24], Parra-Olea [20], Polly [4, 18]), elongation in actinopterygian fish seems to primarily rely on an increase in the number of vertebrae (Ward [16]). For example, in the majority of ambush predators axial elongation was achieved via the addition of abdominal (but not caudal) vertebrae (Maxwell [26]). Other general

trends in the evolution of the vertebral column in fish is a “phyletic tendency for decrease”, i.e. that derived fish tend to have fewer vertebrae (McDowall [27, 28], Lindsey [29]) and a relationship between size and the number of vertebrae (pleomerism: larger species tend to have more vertebrae than smaller species) (Lindsey [30]).

However, apart from the above-mentioned macro-evolutionary patterns, little is known about the adaptive significance of vertebral numbers and their role in evolutionary radiations. Here, we make use of a role model of adaptive radiation, the species-flock of cichlid fishes in East African Lake Tanganyika ([31]). Based on an almost complete taxon sampling [For this study, we collected 4496 specimens of Lake Tanganyika cichlids representing 174 species (i.e., ~90% of the lake’s endemic cichlid fauna) and all of its 53 genera.], we explore the evolution of the vertebral column in one of the largest vertebrate adaptive radiations, with a particular focus on body elongation. We find that elongation is much stronger correlated with the number of caudal than with the number of abdominal vertebrae and that elongation depends on both the addition and prolongation of individual vertebrae. We show that both parts of the vertebral column may evolve independently and that the caudal part is more likely to exhibit developmental abnormalities. The two main parts of the vertebral column correlate differently with ecological factors in teleost fish: The number of abdominal vertebrae shows to correlate negatively with a species’ position within the food web. The number of caudal vertebrae, on the other hand, shows no significant correlations with ecological variables, neither does body elongation. Concerning the total number of vertebrae, the number of abdominal vertebrae and maximal body size, we find conspicuous drops in subclade disparity early in the evolutionary timeline of the radiation. Concerning these traits, disparity was initially mainly distributed within subclades but changed to a pattern where disparity is primarily distributed between subclades still early in the timeline of the radiation. Furthermore, we find pronounced patterns of convergence in vertebral numbers between several distantly related species.

Results

Vertebrae counts and vertebrae, elongation and aspect ratios. We first determined, in a set of 2801 high quality x-ray images representing 174 cichlid species from Lake Tanganyika, the number of abdominal (i.e., all pre-anal vertebrae including occipital vertebrae) and caudal (i.e., post-anal, haemal spine possessing) vertebrae. That way, we uncovered substantial interspecific variation in Lake Tanganyika cichlids with respect to the total number of vertebrae, as well as the number of abdominal and caudal vertebrae (Fig. 1, Fig. 4, Supp. Fig. 3, Supp. Table 2). The total number of vertebrae ranged from 26 in *Astatotilapia burtoni* to 39 in the elongated ambush hunter *Bathybates fasciatus*. The number of abdominal vertebrae spanned from 10 (*Lamprologus meleagris*) to 22 (*Cyprichromis pavo*), while the number of caudal vertebrae ranged from 14 (*Oreochromis tanganicae*) to 24 (*Enantiopus melanogenys*). In 134 out of the 174 species investigated, we additionally observed intra-specific variation in vertebrae number, with the greatest variance (1.8) being present in *Lestradea perspicax*. Most species (162)

exhibited more caudal than abdominal vertebrae while for 12 species the opposite was true.

We then calculated, using these vertebrae counts, the vertebrae ratio (VR; i.e. the number of abdominal vertebrae divided by the number of caudal vertebrae Swain [32]) and the elongation ratio (ER; i.e. the length of an organism divided by the second largest major body axis, in our case body depth (Ward [33]). VR ranged from 0.56 in *Xenotilapia similis* to 1.18 in *Cyprichromis pavo*; ER spans from 2.17 in *Cyphotilapia gibberosa* to 5.24 in *Enantiopus melanogenys* (Fig. 1). We also calculated the vertebrae aspect ratio (AR; i.e. the length of the vertebral centrum divided by its width (Ward [16]) for the 15 most elongated, the 15 medium most and the 15 most short bodied species.

Abdominal but not caudal vertebrae counts correlate with diet. To place the vertebrae counts into an ecological context, we included available data on carbon and nitrogen stable isotope ratios as well as on intestinal tract lengths as proxy for trophic ecology, and performed a phylogenetic generalized least squares (PGLS) analysis (Martins [34]) using a recently published phylogenetic hypothesis [35]. Here, the relative ratio of the rare isotope of carbon ($\partial^{13}C$; available for 75 species from our dataset; [36]) is representative for a species' position along a benthic to limnetic macro-habitat axis, whereas the relative ratio of the rare isotope of nitrogen ($\partial^{15}N$; available for 75 species; [36]) informs about a species' position within the food web; intestinal tract lengths (available for 59 species; [37]) are generally longer in species feeding on plant and algae diet [38]. PGLS revealed a significant correlation between the number of abdominal vertebrae and $\partial^{15}N$ values (R^2=0.137; p<0.01) as well as the length of the intestinal tract (R^2=0.167; p<0.01), whereas no such correlation exists between the number of caudal vertebrae and $\partial^{15}N$ (R^2=0.039; p=0.55) or intestinal tract length (R^2=0.088; p=0.15) (see Table 3 for details).

The number of caudal vertebrae, on the other hand, appears to only correlate with ER (R^2=0.203; p<0.01), which also influences abdominal vertebrae (R^2=0.064; p<0.05). According to our PGLS analyses, there are additional predictors for vertebrae counts: the number of abdominal vertebrae correlates with the maximal body size that a species can reach (data available for 143 species; R^2=0.062; p<0.05); whereas the total number of vertebrae correlates with ER (R^2=0.259; p<0.01), VR (R^2=0.067; p<0.01) and the maximal body size (R^2=0.101; p<0.01).

Body elongation in Lake Tanganyika cichlids. Body elongation in Lake Tanganyikan cichlids may be acquired by both possible mechanisms, i.e. an increase in the number of vertebrae and/or AR is associated with elongation (Fig. 2, Table 3). The analysis in three sets of species revealed that the set with the highest ERs has significantly more vertebrae than both the set of species with intermediate ERs and the set with the smallest ERs (Fig. 2). On the other hand, we also observed a trend that more elongated species have higher ARs (short-bodied species show a significantly smaller AR compared to the set with medium and high ERs).

A modular organization of the vertebral column. Our analyses of vertebrae counts in the adaptive radiation of cichlids from Lake Tanganyika provide strong support for a modular organization of the vertebrate column. We first show that the numbers of abdominal and caudal vertebrae are largely independent from each other (Fig. 1, Table 3) and that species may feature high caudal vertebrae counts despite low abdominal vertebrae counts (upper left areas in Fig. 4A, B) and *vice versa* (lower right areas in Fig. 4A, B). Similarly, the DTT analyses revealed different patterns in trait evolution between abdominal (MDI=0.085) and caudal (MDI=0.003) vertebrae along the phylogeny (Fig. 3, Table 2); and PGLS did not find any effect of the number of caudal vertebrae on the number of abdominal vertebrae (R^2<0.01; p=1) or *vice versa* (R^2<0.01; p=1; see Table 3).

Further evidence for a modular organization of the vertebral column comes from the distribution of developmental abnormalities in the form of fused or deformed vertebrae. Such abnormalities were observed in 1.25 % of the inspected specimens (N=4496) and occur predominantly in the caudal part of the vertebral column in Lake Tanganyika cichlids (chi-squared: P<0.001; t-test: P<0.001) (see also [39], who obtained similar results for medaka). More constraints in the abdominal part due to ecology!!!

Evolutionary analyses

The values for Pagel's λ for all traits were generally high (Table 1) and differed significantly from 0 (meaning no phylogenetic signal at all in the trait data). The values for total number of vertebrae, ER, and maximal body size also differed significantly from 1 (meaning that trait distribution matches a Brownian model), which was not the case for VR, abdominal and caudal vertebrae counts.

DTT analyses revealed, according to the MDI statistics (Table 2), that VR, the number of abdominal vertebrae, the number of caudal vertebrae, the total number of vertebrae, ER and maximal body size deviate positively from the null-model of neutral evolution, i.e. they show larger subclade overlap than predicted by the Brownian model of trait evolution.
Looking at the respective plots (Fig. 3), the total number of vertebrae, the number of abdominal vertebrae and maximal body size feature a conspicuous pattern with high initial subclade disparity followed by a drop and a phase where average subclade disparity generally remains lower than predicted under Brownian motion.

Correlation analyses

In the following, we list the main predictors for vertebrae counts according to correlational analyses as inferred from PGLS (Table 3):

Total number of vertebrae. The number of vertebrae in Lake Tanganyika cichlids is partly determined by the maximal size a species can reach; larger species tend to exhibit more vertebrae than smaller ones. On the other hand, we also found that the vertebrae number is influenced by ER, as species with a higher ER also tend to feature more vertebrae.

Abdominal vertebrae. We found a positive correlation between the number of abdominal vertebrae and the length of the intestinal tract and a negative correlation between the number of abdominal vertebrae and ∂15N values. ER seems to explain some minor parts of the variance in abdominal vertebrae number but no correlation with the number of caudal vertebrae was found.

Caudal vertebrae. Concerning the number of caudal vertebrae, PGLS analyses revealed a significant correlation with ER whereas we did not find any significant correlations between the number of caudal vertebrae and ecological parameters.

ER. PGLS revealed that ER is strongly influenced by vertebrae counts, with caudal vertebrae numbers having a stronger effect on ER than abdominal vertebrae numbers.

VR. We found a negative correlation between VR and ∂15N and a positive correlation between VR and the length of the intestinal tract as well as a minor influence of the total number of vertebrae on VR.

The phylomorphospace analysis of abdominal *versus* caudal vertebrae revealed a large overlap among most 'tribes' (Fig. 1, Supp. Fig. 3). Some 'tribes' or subunits thereof occupied unique areas in morphospace, though. The Cyprichromini, for example, are characterized by intermediate caudal vertebrae numbers, yet very high abdominal vertebrae counts. The Ectodini, on the other hand, are characterized by low to intermediate abdominal vertebrae numbers yet remarkably high caudal vertebrae numbers in many species. Representatives of the Tropheini and Tilapiini show the lowest caudal vertebrae counts, while some Lamprologini species feature the lowest counts for abdominal vertebrae. Also, the Trematocarini show comparatively low numbers of abdominal vertebrae, while the Bathybatini span a wide range of (abdominal) vertebrae numbers but contain some species that show the highest total numbers of vertebrae.

Convergence

Looking at caudal and abdominal vertebrae numbers per specimen (Fig. 4 A), we found some parts of morphospace (e.g. very high numbers of caudal and abdominal vertebrae, respectively) being occupied exclusively by one 'tribe'. Nevertheless, most possible vertebrae compositions seem to be exhibited by multiple 'tribes' (and hence species). These zones therefore contain possible convergent phenotypes. Comparing the actual distribution of vertebral number phenotypes with Brownian motion simulations (Fig. 4 B) we found zones where more species occur than would be expected and these zones contain species from several clades that are not closely related.

Discussion

Vertebrae evolution in the adaptive radiation of cichlids in Lake Tanganyika

Our analyses reveal substantial interspecific variation with respect to both abdominal- and caudal vertebrae numbers in cichlids from Lake Tanganyika

(Fig. 1, Fig. 4, Supp. Fig. 3). Remarkably, the differences between the species with least and most abdominal vertebrae (species averages: 11 to 20.56 = 9.56) and the species with least and most caudal vertebrae (14 to 23.5 = 9.5) are almost the same, suggesting a constraint in the minimum and maximum number of both vertebrae types.

Whereas some 'tribes' (most notably the Lamprologini and Ectodini) display a vast variety of ERs, others (such as the Tropheini and Cyprichromini) show a more narrow intra-tribal distribution of ERs. Overall, ERs are more or less evenly distributed from 2.18 to 5.24. Highly elongated forms, defined here as species with an ER of 4 and greater, are found in five of the 14 cichlid 'tribes' in Lake Tanganyika (Ectodini, Bathybatini, Lamprologini, Limnochromini, Cyprichromini) (Fig. 1, Supp. Fig. 2). While the most elongated species in the Bathybatini, Benthochromini and Lamprologini show relatively high numbers of both abdominal and caudal vertebrae, we observed two distinct strategies for obtaining elongated bodies in the 'tribes' Cyprichromini and Ectodini: the Cyprichromini are generally characterized by intermediate numbers of caudal vertebrae but large numbers of abdominal vertebrae, whereas the elongated members of the Ectodini feature the opposite trend with intermediate numbers of abdominal vertebrae yet large numbers of caudal vertebrae.

Our analyses of vertebrate counts in an entire adaptive radiation provide strong support for a modular organization of the vertebrate column in cichlid fishes in that we show that the numbers of abdominal and caudal vertebrae are largely independent and that species may evolve high numbers of one vertebral type without affecting the numbers of the other type. This is also supported by the DTT analyses, where different patterns for abdominal- and caudal vertebrae evolution were retrieved. Furthermore, PGLS did not find any significant effect of caudal on abdominal vertebral numbers or *vice versa*. Moreover, the module responsible for the development of the caudal vertebrae seems to be less fail-safe than the one organizing the development of the abdominal part of the vertebral column, as developmental abnormalities proved to more frequently affect caudal than abdominal vertebrae in Lake Tanganyikan cichlids (see also [39], who obtained similar results for medaka).

Our analyses reveal that vertebral counts correlate with the maximal body size a species may grow to, i.e. larger species tend to have more vertebrae than smaller species. This phenomenon is known as pleomerism and seems to be a widespread pattern in fish (Lindsey [30]), but explaining only a minor portion of vertebral count variation.

Instead, feeding ecology appears to be partly predictive for vertebrae counts in the adaptive radiation of cichlid fishes in Lake Tanganyika. PGLS analyses revealed a negative correlation between abdominal vertebrae counts and feeding ecology (as approximated by ∂15N values), whereas a positive correlation was found between the number of abdominal vertebrae and the length of the intestinal tract (which is generally longer in species feeding on plant and algae diet; Muschick et al. 2014). Caudal vertebrae, on the other hand, did not correlate significantly with feeding ecology or intestinal tract length. Similarly, only abdominal vertebrae numbers seem to exhibit local adaptation in medaka [39-41].

The negative effect of ∂15N and the positive effect of intestinal tract length on the number of abdominal vertebrae could be explained due to the fact that species ranking lower in the food chain and exhibiting longer intestinal tracts need more space in their abdominal cavity and hence high abdominal vertebrae counts and long digestive tracts co-evolved.

Concerning VR, the negative correlation with ∂15N and the positive with intestinal tract length (backing each other up) lead to a similar interpretation as high vertebrae ratios (meaning many abdominal in comparison to caudal vertebrae) seem to be typical for species ranking rather low in the food chain, exhibiting long digestive tracts.

The question if elongation in Lake Tanganyikan cichlids was achieved by adding more vertebrae or by elongating them could be answered insofar as it seems that both mechanisms played a role. We found significant differences between i.) short bodied and medium/highly elongated species with respect to AR and ii.) short bodied/medium elongated and highly elongated species concerning vertebral numbers. We thus conclude that transitions from a short-bodied to a medium elongated body (or *vice-versa*) was mainly achieved due to alterations of the length of individual vertebrae (AR) while transitions between medium and highly elongated species are mainly attributable to alterations in vertebral numbers. Clearly, the addition of more vertebrae was more important to the evolution of highly elongated body forms than prolonging vertebrae was.
It seems possible that having only a few extremely elongated vertebrae would lead to a stiff body what could be a disadvantage for cichlids living near shore in mostly rocky habitats (e.g. *Julidochromis* species). Furthermore, a flexible caudal peduncle proved to be beneficial for continuous swimming and a flexible trunk is known to facilitate acceleration (Webb [42]), both attributes potentially being beneficial for pelagic piscivores.

Although both abdominal- and caudal vertebrae counts show a positive effect on elongation, correlation analyses show that the effect of the number of caudal vertebrae is stronger. This might be explained by the observation that the caudal part of the vertebral column is straight in most species while the abdominal part often depicts a curvature. Vertebrae added to the bended abdominal part of the vertebral column do not lead as directly to elongation as adding vertebrae to the straight caudal part. Moreover, it seems possible that in some species with a highly bended abdominal part, the addition of more vertebrae would even lead to a deeper bodied fish instead of a more elongated one. This conflicts with previous findings for other actinopterygian fish, i.e. the majority of studied 'ambush predator' clades relies on the addition of abdominal vertebrae for elongation [26].

Convergence

ER and vertebrae numbers do not seem to follow a Brownian model of evolution. Instead, we find recurrently high (respectively low) values for the number of vertebrae all over the phylogeny (see Fig. 1 and Supp. Fig. 3). There is at least some degree of convergence found concerning vertebral counts in Lake Tanganyikan cichlids as demonstrated by a comparison between the number of observed taxa per vertebral composition and the number of taxa expected from Brownian motion simulations (Fig. 4 B). We

find zones in morphospace with much higher numbers of taxa than expected under BM, and that these taxa belong to different ‘tribes’. These zones possibly depict niches that are suitable for several ‘tribes’. This indicates that these zones contain convergent phenotypes in respect to vertebrae numbers. On the other hand, we find non-convergence zones containing fewer taxa than expected, often only occupied by members of single ‘tribes’.

These findings are also supported by our phylomorphospace plot (Supp. Fig. 3), where most ‘tribes’ overlap concerning the number of abdominal and caudal vertebrae and multiple species from different ‘tribes’ (despite high general interspecific diversity) show to exhibit very similar vertebrae numbers and only a few ‘tribes’, like the Cyprichromini, that occupy a unique part of morphospace.

The pattern of ‘tribe’ distribution on the ER axis suggests little phylogenetic constraints. Many ‘tribes’ overlap on this axis and even though e.g. the Tropheini ‘tribe’ is somewhat clustering around low ER values, several species from other ‘tribes’ display similar ER values and the species depicting the lowest value belongs to the Cyphotilapiini ‘tribe’.

In addition to vertebrae number and ER, maximal body size as well seems not to follow a Brownian motion model of evolution although it shows substantial amounts of phylogenetic signal. This confirms our findings from other analyses showing that these traits evolved similarly in different species not necessarily depending on phylogenetic relationships.

Adaptive radiation and early burst

We find evidence for adaptive radiation and a burst of morphological evolution early in the evolution of some of the morphological traits under study, i.e. number of abdominal vertebrae, number of caudal vertebrae, total number of vertebrae and maximal body size. After an initial burst, subclade disparity for these traits remained lower than expected under neutral evolution and only reached values higher than the Brownian motion simulations at certain points in the timeline (and thus lead to low MDI (Table 2)). Low MDI statistics and dropping average subclade disparity are what is generally expected under an ‘early burst’ like process where adaptive zones are initially occupied by rapidly diverging subclades leaving little opportunity for later divergence within subclades (see Harmon [43]). However, as average subclade disparity remains distinctly higher than Brownian motion simulations during a prolonged timespan (until around 0.2 in relative time) and hence leads to positive MDI statistics, the patterns found here might not strictly qualify as early bursts. Nevertheless, the patterns found for maximal body size and, to a lesser extent, the number of caudal vertebrae and the total number of vertebrae clearly reveal a pronounced early divergence that was followed by a period of low disparity within subclades until present. The number of abdominal vertebrae depicts a somehow different pattern with a clear drop after an initial phase of high average subclade disparity but disparity subsequently quickly rising above Brownian motion simulations again.

On the other hand, the DTT plot for ER consistently deviates in positive direction from the null-model of neutral evolution with average subclade

disparity remaining higher than Brownian motion simulations throughout most of the timeline. Larger overlap between subclades than predicted under Brownian-motion simulations like found here are inconsistent with what one would expect in an adaptive radiation scenario with an 'early burst' in the evolution of these traits (see Harmon [43]) and suggests that these traits did not play a major role during the early adaptive radiation of the LT cichlid flock. VR then depicts a pattern of average subcalde disparity being quite in line with the Brownian motion simulations.

Interestingly, we found a recurrent peak near 0.3 in relative time in most of our traits, especially evident e.g. in the ER plot. This may be a sign of a second phase of increased disparity after the initial burst phase. We also find secondary peaks in our DTT plots further towards present as already seen in (Muschick [36]). This may be partly explained by tip over-dispersion due to missing terminal taxa but since our dataset for some traits includes most Lake Tanganyikan cichlid species we do not think this pattern is solely explained by incomplete sampling but may point towards recent morphological advances within cichlid subclades in Lake Tanganyika.

Our findings do not definitely answer the question if evolution proceeded in a radiation in stages scenario (see Streelman [44]) in the Lake Tanganyikan cichlid flock. According to the radiation in stages theory, habitat use should depict the first axis of divergence in vertebrate adaptive radiations. In Lake Malawi cichlids, this first stage of radiation lead to a divergence between sand- and rock-dwelling lineages (Streelman [44], Danley [45]) which can be distinguished by various traits, including body size. Body size is also known to be an important early axis of divergence in sticklebacks (Moser [46]) and might drive assortative mating. It seems possible that body size (and, linked with it, the number of vertebrae) indeed depict an early divergence in Lake Tanganyikan cichlids.

Trophic morphology and other feeding-related traits typically relate to stage two in a radiation in stages scenario, which is followed by divergence according to communication and coloration (stage 3). According to the results presented in this study, it seems possible that the number of abdominal vertebrae, correlating with ∂15N values and intestinal tract length, played a role in diverging events during a longer time span in the radiation when species within subclades diverged further into refined trophic zones within the lake. A process that seems probable given that recurrent peaks appear in DTT plots of all studied traits at similar positions of the relative timeline depicting bursts of subclade disparity substantially after the initial phase of divergence. Moreover, the occurrence of convergent phenotypes within Lake Tanganyika (Muschick [36], this study) belonging to only distantly related 'tribes' indicates that at least some 'tribes' diverged and occupied niches that may in fact have already been occupied by other species at that time. However, further testing of the radiation in stages hypothesis in Lake Tanganyikan cichlids seems necessary to definitely answer the question if the Lake Tanganyikan cichlid radiation proceeded in accordance with the radiation in stages hypothesis, if the ordering of stages might be reversed or if temporally confined stages are present at all.

Materials and Methods

Sampling and vertebrae counts

Between 1982 and 2012, 4496 specimens of Lake Tanganyikan cichlid fish were collected at 426 locations in Zambia, Tanzania and the Democratic Republic of Congo (Supp. Fig. 5). Fish were caught using hand- or gill nets or, in some cases, bought from local fishermen. All specimens were treated with formaldehyde and then preserved in ethanol.

X-ray images of each specimen were taken with a Faxitron 43855 (Faxitron Bioptics, LLC, Tucson, Arizona) using Kodak Industrex MX 125 x-ray films. The analogous x-ray photographs were digitized using a Nikon D5000 with a Macro lens (Nikon, 60 mm) and a background light source; digital images were then edited with Adobe Lightroom 3 (Adobe Inc., San Jose, California, USA). After an initial quality check, 2801 images representing 174 species (i.e. ~90% of Lake Tanganyika's cichlid species) and all of its 53 cichlid genera were selected for further analyses.

For each specimen, we counted the total number of abdominal (i.e., all pre-anal vertebrae including occipital vertebrae) and caudal (i.e., post-anal, haemal spine possessing) vertebrae directly from the photographs. To determine body length and height of each specimen, we used TPSdig2 (Rohlf [47]) and set four homologous landmarks. The anterior ending of the upper jaw (anterior most point) and the onset of the caudal fin (posterior most point) were used to measure standard length, whereas the anterior onset of the dorsal fin and the anterior onset of the pelvic fin were used to determine body height (see Supp. Fig. 1). The x/y coordinates of these landmarks were converted into distance measurements (in mm) using a custom R script. We also used TPSdig2 to set four landmarks on each of the three central-most vertebrae of the abdominal and caudal part of the column in order to assess the anterior and posterior most and the ventral and dorsal most point of the respective vertebral centra.

In addition, we screened all 4496 x-ray images for developmental abnormalities in the vertebral column, such as fused or deformed vertebrae, and recorded the number and location (abdominal or caudal) of the affected vertebrae. To test if abnormalities are disproportionally distributed between the abdominal and caudal part of the vertebral column, we conducted two statistical tests: We first applied a Chi-squared test using a binary coding (abdominal part: normal/abnormal, caudal part: normal/abnormal) and, second, a Welch two sample t-test using frequencies (number of abnormal vertebrae/number of normal vertebrae) for both parts of the vertebral column to account for unequal vertebral numbers.

Vertebrae ratio, elongation ratio and aspect ratio

We first determined the vertebrae ratio (VR) for each species by dividing the number of abdominal through the number of caudal vertebrae (see Swain [32]). We then calculated the elongation ratio (ER), which is defined as the length of an organism divided by the second largest major body axis, in our case body depth (Ward [33]). We aimed for calculating ER for a sample of ten

specimens per species. However, several specimens could not be measured due to suboptimal positioning or incomplete depiction of the fish in the x-ray images (see Supp. Table 1). Finally, we determined the vertebral aspect ratio (AR) by dividing the length of the vertebral centrum by its width (see Ward [16]).

To analyze whether body elongation in LT cichlids was mainly achieved by adding more vertebrae or by prolonging individual vertebrae, we formed three groups containing the 15 most short-bodied, the 15 medium-most and the 15 most elongated species and plotted vertebral number and AR, respectively, using GraphPad Prism version 6.0e (GraphPad Software, La Jolla California USA). A one-way ANOVA was performed followed by Tukey's multiple comparisons test between all three groups.

Ecological data

In order to place the vertebrae counts and measurements into an ecological context, we included data on carbon and nitrogen stable isotope ratios as proxy for trophic ecology as well as data on intestinal tract lengths. The stable isotope data (∂^{15}N, representative for a species' position within the food web and ∂^{13}C, informative for a species' position along a benthic to limnetic macro-habitat axis) for 76 cichlid species were taken from Muschick et al. [36]. Data on the length of the intestinal tracts (whole gut including stomach) were taken from Muschick et al. (2014); additional data were collected directly in the field by measuring the intestinal tracts, to the nearest mm, in 31 additional specimens (see Supp. Table 1). In total, we obtained data for 62 cichlid species and 1 to 14 specimens each. The lengths of the intestinal tracts were then size corrected by dividing these measurements through standard lengths.

When available, the maximum reported size (maximal body size) of a species was taken from the literature ("The cichlid room companion"; Konings [48].), resulting in data for 154 species.

Evolutionary analyses

We first performed a disparity-through-time (DTT) analysis as implemented in the R package Geiger (Harmon [49]) for the number of abdominal and caudal vertebrae, the total number of vertebrae, ER and VR, as well as for maximal body size data on the basis of an all inclusive molecular phylogeny [35]. In a DTT analysis, the observed data are compared to data simulated under a Brownian motion model along the phylogeny. Positive deviations of the data from the simulations indicate a higher trait overlap among subclades than predicted by the model. DTT plots were generated using 1000 simulations under standard settings. The morphological disparity index (MDI) for each trait was calculated following the same procedure. A maximum of 160 species was analyzed here (i.e. all species where trait values and phylogenetic position were known minus two species that are not actually considered part of the radiation due to their vast phylogenetic distance to the other taxa: *Tylochromis polylepis* and *Oreochromis tanganicae* [36]). As our dataset for vertebrae counts comprises almost all species of the cichlid species flock of Lake Tanganyika, we refrained from correcting for tip over-dispersion while we used the first 90 percent for maximal body size (142 species) and ER data (143 species).

We followed a correlation analysis strategy to analyze our trait data, applying a phylogenetic generalized least squares (PGLS) analysis (Martins [34]) as implemented in the R package Caper (Orme [50]) to control for phylogenetic dependence of trait values. PGLS was conducted with a dataset comprising 162 taxa, i.e. all taxa for which trait data plus phylogenetic information was available. P-values were subsequently corrected for multiple testing using a Bonferroni-correction. We applied a maximum likelihood estimate of λ to model the phylogenetic dependency of species trait values (Pagel [51]). Pagel's λ was also calculated for each trait separately, once as implemented in Caper and once using Geiger (Harmon [49]). As both methods led to the same results, only the results obtained from Caper are reported here.

Vertebrae counts from all available specimens (a total of 2801 specimens from 174 species) were used to generate an x-y graph of vertebrae composition using the ggplot2 [52] R package (Fig. 4 A). This vertebrae count data was then transformed into species means and compared to a Brownian motion simulation of trait evolution over our phylogeny. Brownian motion simulations were done using the R package geiger [49] with σ calculated over the root age and extant trait variance. 1000 Brownian motion simulations were conducted with the root value calculated via a parsimony ancestral character state reconstruction in Mesquite [53]. Both abdominal and caudal vertebrae numbers for a set of 160 species were simulated separately and the distribution of simulated trait values was again plotted on an x-y axis and compared to the actual mean values of 160 species (same dataset as for the DTT analyses) (Fig 4 B).

Finally, the same data set was used to generate a phylomorphospace plot using Mesquite (Maddison [53]) and its module Rhetenor. The plot was later modified with Adobe Photoshop CS4 (Version 11.0.2, Adobe Systems, Inc., San Jose, California, USA) for a better visualisation, without changing data points.

We here report vertebrae count data for a total of 174 and ER data for a total of 157 Lake Tanganyikan cichlid species. Maximal overlap between vertebrae data and phylogeny was 162. Maximal overlap between phylogeny, vertebrae count data and ER data was 145 species. *Tylochromis polylepis* and *Oreochromis tanganicae* were excluded from analyses where we were primarily interested in the (time-dependent) course of evolution (i.e. DTT, phylomorphospace, convergence) while for all other (ecology-related) analyses, we used the maximal available species number. Sample sizes per species are available from Supp. Table 1.

References

1. Burke, A.C., Nelson, C.E., Morgan, B.A., and Tabin, C. (1995). Hox genes and the evolution of vertebrate axial morphology. Development *121*, 333-346.
2. Carroll, S.B. (2005). Evolution at two levels: on genes and form. PLoS Biol *3*, e245.
3. Kessel, M., and Gruss, P. (1990). Murine developmental control genes. Science *249*, 374-379.
4. Bohmer, C., Rauhut, O.W., and Worheide, G. (2015). Correlation between Hox code and vertebral morphology in archosaurs. Proc Biol Sci *282*.
5. Bohmer, C., Rauhut, O.W., and Worheide, G. (2015). New insights into the vertebral Hox code of archosaurs. Evol Dev *17*, 258-269.
6. Gomez, C., and Pourquie, O. (2009). Developmental control of segment numbers in vertebrates. J Exp Zool B Mol Dev Evol *312*, 533-544.
7. Gaunt, S.J. (1994). Conservation in the Hox code during morphological evolution. Int J Dev Biol *38*, 549-552.
8. Ford, E. (1937). Vertebral Variation in Teleostean Fishes. Journal of the Marine Biological Association of the United Kingdom *22*, 1-60.
9. Pietsch, T.W. (1978). Evolutionary Relationships of the Sea Moths (Teleostei: Pegasidae) with a Classification of Gasterosteiform Families. Copeia *1978*, 517.
10. Owen, R. (1866). On the Anatomy of Vertebrates: Fishes and reptiles. Longmans, Green *1*.
11. Galis, F. (1999). Why do almost all mammals have seven cervical vertebrae? Developmental constraints,Hox genes, and cancer. Journal of Experimental Zoology *285*, 19-26.
12. Hautier, L., Weisbecker, V., Sanchez-Villagra, M.R., Goswami, A., and Asher, R.J. (2010). Skeletal development in sloths and the evolution of mammalian vertebral patterning. Proc Natl Acad Sci U S A *107*, 18903-18908.
13. Buchholtz, E.A., and Stepien, C.C. (2009). Anatomical transformation in mammals: developmental origin of aberrant cervical anatomy in tree sloths. Evolution & development *11*, 69-79.
14. Narita, Y., and Kuratani, S. (2005). Evolution of the vertebral formulae in mammals: a perspective on developmental constraints. J Exp Zool B Mol Dev Evol *304*, 91-106.
15. Owen, R. (1853). Descriptive catalogue of the osteological series contained in the museum. Taylor and Francis *1*.
16. Ward, A.B., and Brainerd, E.L. (2007). Evolution of axial patterning in elongate fishes. Biological Journal of the Linnean Society *90*, 97-116.
17. Muller, J., Scheyer, T.M., Head, J.J., Barrett, P.M., Werneburg, I., Ericson, P.G., Pol, D., and Sanchez-Villagra, M.R. (2010). Homeotic effects, somitogenesis and the evolution of vertebral numbers in recent and fossil amniotes. Proc Natl Acad Sci U S A *107*, 2118-2123.
18. Polly, P., Head, J., and Cohn, M. (2001). Testing modularity and dissociation: the evolution of regional proportions in snakes. … heterochrony: the evolution of ….

19. Ward, A.B., and Mehta, R.S. (2010). Axial elongation in fishes: using morphological approaches to elucidate developmental mechanisms in studying body shape. Integr Comp Biol *50*, 1106-1119.
20. Parra-Olea, G., and Wake, D.B. (2001). Extreme morphological and ecological homoplasy in tropical salamanders. Proc Natl Acad Sci U S A *98*, 7888-7891.
21. Wiens, J.J., Brandley, M.C., and Reeder, T.W. (2006). Why Does a Trait Evolve Multiple Times within a Clade? Repeated Evolution of Snakeline Body Form in Squamate Reptiles. Evolution *60*, 123-141.
22. Brainerd, E.L., and Patek, S.N. (1998). Vertebral column morphology, C-start curvature, and the evolution of mechanical defenses in tetraodontiform fishes. Copeia, 971-984.
23. Breder, C.M. (1926). The locomotion of fishes, (New York: Office of the Society).
24. Johnson, R.G. (1955). The Adaptive and Phylogenetic Significance of Vertebral Form in Snakes. Evolution *9*, 367-388.
25. Wake, D. (1966). Comparative osteology and evolution of the lungless salamanders, family Plethodontidae.
26. Maxwell, E.E., and Wilson, L.A. (2013). Regionalization of the axial skeleton in the 'ambush predator' guild--are there developmental rules underlying body shape evolution in ray-finned fishes? BMC Evol Biol *13*, 265.
27. McDowall, M. (2003). Variation in vertebral number in galaxiid fishes, how fishes swim and a possible reason for pleomerism. Reviews in Fish Biology and Fisheries *13*, 247-263.
28. McDowall, R.M. (2008). Jordan's and other ecogeographical rules, and the vertebral number in fishes. Journal of Biogeography *35*, 501-508.
29. Lindsey, C.C. (1988). Factors controlling meristic variation. In Fish Physiology, Volume 11B, D.J. Hoar and D.J. Randall, eds., pp. 197-274.
30. Lindsey, C.C. (1975). Pleomerism, the Widespread Tendency Among Related Fish Species for Vertebral Number to be Correlated with Maximum Body Length. Journal of the Fisheries Research Board of Canada *32*, 2453-2469.
31. Salzburger, W., Van Bocxlaer, B., and Cohen, A.S. (2014). Ecology and Evolution of the African Great Lakes and Their Faunas. Annual Review of Ecology, Evolution, and Systematics, Vol 45 *45*, 519-+.
32. Swain, D.P. (1992). Selective Predation for Vertebral Phenotype in Gasterosteus-Aculeatus - Reversal in the Direction of Selection at Different Larval Sizes. Evolution *46*, 998-1013.
33. Ward, A.B., and Azizi, E. (2004). Convergent evolution of the head retraction escape response in elongate fishes and amphibians. Zoology (Jena) *107*, 205-217.
34. Martins, E.P., and Hansen, T.F. (1997). Phylogenies and the comparative method: A general approach to incorporating phylogenetic information into the analysis of interspecific data. American Naturalist *149*, 646-667.
35. Colombo, M., Indermaur, A., Meyer, B.S., and Salzburger, W. (2016). Habitat use and its implications to functional morphology: niche partitioning and the evolution of locomotory morphology in Lake

Tanganyikan cichlids (Perciformes: Cichlidae). Biological Journal of the Linnean Society, n/a-n/a.
36. Muschick, M., Indermaur, A., and Salzburger, W. (2012). Convergent evolution within an adaptive radiation of cichlid fishes. Curr Biol *22*, 2362-2368.
37. Muschick, M., Nosil, P., Roesti, M., Dittmann, M.T., Harmon, L., and Salzburger, W. (2014). Testing the stages model in the adaptive radiation of cichlid fishes in East African Lake Tanganyika. Proc Biol Sci *281*, 1-10.
38. Wagner, C.E., McIntyre, P.B., Buels, K.S., Gilbert, D.M., and Michel, E. (2009). Diet predicts intestine length in Lake Tanganyika's cichlid fishes. Functional Ecology *23*, 1122-1131.
39. Kiso, S., Miyake, T., and Yamahira, K. (2011). Heritability and genetic correlation of abdominal and caudal vertebral numbers in latitudinal populations of the medaka Oryzias latipes. Environmental Biology of Fishes *93*, 185-192.
40. Yamahira, K., Nishida, T., Arakawa, A., and Iwaisaki, H. (2009). Heritability and genetic correlation of abdominal versus caudal vertebral number in the medaka (Actinopterygii: Adrianichthyidae): genetic constraints on evolution of axial patterning? Biological Journal of the Linnean Society *96*, 867-874.
41. Yamahira, K., and Nishida, T. (2009). Latitudinal variation in axial patterning of the medaka (Actinopterygii: Adrianichthyidae): Jordan's rule is substantiated by genetic variation in abdominal vertebral number. Biological Journal of the Linnean Society *96*, 856-866.
42. Webb, P.W. (1984). Body Form, Locomotion and Foraging in Aquatic Vertebrates. American Zoologist *24*, 107-120.
43. Harmon, L.J., Schulte, J.A., 2nd, Larson, A., and Losos, J.B. (2003). Tempo and mode of evolutionary radiation in iguanian lizards. Science *301*, 961-964.
44. Streelman, J.T., and Danley, P.D. (2003). The stages of vertebrate evolutionary radiation. Trends in Ecology & Evolution *18*, 126-131.
45. Danley, P.D., and Kocher, T.D. (2001). Speciation in rapidly diverging systems: lessons from Lake Malawi. Mol Ecol *10*, 1075-1086.
46. Moser, D., Roesti, M., and Berner, D. (2012). Repeated lake-stream divergence in stickleback life history within a Central European lake basin. PloS one *7*.
47. Rohlf, F. (2010). tpsDig, digitize landmarks and outlines. 2.15 Edition. (Department of Ecology and Evolution: State University of New York, Stony Brook, New York.).
48. Konings, A. (1999). Tanganjika-Cichliden in ihrem natürlichen Lebensraum, (cichlid Press).
49. Harmon, L.J., Weir, J.T., Brock, C.D., Glor, R.E., and Challenger, W. (2008). GEIGER: investigating evolutionary radiations. Bioinformatics *24*, 129-131.
50. Orme, D. (2012). The caper package: comparative analysis of phylogenetics and evolution in R.
51. Pagel, M. (1999). Inferring the historical patterns of biological evolution. Nature *401*, 877-884.

52. Ginestet, C. (2011). ggplot2: Elegant Graphics for Data Analysis. Journal of the Royal Statistical Society: Series A (Statistics in Society) *174*, 245-246.
53. Maddison, W.P., and Maddison, D.R. (2011). Mesquite: a modular system for evolutionary analysis. 2.75 Edition.

1.2.2
Figures & Tables

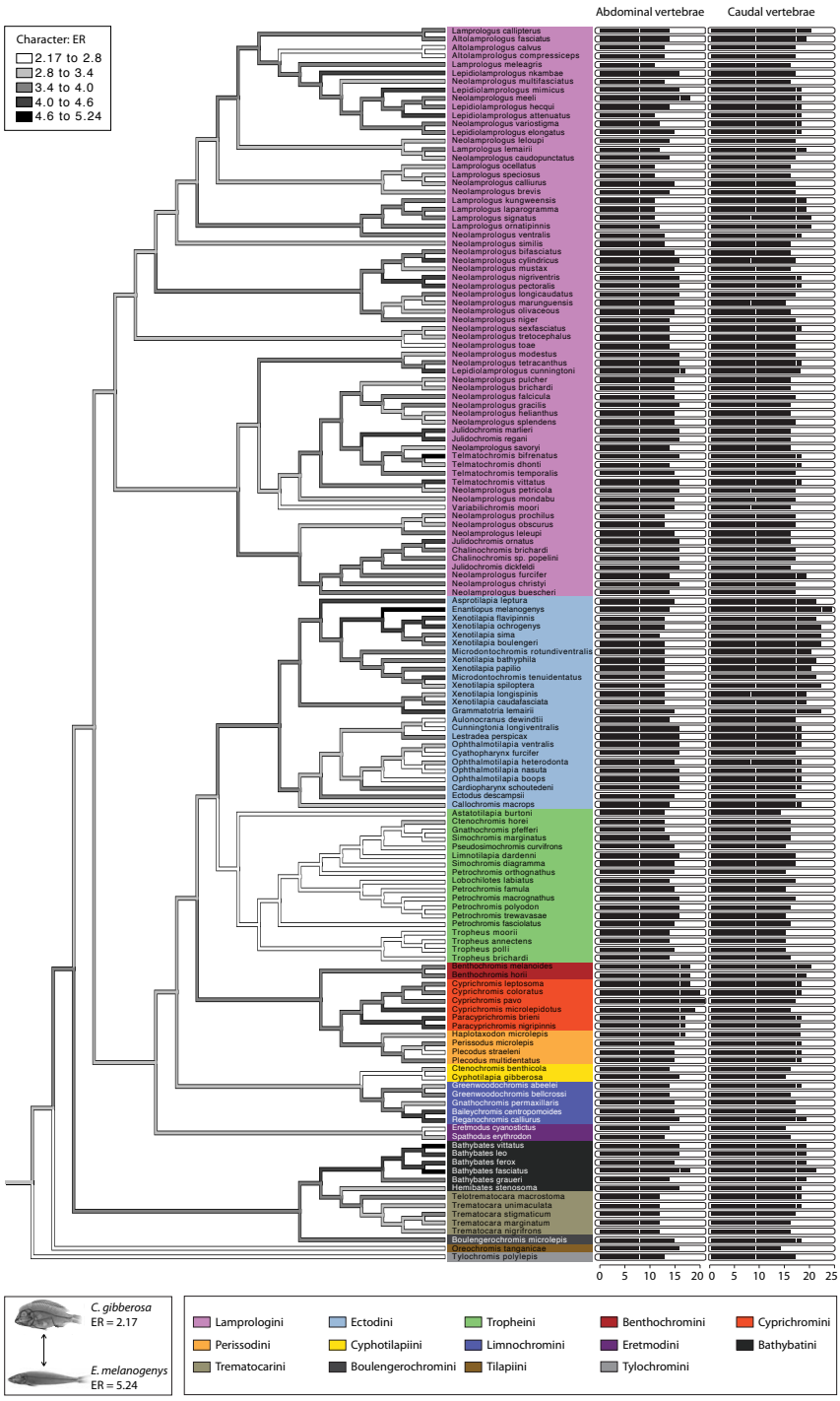

Fig. 1
Ancestral state reconstruction of ER based on a molecular phylogeny including 145 LT cichlid species. The vertebral numbers shown are rounded to whole numbers. ER history was traced using Mesquite with a parsimony reconstruction of ancestral states.
Low respectively high values of both ER and vertebral numbers appear at various positions within the phylogeny.

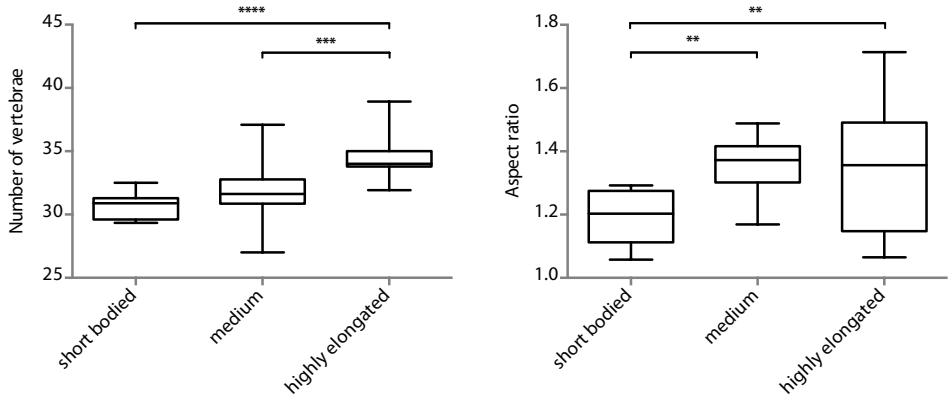

Fig. 2
Significant differences concerning the number of vertebrae were found between short-bodied and highly elongated species (Tukey's multiple comparison test; adjusted p-value: <0.0001) as well as between medium elongated and highly elongated species (p=0.0002). Significant differences concerning AR were found between short-bodied and medium elongated species (Tukey's multiple comparison test; adjusted p-value: 0.0046) as well as between short bodied and highly elongated species (p=0.0073). The graph shows the extent from the 25th to 75th percentiles and median (box) and the minimal and maximal value per group (whiskers).

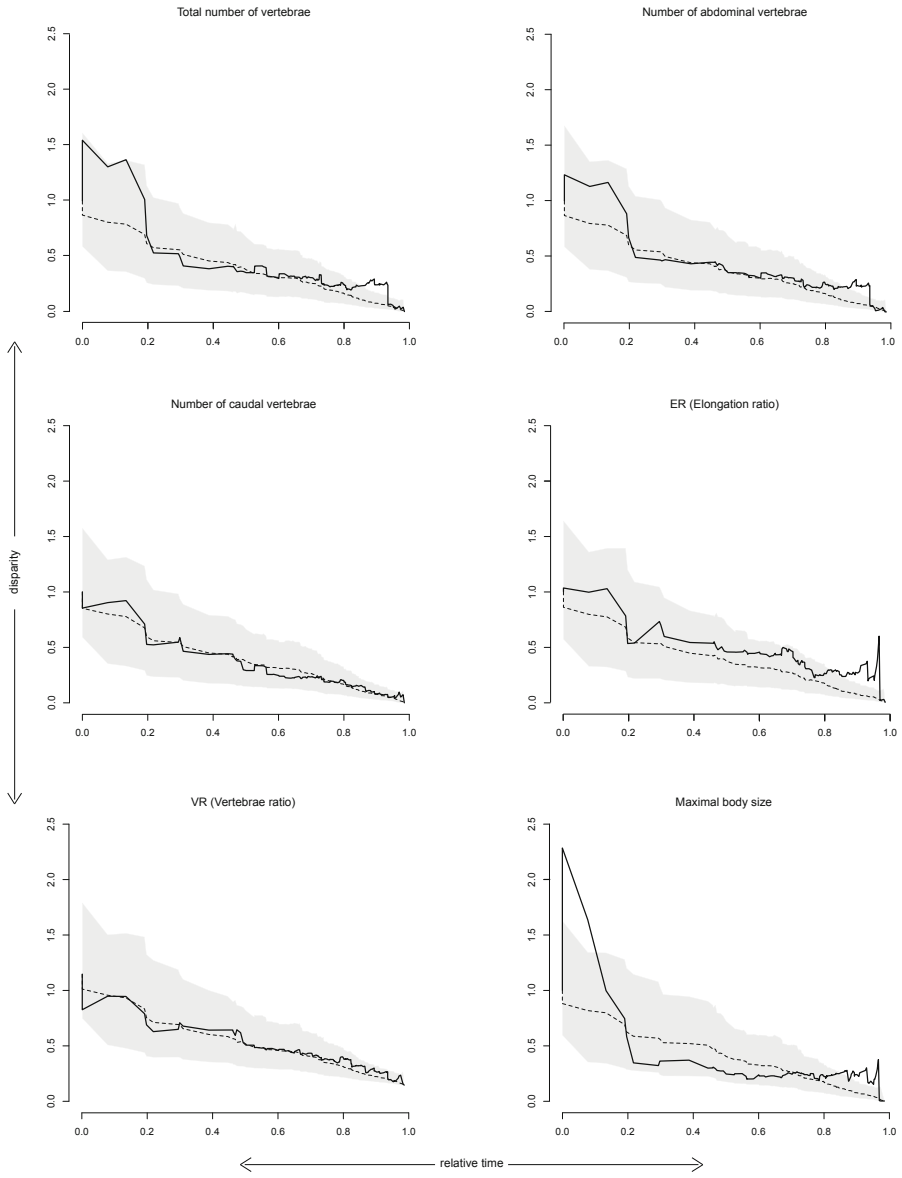

Fig. 3
DTT plots showing average subclade disparity of empirical data through time (black line) as well as the 95% C.I. of 1000 Brownian motion simulations (grey area) and the mean DTT from the simulated datasets (dashed line).
DTT plots for abdominal and caudal vertebrae, total number of vertebrae and maximal body size display bursts of morphological evolution early in the AR. We also found recurrent peaks around 0.3 in relative time for all traits under study meaning that average subclade disparity was elevated for all traits at a particular point in time. Furthermore, we found peaks for all traits later on in the relative time line.
Sample sizes (taxa) were: vertebrae counts: 160, ER: 143, maximal body size: 142.

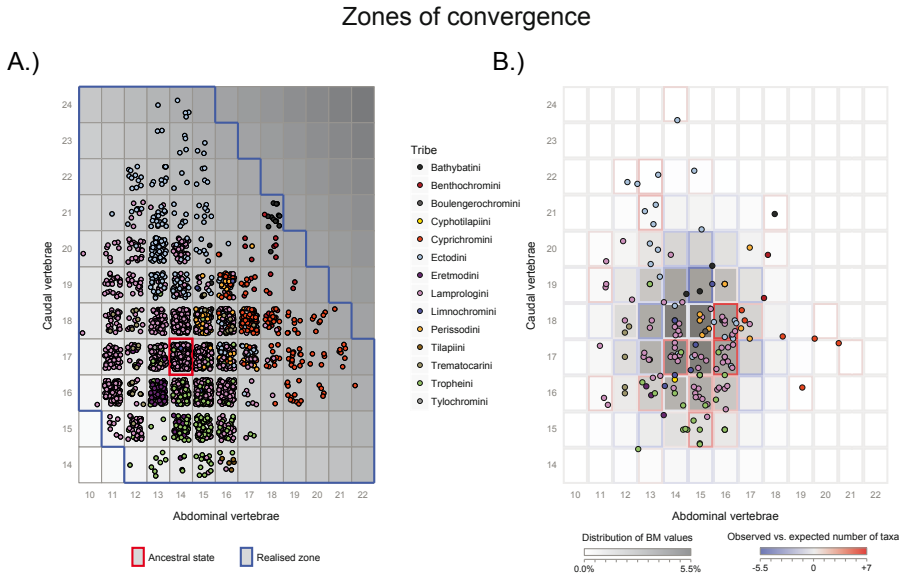

Fig. 4
Zones of possible convergence between LT cichlid species. While we find great overlap between many ‘tribes’ (and taxa), some parts of the morphospace (e.g. very high counts of caudal or abdominal vertebrae) seem to be exclusively occupied by specific ‘tribes’.
A.) Vertebrae count data of 2801 specimens from 174 species. The ancestral state was reconstructed using Mesquite [53]. The realised zone depicts values that were achieved both in terms of individual (abdominal and caudal) and total vertebrae numbers.
B.) Species means of 160 species compared to trait distribution according to 1000 Brownian motion simulations over the same set of taxa (gray shades). The differences between the observed and simulated trait distribution are indicated with blue (fewer taxa than expected) and red (more taxa than expected) frames.

trait	Pagel's lambda	lower boundary p-value	upper boundary p-value	$N_{species}$
Total number of vertebrae	0.965	**<0.0001**	**0.0414**	162
Number of abdominal vertebrae	0.970	**<0.0001**	0.0893	162
Number of caudal vertebrae	0.993	**<0.0001**	0.3284	162
ER	0.931	**<0.0001**	**<0.0001**	145
VR	0.990	**<0.0001**	0.2942	162
Maximal body size	0.960	**<0.0001**	**0.0036**	143

Table 1
Pagels's lambda was calculated as implemented in the R package 'Caper'. Values not significantly different from 0 (lower boundary) indicate that there is no phylogenetic signal whereas values not different from 1 (upper boundary) indicate that trait distribution follows phylogenetic relationships.

trait	MDI	$N_{species}$	MDI range
Total number of vertebrae	0.116	160	100%
Number of abdominal vertebra	0.085	160	100%
Number of caudal vertebrae	0.003	160	100%
ER	0.117	143	90%
VR	0.006	160	100%
Maximal body size	0.060	142	90%

Table 2
Morphological disparity index corresponding to the DTT plots shown in Fig. 6. Low MDI values in combination with DTT plots showing an initial peak and a subsequent drop in average subclade disparity are indicative for a scenario of early divergence in trait evolution. Analyses including substantially less LT cichlid species than currently described were corrected for tip over-dispersion by using only the first 90% of the timeline to calculate MDI.

Total number of vertebrae					
trait	t-value	adjusted p-value	R^2	λ	$N_{Species}$
ER	7.028	**0.000**	0.259	0.899	145
VR	3.307	**0.007**	0.067	0.975	162
Maximal body size	3.982	**0.001**	0.101	0.985	143
δ15N	-0.939	1	0.011	0.993	71
δ13C	0.083	1	0.000	0.995	71
Intestinal tract length	0.649	1	0.006	1	59
Number of abdominal vertebrae					
trait	t-value	adjusted p-value	R^2	λ	$N_{Species}$
Number of caudal vertebrae	0.518	1	0.001	0.971	162
ER	3.112	**0.013**	0.064	0.964	145
Maximal body size	3.044	**0.017**	0.062	1	143
δ15N	-3.480	**0.005**	0.137	0.998	71
δ13C	0.616	1	0.004	0.999	71
Intestinal tract length	3.453	**0.006**	0.167	1	59
Number of caudal vertebrae					
trait	t-value	adjusted p-value	R^2	λ	$N_{Species}$
Number of abdominal vertebrae	0.577	1	0.003	0.993	162
ER	6.004	**0.000**	0.203	0.98	145
Maximal body size	2.269	0.149	0.035	0.995	143
δ15N	1.715	0.545	0.039	1	71
δ13C	-0.418	1	0.003	1	71
Intestinal tract length	-2.304	0.149	0.088	1	59
ER (Elongation ratio)					
trait	t-value	adjusted p-value	R^2	λ	$N_{Species}$
Total number of vertebrae	7.435	**0.000**	0.277	0.839	145
Number of abdominal vertebrae	3.102	**0.019**	0.063	0.933	145
Number of caudal vertebrae	7.549	**0.000**	0.283	0.815	145
VR	-0.924	1	0.006	0.924	145
Maximal body size	0.399	1	0.006	0.923	128
δ15N	-0.323	1	0.001	0.876	66
δ13C	-1.278	1	0.026	0.846	66
Intestinal tract length	-2.029	0.380	0.075	0.863	54
VR (Vertebrae ratio)					
trait	t-value	adjusted p-value	R^2	λ	$N_{Species}$
Total number of vertebrae	3.607	**0.002**	0.072	0.993	162
ER	-0.386	1	0.001	0.988	145
Maximal body size	0.274	1	0.008	1	143
δ15N	-4.608	**0.000**	0.220	1	71
δ13C	0.825	1	0.009	1	71
Intestinal tract length	4.869	**0.000**	0.291	1	59

Table 3
Correlations between traits and ecological parameters according to PGLS analyses that correct for phylogenetic dependency. P-values were adjusted for multiple testing using a Bonferroni correction.

1.2.3
Supporting information

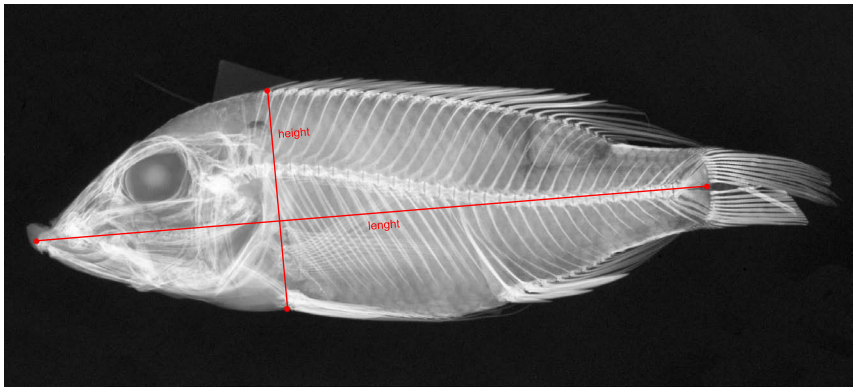

Supp. Figure 1
Landmarks used to assess body height and standard length: The anterior ending of the upper jaw (anterior most point) and the onset of the caudal fin (posterior most point) were used to measure standard length, whereas the anterior onset of the dorsal fin and the anterior onset of the pelvic fin were used to determine body height.

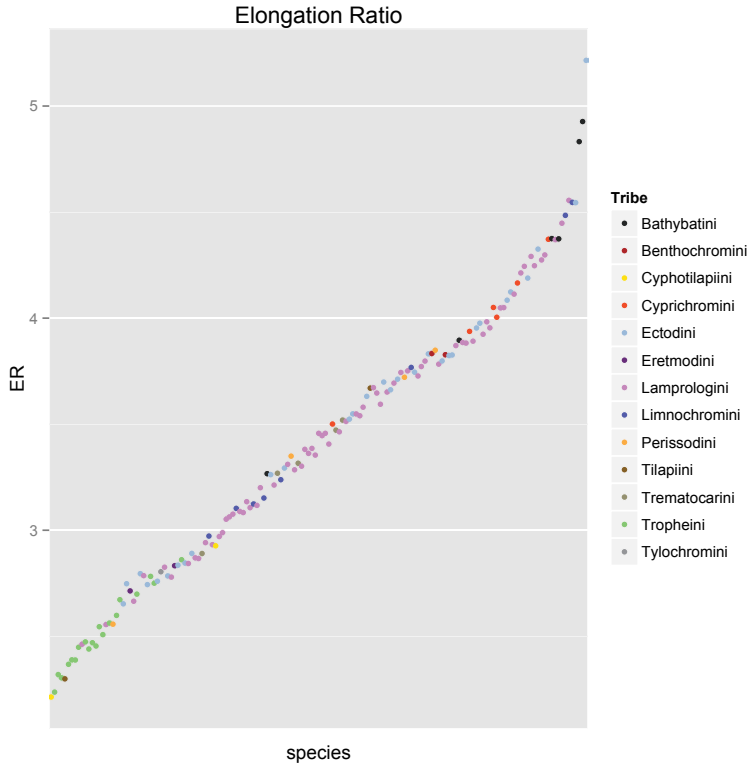

Supp. Figure 2
Elongation ratio data for 157 LT cichlid species showing a smooth distribution of ER values with remarkable gaps only towards the most highly elongated species. Data points are coloured according to ‘tribes’. A jitter of 0.05 was used for better visualisation. Figure was done using the ggplot2 package for R.

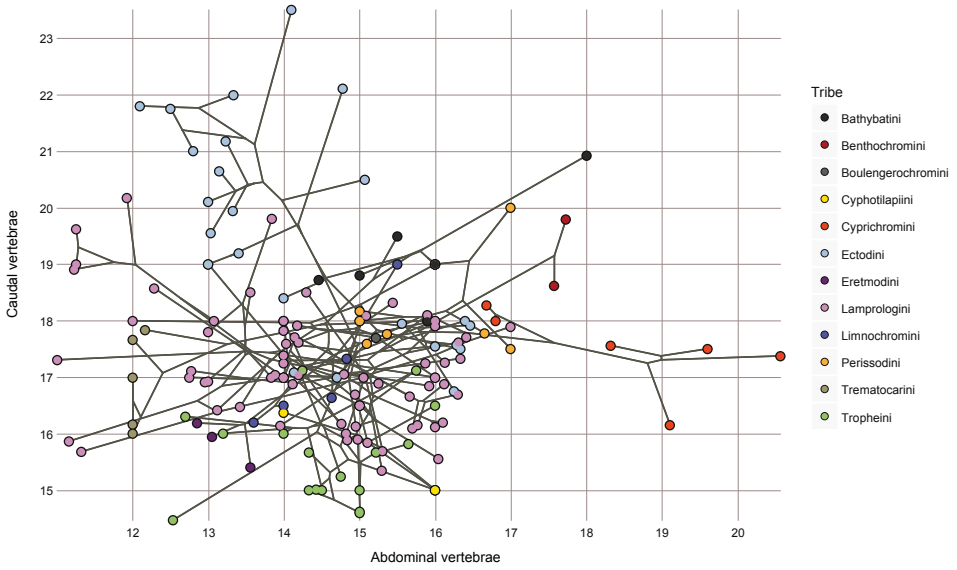

Supp. Figure 3
Phylomorphospace plot done using Mesquite showing abdominal and caudal vertebrae numbers as well as the phylogenetic relationships between taxa. Data points are coloured according to ‘tribes’.

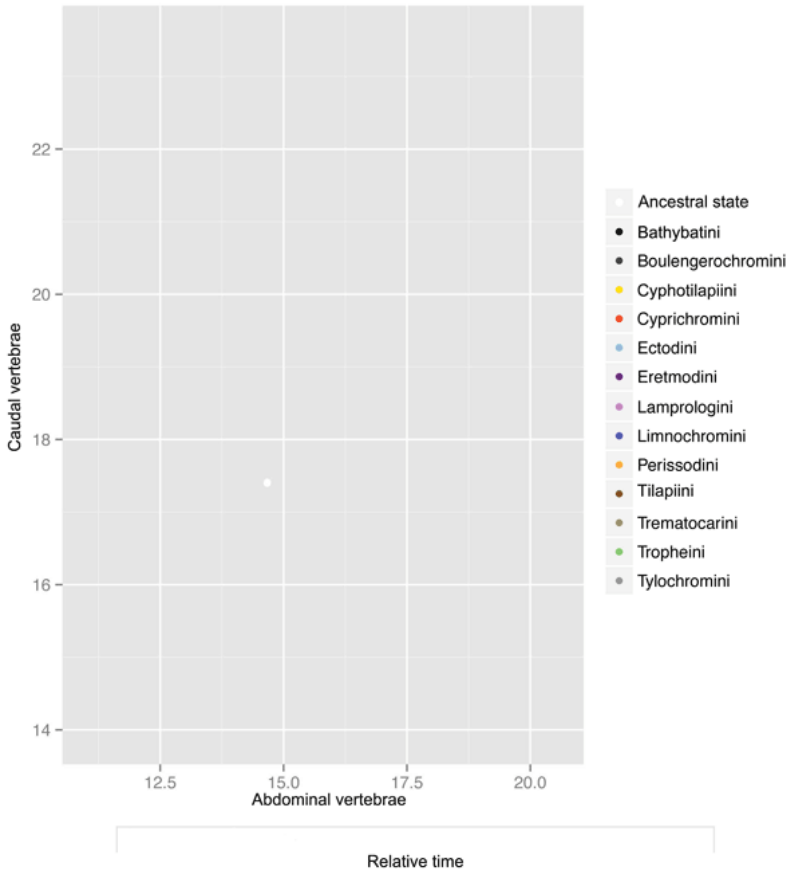

Supp. Figure 4*
Graphics interchange format (GIF) animation showing the development of abdominal and caudal vertebrae numbers over time. Timing of the individual developmental steps is relative to the timing reconstructed from the phylogeny. Ancestral states are depicted in white. Data for this plot was generated using the 'getAncStates' function in the R package Geiger. Single plots were generated using the R package ggplot2.
*shown here is a freeze frame of the animation

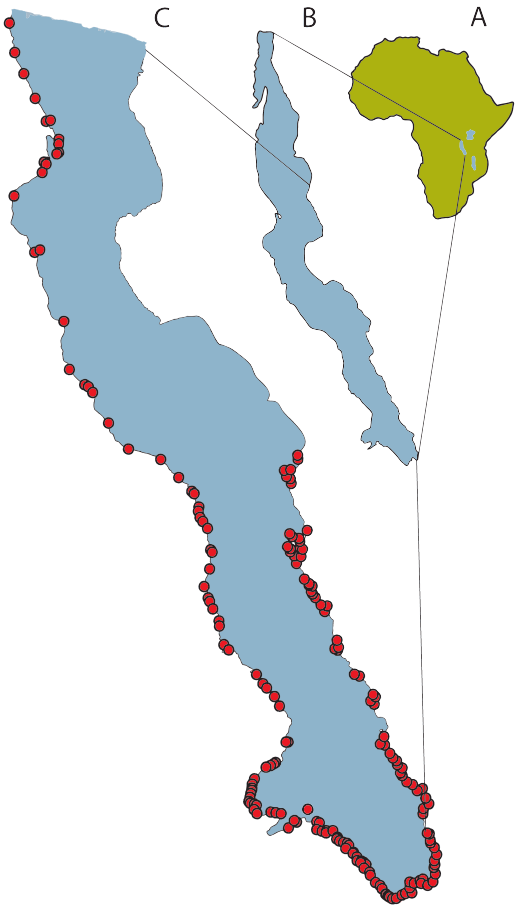

Supp. Figure 5
Map of the sampling localities around the southern part of Lake Tanganyika spanning the countries Zambia, Tanzania and the Democratic Republic of Congo.

	$N_{vertebrae\ counts}$	N_{ER}	$N_{intestinal\ tract}$
Altolamprologus calvus	13	10	1
Altolamprologus compressiceps	25	10	12
Altolamprologus fasciatus	32	10	8
Asprotilapia leptura	14	10	7
Astatotilapia burtoni	15	13	10
Aulonocranus dewindti	23	10	9
Baileychromis centropomoides	6	3	-
Bathybates fasciatus	13	8	2
Bathybates ferox	5	5	-
Bathybates graueri	11	10	6
Bathybates leo	2	1	-
Bathybates minor	2	-	-
Bathybates vittatus	1	1	1
Benthochromis horii	13	10	-
Benthochromis melanoides	10	10	-
Boulengerochromis microlepis	9	10	2
Callochromis macrops	10	10	9
Cardiopharynx schoutedeni	7	5	-
Chalinochromis bifrenatus	5	5	-
Chalinochromis brichardi	10	10	4
Chalinochromis sp. popelini	8	8	-
Ctenochromis benthicola	8	1	-
Ctenochromis horei	10	10	11
Cunningtonia longiventralis	11	10	-
Cyathopharynx foae	4	4	-
Cyathopharynx furcifer	4	4	10
Cyphotilapia gibberosa	7	8	8
Cyprichromis coloratus	10	10	1
Cyprichromis leptosoma	50	-	10
Cyprichromis microlepidotus	19	10	-
Cyprichromis pavo	16	10	-
Ectodus descampsii	10	9	-
Enantiopus melanogenys	10	10	7
Eretmodus cyanostictus	45	10	4
Gnathochromis permaxillaris	11	10	-
Gnathochromis pfefferi	5	5	7
Grammatotria lemairii	9	9	4
Greenwoodochromis bellcrossi	5	1	-
Greenwoodochromis christyi	2	-	-
Haplotaxodon microlepis	23	10	2
Haplotaxodon trifasciatus	2	-	8
Hemibates stenosoma	10	7	-
Interochromis loocki	2	-	11
Julidochromis dickfeldi	10	10	-
Julidochromis marlieri	8	7	-
Julidochromis ornatus	13	10	8
Julidochromis regani	10	10	-
Lamprologus callipterus	61	10	10
Lamprologus congoensis	1	-	-
Lamprologus kungweensis	22	10	-

Lamprologus laparogramma	12	10	-
Lamprologus lemairii	14	10	5
Lamprologus meleagris	67	10	-
Lamprologus mocquardi	1	-	-
Lamprologus ocellatus	86	10	-
Lamprologus ornatipinnis	28	10	-
Lamprologus signatus	8	7	-
Lamprologus speciosus	69	10	-
Lamprologus werneri	1	-	-
Lepidiolamprologus attenuatus	41	10	10
Lepidiolamprologus elongatus	11	9	10
Lepidiolamprologus hecqui	23	10	-
Lepidiolamprologus kendalli	1	-	-
Lepidiolamprologus mimicus	2	2	-
Lepidiolamprologus nkambae	2	2	-
Lepidiolamprologus profundicola	1	-	5
Lestradea perspicax	5	4	-
Limnochromis abeelei	1	1	-
Limnochromis auritus	4	4	-
Limnochromis staneri	4	3	-
Limnotilapia dardenni	8	8	7
Lobochilotes labiatus	8	8	14
Microdontochromis rotundiventralis	9	9	-
Microdontochromis tenuidentatus	14	10	-
Neolamprologus bifasciatus	17	10	-
Neolamprologus brevis	269	10	-
Neolamprologus brichardi	81	10	-
Neolamprologus buescheri	26	9	-
Neolamprologus calliurus	19	10	-
Neolamprologus cancellatus	1	1	-
Neolamprologus caudopunctatus	43	9	10
Neolamprologus christyi	13	10	-
Neolamprologus crassus	2	-	-
Neolamprologus cunningtoni	10	10	1
Neolamprologus cylindricus	3	2	-
Neolamprologus falcicula	4	3	-
Neolamprologus furcifer	10	9	1
Neolamprologus gracilis	25	10	-
Neolamprologus helianthus	39	10	-
Neolamprologus leleupi	17	10	-
Neolamprologus leloupi	65	10	-
Neolamprologus longicaudatus	8	7	-
Neolamprologus marunguensis	17	10	-
Neolamprologus meeli	47	10	-
Neolamprologus modestus	23	10	12
Neolamprologus mondabu	20	10	-
Neolamprologus multifasciatus	33	10	-
Neolamprologus mustax	10	10	2
Neolamprologus niger	13	9	-
Neolamprologus nigriventris	11	9	-
Neolamprologus obscurus	15	9	1

Neolamprologus olivaceous	19	10	-
Neolamprologus pectoralis	13	10	-
Neolamprologus petricola	9	9	-
Neolamprologus prochilus	9	8	3
Neolamprologus pulcher	37	10	9
Neolamprologus savoryi	21	10	11
Neolamprologus sexfasciatus	14	10	8
Neolamprologus similis	23	10	-
Neolamprologus splendens	33	10	-
Neolamprologus tetracanthus	17	10	6
Neolamprologus toae	5	5	-
Neolamprologus tretocephalus	16	9	-
Neolamprologus variostigma	2	2	-
Neolamprologus ventralis	13	10	-
Neolamprologus wauthioni	5	-	-
Ophthalmotilapia boops	18	10	-
Ophthalmotilapia heterodonta	1	1	-
Ophthalmotilapia nasuta	13	10	5
Ophthalmotilapia ventralis	23	10	14
Oreochromis tanganicae	5	5	7
Paracyprichromis brieni	75	10	4
Paracyprichromis nigripinnis	10	10	-
Perissodus eccentricus	3	-	-
Perissodus microlepis	22	10	10
Petrochromis famula	8	7	7
Petrochromis fasciolatus	9	8	-
Petrochromis macrognathus	2	1	13
Petrochromis orthognathus	8	8	-
Petrochromis polyodon	17	10	7
Petrochromis sp. 'Kipili brown'	6	6	-
Petrochromis trewavasae	1	1	-
Plecodus elaviae	6	-	-
Plecodus multidentatus	6	4	-
Plecodus paradoxus	1	-	-
Plecodus straeleni	10	10	5
Pseudosimochromis curvifrons	4	4	9
Reganochromis calliurus	2	1	2
Simochromis babaulti	13	10	-
Simochromis diagramma	10	8	10
Simochromis marginatus	1	1	-
Simochromis pleurospilus	1	-	-
Spathodus erythrodon	37	9	-
Tanganicodus irsacae	21	-	3
Telmatochromis bifrenatus	3	3	-
Telmatochromis brachygnathus	4	4	-
Telmatochromis dhonti	32	10	-
Telmatochromis temporalis	39	10	10
Telmatochromis vittatus	10	10	-
Telotrematocara macrostoma	6	4	-
Trematocara marginatum	6	-	-
Trematocara nigrifrons	1	1	-

Trematocara stigmaticum	1	3	-
Trematocara unimaculatum	3	2	3
Trematocara variabile	7	4	-
Triglachromis otostigma	3	3	-
Tropheus annectens	3	3	-
Tropheus brichardi	3	3	-
Tropheus duboisi	1	1	3
Tropheus moorii	52	10	10
Tropheus polli	5	5	-
Tylochromis polylepis	1	1	3
Variabilichromis moorii	33	10	12
Xenotilapia bathyphila	17	10	-
Xenotilapia boulengeri	6	6	-
Xenotilapia caudofasciata	1	1	-
Xenotilapia flavipinnis	10	10	5
Xenotilapia longispinis	5	4	-
Xenotilapia nigrolabiata	1	2	-
Xenotilapia ochrogenys	4	4	-
Xenotilapia ornatipinnis	7	7	-
Xenotilapia papilio	34	10	-
Xenotilapia sima	10	1	-
Xenotilapia spiloptera	31	10	3
Total	*2801*	*1157*	432

Supp. Table 1
Sample sizes per species for vertebrae counts, ER and intestinal tract length.

Supp. Table 2
Vertebrae count data per specimen for 2801 individuals.
(Not shown here due to vast size)

1.3
The evolution of trophic morphology in a large-scale adaptive radiation of cichlid fishes

Reviewed by AXIOS, suggested for Evolution

HB collected the x-rays. FM and me collected and analysed the data. I then drafted the manuscript. All authors participated in discussing the manuscript and drafting the final version.

The evolution of trophic morphology in a large-scale adaptive radiation of cichlid fishes

Marco Colombo*, Florian Meury*, Heinz H. Büscher & Walter Salzburger

Zoological Institute, University of Basel, Vesalgasse 1, CH 4051, Basel, Switzerland

*These two authors contributed equally to the study

Authors for correspondence:
Marco Colombo
e-mail: marco.colombo@unibas.ch
Walter Salzburger
e-mail: walter.salzburger@unibas.ch

running title: Evolution of cichlid trophic morphology

Abstract

Diversification related to foraging strategies and the trophic apparatus are major axes of divergence in vertebrate adaptive radiations. Here, we investigate divergence of trophic morphology (head shape and relative bite force) throughout the adaptive radiation of cichlid fishes form Lake Tanganyika, using trait data from three quarters of the lake's ~200 endemic cichlid species. We first show that head shape is tightly linked with relative bite force in Lake Tanganyika cichlids and establish a strong correlation between these feeding-related traits and ecology. Our data suggest that elongated head morphologies with anteriorly oriented mouths coincide with the ability to rapidly (yet weakly) move the jaws, which is typical for ram feeders, whereas short and robust snouts with ventrally oriented mouths relate to the ability to slowly (yet forcefully) close the jaws, as is mainly found in species feeding on immobile prey using biting or picking. Furthermore, we show that these trophic traits connected to the strategy of food acquisition diverged early in the adaptive radiation and show the signature of an 'early burst' of morphological diversification. Trophic morphology thus seems to be the first axis of divergence in the Lake Tanganyika cichlid adaptive radiation. This contradicts the 'stages model' of adaptive radiation, which states that diversification should initially occur along macro-habitat related traits. Finally, we identify multiple cases of convergent evolution in trophic morphology within the adaptive radiation of cichlids from Lake Tanganyika.

Keywords

Early burst, radiation in stages, disparity through time, Lake Tanganyika cichlids, convergence

Introduction

Adaptive radiation (AR), a process that is thought to have led to a great deal of the species richness and biodiversity on Earth, is defined as the rapid proliferation of an evolutionary lineage into an array of ecologically and morphologically distinct species as a consequence of their adaptation to various ecological niches due to ecological opportunity [1-5]. Such ecological opportunity may arise from the extinction of antagonists, the colonization of novel (i.e. previously under-colonized) habitats, or following the evolution of 'key innovations' facilitating the exploitation of previously underutilized regions in the adaptive landscape [2,6].

Several general patterns related to morphological evolution in AR have been propagated on the basis of empirical and theoretical research. Among these 'common features' are (*a*) the occurrence of '*early bursts*' in morphological diversification (e.g. [7,8]), (*b*) the progression of morphological diversification in discrete episodes ('*radiation in stages*' model, [9,10]), and (*c*) the repeated generation of morphologically similar forms in ecologically equivalent habitats (i.e. convergence; [3,5]).

The '*early burst*' scenario (*a*) is founded on the assumption that morphological evolution within an AR should initially be rapid in response to the availability of a number of unoccupied ecological niches that the newly forming species can enter; as these niches become more and more filled, the rate of morphological evolution should decrease over the course of the radiation [2,3,7,11]. Although this scenario appears intuitive, such early bursts are rarely observed in comparative data [11] (but see e.g. [12-15]). On the other hand, only few ARs have been studied in sufficient detail and with a sufficiently large taxonomic coverage, and more empirical data are needed, to assess the generality of this and other patterns [16].

The '*radiation in stages*' model (*b*), developed for the AR of cichlid fishes in East African Lake Malawi [10] and later generalized for vertebrate ARs [9], suggests that morphological diversification involves different adaptive axes during discriminable temporal stages. According to this verbal model, the first stage of AR should be characterized by diversification along an axis of macro-habitat specialization, as seen, for example, in three-spine stickleback or crater-lake cichlids that diverged with regard to the exploitation of the benthic and limnetic zones of lakes, respectively [17-19]. Stage two should be dominated by divergence according to micro-habitat and resource use, as is illustrated, for example, by the numerous species of cichlid fishes with distinct mouth morphologies associated with feeding specializations that co-occur within the shallow-water rocky macro-habitat in lakes Malawi [10] and Tanganyika [20]. The third and final stage of AR should involve divergence with respect to sexually selected traits, such as coloration or ornamentation, as observed e.g. in cichlids and anoles. It is important to note that these stages are not thought to be exclusively mediated by one adaptive axis at a time, but rather that one axis predominantly shapes each stage [9]. It is a matter of debate, though, to which extent defined stages are recurrently existent in ARs. Furthermore, the temporal sequence of the three stages seems to vary between ARs for which temporally discriminable stages could be defined: While in Lake Malawi cichlids, the three stages appear to occur in the beforehand mentioned order [9,21], other ARs seem to lack a certain stage, or the sequence of stages relative to each other appears to be reversed [22,23].

Convergent evolution (*c*) describes the independent generation of similar morphologies due to adaptation to similar ecological lifestyles. Many ARs exhibit, alongside often extensive divergence, also a great deal of convergence and it has been suggested that, ultimately, convergence seems to be an inherent feature of divergence

within an AR [5]. Classic examples of convergence in ARs are the recurrently evolving "species-pairs" of stickleback fish in post-glacial lakes [2,24,25], similar ecomorphs of Anoles lizards that evolved on different islands of the Greater Antilles [26,27], and the multiple sets of strikingly similar cichlids – with respect to body shape, trophic morphology and coloration – in the East African Great Lakes [28]. Convergence may, however, also arise within a single AR as reported, for example, for Lake Tanganyikan cichlids [20]. Although convergent evolution provides eminent proof for the action of natural selection [24], it is rarely quantified using comparative data.

Divergence in trophic morphology in correlation with feeding specialization is a central theme in ARs [2], e.g. in *Anolis* lizards with respect to head shape [29], or in three-spine sticklebacks according to gill raker number and length [30,31]. The most famous example for such a phenotype-environment correlation is portrayed by Darwin's finches, which differ greatly in bill shape, size and bite force (e.g. [2,32,33]). In cichlids, the lower pharyngeal jaw apparatus, a second set of tooth-bearing jaws situated in the pharynx [34], has gained considerable attention in this respect (see e.g. [20,23,35-37]), while the oral jaw apparatus, although essential for food acquisition, has been less in the focus of evolutionary research. Similarly, overall body shape, considered to be mainly influenced by macro-habitat related selection pressures [21,23], has been studied in detail [18,20,38,39], whereas studies on time-dependent evolution focusing on head morphology, and, hence, distinguishing between head- and overall body shape, remain scarce (but see [40]).

Here, we make use of an extensive dataset on trophic morphology in one of the role models of AR in vertebrates, the cichlid assemblage of East African Lake Tanganyika. Using a collection of 157 Lake Tanganyikan cichlid species and a corresponding molecular phylogeny, we correlate different morphological traits related to feeding

specializations (trophic and head morphology and relative bite force) with ecological parameters, test for phenotype-environment correlations, and examine the traits under investigation with respect to a time dependence of trait evolution. For the first time, we were thus able to test patterns of trait evolution in an extensive dataset covering about three quarters of all species of a massive cichlid AR, resulting in what is to date among the most complete studies of morphological evolution through time of the trophic apparatus within an AR.

Materials and Methods

Sampling and data acquisition

Sampling was performed by HB between 1982 and 2011 at 426 locations in three adjacent countries (Zambia, Tanzania and the Democratic Republic of Congo) in the central and southern part of Lake Tanganyika. For this study, we used 1125 specimens representing 157 species from all 14 currently recognized Tanganyikan cichlid tribes [20] (see Supplementary file 1). Fish were caught with hand nets or with monofilamentous gill nets; additional specimens were obtained from local fishermen. Specimens were then euthanized with an overdose of Metomidate and immediately fixed in a 4% Formol solution, flushed with water and then permanently stored in 75% EtOH.

All specimens were x-rayed using an industrial X-ray system (Faxitron 43855, Faxitron Bioptics, LLC, Tucson, Arizona 85706 USA) with a tube voltage of 50 kV, a tube current of 3.0 mA and imaged on a Kodak Industrex MX 125 X-ray film. Later on, the pictures were digitized using a Nikon D 5000 digital camera (Nikon Corporation, Tokyo, Japan).

We obtained geometric morphometric landmark data from the digitized images using programs of the tps package [41], which were subsequently analyzed with MorphoJ [42]. We used 15 homologous landmarks to recuperate detailed information on head shape and trophic morphology (see Supplementary file 2). We then performed a canonical variate (CV) analysis with species as the grouping criterion to assess interspecific shape differences. Shape change was then visualized using an outline shape approach

as implemented in MorphoJ [42]; ggplot2 [43] in R (R Development Core Team, 2008) was used to compile morphospace plots using species means for the first two CVs.

Utilizing the same landmark configuration used to recuperate head shape, we measured mean morphological distances between species expressed as procrustes distances, which inform about the distance between two landmark configurations after procrustes superimposition. This strategy was chosen as other measurements of morphological distance, e.g. Mahalanobis distances, are known to be less accurate in cases, such as ours, where the number of landmarks is high, whereas sample sizes per group (i.e. species in our case) are low [44]. Procrustes distances between species were then used to compute a morphological distance genealogy in PAUP* [45] that we then compared to a comprehensive molecular phylogeny based on nuclear and mitochondrial markers [46] using a Kishino-Hasegawa and a Shimodaira test as implemented in PAUP*. Note that procrustes distances were only calculated between species for which a sample size greater than one was available, resulting in a maximal overlap of 128 species between the molecular phylogeny and the morphological distance tree.

We further examined relative bite force (hereafter: 'bite force') as approximated by the lower jaw lever ratio, which is defined as the length of the in-lever divided by the length of the out-lever bone (see [47,48]). To this end, we measured the closing-in lever, the opening-in lever and out-lever (see [48] and figures therein) in the same 1125 x-ray images that were used for the collection of landmark data in the first place. Here, low jaw lever ratios are suggestive for the ability to quickly close the jaw albeit with low to moderate bite force, whereas high ratios are indicative for the ability to close the jaw slowly yet forcefully [47]. Consequently, low in-lever/out-lever ratios are typically

associated with species feeding on immobile prey, whereas high ratios are characteristic for specializations towards feeding on evasive prey [47].

As a proxy for feeding ecology, we used available data on ratios of the stable isotopes of Nitrogen (δ15N) and Carbon (δ13C) [20,23] for a total of 70 species. The ratio of the stable heavy isotope of Nitrogen is commonly used to estimate the position within the food web, while the stable heavy isotope of Carbon is used to estimate the position along a benthic to limnetic axis in lacustrine fish [49-51]. Furthermore, we obtained data on intestinal tract length from [23] that we size-corrected using standard length as size measurement.

Correlations between traits

All data was used for correlation analyses using the CAPER package [52] in R. We once used a classical linear model and then the phylogenetic generalized least squares (PGLS) approach to account for phylogenetic dependence of trait values, making use of the molecular phylogenetic hypothesis mentioned above [46]. Maximal overlap between phylogeny and trait data resulted in a dataset of 145 species for phylogenetically corrected analyses. P-values for both analyses were subsequently corrected for multiple comparisons using a Bonferroni correction. To further test the significance of the association between bite force and head shape we performed a distance based redundancy analysis. To this end, we used morphological distance between taxa as inferred from our morphological distance genealogy and the function capscale() in the R package VEGAN [53] followed by a permutation test using the function anova.cca().

Disparity through time

Both shape and bite force data was also subjected to a disparity through time (DTT) analysis following Harmon et al., 2003 [7]. To this end, we used GEIGER [54] in R and computed 1000 Brownian motion simulations of trait disparity over the phylogeny to compare it with our actual trait data. The morphological disparity index (MDI) was calculated over the first 90% of the relative timeline to correct for tip over-dispersion due to incomplete taxon sampling. We refrained from using real-time estimates for these analyses but instead used a relative timeline as there is no good time calibration available for Lake Tanganyika cichlids. *Tylochromis polylepis* and *Oreochromis tanganicae* were excluded from DTT analyses, as both species are not actually considered part of the AR due to their vast phylogenetic distance to the other taxa [20], thus reducing the sample size to 143 species.

Results

Bite force

Lower jaw lever ratio differed considerably between species and ranged, in the form of a continuum, from 0.365 (*Baileychromis centropomoides*) to 1.325 (*Petrochromis trewavasae*). No apparent clustering around specific lower jaw lever ratios was found although about three quarters of the species have values between 0.365 and 0.663 (maximal difference: 0.298), while the remaining quarter showed values between 0.681 and 1.325 (maximal difference: 0.644) (Fig. 1 A, Supplementary file 1).

Head shape variation

CV1 explained 30.1% of the total shape variation between species. Shape change according to positive CV1 values corresponded with the mouth being shifted downwards, forming a shorter snout; furthermore, the eye was shifted upwards coinciding with a generally deeper head shape (Fig. 2 A). For CV2, explaining 18.5% of the total shape variation, positive values corresponded with the mouth being oriented more anteriorly while the eye was placed more centrally resulting into a more slender head shape. Positive CV3 values, explaining another 12.0% of shape variation, describe a more dorsally oriented mouth position, a conspicuously concave front, and - again - a generally deeper head shape.

A morphospace plot on the basis of mean values per species of the first two CVs (Fig. 2 B) revealed large areas of overlap between tribes, particularly between Lamprologini, Ectodini and Limnochromini. However, several tribes also expand the morphospace in unique directions, e.g. the Tropheini that feature some species with conspicuously robust head shapes (highly positive CV1 values) or the Cyprichromini

that feature particularly anterio-dorsaly oriented and elongated mouth morphologies (negative CV1 and positive CV2 values).

The clustering of species according to morphological distances pertaining head shape variation (Fig. 1 A) indicated a varying degree of phylogenetic constraint on head shape diversity between tribes: while the members of some tribes (e.g. Bathybatini and Cyprichromini) clustered together, other tribes (e.g. Tropheini, Perissodini) showed a scattered distribution across the genealogy. Members of the two largest tribes (Lamprologini, Ectodini) showed a somewhat intermediate distribution with multiple species-clusters appearing at different position within the tree. When compared to the phylogeny based on molecular sequences (Fig. 1 B), both the Kishino-Hasegawa and the Shimodaira test reported highly significant differences ($p < 0.0001$ for both tests), further emphasizing the weak constraint of phylogeny on head shape evolution.

Correlational analyses

Bite force correlated positively with CV1 of head shape according to both PGLS analyses and the linear model, and both traits also correlated positively with intestinal tract length and δ13C values while correlating negatively with δ15N values in both analyses (Tables 1 and 2). CV2 and CV3 of head shape, on the other hand, did not show any significant correlations with bite force, intestinal tract length or stable isotope values. Bite force also showed to be significantly associated with morphological distance between species as inferred from our morphological distance genealogy ($F=56.8$, $p=0.005$).

DTT

Disparity through time analyses revealed patterns consistent with the early burst hypothesis for bite force as well as for head shape CV1 values (Fig. 4). Both traits showed an initial drop in average subclade disparity followed by average subclade disparity remaining substantially lower than Brownian Motion simulations for a prolonged timespan before again raising above the average. Congruently, both traits also exhibited negative MDI values, with MDI for bite force (-0.0640) being slightly more negative than for CV1 of head shape (MDI = -0.0607). Average subclade disparity for bite force rises above simulated values just before 0.8 in relative time, depicts two conspicuous peaks and then drops again. Disparity for CV1 raises around 0.5 in relative time, reaches a plateau-like phase until around 0.8 in relative time and then drops again without showing further peaks towards present time. CV2 and CV3 of head shape (see Supplementary file 3) both showed no evidence for an early burst. Congruently, MDI statistics for both traits remained positive (CV2 = 0.0887, CV3 = 0.1341).

Discussion

In this study, we assess the evolution of trophic morphology in the course of a massive cichlid AR on the basis of one of the largest data sets available to date. We test for correlations between phenotype and environment as an inert feature of AR [2], evidence for early bursts in morphological evolution, patterns of convergence, and a progression of diversification in stages, in which divergence in trophic morphology is predicted to be the second stage after macro-habitat diversification.

Trophic morphology and correlations with ecology

The morphometric examination of head shape in 157 Tanganyikan cichlid species by means of a CVA revealed that CV1 mainly discriminates between short and deep head morphologies with ventrally oriented, large mouths and elongated head morphologies with anteriorly oriented mouths. In fish, long and shallow snouts are typically associated with efficient preying on elusive food items using ram feeding, while short and robust snouts are commonly related to feeding on immobile prey using suction feeding [55-57]. That, in our case, positive CV1 values coincide with the downward orientation of the mouth suggests an additional interpretation of the feeding mode employed by species with short and robust mouths: biting or picking of food items. This partitioning between deep-bodied species featuring ventrally oriented mouths and species featuring elongated (head) morphologies with terminal mouths seems to be pervasive in fish and has been observed in African and Neotropical cichlids [15,40] as well as in other fish [58,59].

Importantly, head shape strongly correlated with bite force, highlighting a connection between deeper and shorter heads and a strong yet slow bite, which is congruent with a specialization towards biting, algae grazing and picking. A correlation between head

shape and bite force is further highlighted by the observation that species that cluster together in the genealogy based on procrustes distances of head shape often show similar values for bite force (Fig. 1 A), irrespective of their phylogenetic background (see also below). This association is also evident in a distance based redundancy analysis. Both head shape and bite force also correlated with δ13C and δ15N stable isotope ratios, as well as with intestinal tract length, suggesting that species with deep head shapes that exhibit strong but slow bites tend to feature (i) a benthic foraging behavior, (ii) rank low in the food web, and (iii) feed on rather nutrient poor food items. On the other hand, species with elongated (i.e. narrower) heads appear to be able to close their jaw at a high velocity and tend to exhibit (i) a limnetic foraging behavior, (ii) stand high in the food web and, (iii) feed primarily on nutrient rich food items.

Interestingly, the correlation of both head shape and bite force appears to be stronger with δ13C stable isotope values than with δ15N. This is somewhat surprising, given that, in fish, head shape is expected to more strongly correlate with a species' position in the food web (approximated by δ15N) than with habitat choice along a benthic-limnetic axis (approximated by δ13C) [18,38,60]. In contrast, our data suggest that head shape is primarily influenced by the feeding strategy, e.g. ram feeding or biting/picking, and only to a lesser extent by the trophic level of ingested food items. Furthermore, head shape and bite force mainly separate species according to a trade-off between fast but weak and slow but forceful closing of the jaw, and thus between the ability to effectively feed on stationary *versus* evasive prey. Accordingly, differences in head shape and bite force are most pronounced between species feeding in the benthic macro-habitat that provides a variety of stationary food items such as algae and 'aufwuchs' but also snails, mussels and fish eggs, and species feeding in the

limnetic macro-habitat that is dominated by evasive food items such as zooplankton and fish.

Early bursts, convergence and the stages model

Our DTT analyses provide strong support for an early burst in trophic morphology (head shape and bite force) in the AR of cichlids from Lake Tanganyika (Fig. 3). An early burst in these two feeding-related traits points towards a scenario in which an early divergence took place between species specialized for feeding on immobile prey exhibiting biting or picking behavior relying on strong but slow bites and species specialized on ram feeding on evasive prey relying on a fast closing of the jaw.

Both traits, head shape and bite force, correlated with δ13C values. Early bursts in these traits could thus be considered to coincide with an early divergence according to benthic *versus* limnetic habitat use in Lake Tanganyika cichlids. DTT analyses of stable isotope values, however, did not reveal signs of such an early divergence [20], nor is an early divergence in habitat use visible within the AR [46]. On the other hand, trophic-related traits seem to have diverged earlier than habitat related traits [23], although no definite hint for an early burst in trophic morphology has been found before. Taken together, the Lake Tanganyikan cichlid assemblage seems to exhibit a scenario in which trophic morphology diverged before habitat preference and that divergence in trophic morphology is more related to *how* a species feeds than to *what* it feeds upon. Similar patterns of early divergence according to trophic morphology and body depth i.e. divergence according to different feeding strategies have been found in South American geophagine cichlids [14,15], and in Antarctic notothenioids [13], also discriminating between elongated and more robust head shapes specialized for feeding on evasive or immobile prey, respectively. Furthermore, divergence according

to head and jaw length was also found in an early-stage adaptive divergence of two cichlid ecomorphs in a Tanzanian crater lake [19].

An early burst in trophic morphology followed by divergence according to habitat-related traits, as observed here, is not fully in agreement with the original 'radiation in stages' hypothesis [9] that states that divergence in ARs should proceed along the axes of habitat choice, foraging morphology, and signaling, in that explicit order. A less strict interpretation of the 'radiation in stages' hypothesis, with a reversed order of the first two stages, would nevertheless be compatible with our findings. Such a "re-ordering" of stages has previously been suggested on the basis of other trophic-related traits (and a much smaller dataset) in Tanganyika cichlids [23], as well as in other ARs, e.g. Old World leaf warblers [22] and early actinopterygians [61].

Our genealogy based on morphological distances (Fig. 1 A) features several instances of distantly related species that cluster together, while many closely related species are well separated. This suggests – together with the observations that this genealogy is significantly different from a molecular phylogeny, and that the different cichlid tribes largely overlap in morphospace (Fig. 2 B) – that there is no strong phylogenetic constraint on head shape and bite force. Instead, similar head shapes and bite forces appear to have evolved repeatedly and convergently in the AR of cichlids in Lake Tanganyika.

Convergence in trophic morphology has been reported in cichlids between the East African Great Lakes [28] and between Neotropical cichlid species [15,62]. Also, patterns of convergence have already been reported for Lake Tanganyika cichlids [20], although for different traits than presented in this study. A recent study including cichlids from Lakes Malawi and Tanganyika recovered patterns of convergence in feeding modes

between these lakes [63]. The study distinguished between two feeding strategies: 'suction feeders' that rely on a rapid expansion of the mouth cavity to pull prey items into the mouth and 'biters' that require direct contact between the fish's jaws and the prey item. While the first strategy presupposes the ability to move the jaws rapidly [64], the second strategy may be exhibited by both species that rely on fast closing of the jaws, i.e. ram feeders and species that rely on a slow but forceful bite, e.g. algae picking species. Albeit using a substantially smaller species count than we use here, the study recovered multiple independent transitions between feeding modes within the lakes.

Although convergence seems to have recurrently arisen in Lake Tanganyika, we also find groups of closely related species clustering together in our morphological genealogy, which is particularly evident for Bathybatini and Cyprichromini or *Xenotilapia* and *Ophthalmotilapia*, indicating that some degree of phylogenetic constraint on head shape/feeding strategy is nevertheless present in some groups. This mixed pattern of convergence and constraint together with the occurrence of 'early bursts' leads to the conclusion that the AR of Lake Tanganyika cichlids proceeded in a pattern of early divergence in trophic morphology that was later followed by convergence between members of different groups.

This is particularly interesting given that the closely related AR of cichlid fish in the neighboring Lake Malawi seems to have followed a sequence of habitat related traits diverging first and trophic related traits diverging subsequently [9,10,21]. What caused these discrepancies in temporal sequence between these two East African Great Lakes remains to be explored. Potentially, genetic constraints in the quasi-monophyletic Lake Malawian cichlid flock [65,66] could have hampered an early divergence in trophic

morphology and food acquisition strategies in Lake Malawi or, not being mutually exclusive, the shallow waters of early Lake Tanganyika [67] did not provide sufficiently different habitats for an early divergence according to habitat use.

Conclusion

We find a continuum of head shapes and correlating bite force estimates attributable to specializations for feeding on elusive *versus* immobile prey in Lake Tanganyika cichlids. Both traits show to be correlated with the position along the bentho-limnetic axis and with traits indicative for the trophic level of a species. Generally, species exhibiting a benthic foraging behavior and/or feeding on nutrient poor food items exhibit deep head shapes and elevated bite force while limnetically feeding species exhibit more narrow head shapes and weak but fast bites. We uncover multiple instances of convergence in head shape and bite force between distantly related species while concurrently these traits show to be conserved in other groups. Taken together, it seems that Lake Tanganyika cichlids underwent early divergence in trophic morphology followed by convergence. Divergence according to feeding strategies likely depicts the first axis of divergence in the AR of Lake Tanganyika cichlids, a scenario that deviates from the proposed sequence for the related AR of Lake Malawi.

Ethics

All experiments have been performed under permits issued by the cantonal veterinary office in Basel.

Data accessibility

The datasets supporting this article have been uploaded as part of the supplementary material.

Competing interests

We have no competing interests.

Authors' contributions

MC participated in conceiving of the study, participated in data analysis and drafted the manuscript. FM conducted the bite force and geometric morphometric measurements and helped analyzing the data. HB collected field data. WS participated in conceiving of the study, coordinated the study and helped drafting the manuscript. All authors gave final approval for publication.

Acknowledgements

X-ray scanning was supported by the group of Michaela Kneissel, Global Head Musculoskeletal Disease Area, Novartis Institutes for BioMedical Research, Basel, Switzerland. The authors would like to thank Leonie Kneipp and Helena Römer for help with data acquisition, Benjamin Koechlin for assistance with digitizing x-ray images, and Jobst Pfänder for valuable suggestions on bite force calculations.

Funding

This study was supported by grants from the Swiss National Science Foundation (SNF) and the European Research Council (ERC; CoG “CICHLID~X”).

References

1 Simpson, G. G. The major features of evolution. *New York, N.Y., Columbia University Press* (1953).

2 Schluter, D. *The ecology of adaptive radiation*. (Oxford University Press, 2000).

3 Gavrilets, S. & Losos, J. B. Adaptive radiation: contrasting theory with data. *Science* **323**, 732-737, doi:10.1126/science.1157966 (2009).

4 Glor, R. E. Phylogenetic Insights on Adaptive Radiation. *Annual Review of Ecology, Evolution, and Systematics, Vol 41* **41**, 251-270, doi:DOI 10.1146/annurev.ecolsys.39.110707.173447 (2010).

5 Berner, D. & Salzburger, W. The genomics of organismal diversification illuminated by adaptive radiations. *Trends Genet* **31**, 491-499, doi:10.1016/j.tig.2015.07.002 (2015).

6 Yoder, J. B. *et al.* Ecological opportunity and the origin of adaptive radiations. *J Evol Biol* **23**, 1581-1596, doi:10.1111/j.1420-9101.2010.02029.x (2010).

7 Harmon, L. J., Schulte, J. A., 2nd, Larson, A. & Losos, J. B. Tempo and mode of evolutionary radiation in iguanian lizards. *Science* **301**, 961-964, doi:10.1126/science.1084786 (2003).

8 McPeek, M. A. The ecological dynamics of clade diversification and community assembly. *Am Nat* **172**, E270-284, doi:10.1086/593137 (2008).

9 Streelman, J. T. & Danley, P. D. The stages of vertebrate evolutionary radiation. *Trends in Ecology & Evolution* **18**, 126-131, doi:10.1016/S0169-5347(02)00036-8 (2003).

10 Danley, P. D. & Kocher, T. D. Speciation in rapidly diverging systems: lessons from Lake Malawi. *Mol Ecol* **10**, 1075-1086, doi:10.1046/j.1365-294X.2001.01283.x (2001).

11 Harmon, L. J. *et al.* Early bursts of body size and shape evolution are rare in comparative data. *Evolution* **64**, 2385-2396, doi:10.1111/j.1558-5646.2010.01025.x (2010).

12 Slater, G. J., Price, S. A., Santini, F. & Alfaro, M. E. Diversity versus disparity and the radiation of modern cetaceans. *Proc Biol Sci* **277**, 3097-3104, doi:10.1098/rspb.2010.0408 (2010).

13 Colombo, M., Damerau, M., Hanel, R., Salzburger, W. & Matschiner, M. Diversity and disparity through time in the adaptive radiation of Antarctic notothenioid fishes. *J Evol Biol* **28**, 376-394, doi:10.1111/jeb.12570 (2015).

14 Lopez-Fernandez, H., Arbour, J. H., Winemiller, K. O. & Honeycutt, R. L. Testing for ancient adaptive radiations in neotropical cichlid fishes. *Evolution* **67**, 1321-1337, doi:10.1111/evo.12038 (2013).

15 Arbour, J. H. & Lopez-Fernandez, H. Ecological variation in South American geophagine cichlids arose during an early burst of adaptive morphological and functional evolution. *Proc Biol Sci* **280**, 20130849, doi:10.1098/rspb.2013.0849 (2013).

16 Gavrilets, S. & Vose, A. Dynamic patterns of adaptive radiation. *Proc Natl Acad Sci U S A* **102**, 18040-18045, doi:10.1073/pnas.0506330102 (2005).

17 Nagel, L. & Schluter, D. Body size, natural selection, and speciation in sticklebacks. *Evolution* **52**, 209-218, doi:Doi 10.2307/2410936 (1998).
18 Barluenga, M., Stolting, K. N., Salzburger, W., Muschick, M. & Meyer, A. Sympatric speciation in Nicaraguan crater lake cichlid fish. *Nature* **439**, 719-723, doi:10.1038/nature04325 (2006).
19 Malinsky, M. *et al.* Genomic islands of speciation separate cichlid ecomorphs in an East African crater lake. *Science* **350**, 1493-1498, doi:10.1126/science.aac9927 (2015).
20 Muschick, M., Indermaur, A. & Salzburger, W. Convergent evolution within an adaptive radiation of cichlid fishes. *Curr Biol* **22**, 2362-2368, doi:10.1016/j.cub.2012.10.048 (2012).
21 Kocher, T. D. Adaptive evolution and explosive speciation: the cichlid fish model. *Nat Rev Genet* **5**, 288-298, doi:10.1038/nrg1316 (2004).
22 Richman, A. D. & Price, T. Evolution of ecological differences in the Old World leaf warblers. *Nature* **355**, 817-821, doi:10.1038/355817a0 (1992).
23 Muschick, M. *et al.* Testing the stages model in the adaptive radiation of cichlid fishes in East African Lake Tanganyika. *Proc Biol Sci* **281**, 1-10, doi:10.1098/rspb.2014.0605 (2014).
24 Schluter, D. & Nagel, L. M. Parallel Speciation by Natural-Selection. *American Naturalist* **146**, 292-301, doi:Doi 10.1086/285799 (1995).
25 Rundle, H. D., Nagel, L., Wenrick Boughman, J. & Schluter, D. Natural selection and parallel speciation in sympatric sticklebacks. *Science* **287**, 306-308, doi:10.1126/science.287.5451.306 (2000).
26 Mahler, D. L., Ingram, T., Revell, L. J. & Losos, J. B. Exceptional convergence on the macroevolutionary landscape in island lizard radiations. *Science* **341**, 292-295, doi:10.1126/science.1232392 (2013).
27 Losos, J. B. Concordant evolution of locomotor behaviour, display rate and morphology in< i> Anolis</i> lizards. *Animal Behaviour* **39**, 879-890 (1990).
28 Kocher, T. D., Conroy, J. A., McKaye, K. R. & Stauffer, J. R. Similar morphologies of cichlid fish in Lakes Tanganyika and Malawi are due to convergence. *Mol Phylogenet Evol* **2**, 158-165, doi:10.1006/mpev.1993.1016 (1993).
29 Beuttell, K. & Losos, J. B. Ecological morphology of Caribbean anoles. *Herpetological Monographs* **13**, 1-28, doi:Doi 10.2307/1467059 (1999).
30 Berner, D., Grandchamp, A. C. & Hendry, A. P. Variable progress toward ecological speciation in parapatry: stickleback across eight lake-stream transitions. *Evolution* **63**, 1740-1753, doi:10.1111/j.1558-5646.2009.00665.x (2009).
31 Berner, D., Roesti, M., Hendry, A. P. & Salzburger, W. Constraints on speciation suggested by comparing lake-stream stickleback divergence across two continents. *Mol Ecol* **19**, 4963-4978, doi:10.1111/j.1365-294X.2010.04858.x (2010).
32 Herrel, A., Podos, J., Huber, S. K. & Hendry, A. P. Bite performance and morphology in a population of Darwin's finches: implications for the evolution of beak shape. *Functional Ecology* **19**, 43-48, doi:DOI 10.1111/j.0269-8463.2005.00923.x (2005).

33 Abzhanov, A., Protas, M., Grant, B. R., Grant, P. R. & Tabin, C. J. Bmp4 and morphological variation of beaks in Darwin's finches. *Science* **305**, 1462-1465, doi:10.1126/science.1098095 (2004).
34 Fryer, G. & Iles, T. D. *The cichlid fishes of the Great Lakes of Africa: their biology and evolution*. (Oliver and Boyd Edinburgh, 1972).
35 Hulsey, C. D. Function of a key morphological innovation: fusion of the cichlid pharyngeal jaw. *Proceedings of the Royal Society B-Biological Sciences* **273**, 669-675, doi:Doi 10.1098/Rspb.2005.3375 (2006).
36 Hulsey, C. D., Roberts, R. J., Lin, A. S., Guldberg, R. & Streelman, J. T. Convergence in a mechanically complex phenotype: detecting structural adaptations for crushing in cichlid fish. *Evolution* **62**, 1587-1599, doi:10.1111/j.1558-5646.2008.00384.x (2008).
37 Burress, E. D. Ecological diversification associated with the pharyngeal jaw diversity of Neotropical cichlid fishes. *J Anim Ecol* **85**, 302-313, doi:10.1111/1365-2656.12457 (2016).
38 Elmer, K. R., Kusche, H., Lehtonen, T. K. & Meyer, A. Local variation and parallel evolution: morphological and genetic diversity across a species complex of neotropical crater lake cichlid fishes. *Philos Trans R Soc Lond B Biol Sci* **365**, 1763-1782, doi:10.1098/rstb.2009.0271 (2010).
39 Klingenberg, C. P., Barluenga, M. & Meyer, A. Body shape variation in cichlid fishes of the Amphilophus citrinellus species complex. *Biological Journal of the Linnean Society* **80**, 397-408, doi:DOI 10.1046/j.1095-8312.2003.00246.x (2003).
40 Cooper, W. J. *et al.* Bentho-pelagic divergence of cichlid feeding architecture was prodigious and consistent during multiple adaptive radiations within African rift-lakes. *PLoS One* **5**, e9551, doi:10.1371/journal.pone.0009551 (2010).
41 tpsDig, digitize landmarks and outlines v. 2.15 (State University of New York, Stony Brook, New York., Department of Ecology and Evolution, 2010).
42 Klingenberg, C. P. MorphoJ: an integrated software package for geometric morphometrics. *Mol Ecol Resour* **11**, 353-357, doi:10.1111/j.1755-0998.2010.02924.x (2011).
43 Wickham, H. *ggplot2: elegant graphics for data analysis*. (Springer New York, 2009).
44 De Maesschalck, R., Jouan-Rimbaud, D. & Massart, D. L. The Mahalanobis distance. *Chemometrics and Intelligent Laboratory Systems* **50**, 1-18, doi:10.1016/s0169-7439(99)00047-7 (2000).
45 PAUP*. Phylogenetic Analysis Using Parsimony (*and Other Methods) v. 4.0 (Sinauer Associates, Sunderland, Massachusetts, 2003).
46 Colombo, M., Indermaur, A., Meyer, B. S. & Salzburger, W. Habitat use and its implications to functional morphology: niche partitioning and the evolution of locomotory morphology in Lake Tanganyikan cichlids (Perciformes: Cichlidae). *Biological Journal of the Linnean Society*, n/a-n/a, doi:10.1111/bij.12754 (2016).
47 Wainwright, P. C. & Richard, B. A. Predicting Patterns of Prey Use from Morphology of Fishes. *Environmental Biology of Fishes* **44**, 97-113, doi:Doi 10.1007/Bf00005909 (1995).

48 Pfaender, J., Miesen, F. W., Hadiaty, R. K. & Herder, F. Adaptive speciation and sexual dimorphism contribute to diversity in form and function in the adaptive radiation of Lake Matano's sympatric roundfin sailfin silversides. *J Evol Biol* **24**, 2329-2345, doi:10.1111/j.1420-9101.2011.02357.x (2011).
49 DeNiro, M. J. & Epstein, S. Influence of diet on the distribution of carbon isotopes in animals. *Geochimica et Cosmochimica Acta* **42**, 495-506, doi:10.1016/0016-7037(78)90199-0 (1978).
50 Hobson, K. A., Piatt, J. F. & Pitocchelli, J. Using Stable Isotopes to Determine Seabird Trophic Relationships. *Journal of Animal Ecology* **63**, 786-798, doi:Doi 10.2307/5256 (1994).
51 Post, D. M. Using stable isotopes to estimate trophic position: Models, methods, and assumptions. *Ecology* **83**, 703-718, doi:Doi 10.2307/3071875 (2002).
52 Orme, D. The caper package: comparative analysis of phylogenetics and evolution in R. (2012).
53 vegan: Community Ecology Package (2013).
54 Harmon, L. J., Weir, J. T., Brock, C. D., Glor, R. E. & Challenger, W. GEIGER: investigating evolutionary radiations. *Bioinformatics* **24**, 129-131, doi:10.1093/bioinformatics/btm538 (2008).
55 Webb, P. W. Body and Fin Form and Strike Tactics of Four Teleost Predators Attacking Fathead Minnow (Pimephales promelas) Prey. *Canadian Journal of Fisheries and Aquatic Sciences* **41**, 157-165, doi:10.1139/f84-016 (1984).
56 Norton, S. F. & Brainerd, E. L. Convergence in the Feeding Mechanics of Ecomorphologically Similar Species in the Centrarchidae and Cichlidae. *Journal of Experimental Biology* **176**, 11-29 (1993).
57 Huskey, S. H. & Turingan, R. G. Variation in prey-resource utilization and oral jaw gape between two populations of largemouth bass, Micropterus salmoides. *Environmental Biology of Fishes* **61**, 185-194, doi:Doi 10.1023/A:1011095526939 (2001).
58 Sandlund, O. T. *et al.* The Arctic Charr Salvelinus alpinus in Thingvallavatn. *Oikos* **64**, 305, doi:10.2307/3545056 (1992).
59 de Graaf, M., Dejen, E., Osse, J. W. M. & Sibbing, F. A. Adaptive radiation of Lake Tana's (Ethiopia) Labeobarbus species flock (Pisces, Cyprinidae). *Marine and Freshwater …* (2008).
60 Hulsey, C. D., Roberts, R. J., Loh, Y. H., Rupp, M. F. & Streelman, J. T. Lake Malawi cichlid evolution along a benthic/limnetic axis. *Ecol Evol* **3**, 2262-2272, doi:10.1002/ece3.633 (2013).
61 Sallan, L. C. & Friedman, M. Heads or tails: staged diversification in vertebrate evolutionary radiations. *Proc Biol Sci* **279**, 2025-2032, doi:10.1098/rspb.2011.2454 (2012).
62 Lopez-Fernandez, H. *et al.* Morphology and efficiency of a specialized foraging behavior, sediment sifting, in neotropical cichlid fishes. *PLoS One* **9**, e89832, doi:10.1371/journal.pone.0089832 (2014).
63 McGee, M. D. *et al.* in *Replicated divergence in cichlid radiations mirrors a major vertebrate innovation.*1822 edn 20151413 (The Royal Society).
64 Wainwright, P. *et al.* Suction feeding mechanics, performance, and diversity in fishes. *Integr Comp Biol* **47**, 96-106, doi:10.1093/icb/icm032 (2007).

65 Moran, P., Kornfield, I. & Reinthal, P. N. Molecular Systematics and Radiation of the Haplochromine Cichlids (Teleostei, Perciformes) of Lake Malawi. *Copeia* **1994**, 274-288, doi:10.2307/1446977 (1994).
66 Joyce, D. A. *et al.* Repeated colonization and hybridization in Lake Malawi cichlids. *Curr Biol* **21**, R108-109, doi:10.1016/j.cub.2010.11.029 (2011).
67 Salzburger, W., Van Bocxlaer, B. & Cohen, A. S. Ecology and Evolution of the African Great Lakes and Their Faunas. *Annual Review of Ecology, Evolution, and Systematics, Vol 45* **45**, 519-+, doi:10.1146/annurev-ecolsys-120213-091804 (2014).

1.3.2
Figures & Tables

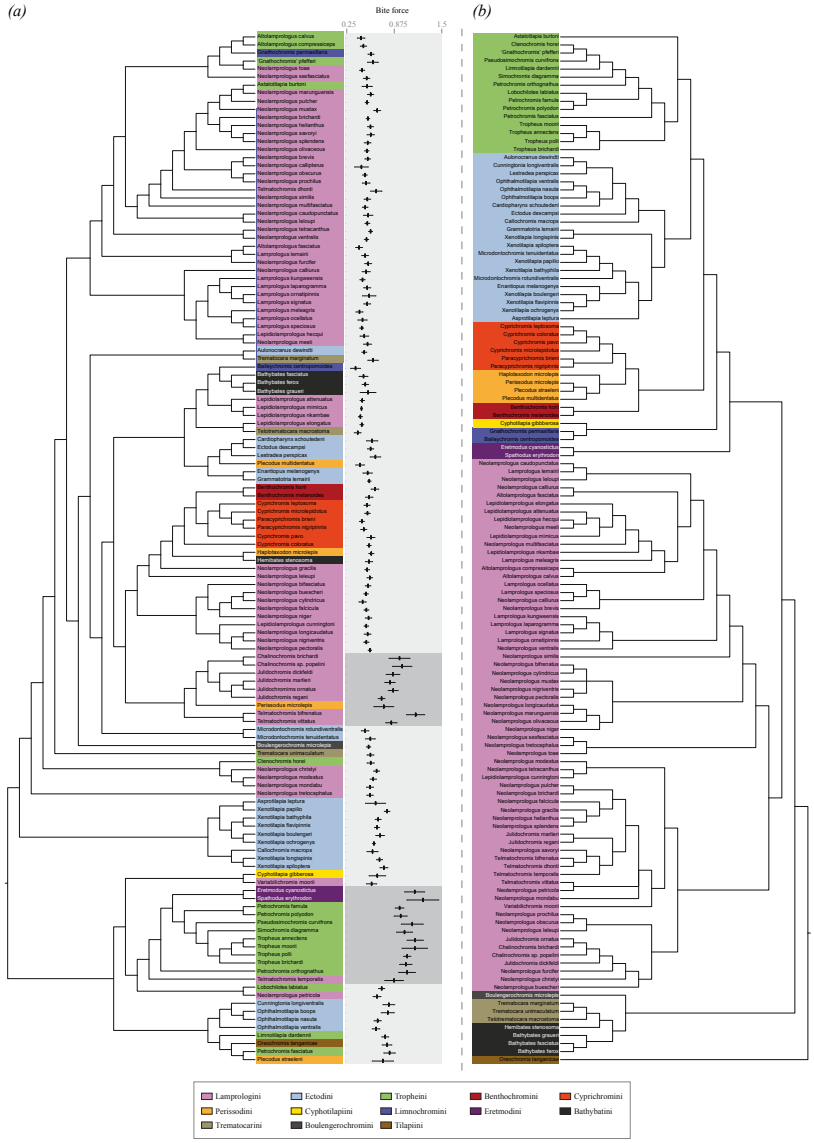

Figure 1. Genealogy based on morphological distances in head shape (*a*) *versus* a molecular phylogeny based on mitochondrial (ND2) and nuclear DNA sequences (42 genes; see [46]) (*b*). Both genealogies include the same 128 Lake Tanganyikan cichlid species. Species are color coded according to tribes; mean bite force estimates per species are depicted in (*a*) including standard deviations. Two clusters of species that show consistently high bite force estimates are highlighted in dark grey.

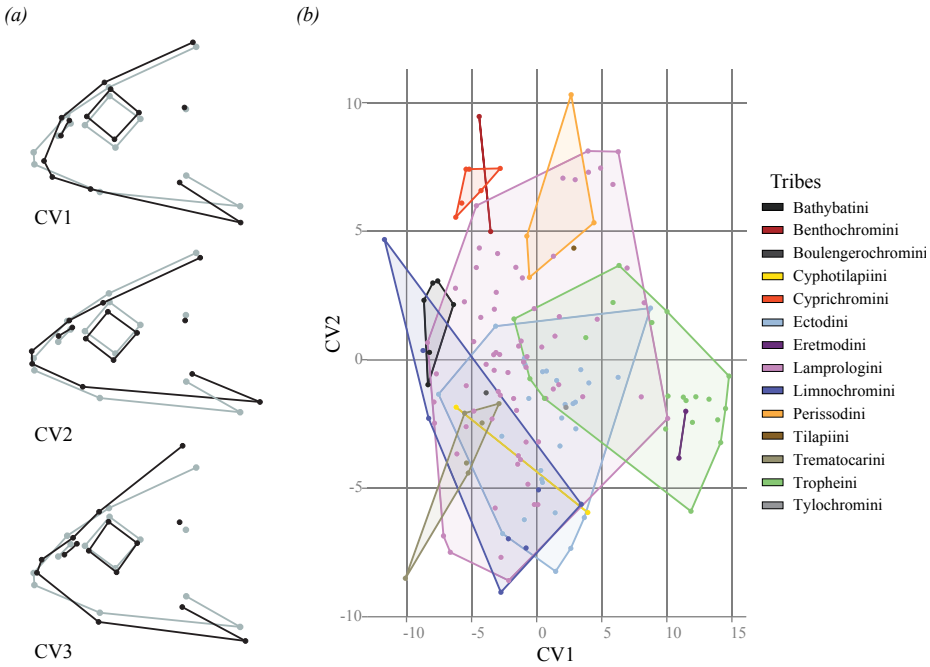

Figure 2. Head shape in Lake Tanganyika cichlids by means of a CVA. (a) Change of head shape according to CV axis 1 to 3. The black lines indicate shape change in the direction of positive values in relation to neutral CV values, which are depicted in grey. (b) Morphospace occupation according to the first two CVs. Species mean values are depicted for all 157 species analyzed and color-coded according to tribes. There appears to be large areas of overlap between different tribes, although certain areas of the morphospace are occupied by members of only one tribe.

CV1 accounted for 30.1% of total variation in the dataset, whereas CV2 accounted for 18.5% and CV3 for 12%.

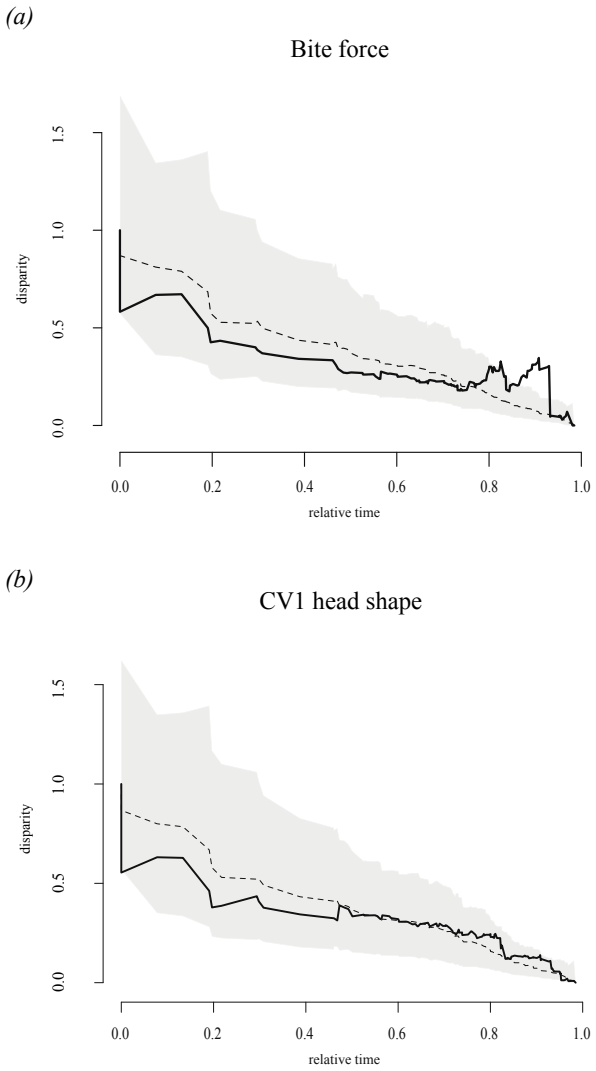

Figure 3. Disparity-through time (DTT) plots of bite force (*a*) and CV1 of head shape (*b*). The DTT plots show the average subclade disparity of the empirical data through time (black line), as well as the 95% confidence interval of 1000 Brownian motion simulations (grey area) and the mean DTT from the simulated datasets (dashed line). Bite force and CV1 of head shape both show patterns consistent with an early burst in morphological diversification. Accordingly, MDI statistics for both traits remained negative (bite force: -0.0640, CV1 of head shape: -0.0607).

Table 1. Correlation analyses of head shape and bite force according to a classic linear model.

CV1 head shape

	t-value	adjusted p~	R^2	$N_{species}$
Bite force	23.27	**0.000**	0.78	157
Intestinal tract length	7.38	**0.000**	0.51	54
δ15N	-5.89	**0.000**	0.34	70
δ13C	9.48	**0.000**	0.57	70

CV2 head shape

	t-value	adjusted p~	R2	Nspecies
Bite force	1.03	1	0.01	157
Intestinal tract length	-0.95	1	0.02	54
δ15N	-0.39	1	0.00	70
δ13C	0.35	1	0.00	70

CV3 head shape

	t-value	adjusted p~	R^2	$N_{species}$
Bite force	0.12	1	0.00	157
Intestinal tract length	2.12	0.155	0.08	54
δ15N	-0.76	1	0.01	70
δ13C	0.43	1	0.00	70

Bite force

	t-value	adjusted p~	R^2	$N_{species}$
CV1 head shape	23.27	**0.000**	0.78	157
CV2 head shape	1.03	1	0.01	157
CV3 head shape	0.12	1	0.00	157
Intestinal tract length	6.09	**0.000**	0.42	54
δ15N	-5.43	**0.000**	0.30	70
δ13C	9.13	**0.000**	0.55	70

Table 2. Correlation analysis of head shape and bite force corrected for phylogenetic dependence of trait values.

CV1 head shape

	t-value	adjusted p~	R^2	lambda	$N_{species}$
Bite force	16.02	**0.00**	0.64	0.83	145
Intestinal tract length	5.65	**0.00**	0.38	0.69	54
δ15N	-4.51	**0.00**	0.24	0.72	66
δ13C	9.32	**0.00**	0.58	0.00	66

CV2 head shape

	t-value	adjusted p~	R^2	lambda	$N_{species}$
Bite force	0.28	1	0.00	0.95	145
Intestinal tract length	-0.64	1	0.01	0.95	54
δ15N	-0.81	1	0.01	0.93	66
δ13C	-0.45	1	0.00	0.93	66

CV3 head shape

	t-value	adjusted p~	R^2	lambda	$N_{species}$
Bite force	-2.00	0.19	0.03	0.96	145
Intestinal tract length	1.38	0.69	0.04	0.93	54
δ15N	0.29	1	0.00	0.93	66
δ13C	-1.60	0.46	0.04	0.94	66

Bite force

	t-value	adjusted p~	R^2	lambda	$N_{species}$
CV1 head shape	16.68	**0.00**	0.66	0.74	145
CV2 head shape	0.17	1	0.00	0.93	145
CV3 head shape	-1.93	0.33	0.03	0.93	145
Intestinal tract length	4.89	**0.00**	0.31	0.83	54
δ15N	-4.48	**0.00**	0.24	0.72	66
δ13C	7.88	**0.00**	0.49	0.46	66

1.3.3
Supporting information

Supplementary file 1

Mean species values and sample sizes for bite force and geometric morphometric measurements per species.

Species	Tribe	bite force ratio	StdDev bite force	Samplesize bite force	CV1	CV2	CV3	Samplesize morphometrics
Bathybates fasciatus	Bathybatini	0.47	0.058	10	-7.981	2.983	-0.970	10
Bathybates ferox	Bathybatini	0.495	0.042	5	-8.353	-0.973	-2.147	4
Bathybates graueri	Bathybatini	0.53	0.104	10	-8.230	0.285	-1.636	10
Bathybates leo	Bathybatini	0.506	NA	1	-8.660	2.312	-1.160	1
Bathybates vittatus	Bathybatini	0.609	NA	1	-7.604	3.064	-3.140	1
Hemibates stenosoma	Bathybatini	0.542	0.047	6	-6.387	2.144	3.089	6
Benthochromis horii	Benthochromini	0.62	0.05	10	-4.414	9.460	2.674	10
Benthochromis melanoides	Benthochromini	0.546	0.049	10	-3.535	4.984	5.220	10
Boulengerochromis microlepis	Boulengerochromii	0.537	0.028	10	-3.881	-1.287	-0.390	10
Ctenochromis benthicola	Cyphotilapiini	0.551	NA	1	-6.185	-1.849	-0.851	1
Cyphotilapia gibberosa	Cyphotilapiini	0.653	0.109	7	3.924	-5.944	3.810	7
Cyprichromis coloratus	Cyprichromini	0.544	0.028	10	-2.799	7.440	3.404	10
Cyprichromis leptosoma	Cyprichromini	0.517	0.04	10	-4.276	6.577	1.386	10
Cyprichromis microlepidotus	Cyprichromini	0.523	0.036	10	-5.424	7.410	-0.122	10
Cyprichromis pavo	Cyprichromini	0.568	0.052	10	-5.187	7.409	1.578	10
Paracyprichromis brieni	Cyprichromini	0.449	0.032	10	-5.755	6.091	-0.244	10
Paracyprichromis nigripinnis	Cyprichromini	0.474	0.04	6	-6.218	5.541	0.206	6
Asprotilapia leptura	Ectodini	0.629	0.132	10	8.748	2.007	-8.094	10
Aulonocranus dewindti	Ectodini	0.481	0.032	10	-2.679	-2.977	2.644	10
Callochromis macrops	Ectodini	0.589	0.073	8	0.387	-4.649	-3.126	8
Cardiopharynx schoutedeni	Ectodini	0.584	0.074	4	0.454	-0.467	1.444	4
Cunningtonia longiventralis	Ectodini	0.804	0.077	10	3.390	-0.388	2.531	10
Cyathopharynx foae	Ectodini	0.64	0.081	4	2.186	-1.739	2.366	4
Cyathopharynx furcifer	Ectodini	0.495	NA	1	1.535	-0.807	3.409	1
Ectodus descampsii	Ectodini	0.563	0.04	10	-0.943	0.056	-0.983	10
Enantiopus melanogenys	Ectodini	0.524	0.061	10	-7.537	-1.345	-2.573	10
Grammatotria lemairii	Ectodini	0.547	0.023	9	-3.152	1.303	-2.010	9
Lestradea perspicax	Ectodini	0.627	0.069	4	0.754	-0.443	-1.927	4
Microdontochromis rotundiventralis	Ectodini	0.491	0.05	14	-0.605	-1.508	-0.342	14
Microdontochromis tenuidentatus	Ectodini	0.561	0.065	10	-0.889	-0.198	-0.531	10
Ophthalmotilapia boops	Ectodini	0.789	0.086	5	6.259	-0.686	0.622	5
Ophthalmotilapia heterodonta	Ectodini	0.572	NA	1	1.922	-2.269	2.805	1
Ophthalmotilapia nasuta	Ectodini	0.656	0.047	9	4.007	-0.903	2.141	9
Ophthalmotilapia ventralis	Ectodini	0.635	0.051	10	2.798	-1.708	1.736	10
Xenotilapia bathyphila	Ectodini	0.663	0.039	10	0.318	-4.309	-4.565	10
Xenotilapia boulengeri	Ectodini	0.689	0.056	5	1.422	-5.955	-5.643	5
Xenotilapia caudafasciata	Ectodini	0.584	NA	1	-2.618	-6.766	-4.245	1
Xenotilapia flavipinnis	Ectodini	0.648	0.033	10	0.449	-4.776	-5.173	10
Xenotilapia longispinis	Ectodini	0.681	0.039	3	1.790	-3.357	-2.561	3

Xenotilapia nigrolabiata	Ectodini	0.693	NA	1	3.663	-6.139	-6.315	1
Xenotilapia ochrogenys	Ectodini	0.608	0.02	3	-0.949	-6.223	-6.935	3
Xenotilapia ornatipinnis	Ectodini	0.609	0.075	7	2.620	-7.340	-5.741	7
Xenotilapia papilio	Ectodini	0.781	0.037	10	2.976	-1.653	-5.358	10
Xenotilapia sima	Ectodini	0.645	NA	1	1.458	-8.235	-9.572	1
Xenotilapia spiloptera	Ectodini	0.739	0.053	10	3.005	-2.687	-2.623	10
Eretmodus cyanostictus	Eretmodini	1.143	0.131	10	10.928	-3.826	-0.025	10
Spathodus erythrodon	Eretmodini	1.251	0.21	10	11.453	-2.007	-1.277	10
Altolamprologus calvus	Lamprologini	0.439	0.051	10	-7.159	-6.854	4.406	10
Altolamprologus compressiceps	Lamprologini	0.469	0.041	10	-6.634	-7.491	5.411	10
Altolamprologus fasciatus	Lamprologini	0.412	0.045	10	-7.888	-1.646	-2.113	10
Chalinochromis brichardi	Lamprologini	0.944	0.138	10	5.857	6.817	-3.127	10
Chalinochromis sp. popelini	Lamprologini	0.98	0.127	8	4.910	7.454	-4.528	8
Julidochromis dickfeldi	Lamprologini	0.858	0.09	10	3.980	7.292	-4.636	10
Julidochromis marlieri	Lamprologini	0.819	0.068	7	2.959	7.003	-5.465	7
Julidochromis ornatus	Lamprologini	0.86	0.065	10	3.947	8.117	-5.244	10
Julidochromis regani	Lamprologini	0.708	0.044	10	2.015	7.061	-5.307	10
Julidochromis sp. bifrenatus	Lamprologini	0.943	0.108	5	6.267	8.092	-4.333	5
Lamprologus callipterus	Lamprologini	0.505	0.053	10	-1.546	-1.973	-0.954	10
Lamprologus kungweensis	Lamprologini	0.457	0.034	6	0.142	-3.196	-1.815	6
Lamprologus laparogramma	Lamprologini	0.519	0.046	8	-1.458	-4.067	-1.983	8
Lamprologus lemairii	Lamprologini	0.491	0.044	10	-6.131	-3.665	-2.222	10
Lamprologus meleagris	Lamprologini	0.417	0.047	10	-3.186	-5.770	-1.881	10
Lamprologus ocellatus	Lamprologini	0.457	0.061	10	-2.151	-8.590	-0.904	10
Lamprologus ornatipinnis	Lamprologini	0.545	0.089	10	0.093	-5.638	-2.327	10
Lamprologus signatus	Lamprologini	0.519	0.045	6	-0.675	-4.844	-2.216	6
Lamprologus speciosus	Lamprologini	0.446	0.025	10	-2.743	-7.688	-0.808	10
Lepidiolamprologus attenuatus	Lamprologini	0.454	0.029	10	-4.839	0.704	-2.420	10
Lepidiolamprologus cunningtoni	Lamprologini	0.508	0.029	10	-3.104	2.620	-2.060	10
Lepidiolamprologus elongatus	Lamprologini	0.448	0.025	10	-5.411	-1.012	-2.174	10
Lepidiolamprologus hecqui	Lamprologini	0.481	0.056	10	-1.240	-3.887	-1.155	10
Lepidiolamprologus mimicus	Lamprologini	0.444	0.012	2	-7.706	-0.551	-2.662	2
Lepidiolamprologus nkambae	Lamprologini	0.43	0.026	2	-8.383	0.664	-4.618	2
Neolamprologus bifasciatus	Lamprologini	0.531	0.037	7	-5.552	2.254	-0.426	7
Neolamprologus brevis	Lamprologini	0.525	0.036	10	-0.181	-5.634	6.587	10
Neolamprologus brichardi	Lamprologini	0.529	0.023	10	-1.387	0.530	4.268	10
Neolamprologus buescheri	Lamprologini	0.504	0.029	10	-6.239	2.779	-1.321	10
Neolamprologus calliurus	Lamprologini	0.443	0.09	10	-0.814	-3.204	5.940	10
Neolamprologus cancellatus	Lamprologini	0.61	NA	1	1.696	-0.971	-6.719	1
Neolamprologus caudopunctatus	Lamprologini	0.531	0.062	10	-1.008	-0.090	1.885	10

Neolamprologus christyi	Lamprologini	0.642	0.038	10	0.390	0.492	-2.630	10
Neolamprologus cylindricus	Lamprologini	0.458	0.048	2	-4.632	5.990	-4.606	2
Neolamprologus falcicula	Lamprologini	0.509	0.032	3	-3.250	1.962	-1.866	3
Neolamprologus furcifer	Lamprologini	0.532	0.045	10	-3.883	-0.182	-4.222	10
Neolamprologus gracilis	Lamprologini	0.519	0.031	10	-1.096	3.182	3.012	10
Neolamprologus helianthus	Lamprologini	0.562	0.038	10	-3.127	0.280	3.553	10
Neolamprologus leleupi	Lamprologini	0.552	0.036	9	-3.002	4.129	-0.855	9
Neolamprologus leloupi	Lamprologini	0.521	0.032	10	-0.812	-0.297	2.071	10
Neolamprologus longicaudatus	Lamprologini	0.524	0.044	7	-4.635	3.586	-3.006	7
Neolamprologus marunguensis	Lamprologini	0.564	0.041	10	1.740	1.677	5.667	10
Neolamprologus meeli	Lamprologini	0.523	0.052	10	-1.408	-3.733	-1.268	10
Neolamprologus modestus	Lamprologini	0.599	0.041	10	1.405	0.916	-1.105	10
Neolamprologus mondabu	Lamprologini	0.555	0.046	10	-0.187	1.987	-1.551	10
Neolamprologus multifasciatus	Lamprologini	0.493	0.036	10	-1.772	-1.510	2.041	10
Neolamprologus mustax	Lamprologini	0.651	0.046	10	1.288	4.024	1.297	10
Neolamprologus niger	Lamprologini	0.537	0.042	9	-4.296	1.645	-1.712	9
Neolamprologus nigriventris	Lamprologini	0.508	0.034	6	-4.404	4.345	-3.545	6
Neolamprologus obscurus	Lamprologini	0.489	0.03	10	-4.822	-2.002	3.353	10
Neolamprologus olivaceous	Lamprologini	0.514	0.029	10	-1.188	0.724	3.708	10
Neolamprologus pectoralis	Lamprologini	0.554	0.023	9	-1.602	3.593	-4.752	9
Neolamprologus petricola	Lamprologini	0.648	0.052	9	4.652	1.572	-1.266	9
Neolamprologus prochilus	Lamprologini	0.506	0.05	7	-5.420	-2.606	3.343	7
Neolamprologus pulcher	Lamprologini	0.517	0.024	10	-0.744	0.121	4.781	10
Neolamprologus savoryi	Lamprologini	0.565	0.048	10	-3.265	-0.413	3.468	10
Neolamprologus sexfasciatus	Lamprologini	0.511	0.042	10	-3.429	-2.304	-0.088	10
Neolamprologus similis	Lamprologini	0.522	0.043	10	-2.206	-0.499	2.081	10
Neolamprologus splendens	Lamprologini	0.525	0.044	10	-3.305	0.195	3.562	10
Neolamprologus tetracanthus	Lamprologini	0.563	0.025	10	-2.844	0.202	-1.729	10
Neolamprologus toae	Lamprologini	0.453	0.032	5	-2.953	-1.236	0.613	5
Neolamprologus tretocephalus	Lamprologini	0.556	0.042	10	1.278	-1.141	-2.433	10
Neolamprologus variostigma	Lamprologini	0.503	NA	1	-7.847	-2.467	0.823	1
Neolamprologus ventralis	Lamprologini	0.51	0.028	6	-2.797	-1.382	0.466	6
Telmatochromis bifrenatus	Lamprologini	1.156	0.119	3	6.947	3.565	-3.758	3
Telmatochromis brachygnathus	Lamprologini	1.039	0.101	4	10.064	-2.286	-1.696	4
Telmatochromis dhonti	Lamprologini	0.638	0.075	10	0.708	-1.507	0.962	10
Telmatochromis temporalis	Lamprologini	0.873	0.123	10	8.037	-1.445	-1.354	10
Telmatochromis vittatus	Lamprologini	0.837	0.074	10	8.258	2.216	-3.216	10
Variabilichromis moorii	Lamprologini	0.576	0.068	10	3.537	-1.439	4.973	10
Baileychromis centropomoides	Limnochromini	0.365	0.066	3	-11.694	4.675	-4.502	3
Gnathochromis permaxillaris	Limnochromini	0.568	0.039	10	-2.749	-9.047	-5.505	10

Greenwoodochromis abeelei	Limnochromini	0.47	NA	1	-2.173	-6.965	-3.037	1
Greenwoodochromis bellcrossi	Limnochromini	0.53	NA	1	-8.728	0.357	3.668	1
Limnochromis auritus	Limnochromini	0.637	0.035	4	3.426	-5.623	-2.890	4
Limnochromis staneri	Limnochromini	0.613	0.023	2	-0.814	-7.324	1.883	2
Reganochromis calliurus	Limnochromini	0.457	NA	1	-8.300	-2.280	-4.535	1
Triglachromis otostigma	Limnochromini	0.485	0.045	2	0.142	-5.062	0.989	2
Haplotaxodon microlepis	Perissodini	0.574	0.034	10	-0.757	4.808	4.743	10
Perissodus microlepis	Perissodini	0.737	0.131	10	2.649	10.308	0.551	10
Plecodus multidentatus	Perissodini	0.425	0.057	4	-0.557	3.202	-0.892	4
Plecodus straeleni	Perissodini	0.725	0.14	8	4.402	5.329	4.681	8
Oreochromis tanganicae	Tilapiini	0.78	0.063	5	2.854	4.339	10.012	5
Telotrematocara macrostoma	Trematocarini	0.393	0.045	4	-10.086	-8.503	0.524	4
Trematocara marginatum	Trematocarini	0.596	0.069	2	-2.896	-1.708	-1.007	2
Trematocara nigrifrons	Trematocarini	0.421	NA	1	-5.395	-4.019	1.625	1
Trematocara stigmaticum	Trematocarini	0.564	NA	1	-5.537	-2.081	-0.888	1
Trematocara unimaculatum	Trematocarini	0.562	0.045	3	-4.193	-2.458	-1.544	3
Trematocara variabile	Trematocarini	0.457	0.026	3	-5.258	-4.406	0.936	3
Astatotilapia burtoni	Tropheini	0.519	0.067	12	0.599	-1.506	6.573	13
Ctenochromis horei	Tropheini	0.564	0.047	9	-1.744	1.585	1.138	9
Gnathochromis pfefferi	Tropheini	0.594	0.071	5	-0.524	-0.739	0.164	5
Limnotilapia dardenni	Tropheini	0.755	0.045	8	5.865	2.225	2.501	8
Lobochilotes labiatus	Tropheini	0.708	0.041	8	3.774	0.859	0.618	7
Petrochromis famula	Tropheini	0.945	0.056	7	10.090	-1.415	4.688	7
Petrochromis fasciolatus	Tropheini	0.813	0.076	6	6.329	3.665	6.552	6
Petrochromis macrognathus	Tropheini	1.112	NA	1	12.227	-1.442	0.944	1
Petrochromis orthognathus	Tropheini	1.043	0.11	8	10.018	1.871	3.128	8
Petrochromis polyodon	Tropheini	0.959	0.086	7	11.268	-1.458	2.022	7
Petrochromis sp. 'Kipili brown'	Tropheini	0.925	0.076	6	8.849	1.445	5.082	6
Petrochromis trewavasae	Tropheini	1.325	NA	1	11.851	-5.895	2.126	1
Pseudosimochromis curvifrons	Tropheini	1.112	0.144	4	13.908	-2.338	1.603	4
Simochromis babaulti	Tropheini	0.955	0.064	9	11.478	-1.589	0.784	9
Simochromis diagramma	Tropheini	1.01	0.105	7	11.967	-2.438	1.151	7
Simochromis marginatus	Tropheini	0.993	NA	1	9.906	-2.696	0.965	1
Tropheus annectens	Tropheini	1.151	0.107	3	14.136	-3.223	1.257	3
Tropheus brichardi	Tropheini	1.027	0.081	3	13.241	-1.538	-0.733	3
Tropheus moorii	Tropheini	1.144	0.167	10	14.509	-1.900	1.022	10
Tropheus polli	Tropheini	1.046	0.047	5	14.777	-0.639	1.251	5
Tylochromis polylepis	Tylochromini	0.714	NA	1	2.251	-1.856	1.201	1
				1125				1124

Supplementary file 2

Landmark distribution used for the assessment of head shape.

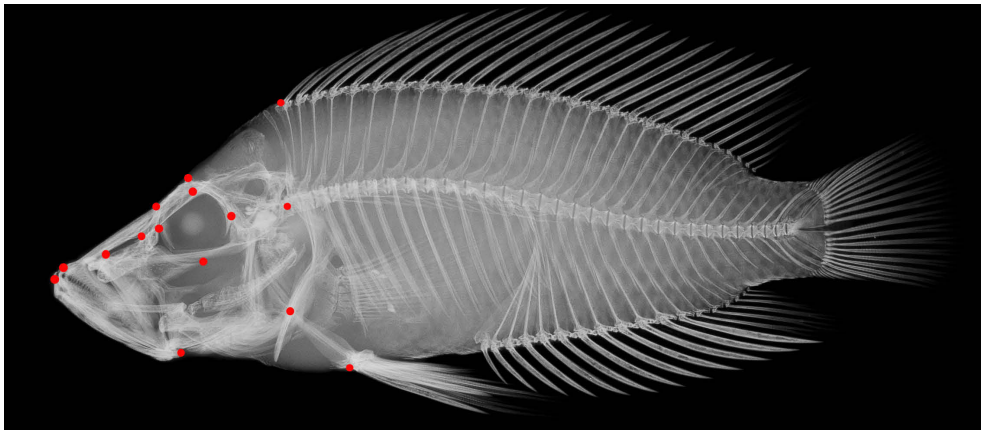

Supplementary file 3

DTT plots of CV2 and CV3 of head shape.

DTT plots showing average subclade disparity of empirical data through time (black line) as well as the 95% confidence interval of 1000 Brownian motion simulations (grey area) and the mean DTT from the simulated datasets (dashed line).

Both plots did not show signs of an 'early burst' process.

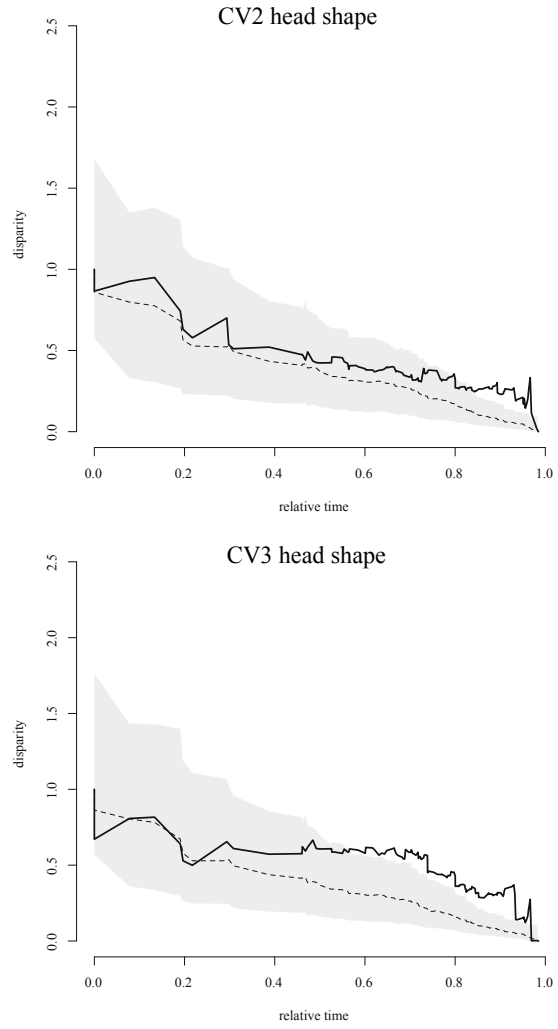

Supplementary file 4

Procrustes coordinates for the 15 landmarks used for morphometric analyses.

(not shown here due to vast size)

1.4

Habitat use and its implications to functional morphology: niche partitioning and the evolution of locomotory morphology in Lake Tanganyikan cichlids (Perciformes: Cichlidae)

Biological Journal of the Linnean Society

I collected and analysed the data and drafted the manuscript. AI provided ecological data and BM computed the molecular phylogeny. All authors participated in discussing the manuscript and drafting the final version.

The LINNEAN SOCIETY of London BIOLOGICAL Journal of the Linnean Society

Biological Journal of the Linnean Society, 2016, ••, ••–••. With 3 figures.

Habitat use and its implications to functional morphology: niche partitioning and the evolution of locomotory morphology in Lake Tanganyikan cichlids (Perciformes: Cichlidae)

MARCO COLOMBO[1]*, ADRIAN INDERMAUR[1], BRITTA S. MEYER[1,2] and WALTER SALZBURGER[1]

[1]*Zoological Institute, University of Basel, Vesalgasse 1, CH 4051, Basel, Switzerland*
[2]*Marine Ecology, Evolutionary Ecology of Marine Fishes, GEOMAR Helmholtz Centre for Ocean Research Kiel, Düsternbrooker Weg 20, D-24105, Kiel, Germany*

Received 8 October 2015; revised 11 November 2015; accepted for publication 12 November 2015

Animal locomotory morphology, i.e. morphological features involved in locomotion, is under the influence of a diverse set of ecological and behavioral factors. In teleost fish, habitat choice and foraging strategy are major determinants of locomotory morphology. In this study, we assess the influence of habitat use and foraging strategy on important locomotory traits, namely the size of the pectoral and caudal fins and the weight of the pectoral fin muscles, as applied to one of the most astonishing cases of adaptive radiation: the species flock of cichlid fishes in East African Lake Tanganyika. We also examine the course of niche partitioning along two main habitat axes, the benthic vs. limnetic and the sandy vs. rocky substrate axis. The results are then compared with available data on the cichlid adaptive radiation of neighbouring Lake Malawi. We find that pectoral fin size and muscle weight correlate with habitat use within the water column, as well as with substrate composition and foraging strategies. Niche partitioning along the benthic–limnetic axis in Lake Tanganyikan cichlids seems to follow a similar course as in Lake Malawi, while the course of habitat use with respect to substrate composition appears to differ between the cichlid assemblages of these two lakes. © 2016 The Linnean Society of London, *Biological Journal of the Linnean Society*, 2016, **00**, 000–000.

ADDITIONAL KEYWORDS: adaptive radiation – disparity through time – fish – locomotion.

INTRODUCTION

Locomotion and related morphological features (i.e. 'locomotory morphologies') occur in nearly all animal taxa. Vertebrates display a compelling diversity of locomotion strategies that involve a variety of body parts such as limbs, fins or, as seen for example in snakes or eels, the entire body. Locomotion and locomotory morphologies often correlate with the habitat in which a given species lives and forages. A classic textbook example for this correlation is lizards of the genus *Anolis*, in which limb lengths correlate with twig diameters (Losos, 1990; Irschick & Losos, 1999; Mattingly & Jayne, 2004; Vanhooydonck, Herrel & Irschick, 2006). Moreover, the same set of forms showing a strong correspondence between limb lengths and twig diameters evolved repeatedly and convergently on different islands of the Caribbean (Losos, 1990; Losos *et al.*, 1998; Mahler *et al.*, 2013). This phenomenon is generally regarded as a strong indicator for the importance of natural selection in shaping this correlation. Other vertebrate taxa rely on different body parts to generate movement, yet show similar correlations between morphology and habitat. Wing length in birds, for example, is often correlated with habitat structure, with species living in habitats characterized by dense vegetation exhibiting shorter wings than species living in open areas [reviewed by Hamilton (1961)]. Fish, conversely, often show a phenotype–environment correlation between fin morphology and benthic or limnetic habitat use [e.g. Malmquist (1992) and Dynes *et al.* (1999) for Arctic and brook charr,

*Corresponding author. E-mail: marco.colombo@unibas.ch

Hulsey *et al.* (2013) for cichlids and Robinson, Wilson & Margosian (2000) for pumpkinseed sunfish].

Most available studies in fish have investigated intraspecific variation, while studies linking divergence along a benthic–limnetic axis with repeated changes in locomotory morphology in more complex multi-species systems remain scarce. Notable exceptions are a study on selection towards different adaptive optima in locomotor phenotypes in neotropical geophagine cichlids (Astudillo-Clavijo, Arbour & Lopez-Fernandez, 2015) and the study by Hulsey *et al.* (2013), who examined the evolution of locomotory morphology in 24 species of Lake Malawi cichlids. The latter study found that benthic species exhibit larger pectoral fins and more massive, i.e. heavier, pectoral muscles compared with limnetic ones. Interestingly, the repeated shift between limnetic and benthic lifestyles in Lake Malawi cichlids seems to have been accompanied by convergent modifications in locomotory morphology (Hulsey *et al.*, 2013). Overall, however, habitat shifts along the benthic to limnetic axis, and the associated adaptations in locomotory morphology, have gained relatively limited attention in the study of East African Great Lake cichlids, although such habitat shifts have played an important role in shaping cichlid diversity in all three Great Lakes (Cooper *et al.*, 2010; Muschick, Indermaur & Salzburger, 2012; Hulsey *et al.*, 2013; Muschick *et al.*, 2014 and reviewed in Burress, 2015) as well as in various small crater lakes in Africa and Central America (Schliewen, Tautz & Paabo, 1994; Barluenga *et al.*, 2006). The species assemblages in Lake Victoria, Lake Malawi and Lake Tanganyika, which collectively are the most species-rich adaptive radiations in vertebrates (Salzburger, Van Bocxlaer & Cohen, 2014), contain extreme forms adapted to benthic or limnetic lifestyles (Cooper *et al.*, 2010). These mirror benthic–limnetic shifts that have occurred in a wide range of other fish groups including sunfishes, whitefishes, perch, charr and stickleback (Malmquist, 1992; Dynes *et al.*, 1999; Robinson *et al.*, 2000; Rundle *et al.*, 2000; Hjelm *et al.*, 2001; Gillespie & Fox, 2003; Amundsen *et al.*, 2004; Ostbye *et al.*, 2006).

Teleost fish, which constitute at least 50% of all known vertebrate species, exhibit a variety of swimming modes, often coupled with distinct body and fin morphologies. These locomotion strategies range, in the form of a continuum, from anguilliform to sub-carangiform, carangiform and thunniform swimming modes (Webb, 1984a, b; Blake, 2004). The anguilliform swimming mode usually involves more than two lateral flexures present along the fish's body at a time. Moving over sub-carangiform and carangiform swimming, the number of bends decreases continuously until, in thunniform swimming, the caudal fin and peduncle remain the only body parts involved in generating thrust (McDowall, 2003). In addition, there are some highly specialized swimming modes, such as ostraciform, which are found in few specialized groups only (i.e. Tetraodontiformes). On the basis of the observation that benthic species exhibit larger pectoral fins and muscles in many fish taxa (Malmquist, 1992; Dynes *et al.*, 1999; Robinson *et al.*, 2000; Hulsey *et al.*, 2013), it has been hypothesized that limnetic species may continuously make use of other locomotory structures, for example their caudal fin, to generate thrust (Hulsey *et al.*, 2013).

Specialization according to macro-habitat use is generally interpreted as the first step in the so-called 'stages model' of adaptive radiation, which was first developed for Lake Malawi cichlids (Danley & Kocher, 2001) and later generalized for vertebrates (Streelman & Danley, 2003). The second stage after macro-habitat specialization would be divergence according to trophic morphology, followed by diversification with respect to communication and coloration traits (stage 3) [reviewed in Gavrilets & Losos (2009)].

Another connection exists between locomotory morphology and feeding strategy in many animal taxa (Irschick & Losos, 1998; Domenici, 2001; Dean & Lannoo, 2003; Higham, 2007b). In fish, precise maneuvering while feeding is an important aspect of prey acquisition. In suction feeding species, for example, accurate positioning of the mouth relative to the prey item is essential, and pectoral fins play a crucial role in deceleration while maintaining approach stability. Therefore, fish that feature limited suction feeding abilities with respect to the water volume ingested often feature larger pectoral fins, thereby increasing their maneuverability and ability to correctly focus their attack on a prey item (Higham, 2007b).

Finally, fin size and morphology (including pigmentation patterns) can also be under the influence of sexual selection in fish. In many cichlids, for example, males, but not females, show enlarged or elongated and often elaborately colored paired (e.g. pectoral) or unpaired (e.g. anal, caudal) fins (Konings, 2015).

Against this background we investigate the cichlid assemblage of Lake Tanganyika to test whether or not pectoral and caudal fin sizes correlate with: (1) habitat use along a benthic–limnetic axis as found in other fish species and assemblages, (2) sandy–rocky habitat use, and (3) foraging mode. Furthermore, we use a wider sample of Lake Tanganyikan cichlids and a direct characterization of habitat use per species to examine bentho-limnetic and sandy–rocky habitat use through time and then compare it to patterns previously found in other teleost adaptive

radiations. Specifically, we test for evidence for an early divergence in habitat use leading to distinct lineages adapted to live on particular substrates as proposed by the radiation in stages model. It has previously been suggested that the three East African cichlid radiations depict, to some extent, replicated radiation events (Kocher *et al.*, 1993; Santos & Salzburger, 2012). Demonstrating temporal similarities or discrepancies in the process of adaptation and speciation between these three cichlid flocks should thus be interesting in the light of the ongoing quest to answer the question on whether there are general temporal patterns emerging in the course of adaptive radiations.

MATERIAL AND METHODS

In 2013 and 2014, we collected a total of 546 mature specimens representing 28 Lake Tanganyikan cichlid species in the southern part of Lake Tanganyika, Zambia. The samples include a phylogenetically and ecologically diverse set of species from 11 out of the 14 described Lake Tanganyikan cichlid tribes (Muschick *et al.*, 2012) (see Supporting Information, Table S1). Fish were caught using gill nets or, for some deep-water species, obtained from local fishermen. After euthanasia with clove oil, the sex of each specimen was determined, specimens were measured (standard and total length and weight were recorded) and photographed in a standardized way laying flat on the right side. We then dissected each specimen in the field and extracted all four pectoral adductor muscles (*arrector dorsalis*, *adductor radialis*, *adductor medialis* and *adductor superficialis*) of both pectoral fins. The four pectoral adductor muscles function together to pull the fin posteriorly. We refrained from examining the four pectoral abductor muscles that function to pull the fin anteriorly, as it has previously been shown that the forces of these two sets of muscles likely counterbalance each other and show fairly similar weights (Thorsen & Westneat, 2005; Hulsey *et al.*, 2013). All four muscles were measured together, but separately for each pectoral fin. Each set of muscles was measured twice and the mean of both measurements was taken for further analyses to increase measurement robustness. Concurrently, both pectoral fins and the caudal fin were separated from the fish's body, cleaned from dirt and mucus, and dyed with Indian ink to increase contrast. Each set of fins per specimen was then placed on a Styrofoam plate covered with an individual piece of white paper together with a premeasured reference plate of known area. Fins were spread using pins in a naturally erect position, i.e. in a maximal expanded position without over-expanding/damaging the fins. Each set of fins was then photographed using a Nikon D5000 digital camera (Nikon Corporation, Tokyo, Japan). Later on, each digital image was analyzed using the software FinPix, specifically written for this purpose (available under http://www.salzburgerlab.org/publications/software). More precisely, this software calculates the area of each fin (mm^2) by comparing the number of pixels constituting each fin with the number of pixels constituting a reference plate of known size. To do so, the program subdivides the picture into three sectors: (1) the upper half of the sheet in landscape orientation containing the left and right pectoral fins and the caudal fin, in that order, (2) the lower left quarter containing the reference area and (3) the lower right quarter, which is ignored by the program but may be used to add for example the specimen number or further annotations. First, the program searches for the reference area in the lower left quarter using the contrast between the white paper sheet and the black reference plate and subsequently counts the number of pixels that constitute this reference area. Next, the program consecutively searches, from left to right, the individual fins in the upper half of the sheet using the same method. Again, the number of pixels constituting each fin is counted and finally, by comparing the number of pixels constituting each individual fin and the number of pixels constituting the reference area of known size, the program calculates the area of each fin and provides a table containing the individual measurements. Given the high resolution of the digital images and the sharp contrast between ink-dyed fins and the white background, this method allows a highly accurate measurement of fin area. In addition, the program provides pictures with the pixels that were actually counted. The areas counted are highlighted in red giving the user the opportunity to cross-check whether the measurements had been performed correctly.

All trait measurements were screened for potential methodical problems (e.g. not fully expanded fins, imperfectly dissected muscles) or apparent measurement errors. If methodical problems or measurement errors were detected, individual trait measurements were excluded from further analyses. After this procedure, our dataset consisted of 530–536 individual values per trait and 8–23 specimens per species (see Supporting Information, Table S1). After this initial quality check, the average of the right and left pectoral muscle mass, the average of the right and left pectoral fin area and the caudal fin area were recorded for each specimen separately. Fifteen pectoral fin area and 15 pectoral muscle mass measurements were solely based on the left or right fin apparatus, respectively, as trait values were only available for one side.

To compute phylogenetically size-corrected values of traits (Revell, 2009) we used a modified version of the 'phyl.resid' function in the phytools package (Revell, 2012) in R (R Development Core Team, 2008) that allows for multiple individuals per species (Lopez-Fernandez *et al.*, 2014). We used the weight of an individual specimen to size-correct the muscle mass or centroid size (which is, in this case, essentially a measurement of the body area, see Supporting Information, Fig. S1) to size-correct the fin areas. Centroid size was calculated using tpsDig (Rohlf, 2010) and MorphoJ (Klingenberg, 2011), on the basis of nine landmarks distributed over the fish's body (Supporting Information, Fig. S1). Species were later individually tested for sexual dimorphism in all traits using a *t*-test in PRISM v.6.0e (GraphPad Software, La Jolla, CA, USA, www.graphpad.com). Furthermore, we used stable isotope data for the rare isotopes of Nitrogen and Carbon from Muschick *et al.* (2012) to further assess each species' position along the bentho-limnetic axis (Carbon) as well as each species' position within the food web (Nitrogen) [e.g. DeNiro & Epstein (1978); Hobson, Piatt & Pitocchelli (1994); Post (2002)]. As stable isotope data were not available for *Bathybates leo* and *Hemibates stenosoma,* analyses incorporating stable isotope values could only be conducted in 26 out of the 28 species. We further used data on intestinal tract length from Muschick *et al.* (2014) that we size-corrected using standard length as size measurement following the same procedure as described above. Again, data were not available for all species in our dataset, which reduced the species number to 24 when incorporating intestinal tract lengths (data were missing for *Bathybates graueri*, *Gnathochromis permaxillaris*, *Hemibates stenosoma* and *Trematocara marginatum*).

Additionally to this first dataset, we generated a second dataset containing 159 Lake Tanganyikan cichlid species grouped into categories according to their position on a benthic to limnetic axis and to whether a species prefers sandy or rocky habitats (see Fig. 1 and Supporting Information, Table S2). Information on habitat use was compiled from several literature sources as well as our own transect data. The species were then categorized into four discrete categories according to benthic to limnetic habitat use (benthic, semi-benthic, semi-limnetic, limnetic) and two categories (sandy or rocky) according to their substrate preference by one of the authors (AI) (Coulter, 1991; Hori *et al.*, 1993; Muschick *et al.*, 2012; Konings, 2015). Species categorized as semi-benthic or semi-limnetic, respectively, are species that are mainly associated with one macro-habitat but can occasionally also be encountered in the other macro-habitat.

In a next step, we created a new phylogenetic hypothesis for East African cichlids (196 taxa) on the basis of mitochondrial and nuclear sequence data obtained from GenBank (see Supporting Information, Fig. S2; Tables S5 and S6). To this end, we used nuclear sequence data from 42 genes (Meyer & Salzburger, 2012; Meyer, Matschiner & Salzburger, 2015) as backbone, and combined it with sequences of the mitochondrial NADH dehydrogenase subunit 2 (ND2) of 195 taxa, leading to a concatenated dataset of 18 592 bp in length and the most comprehensive phylogeny of cichlid fishes for Lake Tanganyika to date. As the nuclear data were only available for 45 taxa, we ended up with a proportion of gaps and undetermined positions of 72.85%. However, it has previously been shown that such a large proportion of missing data can still lead to reliable phylogenetic estimates (Wiens & Morrill, 2011). Model choice and data partitioning was done with PartitionFinder (Lanfear *et al.*, 2012). The resulting 18 partitions and models were subsequently used in the program GARLI version 2.0 (Zwickl, 2006) on the CIPRES Science Gateway (Miller, Pfeiffer & Schwartz, 2010) to perform a phylogenetic inference. The optimal tree was searched in 50 replicates, and 339 nonparametric bootstrap runs were conducted for confidence assessment, both using *Tylochromis polylepis* as outgroup (see Salzburger *et al.*, 2002). Models of the 18 partitions were allowed to differ and rates of subsets to change proportionally to one another (link models = 0; subset specific rates = 1). The resultant tree was then trimmed using ape (Paradis, Claude & Strimmer, 2004) in R to match the species for which trait data were available. Note that, for this study, we were not primarily interested in the phylogenetic hypothesis *per se*, but instead, used it to correct for phylogenetic signal and to reconstruct habitat use through time (see below).

We then applied correlational analyses in R on the dataset consisting of 28 species, once using a classical linear model and once using phylogenetic generalized least squares (PGLS) to correct for phylogenetic dependence of trait values. PGLS analyses were done using the R package caper (Orme, 2012) and a phylogeny trimmed to match the species sample of the trait dataset. *P*-values were subsequently corrected for multiple comparisons using a Bonferroni correction. We tested all species for sexual dimorphism in trait values as this could influence our correlational analyses. Significant sexual dimorphism regarding fin sizes and/or muscle mass was detected in only one out of 28 studied species: in *Enantiopus melanogenys*, females exhibited significantly larger pectoral fins than their male conspecifics ($P < 0.0028$). To account for this dimorphism, we created a secondary dataset excluding

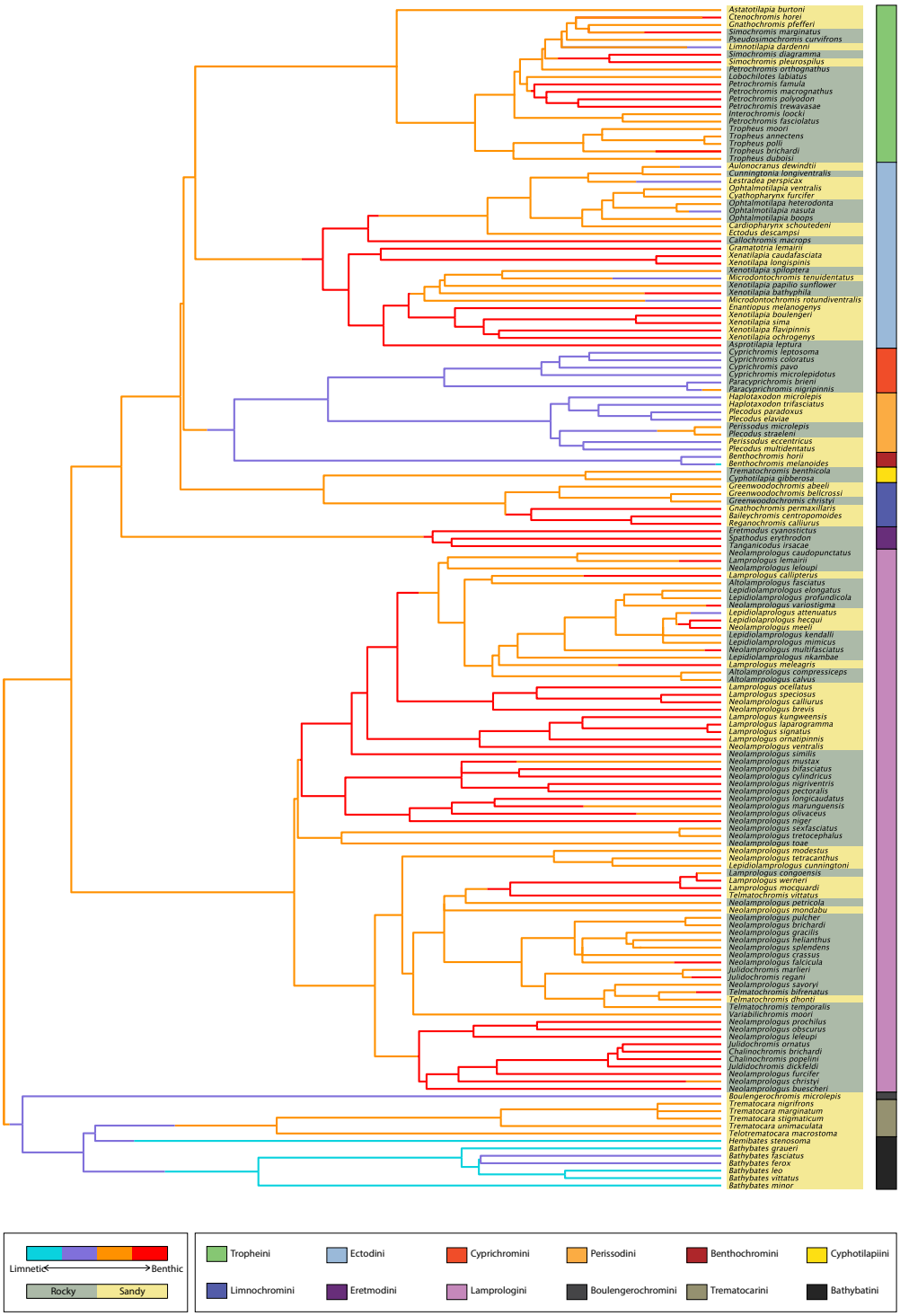

Figure 1. Ancestral character state reconstruction of 159 Lake Tanganyikan cichlid species according to a species' position along the benthic–limnetic axis (four categories). Preferences for rocky or sandy habitats are highlighted by grey and yellow boxes, respectively. The phylogenetic hypothesis presented here is inferred with a maximum likelihood approach using GARLI and is based mainly on mitochondrial ND2 sequences for all species and 42 nuclear markers where available.

pectoral fin area measurements of *Enantiopus melanogenys* and applied the same correlational analyses as on the original dataset (see Supporting Information, Tables S3 and S4). As the results were fairly similar, we here primarily rely on the results of the complete dataset for further interpretation (but see Discussion and Supporting Information). An ancestral character state reconstruction according to a species position along the benthic to limnetic axis in four categories (Fig. 1) was done with SIMMAP version 1.5.2 (Bollback, 2006) with an empirical prior and a linear ordering of states, setting the rate parameter to 'branch length prior'. The resultant figure was later modified in Adobe Illustrator CS 4 version 14.0.0 (Adobe Systems Inc., San José, CA, USA).

On the first dataset, consisting of 28 species, we again used PRISM to compare the four groups according to a species' position on the benthic to limnetic axis using an ordinary one-way ANOVA and Tukey's multiple comparisons test on pectoral fin area, caudal fin area and muscle mass, respectively, to compare benthic and limnetic groups. We further performed a *t*-test to contrast the group categorized as preferring sandy habitats with the group characterized as preferring rocky habitats.

Finally, we conducted two separate disparity through time (DTT) analyses using 159 species' grouping according to benthic/limnetic and sandy/rocky habitat use following Harmon *et al.* (2003). To this end, we used GEIGER (Harmon *et al.*, 2008) in R with the number of unique character states ('num.states', currently the only option for discrete character data) as disparity index. We computed 1000 Brownian motion simulations of trait disparity over the phylogeny and compared it with our actual habitat use data. We then calculated the morphological disparity index (MDI) over the first 75% of the relative timeline to correct for tip over-dispersion due to incomplete taxon sampling.

RESULTS

Phylogenetic analysis

With respect to the relationships between tribes, the phylogenetic hypothesis presented here (Fig. 1; Supporting Information, Fig. S2 for the complete phylogeny including bootstrap values) largely agrees with a recent multilocus nuclear phylogenetic hypothesis for Lake Tanganyika cichlids (Meyer *et al.*, 2015), which is not unexpected given that we used the nuclear data from this study. As in Meyer *et al.* (2015), the Boulengerochromini, Bathybatini and Trematocarini form a basal clade, a sister group to the Lamprologini and all remaining tribes that exclusively consist of mouthbrooding lineages. Within these, the Eretmodini branched off first [see Fig. 2B and discussion in Meyer *et al.* (2015)], followed by the Limnochromini and Cyphotilapiini, a clade formed by the Perissodini and Cyprichromini, the Ectodini and the Tropheini (as part of the Haplochromini). The internal branches, especially between the mouthbrooding tribes, are rather short suggesting a rapid period of lineage formation. This result is congruent with all previous analyses [e.g. Salzburger *et al.* (2002); Clabaut, Salzburger & Meyer (2005); Day, Cotton & Barraclough (2008)]. Regarding the placement of taxa within the tribes, our phylogeny is consistent with earlier studies based on mitochondrial DNA markers (Salzburger *et al.*, 2002; Day *et al.*, 2008; Sturmbauer *et al.*, 2010), which is also not unexpected, given that we largely relied on data from these studies for the mitochondrial DNA part of the concatenated sequence alignment. Overall, we feel confident about using our new phylogenetic hypothesis to correct for phylogenetic signal in the trait data and for the DTT analyses.

Correlational analyses

Both correlational analyses, PGLS and the classical linear model, revealed a significant positive correlation between pectoral muscle mass and fin area. Both analyses also revealed a strong positive correlation between pectoral and caudal fin area and, to a lesser extend, between pectoral muscle mass and caudal fin area (Tables 1 and 2). Pectoral fin area also correlated positively with intestinal tract length in both analyses, whereas we observed a negative correlation between pectoral fin area and δ15N stable isotope measurements in the linear model; however, this correlation disappears in the PGLS analysis [yet is still evident in both the linear model and PGLS when excluding the sexually dimorphic *E. melanogenys* (Supporting Information, Tables S3 and S4)]. Pectoral muscle mass, correlating with pectoral fin area, showed a similar pattern: we also found a negative correlation with δ15N and a positive one with intestinal tract length with the difference that the correlation also holds in the PGLS analysis of the complete dataset. Caudal fin area, which correlated with pectoral fin area as well as pectoral muscle mass, showed positive correlations with intestinal tract length in both analyses.

Habitat use

Characterization of habitat use in 159 Lake Tanganyikan cichlid species led to six species being characterized as limnetic, 22 as semi-limnetic, 67 as semi-benthic and 64 as benthic. From the same pool

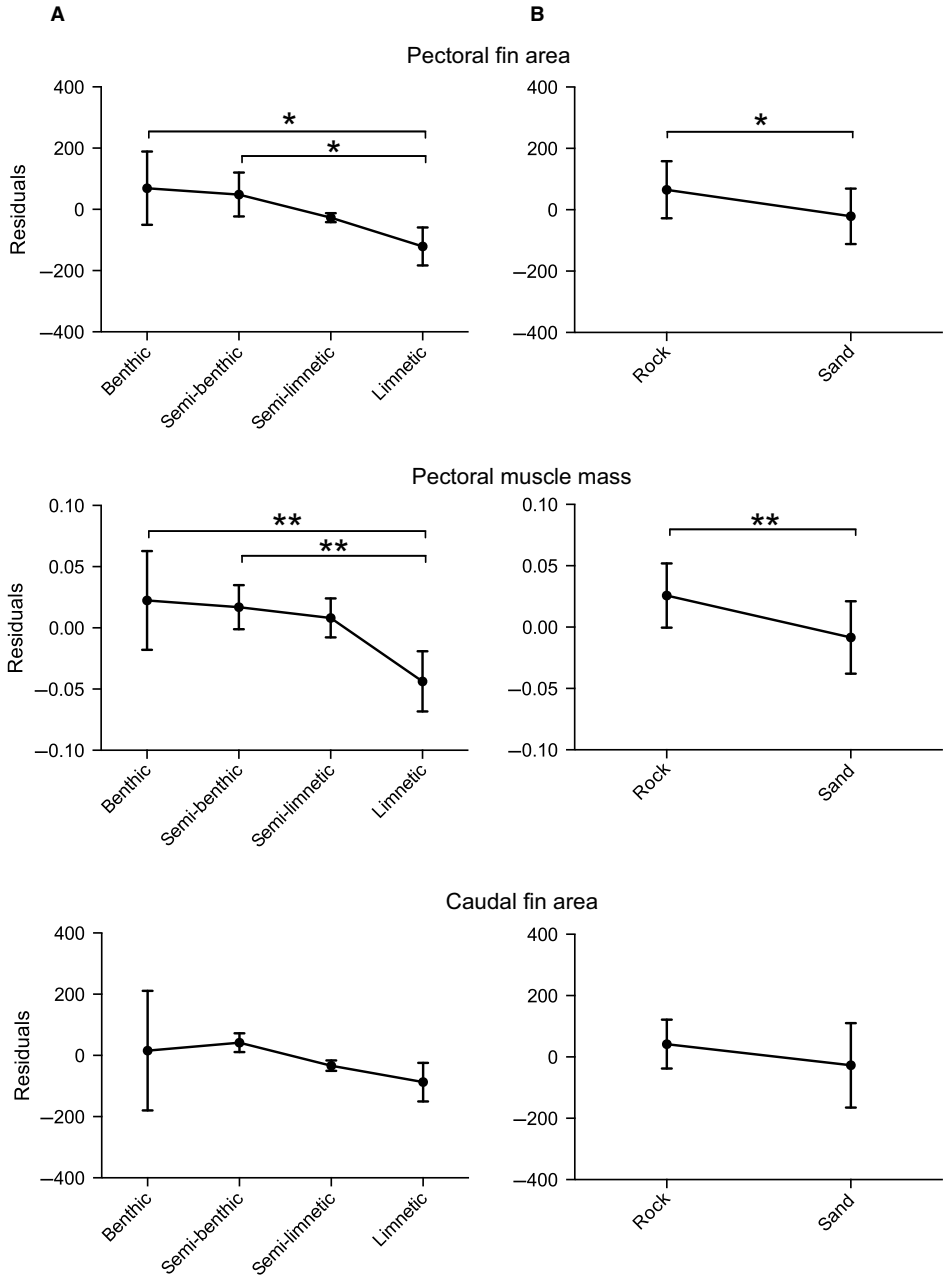

Figure 2. Comparison between species grouped according to habitat preferences. A, One-way ANOVA with grouping according to a species' position along a benthic to limnetic axis, revealing a gradient towards smaller pectoral fins and muscles with an increasingly limnetic habitat use. Significant differences were detected in pectoral fin area and muscle mass between the benthic and semi-benthic groups and the limnetic group. B, Student's *t*-test between species grouped according to either sandy or rocky habitat use, revealed significantly smaller pectoral fins and lighter muscles in species preferring sandy habitats. *$P < 0.05$, **$P < 0.01$.

of species, 90 can be regarded as exhibiting an association with rocky substrate and 69 as exhibiting a lifestyle connected to sandy substrate (Fig. 1; Supporting Information Table S2).

Tukey's multiple comparisons test following a one-way ANOVA between our four groups according to a species' position along a benthic to limnetic axis revealed increasingly smaller pectoral fins and

Table 1. Results of a correlation analysis according to a classic linear model

	t-Value	Adjusted *P*-value	R^2	$N_{species}$
Pectoral fin area				
Pectoral muscle mass	7.431	**0.000**	0.680	28
Caudal fin area	6.121	**0.000**	0.590	28
δ15N	−2.865	**0.043**	0.255	26
δ13C	2.705	0.062	0.234	26
Intestinal tract length	5.063	**0.000**	0.538	24
Caudal fin area				
Pectoral muscle mass	3.502	**0.008**	0.321	28
Pectoral fin area	6.121	**0.000**	0.590	28
δ15N	−1.226	1	0.059	26
δ13C	1.787	0.433	0.118	26
Intestinal tract length	3.908	**0.004**	0.410	24
Pectoral muscle mass				
Pectoral fin area	7.431	**0.000**	0.680	28
Caudal fin area	3.502	**0.008**	0.321	28
δ15N	−3.029	**0.029**	0.277	26
δ13C	2.730	0.058	0.237	26
Intestinal tract length	4.426	**0.001**	0.471	24

P-values were corrected for multiple comparisons using a Bonferroni correction. Bold values indicate *P*-values < 0.05 after Bonferroni correction.

Table 2. Results of a correlation analysis corrected for phylogenetic dependence of trait values using PGLS

	t-Value	Adjusted *P*-value	R^2	λ	$N_{species}$
Pectoral fin area					
Pectoral muscle mass	6.184	**0.000**	0.595	0.975	28
Caudal fin area	5.055	**0.000**	0.496	1	28
δ15N	−2.325	0.144	0.184	1	26
δ13C	0.856	1	0.030	1	26
Intestinal tract length	4.118	**0.002**	0.435	1	24
Caudal fin area					
Pectoral muscle mass	3.502	**0.008**	0.321	0	28
Pectoral fin area	6.121	**0.000**	0.590	0	28
δ15N	−1.226	1	0.059	0	26
δ13C	1.787	0.433	0.118	0	26
Intestinal tract length	3.908	**0.004**	0.410	0	24
Pectoral muscle mass					
Pectoral fin area	6.365	**0.000**	0.609	0.838	28
Caudal fin area	2.782	**0.050**	0.229	0.773	28
δ15N	−2.914	**0.038**	0.261	0.639	26
δ13C	2.730	0.058	0.237	0	26
Intestinal tract length	4.196	**0.002**	0.445	1	24

P-values were corrected for multiple comparisons using a Bonferroni correction. Bold values indicate *P*-values < 0.05 after Bonferroni correction.

lighter pectoral fin muscles towards a more limnetic lifestyle. For both traits, we detected significant differences between both the group exhibiting a benthic lifestyle and the group exhibiting a semi-benthic lifestyle when compared to the group exhibiting a limnetic lifestyle (Fig. 2; Table 3A). We found similar results when comparing species grouped according to their habitat use (rocky vs. sandy): both pectoral fin area and muscle mass showed significantly smaller values for species exhibiting a lifestyle connected to sandy habitats (Fig. 2; Table 3B).

Plotting benthic to limnetic habitat use over the most inclusive molecular phylogeny for Lake Tanganyikan cichlid species available revealed a rather disparate habitat use distribution (Fig. 1). There were only a few tribes featuring only benthic or limnetic living species, respectively. However, the Bathybatini exclusively consist of limnetic or semi-limnetic species, while, conversely, the Eretmodini and Limnochromini feature only benthic or semi-benthic species. Only Cyphotilapiini, Eretmodini, Boulengerochromini and Trematocarini, which were represented by one to five species per tribe in our phylogeny, exhibited a uniform habitat use with all species falling into the same habitat category. Of these tribes, only the Eretmodini showed a strictly benthic habitat use, while the species of the other 'uniform' tribes all fell into intermediate categories. All other tribes are non-uniform and show within-tribe diversity related to habitat use with species falling into two to three categories within a tribe. Nevertheless, no tribe was found to feature all four habitat categories. We observed a similar pattern associated with habitat use according to sandy or rocky substrate: The species-rich tribes feature species from both categories and only the rather species-poor tribes feature species restricted to either rocky or sandy substrate, i.e. the Cyprichromini, Benthochromini, Cyphotilapiini, Eretmodini, Boulengerochromini, Trematocarini and Bathybatini.

Table 3. Test statistics corresponding to the comparison between species grouped according to habitat preferences (Fig. 2). (A) Tukey's multiple comparisons test following a one-way ANOVA with grouping according to a species' position along a benthic to limnetic axis. (B) Student's *t*-test between species grouped according to either sandy or rocky habitat preference

A				B			
Comparison	Difference between means	Summary	Adjusted *P*-value	Comparison	Difference between means	Summary	*P*-value
Pectoral fin area							
Benthic vs. semi-benthic	20.60	ns	0.947	Sand vs. rock	−86.39	*	**0.021**
Benthic vs. semi-limnetic	96.04	ns	0.366				
Benthic vs. limnetic	190.10	*	**0.016**				
Semi-benthic vs. semi-limnetic	75.45	ns	0.519				
Semi-benthic vs. limnetic	169.50	*	**0.023**				
Semi-limnetic vs. limnetic	94.05	ns	0.543				
Pectoral muscle mass							
Benthic vs. semi-benthic	0.0055	ns	0.967	Sand vs. rock	−0.03415	*	**0.015**
Benthic vs. semi-limnetic	0.0143	ns	0.861				
Benthic vs. limnetic	0.0661	**	**0.007**				
Semi-benthic vs. semi-limnetic	0.0088	ns	0.955				
Semi-benthic vs. limnetic	0.0606	**	**0.008**				
Semi-limnetic vs. limnetic	0.0518	ns	0.112				
Caudal fin area							
Benthic vs. semi-benthic	−26.03	ns	0.950	Sand vs. rock	−69.05	ns	0.560
Benthic vs. semi-limnetic	48.97	ns	0.911				
Benthic vs. limnetic	102.90	ns	0.520				
Semi-benthic vs. semi-limnetic	75.00	ns	0.708				
Semi-benthic vs. limnetic	129.00	ns	0.276				
Semi-limnetic vs. limnetic	53.98	ns	0.930				

ns, non-significant, *$P < 0.05$, **$P < 0.01$. Significant *P*-values are depicted in bold.

Disparity through time

DTT analyses of habitat use (rocky vs. sandy and benthic vs. limnetic) both showed no signs of an early burst (Fig. 3), with MDI statistics for both analyses being positive (rocky vs. sandy, MDI = 0.1734; benthic vs. limnetic, MDI = 0.0316). Nevertheless, we detected periods where average subclade disparity remains lower than predicted by Brownian motion simulations: just at the onset of the radiation for rocky vs. sandy habitat use and around 0.2 in relative time for benthic vs. limnetic habitat use. However, following these valleys, average subclade disparity consistently remains higher than predicted, indicating elevated disparity within subclades.

DISCUSSION

In the present study, we analyzed pectoral and caudal fin size and pectoral fin muscle weight in the species flock of cichlid fishes form Lake Tanganyika, and correlated it with ecological and behavioral traits to test hypotheses regarding phenotype-environment correlations, previously established in other, mostly species-poor fish assemblages. Further, we tested hypotheses on habitat use and its diversification through time. Namely, that habitat use according to sandy and rocky habitat use represents the first axis of divergence while habitat use along the benthic–limnetic axis diverged over a prolonged time span. These scenarios were previously discussed for example in Lake Malawi cichlids. If habitat use indeed represents the first axis of divergence in Lake Tanganyikan cichlids, an 'early burst'-like pattern should be visible in our DTT plots.

Correlation between pectoral fin area and muscle mass in Lake Tanganyikan cichlids was shown to be significant and comparable with the outcome of a similar study in Lake Malawi cichlids (Hulsey *et al.*, 2013). Both the classical linear model and PGLS analyses revealed correlations between the area of the pectoral fins and the mass of the muscles that are used to move the respective fins through the water (Tables 1 and 2). This correlation becomes even stronger when excluding the sexually dimorphic

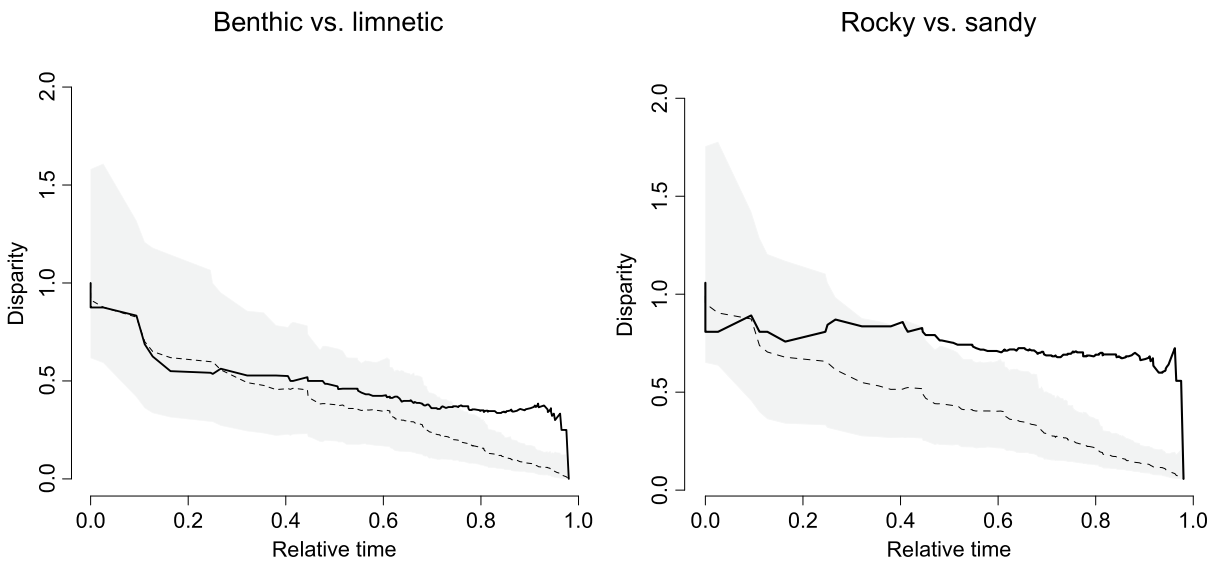

Figure 3. Disparity through time plots according to habitat preference along the benthic–limnetic axis (left, four categories, MDI = 0.0316) and rocky vs. sandy habitat preference (right, two categories, MDI = 0.1734). Average subclade disparity remains generally higher than the mean of 1000 Brownian motion simulations, indicating elevated disparity within subclades.

E. melanogenys (Supporting Information, Tables S3 and S4). Moreover, pectoral fin area and muscle mass showed very similar correlations with ecological factors and habitat use (discussed below). Larger pectoral fins coupled with heavier pectoral fin muscles should directly lead to increased maneuverability and a more efficient deceleration, also during prey capture (Higham, 2007a, b). To decelerate, fish commonly use their extended pectoral, caudal and median fins to increase drag (Drucker & Lauder, 2002; Rice & Westneat, 2005; Higham, 2007a). Conversely, a more powerful pectoral apparatus should lead to increased locomotory performance, when used to generate thrust.

Of 159 characterized Lake Tanganyikan cichlid species, 28 species exhibited a limnetic or semi-limnetic habitat association, whereas 131 species had a benthic or semi-benthic habitat association. This suggests that the structured and diverse benthic macro-habitat provides far more niches for species diversification than the rather uniform limnetic macro-habitat. A more equal distribution is found regarding substrate preference, for which 90 species can be regarded as being associated with rocky substrate and 69 species with sandy substrate. Again, the higher number of species preferring rocky substrates indicates that the densely structured rocky habitat likely provides more niches for species to forage in than the more uniform sandy habitat.

The most pronounced axis of divergence between closely related fish taxa often coincides with adaptations to a benthic vs. a limnetic lifestyle (Schluter, 1993; Rundle *et al.*, 2000; Barluenga *et al.*, 2006; Machado-Schiaffino *et al.*, 2015). Most of these shifts are accompanied by alterations of the feeding apparatus and the general body shape including fin morphology. In Arctic (*Salvelinus alpinus*) and brook charr (*Salvelinus fontinalis*), for example, pronounced differences exist between limnetic and benthic morphs, *inter alia* involving locomotory morphology (Malmquist, 1992; Dynes *et al.*, 1999). Limnetic morphs exhibit shorter pectoral fins and a more fusiform body, whereas benthic forms feature longer pectoral fins and a deeper body. Moreover, it has been shown that the limnetic morph feeds more effectively on plankton, suggesting that the beforehand mentioned morphological differences are adaptive to a planktivorous diet. In addition, morphologically distinct benthic and limnetic morphs are thought to have mediated reproductive isolation in Arctic charr (Jonsson & Jonsson, 2001), as well as in threespine stickleback (Rundle *et al.*, 2000; Boughman, 2001), thus providing a possible mechanism for speciation along this major ecological axis. In perch (*Perca fluviatilis*), benthic and limnetic morphs differ in body depth, with the benthic morph showing a deeper body than its limnetic conspecific (Hjelm *et al.*, 2001). The same was found for pumpkinseed sunfish (*Lepomis gibbosus*), in which some populations additionally show divergence in pectoral fin size: benthic morphs have larger fins in some populations (Robinson *et al.*, 2000) but not in others

(Gillespie & Fox, 2003). Similarly, neotropical geophagine cichlids exhibit an early divergence in locomotor phenotypes towards two distinct adaptive peaks: one that includes deep-bodied, predominantly benthically feeding fish and one including mostly ram-feeding species with streamlined bodies (Astudillo-Clavijo *et al.*, 2015).

We found a gradient towards smaller pectoral fins and lighter muscles with increasingly limnetic lifestyle, with significant differences in pectoral fin area and muscle mass between benthic and semi-benthic species and the limnetic species group (Fig. 2A and Table 3). Differences concerning pectoral fin area and muscle mass seem to be partially explained by differences in benthic vs. limnetic habitat use. A similar pattern has been documented for Lake Malawi cichlids (Hulsey *et al.*, 2013). More generally, morphological differences influencing locomotion connected with benthic vs. limnetic lifestyles have been demonstrated for various temperate water species (Malmquist, 1992; Schluter, 1993; Dynes *et al.*, 1999; Robinson *et al.*, 2000; Svanback & Eklov, 2004).

In this study, we provide evidence that foraging strategy influences fin morphology in Lake Tanganyikan cichlids. Both δ15N values (a measure for a species' position within the food web) and intestinal tract length (with longer intestinal tract length pointing towards a more herbivorous diet) correlated strongly with pectoral fin area and muscle mass (although the correlation between pectoral fin area and δ15N appeared weaker in the PGLS analysis of the complete dataset). A similar correlation was found between intestinal tract length and caudal fin area, further emphasizing the association between feeding and locomotion. Species ranking lower in the food web exhibit larger pectoral and caudal fins.

Pectoral fins play a crucial role in maneuvering in fish and are essential in turning, fine correction, rapid acceleration, deceleration, backward swimming and stationary hovering (Webb, 2006). Herbivores require a more precise maneuvering during foraging to feed effectively along substrata with varying topologies and at varying angles (Webb, 1984a; Rice & Westneat, 2005) and thus likely require larger fins to meet the demands of this foraging strategy. Furthermore, efficient deceleration, mainly relying on movements of the pectoral fins, is crucial when feeding from substrate as it prevents collisions that could otherwise harm the fish (Rice & Westneat, 2005; Higham, 2007a). The correlation between foraging strategy and locomotory morphology is probably connected with the correlation between locomotory morphology and benthic vs. limnetic habitat use (see above), as herbivorous species seem to be more common in benthic habitats due to higher availability of suitable food items (Hori *et al.*, 1993; Muschick *et al.*, 2012).

We also found a gradient towards smaller pectoral fins and lighter pectoral muscles in species living on sandy substrate as compared to species living in rocky habitats, with the former exhibiting significantly smaller pectoral fins and lighter pectoral muscles (Fig. 2B and Table 3). This discrepancy likely evolved due to increased demands on maneuverability when foraging in a complex, rocky environment, both in terms of precise swimming in-between rocks and cavities, as well as braking to prevent collisions with sharp-edged rocks when feeding from the substrate.

Given the apparent correlation between benthic habitat use and enlarged pectoral fins in various fish species (Malmquist, 1992; Dynes *et al.*, 1999; Robinson *et al.*, 2000; Hulsey *et al.*, 2013) one could expect that limnetic living species make increased use of other locomotory features such as the caudal fin. If this is the case in Lake Tanganyika cichlids, it is not reflected by caudal fin size as we did not find any evidence for limnetic species having larger caudal fins (Fig. 2A and Table 3A). Moreover, we found a strong correlation between pectoral and caudal fin area (and pectoral muscle mass), which might be due to a constraint in fin size evolution, i.e. that the evolution of larger pectoral fins positively influences the size of the caudal fin or *vice versa*. This result would mean that pectoral and caudal fin sizes are regulated in common, possibly by the same set of genes.

There was only one species with significant sexual dimorphism concerning pectoral fin size, namely *Enantiopus melanogenys*. This species is found predominantly on open sand plains and hence has little need for enhanced maneuverability. It is also a lek forming species with males competing in large and dense aggregations. Sexual dimorphism is hence relatively pronounced in coloration, body size and also the patterning and size of the unpaired fins. Combined with a relative low ecological selection pressure on pectoral (paired) fins and maneuverability this might account for the intersexual differences in this species.

We did not find any evidence for an early burst of diversification, defined as a rapid initial diversification followed by a drop in evolutionary rate as ecological space becomes filled (Schluter, 2000; Harmon *et al.*, 2003, 2010) in Lake Tanganyikan cichlids in terms of habitat use – neither according to habitat use towards rocky vs. sandy substrate nor along the benthic to limnetic axis. Early divergence with respect to macro-habitat use would be expected under the 'radiation in stages' model, and would have led to a persistent deep split in the phylogeny according to habitat use. This is because the

available niches would have been filled during the initial phases of divergence, leaving little opportunity for subsequent habitat changes within subclades. Such a persistent split, for example into rock dwelling and sand dwelling lineages, as found in Lake Malawi cichlids (Danley & Kocher, 2001; Streelman & Danley, 2003), is not visible in the Lake Tanganyikan cichlid assemblage. DTT analyses and MDI statistics of sandy vs. rocky habitat use show no sign of an early, continuous split according to these categories (Fig. 3).

Another pattern becomes evident when inspecting sandy vs. rocky habitat use plotted onto the phylogeny (Fig. 1): There is little clustering of habitat use according to phylogenetic relationships. We therefore conclude that discrepancies in habitat use between Lake Tanganyika cichlid species are not the result of an early burst at the onset of the radiation but, contrary to the pattern discussed for Lake Malawi, evolved over a prolonged timespan with habitat shifts recurrently occurring within subclades. This discrepancy in the timing of niche partitioning might be explained by differences in the origin and history of these two cichlid assemblages. In contrast to the quasi-monophyletic Lake Malawian cichlid species flock, the Lake Tanganyika assemblage was presumably seeded by several cichlid lineages and diversified into a variety of tribes (Salzburger *et al.*, 2002), possibly facilitating niche sharing and niche co-occupation by phylogenetically distinct species (Muschick *et al.*, 2012). A similar pattern of recurrent habitat shifts was found for habitat use along the benthic–limnetic axis: We did not find any signs of an early divergence leading to distinct lineages along this axis, but rather a pattern of recurrent shifts in habitat use within subclades. This is in accordance with findings concerning the Lake Malawi cichlid species flock (Hulsey *et al.*, 2013). Similarly, Muschick *et al.* (2014) found no evidence for a temporal ordering of trait evolution according to the 'radiation in stages' model in Lake Tanganyikan cichlids. Compared with traits associated with foraging, macro-habitat-related traits show less phylogenetic signal and a more accelerated rate of trait evolution across the radiation, indicating that traits associated with feeding actually diverged earlier than macro-habitat-related traits. Other studies did not recover an 'early burst' in two components of trophic morphology in Lake Tanganyika cichlids, the shape of the lower pharyngeal jaw (Muschick *et al.*, 2012) and operculum shape (Wilson *et al.*, 2015).

Taken together, we show that specializations in habitat use, both with respect to rocky vs. sandy and benthic vs. limnetic, occurred repeatedly within the cichlid species flock of Lake Tanganyika, and that habitat use shows little phylogenetic constraints. Furthermore, these shifts in habitat use are accompanied by convergent modification of the locomotory system with species preferring benthic and rocky habitats exhibiting larger pectoral fins and heavier muscles. This could mainly be explained by increased demands regarding maneuverability required for foraging in these habitats and/or feeding and grazing between rocks. In addition to this correlation with habitat use, and probably connected to it, locomotory morphology of Lake Tanganyikan cichlids was shown to be influenced by foraging strategies with herbivorous species ranking lower in the food web, exhibiting larger pectoral fins and muscles.

ACKNOWLEDGEMENTS

The authors would like to thank Astrid Böhne, Nicolas Boileau, Marie Dittmann, Isabel Keller, Florian Meury, Fabrizia Ronco and Attila Rüegg for their help during fieldwork, Matthias Wyss for writing the FinPix software and five anonymous reviewers for their helpful comments and suggestions. This project was supported by funding from the Swiss National Science Foundation (SNF) Sinergia program, granted to WS, Marcelo R. Sánchez-Villagra and Heinz Furrer (Universität Zürich) (CRSII3-136293) and the European Research Council (ERC; CoG 'Cichlid~X') to WS.

REFERENCES

Amundsen PA, Knudsen R, Klemetsen A, Kristoffersen R. 2004. Resource competition and interactive segregation between sympatric whitefish morphs. *Annales Zoologici Fennici* **41:** 301–307.

Astudillo-Clavijo V, Arbour JH, Lopez-Fernandez H. 2015. Selection towards different adaptive optima drove the early diversification of locomotor phenotypes in the radiation of Neotropical geophagine cichlids. *BMC Evolutionary Biology* **15:** 77.

Barluenga M, Stolting KN, Salzburger W, Muschick M, Meyer A. 2006. Sympatric speciation in Nicaraguan crater lake cichlid fish. *Nature* **439:** 719–723.

Blake RW. 2004. Fish functional design and swimming performance. *Journal of Fish Biology* **65:** 1193–1222.

Bollback JP. 2006. SIMMAP: stochastic character mapping of discrete traits on phylogenies. *BMC Bioinformatics* **7:** 88.

Boughman JW. 2001. Divergent sexual selection enhances reproductive isolation in sticklebacks. *Nature* **411:** 944–948.

Burress ED. 2015. Cichlid fishes as models of ecological diversification: patterns, mechanisms, and consequences. *Hydrobiologia* **748:** 7–27.

Clabaut C, Salzburger W, Meyer A. 2005. Comparative phylogenetic analyses of the adaptive radiation of Lake Tanganyika cichlid fish: nuclear sequences are less

homoplasious but also less informative than mitochondrial DNA. *Journal of Molecular Evolution* **61:** 666–681.

Cooper WJ, Parsons K, McIntyre A, Kern B, McGee-Moore A, Albertson RC. 2010. Bentho-pelagic divergence of cichlid feeding architecture was prodigious and consistent during multiple adaptive radiations within African rift-lakes. *PLoS ONE* **5:** e9551.

Coulter GW. 1991. *Lake Tanganyika and its life*. London: Oxford University Press/Natural History Museum.

Danley PD, Kocher TD. 2001. Speciation in rapidly diverging systems: lessons from Lake Malawi. *Molecular Ecology* **10:** 1075–1086.

Day JJ, Cotton JA, Barraclough TG. 2008. Tempo and mode of diversification of lake Tanganyika cichlid fishes. *PLoS ONE* **3:** e1730.

Dean MN, Lannoo MJ. 2003. Suction feeding in the pipid frog, *Hymenochirus boettgeri*: kinematic and behavioral considerations. *Copeia* **2003:** 879–886.

DeNiro MJ, Epstein S. 1978. Influence of diet on the distribution of carbon isotopes in animals. *Geochimica et Cosmochimica Acta* **42:** 495–506.

Domenici P. 2001. The scaling of locomotor performance in predator-prey encounters: from fish to killer whales. *Comparative Biochemistry and Physiology Part A Molecular Integrative Physiology* **131:** 169–182.

Drucker EG, Lauder GV. 2002. Wake dynamics and locomotor function in fishes: interpreting evolutionary patterns in pectoral fin design. *Integrative and Comparative Biology* **42:** 997–1008.

Dynes J, Magnan P, Bernatchez L, Rodriguez MA. 1999. Genetic and morphological variation between two forms of lacustrine brook charr. *Journal of Fish Biology* **54:** 955–972.

Gavrilets S, Losos JB. 2009. Adaptive radiation: contrasting theory with data. *Science* **323:** 732–737.

Gillespie GJ, Fox MG. 2003. Morphological and life-history differentiation between littoral and pelagic forms of pumpkinseed. *Journal of Fish Biology* **62:** 1099–1115.

Hamilton TH. 1961. The adaptive significances of intraspecific trends of variation in wing length and body size among bird species. *Evolution* **15:** 180–195.

Harmon LJ, Schulte JA 2nd, Larson A, Losos JB. 2003. Tempo and mode of evolutionary radiation in iguanian lizards. *Science* **301:** 961–964.

Harmon LJ, Weir JT, Brock CD, Glor RE, Challenger W. 2008. GEIGER: investigating evolutionary radiations. *Bioinformatics* **24:** 129–131.

Harmon LJ, Losos JB, Jonathan Davies T, Gillespie RG, Gittleman JL, Bryan Jennings W, Kozak KH, McPeek MA, Moreno-Roark F, Near TJ, Purvis A, Ricklefs RE, Schluter D, Schulte Ii JA, Seehausen O, Sidlauskas BL, Torres-Carvajal O, Weir JT, Mooers AO. 2010. Early bursts of body size and shape evolution are rare in comparative data. *Evolution* **64:** 2385–2396.

Higham TE. 2007a. Feeding, fins and braking maneuvers: locomotion during prey capture in centrarchid fishes. *Journal of Experimental Biology* **210:** 107–117.

Higham TE. 2007b. The integration of locomotion and prey capture in vertebrates: morphology, behavior, and performance. *Integrative and Comparative Biology* **47:** 82–95.

Hjelm J, Svanback R, Bystrom P, Persson L, Wahlstrom E. 2001. Diet-dependent body morphology and ontogenetic reaction norms in Eurasian perch. *Oikos* **95:** 311–323.

Hobson KA, Piatt JF, Pitocchelli J. 1994. Using stable isotopes to determine seabird trophic relationships. *The Journal of Animal Ecology* **63:** 786.

Hori M, Gashagaza MM, Nshombo M, Kawanabe H. 1993. Littoral fish communities in Lake Tanganyika – irreplaceable diversity supported by intricate interactions among species. *Conservation Biology* **7:** 657–666.

Hulsey CD, Roberts RJ, Loh YH, Rupp MF, Streelman JT. 2013. Lake Malawi cichlid evolution along a benthic/limnetic axis. *Ecology and Evolution* **3:** 2262–2272.

Irschick DJ, Losos JB. 1998. A comparative analysis of the ecological significance of maximal locomotor performance in Caribbean Anolis lizards. *Evolution* **52:** 219–226.

Irschick DJ, Losos JB. 1999. Do lizards avoid habitats in which performance is submaximal? the relationship between sprinting capabilities and structural habitat use in Caribbean anoles. *The American Naturalist* **154:** 293–305.

Jonsson B, Jonsson N. 2001. Polymorphism and speciation in Arctic charr. *Journal of Fish Biology* **58:** 605–638.

Klingenberg CP. 2011. MorphoJ: an integrated software package for geometric morphometrics. *Molecular Ecology Resources* **11:** 353–357.

Kocher TD, Conroy JA, McKaye KR, Stauffer JR. 1993. Similar morphologies of cichlid fish in Lakes Tanganyika and Malawi are due to convergence. *Molecular Phylogenetics and Evolution* **2:** 158–165.

Konings A. 2015. *Tanganyika Cichlids in their natural habitat*. El Paso, TX: Cichlid Press.

Lanfear R, Calcott B, Ho SY, Guindon S. 2012. PartitionFinder: combined selection of partitioning schemes and substitution models for phylogenetic analyses. *Molecular Biology and Evolution* **29:** 1695–1701.

Lopez-Fernandez H, Arbour J, Willis S, Watkins C, Honeycutt RL, Winemiller KO. 2014. Morphology and efficiency of a specialized foraging behavior, sediment sifting, in neotropical cichlid fishes. *PLoS ONE* **9:** e89832.

Losos JB. 1990. Concordant evolution of locomotor behaviour, display rate and morphology in *Anolis* lizards. *Animal Behaviour* **39:** 879–890.

Losos JB, Jackman TR, Larson A, Queiroz K, Rodriguez-Schettino L. 1998. Contingency and determinism in replicated adaptive radiations of island lizards. *Science* **279:** 2115–2118.

Machado-Schiaffino G, Kautt AF, Kusche H, Meyer A. 2015. Parallel evolution in Ugandan crater lakes: repeated evolution of limnetic body shapes in haplochromine cichlid fish. *BMC Evolutionary Biology* **15:** 9.

Mahler DL, Ingram T, Revell LJ, Losos JB. 2013. Exceptional convergence on the macroevolutionary landscape in island lizard radiations. *Science* **341:** 292–295.

Malmquist HJ. 1992. Phenotype-specific feeding behaviour of two arctic charr Salvelinus alpinus morphs. *Oecologia* **92:** 354–361.

Mattingly WB, Jayne BC. 2004. Resource use in arboreal habitats: structure affects locomotion of four ecomorphs of Anolis lizards. *Ecology* **85:** 1111–1124.

McDowall M. 2003. Variation in vertebral number in galaxiid fishes, how fishes swim and a possible reason for pleomerism. *Reviews in Fish Biology and Fisheries* **13:** 247–263.

Meyer BS, Salzburger W. 2012. A novel primer set for multilocus phylogenetic inference in East African cichlid fishes. *Molecular Ecology Resources* **12:** 1097–1104.

Meyer BS, Matschiner M, Salzburger W. 2015. A tribal level phylogeny of Lake Tanganyika cichlid fishes based on a genomic multi-marker approach. *Molecular Phylogenetics and Evolution* **83:** 56–71.

Miller MA, Pfeiffer W, Schwartz T. 2010. Creating the CIPRES Science Gateway for inference of large phylogenetic trees. *Gateway Computing Environments Workshop (GCE)* **2010:** 1–8.

Muschick M, Indermaur A, Salzburger W. 2012. Convergent evolution within an adaptive radiation of cichlid fishes. *Current Biology* **22:** 2362–2368.

Muschick M, Nosil P, Roesti M, Dittmann MT, Harmon L, Salzburger W. 2014. Testing the stages model in the adaptive radiation of cichlid fishes in East African Lake Tanganyika. *Proceedings of the Royal Society of London B: Biological Sciences* **281:** 1–10.

Orme D. 2012. *The caper package: comparative analysis of phylogenetics and evolution in R*.

Ostbye K, Amundsen PA, Bernatchez L, Klemetsen A, Knudsen R, Kristoffersen R, Naesje TF, Hindar K. 2006. Parallel evolution of ecomorphological traits in the European whitefish *Coregonus lavaretus* (L.) species complex during postglacial times. *Molecular Ecology* **15:** 3983–4001.

Paradis E, Claude J, Strimmer K. 2004. APE: analyses of phylogenetics and evolution in R language. *Bioinformatics* **20:** 289–290.

Post DM. 2002. Using stable isotopes to estimate trophic position: models, methods, and assumptions. *Ecology* **83:** 703–718.

R Development Core Team. 2008. *R: A language and environment for statistical computing*. Vienna, Austria: R Foundation for Statistical Computing. URL http://www.R-project.org. ISBN 3-900051-07-0.

Revell LJ. 2009. Size-correction and principal components for interspecific comparative studies. *Evolution* **63:** 3258–3268.

Revell LJ. 2012. phytools: an R package for phylogenetic comparative biology (and other things). *Methods in Ecology and Evolution* **3:** 217–223.

Rice AN, Westneat MW. 2005. Coordination of feeding, locomotor and visual systems in parrotfishes (Teleostei: Labridae). *Journal of Experimental Biology* **208:** 3503–3518.

Robinson BW, Wilson DS, Margosian AS. 2000. A pluralistic analysis of character release in pumpkinseed sunfish (*Lepomis gibbosus*). *Ecology* **81:** 2799–2812.

Rohlf F. 2010. *tpsDig, digitize landmarks and outlines, 2.15 edn*. Stony Brook, New York: Department of Ecology and Evolution: State University of New York.

Rundle HD, Nagel L, Wenrick Boughman J, Schluter D. 2000. Natural selection and parallel speciation in sympatric sticklebacks. *Science* **287:** 306–308.

Salzburger W, Meyer A, Baric S, Verheyen E, Sturmbauer C. 2002. Phylogeny of the Lake Tanganyika cichlid species flock and its relationship to the Central and East African haplochromine cichlid fish faunas. *Systematic Biology* **51:** 113–135.

Salzburger W, Van Bocxlaer B, Cohen AS. 2014. Ecology and evolution of the African Great Lakes and their faunas. *Annual Review of Ecology, Evolution, and Systematics* **45:** 519–545.

Santos ME, Salzburger W. 2012. How cichlids diversify. *Science* **338:** 619–621.

Schliewen UK, Tautz D, Paabo S. 1994. Sympatric speciation suggested by monophyly of crater lake cichlids. *Nature* **368:** 629–632.

Schluter D. 1993. Adaptive radiation in sticklebacks – size, shape, and habitat use efficiency. *Ecology* **74:** 699–709.

Schluter D. 2000. *The ecology of adaptive radiation*. New York, USA: Oxford University Press.

Streelman JT, Danley PD. 2003. The stages of vertebrate evolutionary radiation. *Trends in Ecology & Evolution* **18:** 126–131.

Sturmbauer C, Salzburger W, Duftner N, Schelly R, Koblmuller S. 2010. Evolutionary history of the Lake Tanganyika cichlid tribe Lamprologini (Teleostei: Perciformes) derived from mitochondrial and nuclear DNA data. *Molecular Phylogenetics and Evolution* **57:** 266–284.

Svanback R, Eklov P. 2004. Morphology in perch affects habitat specific feeding efficiency. *Functional Ecology* **18:** 503–510.

Thorsen DH, Westneat MW. 2005. Diversity of pectoral fin structure and function in fishes with labriform propulsion. *Journal of Morphology* **263:** 133–150.

Vanhooydonck B, Herrel A, Irschick DJ. 2006. Out on a limb: the differential effect of substrate diameter on acceleration capacity in Anolis lizards. *Journal of Experimental Biology* **209:** 4515–4523.

Webb PW. 1984a. Body form, locomotion and foraging in aquatic vertebrates. *American Zoologist* **24:** 107–120.

Webb PW. 1984b. Form and function in fish swimming. *Scientific American* **251:** 72–82.

Webb PW. 2006. Stability and maneuverability. *Fish Biomechanics* **23:** 281–332.

Wiens JJ, Morrill MC. 2011. Missing data in phylogenetic analysis: reconciling results from simulations and empirical data. *Systematic Biology* **60:** 719–731.

Wilson LAB, Colombo M, Sanchez-Villagra MR, Salzburger W. 2015. Evolution of opercle shape in cichlid fishes from Lake Tanganyika - adaptive trait interactions in extant and extinct species flocks. *Scientific Reports* **5:** 16909.

Zwickl DJ. 2006. *Genetic algorithm approaches for the phylogenetic analysis of large biological sequence datasets under the maximum likelihood criterion*. Austin, TX: The University of Texas at Austin.

SUPPORTING INFORMATION

Additional Supporting Information may be found in the online version of this article at the publisher's website:

Figure S1. Position of nine landmarks over the fish's body used to assess centroid size on each specimen. The picture shows *Gnathochromis permaxillaris*.
Figure S2. New phylogenetic hypothesis including 196 East African cichlid species. Bootstrap support values are indicated at nodes. The phylogeny is based on mitochondrial (ND2) sequences obtained from GenBank (see Supporting Information, Table S5) and nuclear sequence data (42 genes) obtained from Meyer *et al.* (2015); Meyer & Salzburger (2012) and GenBank (Supporting Information, Table S6).
Table S1. Sample sizes per species for fin area and muscle weight measurements.
Table S2. Characterization of 159 Lake Tanganyikan cichlid species according to benthic–limnetic and sandy–rocky habitat use.
Table S3. Results of a correlation analysis according to a classic linear model excluding the sexually dimorphic *Enantiopus melanogenys*.
Table S4. Results of a correlation analysis corrected for phylogenetic dependence of trait values using PGLS excluding the sexually dimorphic *Enantiopus melanogenys*.
Table S5. Listed are the used ND2 sequences with species name and accession number: first are the species for which nuclear markers are also available [from Meyer & Salzburger (2012) and Meyer *et al.* (2015)]; then followed by other available species (alphabetically ordered) with ND2. It is indicated if the species was used for further analyses.
Table S6. Additional sequences for nuclear loci downloaded from GenBank.

1.4.2
Supporting information

Figure S1. Position of nine landmarks over the fish's body used to assess centroid size on each specimen. The picture shows Gnathochromis permaxillaris.

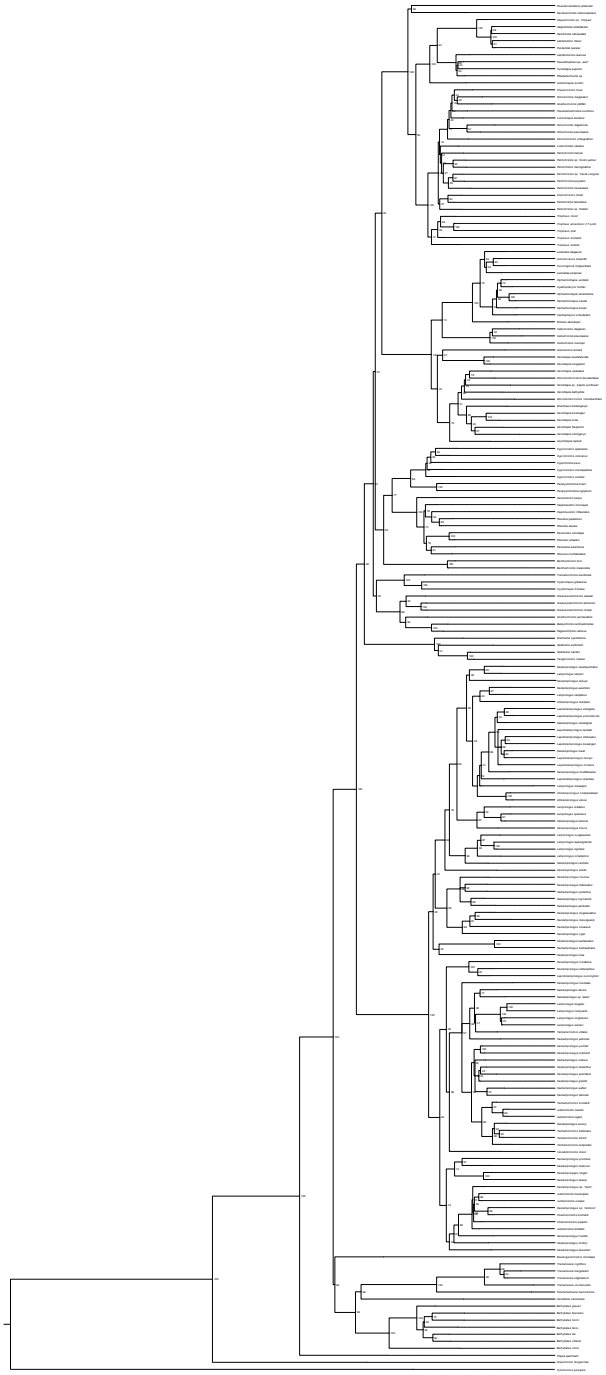

Figure S2. New phylogenetic hypothesis including 196 East African cichlid species. Bootstrap support values are indicated at nodes. The phylogeny is based on mitochondrial (ND2) sequences obtained from GenBank (see Supporting Information, Table S5) and nuclear sequence data (42 genes) obtained from Meyer et al. (2015); Meyer & Salzburger (2012) and GenBank (Supporting Information, Table S6).

Species	Tribe	Pectoral fin area	Pectoral muscle mass	Caudal fin area
Altolamprologus compressiceps	Lamprologini	19	20	20
Astatotilapia burtoni	Tropheini	22	21	22
Bathybates graueri	Bathybatini	20	20	20
Bathybates leo	Bathybatini	21	23	21
Boulengerochromis microlepis	Boulengerochromini	21	21	21
Cyphotilapia gibberosa	Cyphotilapiini	11	11	11
Cyathopharynx furcifer	Ectodini	21	22	21
Cyprichromis leptosoma	Cyprichromini	19	20	18
Enantiopus melanogenys	Ectodini	19	19	19
Eretmodus cyanostictus	Eretmodini	21	21	21
Gnathochromis permaxillaris	Limnochromini	22	22	22
Grammatotria lemairii	Ectodini	8	8	8
Hemibates stenosoma	Bathybatini	21	20	21
Interochromis loocki	Tropheini	20	20	20
Julidochromis ornatus	Lamprologini	20	15	20
Lamprologus lemairii	Lamprologini	21	21	21
Lepidiolamprologus attenuatus	Lamprologini	21	21	22
Lepidiolamprologus elongatus	Lamprologini	20	20	20
Lobochilotes labiatus	Tropheini	22	22	22
Neolamprologus tetracanthus	Lamprologini	20	19	20
Ophthalmotilapia ventralis	Ectodini	20	18	20
Perissodus microlepis	Perissodini	21	22	22
Petrochromis polyodon	Tropheini	20	20	20
Plecodus straeleni	Perissodini	12	12	11
Trematocara marginatum	Trematocarini	12	9	12
Tropheus moorii	Tropheini	21	21	21
Variabilichromis moorii	Lamprologini	18	21	19
Xenotilapia spiloptera	Ectodini	19	21	21
Total:		**532**	**530**	**536**

Table S1. Sample sizes per species for fin area and muscle weight measurements.

Species	benthic(1)-limnetic(4)	rock(r)-sand(s)
Altolamprologus calvus	2	r
Altolamprologus compressiceps	2	r
Altolamprologus fasciatus	2	r
Asprotilapia leptura	1	r
Astatotilapia burtoni	2	s
Aulonocranus dewindti	3	s
Baileychromis centropomoides	1	s
Bathybates fasciatus	3	s
Bathybates ferox	3	s
Bathybates graueri	4	s
Bathybates leo	4	s
Bathybates minor	4	s
Bathybates vittatus	4	s
Benthochromis horii	3	s

Benthochromis melanoides	4	s
Boulengerochromis microlepis	3	s
Callochromis macrops	1	r
Cardiopharynx schoutedeni	2	s
Chalinochromis brichardi	1	r
Chalinochromis popelini	1	r
Ctenochromis benthicola	2	r
Ctenochromis horei	1	s
Cunningtonia longiventralis	2	r
Cyathopharynx foae	3	s
Cyathopharynx furcifer	2	s
Cyphotilapia gibberosa	2	r
Cyprichromis coloratus	3	r
Cyprichromis leptosoma	3	r
Cyprichromis microlepidotus	3	r
Cyprichromis pavo	3	r
Ectodus descampsi	2	s
Enantiopus melanogenys	1	s
Eretmodus cyanostictus	1	r
Gnathochromis permaxillaris	1	s
Gnathochromis pfefferi	2	s
Grammatotria lemairii	1	s
Greenwoodochromis abeelei	2	s
Greenwoodochromis bellcrossi	2	s
Greenwoodochromis christyi	2	r
Haplotaxodon microlepis	3	s
Haplotaxodon trifasciatus	3	s
Hemibates stenosoma	4	s
Interochromis loocki	2	r
Julidochromis bifrenatus	1	r
Julidochromis dickfeldi	1	r
Julidochromis marlieri	2	r
Julidochromis ornatus	1	r
Julidochromis regani	1	r
Lamprologus callipterus	1	s
Lamprologus congoensis	2	r

Lamprologus kungweensis	1	s
Lamprologus laparogramma	1	s
Lamprologus lemairii	1	r
Lamprologus meleagris	1	s
Lamprologus mocquardi	1	s
Lamprologus ocellatus	1	s
Lamprologus ornatipinnis	1	s
Lamprologus signatus	1	s
Lamprologus speciosus	1	s
Lamprologus werneri	1	s
Lepidiolamprologus attenuatus	3	s
Lepidiolamprologus elongatus	2	r
Lepidiolamprologus hecqui	1	s
Lepidiolamprologus kendalli	2	r
Lepidiolamprologus mimicus	2	r
Lepidiolamprologus nkambae	2	r
Lepidiolamprologus profundicola	2	r
Lestradea perspicax	3	s
Limnochromis auritus	1	s
Limnochromis staneri	2	s
Limnotilapia dardenni	3	s
Lobochilotes labiatus	2	r
Microdontochromis rotundiventralis	3	s
Microdontochromis tenuidentatus	3	s
Neolamprologus bifasciatus	1	r
Neolamprologus brevis	1	s
Neolamprologus brichardi	2	r
Neolamprologus buescheri	1	r
Neolamprologus calliurus	1	s
Neolamprologus cancellatus	1	r
Neolamprologus caudopunctatus	2	r
Neolamprologus christyi	2	r
Neolamprologus crassus	2	r
Neolamprologus cunningtoni	2	s
Neolamprologus cylindricus	1	r
Neolamprologus falcicula	1	r

Neolamprologus furcifer	1	r
Neolamprologus gracilis	2	r
Neolamprologus helianthus	2	r
Neolamprologus leleupi	1	r
Neolamprologus leloupi	2	r
Neolamprologus longicaudatus	1	r
Neolamprologus marunguensis	2	r
Neolamprologus meeli	1	s
Neolamprologus modestus	2	s
Neolamprologus mondabu	2	s
Neolamprologus multifasciatus	1	r
Neolamprologus mustax	2	r
Neolamprologus niger	1	r
Neolamprologus nigriventris	1	r
Neolamprologus obscurus	1	r
Neolamprologus olivaceous	2	r
Neolamprologus pectoralis	1	r
Neolamprologus petricola	2	r
Neolamprologus prochilus	1	r
Neolamprologus pulcher	2	r
Neolamprologus savoryi	2	r
Neolamprologus sexfasciatus	2	r
Neolamprologus similis	1	r
Neolamprologus splendens	2	r
Neolamprologus tetracanthus	2	s
Neolamprologus toae	2	r
Neolamprologus tretocephalus	2	r
Neolamprologus variostigma	1	r
Neolamprologus ventralis	1	s
Neolamprologus wauthioni	NA	s
Ophthalmotilapia boops	2	r
Ophthalmotilapia heterodonta	2	r
Ophthalmotilapia nasuta	3	r
Ophthalmotilapia ventralis	2	r
Oreochromis tanganicae	3	s
Paracyprichromis brieni	3	r

Paracyprichromis nigripinnis	2	r
Perissodus eccentricus	3	s
Perissodus microlepis	2	r
Perissodus paradoxus	3	s
Petrochromis famula	1	r
Petrochromis fasciolatus	2	r
Petrochromis macrognathus	1	r
Petrochromis orthognathus	2	r
Petrochromis polyodon	1	r
Petrochromis sp. 'Kipili brown'	2	r
Petrochromis trewavasae	1	r
Plecodus elaviae	3	s
Plecodus multidentatus	3	s
Plecodus straeleni	2	r
Pseudosimochromis curvifrons	2	r
Reganochromis calliurus	1	s
Simochromis babaulti	1	s
Simochromis diagramma	1	r
Simochromis marginatum	1	r
Simochromis pleurospilus	1	s
Spathodus erythrodon	1	r
Tanganicodus irsacae	1	r
Telmatochromis bifrenatus	1	r
Telmatochromis brachygnathus	1	r
Telmatochromis dhonti	2	s
Telmatochromis temporalis	2	r
Telmatochromis vittatus	1	s
Telotrematocara macrostoma	2	s
Trematocara marginatum	2	s
Trematocara nigrifrons	2	s
Trematocara stigmaticum	2	s
Trematocara unimaculata	2	s
Trematocara variabilae	2	s
Triglachromis otostigma	1	s
Tropheus annectens	2	r
Tropheus brichardi	1	r

Tropheus duboisi	2	r
Tropheus moorii	1	r
Tropheus polli	2	r
Tylochromis polylepis	2	s
Variabilichromis moorii	2	r
Xenotilapia bathyphila	1	s
Xenotilapia boulengeri	1	s
Xenotilapia caudafasciata	1	s
Xenotilapia flavipinnis	1	s
Xenotilapia longispinis	1	s
Xenotilapia nigrolabiata	1	s
Xenotilapia ochrogenys	1	s
Xenotilapia ornatipinnis	1	s
Xenotilapia papilio	2	r
Xenotilapia sima	1	s
Xenotilapia spiloptera	2	r

Table S2. Characterization of 159 Lake Tanganyikan cichlid species according to benthic–limnetic and sandy– rocky habitat use.

Pectoral fin area				
	t-value	adjusted p-value	R^2	$N_{species}$
Pectoral muscle mass	7.859	**0.000**	0.712	27
Caudal fin area	5.779	**0.000**	0.572	27
δ15N	-3.630	**0.007**	0.364	25
δ13C	2.838	**0.047**	0.259	25
Intestinal tract length	5.105	**0.000**	0.554	23
Caudal fin area				
	t-value	adjusted p-value	R^2	$N_{species}$
Pectoral fin area	5.779	**0.000**	0.572	27
Pectoral muscle mass				
	t-value	adjusted p-value	R^2	$N_{species}$
Pectoral fin area	7.859	**0.000**	0.712	27

Table S3. Results of a correlation analysis according to a classic linear model excluding the sexually dimorphic *Enantiopus melanogenys*.

Pectoral fin area					
	t-value	adjusted p-value	R^2	lambda	$N_{species}$
Pectoral muscle mass	7.083	**0.000**	0.667	0.964	27
Caudal fin area	4.498	**0.001**	0.447	1	27
δ15N	-2.967	**0.034**	0.277	0.997	25
δ13C	0.952	1	0.038	1	25
Intestinal tract length	4.175	**0.002**	0.454	1	23
Caudal fin area					
	t-value	adjusted p-value	R^2	lambda	$N_{species}$
Pectoral fin area	5.779	**0.000**	0.572	0	27
Pectoral muscle mass					
	t-value	adjusted p-value	R^2	lambda	$N_{species}$
Pectoral fin area	7.218	**0.000**	0.676	0.880	27

Table S4. Results of a correlation analysis corrected for phylogenetic dependence of trait values using PGLS excluding the sexually dimorphic Enantiopus melanogenys.

Table S5. Listed are the used ND2 sequences with species name and accession number: first are the species for which nuclear markers are also available [from Meyer & Salzburger (2012) and Meyer et al. (2015)]; then followed by other available species (alphabetically ordered) with ND2. It is indicated if the species was used for further analyses.
(not shown here due to vast size)

Table S6. Additional sequences for nuclear loci downloaded from GenBank.
(not shown here due to vast size)

1.5
Evolution of opercle bone shape in cichlid fishes from Lake Tanganyika - adaptive trait interactions in extant and extinct species flocks

Scientific Reports

I provided the raw data and helped analyzing the results and drafting the manuscript. LW conducted the geometric morphometric analyses and drafted the manuscript. All authors participated in discussing the manuscript and drafting the final version.

SCIENTIFIC REPORTS

OPEN

Evolution of opercle shape in cichlid fishes from Lake Tanganyika - adaptive trait interactions in extant and extinct species flocks

Received: 14 June 2015
Accepted: 22 October 2015
Published: 20 November 2015

Laura A. B. Wilson[1], Marco Colombo[2], Marcelo R. Sánchez-Villagra[3] & Walter Salzburger[2]

Phenotype-environment correlations and the evolution of trait interactions in adaptive radiations have been widely studied to gain insight into the dynamics underpinning rapid species diversification. In this study we explore the phenotype-environment correlation and evolution of operculum shape in cichlid fishes using an outline-based geometric morphometric approach combined with stable isotope indicators of macrohabitat and trophic niche. We then apply our method to a sample of extinct saurichthyid fishes, a highly diverse and near globally distributed group of actinopterygians occurring throughout the Triassic, to assess the utility of extant data to inform our understanding of ecomorphological evolution in extinct species flocks. A series of comparative methods were used to analyze shape data for 54 extant species of cichlids (N = 416), and 6 extinct species of saurichthyids (N = 44). Results provide evidence for a relationship between operculum shape and feeding ecology, a concentration in shape evolution towards present along with evidence for convergence in form, and significant correlation between the major axes of shape change and measures of gut length and body elongation. The operculum is one of few features that can be compared in extant and extinct groups, enabling reconstruction of phenotype-environment interactions and modes of evolutionary diversification in deep time.

Understanding how organismal diversity is generated and maintained, why some groups diversify when others remain relatively unchanged over geological time, and how organisms adapt to and interact with the environment are key challenges in evolutionary biology. Adaptive radiations, defined as rapid and extensive diversifications from an ancestral species that result in descendants adapted to exploit a wide array of ecological niches[1,2], are widely recognized as fundamental subjects of investigations into organismal diversification.

The species flocks of cichlid fishes from the East African Great Lakes collectively represent an unparalleled example of adaptive radiation in vertebrates[3–6]. In all of the three major lakes, one or several species have radiated to produce flocks comprising more than 500 species each in Lakes Malawi and Victoria, and at least 200 species in Lake Tanganyika (LT)[7], which is the oldest of the three with an estimated age of around nine to 12 million years[8,9]. Unlike the quasi-monophyletic haplochromine species flocks in Lakes Malawi and Victoria, the species flock in Tanganyika consists of several ancient lineages that radiated in parallel[9–11]. Molecular markers have been used to reconstruct the recent history of the LT radiation, revealing that the LT species flock was established in a series of cladogenic events that coincided with changes in the lake's environment. An initial diversification event by seeding lineages occurred around the early stage of lake formation, represented by several shallow protolakes at around

[1]School of Biological, Earth and Environmental Sciences, University of New South Wales, Sydney, NSW 2052, Australia. [2]Zoological Institute, University of Basel, Vesalgasse 1, CH 4051, Basel, Switzerland. [3]Paläontologisches Institut und Museum, Karl-Schmid Strasse 4, CH 8006, Zürich, Switzerland. Correspondence and requests for materials should be addressed to L.A.B.W. (email: laura.wilson@unsw.edu.au) or W.S. (email: walter.salzburger@unibas.ch)

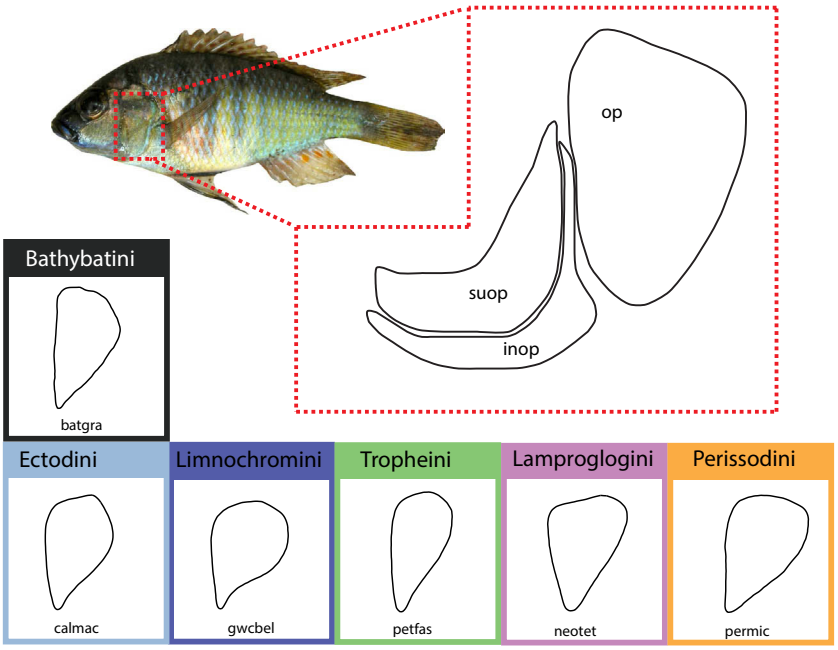

Figure 1. Photograph of *Astatotilapia burtoni* (astbur) showing the position of the operculum. Illustration of the operculum (op), and adjacent bones of the suboperculum (suop) and interoperculum (inop) are not to scale. Examples of operculum shape for several of the groups examined in this study are provided in the labelled, colored boxes. Species illustrated are: *Bathybates graueri* (batgra), *Callochromis macrops* (calmac), *Greenwoodochromis bellcrossi* (gwcbel), *Petrochromis famula* (petfas), *Neolamprologus tetracanthus* (neotet), and *Perissodus microlepis* (permic).

9–12 MYA[8,9]. A subsequent diversification, involving seven ancient lineages and referred to as the 'primary lacustrine radiation', occurred around the time that the protolakes became deeper and joined to form a single deep lake, around 5–6 MYA[9]. LT cichlids are the most morphologically, ecologically and behaviorally diverse of the three lake flocks, and a number of studies have explored evolutionary patterns in the group. These include coloration patterns[12,13], parental care strategies[14–16], patterns of mouth morphology[17–19], and brain and body size evolution[18–22].

Among the morphological traits examined in LT cichlids so far, most comprise combinations of linear measurement or scored character data and, with the notable exception of body shape and size measures, few traits are directly amenable to comparison with other species flocks, such as sticklebacks and Antarctic notothenioids, which represent radiations of different geological age that have occurred in different environmental settings (marine, lacustrine, riverine). Uncovering commonalities in trait complex evolution in phylogenetically, morphologically and ecologically distinct species flocks would be highly desirable in assessing key questions underpinning how adaptive radiation progresses. Issues include the general extent to which diversification occurs in stages[23,24], recently tested in LT cichlids by Muschick and colleagues[19], and how well an early burst model, which predicts that major ecological differences occur early in a clades' history[25], fits adaptive radiation in fishes (see e.g.[26]). Illuminating trait patterning in deep time would be equally valuable, by focusing attention towards searching for traits that may also be measured in extinct species flocks (e.g.[25,27]).

In this paper, we build upon our earlier geometric morphometric investigations of operculum shape in extant[28] and extinct species flocks[29] by quantifying evolutionary patterns in this trait for an extensive sample of LT cichlids. The operculum is a flat and slightly curved bone plate that, together with the suboperculum, makes up the gill cover in osteichthyans (Fig. 1). It forms a ball-and-socket connection with the hyomandibula, which enables inward-outward movement of the gill cover to expand and compress the opercular chamber during the suction pump phase of the respiratory cycle[30,31]. In cichlids, the operculum is connected to the neurocranium (via m. levator operculi) and the gill cover complex forms a second mechanism assisting in mouth opening[32]. The considerable diversity in operculum shape and size among osteichthyans has been attributed to the important role of this bone in respiration and the jaw opening mechanism of some fishes through its functional connectivity to the lower jaw[33]. Owing to these properties, and further supported by insight from studies of operculum morphogenesis in zebrafish that have illuminated genetic pathways influencing its shape and size (e.g.[34,35]), the operculum has been

the subject of several investigations, particularly in the threespine sticklebacks[33,36,37]. The occurrence of a parallel divergence in operculum shape following a 'dilation-diminution model', defined as dorsal-ventral compression coupled with anterior-posterior extension of the outline shape[33], has been demonstrated to be a widespread phenomenon between oceanic and freshwater threespine sticklebacks[38–40]. Differences in operculum shape have also been found between sticklebacks inhabiting deep lakes, shallow lakes and streams, indicating a functional difference among phenotypes[37]. Recent analysis of operculum shape in Antarctic notothenioids, using phylogenetic comparative methods, revealed also a general trend in shape change along a macrohabitat-related axis (benthic-pelagic[28]), further highlighting the utility of this trait in assessing ecomorphological interactions on a broad scale. That earlier study revealed evolutionary patterns in shape best fit a model of directional selection (Ornstein-Uhlenbeck), and did not support an early burst model of adaptive radiation in notothenioids[28]. Importantly, the operculum is one of only few morphological features that can be studied in fossil groups because it is commonly well preserved.

The extent to which observed patterns in operculum shape evolution among extant species flocks may be similarly recovered in extinct species flocks requires considerable further effort to understand. Previously operculum shape evolution has been studied in a subset of the diverse species flock of *Saurichthys* (>35 species[41]), a near globally distributed genus of actinopterygian fishes that occurred from the Late Permian (245 MYA) to the Early Jurassic (176 MYA)[42]. Being the presumably first group of fishes to have evolved an elongated, slender body plan, saurichthyids have been reconstructed as bearing physical resemblance to the modern day garfish, likely a fast-swimming predator, and are known to have occupied both marine and freshwater realms[42]. Owing to their rather distinctive morphology, saurichthyids have been quite well-documented in the fossil record[41] and particularly a number of exceptionally preserved specimens are known from the UNESCO site of Monte San Giorgio in Switzerland, allowing for detailed study of axial elongation patterns[43,44]. Similar to the dilation-diminution model uncovered in studies by Kimmel and colleagues, species-specific change in operculum shape among members of the genus *Saurichthys* was concentrated to a narrowing along the anterior-posterior margin antagonistically coupled with perpendicular extension along the dorsal-ventral axis[29].

As a preliminary pathway to uniting evolutionary patterns for trait data in extinct and extant species flocks, we here place our earlier data on opercle shape and body elongation in *Sauricthys*[29,44] within the framework of a much larger sample of LT cichlid data, for which we are able to measure the same traits, and complement those with additional ecological variables. The species flock of *Saurichthys* was chosen as example for this study because it possesses several favorable attributes. The saurichthyids are a distinctive group that is well-documented from Triassic deposits in Europe, particularly the Besano and Cassina formations (Monte San Giorgio, Switzerland) and the Prosanto formation (Ducan-Landwasser, Switzerland), thereby allowing for detailed palaeoecological, faunal and stratigraphical information to be extracted for numerous species (e.g.[45]), and ultimately enabling temporal changes in morphological disparity to be quantified. Previous work on the operculum of *Saurichthys*[29,46,47] has indicated that opercle shape is a key feature for distinguishing among several species, and considerable variation in opercle shape has been linked to behavioural differences. A comprehensive examination of operculum variation and evolution in saurichthyids is of particular interest for understanding ecomorphotype segregation for sympatric groups[47].

Our cichlid dataset contains a considerable proportion of species present in LT (Fig. 2), including the most abundant ones that coexist in the southern basin of the lake[19], and spans the majority of LT cichlid tribes. Ecological diversity is well represented in the sample, which includes epilithic algae grazers, scale eaters, fish hunters, invertebrate pickers and species that dwell in sandy, rocky or open water areas. Using the LT cichlid data set, we apply phylogenetic comparative methods to a) examine the patterns of opercle shape and size disparity over time; b) test for phenotype-environment correlations between operculum shape and size using stable isotope data as proxy for macrohabitat and trophic niche; c) examine whether operculum shape and size are related to recognized adaptive trait complexes and assess the utility of those interactions for data from fossil species; and d) test the fit of competing macroevolutionary models to our data.

Results

Operculum shape and form space. Phylomorphospace plots indicated a considerable amount of variation in operculum shape and overlap between members of different tribes (Fig. 3). The first PC axis (43.9% variance) separated Bathybatini plus the lamprologine *A. calvus* (Fig. 3A (i)) from the other groups. Positive PC1 scores, exhibited by members of Bathybatini, reflected compression along the anterior dorsal and posterior ventral margin of the operculum along with extension along the posterior dorsal and anterior ventral margin (Fig. 3A). Negative scores along PC2 (20.4%) reflected a widening of the operculum along the anterior-posterior axis and a shortening along the dorsal-ventral axis, whereas positive scores reflected the reverse. Generally, some separation along this axis is evident between Lamprologini (negative scores) and Tropheini (positive scores), overlapping with Ectodini, as for example the second most extreme positive value is represented by a member of the latter tribe (*O. ventralis*: ophven). Noteworthy is that the PC1-PC2 plot (Fig. 3A) shows more or less complete overlap in morphospace occupation for Tropheini and Ectodini relative to different regions of morphospace occupied by Lamprologini and Bathybatini. A division in morphospace occupation is also visible for members of Lamprologini wherein members of *Neolamprologus* have negative scores along PC2 and are separated

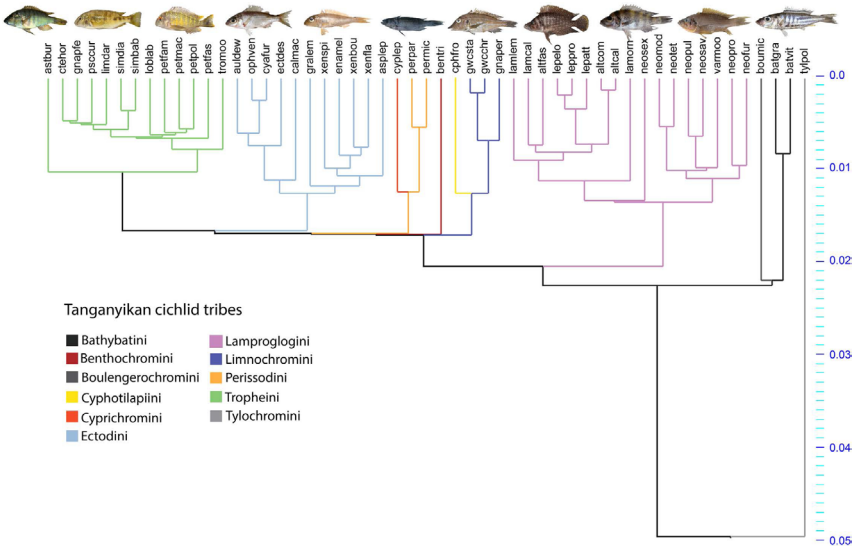

Figure 2. Phylogenetic relationships among the species studied here, pruned from the phylogeny of Muschick *et al.* (2012) which was based on two nuclear (*erdnrb1*, *phpt1*) and one mitochondrial (ND2) marker and the GTR+G model of molecular evolution. See Supplementary Table 1 for full details of species acronyms. Images shown are, from left to right: *Astatotilapia burtoni* (asbur), *Simochromis babaulti* (simbab), *Tropheus moori* (tromoo), *Cyathopharynx furcifer* (cyafur), *Xenotilapia spiloptera* (xenspi), *Perissodus microlepis* (permic), *Gnathochromis permaxillaris* (gnaper), *Altolamprologus calvus* (altcal), *Neolamprologus sexfasciatus* (neosex), *Neolamprologus pulcher* (neopul) and *Bathybates graueri* (batgra).

from other species in Lamprologini, belonging to *Lamprologus*, *Altolamprologus* and *Lepidolamprologus*. PC3 (12.5%) largely reflected shape changes occurring along the dorsal edge of the bone, resulting in a more asymmetrical shape of the bone at the dorsal margin, either angled with more bone extending on the anterior (negative PC3 score) or posterior (positive PC3 score) side (Fig. 3B). PC3 resulted in some minor separation between Tropheini and Ectodini (slightly higher PC3 scores).

The projection of shape data into form space, including centroid size, resulted in two PC axes comprising more than 95% of the sample variance. PC1 contains size-related shape change, accounting for 92.4% of sample variance. This reflects a change from species with smaller bones exhibiting expansion and compression along the posterior and anterior margin of the operculum (e.g. *Altolamprologus compressiceps* [altcom], *Lamprologus ornatipinnis* [lamorn] and *A. fasciatus* [altfas]), respectively, to species with larger bones showing expansion of the dorsal anterior margin and compression of the dorsal posterior margin (e.g. *Bathybates vittatus* [batvit], *B. graueri* [batgra], and *Benthrochromis tricoti* [bentri]) (Supplementary Fig. 1).

Operculum shape patterns associated with feeding ecology. CVA for feeding preference groupings resulted in a clear separation along CV1 (43.5%) between microvertebrate/algae eaters (negative scores) and piscivores (positive scores), with generalist and benthic invertebrate feeders occupying an intermediate position between the two. CV1 largely reflected shape change along the posterior margin of the operculum, with piscivores having a dorsally-broader bone that tapers postero-ventrally. CV2 (18.0%) separates the scale eaters (*Perissodus*) and zooplankton feeders, both of which are located at the positive end of CV2, from piscivores and generalist feeders, which both have negative scores for CV2 (Fig. 4A). CV2 shows that *Perissodus* and zooplankton feeders typically have a more anteriorly widened bone compared to species occupying the negative end of that axis.

CVA conducted on feeding mode revealed a clear separation between all feeding mode categories with the exception of benthic invertebrate pickers and suction groups that overlapped almost completely in CV1-CV2 morphospace (Fig. 4B). CV1 (34.9%) separated the rockpicking group (negative scores) from the scale group (positive scores), with other groups distributed in between those two extremal categories. Similar to the CVA of feeding preference, CV1 distinguished *Perissodus* as having opercles that were widened along the dorsal anterior-posterior margin. CV2 (26.7%) clearly separated the ram and suction feeders, which are shown to have a dorsally flattened opercle margin and general wider bone, from species that sandpick, algaepick and rockpick (Fig. 4B). Results of Procrustes ANOVA indicated

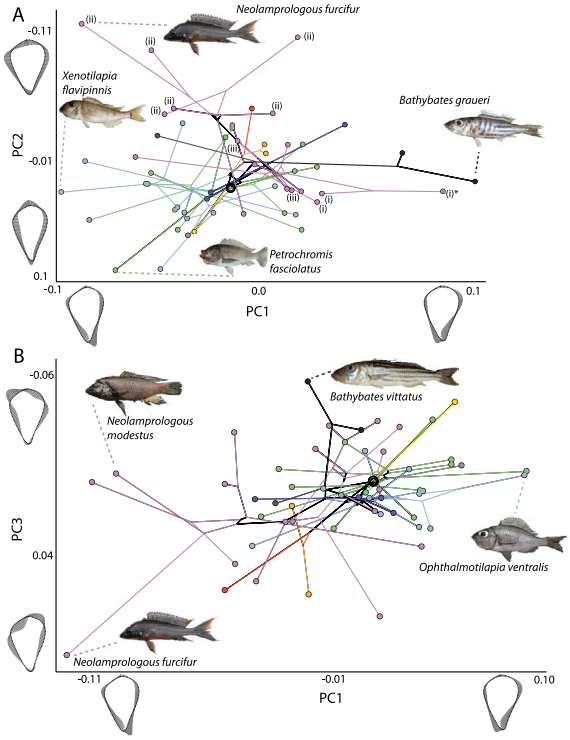

Figure 3. Phylomorphospace projections of cichlid relationships into operculum shape space, showing (A) PC1 vs. PC2 and (B) PC1 vs. PC3. Branches are colored by tribe (see Fig. 2), and the root is denoted by concentric ellipses. Patterns of outline shape change associated with each axis are illustrated using mean shape models and vector displacements. Labelled groups (i) *Altolamprologous*, (ii) *Neolamprologous*, (iii) *Lepidolamprologous* and taxon (i)* *Altolamprologous calva* are referred to in the text. Images of fish are not to scale.

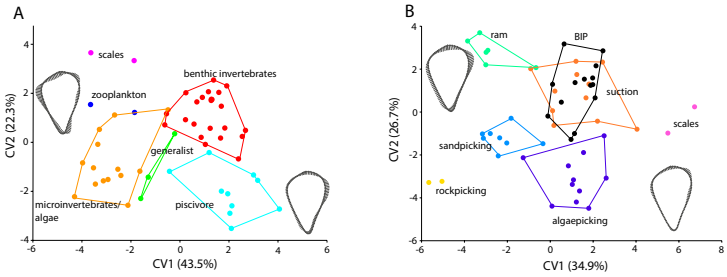

Figure 4. Results of Canonical Variates (CV) Analysis for operculum shape data, showing species mean values, grouped according to (A) feeding preference and (B) feeding mode categories.

a significant effect of both feeding mode ($F_{5,410} = 3.70$, $P < 0.001$) and feeding preference on operculum size and shape ($F_{5,410} = 6.49–10.63$, $P < 0.001$).

Correlation between operculum shape and ecological trait and niche data. Correlations were computed using phylogenetically corrected regressions for operculum shape and form space axes, and centroid size against isotope values, gut length, gill raker traits and ER. Overall, significant results were limited to a subset of the investigated variables, with no significant relationship between operculum size or shape and gill raker numbers (grnDa, grnVa) or values of $\delta_{13}C$. Gut length data were found to be significantly correlated with PC2 ($P = 0.003$, correlation $= -0.16$; Fig. 5B), mainly reflecting a distinction between members of Lamprologini, having low scores along PC2 and shorter intestine length relative

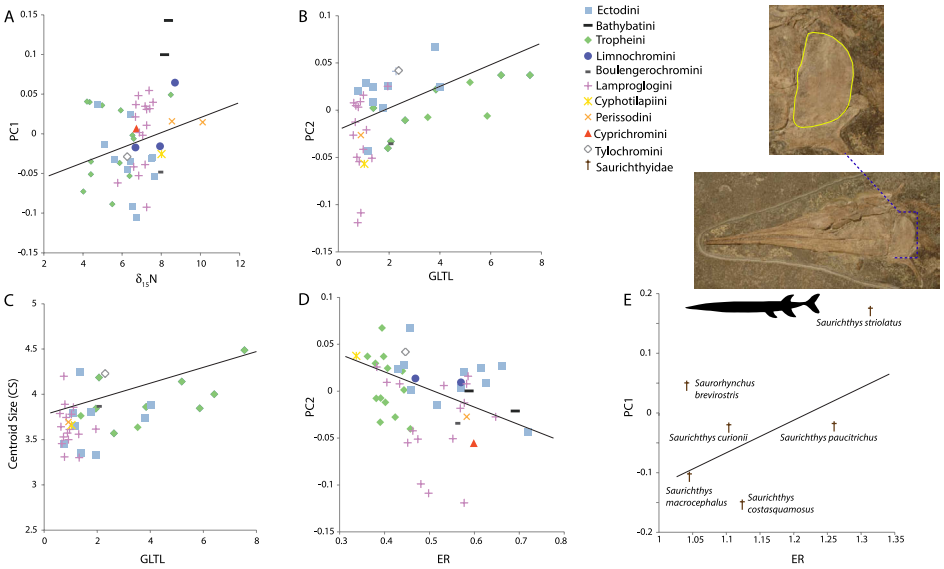

Figure 5. Phenotype-environment correlations for selected (significant) trait interactions, regression lines are produced using the Phylogenetic Generalized Least Squares (PGLS) model. Species mean values for centroid size and PC (axes 1 or 2) scores from a PCA of operculum shape data were plotted against mean values for: (**A**) $\delta_{15}N$, which is a proxy for trophic level wherein larger values reflect a higher trophic position; (**B**,**C**) gut length standardized by total length (GLTL); (**D**) Elongation Ratio (ER), and (**E**) Elongation Ratio for specimens belonging to the extinct species flock of saurichthyids (denoted by †). A generalized sketch of the elongate body plan of saurichthyids is shown (modified from[27]), and inset a photograph of *S. macrocephalus* T4106 (Paläontologisches Institut und Museum, Zürich; photo: Rosi Roth). The dashed line indicates the position of the operculum, highlighted inset by a colored outline.

to body length, and Tropheini, typically possessing longer relative intestine lengths and positive scores along PC2. A significant relationship was also found between GLTL and PC1 of form space ($P = 0.017$, correlation $= 0.016$), and centroid size ($P = 0.022$, correlation $= -0.16$; Fig. 4C). PC2 and ER were also found to be correlated ($P = 0.041$, correlation $= -0.54$; Fig. 5D) with more elongate species (greater values for ER) having generally more negative PC2 scores. We also examined plots of the relationship between operculum shape and ER for the six saurichthyid species. Both PC1 ($P = 0.06$, correlation $= 0.56$) and PC2 ($P = 0.32$, correlation $= -0.26$) were correlated with ER, however these correlations were not significant. The saurichthyids were more elongate (ER values of < 2) than the LT cichlids studied here, and PC1 (shown in Fig. 5E) for the saurichthyid data set expressed the same mode of shape change captured by PC2 of the LT cichlids (see shape models bordering PC2 on Fig. 3A). Among the fossil taxa, PC1 variance showed some phylogenetic grouping (Supplementary Fig. 2) and is likely explained by the large variance in body size in the sample. Apart from the small-bodied *Saurichthys striolatus* (100–180 mm[48]) (Fig. 5E), the sample included several large-bodied species (e.g. *S. costasquamosus,* >1 meter[41]). The relationship between ER and size-related shape change of the operculum requires a thorough examination in other extinct species flock. Our results recover a common pattern of size-related shape change for the two species flocks, holding promise for future examination of macroevolutionary dynamics for this trait.

Macroevolutionary model test of operculum shape and size evolution. Model fitting results indicated that PC axes of operculum shape showed best fit to different models. In contrast to the other shape variables, PC1 was best fit by the WN model, however AICc values showed very small magnitudes of difference between that model and all others (ΔAICc $= 0.26$–0.49), apart from BM, which was least favored (ΔAICc $= 5.20$) (Table 1). Pagel's λ was marginally best supported for PC2 and both BM and WN fit least well (ΔAICc $= 4.97$–4.99) (Table 1). Again, differences were quite small for AICc values among OU, EB, Pagel's δ and Pagel's λ indicating a single model could not be clearly distinguished as best fit. PC3 and centroid size fit best to Pagel's δ and, of the three shape axes examined, PC3 showed the most difference in fit across the tested models (Table 1).

Blomberg's *K* values were less than 1 for all examined axes of shape space, and for centroid size (Table 2). Values of <1 for the *K* statistic indicate less phylogenetic signal than expected under a Brownian motion, whereas values of >1 would indicate close relatives are more similar in operculum

Variable	PC1				PC2				PC3				Centroid size			
Model	LogL	AICc	dAICc	Akaike Weight	LogL	AICc	dAICc	Akaike Weight	LogL	AICc	dAICc	Akaike Weight	LogL	AICc	dAICc	Akaike Weight
BM	77.53	−150.81	5.20	0.017	92.59	−180.93	4.97	0.021	105.25	−206.25	1.91	0.134	26.24	−48.22	1.66	0.106
OU	81.11	−155.71	0.29	0.193	96.09	−185.68	0.22	0.231	105.42	−204.33	3.82	0.051	28.10	−49.70	0.19	0.222
WN	80.13	−156.00	0.00	0.224	92.57	−180.90	4.99	0.021	105.27	−206.30	1.86	0.137	24.50	−44.75	5.13	0.019
δ	81.13	−155.74	0.26	0.197	96.13	−185.74	0.16	0.238	107.33	−208.16	0.00	0.347	28.20	−49.88	0.00	0.244
EB[1]	81.11	−155.71	0.29	0.194	96.10	−185.68	0.22	0.230	107.14	−207.77	0.39	0.286	28.10	−49.70	0.19	0.223
λ	—	−155.52	0.49	0.175	—	−185.90	0.00	0.258	—	−204.10	4.06	0.046	—	−49.36	0.53	0.187

Table 1. Results of macroevolutionary models fit to axes of operculum shape (PC1-PC3) and centroid size data: Brownian Motion (BM), Ornstein-Uhlenbeck (OU), White noise (WN), Pagel's delta (δ) and lambda (λ), Early Burst (EB). Akaike weight values were calculated using AICc (AIC corrected for sample size). Delta (d) AICc is calculated as the difference between the candidate model AICc and the AICc for the best fitting model (i.e. the one with the lowest AICc). [1]Alpha (α) values were 193.02 (PC1), 160.02 (PC2), 150.30 (PC3) and 106.94 (centroid size)

Variable				
Test	PC1	PC2	PC3	Centroid Size
Blomberg's K Statistic	0.337	0.415	0.392	0.592
P	0.021	0.004	0.007	0.004
Pagel's λ	0.746	0.777	0.945	0.851

Table 2. Results of tests for phylogenetic signal in axes of operculum shape data (PC1-PC3) and centroid size data.

traits than expected given the topology and branch lengths. Values ranged from *K* of 0.34 (PC1) to 0.59 (centroid size). Generally, values of *K* were quite low for PC axes, and lowest for PC1, reflected also in the low Akaike weight (probability 0.02) of that model. Our reported range of 0.34 (PC1) to 0.42 (PC2) for *K* corresponds well with that of earlier reported values for PC axes of body shape (range = 0.41–0.44), and is lower than that for PC axes of lower pharyngeal jaw (LPJ) shape (range = 0.48–0.67) (Table S3[19]). Pagel's λ values for quantifying phylogenetic signal in the data indicate a continual increase from λ = 0.75 for PC1 to λ = 0.95 for PC3 (Table 2). Values of λ range from 0, reflecting a star phylogeny and no phylogenetic signal, to 1, which recovers the Brownian motion model. Since a Pagel's λ value of 1 would recover the BM model, the latter result is also reflected in the substantially larger Akaike weight for the BM model fit to PC3 (probability 0.13), than the other axes (<0.03). Previous quantification of phylogenetic signal in shape data recovered similar Pagel's λ values, ranging from λ = 0.44–0.88 for body shape and λ = 0.83–0.95 for LPJ shape[19].

Values for α from EB model fitting were positive for all shape axes and centroid size, indicating acceleration in trait evolution. Pagel's δ values were also greater than 1 for all measured axes and centroid size (range 5.06–8.67); δ values >1 indicate a concentration of evolution in the operculum shape and size traits towards present. If Pagel's δ values were <1 this would indicate that branch lengths are transformed to become increasingly shorter towards the tips, meaning that trait change occurred mainly along basal branches. Operculum shape appears to be evolving more rapidly than size, as indicated by larger values for α. The time-dependent models were not better fit than alternative tested models in the case of centroid size. In contrast, for PC1 and PC2, Pagel's δ, EB and OU appear to be considerably better supported (ΔAICc >4) then the BM model (Table 1).

Pairwise distance-contrast plots indicate a general trend that is compatible with convergence, showing most species pairs occupy the quadrant of the plot represented by small morphological distances yet large phylogenetic distance (Fig. 6). Similarly, for a considerable number of species pair comparisons the observed interspecific similarity is slightly greater than expected under BM given the phylogenetic distance between the species pair (Fig. 6B). Results of pairwise comparison between the observed data and simulated data resulted in 87 species pairs being more similar than expected under BM, which is around three times more than expected by chance from the model. These pairs include a number of comparisons between members of Limnochromini and Lamproglogini.

Disparity through time. Disparity through time analyses resulted in generally similar patterns of average clade disparities for shape and size across the time slices plotted (Fig 7). Shape disparity

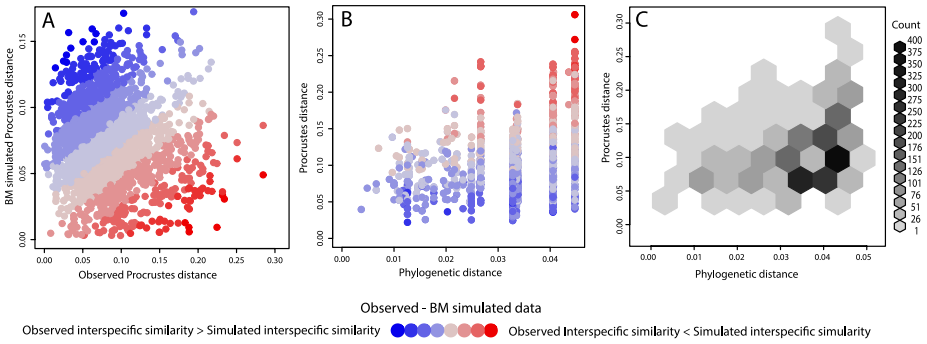

Figure 6. Pairwise distance-contrast plots, (A) colored using the difference between observed and simulated interspecific morphological distance, (B) showing the relationship between phylogenetic and morphological distance for all species pairwise comparisons data points, and for (C) binned values using N = 8 hexagonal bins. Interspecific morphological distances were simulated using Brownian motion to assess the relative similarity in shape between species pairs compared to that expected under neutral evolution on the given phylogeny.

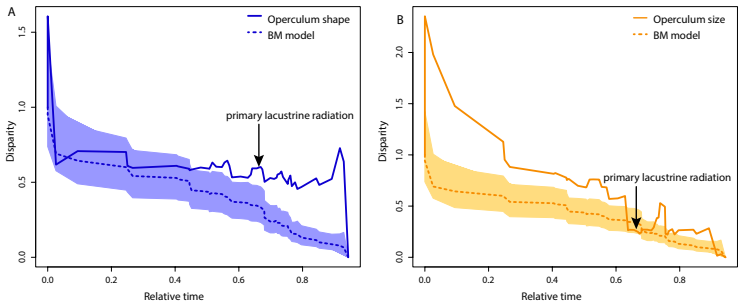

Figure 7. Disparity Through Time (DTT) plots for operculum shape (A) and centroid size (B) data. Mean values were used for each species, following the relationships depicted in Fig. 2. Disparity along the Y axis is the average subclade disparity divided by total clade disparity and is calculated at each internal node of the tree. The dotted lines represent values of trait disparity expected under Brownian motion by simulating operculum size and shape evolution 10000 times each across the tree. For relative time values 0.0 represents the root and 1.0 the tip of the phylogeny. Shaded areas on each plot indicate the 95% confidence interval for the simulations. The approximate timing of the primary lacustrine radiation, a synchronous diversification within several lineages that is thought to have coincided with the establishment of deep-water conditions in a clear lacustrine habitat[8–10] is indicated.

remained relatively stable through time (Fig. 7A), whereas size disparity (Fig. 7B) tended to decline over time until reaching a plateau around 0.65 relative time, followed by a subsequent increase. Both shape and size disparity deviated positively from simulations under BM, indicating a slightly greater amount of overlap in morphospace among sublades than would be expected under neutral evolution. Values for MDI were deviated significantly from BM simulations for both shape ($P = 0.0049$) and size ($P < 0.001$). The morphological disparity index (MDI), which indicates the amount of difference in disparity between observed trait data and data expected under BM, was greater for operculum size (MDI = 0.35) than for shape data (MDI = 0.15). Neither plots show clear evidence for an Early Burst in these traits, which is in accordance with the above reported α values for the EB calculations and the Pagel's δ values, which together point towards more evolutionary change in the recent fauna for operculum size and shape.

Discussion

The species flock of LT cichlids is well-recognized as an ideal model system for studying how organismal diversity emerges[5,49,50]. The operculum, a functionally-important craniofacial element for which comparative data are available from other extant species flocks and may be acquired from extinct species flocks, is here studied in a comprehensive sample of LT cichlids. Our results indicate (a) a similar mode of operculum shape change to that previously uncovered for other species flocks; (b) stability in the patterns of shape disparity through time, whereas size disparity tended to decline followed by a subsequent increase

around the time of the "primary lacustrine radiation"[10]; (c) a lack of unequivocal support for a single evolutionary model, yet suggested that operculum shape evolution fit well to time-dependent models (Pagel's δ); (d) evidence for differences in operculum shape relating to feeding preference and feeding mode, especially between piscivores and algivores, providing preliminary support for the potential utility of this trait in dietary inference; and (e) a significant relationship between operculum shape and several traits, including measures of elongation, which may also be potentially recovered for extinct species flocks.

Relationship between operculum shape and feeding ecology. It has recently been shown that evolutionary shape change between anadromous and lacustrine sticklebacks reflects the pattern of morphological development of the opercle, namely a broadening of the anterior-posterior axis of the operculum coupled with a narrowing of the dorsal-ventral axis in freshwater sticklebacks[40], which was further confirmed in other populations[37]. This main mode of shape change is reflected among the cichlids sampled here along PC2, which is found to correlate significantly with body elongation (ER) as well as standardized measures of gut length (GLTL). Together, the results for GLTL and $\delta_{15}N$ point towards support for a relationship between operculum shape and feeding, which is shown by the results of the Procrustes ANOVAs and CVAs using feeding mode and preference (Fig. 4), and further suggested by the correlation of operculum traits with gill raker length, an additional trait that is connected to feeding, particularly processing of food items in the buccal cavity. A benthic-limnetic trend is evident in the results of the CVA based on dietary groupings, and the main axis that results in discrimination between algivore and piscivore species (CV1) reflects a similar mode of shape change to that recovered along PC1, namely an extension of the posterior edge of the operculum to create a bone that is more dorsally-broad, and triangular in shape. The ER~PC2 plot indicates that this broadening occurs in more elongate species, which have more negative PC2 scores and generally tend to be limnetic, feeding on fish or larger zooplankton. Conversely, deeper bodied species tend to be benthic, eating mainly algae, copepods and other small invertebrates, and have higher scores along PC2, reflecting a narrow operculum. In complement, results from the CVA based on feeding mode also clearly separate ram and suction feeders, which possess generally more broad opercles with a dorsally-flattened margin, from species that pick food from substrate and generally have a narrower bone.

Interspecific variation in operculum shape has previously been associated to a species' position along the benthic-pelagic axis in the species flock of Antarctic notothenioids[29]. That study, however, also revealed a high level of phylogenetic structuring of shape space, a pattern not recovered among the LT cichlids. Beyond a number of studies that have identified high levels of variation in cichlid trophic apparatus[51–54], a correspondence between aspects of craniofacial shape and feeding ecology has been previously shown for LT cichlids, particularly focusing on the evolution of Lower Pharyngeal Jaw (LPJ) shape[18]. Muschick and colleagues[18] demonstrated that LPJ shape was highly similar among species with the same diet, and generally found a high level of convergence in LPJ as well as body shape. The latter was further demonstrated by comparisons between phylogenetic and morphological distances for species pairs, which clearly showed that LPJ and body shape was similar for species pairs that were phylogenetically distant from one another. In corroboration with the findings of Muschick *et al.*[18], we find a relationship between operculum shape and feeding ecology, and evidence of convergence, though less marked than that detected for LPJ shape. Results of our pairwise distance-contrast plots indicated that more distantly related species were morphologically more similar than expected under neutral evolution (convergence) but also some species pairs showed divergence. The comparatively greater amount of convergence for LPJ shape in part reflects the unique functionality afforded by the pharyngeal jaw complex, which is recognized as an evolutionary key innovation in cichlids[53], but also suggests there may be some difference in trophic trait rate diversification, which is further suggested by considering the disparity through time results. We find operculum shape and size disparity through time to be overall relatively constant with an increase towards present, in contrast to earlier findings for LPJ shape which showed a more marked elevation of disparity through time compared to neutral evolution, and also a continual decline in disparity to the present[18]. A direct explanation for these differences is not immediately obvious. They may reflect the differential importance of operculum shape to feeding, plus the potential role of the LPJ in courtship thus placing the trait under both natural and sexual selection[55,56]. While it is clear that operculum shape can evolve rapidly on a short time scale[37], and there is evidence for strong directional selection along a specific axis of shape change that is not consistently biased by genetic architecture[39], the uncovered shape changes, especially a broadening along the longitudinal axis of the bone, requires further investigation. Further, the DTT results also show no evidence for an 'early burst' scenario, which is consistent with a general scarcity of evidence for transient bursts of morphological evolution across a wide variety of animal clades[57,58].

Extracting general patterns on adaptive radiations in fishes. The correspondence of our recovered axes of shape variance in the operculum with those for other species flocks, and particularly for the extinct species flock of saurichthyid fishes, is encouraging in light of the quest for traits that may be studied across different radiations and in deep time. The importance of viewing adaptive radiation as a process, to assess axes of divergence through a global morphospace, rather than to elucidate patterns of diversity in a flock-specific morphospace is underscored by several studies that have uncovered convergence in axes of morphological diversification, for example across the cichlid radiations occurring

in each of the East African Great Lakes[54,59]. One limiting aspect to this endeavor is that fewer characters may be examined in fossil species. To this end, study of the operculum, a bone that is commonly well-preserved, presents a promising source for continued research effort. Particularly, the discrimination of feeding mode and preference groups based on opercle shape could act as useful tools for inferring feeding ecology in fossil species, and may allow a more nuanced understanding of trophic niche exploitation in extinct species flocks.

Furthermore, that we find a relationship between operculum shape and body elongation is also encouraging for elucidating general patterns of morphological diversification in species flocks. Body elongation has been previously shown to be a major axis of body shape evolution in cichlids[19] and in other fish groups, reflecting macrohabitat adaptation[44,53,60]. Recently, Maxwell and colleagues[47] found a correlation between measures of opercle depth/length and body elongation among 10 saurichthyid species, suggesting that opercular depth may be constrained by a long, slender body and hypothesized that an axial length increase would necessitate an increased gill area to cope with increased metabolic requirements related to increased body mass in a more elongate form. This result is concordant with our findings, and shows that an interaction between elongation and opercle shape is present in at least one other species flock. This relationship, if uncovered as a general feature, may suggest that investigation of the operculum in fossils could provide insight into the evolution of elongation for specimens without fully preserved axial skeletons.

Conclusions

We investigated patterns of operculum shape and size evolution in the cichlid fishes from Lake Tanganyika, and compare the patterns with those of an extinct species flock. Our results show that the major modes of operculum shape change among cichlids corresponds with those for other species flocks, and also for a sample of the Mesozoic saurichthyid fishes. Operculum shape patterns are found to be related to feeding, which may be used to gain insight into niche occupation and feeding ecology in fossil taxa, and to body elongation. We do not find evidence for an early burst of operculum trait evolution, instead recovering more support for a concentration of shape evolution towards present, and an increase in disparity around the time of the primary lacustrine radiation.

Methods

Study sample. The study sample comprised 416 specimens (54 species), representing 31 genera (of 53) and 11 of the 14 tribes present in the lake[10] (Fig. 2). Additionally, we include data from 44 specimens, representing 5 species of saurichthyid fishes, previously collected by Wilson and colleagues[29]: *Saurichthys striolatus*, *S. costasquamosus*, *S. curionii*, *S. paucitrichus*, and *S. macrocephalus*. We collect new data for two specimens of *Saurorhynchus brevirostris*, housed at the Bayerische Staatssammlung für Paläontologie und Geologie München (Munich, Germany), and the Urweltmuseum Hauff (Holzmaden, Germany). These six species encapsulate the full range of body size variation within the clade, including both small-bodied *Saurichthys striolatus* (100–180 mm[48]), and several large-bodied species (e.g. *S. costasquamosus,* $>$ 1 meter[41]), as well as spanning deposits from the Early Jurassic to the Late Triassic (Table 2[42]). Sampling was chosen to maximize usage of available data for body elongation[44], and thereby enable direct comparison with cichlid data (see below) (Supplementary Table 1). Our dataset contains a considerable proportion of species present in LT (Fig. 2), including the most abundant ones that coexist in the southern basin of the lake[19], and spans the majority of LT cichlid tribes. Ecological diversity is well represented in the sample, which includes epilithic algae grazers, scale eaters, fish hunters, invertebrate pickers and species that dwell in sandy, rocky or open water areas.

Geometric morphometric data collection. Each specimen was photographed according to a standard procedure that has been used previously for geometric morphometric studies of the operculum[28,29] and whole body shape[18]. For the cichlids, a Nikon D5000 digital camera mounted on a tripod, with the camera lens positioned parallel to the plane of the fish in lateral view, was used to capture the left side of head (see procedure described by Muschick and colleagues[18]), and for the saurichthyid specimens a similar protocol was performed followed by re-orientation of the image in Photoshop CS6 to correspond with life position (see[29]). Following the same approach as our previous studies[28,29], the outline of each opercle was captured by 100 equi-distant semilandmarks collected using the software tpsDig[61]. This involved resampling the length of the outline clockwise, beginning at a homologous start point, defined by a type II[62] landmark located at the maximum of curvature of the dorsal margin of the opercle (see Fig. 2 in[29] for precise scheme, and[63] for details on sampling simple closed curves). Coordinate points (x, y) were exported and centroid size was calculated for each specimen. Prior to analysis and ordination, landmarks were Procrustes superimposed to remove the effects of scale, translation and rotation.

Landmark data for all LT cichlid species were entered into Principal Component Analysis (PCA) to extract axes of maximum shape variance in the sample, and the broken stick model[64] was used to assess significance of variance. A PCA was also conducted in Procrustes Form space for all cichlids, in which Procrustes shape coordinates plus the natural logarithm of centroid size are used as input[65]. We acknowledge that there are some concerns with the use of PC axes as proxies for phenotypic traits in the context of comparative methods (see[66] for discussion), and our use of a comprehensive sampling of the ecomorphologcial diversity in LT cichlids helps to reduce any potential bias associated with the treatment

of autocorrelated data from a PCA. Following Sidlauskas[67], phylomorphospaces were constructed using PC axes and the plot tree 2D algorithm in the Rhetenor module of the software Mesquite[68]. For phylomorphospace ordinations, phylogenetic relationships for the 54 species in this study were derived from a pruned version of the phylogeny constructed by Muschick and colleagues[18], which was based on sequences for one mitochondrial (ND2) and two nuclear (*ednrb1*, *phpt*) markers (Fig. 2).

Landmark data for all saurichthyid specimens (N = 44) were inputted into a separate PCA to extract the main axes of shape variance, and mean PC scores for six saurichthyid species were used in subsequent data plots.

Exploration of operculum shape patterns associated with feeding preference and mode. Canonical variates analysis (CVA) of species' mean landmark data was used to visualize the extent to which operculum shape reflected feeding preference and feeding mode groupings in LT cichlids. Data for feeding preference were collated from the literature[69–76]. Each species was assigned a feeding preference representing one of six categories: microinvertebrates/algae, zooplankton, benthic invertebrates, piscivore, scales, and 'generalist', which was used for opportunistic feeders (Supplementary Table 1). Each species was also assigned to one of seven feeding mode categories, these were: ram, sandpicking, rockpicking, scales, algaepicking, suction and benthic invertebrate picking (BIP). Procrustes ANOVAs were conducted on landmark data for all LT cichlid specimens to assess the effect of feeding preference and mode on operculum shape and size (e.g. [77]).

Correlation between operculum shape and ecological trait and niche data. Seven traits were used as covariates in this study: $\delta_{13}C$, $\delta_{15}N$, gill raker number on the ventral arch, gill raker number on the dorsal arch, average gill raker length, and gut length[19], and elongation ratio (ER) (Colombo *et al.* in prep). All seven traits were available for LT cichlids, and ER was available for the fossil saurichthyid sample. Stable isotopes for $\delta_{13}C$ and $\delta_{15}N$ were used as proxies for specialization along the benthic-limnetic axis (macrohabitat) and tropic niche (microhabitat), respectively[78]. Features of the gill rakers, the bony processes that project from the gill arches, have been recently examined for LT cichlids, including number of gill rakers on the ventral arch (grnVa) and dorsal arch (grnDa), as well as mean gill raker length measured in millimeters (mean_rl) (see [19]). Plasticity in intestinal length in response to quality of diet has previously been shown for LT cichlids; species that have low quality (nutrient poor) diets (e.g. algivores) have longer intestines to maximize the extraction of nutrients and energy from dietary material[76]. Gut length data (GLTL) were standardized against total body length for comparison across taxa. Elongation ratio (ER) is defined as the standard length of the body divided by its second largest major axis, which for the here measured cichlids refers to body depth (see Colombo *et al.* in prep). Elongation ratio (ER) data were taken from Maxwell and Wilson[44] (therein referred to as 'fineness ratio') for saurichthyid species.

Using species mean values, interactions between operculum shape (PC1 and PC2) and form (PC1) space axes and centroid size in relation to the above seven traits were examined using Phylogenetic generalized least squares (PGLS) regression. PGLS takes phylogenetic relationships into account, assuming that the evolution of residual traits follows a neutral model (Brownian motion)[79,80]. PGLS was implemented in version 3.1.2 of R[81] using the package *nlme*[82] (version 3.1–118). These analyses were conducted on a reduced data set for which all ecological variables were available (N = 38–49 species). PGLS regressions were also conducted for operculum shape (PC1 and PC2) and ER, using phylogenetic relationships taken from Maxwell *et al.* [43].

Macroevolutionary model tests of operculum shape and size evolution. Several models were fit to the LT cichlid operculum shape data (axes PC1-PC3) and centroid size data, using the fitContinuous() function in the R package *Geiger*[83] (version 2.0.3). Model fit was assessed using sample-size corrected Akaike Information Criterion (AICc), and Akaike weight values were calculated to express proportional support for each model[84]. To enable direct comparison with a previous, comprehensive study of ecological and shape trait data in LT cichlids[19], we fit Brownian motion (BM), Ornstein-Uhlenbeck (OU), and white noise (WN) models to evaluate the general process of operculum size and shape trait evolution. Under BM, trait evolution is simulated as a random walk through trait space, and phenotypic difference between sister taxa is expected to grow proportional to the sum of branch lengths between them. The OU model describes trait evolution under stabilizing selection, whereby there is attraction to a selective optimum, the strength of attraction to this selective optimum (i.e. the strength of selection) is measured using the alpha parameter. Under the WN model, equating to OU with an alpha of infinity, data are assumed to arise from a single normal distribution with no phylogenetically induced covariance among species values.

The time-dependence of trait evolution was assessed using Pagel's δ model[85] and the Early Burst (EB) model, also called the ACDC model (accelerating-decelerating[86]). Pagel's δ model was used to evaluate whether changes in operculum trait data mainly occurred near the root (early) or tips (late) of the phylogeny. Values of <1 for δ indicate that branch lengths of the phylogeny are transformed to become increasingly shorter towards the tips and hence trait change occurred mainly along basal branches, whereas values of >1 for δ indicate trait evolution was more concentrated in younger subclades. The EB model measures, using the rate change parameter alpha, the acceleration or deceleration of evolution

through time. Negative values of α reflect a rate deceleration in trait evolution whereas positive values indicate acceleration in trait evolution rate.

To quantify phylogenetic signal in operculum shape (axes PC1-PC3) and centroid size data, Blomberg's *K* statistic[86] was calculated using the R package *Picante*[87] (version 1.6–2). Values of >1 for the *K* statistic indicate that close relatives are more similar in operculum traits than expected given the topology and branch lengths, whereas values of <1 indicate less phylogenetic signal than expected under a Brownian motion model[86]. Pagel's λ, a branch length transformation model, was calculated to assess the extent to which the phylogeny predicts covariance in operculum shape and size for the species here examined[84]. Values of λ range from 0, reflecting a star phylogeny and no phylogenetic signal, to 1, which recovers the Brownian motion model.

Pairwise distance-contrast plots were constructed following a similar approach to Muschick and colleagues[18] to assess whether differences in operculum shape were smaller between species pairs than were phylogenetic distances, which would indicate convergent evolution. *Tylochromis polylepis* (tylpol) was removed from the data set due to its large distance from other taxa[18]. Morphological and phylogenetic distances between species pairs were calculated and plotted against one another. Morphological distances were calculated by extracting a variance-covariance matrix of Procrustes distances between each species. A Phylogenetic distance matrix was extracted using the cophenetic() function in R. To compare the observed data with that expected under BM, which would predict a correlation between phylogenetic and morphological distance (divergence), shape data were simulated on the phylogeny. An evolutionary variance-covariance matrix was extracted for operculum shape data using the ratematrix() function in R[88] using *Geiger*[83] (version 2.0.3). The function sim.char() was then used to simulate neutral trait evolution under BM. The simulated pairwise comparisons were then compared to the observed data by subtracting the simulated data from the observed data. This resulted in negative values when species were more similar in shape in the actual data than the data simulated given their phylogenetic distance, and positive values when species were more similar in the simulated data. We used this vector to color-code our plots, and additionally conducted a test for pairwise comparison between the observed data and the simulated data. We generated a 95% confidence interval for the simulated data using 1000 bootstrap replicates, and counted the number of species pairs in the observed data that had a smaller value than the lower 95% threshold value of the simulated data.

Disparity through time analysis. To evaluate how operculum size and shape disparity changed through time, disparity through time (DTT) analyses were implemented in the R package *Geiger*[83] (version 2.0.3) for centroid size and PC axes. Morphological Disparity Index (MDI) values were calculated to quantify overall difference in the observed trait disparity compared to that expected under Brownian motion by simulating operculum size and shape evolution 10,000 times across the tree. The function dttFullCIs() was used, following Slater *et al.*[89] to create 95% confidence intervals on the simulations and to test whether the values for MDI differed significantly from the BM simulations. Default settings of nsmims = 10,000 were used to obtain a stable *P* value. To correct for tip over dispersion, MDI values were calculated over the first 90% of the phylogeny.

References

1. Schluter, D. *The Ecology of Adaptive Radiation*. (Oxford University Press, 2000).
2. Losos, J. B. Adaptive Radiation, Ecological Opportunity, and Evolutionary Determinism. *Am. Nat.* **175,** 623–639, doi: 10.1086/652433 (2010).
3. Kocher, T. D. Adaptive evolution and explosive speciation: the cichlid fish model. *Nat. Rev. Genet.* **5,** 288–298 (2004).
4. Seehausen, O. African cichlid fish: a model system in adaptive radiation research. *P. Roy. Soc. Lond. B Bio.* **273,** 1987–1998, doi: 10.1098/rspb.2006.3539 (2006).
5. Santos, M. E. & Salzburger, W. How cichlids diversify. *Science* **338,** 619–621 (2012).
6. Salzburger, W., Van Bocxlaer, B. & Cohen, A. S. African Great Lakes and their faunas. *Annu. Rev. Ecol. Syst.* **45,** 519–545 (2014).
7. Turner, G. F., Seehausen, O., Knight, M. E., Allender, C. J. & Robinson, R. L. How many species of cichlid fishes are there in African lakes? *Mol. Ecol.* **10,** 793–806, doi: 10.1046/j.1365-294x.2001.01200.x (2001).
8. Cohen, A. S., Lezzar, K. E., Tiercelin, J. J. & Soreghan, M. New palaeogeographic and lake-level reconstructions of Lake Tanganyika: Implications for tectonic, climatic and biological evolution in a rift lake. *Basin Res.* **9,** 107–132, doi: 10.1046/j.1365-2117.1997.00038.x (1997).
9. Salzburger, W., Meyer, A., Baric, S., Verheyen, E. & Sturmbauer, C. Phylogeny of the Lake Tanganyika Cichlid species flock and its relationship to the Central and East African Haplochromine Cichlid fish faunas. *Syst. Biol.* **51,** 113–135, doi: 10.1080/106351502753475907 (2002).
10. Koblmüller, S., Sefc, K. M. & Sturmbauer, C. The Lake Tanganyika cichlid species assemblage: recent advances in molecular phylogenetics. *Hydrobiologia* **615,** 5–20, doi: 10.1007/s10750-008-9552-4 (2008).
11. Meyer, B. S., Matschiner, M. & Salzburger, W. A tribal level phylogeny of Lake Tanganyika cichlid fishes based on a genomic multi-marker approach. *Mol. Phylogenet. Evol.* **83,** 56–71 (2015).
12. Duftner, N. *et al.* Parallel evolution of facial stripe patterns in the *Neolamprologus brichardi/pulcher* species complex endemic to Lake Tanganyika. *Mol. Phylogenet. Evol.* **45,** 706–715 (2007).
13. Wagner, C. A., Harmon, L. J. & Seehausen, O. Ecological opportunity and sexual selection together predict adaptive radiation. *Nature* **487,** 366–369 (2012).
14. Koblmüller, S., Salzburger, W. & Sturmbauer, C. Evolutionary relationships in the sand-dwelling cichlid lineage of Lake Tanganyika suggest multiple colonization of rocky habitats and convergent origin of biparental mouthbrooding. *J. Mol. Evol.* **58,** 79–96 (2004).
15. Duponchelle, F., Paradis, E., Ribbink, A. J. & Turner, G. F. Parallel life history evolution in mouthbrooding cichlids from the African Great Lakes. *P. Natl. Acad. Sci. USA* **105,** 15475–15480, doi: 10.1073/pnas.0802343105 (2008).

16. Kidd, M. R., Duftner, N., Koblmueller, S., Sturmbauer, C. & Hofmann, H. A. Repeated Parallel Evolution of Parental Care Strategies within Xenotilapia, a Genus of Cichlid Fishes from Lake Tanganyika. *Plos One* **7,** doi: 10.1371/journal.pone.0031236 (2012).
17. Colombo, M. *et al.* The ecological and genetic basis of convergent thick-lipped phenotypes in cichlid fishes. *Mol. Ecol.* **22,** 670–684 (2013).
18. Muschick, M., Indermaur, A. & Salzburger, W. Convergent evolution within an adaptive radiation of cichlid fishes. *Curr. Biol.* **22,** 2362–2368 (2012).
19. Muschick, M. *et al.* Testing the stages model in the adaptive radiation of cichlid fishes in East African Lake Tanganyika. *P. Roy. Soc. Lond. B Bio*. **281,** doi: 10.1098/rspb.2014.0605 (2014).
20. Chakrabarty, P. Testing conjectures about morphological diversity in cichlids of lakes Malawi and Tanganyika. *Copeia* **2,** 359–373 (2005).
21. Clabaut, C., Bunje, P. M. E., Salzburger, W. & Meyer, A. Geometric morphometric analyses provide evidence for the adaptive character of the Tanganyikan cichlid fish radiations. *Evolution* **61,** 560–578, doi: 10.1111/j.1558-5646.2007.00045.x (2007).
22. Gonzalez-Voyer, A., Winberg, S. & Kolm, N. Distinct evolutionary patterns of brain and body size during adaptive radiation. *Evolution* **63,** 2266–2274, doi: 10.1111/j.1558-5646.2009.00705.x (2009).
23. Danley, P. D. & Kocher, T. D. Speciation in rapidly diverging systems: lessons from Lake Malawi. *Mol. Ecol.* **10,** 1075–1086 (2001).
24. Streelman, J. T. & Danley, P. D. The stages of vertebrate evolutionary radiation. *Trends Ecol. Evol.* **18,** 126–131 (2003).
25. Gavrilets, S. & Losos, J. B. Adaptive radiation: contrasting theory with data. *Science* **323,** 732–737 (2009).
26. Colombo, M., Damerau, M., Hanel, R., Salzburger, W. & Matschiner, M. Diversity and disparity through time in the adaptive radiation of Antarctic notothenioid fishes. *J. Evol. Biol.* **28,** 376–394, doi: 10.1111/jeb.12570 (2015).
27. Schmid, L. & Sánchez-Villagra, M. R. Potential Genetic Bases of Morphological Evolution in the Triassic Fish Saurichthys. *Journal of Experimental Zoology Part B-Molecular and Developmental Evolution* **314B,** 519–526, doi: 10.1002/jez.b.21372 (2010).
28. Wilson, L. A. B., Colombo, M., Hanel, R., Salzburger, W. & Sánchez-Villagra, M. R. Ecomorphological disparity in an adaptive radiation: opercular bone shape and stable isotopes in Antarctic icefishes. *Ecol. Evol*. **3,** 3166–3182, doi: 10.1002/ece3.708 (2013a).
29. Wilson, L. A. B., Furrer, H., Stockar, R. & Sánchez-Villagra, M. R. A quantitative evaluation of evolutionary patterns in opercle bone shape in *Saurichthys* (Actinopterygii: Saurichthyidae). *Palaeontology* **56,** 901–915, doi: 10.1111/pala.12026 (2013b).
30. Hughes, G. M. A comparative study of gill ventilation in marine teleosts. *J. Exp. Biol.* **37,** 28–45 (1960).
31. Anker, G. C. Morphology and kinetics of the head of the stickleback, *Gasterosteus aculeatus*. *T. Zool. Soc. Lond.* **32,** 311–416 (1974).
32. Baerends, G. P. & Roon, J. M. B.-V. An Introduction to the Study of the Ethology of the Cichlid Fishes. *Behaviour* Supplement I, 1–243 (1950).
33. Kimmel, C. B., Aguirre, W. E., Ullmann, B., Currey, M. & Cresko, W. A. Allometric change accompanies opercular shape evolution in Alaskan threespine sticklebacks. *Behaviour* **145,** 669–691, doi: 10.1163/156853908792451395 (2008).
34. Cubbage, C. C. & Mabee, P. M. Development of the cranium and paired fins in the zebrafish *Danio rerio* (Ostariophysi, cyprinidae). *J. Morph*. **229,** 121–160 (1996).
35. Kimmel, C. B., DeLaurier, A., Ullmann, B., Dowd, J. & McFadden, M. Modes of Developmental Outgrowth and Shaping of a Craniofacial Bone in Zebrafish. *Plos One* **5,** doi: 10.1371/journal.pone.0009475 (2010).
36. Kimmel, C. B. Skull developmental modularity: a view from a single bone - or two. *J. Appl. Ichthyol.* **30,** 600–607, doi: 10.1111/jai.12508 (2014).
37. Arif, S., Aguirre, W. E. & Bell, M. A. Evolutionary diversification of opercle shape in Cook Inlet threespine stickleback. *Biol. J. Linn. Soc.* **97,** 832–844 (2009).
38. Kimmel, C. B. *et al.* Evolution and development of facial bone morphology in threespine sticklebacks. *P. Natl. Acad. Sci. USA* **102,** 5791–5796, doi: 10.1073/pnas.0408533102 (2005).
39. Kimmel, C. B. *et al.* Independent axes of genetic variation and parallel evolutionary divergence of opercle bone shape in Threespine stickleback. *Evolution* **66,** 419–434, doi: 10.1111/j.1558-5646.2011.01441.x (2012a).
40. Kimmel, C. B., Hohenlohe, P. A., Ullmann, B., Currey, M. & Cresko, W. A. Developmental dissociation in morphological evolution of the stickleback opercle. *Evol. Dev.* **14,** 326–337, doi: 10.1111/j.1525-142X.2012.00551.x (2012b).
41. Mutter, R. J., Cartanya, J. & Basaraba, S. A. in *Mesozoic fishes 4. Homology and phylogeny* (eds G. Arratia, H.-P. Schultze, & M. V. H. Wilson) 103–127 (Dr. Friederich Pfeil, 2008).
42. Romano, C., Kogan, I., Jenks, J., Jerjen, I. & Brinkmann, W. Saurichthys and other fossil fishes from the late Smithian (Early Triassic) of Bear Lake County (Idaho, USA), with a discussion of saurichthyid palaeogeography and evolution. *B. Geosci.* **87,** 543–570, doi: 10.3140/bull.geosci.1337 (2012).
43. Maxwell, E. E., Furrer, H. & Sanchez-Villagra, M. R. Exceptional fossil preservation demonstrates a new mode of axial skeleton elongation in early ray-finned fishes. *Nat. Comm*. **4,** doi: 10.1038/ncomms3570 (2013).
44. Maxwell, E. E. & Wilson, L. A. B. Regionalization of the axial skeleton in the 'ambush predator' guild - are there developmental rules underlying body shape evolution in ray-finned fishes? *BMC Evol. Biol.* **13,** doi: 10.1186/1471-2148-13-265 (2013).
45. Furrer, H., Schaltegger, U., Ovtcharova, M. & Meister, P. U-Pb zircon age of volcanic layers in Middle Triassic platform carbonates of the Austroalpine Silvretta nappe (Switzerland). *Swiss J. Geosci.* **101,** 595–603 (2008).
46. Rieppel, O. A new species of the genus *Saurichthys* (pisces: Actinopterygii) from the Middle Triassic of Monte San Giorgio (Switzerland), with comments on the phylogenetic interrelationships of the genus. *Palaeontographica Abteilung A-Palaozoologie-Stratigraphie* **221,** 63–94 (1992).
47. Maxwell, E. E., Romano, C., Wu, F. & Furrer, H. Two new species of *Saurichthys* (Actinopterygii: Saurichthyidae) from the Middle Triassic of Monte San Giorgio, Switzeralnd, with implication for the phylogenetic relationships of the Genus. *Zool. J. Linn. Soc.* **173,** 887–912 (2015).
48. Griffith, J. On the anatomy of two saurichthyid fishes, *Saurichthys striolatus* (Bronn) and *S. curionii* (Bellotti). *P. Zool. Soc. Lond*. **132,** 587–606 (1959).
49. Kornfield, I. & Smith, P. F. African cichlid fishes: Model systems for evolutionary biology. *Annu. Rev. Ecol. Syst.* **31,** 163–196, doi: 10.1146/annurev.ecolsys.31.1.163 (2000).
50. Salzburger, W. & Meyer, A. The species flocks of East African cichlid fishes: recent advances in molecular phylogenetics and population genetics. *Naturwissenschaften* **91,** 277–290 (2004).
51. Streelman, J. T., Webb, J. F., Albertson, R. C. & Kocher, T. D. The cusp of evolution and development: a model of cichlid tooth shape diversity. *Evol. Dev.* **5,** 600–608, doi: 10.1046/j.1525-142X.2003.03065.x (2003).
52. Albertson, R. C., Streelman, J. T., Kocher, T. D. & Yelick, P. C. Integration and evolution of the cichlid mandible: The molecular basis of alternate feeding strategies. *P. Natl. Acad. Sci. USA* **102,** 16287–16292, doi: 10.1073/pnas.0506649102 (2005).
53. Barluenga, M., Stölting, K. N., Salzburger, W., Muschick, M. & Meyer, A. Sympatric speciation in Nicaraguan crater lake cichlid fish. *Nature* **439,** 719–723, doi: http://www.nature.com/nature/journal/v439/n7077/suppinfo/nature04325_S1.html (2006).
54. Cooper, W. J. *et al.* Bentho-Pelagic Divergence of Cichlid Feeding Architecture Was Prodigious and Consistent during Multiple Adaptive Radiations within African Rift-Lakes. *PLoS ONE* **5,** e9551, doi: 10.1371/journal.pone.0009551 (2010).

55. Hulsey, C. D. Function of a key morphological innovation: fusion of the cichlid pharyngeal jaw. *P. Roy. Soc. Lond. B Bio* **273,** 669–675, doi: 10.1098/rspb.2005.3375 (2006).
56. Salzburger, W. The interaction of sexually and naturally selected traits in the adaptive radiations of cichlid fishes. *Mol. Ecol.* **18,** 169–185, doi: 10.1111/j.1365-294X.2008.03981.x (2009).
57. Harmon, L. J. *et al.* Early bursts of body size and shape evolution are rare in comparative data. *Evolution* **64,** 2385–2396, doi: 10.1111/j.1558-5646.2010.01025.x (2010).
58. Sallan, L. C. & Friedman, M. Heads or tails: staged diversification in vertebrate evolutionary radiations. *P. Roy. Soc. Lond. B Bio* **279,** 2025–2032 (2012).
59. Young, K. A., Snoeks, J. & Seehausen, O. Morphological Diversity and the Roles of Contingency, Chance and Determinism in African Cichlid Radiations. *PLoS ONE* **4,** e4740, doi: 10.1371/journal.pone.0004740 (2009).
60. Krabbenhoft, T. J., Collyer, M. L. & Quattro, J. M. Differing evolutionary patterns underlie convergence on elongate morphology in endemic fishes of Lake Waccamaw, North Carolina. *Biol. J. Linn. Soc.* **98,** 636–645 (2009).
61. Digitize landmarks and outlines tpsDig 2.17 (Rohlf, FJ, Department of Ecology & Evolution, SUNY at Stony Brook, 2013).
62. Bookstein, F. L. *Morphometric tools for landmark data*. (Cambridge University Press, 1991).
63. MacLeod, N. Generalizing and extending the eigenshape method of shape space visulization and analysis. *Paleobiology* **25,** 107–138 (1999).
64. Jackson, D. A. Stopping rules in principal components analysis – a comparison of heuristic and statistical approaches. *Ecology* **74,** 2204–2214, doi: 10.2307/1939574 (1993).
65. Mitteroecker, P. & Gunz, P. Advances in Geometric Morphometrics. *Evol. Biol.* **36,** 235–247, doi: 10.1007/s11692-009-9055-x (2009).
66. Uyeda, J. C., Caetano, D. S. & Pennell, M. W. Comparative Analysis of Principal Components Can be Misleading. *Syst. Biol.* **64,** 677–689, doi: 10.1093/sysbio/syv019 (2015).
67. Sidlauskas, B. Continuous and arrested morphological diversification in sister clades of characiform fishes: a phylomorphospace approach. *Evolution* **62,** 3135–3156, doi: 10.1111/j.1558-5646.2008.00519.x (2008).
68. Mesquite: a modular system for evolutionary analysis v. 2.75 (2011).
69. Hori, M., Yamaoka, K. & Takamura, K. Abundance and micro-distribution of cichlid fishes on a rocky shore of Lake Tanganyika. *African Studies Monograph* **3,** 25–38 (1983).
70. Maréchal, C. & Poll, M. in *Check-list of the freshwater fishes of Africa (CLOFFA)* Vol. 4 (eds J. Daget, J.-P. Gosse, G. G. Teugels, & D. F. E. Thys van den Audenaerde) 32–35 (ISNB, 1991).
71. Sturmbauer, C. & Meyer, A. Mitochondrial phylogeny of the endemic mouthbrooding lineages of cichlid fises from Lake Tanganyika in Eastern Africa. *Mol. Biol. Evol.* **10,** 751–768 (1993).
72. Konings, A. *Tanganyika cichlids in their natural habitat*. (Cichlid Press, 1998).
73. Clabaut, C., Bunje, P. M. E., Salzburger, W. & Meyer, A. Geometric morphometric analyses provide evidence for the adaptive character of the Tanganyikan cichlid fish radiations. *Evolution* **61,** 560–578, doi: 10.1111/j.1558-5646.2007.00045.x (2007).
74. Takahashi, R., Watanabe, K., Nishida, M. & Hori, M. Evolution of feeding specialization in Tanganyikan scale-eating cichlids: a molecular phylogenetic approach. *BMC Evol. Biol.* **7,** 195 (2007).
75. Wagner, C. E. & McCune, A. R. Contrasting patterns of spatial genetic structure in sympatric rock-dwelling cichlid fishes. *Evolution* **63,** 1312–1326, doi: 10.1111/j.1558-5646.2009.00612.x (2009).
76. Wagner, C. E., McIntyre, P. B., Buels, K. S., Gilbert, D. M. & Michel, E. Diet predicts intestine length in Lake Tanganyika's cichlid fishes. *Funct. Ecol.* **23,** 1122–1131, doi: 10.1111/j.1365-2435.2009.01589.x (2009).
77. Klingenberg, C. P., Barluenga, M. & Meyer, A. Shape analysis of symmetric structures: Quantifying variation among individuals and asymmetry. *Evolution* **56,** 1909–1920 (2002).
78. Post, D. M. Using stable isotopes to estimate trophic position: Models, methods, and assumptions. *Ecology* **83,** 703–718, doi: 10.2307/3071875 (2002).
79. Rohlf, F. J. Comparative methods for the analysis of continuous variables: Geometric interpretations. *Evolution* **55,** 2143–2160 (2001).
80. Butler, M. A. & King, A. A. Phylogenetic comparative analysis: A modeling approach for adaptive evolution. *Am. Nat.* **164,** 683–695, doi: 10.1086/426002 (2004).
81. R Core Team. R: A language and environment for statistical computing. R Foundation for Statistical Computing, Vienna, Austria. http://www.R-project.org/ (2013).
82. Pinheiro, J., Bates, D., DebRoy, S., Sarkar, D. & R Core Team. nlme: Linear and Nonlinear Mixed Effects Models. R package version 3.1-119, http://CRAN.R-project.org/package=nlme (2015).
83. Harmon, L. J., Weir, J. T., Brock, C. D., Glor, R. E. & Challenger, W. GEIGER: investigating evolutionary radiations. *Bioinformatics* 24, 129–131, doi: 10.1093/bioinformatics/btm538 (2008).
84. Hunt, G. & Carrano, M. T. in *Quantitative Methods in Paleobiology* Vol. 16 (eds J Alroy & G Hunt) 245–269 (The Paleontological Society Papers, 2010).
85. Pagel, M. Inferring the historical patterns of biological evolution. *Nature* **401,** 877–884, doi: 10.1038/44766 (1999).
86. Blomberg, S. P., Garland, T. & Ives, A. R. Testing for phylogenetic signal in comparative data: Behavioral traits are more labile. *Evolution* **57,** 717–745, doi: 10.1111/j.0014-3820.2003.tb00285.x (2003).
87. Kembel, S. W. *et al.* Picante: R tools for integrating phylogenies and ecology. *Bioinformatics* **26,** 1463–1464 (2010).
88. Revell, L. J., Johnson, M. A., Schulte, J. A., II, Kolbe, J. J. & Losos, J. B. A phylogenetic test for adaptive convergence in rock-dwelling lizards. *Evolution* **61,** 2898–2912, doi: 10.1111/j.1558-5646.2007.00225.x (2007).
89. Slater, G. J., Price, S. A., Santini, F. & Alfaro, M. E. Diversity versus disparity and the radiation of modern cetaceans. *P. Roy. Soc. Lond. B Bio* **277,** 3097–3104, doi: 10.1098/rspb.2010.0408 (2010).

Acknowledgements

We thank Erin Maxwell (Staatliches Museum für Naturkunde Stuttgart) for kindly providing several photographs of *S. brevirostris*, as well as Thomas Brühweiler (University of Zürich) and Adrian Indermaur (University of Basel) for help with data collection and categorization. This project is supported by funding from the Swiss National Science Foundation (SNF) Sinergia program, granted to WS, MRS-V and Heinz Furrer (Universität Zürich) (CRSII3-136293), and a CoG "CICHLID~X" from the European Research Council (ERC) to WS. LABW is supported by the SNF Advanced Mobility Postdoc scheme (P300P3_151189).

Author Contributions

L.A.B.W. performed research, analyzed data and drafted the manuscript; M.C. contributed to data collection and provided elongation data; M.R.S.-V. and W.S. conceived the study. All authors contributed to manuscript drafts, and approved the final version.

Additional Information

Supplementary information accompanies this paper at http://www.nature.com/srep

Competing financial interests: The authors declare no competing financial interests.

How to cite this article: Wilson, L. A. B. *et al.* Evolution of opercle shape in cichlid fishes from Lake Tanganyika - adaptive trait interactions in extant and extinct species flocks. *Sci. Rep.* **5**, 16909; doi: 10.1038/srep16909 (2015).

1.5.2
Supporting information

Supplementary Information

Evolution of opercle shape in cichlid fishes from Lake Tanganyika - adaptive trait interactions in extant and extinct species flocks

Laura A. B. Wilson, Marco Colombo, Marcelo R. Sánchez-Villagra, Walter Salzburger

Contents

Supplementary Table 1. List of species examined in this study.

Short name	Tribe	Species	N	Feeding preference	Feeding mode
altcal	Lamprologini	*Altolamprologus calvus*	3	benthic invertebrates	Suction
altcom	Lamprologini	*Altolamprologus compressiceps*	35	benthic invertebrates	Suction
altfas	Lamprologini	*Altolamprologus fasciatus*	20	benthic invertebrates	Suction
asplep	Ectodini	*Asprotilapia leptura*	9	microinvertebrates/ algae	Rockpicking
astbur	Tropheini	*Astatotilapia burtoni*	17	generalist	BIP
auldew	Ectodini	*Aulonocranus dewindtii*	31	microinvertebrates/ algae	BIP
batgra	Bathybatini	*Bathybates graueri*	4	piscivore	Ram
batvit	Bathybatini	*Bathybates vittatus*	3	piscivore	Ram
bentri	Benthochromini	*Benthochromis tricoti*	8	zooplankton	Suction
boumic	Boulengerochromini	*Boulengerochromis microlepis*	15	piscivore	Ram
calmac	Ectodini	*Callochromis macrops*	9	benthic invertebrates	Sandpicking
cphgib	Cyphotilapiini	*Cyphotilapia gibberosa*	13	piscivore	BIP
ctehor	Tropheini	*Ctenochromis horei*	9	generalist	BIP
cyafur	Ectodini	*Cyathopharynx furcifer*	23	microinvertebrates/ algae	Algaescraping
cyplep	Cyprichromini	*Cyprichromis leptosoma*	3	zooplankton	Suction
ectdes	Ectodini	*Ectodus descampsii*	3	generalist	Sandpicking
enamel	Ectodini	*Enantiopus melanogenys*	7	benthic invertebrates	Sandpicking
gnaper	Limnochromini	*Gnathochromis permaxillaris*	10	benthic invertebrates	Suction
gnapfe	Tropheini	*Gnathochromis pfefferi*	9	benthic invertebrates	Suction
gralem	Ectodini	*Grammatotria lemairii*	10	benthic invertebrates	Sandpicking
gwcbel	Limnochromini	*Greenwoodochromis bellcrossi*	6	piscivore	Suction
gwcchr	Limnochromini	*Greenwoodochromis christyi*	4	piscivore	BIP
intloo	Tropheini	*Interochromis loocki*	9	microinvertebrates/ algae	Algaescraping
lamcal	Lamprologini	*Lamprologus callipterus*	7	benthic invertebrates	BIP
lamlem	Lamprologini	*Lamprologus lemairii*	4	piscivore	Suction
lamorn	Lamprologini	*Lamprologus ornatipinnis*	4	benthic invertebrates	BIP
lepatt	Lamprologini	*Lepidiolamprologus attenuatus*	11	piscivore	Ram
lepelo	Lamprologini	*Lepidiolamprologus elongatus*	12	piscivore	Ram
leppro	Lamprologini	*Lepidolamprologus profundicola*	5	piscivore	Ram
limdar	Tropheini	*Limnotilapia dardenni*	15	microinvertebrates/ algae	Sandpicking
loblab	Tropheini	*Lobochilotes labiatus*	6	benthic invertebrates	Suction
neofur	Lamprologini	*Neolamprologus furcifer*	1	benthic invertebrates	BIP
neomod	Lamprologini	*Neolamprologus modestus*	7	benthic invertebrates	BIP
neopro	Lamprologini	*Neolamprologus prochilus*	3	benthic invertebrates	Suction
neopul	Lamprologini	*Neolamprologus pulcher*	8	benthic invertebrates	BIP
neosav	Lamprologini	*Neolamprologus savoryi*	2	benthic invertebrates	BIP
neosex	Lamprologini	*Neolamprologus sexfasciatus*	8	benthic invertebrates	BIP
neotet	Lamprologini	*Neolamprologus tetracanthus*	7	benthic invertebrates	BIP

ophven	Ectodini	*Ophthalmotilapia ventralis*	7	microinvertebrates/ algae	Algaescraping
permic	Perissodini	*Perissodus microlepis*	3	scales	Scales
perpar	Perissodini	*Perissodus paradoxus*	3	scales	Scales
petfam	Tropheini	*Petrochromis famula*	4	microinvertebrates/ algae	Algaescraping
petfas	Tropheini	*Petrochromis fasciolatus*	2	microinvertebrates/ algae	Algaescraping
petmac	Tropheini	*Petrochromis macrognathus*	1	microinvertebrates/ algae	Algaescraping
petpol	Tropheini	*Petrochromis polyodon*	4	microinvertebrates/ algae	Algaescraping
psccur	Tropheini	*Pseudosimochromis curvifrons*	4	microinvertebrates/ algae	Algaescraping
simbab	Tropheini	*Simochromis babaulti*	3	microinvertebrates/ algae	Algaescraping
simdia	Tropheini	*Simochromis diagramma*	2	microinvertebrates/ algae	Algaescraping
tromoo	Tropheini	*Tropheus moori*	10	microinvertebrates/ algae	Algaescraping
tylpol	Tylochromini	*Tylochromis polylepis*	2	benthic invertebrates	Sandpicking
varmoo	Lamprologini	*Variabilichromis moori*	2	benthic invertebrates	BIP
xenfla	Ectodini	*Xenotilapia flavipinnis*	2	benthic invertebrates	Sandpicking
xenbou	Ectodini	*Xenotilapia boulengeri*	4	benthic invertebrates	Sandpicking
xenspi	Ectodini	*Xenotilapia spiloptera*	3	benthic invertebrates	Rockpicking
		Saurorhynchus brevirostris	2		
		Saurichthys costasquamosus	4		
		Saurichthys curionii	15		
		Saurichthys macrocephalus	3		
		Saurichthys paucitrichus	1		
		Saurichthys striolatus	19		
TOTAL			**460**		

Supplementary Fig. 1. Phylomorphospace of PC1 and PC2 for form (shape + centroid size) space of opercular landmarks collected on specimens of Lake Tanganyikan cichlid fish.

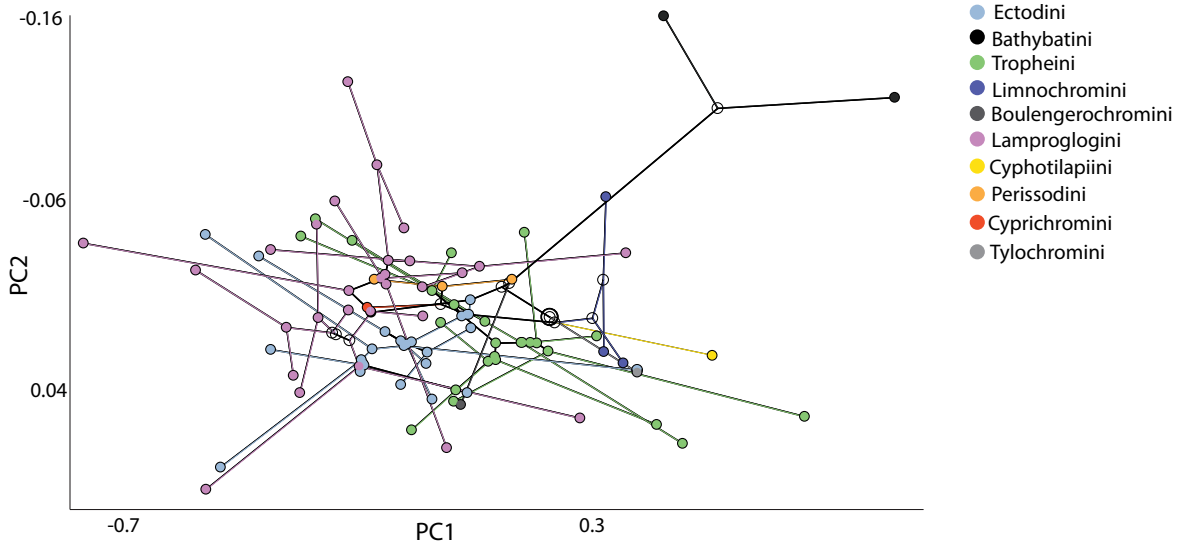

Supplementary Fig. 2. Ordination of PC1 (76.9%) and PC2 (8.7%) from PCA of opercular landmarks for members of the Saurichthyidae species flock.

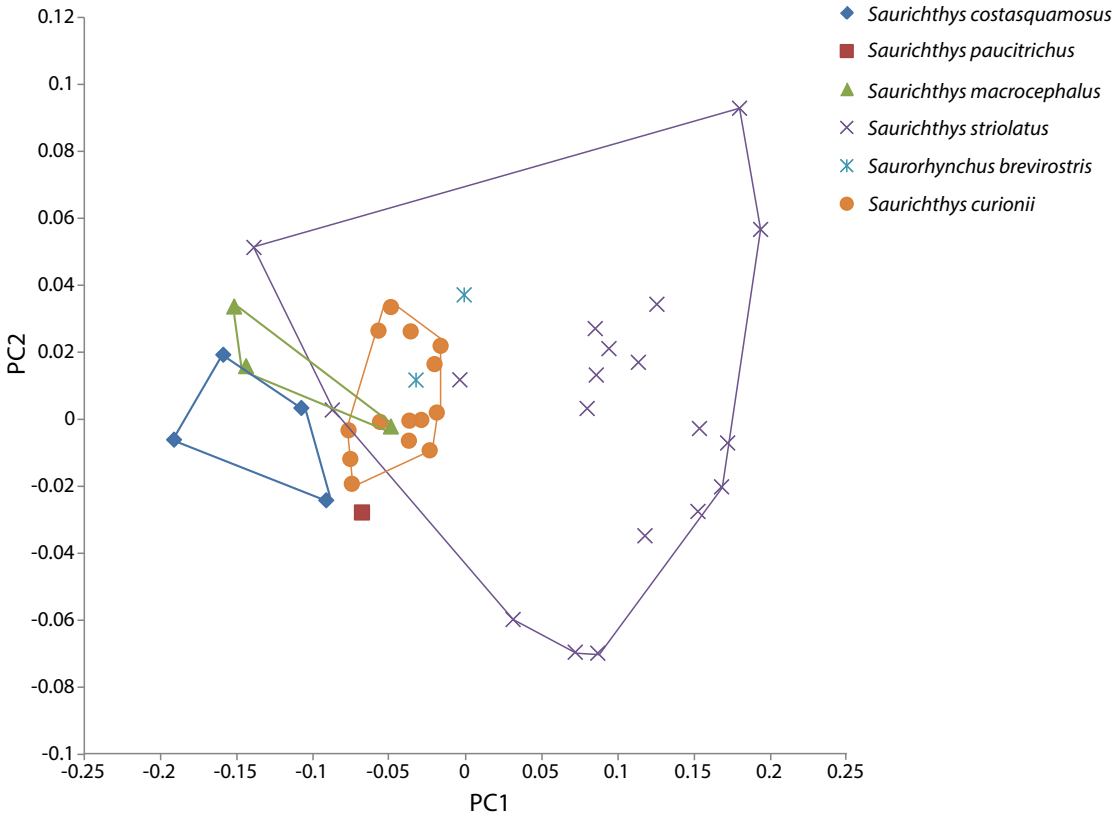

1.6

Depth-dependent abundance of Midas Cichlid fish (*Amphilophus* spp.) in two Nicaraguan crater lakes

Hydrobiologia

I helped collecting the data and discussed the manuscript. MD and MR analysed the data and drafted the manuscript.

Hydrobiologia (2012) 686:277–285
DOI 10.1007/s10750-012-1024-1

PRIMARY RESEARCH PAPER

Depth-dependent abundance of Midas Cichlid fish (*Amphilophus* spp.) in two Nicaraguan crater lakes

Marie Theres Dittmann · Marius Roesti · Adrian Indermaur · Marco Colombo · Martin Gschwind · Isabel Keller · Robin Kovac · Marta Barluenga · Moritz Muschick · Walter Salzburger

Received: 4 July 2011 / Revised: 2 February 2012 / Accepted: 5 February 2012 / Published online: 22 February 2012

Abstract The Midas Cichlid species complex (*Amphilophus* spp.) in Central America serves as a prominent model system to study sympatric speciation and parallel adaptive radiation, since small arrays of equivalent ecotype morphs have evolved independently in different crater lakes. While the taxonomy and evolutionary history of the different species are well resolved, little is known about basic ecological parameters of Midas Cichlid assemblages. Here, we use a line transect survey to investigate the depth-dependent abundance of *Amphilophus* spp. along the shores of two Nicaraguan crater lakes, Apoyo and Xiloá. We find a considerable higher density of Midas cichlids in Lake Xiloá as compared to Lake Apoyo, especially at the shallowest depth level. This might be due to the higher eutrophication level of Lake Xiloá and associated differences in food availability, and/or the presence of a greater diversity of niches in that lake. In any case, convergent forms evolved despite noticeable differences in size, age, eutrophication level, and carrying capacity. Further, our data provide abundance and density estimates for Midas Cichlid fish, which serve as baseline for future surveys of these ecosystems and are also relevant to past and future modeling of ecological speciation.

Keywords Sympatric speciation · Parallel adaptive radiation · Fish density estimates · Crater Lake Apoyo · Crater Lake Xiloá · Ecology

Marie Theres Dittmann and Marius Roesti contributed equally to this study.

Handling editor: Christian Sturmbauer

Electronic supplementary material The online version of this article (doi:10.1007/s10750-012-1024-1) contains supplementary material, which is available to authorized users.

M. T. Dittmann · M. Roesti · A. Indermaur · M. Colombo · M. Gschwind · I. Keller · R. Kovac · M. Muschick · W. Salzburger (✉)
Zoological Institute, University of Basel, Vesalgasse 1, 4051 Basel, Switzerland
e-mail: walter.salzburger@unibas.ch

Present Address:
M. T. Dittmann
Group of Animal Nutrition, Institute of Agricultural Science, Swiss Federal Institute of Technology, Universitätsstrasse 2, 8092 Zurich, Switzerland

I. Keller
IFM-Geomar, Evolutionsbiologie, Düstenbrooker Weg 20, 24105 Kiel, Germany

M. Barluenga
Museo Nacional de Ciencias Naturales, CSIC, José Gutierrez Abascal 2, 28006 Madrid, Spain

Introduction

The species flocks of cichlid fishes in the East African Great Lakes Victoria, Malawi, and Tanganyika are prime model systems in evolutionary biology and, particularly, in research focusing on speciation,

adaptive radiation, and parallel evolution (reviewed in Kocher, 2004; Salzburger, 2009; Sturmbauer et al., 2011). One of the most outstanding features of the East African cichlid assemblages is their species richness, with each of the Great Lakes harboring hundreds of endemic species. The downside of this unparalleled diversity is that these species flocks are notoriously difficult to study in their entirety, which makes it attractive to study simpler cichlid communities in smaller water bodies. In the last years surveys of crater lakes cichlids proved especially fruitful, mostly due to the degree of isolation of their cichlid assemblages (Schliewen et al., 1994; Barluenga & Meyer, 2004; Barluenga et al., 2006). The probably best-studied cichlids in volcanic crater lakes belong to the Midas Cichlid species complex (*Amphilophus* spp.), which is native to Central America. Midas cichlids are abundant in the large lakes of Nicaragua (Lake Nicaragua and Lake Managua) and associated rivers in Nicaragua and northern Costa Rica. Interestingly, Midas Cichlids have also colonized various volcanic crater lakes in the area (Barlow, 1976; Barluenga & Meyer, 2004, 2010), which emerge when calderas of extinct volcanoes of the 'Pacific Ring of Fire' become filled with water.

This study focuses on the *Amphilophus* assemblages in two of these crater lakes, Apoyo and Xiloá, which contain two independent, yet ecologically and morphologically very similar sets of Midas cichlid species (Elmer et al., 2010; Geiger et al., 2010a). The lakes are similar in some aspects, such as their volcanic origin, but they do differ in others (Barlow, 1976; Sussman, 1985; Waid et al., 1999; McKaye et al., 2002; Barluenga & Meyer, 2010): With a surface area of 21.1 km^2 and a maximum depth of 142 m, Lake Apoyo is larger and deeper than Lake Xiloá, which has a surface area of 3.8 km^2 and a maximum depth of 89 m (Table 1). Also, compared to the nutrient-rich Lake Xiloá, Lake Apoyo is oligotrophic. Furthermore, they differ in the number of cichlid species. Crater Lake Apoyo is suggested to harbor six endemic species of the *Amphilophus* complex (Barlow, 1976; Stauffer et al., 2008; Geiger et al., 2010b) (Supplementary Table 1), which most likely go back to a seeding lineage from adjacent Lake Nicaragua (Barluenga et al., 2006); together with *Parachromis managuense* and the recently introduced African species *Oreochromis aureus* and *O. niloticus*, these are the only cichlids found in this lake. In Lake Xiloá three to four endemic species of the *Amphilophus* species complex are described (McKaye et al., 2002; Stauffer & McKaye, 2002) (Supplementary Table 1), which derive from the close-by Lake Managua stocks (Barluenga & Meyer, 2010). In addition to the Midas Cichlid fish, Lake Xiloá is inhabited by eight additional cichlid species, which either migrated naturally from nearby Lake Managua, or were introduced by humans, as might be the case for *Parachromis managuense* (Kullander & Hartel, 1997).

Table 1 General descriptors of size, depth, age, visibility, fish density, and population size of the crater lakes Apoyo and Xiloá

	Apoyo	Xiloá
Surface area (km^2)	21.1[a]	3.8[a]
Maximum depth (m)	142[a]	89[a]
Age (year)	<23.000[a]	ca. 10.000[a]
Secchi depth (m)	5–7	3
Cichlid density along shore (individuals per 10 m transect)	11.3	19.9
Total number of *Amphilophus* spp. along shore (estimated)	83.000	66.000

[a] Barluenga & Meyer (2010)

Here, we present a comparative study of cichlid abundance and density estimates in the two Central American calderas Lake Apoyo and Lake Xiloá. The set-up consisting of two rather similar crater lakes seeded independently by more or less the same ancestral line that subsequently radiated in parallel appears ideal to disentangle the biotic and abiotic factors influencing parallel adaptive radiation, particularly in its early stages. Many adaptive radiations appear to proceed in discrete stages starting with an initial diversification into macrohabitats (Streelman & Danley, 2003; Gavrilets & Losos, 2009), which—in fishes—is often associated with differentiation along the benthic-limnetic (pelagic) axis (Schluter & McPhail, 1992; Gíslason et al., 1999; Barluenga et al., 2006; Rutschmann et al., 2011). That independent adaptive radiations of the same group of organisms in similar ecological settings often result in similar morphologies is generally taken as strong evidence for natural selection (and the importance of ecology in speciation) (see Schluter & Nagel, 1995; Losos et al., 1998). On the other hand, the degree of similarity observed in convergent species pairs of cichlids has led some authors to question whether natural selection alone is sufficient to produce such matching morphologies, or whether genetic or developmental constraints have

contributed to the evolution of convergent forms (see, e.g., Brakefield, 2006). Even in the genomic era it is difficult to determine the relative contribution of natural selection and developmental channeling to parallel evolution. One possibility is to apply genetic and genomic experiments (reviewed in: Brakefield, 2006; Arendt & Reznick, 2008). In addition, one should inspect parallel radiations with respect to key ecological parameters. Under the assumption that ecology is the driving force behind parallel adaptive radiation, it is expected that not only the outcome of the radiations should be the same, but that the radiations should also follow the same steps and should show the same (ecological) characteristics. In the case of the parallel radiations of the Midas Cichlid in crater lakes Apoyo and Xiloá, the outcome in form of morphologically equivalent species is obviously quite similar (Fig. 1) and there is evidence that the radiations progressed in a similar fashion (Barluenga et al., 2006; Barluenga & Meyer, 2010; Elmer et al., 2010). It is not known, however, whether the communities in the seemingly similar crater lakes Apoyo and Xiloá are also similar in terms of ecological parameters such as fish densities and depth distributions.

In this study, we applied transect surveys to record the abundance of *Amphilophus* spp. in crater lakes Apoyo and Xiloá. Applying SCUBA diving and snorkeling, fish were counted at different locations and depth levels to provide data on densities of cichlids in both lakes. We hypothesized that the

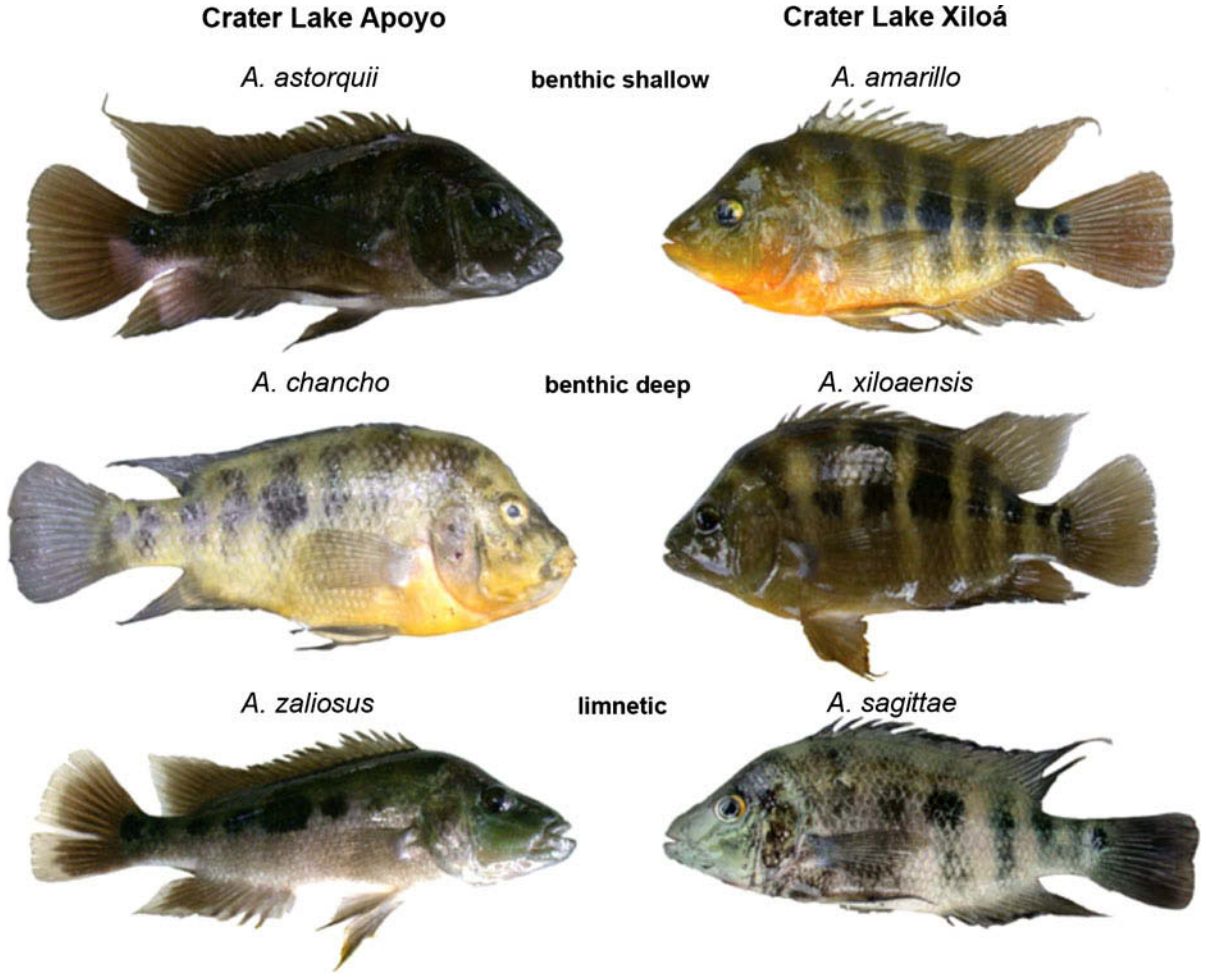

Fig. 1 Convergent phenotypes that evolved independently in the two Nicaraguan crater lakes Apoyo and Xiloá. Three species pairs are shown: benthic species using the shallow areas of the lakes; benthic species using the deeper areas of the lakes; and limnetic species inhabiting the open water column

density and distribution of Midas cichlids should be rather similar in both crater lakes due to their similar mode of origin and structure. In addition, this study aims to add ecological data in the form of abundance estimates for *Amphilophus* spp. to theoretical studies on sympatric and/or ecological speciation. Gavrilets et al. (2007), for example, investigated under which biological conditions rapid colonization of a new niche followed by sympatric or parapatric speciation in Lake Apoyo is theoretically possible. However, in their models, Gavrilets et al. (2007) were lacking empirical data on several important biological parameters (including abundance estimates). Finally, knowledge of the natural abundance of a population, species, or species group is fundamental not only to biological research but also to the management of wildlife populations. This is important in the case of crater lakes Apoyo and Xiloá, too, where cichlid fishes make up the main fraction of the ichthyofauna and provide a valuable food resource for local people (Schuster, 1957; Lin, 1961; Barlow, 1976). Importantly, through the recent introduction of African tilapiine cichlid species (*Oreochromis* spp.), the endemic cichlids of Lake Apoyo are thought to be threatened (McKaye et al., 1995; McCrary et al., 2001; Barluenga & Meyer, 2004), calling for an evaluation of the conservation status of the endemic faunas in the two crater lakes. Our data should, thus, provide important baseline references, with which upcoming impacts on the native cichlid abundance can be assessed.

Materials and methods

Study area and period

Field work was carried out in the two crater lakes Apoyo and Xiloá in Nicaragua, Central America, in September 2009. Diving was performed during the day by almost invariably good weather conditions. At the time of the study, water temperatures ranged between 29 and 31°C on all surveyed depth levels in both lakes. Transect sites were chosen randomly in both lakes, balanced, however, for different geographical locations within each lake (Supplementary Table 2). As crater lakes have a relatively homogenous habitat structure, the transects are representative of the habitat composition in each lake.

Transect surveys

We used fish counts along line transects to compare the depth-dependent abundance and density of *Amphilophus* spp. between the two lakes. Six transects were studied in the larger Lake Apoyo and four transects in the smaller Lake Xiloá. The start and end coordinates of each transect were taken with a handheld GPS from a boat (Supplementary Table 2). Depth levels at 10, 15, and 20 m were covered for each transects by a SCUBA diving buddy pair, whereas the 5 m depth level was covered by snorkelers (whenever the visibility was sufficient).

Transect length was determined by the distance covered during 10–15 min of diving (depending on the available air). Diving pace was moderate but varied between transects according to visibility and the quantity of fish that had to be counted, leading to variation in the lengths of the different transects. After having covered a transect one way, buddy pairs remained at their set depth level for 10 min to leave enough time for the fish to restore an undisturbed distribution. The end of each transect was marked with a buoy, which enabled the recording of the GPS coordinates. Buddy pairs then returned along the line transect back to the starting point. Diving was performed at 2 m above the substrate whereby dive buddies were swimming beside each other, individually counting all *Amphilophus* spp. individuals larger than ca. 5 cm within a visual field of about 4 m distance and 2 m to either side of the transect line. Snorkelers covering the 5 m depth used the same method and tried to remain at a depth of 3 m as much as possible. Owing to the difficulty to clearly identify species in sub-adult or non-breeding life stages underwater and the ongoing debate and steady changes in species classification, the overall number of *Amphilophus* spp. individuals was counted and no attempts were made to distinguish species, hybrids, or morphotypes (e.g., Barlow, 1976; McKaye et al., 2002; Bunje et al., 2007; Stauffer et al., 2008). In this visual survey a minimal bias among and within observers is expected due to individual survey differences (Thompson & Mapstone, 1997). To remove such potential confounding effects, observers alternated between different depth levels and in buddy pair partners at consecutive transects. The total number of dives over all transects was 36 (including each two persons diving back and forth), resulting in 144 single transect records.

In addition, Secchi depth measurements were taken from a boat to determine the water transparency at several random locations in both lakes.

Data analysis

To determine the average number of *Amphilophus* spp. individuals for every transect at each depth level separately, we averaged the fish counts by the two buddy team partners including the replicates from diving back and forth (Supplementary Table 3). We then calculated the average numbers of individuals per 10 m transect length for each depth level for every transect (Fig. 2), which we tested for normal distribution by applying a Shapiro–Wilk test. Using this data we tested for an overall difference in the density of *Amphilophus* spp. between lakes using Mann–Whitney U tests. We further applied a linear mixed model (LMM, LME4 package, Bates et al., 2011) to test for a difference in number and depth-distribution of individuals between the lakes by including the number of individuals counted per 10 m as the dependent variable, and lake and depth level as predictors. Assumptions of the LMM were visually checked. Since we assumed a potential difference in the depth-distribution of individuals between lakes, we included the interaction of lake and depth in the model. Furthermore, to correct for dependence in our data, we included transect as random factor. To further explore the data for effects not captured by the LMM, we applied separate Mann–Whitney U Tests for each depth level to test for depth-dependent differences in fish abundance between lakes. To roughly estimate the total number of Midas cichlids for both lakes, the numbers of fish per 10 m were extrapolated to the total circumference of the lake. This was calculated by summing up the average number of individuals at all four depth levels (Suppl. Table 3) multiplied by the circumference of the lake. All analyses was performed using R 2.9.2 (R Foundation for Statistical Computing, Vienna, Austria).

Results

The average number of *Amphilophus* spp. individuals per 10 m transect length in Apoyo across all transects and depth levels was 11.3 (min = 0, max = 37, SD = 9.5), which did not differ significantly from Lake Xiloá with 19.9 fish per 10 m transect length (min = 3, max = 55, SD = 15.7) (Mann–Whitney U test, $N = 36$, $p = 0.112$). The LMM did not reveal a significant interaction between lake and depth ($t = 0.1692$, $p = 0.169$) (Fig. 2). However, testing for single depth levels between the lakes revealed a marginally significant difference at the 5 m depth level (Mann–Whitney U test, $N = 10$, $W = 18$, $p = 0.050$). The pairwise comparison of numbers of fish per 10 m transect at the other depth levels exhibited no significant difference between the lakes (Mann–Whitney U test, 10 m: $N = 10$, $p = 0.394$; 15 m: $N = 10$, $p = 0.796$; 20 m: $N = 8$, $p = 0.180$).

Extrapolating the average number of *Amphilophus* spp. individuals of all transects and depth levels to the total circumference in both lakes (Apoyo approx. 18.2 km; Xiloá approx. 8.3 km) revealed a similar

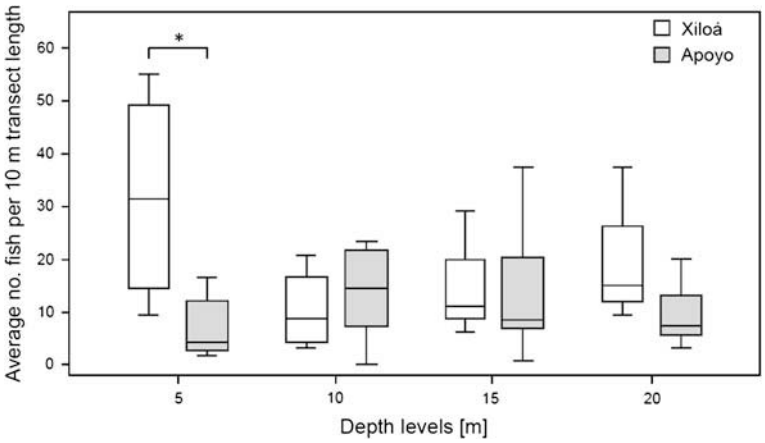

Fig. 2 Average number of *Amphilophus* spp. individuals per 10 m transect at each depth level for Lake Xiloá and Lake Apoyo. "*" denotes a marginally significant difference in cichlid fish density between the lakes (Mann–Whitney U test, $N = 10$, $p = 0.050$)

total number of fish in both lakes along the shoreline: ca. 83.000 individuals (13.000 to 150.000) in Lake Apoyo and ca. 66.000 individuals (13.000 to 120.000) in Lake Xiloá.

The Secchi depth, measured randomly several times in both lakes, ranged between 5 and 7 m in Lake Apoyo, compared to an approximately constant Secchi depth of 3 m in Lake Xiloá.

Discussion

Benefits of fish abundance estimates are diverse. The comparison of fish abundances between comparable ecosystems (e.g., between lakes) that differ in only few and well-defined ecological factors, allows to draw general conclusions on the possible impact of these factors on fish abundances and the composition and evolution of communities. This is especially the case when members of the same lineage radiated in parallel. Furthermore, in conservation biology and wildlife management, for example, changes in abundance of a fish species or population in a specific area may give an estimate for its "ecological health". This allows to define appropriate conservation strategies as well as to evaluate the (long-term) effects of habitat or species-specific conservation actions (Cheal & Thompson, 1997; Witmer, 2005). To estimate the impact of naturally induced (e.g., by a hurricane) or human-induced (e.g., by industrial fishery) changes on fish abundance, a baseline abundance needs to be established against which future levels of impact can be assessed (Jennings & Blanchard, 2004; Silvano et al., 2009). Then, abundance estimates are valuable to evaluate the relative importance and status of a fish species in an ecosystem, such as in a predator–prey relationship in the food web. Finally, mathematical modeling in fields such as evolutionary biology provides more accurate, theoretical insights into biological processes. Most often, however, theoretical approaches lack data from empirical work such as abundance estimates that would allow to make biologically reasonable assumptions and to apply mathematical models to particular case studies (see, e.g., Gavrilets et al., 2007).

The above reasons have been the motivation for this comparative study of Midas cichlid fish (*Amphilophus* spp.) abundance and density estimates in the two comparable Nicaraguan crater lakes, Apoyo and Xiloá. Despite the lack of statistical significance, our data reveal an almost twofold higher density of cichlid fish along the shoreline in Lake Xiloá as compared to Lake Apoyo. At a depth of 5 m, we found a more than fourfold higher density of Midas cichlids in Lake Xiloá (Fig. 2). Overall, however, as a consequence of the higher density of fish in the smaller lake Xiloá, the absolute numbers of *Amphilophus* spp. are relatively similar in both lakes—at least along the shore habitat covered by our survey.

Differences in food availability could explain the different densities of *Amphilophus* spp. between the two crater lakes. Indeed, the two lakes differ in their level of eutrophication: Lake Apoyo is an oligotrophic environment, whereas Lake Xiloá is relatively more eutrophic. But why would higher fish densities then only be found at shallow areas and not throughout Lake Xiloá? Eutrophication leads to a considerable reduction of ambient light at deeper waters (e.g. Koch, 2001), which can restrict photosynthesis to the shallow waters where sufficient ambient light is available for primary production (see Secchi depth in Table 1). This can directly (e.g., algae-feeders) or indirectly (e.g., through the food web) lead to higher fish densities in the shallow area. Higher fish densities in more turbid waters may also be explained by the reduced performance of predators, such as birds, which under turbid conditions have more difficulties to spot fish. It has previously been shown that reduced visibility can influence color-recognition in cichlids, and, hence, may have an impact on intraspecific (and interspecific) species recognition and communication (see, e.g., Seehausen, 1997, 2008). Whether this is also the case in Nicaraguan crater lakes remains to be tested.

An alternative explanation for the higher density of cichlids in Lake Xiloá could be the availability of ecologically more diverse niches in this lake, e.g., in the shallow area where differences in the densities of *Amphilophus* spp. are greatest. This could also explain the higher variance in fish counts at the 5 m depth level in Lake Xiloá compared to the other depth levels. Perhaps it is a combination of both factors, eutrophication and habitat complexity, that leads to higher fish densities in Lake Xiloá. A more thorough analysis of the habitat structure would be necessary to clarify this point. Furthermore, there is no knowledge on fish densities in deeper and open waters, which would allow a comprehensive comparison of both lakes. Such fish counts at deeper waters seem particularly

interesting, since we observed a distinct and clear water layer below a depth of 35 m in Lake Xiloá.

Crater lakes Apoyo and Xiloá are inhabited by a similar set of convergent *Amphilophus* ecotype morphs (Fig. 1) making the Midas Cichlid complex an ideal system to study parallel evolution (see, e.g., McKaye et al., 2002; Barluenga et al., 2006; Elmer et al., 2010). While taxonomy, morphology, and evolutionary history of the species complex is largely resolved (see Barluenga et al., 2006; Barluenga & Meyer, 2010; Elmer et al., 2010; Geiger et al., 2010a, b), little is known about basic ecological parameters such as the relative densities of the different species. Our study is the first to provide such data. We uncover a rather similar overall number of *Amphilophus* spp. individuals in both lakes, but also account differences in densities, especially in the shallow area (see above). Interestingly, the shallow areas of Lake Xiloá are not only characterized by larger densities of Midas cichlids, but also by the presence of additional cichlid species (see Supplementary Table 1). It remains unclear whether these never arrived in Lake Apoyo (e.g., because of the larger distance to a large lake), or whether these could not establish themselves there (e.g., because of the eutrophic situation). In any case, convergent phenotypes evolved in both crater lakes despite noticeable differences in size and age of the respective lake (see Table 1), in community structure (the presence/absence of other cichlid species; Supplementary Table 1), and in fish densities (Fig. 2). This corroborates the view that the initial steps of ecological speciation in fish species flocks follow similar pathways in form of a splitting into benthic and limnetic types (see, e.g., Schluter & McPhail, 1992; Salzburger, 2009), which does not seem to be dependent on phylogenetic background and parameters such as size or age of a lake or level of eutrophication. Apparently, it is enough that a benthic-limnetic axis is present in a lake (see Barluenga et al., 2006).

The Midas cichlid fauna from Lake Apoyo represents one of the most famous examples for sympatric speciation (Barluenga et al., 2006), and has attracted theoretical modeling work. Gavrilets et al. (2007), for example, investigated whether at all and under which ecological conditions sympatric speciation is likely to have occurred in lake Apoyo. One of the parameters incorporated into the model of Gavrilets et al. (2007) was the carrying capacity (K) of Lake Apoyo. Carrying capacity stands for the maximum number of individuals that can live in a particular environment given the available nutrients and without causing detrimental effects. Gavrilets et al. (2007) concluded that intermediate carrying capacities ($K = 16.000$) are propensive for sympatric speciation, whereas large carrying capacities ($K = 32.000$–51.200, depending on the model) would rather lead to the evolution of a single, generalistic species. Our estimates of K (ca. 83.000 and ca. 66.000 individuals in Lakes Apoyo and Xiloá, respectively) lie above these numbers, although these estimates refer to counts at four depth levels along the shoreline only and nothing is known about fish densities below 20 m. One also has to consider that Gavrilets et al. (2007) assumed the presence of a single age class (i.e., generation) at a given time. Our counts certainly included members from different age classes, although we lack detailed information on age distribution. Taken together, the carrying capacities assumed by Gavrilets et al. (2007) to model sympatric speciation in Lake Apoyo seem to be slightly—however not substantially—underestimated compared to our findings and it would now be interesting to evaluate what effect this has on available models.

Although a reproducing population of invasive *Oreochromis* spp. (tilapias) has been reported for Lake Apoyo in previous studies (McKaye et al., 1995; McCrary et al., 2001), we did not observe any tilapiine species during our fieldwork. These African cichlids were reported to feed on stonewort beds (*Chara* spp.) and are likely to account for the temporal elimination of these algae in Lake Apoyo (McKaye et al., 1995; McCrary et al., 2001, Canonico et al., 2005). However, we found extensive stonewort beds in Lake Apoyo. This suggests that tilapia populations might have failed to establish permanently in an oligotrophic environment such as Lake Apoyo.

Conclusions

Our study gives estimates of cichlid fish densities in two crater lakes in Nicaragua, Apoyo and Xiloá. We find that parallel ecotype morphs evolved despite noticeable differences in size, age, eutrophication level, and carrying capacity. We provide ecological data for understanding the carrying capacity of the systems in order to apply it to modeling sympatric/parapatric speciation. Furthermore, it sets baseline abundance estimates for cichlid fish in Nicaraguan

crater lakes, to which future ecological health assessments of these lakes can be compared.

Acknowledgments We are grateful to C. Heule, N. Hue and A. Theis for assisting us with diving; B. Christ and T. Suter for their helping hand at dive sites; the Ministerio del Ambiente y los Recursos Naturales Nicaragua (MARENA) for research permits; E. P. van den Berghe for logistical help and scientific expertise; and two anonymous referees, Associated Editor C. Sturmbauer and the Editor K. Martens for valuable comments on the manuscript; T. Roth for statistical support, and the "Fuerzas Armadas de Nicaragua" for boat cruises and air supply. This project was funded by grants from the European Research Council (ERC) and the Swiss NSF.

References

Arendt, J. & D. Reznick, 2008. Convergence and parallelism reconsidered: what have we learned about the genetics of adaptation? Trends in Ecology & Evolution 23: 26–32.

Barlow, G. W., 1976. The Midas cichlid in Nicaragua. In Thorson, T. B. (ed.), Investigations of the Ichthyofauna of Nicaraguan Lakes, University of Nebraska-Lincoln: 333–358.

Barluenga, M. & A. Meyer, 2004. The Midas cichlid species complex: incipient sympatric speciation in Nicaraguan cichlid fishes. Molecular Ecology 13: 2061–2076.

Barluenga, M. & A. Meyer, 2010. Phylogeography, colonization and population history of the Midas cichlid species complex (*Amphilophus* spp.) in the Nicaraguan crater lakes. BMC Evolutionary Biology 10: 326.

Barluenga, M., K. N. Stölting, W. Salzburger, M. Muschick & A. Meyer, 2006. Sympatric speciation in Nicaraguan Crater Lake cichlid fish. Nature 439: 719–723.

Bates, D., M. Mächler & B. Bolker, 2011. LME4: linear mixed-effects model using S4 classes. R package, v. 0.999375-40. http://cran.r-project.org.

Brakefield, P. M., 2006. Evo-devo and constraints on selection. Trends in Ecology & Evolution 21: 362–368.

Bunje, P. M., M. Barluenga & A. Meyer, 2007. Sampling genetic diversity in the sympatrically and allopatrically speciating Midas cichlid species complex over a 16 year time series. Bmc Evolutionary Biology 7: 25.

Canonico, G. C., A. Arthington, J. K. McCrary & M. L. Thieme, 2005. The effects of introduced tilapias on native biodiversity. Aquatic Conservation: Marine and Freshwater Ecosystems 15: 463–483.

Cheal, A. J. & A. A. Thompson, 1997. Comparing visual counts of coral reef fish: implications of transect width and species selection. Marine Ecology Progress Series 158: 241–248.

Elmer, K. R., H. Kusche, T. K. Lehtonen & A. Meyer, 2010. Local variation and parallel evolution: morphological and genetic diversity across a species complex of Neotropical Crater Lake cichlid fishes. Philosophical Transactions of the Royal Society London B 365: 1763–1782.

Gavrilets, S., A. Vose, M. Barluenga, W. Salzburger & A. Meyer, 2007. Case studies and mathematical models of ecological speciation. 1. Cichlids in a crater lake. Molecular Ecology 16: 2893–2909.

Gavrilets, S. & J. B. Losos, 2009. Adaptive radiation: contrasting theory with data. Science 323: 732–737.

Geiger, M. F., J. K. McCrary & U. K. Schliewen, 2010a. Not a simple case – A first comprehensive phylogenetic hypothesis for the Midas cichlid complex in Nicaragua (Teleostei: Cichlidae: Amphilophus). Molecular Phylogenetics and Evolution 56: 1011–1024.

Geiger, M. F., J. K. McCrary & J. R. Stauffer, 2010b. Description of two new species of the Midas cichlid complex (Teleostei: Cichlidae) from Lake Apoyo, Nicaragua. Proceedings of the Biological Society of Washington 123: 159–173.

Gíslason, D., M. M. Ferguson, S. Skúlason & S. S. Snorrason, 1999. Rapid and coupled phenotypic and genetic divergence in Icelandic Arctic charr (*Salvelinus alpinus*). Canadian Journal of Fisheries and Aquatic Sciences 56: 2229–2234.

Jennings, S. & J. Blanchard, 2004. Fish abundance with no fishing: predictions based on macroecological theory. Journal of Animal Ecology 73: 632–642.

Koch, E. W., 2001. Beyond light: physical, geological and geochemical parameters as possible submersed aquatic vegetation habitat requirements. Estuaries 24: 1–17.

Kocher, T. D., 2004. Adaptive evolution and explosive speciation: the cichlid fish model. Nature Reviews Genetics 5: 288–298.

Kullander, S. & K. E. Hartel, 1997. The systematic status of cichlid genera described by Louis Agassiz in 1859: Amphilophus, Baiodon, Hypsophyrs and Parachromis (Teleostei: Cichlidae). Ichthyological Explorations of Freshwaters 7: 193–202.

Lin, S. Y., 1961. Informe al goberino de Nicaragua sobre el desarrollo de un proyecto de pesquerías continentals en dicho país. Informe F. A. O. 1347: 1–21.

Losos, J. B., T. R. Jackman, A. Larson, K. Queiroz & L. Rodriguez-Schettino, 1998. Contingency and determinism in replicated adaptive radiations of island lizards. Science 279: 2115–2118.

McCrary, J. K., E. P. van den Berghe, K. R. McKaye & L. J. Lopez Perez, 2001. Tilapia cultivation: a threat to native species in Nicaragua. Encuentro 58: 9–19.

McKaye, K. R., J. D. Ryan, J. R. Stauffer, L. J. Lopez Perez & E. P. van den Berghe, 1995. African tilapia in Lake Nicaragua: ecosystem in transition. BioScience 45: 406–411.

McKaye, K. R., J. R. Stauffer, E. P. van den Berghe, R. Vivas, L. J. Lopez Perez, J. K. McCrary, R. Waid, A. Konings, W. J. Lee & T. D. Kocher, 2002. Behavioral, morphological and genetic evidence of divergence of the Midas Cichlid species complex in two Nicaraguan crater lakes. Cuadernos de Investigación de la UCA 12: 19–47.

Rutschmann, S., M. Matschiner, M. Damerau, M. Muschick, M. F. Lehmann, R. Hanel & W. Salzburger, 2011. Parallel ecological diversification in Antarctic notothenioid fishes as evidence for adaptive radiation. Molecular Ecology 20: 4707–4721.

Salzburger, W., 2009. The interaction of sexually and naturally selected traits in the adaptive radiations of cichlid fishes. Molecular Ecology 18: 169–185.

Schliewen, U. K., D. Tautz & S. Paabo, 1994. Sympatric speciation suggested by monophyly of crater lake cichlids. Nature 368: 629–632.

Schluter, D. & J. D. McPhail, 1992. Ecological character displacement and speciation in sticklebacks. American Naturalist 140: 85–108.

Schluter, D. & L. Nagel, 1995. Parallel speciation by natural selection. American Naturalist 140: 292–301.

Schuster, W. H., 1957. Informe al goberino de Nicaragua sobre fomento de la pesca contonental. Informe F. A. O. 607: 1–13.

Seehausen, O., 1997. Cichlid fish diversity threatened by eutrophication that curbs sexual selection. Science 277: 1808–1811.

Seehausen, O., Y. Terai, I. S. Magalhaes, K. L. Carleton, H. D. J. Mrosso, R. Miyagi, I. van der Sluijs, et al., 2008. Speciation through sensory drive in cichlid fish. Nature 455: 620–626.

Silvano, R. A. M., M. Ramires & J. Zuanon, 2009. Effects of fisheries management on fish communities in the floodplain lakes of a Brazilian Amazonian Reserve. Ecology of Freshwater Fish 18: 156–166.

Stauffer, J. R. & K. R. McKaye, 2002. Descriptions of three new species of cichlid fishes (Teleostei: Cichlidae) from Lake Xiloá, Nicaragua. Cuadernos de Investigacíon de la Universidad Centroamericana 12: 1–18.

Stauffer, J. R., J. K. McCrary & K. E. Black, 2008. Three new species of cichlid fishes (Teleostei: Cichlidae) from Lake Apoyo, Nicaragua. Proceedings of the Biological Society Washington 121: 117–129.

Streelman, J. T. & P. D. Danley, 2003. The stages of vertebrate evolutionary radiation. Trends in Ecology & Evolution 18: 126–131.

Sturmbauer, C., M. Husemann & P. D. Danley, 2011. Explosive speciaiton and adaptive radiation of East African cichlid fishes. In Zachos, F. E. & J. C. Habel (eds.), Biodiversity Hotspots: Distribution and Protection of Conservation Priority Areas. Springer: 333–362.

Sussman, D., 1985. Apoyo caldera, Nicaragua: a major quaternary silicic eruptive center. Journal of Volcanology and Geothermal Research 24: 249–282.

Thompson, A. A. & B. D. Mapstone, 1997. Observer effects and training in underwater visual surveys of reef fishes. Marine Ecology Progress Series 154: 53–63.

Waid, R. M., R. L. Raesly, K. R. McKaye & J. K. McCrary, 1999. Zoogeografía íctica de lagunas cratéricas de Nicaragua. Encuentro 51: 65–80.

Witmer, G. W., 2005. Wildlife population monitoring: some practical considerations. Wildlife Research 32: 259.

1.6.2
Supporting information

Supplementary Table 1: Cichlid fish diversity in lakes Apoyo and Xiloá.

Lake Apoyo – Midas cichlid species (endemic)
Amphilophus zaliosus Barlow and Munsey 1976
Amphilophus flaveolus Stauffer *et al.* 2008
Amphilophus chancho Stauffer *et al.* 2008
Amphilophus astorquii Stauffer *et al.* 2008
Amphilophus globosus Geiger *et al.* 2010
Amphilophus supercilius Geiger *et al.* 2010
Lake Apoyo – other cichlid species (introduced)
Parachromis managuense Kallander 1997
Oreochromis aureus Steindachner 1864
Oreochromis niloticus Linnaeus 1758
Lake Xiloá – Midas cichlid species (endemic)
Amphilophus xiloaensis Stauffer and McKaye 2002
Amphilophus amarillo Stauffer and McKaye 2002
Amphilophus sagittae Stauffer and McKaye 2002
Amphilophus sp. "Fat lips" (Stauffer and McKaye 2002, undescribed)
Lake Xiloá – other cichlid species (native)
Astatoheros longimanus Jordan *et al.* 1930
Archocentrus centrarchus Jordan *et al.* 1930
Amphilophus rostratus Kullander 1996
Parachromis dovii Kullander *et al.* 1997
Hypsophrys nicaraguensis Kullander *et al.* 1997
Parachromis managuense Kullander *et al.* 1997
Hypsophrys nematopus Chakrabarty *et al.* 2007
Amantitlania siquia Schmitter-Soto 2007

Supplementary Table 2: Coordinates and length of the transects in lakes Apoyo and Xiloá. Lengths were calculated by measuring start and end coordinates of each transect with a GPS device.

Lake	Transect	Start coordinate	Length [m]
Apoyo	1	11°54,554' N / 86°02,467' W	120
	2	11°54,183' N / 86°01.791' W	115
	3	11°55,626' N / 86°00,854' W	80
	4	11°56,196' N / 86°01,371' W	80
	5	11°56,002' N / 86°03,391' W	80
	6	11°92,538' N / 86°05,557' W	80
Xiloá	1	12°23,120' N / 86°31,857' W	40
	2	12°23,081' N / 86°32,259' W	40
	3	12°21.483' N / 86°32,548' W	50
	4	12°21.428' N / 86°31,510' W	50

Supplementary Table 3: Averaged numbers of cichlid fish per 10 m transect for each transect and depth level. Numbers are the averaged fish counts by the two buddy team partners including the replicates from diving back and forth.

Lake	Transect	Depth [m]				
		5	10	15	20	total
Apoyo	1	-	7.0	6.6	5.7	6.4
	2	12.3	21.7	9.9	13.2	14.3
	3	2.4	23.0	37.3	-	20.9
	4	16.2	21.8	20.4	20.1	19.6
	5	4.3	0.0	0.6	3.2	2.0
	6	1.6	6.9	6.8	7.2	5.6
	total	7.4	14.7	15.0	8.7	11.4
Xiloá	1	43.3	12.6	29.1	9.6	23.7
	2	55.0	5.5	-	37.3	32.6
	3	19.4	20.9	11.2	-	17.2
	4	9.7	3.2	6.4	15.1	8.6
	total	31.9	10.6	15.6	20.7	19.7

Part 2
The adaptive radiation of Antarctic notothenioids

2.1

The Adaptive Radiation of Notothenioid Fishes in the Waters of Antarctica

Extremophile Fishes - Ecology, Evolution, and Physiology of Teleosts in Extreme Environments

I wrote subsection 5: “The Adaptive Character of the Notothenioid Radiation “, helped creating the figure and discussed the manuscript. All authors wrote different subsections and/or participated in discussing the manuscript. MM assembled the different subsections and drafted the final version of the manuscript.

The Adaptive Radiation of Notothenioid Fishes in the Waters of Antarctica

Michael Matschiner, Marco Colombo, Malte Damerau, Santiago Ceballos, Reinhold Hanel, and Walter Salzburger

Abstract Fishes of the perciform suborder Notothenioidei, which dominate the ichthyofauna in the freezing waters surrounding the Antarctic continent, represent one of the prime examples of adaptive radiation in a marine environment. Driven by unique adaptations, such as antifreeze glycoproteins that lower their internal freezing point, notothenioids have not only managed to adapt to sub-zero temperatures and the presence of sea ice, but also diversified into over 130 species. We here review the current knowledge about the most prominent notothenioid characteristics, how these evolved during the evolutionary history of the suborder, how they compare between Antarctic and non-Antarctic groups of notothenioids, and how they could relate to speciation processes.

1 Antarctic Waters: An Extreme Environment

Antarctica represents an isolated "continental island," separated from other continental shelves by the Antarctic Circumpolar Current (ACC) that reaches the ocean floor (Foster 1984) and transports more water than any other ocean current on Earth (Tomczak and Godfrey 2003). The Antarctic Polar Front (APF), located between 50 and 60°S, thermally isolates the continent (Gordon 1971) and poses an

M. Matschiner (✉) • W. Salzburger (✉)
Zoological Institute, University of Basel, Vesalgasse 1, 4051 Basel, Switzerland

Centre for Ecological and Evolutionary Synthesis (CEES), Department of Biosciences, University of Oslo, Oslo, Norway
e-mail: michaelmatschiner@mac.com; walter.salzburger@unibas.ch

M. Colombo
Zoological Institute, University of Basel, Vesalgasse 1, 4051 Basel, Switzerland

M. Damerau • R. Hanel
Thünen Institute of Fisheries Ecology, Palmaille 9, 22767 Hamburg, Germany

S. Ceballos
Zoological Institute, University of Basel, Vesalgasse 1, 4051 Basel, Switzerland

Centro Austral de Investigaciones Científicas (CADIC), Bernardo A. Houssay 200, cp 9410 Ushuaia, Tierra Del Fuego, Argentina

R. Riesch et al. (eds.), *Extremophile Fishes*, DOI 10.1007/978-3-319-13362-1_3

additional physical barrier to marine organisms (Shaw et al. 2004). As a result, Antarctic waters are unique marine environments, characterized by sub-zero temperatures and the widespread presence of sea ice. At high latitudes, temperatures remain close to the freezing point of seawater at −1.86 °C throughout the year (Eastman 1993). Due to the weight of the continental ice cap, the Antarctic shelf is eight times deeper than the world average (Anderson 1999). Many potential shallow water habitats are covered by ice foots and anchor ice, and gigantic icebergs regularly rework the bottom topography as deep as 550 m below sea level, so that these habitats are constantly in a state of change or recovery (Barnes and Conlan 2007). Even at depths below 400 m, water temperatures can remain near the freezing point throughout the year (Cheng and Detrich 2007). As a consequence, Antarctic waters are among the thermally most stable habitats on Earth. Nevertheless, they are subject to strong seasonality in light conditions, which in turn influences primary production and nutrient availability (Clarke 1988). Taken together, sub-zero temperatures, the continuous presence of sea ice, and extreme seasonality pose great ecophysiological challenges for marine organisms living in Antarctic waters.

Due to the harsh environment and the isolation by the APF, only a few groups of teleost fishes have managed to successfully colonize Antarctic waters. Out of a diversity of about 28,000 teleost species worldwide (Nelson 2006), less than 400 are known to occur in Antarctica (Eastman 2005). The bulk of the Antarctic fish diversity (~90 %; Eastman 2005) belongs to three different taxonomic groups, which have all been assigned to the recently redefined order Perciformes (Betancur-R et al. 2013): the suborder Notothenioidei (107 species; see below), the family Liparidae (~150 species; Stein 2012), and family Zoarcidae (28 species; Matallanas 2008). The two largest of these groups (Notothenioidei and Liparidae) occupy mostly non-overlapping habitats, as liparids are almost exclusively found in the deep sea below ~800 m depth and are of low abundance (Stein 2012), whereas Antarctic notothenioids dominate the continental shelf and upper slope in terms of vertebrate species number (~50 %) and biomass (90–95 %) (Eastman and Clarke 1998). As most scientific sampling to date has focused on depths shallower than 1,000 m, the Antarctic liparid diversity is greatly understudied, and new species are still frequently described (Stein 2012). Nevertheless, it seems clear that Antarctic Liparidae represent a polyphyletic group resulting from multiple independent invasions from the north (Balushkin 2012), so that they are considered a secondary Antarctic group (Stein 2012). In contrast, the similarly species-rich Antarctic notothenioids apparently evolved in situ on the continental shelf and have been described as a rare example of a marine "species flock."

The species flock concept was developed more than 100 years ago by botanists to describe assemblages of closely related taxa that "flock together," i.e., coexist in the same area, and later adopted by ichthyologists for the particularly diverse cichlid fishes of the East African Great Lakes and other lacustrine evolutionary radiations (Salzburger et al. 2014). The key features of a species flock are thus, besides species richness, the common ancestry of its members, a clear-cut

geographic circumscription, and, hence, high levels of endemicity. Most, if not all, species flocks are the product of adaptive radiations (Eastman and McCune 2000; Salzburger and Meyer 2004), and as we will describe below in more detail, Antarctic notothenioid fishes represent what is arguably the most spectacular example of an extant adaptive radiation in the marine realm.

2 Taxonomy of Notothenioids

The Notothenioidei have been taxonomically classified into 8 different families and 136 species (Eastman and Eakin 2000; Table 1, continuously updated by Eastman and Eakin and available at http://www.oucom.ohiou.edu/dbms-eastman/; version Oct. 18, 2013). Five families are predominantly Antarctic and three occur in the coastal waters of New Zealand, Australia, South America, and subantarctic islands (Fig. 1a). The most widely distributed family is Bovichtidae, consisting of nine

Table 1 All non-Antarctic notothenioids with presumed Antarctic ancestry and presence of AFGP

Family/genus and species	Occurrence	AFGP
Nototheniidae		
Dissostichus eleginoides	SA, NZ, SG	No
Notothenia angustata	NZ	Yes
Notothenia microlepidota	NZ	Yes
Paranotothenia magellanica	SA	Yes
Lepidonotothen macrophthalma	SA	?
Patagonotothen brevicauda	SA	?
Patagonotothen canina	SA	?
Patagonotothen cornucola	SA	?
Patagonotothen elegans	SA	?
Patagonotothen guntheri	SA, SG	No
Patagonotothen jordani	SA	?
Patagonotothen kreffti	SA	?
Patagonotothen longipes	SA	?
Patagonotothen ramsayi	SA	No
Patagonotothen sima	SA	?
Patagonotothen squamiceps	SA	?
Patagonotothen tessellata	SA	No
Patagonotothen trigramma	SA	?
Patagonotothen thompsoni	SA	?
Patagonotothen wiltoni	SA	?
Harpagiferidae		
Harpagifer bispinis	SA	?
Channichthyidae		
Champsocephalus esox	SA	Yes

SA South America, *NZ* New Zealand, *SG* South Georgia, ? AFG possession unknown

species in three genera. Only one of these, *Bovichtus elongatus*, is found in Antarctica at the tip of the Antarctic Peninsula, while all other bovichtid species occur north of the ACC. Two notothenioid families are monotypic, and limited to temperate habitats. *Pseudaphritis urvillii* is the only member of the family Pseudaphritidae and occurs in southeast Australia and Tasmania. It is one of very few species of notothenioids that inhabits freshwaters such as slow-flowing streams and estuaries. The second monotypic family, Eleginopsidae, is represented by *Eleginops maclovinus*, which is distributed on the shelf areas of Patagonia and the Falkland Islands and commonly fished commercially in Chile and Argentina, where it is known as "róbalo." The remaining five families Nototheniidae, Bathydraconidae, Harpagiferidae, Artedidraconidae, and Channichthyidae represent the bulk of the notothenioid species diversity, including at least 125 species, most of which occur only in Antarctic waters. The exception to this are 22 non-Antarctic species of the genera *Lepidonotothen*, *Notothenia*, *Paranotothenia*, *Champsocephalus*, *Harpagifer*, *Dissostichus,* and *Patagonotothen* (see Table 1), which secondarily escaped the Southern Ocean to colonize the coastal waters of New Zealand and South America (Cheng et al. 2003).

3 Characteristics of Notothenioids

The diversification of Notothenioidei has been accompanied by a number of physiological innovations. In their ice-laden environment, the greatest ecophysiological challenge for ectotherm organisms is to prevent freezing of blood and body tissue. As marine teleost fishes have a higher colligative freezing point than seawater, contact with sea ice would lead to rapid freezing of body fluids (Cheng and Detrich 2007), which is lethal for almost all vertebrates. Thus, arguably the most important innovation of Antarctic notothenioids are antifreeze glycoproteins (AFGPs) that effectively lower their freezing point and thus prevent freezing upon contact with sea ice. AFGPs are present in all notothenioids of the five predominantly Antarctic families, with the exception of the nototheniid genus *Patagonotothen* that secondarily escaped to continental shelves of South America (Near et al. 2012). The AFGPs evolved from a pancreatic trypsinogen gene and are usually composed of 4–56 repeats of a threonine–alanine–alanine tripeptide, with threonine residues being O-glycosylated by disaccharides (Hsiao et al. 1990; Chen et al. 1997a). According to size differences, AFGPs are grouped into eight distinct types, with molecular weights between 2.6 and 33.7 kDa (DeVries and Cheng 2005). They are synthesized in the exocrine pancreas as large polyprotein precursors that are cleaved post-translationally to produce the eight different types of AFGPs (Hsiao et al. 1990; Evans et al. 2012). From the exocrine pancreas, AFGPs are discharged into the gastrointestinal tract (Cheng et al. 2006), where they bind to ice crystals ingested with food or water, and inhibit their growth until they are excreted along with feces (see Fig. 1b). Free AFGPs are resorbed via the rectal epithelium and enter the blood and the interstitial fluid. Blood-borne AFGPs reach

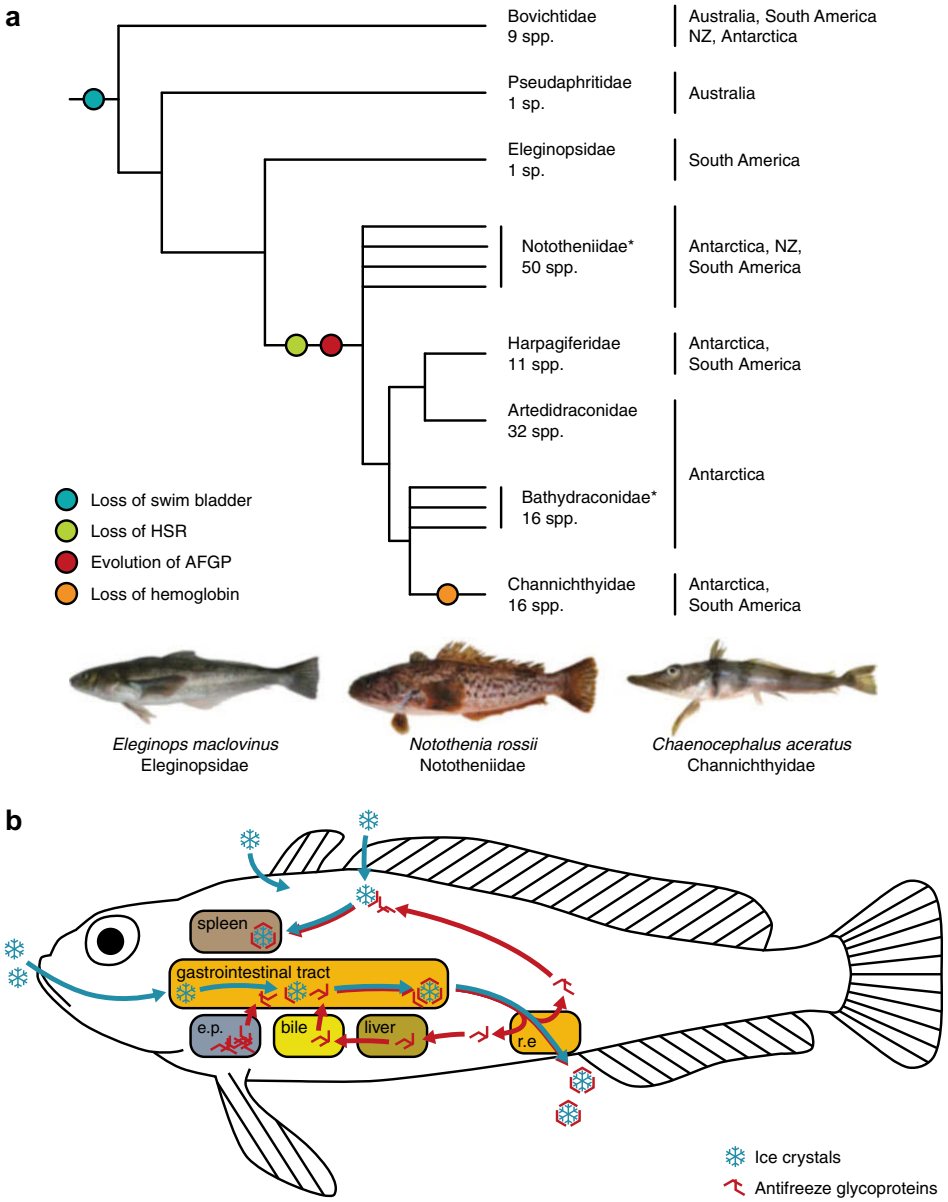

Fig. 1 (**a**) A simplified cladogram showing relations between notothenioid families, their species richness, and distribution. Major evolutionary innovations and losses (see main text) are marked by *circles* (*Asterisks* indicate presumably non-monophyletic families. *HSR* heat-shock response, *AFGP* antifreeze glycoproteins). (**b**) Schematic representation of the function of AFGP in notothenioids (*Blue-green arrows* indicate points of entry and transport of ice crystals, *red arrows* show AFGP pathways. For details see main text)

the bile via the liver and are discharged again into the gastrointestinal tract. Ice crystals present in the circulatory system usually enter the body through the epithelium, as endogenous ice nucleators are apparently absent in notothenioid fishes (Evans et al. 2011). It has been shown that larvae with low levels of AFGPs survive in ice-laden waters as long as the epithelium is intact, thus highlighting the important role of the epithelium as a protection against freezing (Cziko et al. 2006). In addition, external mucus of adult notothenioids contains AFGPs, which inhibit ice growth on the body surface, and thus prevent injury of the epithelium (albeit the mechanisms by which AFGPs are incorporated in the mucus are still unknown; Evans et al. 2011). If, despite these protective mechanisms, ice enters through the body surface, it is adsorbed by AFGPs of the blood and the interstitial fluid and transported to the spleen, where it is stored in ellipsoidal macrophages (Præbel et al. 2009; Evans et al. 2012). As no mechanism is known for the disposal of AFGP-bound ice from the spleen, it is assumed that ice accumulates in the spleen until seasonal warming events allow melting (Evans et al. 2011).

In a remarkable case of convergent evolution, near-identical AFGPs have independently emerged in at least seven Arctic species of the family Gadidae (Chen et al. 1997b; Zhuang 2013). As in notothenioids, gadid AFGP contains a large number of threonine–alanine–alanine tripeptide repeats, but apparently evolved from noncoding DNA through recruitment of an upstream regulatory sequence, rather than from a precursor gene as in notothenioids (Zhuang 2013). Different types of non-glycosylated antifreeze proteins (AFP) are known from distantly related Arctic and Antarctic fish groups, such as Zoarcidae (eelpouts), Labridae (cunner), Cottidae (sculpins), Hemitripteridae (sea ravens), Osmeridae (smelt), and Clupeidae (herring) (Cheng and DeVries 1989; Fletcher et al. 2001). The latter three lineages possess highly conserved sequences in both exons and introns of AFP genes despite an evolutionary distance of ~250 million years (Ma) (Betancur-R et al. 2013), which led Graham et al. (2008) to suggest sperm-mediated lateral gene flow as the mean of AFP acquisition. In this scenario, fish sperm would absorb foreign DNA from seawater, followed by partial integration into the sperm nucleus. Regardless of the mode of transfer, the presence of highly conserved AFP genes in distantly related lineages highlights the strong natural selection for freeze protection in sub-zero environments.

Besides AFGPs, another general feature found in all notothenioids is the lack of a swim bladder. For this reason, most notothenioids are heavier than seawater and dwell on or near the seafloor. However, several notothenioid lineages, including the genera *Aethotaxis*, *Pleuragramma*, and *Dissostichus*, have independently colonized the water column in a trend termed pelagization (Klingenberg and Ekau 1996; Rutschmann et al. 2011). If these fishes were not neutrally buoyant, continuous investment of muscular energy would be required to provide hydrodynamic uplift. Therefore, these species evolved a plethora of morphological adaptations to compensate for the lack of a swim bladder and attain neutral buoyancy (see below). To name but a few of these adaptations, some pelagic species have reduced ossification of the vertebral column and other body components, the scales of *Pleuragramma*

and *Dissostichus* are only weakly mineralized in order to save weight, and *Pleuragramma* further deposits lipids in large assemblages of adipose cells to decrease overall density and to produce static uplift (Eastman 1993; Fernández et al. 2012).

In addition to the loss of the swim bladder, at least some notothenioid species have lost a second trait that is otherwise ubiquitous: The expression of heat-shock proteins (HSPs) as a response to elevated temperatures is regarded a universal characteristic of nearly all organisms, but is absent in the highly cold-adapted stenothermal nototheniid *Trematomus bernacchii* (Hofmann et al. 2000). Further research revealed that the absence of the heat-shock response (HSR) in *T. bernacchii*, as well as in a second member of the same genus, *T. borchgrevinki*, is not due to a loss of HSPs itself, but, on the contrary, due to a constitutive upregulation of Hsp70, which is attributed to permanent cold-stress conditions (Place et al. 2004; Place and Hofmann 2005). Subsequently, this finding has been extended to a representative of the Harpagiferidae, *Harpagifer antarcticus*, suggesting that the loss of the HSR affects most notothenioids and occurred just once during their diversification (Clark et al. 2008). Despite the lack of the classic heat-shock response, notothenioids have recently been shown to retain the ability to acclimatize to elevated temperatures of up to 13–18 °C, yet the molecular mechanisms of this heat hardening remain unknown (Bilyk and DeVries 2011; Bilyk et al. 2012).

Another exceptional loss affecting part of the notothenioid radiation, namely the members of the most derived family, the Channichthyidae, is the lack of the ability to synthesize hemoglobin (Ruud 1954; Eastman 1993). The Channichthyidae are thus the only vertebrate group without oxygen-bearing blood pigments. While the absence of hemoglobin apparently results from the loss of the β-globin subunit gene due to a single deletion event (di Prisco et al. 2002), truncated and inactive remnants of the α-globin gene are retained in the channichthyid genomes (Cocca et al. 1995; Near et al. 2006). Since the oxygen-carrying capacity of the hemoglobin-less phenotype is reduced by a factor of 10, the Channichthyidae evolved compensational features such as an increased blood volume that is 2–4 times that of comparable teleosts, a large stroke volume and cardiac output, and relatively large diameters of arteries and capillaries (Eastman 1993). The adaptive value and evolutionary cause of the loss of hemoglobin remain uncertain (Sidell and O'Brien 2006), but could potentially be related to low iron availability in the Southern Ocean (von der Heyden et al. 2012).

4 Notothenioid Phylogeography

The sister lineages of Notothenioidei have long been uncertain (Dettaï and Lecointre 2004), but molecular phylogenetic analyses that have recently become available support the placement of notothenioids within a redefined order of Perciformes that also contains the suborders Serranoidei, Percoidei, Scorpaenoidei,

Triglioidei, Cottioidei, and the two families Percophidae and Platycephalidae (Betancur-R et al. 2013; Lautrédou et al. 2013). Within this order, relationships remain poorly resolved, but close affinities of Notothenioidei with Percophidae, Trachinidae, and Percidae have repeatedly been suggested (Matschiner et al. 2011; Lautrédou et al. 2013). Of the three families, Trachinidae and some members of Percidae are also characterized by the lack of a swim bladder (Lewis 1976; Evans and Page 2003), which could thus represent a shared loss between notothenioids and their sister lineage(s), depending on the precise interrelationships of these groups.

Within notothenioids, all molecular phylogenies to date agree on the sequence of the basal splits: the basal Bovichtidae are the sister group of all other notothenioid families, and the monotypic families; Pseudaphritidae and Eleginopsidae diverged before the diversification of the five predominantly Antarctic families (Balushkin 1992; Bargelloni et al. 2000; Near et al. 2004; Near and Cheng 2008; Matschiner et al. 2011; Rutschmann et al. 2011; Near et al. 2012; Betancur-R et al. 2013). Uncertainty remains only regarding the placement of the monotypic genus *Halaphritis*, which appears to be endemic to southeastern Australia and Tasmania. Only seven specimens are known of *H. platycephala*, and DNA could not be extracted from this species (Last et al. 2002). Morphologically, *H. platycephala* superficially resembles the sympatrically occurring pseudaphritid *Pseudaphritis urvillii*, but was provisionally assigned to the Bovichtidae, as it shares almost all diagnostic characters defining this family (Last et al. 2002).

Regardless of the exact affinities of *Halaphritis* with Bovichtidae and Pseudaphritidae, three out of the four most ancestral genera of notothenioids (the monotypic bovichtid genus *Cottoperca* being the exception) occur in, or are even endemic to Australian waters, suggesting that the initial diversification of the suborder took place in this region (Balushkin 2000; Matschiner et al. 2011). This scenario was supported by the time-calibrated molecular phylogeny of Matschiner et al. (2011), who found that the separation of bovichtid and pseudaphritid ancestors may have coincided with shelf area fragmentation between Australia and New Zealand around 70 Ma ago, and that the divergence between Pseudaphritidae and more derived Notothenioidei could have been caused by the breakup of Australia and Antarctica that became complete only around 32 Ma (Barker et al. 2007). According to this hypothesis, individual bovichtid lineages that occur in South America and the island of Tristan da Cunha could have arrived with paleogene currents, owing to their extended pelagic larval durations (Balushkin 2000; Matschiner et al. 2011). The same time-calibration further supports a vicariant separation of the South American Eleginopsidae from the five predominantly Antarctic families in the Eocene, before the opening of the Drake Passage around 41 Ma (Scher and Martin 2006).

Subsequent to the opening of both the Tasman Gateway and the Drake Passage, the onset of the ACC led to thermal isolation of the Antarctic continent and, in combination with declining atmospheric carbon dioxide (DeConto and Pollard 2003; Scher and Martin 2006), to a decrease in water temperatures by up to 4 °C (Nong et al. 2000), resulting in widespread Antarctic continental glaciation at the

time of the Eocene–Oligocene transition 34–33 Ma. Whereas the drop to sub-zero temperatures may have been delayed in the marine environment compared to continental Antarctica, there is evidence for sea ice since the early Oligocene. Deposits in offshore drill cores show that since that time, glaciers have repeatedly extended well onto the continental shelf (Cape Roberts Science Team 2000). Sea ice-dependent diatoms have been found in Oligocene sediments (Olney et al. 2009), and widespread ice-rafting occurred as early as 33.6 Ma (Zachos et al. 1996). Freezing conditions in Antarctic waters have been episodic before the middle Miocene climate transition (MMCT) around 14 Ma (Shevenell et al. 2004); however, even seasonal presence of sea ice during cold events of the Oligocene and early Miocene (Naish et al. 2001) must have had a strong impact on the marine fauna of Antarctica.

Fossil evidence from the La Meseta Formation of Seymour Island, off the Antarctic Peninsula, shows that a diverse temperate ichthyofauna existed in the Late Eocene, when Antarctic water temperatures ranged between 10 and15 °C (Eastman 1993; Claeson et al. 2012). Even though ancestral notothenioid lineages were probably present in Antarctic waters during the Eocene, only a single putative notothenioid fossil is known from the La Meseta Formation. *Proeleginops grandeastmanorum* has originally been described as a gadiform (Eastman and Grande 1991), but was subsequently claimed to represent an early member of Eleginopsidae (Balushkin 1994). The fossil has been used to time-calibrate the molecular phylogeny of Near (2004); however, its taxonomic assignment remains questionable. The type locality is specified as RV-8200 and reported to be about 40 Ma (Eastman and Grande 1991). However, according to Long (1992), RV-8200 lies in the lower section of "Tertiary Eocene La Meseta" (Telm) 4, the age of which has recently been reevaluated and is now considered to be 52.5–51.0 Ma (Ivany et al. 2008). This age is substantially older than the mean molecular date estimate for the origin of Eleginopsidae (42.9 Ma) in the study of Matschiner et al. (2011). In their molecular analysis, Matschiner et al. (2011) deliberately excluded *P. grandeastmanorum* as a time constraint due to its debated taxonomic assignment. The presumed fit of their results with the fossil's age (there assumed to be 40 Ma) supported the interpretation of *P. grandeastmanorum* as a notothenioid; however, this does not hold if the fossil is in fact 52.5–51 Ma old. Thus, Notothenioidei may not be represented at all in the Eocene fossil record of the La Meseta Formation, even though a large number of other fishes are found at the same location.

According to the time-calibrated molecular phylogeny of Matschiner et al. (2011), the diversification of the five predominantly Antarctic notothenioid families began near the Oligocene–Miocene boundary, about 24 Ma. Their study agrees with almost all other molecular phylogenies of notothenioids in finding the most basal divergences of Antarctic notothenioids within a paraphyletic family Nototheniidae (Bargelloni et al. 2000; Near and Cheng 2008; Rutschmann et al. 2011; Near et al. 2012; Dettai et al. 2012; Betancur-R et al. 2013). However, uncertainty remains regarding the sister group of all other Antarctic notothenioids, with different analyses recovering either the genus *Gobionotothen* (Matschiner et al. 2011; Near and Cheng 2008; Near et al. 2012), *Aethotaxis* (Rutschmann

et al. 2011; Betancur-R et al. 2013), a clade composed of *Aethotaxis* and *Dissostichus* (Near and Cheng 2008; Near et al. 2012; Dettai et al. 2012), or the combined genera *Pleuragramma*, *Aethotaxis*, and *Dissostichus*, in this position (Near et al. 2012).

Individual groups within Nototheniidae receive overwhelming support from molecular analyses, such as the species-rich Trematominae that are composed of the genera *Trematomus*, *Lepidonotothen*, *Patagonotothen*, *Pagothenia* (now included in *Trematomus*; Near et al. 2012), and *Cryothenia* (Janko et al. 2011; Lautrédou et al. 2012), or the clade combining *Notothenia* and *Paranotothenia* (Dettai et al. 2012). Similarly, the more derived families Artedidraconidae, Harpagiferidae, and Channichthyidae appear nested within the paraphyletic Nototheniidae, but are themselves strongly supported to be monophyletic (Derome et al. 2002; Johnston et al. 2003; Rutschmann et al. 2011; Near et al. 2012; Dettai et al. 2012). The same cannot be claimed for the family Bathydraconidae. Monophyly of a clade combining Bathydraconidae and Channichthyidae has not been questioned; however, most analyses recover Channichthyidae nested within Bathydraconidae, thus rendering the latter family paraphyletic (Derome et al. 2002; Near et al. 2012; Dettai et al. 2012; Betancur-R et al. 2013).

5 The Adaptive Character of the Notothenioid Radiation

Adaptive radiation is the rapid origin of an array of morphologically and ecologically distinct species from a common ancestor, as a consequence of the adaptation to distinct ecological niches (Schluter 2000; Gavrilets and Losos 2009). Adaptive radiations typically occur after an ancestral species conquers a new, island-type environment with many open niches ("ecological opportunity"), after the extinction of antagonists, liberating previously occupied niches (another form of opportunity), or following the evolution of a novel trait (a so-called key innovation) allowing to effectively exploit new niches (Schluter 2000; Gavrilets and Vose 2005; Yoder et al. 2010). Schluter (2000) defined four main criteria of an adaptive radiation: common ancestry, rapid diversification, phenotype-environment correlation, and trait utility. In the following, we discuss these criteria with respect to the notothenioid species flock:

The first two criteria, common ancestry and rapid diversification, were highlighted by several studies investigating notothenioid phylogeny and diversification rates (Eastman 2005; Matschiner et al. 2011; Near et al. 2012). However, diversification rates seem to be lower in notothenioids compared to other adaptive radiations like the East African cichlid fishes (Rutschmann et al. 2011). It has been suggested that this inequality is due to the lack of habitat heterogeneity, the absence of certain prime inshore habitats in the Antarctic shelf area, enhanced long-range migration ability of pelagic larval stages (Damerau et al. 2014), the absence of genetic population structuring over large distances (see below), and that the

notothenioid radiation may not yet have reached its final stage (see Rutschmann et al. 2011, and references therein).

Phenotype–environment correlation and trait utility in notothenioids are best understood with regard to pelagization (the shift from a benthic to a pelagic lifestyle) that has arisen independently in several notothenioid clades (Klingenberg and Ekau 1996; Rutschmann et al. 2011). This shift, referred to as "the hallmark of the notothenioid radiation" (Eastman 2000), was facilitated by adaptations enabling various species to exploit previously unoccupied niches in the water column. Starting from a benthic ancestor, substantial morphological diversification led to phenotypes suited for foraging modes of pelagic or partially pelagic zooplanktivory and piscivory (Eastman 2000). Notothenioids diversified to fill these niches while at the same time also remaining the dominant benthic group of vertebrates (Eastman 2000).

Various morphological and physiological adjustments were needed for species to be able to colonize the water column, mainly to achieve effective swimming performance and to compensate the lack of a swim bladder that most other teleosts use to regulate their buoyancy (Klingenberg and Ekau 1996). Several notothenioid species achieved neutral buoyancy by reducing the mineralization of the skeleton and scales (a pedomorphic trait; Balushkin 2000; Eastman 2000), and by the accumulation of lipid deposits (Eastman 2000). While pelagization has occurred independently in several notothenioid clades (see e.g. Rutschmann et al. 2011), the most complete examples can be found within the family Nototheniidae, where about half of the species occupy the ancestral benthic habitat, whereas the other half adopted a semipelagic, epibenthic, cryopelagic, or pelagic lifestyle (Eastman 2005). Pelagization may be best depicted by *Pleuragramma antarctica,* a sardine-like zooplankton feeder. Morphological adaptations to a life in the water column are highly pronounced in this species, and it evolved to become the dominant species in the water column and the key species in the high-Antarctic food web (Eastman 2005), with several species of channichthyids (*Chionodraco hamatus, Chionodraco myersi, Dacodraco hunteri, Neopagetopsis ionah*) feeding almost exclusively on this species (La Mesa et al. 2004). On the High Antarctic shelf, *Pleuragramma antarctica* is the most important prey item for *Dissostichus mawsoni*, and top predators like penguins, Weddell seals (*Leptonychotes weddellii*), and minke whales (*Balaenoptera bonaerensis*) also greatly rely on *Pleuragramma antarctica* as a food source (Eastman 1985; La Mesa et al. 2004). *Pleuragramma antarctica* has become the dominant species of the midwater fish fauna, with over 90 % both in abundance and biomass (La Mesa et al. 2004), and this dominance can be attributed to a wide range of highly specialized morphological adaptations.

Pleuragramma antarctica evolved neutral buoyancy by driving the abovementioned adaptations (reduced mineralization of the skeleton and lipid deposits) to a degree of completion unreached by any other notothenioid species. Lipid, more precisely triglyceride, is stored in intermuscular and subcutaneous sacs. Translucent sacs containing lipid are present between the muscle masses at the bases of the dorsal and anal fins. Furthermore, smaller subcutaneous sacs can be found at the sides of the body (DeVries and Eastman 1978; Eastman 1993).

The skeleton of *P. antarctica* is pedomorphic and reduced, including the reduction of vertebrae and the persistence of the notochord in adult specimens (Eastman 1993).

Adaptations for a life in the water column other than the reduction of buoyancy include morphological changes to alter feeding and swimming performance. *Pleuragramma antarctica* possesses short, protractile jaws featuring a single row with few but large oral teeth suited for suction feeding on planktonic prey (Albertson et al. 2010). Notothenioids living in the water column generally tend to have more elongated, slimmer bodies, but smaller heads than benthic feeders (Klingenberg and Ekau 1996)—the latter probably due to planktonic prey generally being smaller than benthic prey (Klingenberg and Ekau 1996, and references therein). Analyses of the shape of the operculum (Wilson et al. 2013) have furthermore shown that members of the Channichthyidae and Nototheniidae evolved broadly similar opercle shapes in relation to their position along the benthic-pelagic axis and that benthic species generally have an extended posterior margin of the opercle compared to pelagic species, probably reflecting the generally larger head width of benthic notothenioids.

Ecological diversification along the benthic–pelagic axis is also reflected in carbon isotope levels, which can be used to approximate the habitat type. The lowest ∂^{13}C values are found in more pelagic species like *Chaenodraco wilsoni*, *Champsocephalus gunnari*, and *Pleuragramma antarctica*, while strictly benthic notothenioids like *Gobionotothen gibberifrons*, *Lepidonotothen nudifrons*, and *Pogonophryne scotti* occupy the upper end of the range (Rutschmann et al. 2011). Carbon isotopic levels further correlate with nitrogen isotope amounts in notothenioids, indicating a connection between habitat and trophic levels. With the exception of the pelagic top predator *Dissostichus mawsoni*, the highest ∂^{15}N values are found almost exclusively in benthic species. Remarkably, very similar ranges of isotope signatures are present in at least two notothenioid families, Nototheniidae and Channichthyidae, suggesting convergent ecological evolution along habitat and trophic axes, which is considered characteristic for adaptive radiation (Muschick et al. 2012).

Other than buoyancy adaptations, a second trait that serves well to illustrate both phenotype–environment correlation and trait utility in notothenioids are AFGPs. As these proteins are present in all Antarctic notothenioid clades they are commonly thought to have evolved only once prior to the notothenioid radiation (Chen et al. 1997a; Cheng et al. 2003). The utility of AFGPs in the Antarctic environment is obvious, as these proteins are essential to prevent the formation of ice crystals within the fish's body, and thus are needed for the survival of notothenioids in sub-zero waters (as described above). A correlation between the phenotype and the environment could also be demonstrated in a case study of 11 channichthyid species, where freeze avoidance due to AFGP expression was found to be greater in species occurring at higher latitudes (and thus at colder water temperatures; Bilyk and DeVries 2010). Thus, the four criteria outlined by Schluter (2000) for the detection of adaptive radiation are all fulfilled by Antarctic notothenioids, whereby

the latter two criteria (phenotype–environment correlation and trait utility) apply to even more than one notothenioid characteristic.

The evolution of AFGPs is often viewed as a "key-innovation" (see Schluter 2000 for more details on the term), meaning that the emergence of this trait allowed notothenioids to effectively exploit new niches and therefore triggered the notothenioid adaptive radiation (Matschiner et al. 2011). It has been hypothesized that the drop to sub-zero water temperatures around Antarctica led to the extinction of most of the previously existing ichthyofauna (Eastman 1993), which enabled notothenioids to diversify and occupy the subsequently vacant niches (Matschiner et al. 2011). However, diversification rate analyses have recently suggested that major pulses of lineage diversification within notothenioid clades, responsible for a large share of the notothenioid species richness, occurred substantially later than the origin of AFGPs, thus suggesting that the key innovation of AFGPs may not have been the only driver of the notothenioid radiation (Near et al. 2012).

6 Non-Antarctic Notothenioids

The non-Antarctic notothenioids comprise two main groups of fishes: basal lineages that diverged before the isolation of Antarctica (families Eleginopsidae, Pseudaphritidae, and Bovichtidae), which therefore never experienced the "Antarctic permanent cold conditions" during their evolutionary history, and a more derived group that presumably originated from northward dispersal events of Antarctic ancestors (belonging to families Nototheniidae, Harpagiferidae, and Channichthyidae). The comparison between Antarctic and non-Antarctic notothenioids may be important to better understand the numerous unique traits that notothenioids have evolved in Antarctic waters. In addition, the specific comparison with non-Antarctic notothenioids of Antarctic ancestry may allow the identification of features that allow them to inhabit cold-temperate waters outside the APF. The knowledge about these latter traits may be a key to better understand how evolution in the stable cold waters of Antarctica has constrained the ability of Antarctic notothenioids to deal with environmental changes and global warming.

So far, phylogenetic analyses have identified seven genera (represented by 22 species) that are nested within the Antarctic notothenioid clade, but occur north of the border drawn by the APF (Table 1). There are still many uncertainties about the phylogenetic relationships between and within these seven genera, though. Nonetheless, there is some evidence that supports monophyly of a clade combining *Paranotothenia magellanica* and the two non-Antarctic *Notothenia* species (Cheng et al. 2003). Likewise, *Lepidonotothen macrophthalma*, the only non-Antarctic representative of the genus, has never been included in a molecular phylogeny, but is morphologically closely related to *L. squamifrons* (Balushkin 2000; Pequeño 2000), which was found to be the sister taxon of the genus *Patagonotothen* (Dettai et al. 2012; Near et al. 2012). Thus, there is the possibility that *L. macrophthalma* and the genus *Patagonotothen* form a monophyletic group

as well. The remaining components of the group of non-Antarctic notothenioids are strongly supported as non-monophyletic (Rutschmann et al. 2011; Dettai et al. 2012; Near et al. 2012). Therefore, the most parsimonious explanation would involve at least five putative ancestors that dispersed northward across the APF. Three would belong to the family Nototheniidae, the most basal one of the five Antarctic notothenioids families, and the other two are members of the more derived high-Antarctic families Harpagiferidae and Channichthyidae.

Some authors have suggested that the "escapes" of these ancestors from the Antarctic waters may be linked to temporally northwards movements of the APF (Bargelloni et al. 2000; Cheng et al. 2003; Coppes Petricorena and Somero 2007). If the five putative escapes are linked to paleoceanographic events, it seems that at least two different events would be involved. The divergence between the Antarctic and non-Antarctic sister lineages of the family Nototheniidae apparently took place more than 7 Ma (Near 2004; Near et al. 2012), whereas the divergence of *Champsocephalus esox* and its Antarctic sister taxon *C. gunnari* was estimated at around 4–1.7 Ma (Near et al. 2004; Stankovic et al. 2002). An estimation of the divergence time between the South American *Harpagifer bispinis* and its closest relative from Antarctica, *H. antarcticus,* is still lacking, albeit their very similar morphology (Gon and Heemstra 1990) may suggest a recent divergence, probably closer in time to the separation of non-Antarctic Channichthyidae than to that of non-Antarctic nototheniids.

The Antarctic ancestry of these non-Antarctic notothenioids led to the prediction that these species might have AFGP genes or at least its remnants in their genomes. The occurrence of AFGP in non-Antarctic notothenioids from South America and New Zealand waters has already been examined in eight species (Cheng and Detrich 2007), confirming its presence in four of them (Table 1). The most parsimonious explanation for the apparent absence of AFGP in *Dissostichus eleginoides* and three species of *Patagonotothen* involves at least two independent losses or severe mutations of this gene. On the other hand, whereas the Antarctic notothenioids lost the HSR, the New Zealand notothenioid *Notothenia angustata* is able to upregulate the transcription of hsp70 in response to heat shock (Hofmann et al. 2005).

One of the main differences in the evolutionary history between non-Antarctic and Antarctic notothenioids is that the former evolved in the presence of fish groups that are absent or uncommon in Antarctic waters. Therefore, these lineages likely experienced more competition compared with the Antarctic notothenioids, limiting the occupation of niches distinct from the original benthic one. In agreement with this idea, no evidence for diverse static buoyancy values was found in non-Antarctic notothenioids that would allow them to occupy different areas in the water column in the same way as Antarctic notothenioids (Fernández et al. 2012). Comparison of Antarctic and non-Antarctic sister taxa with modern genomic technology may help to identify the genetic changes underlying the transition across the APF, and reveal whether or not they led to adaptations in a similar fashion in different notothenioid families.

The main radiation of notothenioids occurred in an Antarctic environment, and thus the bulk of notothenioids species inhabit the Southern Ocean within the APF. Nonetheless, the second-most species-rich genus is found almost exclusively in non-Antarctic waters: the genus *Patagonotothen* with so far 15 described species is only surpassed in diversity by the Antarctic genus *Pogonophryne* that contains 24 species. The 15 *Patagonotothen* species occur in southern South America with the only exception being *P. guntheri,* which has a trans-APF distribution and it is also found in South Georgia. Morphological analysis suggests that *P. guntheri* may be considered as a derived species within the genus (Balushkin 1992). Thus its presence within the APF is probably a derived character rather than an ancestral one.

The age of the most recent common ancestor of the *Patagonotothen* genus was estimated to be around 5 Ma (Near et al. 2012). This implies a rather rapid radiation of the 15 species, whereby the drivers of this radiation remain unknown but are likely unrelated to the key innovation hypothesis for AFGP. The inshore fish fauna of southern South America seems to be characterized by generally low diversity (Ojeda et al. 2000), which could have facilitated the *Patagonotothen* expansion. A similar radiation in the same region is the one exhibited by the species of the mollusc genus *Nacella*. In this case it has been proposed that the currently overlapping distributions of *Nacella* species and their close genetic relationships could be explained by allopatric speciation, or at least incipient separation, in separate refugia during glaciations, followed by geographical re-expansion and ecological separation (González-Wevar et al. 2011). A similar scenario could explain the *Patagonotothen* radiation; however, more research on this group will be needed to support this hypothesis.

7 Demography and Population Structure in Antarctic Notothenioids

Whereas phylogenies can inform about the macroevolutionary history of Antarctic notothenioids, the underlying forces of speciation processes are commonly linked to ecological factors that often act on a far more microevolutionary timescale (Nosil 2012). Understanding the population dynamics of species, especially the factors modulating demography and gene flow among populations, is therefore crucial for the understanding of the adaptive radiation of notothenioids. Molecular genetic signatures left by past and present demographic events, such as population size changes or migration, allow us to disentangle the importance of biotic and abiotic factors that influence differentiation processes on the population level.

For polar organisms including notothenioid fishes, it has often been hypothesized that population size changes are driven by glaciation cycles associated with severe implications for species' survival and distribution (Kennett 1982; Eastman 1993; Petit et al. 1999). During major glacial periods, the Antarctic ice sheet

extended as far as the edge of the continental shelf (Ingólfsson 2004; Gersonde et al. 2005), sometimes eradicating Antarctic marine bottom communities on the large scale (Thatje et al. 2005) and "bulldozing the surviving fauna to the deep continental margin" (Barnes and Conlan 2007). As a result, populations were periodically isolated in remaining ice-free refugia (Barnes et al. 2006), which was suggested as a key mechanism for allopatric speciation (Hewitt 1996; Rogers 2007), and is expected to result in population expansions subsequent to glacial retreat. The use of population level molecular data allows the investigation of past population size changes, and in fact has provided evidence for demographic expansions in multiple notothenioid fishes (Zane et al. 2006; Janko et al. 2007; Matschiner et al. 2009), which highlights the impact of glacial cycles on notothenioid populations.

The extent to which population fragmentation leads to differentiation and allopatric speciation in notothenioid fishes remains unclear, but is strongly linked to their potential for long-distance gene flow. While distances between isolated notothenioid populations are on the order of thousands of kilometers (Matschiner et al. 2009), notothenioid fishes are characterized by extended pelagic larval stages that may last between a few months and more than 1 year (Loeb et al. 1993; La Mesa and Ashford 2008). This, in combination with the strong current of the ACC endows the propagules of many species with a great potential for long-distance dispersal (Damerau et al. 2014). Hence, high levels of gene flow could be expected between distant notothenioid populations, which might counteract differentiation and allopatric speciation events.

Since the advent of DNA sequencing and genotyping technologies, estimates of population connectivity have been inferred based on population genetic tools, which measure the distribution of genetic variation among populations. To date, at least 29 population genetic studies have been published for 22 notothenioid species (see references in Volckaert et al. 2012, as well as Carvalho and Warren 1991; Smith and Gaffney 2000; Damerau et al. 2012; Agostini et al. 2013; Damerau et al. 2014). The results of these studies were highly variable and depended clearly on sampling designs and applied marker types (see Table 3 in Matschiner et al. 2009). Nonetheless, an overall trend uncovered by these studies is the decrease of genetic homogeneity among populations with distance, indicating an isolation-by-distance relationship. On a regional scale (within a few hundred kilometers), the vast majority of species showed genetic homogeneity. Even population differentiations within ocean sectors are predominantly insignificant, sometimes over several thousand kilometers. Although a marginal majority of studies revealed significant population differentiations between ocean sectors, many populations of species with circum-Antarctic distributions showed no significant differentiation, as, for example, in the bentho-pelagic Antarctic toothfish *Dissostichus mawsoni* (Smith and Gaffney 2005) or the truly pelagic Antarctic silverfish *Pleuragramma antarctica* (Zane et al. 2006). Moreover, populations of strictly benthic species, such as *Gobionotothen gibberifrons*, which is confined to shelf areas as adults, were not significantly differentiated over their distribution range on subantarctic islands (Matschiner et al. 2009).

The seemingly high levels of gene flow among populations separated by deep ocean over large geographic scales, but connected by currents like the ACC, regardless of the adult life strategy, suggest that gene flow is mediated via dispersal of pelagic developmental stages such as eggs, larvae, or juveniles. This finding is corroborated by genetic breaks that have been found over much shorter geographic distances, where oceanographic barriers exist. For example, populations of *D. eleginoides* are not significantly differentiated over large parts of its circumpolar distribution range, whereas populations that are geographically close but separated by the APF show little connectivity (Shaw et al. 2004; Rogers et al. 2006). Hence, oceanographic features are an important factor regulating population connectivity of notothenioids by either enhancing or attenuating larval dispersal, as has also been shown in species from warmer waters with distinctly shorter pelagic larval stages (e.g. Taylor and Hellberg 2003; Bay et al. 2006; Cowen and Sponaugle 2009). However, the general validity of the observed patterns is limited by varying sampling designs, genetic marker types, and species' biogeography, what makes general inferences about gene flow by larval dispersal a challenging task.

8 Conclusions and Outlook

It has been 60 years since notothenioid fishes were first brought to the attention of a broader scientific community, with Johan T. Ruud's (1954) publication in *Nature* demonstrating the loss of hemoglobin as the cause of the colorlessness of the blood of channichthyids. Our knowledge about the nature of the notothenioid evolution has greatly increased over the recent decades, especially since the advent of molecular sequencing technology, but important questions of the notothenioid radiation remain to be answered. While recent phylogenetic work (Rutschmann et al. 2011; Near et al. 2012; Lautrédou et al. 2012) helped to identify multiple well-supported clades such as Trematominae, Artedidraconidae, and Channichthyidae, the same studies also disagreed with respect to more basal notothenioid relationships and thus highlight the need for more comprehensive sequence data sets. Due to ongoing sampling efforts in combination with rapid improvements in sequencing technologies and methodological advances, we may soon be able to address these questions. Through combination of population level and species level sequence data, approaches like the multi-marker coalescent model implemented in *BEAST (Heled and Drummond 2010) are able to account for incomplete lineage sorting, which is common in rapidly diversifying clades (Koblmüller et al. 2010), and could be the cause of incompatibilities between published phylogenies. To date, family-level relationships within Bovichtidae and Harpagiferidae have not been investigated in detail, but could provide valuable insights into the geographic origin and the early phylogeography of the notothenioid radiation. Finally, thanks to the rapidly decreasing cost of next generation sequencing, genome-size data sets may soon be available for notothenioid fishes and permit investigations into the molecular basis of notothenioid adaptations.

Other than molecular data, recent studies have begun to systematically quantify morphological and physiological characteristics (Rutschmann et al. 2011; Near et al. 2012; Wilson et al. 2013), a trend that will continue to give us increasingly well-resolved descriptions of ecological niches occupied by notothenioid taxa. In addition, more behavioral data can be acquired through continuing field expeditions equipped with remotely operated underwater vehicles. In combination, these data will allow us to better understand the axes along which the notothenioid radiation has proceeded (and continues to proceed), as well as the molecular adaptations that enabled their tremendous evolutionary success.

Acknowledgements We thank the editors and Joseph Eastman for valuable comments on the manuscript. The authors of this book chapter have been supported by funding from the Swiss National Science Foundation (SNF grants PBBSP3-138680 to MM and CRSII3-136293 to WS), the European Research Council (Starting Grant "INTERGENADAPT" to WS), the Volkswagen Foundation (grant I/83 548 to MM), and the German Research Foundation (grant HA 4328/4 to RH).

References

Agostini C, Papetti C, Patarnello T et al (2013) Putative selected markers in the *Chionodraco* genus detected by interspecific outlier tests. Polar Biol 36:1509–1518

Albertson RC, Yan Y-L, Titus TA et al (2010) Molecular pedomorphism underlies craniofacial skeletal evolution in Antarctic notothenioid fishes. BMC Evol Biol 10:4

Anderson JB (1999) Antarctic marine geology. Cambridge University Press, Cambridge

Balushkin AV (1992) Classification, phylogenetic relationships, and origins of the families of the suborder Notothenioidei (Perciformes). J Ichthyol 32:90–110

Balushkin AV (1994) Fossil notothenioid, and not gadiform, fish *Proeleginops grandeastmanorum* gen. sp. nov. (Perciformes, Notothenioidei, Eleginopidae) from the late Eocene found in Seymour Island (Antarctica). Voprosy Ikhtiologii 34:298–307

Balushkin AV (2000) Morphology, classification, and evolution of notothenioid fishes of the Southern Ocean (Notothenioidei, Perciformes). J Ichthyol 40:S74–S109

Balushkin AV (2012) *Volodichthys* gen. nov. new species of the primitive snailfish (Liparidae: Scorpaeniformes) of the southern hemishpere. Description of new species V. *Solovjevae* sp. nov. (Cooperation Sea, the Antarctic). J Ichthyol 52:1–10

Bargelloni L, Marcato S, Zane L, Patarnello T (2000) Mitochondrial phylogeny of notothenioids: a molecular approach to Antarctic fish evolution and biogeography. Syst Biol 49:114–129

Barker PF, Filippelli GM, Florindo F, Martin EE, Scher HD (2007) Onset and role of the Antarctic circumpolar current. Deep Sea Res Pt II 54:2388–2398

Barnes DKA, Conlan KE (2007) Disturbance, colonization and development of Antarctic benthic communities. Philos Trans R Soc B 362:11–38

Barnes DKA, Hodgson DA, Convey P, Allen CS, Clarke A (2006) Incursion and excursion of Antarctic biota: past, present and future. Global Ecol Biogeogr 15:121–142

Bay LK, Crozier RH, Caley MJ (2006) The relationship between population genetic structure and pelagic larval duration in coral reef fishes on the Great Barrier Reef. Mar Biol 149:1247–1256

Betancur-R R, Broughton RE, Wiley EO et al (2013) The Tree of Life and a new classification of bony fishes. PLoS Curr 5:18

Bilyk KT, DeVries AL (2010) Freezing avoidance of the Antarctic icefishes (Channichthyidae) across thermal gradients in the Southern Ocean. Polar Biol 33:203–213

Bilyk KT, DeVries AL (2011) Heat tolerance and its plasticity in Antarctic fishes. Comp Biochem Physiol A 158:382–390

Bilyk KT, Evans CW, DeVries AL (2012) Heat hardening in Antarctic notothenioid fishes. Polar Biol 35:1447–1451

Carvalho GR, Warren M (1991) Genetic population structure of the mackerel icefish, *Champsocephalus gunnari*, in Antarctic waters. Document WG-FSA-91/22. CCAMLR working paper

Chen L, DeVries AL, Cheng C-HC (1997a) Evolution of antifreeze glycoprotein gene from a trypsinogen gene in Antarctic notothenioid fish. Proc Natl Acad Sci U S A 94:3811–3816

Chen L, DeVries AL, Cheng C-HC (1997b) Convergent evolution of antifreeze glycoproteins in Antarctic notothenioid fish and Arctic cod. Proc Natl Acad Sci U S A 94:3817–3822

Cheng C-HC, Detrich HW III (2007) Molecular ecophysiology of Antarctic notothenioid fishes. Philos Trans R Soc B 362:2215–2232

Cheng C-HC, DeVries AL (1989) Structures of antifreeze peptides from the Antarctic eel pout, *Austrolycicthys brachycephalus*. Biochim Biophys Acta 997:55–64

Cheng C-HC, Chen L, Near TJ, Jin Y (2003) Functional antifreeze glycoprotein genes in temperate-water New Zealand nototheniid fish infer an Antarctic evolutionary origin. Mol Biol Evol 20:1897–1908

Cheng C-HC, Cziko PA, Evans CW (2006) Nonhepatic origin of notothenioid antifreeze reveals pancreatic synthesis as common mechanism in polar fish freezing avoidance. Proc Natl Acad Sci U S A 103:10491–10496

Claeson KM, Eastman JT, MacPhee RDE (2012) Definitive specimens of Merlucciidae (Gadiformes) from the Eocene James Ross Basin of Isla Marambio (Seymour Island), Antarctic Peninsula. Antarct Sci 24:467–472

Clark MS, Fraser KPP, Burns G, Peck LS (2008) The HSP70 heat shock response in the Antarctic fish *Harpagifer antarcticus*. Polar Biol 31:171–180

Clarke A (1988) Seasonality in the Antarctic marine environment. Comp Biochem Physiol B 90:461–473

Cocca E, Ratnayake-Lecamwasam M, Parker SK et al (1995) Genomic remnants of alpha-globin genes in the hemoglobinless Antarctic icefishes. Proc Natl Acad Sci U S A 92:1817–1821

Coppes Petricorena ZL, Somero GN (2007) Biochemical adaptations of notothenioid fishes: comparisons between cold temperate South American and New Zealand species and Antarctic species. Comp Biochem Physiol A 147:799–807

Cowen RK, Sponaugle S (2009) Larval dispersal and marine population connectivity. Ann Rev Mar Sci 1:443–466

Cziko PA, Evans CW, Cheng C-HC, DeVries AL (2006) Freezing resistance of antifreeze-deficient larval Antarctic fish. J Exp Biol 209:407–420

Damerau M, Matschiner M, Salzburger W, Hanel R (2012) Comparative population genetics of seven notothenioid fish species reveals high levels of gene flow along ocean currents in the southern Scotia Arc, Antarctica. Polar Biol 35:1073–1086

Damerau M, Matschiner M, Salzburger W, Hanel R (2014) Population divergences despite long pelagic larval stages: lessons from crocodile icefishes (Channichthyidae). Mol Ecol 23:284–299

DeConto RM, Pollard D (2003) Rapid Cenozoic glaciation of Antarctica induced by declining atmospheric CO_2. Nature 421:245–249

Derome N, Chen W-J, Dettaï A, Bonillo CÉ, Lecointre G (2002) Phylogeny of Antarctic dragonfishes (Bathydraconidae, Notothenioidei, Teleostei) and related families based on their anatomy and two mitochondrial genes. Mol Phylogenet Evol 24:139–152

Dettaï A, Lecointre G (2004) In search of notothenioid (Teleostei) relatives. Antarct Sci 16:71–85

Dettai A, Berkani M, Lautrédou A-C et al (2012) Tracking the elusive monophyly of nototheniid fishes (Teleostei) with multiple mitochondrial and nuclear markers. Mar Genomics 8:49–58

DeVries AL, Cheng CH (2005) Antifreeze proteins and organismal freezing avoidance in polar fishes. In: Farrell AP, Steffensen JF (eds) Fish physiology, vol 22. Academic Press, San Diego, CA, pp 155–201

DeVries AL, Eastman JT (1978) Lipid sacs as a buoyancy adaptation in an Antarctic fish. Nature 271:352–353

di Prisco G, Cocca E, Parker SK, Detrich HW III (2002) Tracking the evolutionary loss of hemoglobin expression by the white-blooded Antarctic icefishes. Gene 295:185–191

Eastman JT (1985) The evolution of neutrally buoyant notothenioid fishes: their specializations and potential interactions in the Antarctic marine food web. In: Siegfried WR, Condy PR, Laws RM (eds) Antarctic nutrient cycles and food webs. Springer, Berlin, pp 430–436

Eastman JT (1993) Antarctic fish biology: evolution in a unique environment. Academic Press, San Diego, CA

Eastman JT (2000) Antarctic notothenioid fishes as subjects for research in evolutionary biology. Antarct Sci 12:276–287

Eastman JT (2005) The nature of the diversity of Antarctic fishes. Polar Biol 28:93–107

Eastman JT, Clarke A (1998) A comparison of adaptive radiations of Antarctic fish with those of nonAntarctic fish. In: di Prisco G, Pisano E, Clarke A (eds) Fishes of Antarctica. A biological overview. Springer, Milano, pp 3–26

Eastman JT, Eakin RR (2000) An updated species list for notothenioid fish (Perciformes; Notothenioidei), with comments on Antarctic species. Arch Fish Mar Res 48:11–20

Eastman JT, Grande L (1991) Late Eocene gadiform (Teleostei) skull from Seymour Island, Antarctic Peninsula. Antarct Sci 3:87–95

Eastman JT, McCune AR (2000) Fishes on the Antarctic continental shelf: evolution of a marine species flock? J Fish Biol 57:84–102

Evans JD, Page LM (2003) Distribution and relative size of the swim bladder in *Percina*, with comparisons to *Etheostoma*, *Crystallaria*, and *Ammocrypta* (Teleostei: Percidae). Environ Biol Fish 66:61–65

Evans CW, Gubala V, Nooney R et al (2011) How do Antarctic notothenioid fishes cope with internal ice? A novel function for antifreeze glycoproteins. Antarct Sci 23:57–64

Evans CW, Hellman L, Middleditch M et al (2012) Synthesis and recycling of antifreeze glycoproteins in polar fishes. Antarct Sci 24:259–268

Fernández DA, Ceballos SG, Malanga G, Boy CC, Vanella FA (2012) Buoyancy of sub-Antarctic notothenioids including the sister lineage of all other notothenioids (Bovichtidae). Polar Biol 35:99–106

Fletcher GL, Hew C-L, Davies PL (2001) Antifreeze proteins of teleost fishes. Annu Rev Physiol 63:359–390

Foster TD (1984) The marine environment. In: Laws RM (ed) Antarctic ecology, vol 2. Academic Press, London, pp 345–371

Gavrilets S, Losos JB (2009) Adaptive radiation: contrasting theory with data. Science 323:732–737

Gavrilets S, Vose A (2005) Dynamic patterns of adaptive radiation. Proc Natl Acad Sci U S A 102:18040–18045

Gersonde R, Crosta X, Abelmann A, Armand L (2005) Sea-surface temperature and sea ice distribution of the Southern Ocean at the EPILOG Last Glacial Maximum—a circum-Antarctic view based on siliceous microfossil records. Quaternary Sci Rev 24:869–896

Gon O, Heemstra PC (1990) Fishes of the Southern Ocean. J.L.B. Smith Institute of Ichthyology, Grahamstown

González-Wevar CA, Nakano T, Cañete JI, Poulin E (2011) Concerted genetic, morphological and ecological diversification in *Nacella* limpets in the Magellanic Province. Mol Ecol 20:1936–1951

Gordon AL (1971) Oceanography of Antarctic waters. In: Reid JL (ed) Antarctic oceanology I. American Geophysical Union, Washington, DC, pp 169–203

Graham LA, Lougheed SC, Ewart KV, Davies PL (2008) Lateral transfer of a lectin-like antifreeze protein gene in fishes. PLoS One 3:e2616

Heled J, Drummond AJ (2010) Bayesian inference of species trees from multilocus data. Mol Biol Evol 27:570–580

Hewitt GM (1996) Some genetic consequences of ice ages, and their role in divergence and speciation. Biol J Linn Soc 58:247–276

Hofmann GE, Buckley BA, Airaksinen S, Keen JE, Somero GN (2000) Heat-shock protein expression is absent in the Antarctic fish *Trematomus bernacchii* (family Nototheniidae). J Exp Biol 203:2331–2339

Hofmann GE, Lund SG, Place SP, Whitmer AC (2005) Some like it hot, some like it cold: the heat shock response is found in New Zealand but not Antarctic notothenioid fishes. J Exp Mar Biol Ecol 316:79–89

Hsiao K-C, Cheng C-HC, Fernandes IE, Detrich HW III, DeVries AL (1990) An antifreeze glycopeptide gene from the antarctic cod *Notothenia coriiceps neglecta* encodes a polyprotein of high peptide copy number. Proc Natl Acad Sci U S A 87:9265–9269

Ingólfsson Ó (2004) Quaternary glacial and climate history of Antarctica. Dev Quaternary Sci 2C:3–44

Ivany LC, Lohmann KC, Hasiuk F et al (2008) Eocene climate record of a high southern latitude continental shelf: Seymour Island, Antarctica. Geol Soc Am Bull 120:659–678

Janko K, Lecointre G, DeVries AL et al (2007) Did glacial advances during the Pleistocene influence differently the demographic histories of benthic and pelagic Antarctic shelf fishes? Inferences from intraspecific mitochondrial and nuclear DNA sequence diversity. BMC Evol Biol 7:220

Janko K, Marshall C, Musilová Z et al (2011) Multilocus analyses of an Antarctic fish species flock (Teleostei, Notothenioidei, Trematominae): phylogenetic approach and test of the early-radiation event. Mol Phylogenet Evol 60:305–316

Johnston IA, Fernández DA, Calvo J et al (2003) Reduction in muscle fibre number during the adaptive radiation of notothenioid fishes: a phylogenetic perspective. J Exp Biol 206:2595–2609

Kennett JP (1982) Marine geology. Prentice Hall, Englewood Cliffs, NJ

Klingenberg CP, Ekau W (1996) A combined morphometric and phylogenetic analysis of an ecomorphological trend: pelagization in Antarctic fishes (Perciformes: Nototheniidae). Biol J Linn Soc 59:143–177

Koblmüller S, Egger B, Sturmbauer C, Sefc KM (2010) Rapid radiation, ancient incomplete lineage sorting and ancient hybridization in the endemic Lake Tanganyika cichlid tribe Tropheini. Mol Phylogenet Evol 55:318–334

La Mesa M, Ashford J (2008) Age and early life history of juvenile Scotia Sea icefish, *Chaenocephalus aceratus*, from Elephant and the South Shetland Islands. Polar Biol 31:221–228

La Mesa M, Eastman JT, Vacchi M (2004) The role of notothenioid fish in the food web of the Ross Sea shelf waters: a review. Polar Biol 27:321–338

Last PR, Balushkin AV, Hutchins JB (2002) *Halaphritis platycephala* (Notothenioidei: Bovichtidae): a new genus and species of temperate icefish from Southeastern Australia. Copeia 2002:433–440

Lautrédou A-C, Hinsinger DD, Gallut C et al (2012) Phylogenetic footprints of an Antarctic radiation: the Trematominae (Notothenioidei, Teleostei). Mol Phylogenet Evol 65:87–101

Lautrédou A-C, Motomura H, Gallut C et al (2013) New nuclear markers and exploration of the relationships among Serraniformes (Acanthomorpha, Teleostei): the importance of working at multiple scales. Mol Phylogenet Evol 67:140–155

Lewis DB (1976) Studies of the biology of the lesser weever. J Fish Biol 8:127–138

Loeb VJ, Kellermann AK, Koubbi P, North AW, White MG (1993) Antarctic larval fish assemblages: a review. Bull Mar Sci 53:416–449

Long DJ (1992) Sharks from the La Meseta Formation (Eocene), Seymour Island, Antarctic Peninsula. J Vertebr Paleontol 12:11–32
Matallanas J (2008) Description of *Gosztonyia antarctica*, a new genus and species of Zoarcidae (Teleostei: Perciformes) from the Antarctic Ocean. Polar Biol 32:15–19
Matschiner M, Hanel R, Salzburger W (2009) Gene flow by larval dispersal in the Antarctic notothenioid fish *Gobionotothen gibberifrons*. Mol Ecol 18:2574–2587
Matschiner M, Hanel R, Salzburger W (2011) On the origin and trigger of the notothenioid adaptive radiation. PLoS One 6:e18911
Muschick M, Indermaur A, Salzburger W (2012) Convergent evolution within an adaptive radiation of cichlid fishes. Curr Biol 22:2362–2368
Naish TR, Woolfe KJ, Barrett PJ et al (2001) Orbitally induced oscillations in the East Antarctic ice sheet at the Oligocene/Miocene boundary. Nature 413:719–723
Near TJ (2004) Estimating divergence times of notothenioid fishes using a fossil-calibrated molecular clock. Antarct Sci 16:37–44
Near TJ, Cheng C-HC (2008) Phylogenetics of notothenioid fishes (Teleostei: Acanthomorpha): inferences from mitochondrial and nuclear gene sequences. Mol Phylogenet Evol 47:1–9
Near TJ, Pesavento JJ, Cheng C-HC (2004) Phylogenetic investigations of Antarctic notothenioid fishes (Perciformes: Notothenioidei) using complete gene sequences of the mitochondrial encoded 16S rRNA. Mol Phylogenet Evol 32:881–891
Near TJ, Parker SK, Detrich HW III (2006) A genomic fossil reveals key steps in hemoglobin loss by the Antarctic icefishes. Mol Biol Evol 23:2008–2016
Near TJ, Dornburg A, Kuhn KL et al (2012) Ancient climate change, antifreeze, and the evolutionary diversification of Antarctic fishes. Proc Natl Acad Sci U S A 109:3434–3439
Nelson JS (2006) Fishes of the world. John Wiley, Hoboken, NJ
Nong GT, Najjar RG, Seidov D, Peterson WH (2000) Simulation of ocean temperature change due to the opening of Drake Passage. Geophys Res Lett 27:2689–2692
Nosil P (2012) Ecological speciation. Oxford University Press, New York, NY
Ojeda FP, Labra FA, Muñoz AA (2000) Biogeographic patterns of Chilean littoral fishes. Revista Chilena de Historia Natural 73:625–641
Olney MP, Bohaty SM, Harwood DM (2009) *Creania lacyae* gen. nov et sp. nov and *Synedropsis cheethamii* sp. nov., fossil indicators of Antarctic sea ice? Diatom Res 24:357–375
Pequeño RG (2000) Peces del crucero Cimar-Fiordo 3, a los canales del sur de Magallanes (ca. 55°S), Chile. Ciencia y Tecnología del Mar 23:83–94
Petit JR, Jouzel J, Barkov NI et al (1999) Climate and atmospheric history of the past 420,000 years from the Vostok ice core, Antarctica. Nature 399:429–436
Place SP, Hofmann GE (2005) Constitutive expression of a stress-inducible heat shock protein gene, hsp70, in phylogenetically distant Antarctic fish. Polar Biol 28:261–267
Place SP, Zippay ML, Hofmann GE (2004) Constitutive roles for inducible genes: evidence for the alteration in expression of the inducible hsp70 gene in Antarctic notothenioid fishes. Am J Physiol-Reg I 287:R429–R436
Præbel K, Hunt B, Hunt LH, DeVries AL (2009) The presence and quantification of splenic ice in the McMurdo Sound Notothenioid fish, *Pagothenia borchgrevinki* (Boulenger, 1902). Comp Biochem Physiol A 154:564–569
Rogers AD (2007) Evolution and biodiversity of Antarctic organisms: a molecular perspective. Philos Trans R Soc B 362:2191–2214
Rogers AD, Morley S, Fitzcharles E, Jarvis K, Belchier M (2006) Genetic structure of Patagonian toothfish (*Dissostichus eleginoides*) populations on the Patagonian Shelf and Atlantic and western Indian Ocean Sectors of the Southern Ocean. Mar Biol 149:915–924
Rutschmann S, Matschiner M, Damerau M et al (2011) Parallel ecological diversification in Antarctic notothenioid fishes as evidence for adaptive radiation. Mol Ecol 20:4707–4721
Ruud JT (1954) Vertebrates without erythrocytes and blood pigment. Nature 173:848–850
Salzburger W, Meyer A (2004) The species flocks of East African cichlid fishes: recent advances in molecular phylogenetics and population genetics. Naturwissenschaften 91:277–290

Salzburger W, Van Bocxlaer B, Cohen AS (2014) Ecology and evolution of the African Great Lakes and their faunas. Annu Rev Ecol Evol Syst 45:519–545

Scher HD, Martin EE (2006) Timing and climatic consequences of the opening of Drake Passage. Science 428:428–430

Schluter D (2000) The ecology of adaptive radiation. Oxford University Press, New York, NY

Shaw PW, Arkhipkin AI, Al-Khairulla H (2004) Genetic structuring of Patagonian toothfish populations in the Southwest Atlantic Ocean: the effect of the Antarctic Polar Front and deep-water troughs as barriers to genetic exchange. Mol Ecol 13:3293–3303

Shevenell AE, Kennett JP, Lea DW (2004) Middle Miocene Southern Ocean cooling and Antarctic cryosphere expansion. Science 305:1766–1770

Sidell BD, O'Brien K (2006) When bad things happen to good fish: the loss of hemoglobin and myoglobin expression in Antarctic icefishes. J Exp Biol 209:1791–1802

Smith P, Gaffney PM (2000) Toothfish stock structure revealed with DNA methods. Water Atmos 8:17–18

Smith PJ, Gaffney PM (2005) Low genetic diversity in the Antarctic toothfish (*Dissostichus mawsoni*) observed with mitochondrial and intron DNA markers. CCAMLR Sci 12:43–51

Stankovic A, Spalik K, Kamler E, Borsuk P, Weglenski P (2002) Recent origin of sub-Antarctic notothenioids. Polar Biol 25:203–205

Stein DL (2012) Snailfishes (Family Liparidae) of the Ross Sea, Antarctica, and closely adjacent waters. Zootaxa 3285:1–120

Taylor MS, Hellberg ME (2003) Genetic evidence for local retention of pelagic larvae in a Caribbean reef fish. Science 299:107–109

Team CRS (2000) Studies from the Cape Roberts project, Ross Sea, Antarctica. Initial report on CRP-3. Terra Antarctica 7:1–209

Thatje S, Hillenbrand C-D, Larter R (2005) On the origin of Antarctic marine benthic community structure. Trends Ecol Evol 20:534–540

Tomczak M, Godfrey JS (2003) Regional oceanography: an introduction. Daya Publishing House, Delhi

Volckaert FAM, Rock J, Putte AP (2012) Connectivity and molecular ecology of Antarctic fishes. In: di Prisco G, Verde C (eds) Adaptation and evolution in marine environments, vol 1. Springer, Berlin, pp 75–96

von der Heyden BP, Roychoudhury AN, Mtshali TN, Tyliszczak T, Myneni SCB (2012) Chemically and geographically distinct solid-phase iron pools in the Southern Ocean. Science 338:1199–1201

Wilson LAB, Colombo M, Hanel R, Salzburger W, Sánchez-Villagra MR (2013) Ecomorphological disparity in an adaptive radiation: opercular bone shape and stable isotopes in Antarctic icefishes. Ecol Evol 3:3166–3182

Yoder JB, Clancey E, Des Roches S et al (2010) Ecological opportunity and the origin of adaptive radiations. J Evol Biol 23:1581–1596

Zachos JC, Quinn TM, Salamy KA (1996) High resolution (10^4 years) deep-sea foraminiferal stable isotope records of the Eocene-Oligocene climate transition. Paleoceanography 11:251–266

Zane L, Bargelloni L, Bortolotto E et al (2006) Demographic history and population structure of the Antarctic silverfish *Pleuragramma antarcticum*. Mol Ecol 15:4499–4511

Zhuang X (2013) Creating sense from non-sense DNA: de novo genesis and evolutionary history of antifreeze glycoprotein gene in northern cod fishes (Gadidae). Dissertation, School of Integrative Biology, University of Illinois at Urbana-Champaign

2.2

Diversity and disparity through time in the adaptive radiation of Antarctic notothenioid fishes

Journal of Evolutionary Biology

I collected the specimens and collected and analysed the geometric morphometric data. MM and myself did the disparity through time analyses and drafted the manuscript. MM conducted the simulations, all authors then participated in discussing the manuscript and drafting the final version.

JOURNAL OF Evolutionary Biology

doi: 10.1111/jeb.12570

Diversity and disparity through time in the adaptive radiation of Antarctic notothenioid fishes

M. COLOMBO*, M. DAMERAU†, R. HANEL†, W. SALZBURGER*‡ & M. MATSCHINER*‡

*Zoological Institute, University of Basel, Basel, Switzerland
†Thünen Institute of Fisheries Ecology, Hamburg, Germany
‡Centre for Ecological and Evolutionary Synthesis (CEES), Department of Biosciences, University of Oslo, Oslo, Norway

Keywords:

adaptive radiation;
early burst;
geometric morphometrics;
incomplete lineage sorting;
species tree.

Abstract

According to theory, adaptive radiation is triggered by ecological opportunity that can arise through the colonization of new habitats, the extinction of antagonists or the origin of key innovations. In the course of an adaptive radiation, diversification and morphological evolution are expected to slow down after an initial phase of rapid adaptation to vacant ecological niches, followed by speciation. Such 'early bursts' of diversification are thought to occur because niche space becomes increasingly filled over time. The diversification of Antarctic notothenioid fishes into over 120 species has become one of the prime examples of adaptive radiation in the marine realm and has likely been triggered by an evolutionary key innovation in the form of the emergence of antifreeze glycoproteins. Here, we test, using a novel time-calibrated phylogeny of 49 species and five traits that characterize notothenioid body size and shape as well as buoyancy adaptations and habitat preferences, whether the notothenioid adaptive radiation is compatible with an early burst scenario. Extensive Bayesian model comparison shows that phylogenetic age estimates are highly dependent on model choice and that models with unlinked gene trees are generally better supported and result in younger age estimates. We find strong evidence for elevated diversification rates in Antarctic notothenioids compared to outgroups, yet no sign of rate heterogeneity in the course of the radiation, except that the notothenioid family Artedidraconidae appears to show secondarily elevated diversification rates. We further observe an early burst in trophic morphology, suggesting that the notothenioid radiation proceeds in stages similar to other prominent examples of adaptive radiation.

Introduction

Adaptive radiation, that is the evolution of a multitude of species as a consequence of the adaptation to new ecological niches, is considered to be responsible for much of the diversity of life on Earth (Simpson, 1953; Schluter, 2000). In general, adaptive radiation is thought to result from ecological opportunity in the form of vacant ecological niches that may have become available due to the colonization of new habitats, the extinction of antagonists or the emergence of evolutionary key innovations that allow the invasion of new adaptive zones (Heard & Hauser, 1995; Schluter, 2000; Yoder *et al.*, 2010). Starting from a single ancestor, adaptively radiating groups are expected to differentiate into an array of morphologically and ecologically diverse species filling multiple available ecological niches. Mathematical models of adaptive radiation predict that rates of diversification and morphological evolution are inversely correlated with available niche space, thus leading to a slowdown in diversification rates as niche space becomes increasingly filled (Gavrilets & Vose, 2005; Gavrilets & Losos, 2009). As a result, both speciation events and morphological change would be concentrated in an 'early burst' near the

Correspondence: Walter Salzburger and Michael Matschiner, Zoological Institute, University of Basel, Vesalgasse 1, Basel 4051, Switzerland. Tel.: +41 61 267 03 03; fax: +41 61 267 03 01; e-mails: walter.salzburger@unibas.ch and michaelmatschiner@mac.com

beginning of the history of an adaptive radiation (Simpson, 1953; Erwin, 1994; Losos & Miles, 2002).

Temporally declining rates of speciation are often observed in molecular phylogenies of radiating clades, including Anolis lizards of the Caribbean islands (Rabosky & Glor, 2010), North American wood warblers (Rabosky & Lovette, 2008), squamates (Burbrink *et al.*, 2012), Neotropical cichlid fishes (López-Fernández *et al.*, 2013) and bats (Yu *et al.*, 2014). In addition, inverse relationships between radiation age and species counts have been found in the replicate adaptive radiations of *Tetragnatha* spiders on the Hawaiian islands (Gillespie, 2004), and in those of cichlid fishes in East African Rift lakes (Seehausen, 2006). This suggests that not only speciation rates, but also the total number of species can decline subsequently to an early burst, a phenomenon termed 'overshooting' (Gavrilets & Losos, 2009).

However, most empirical support for early bursts in morphological disparity derives from paleontological studies, which show that fossil groups often obtain maximum disparity early in their history, followed by subsequent decline (Foote, 1997). Several methods have been developed to infer early bursts in disparity from extant species on the basis of phylogenetic analyses (Harmon *et al.*, 2003, 2010; Slater & Pennell, 2014). In practice, however, these methods often fail to detect early bursts in morphological diversification in even the most prominent examples of adaptive radiation (Harmon *et al.*, 2010; but see Mahler *et al.*, 2010; Slater *et al.*, 2010; López-Fernández *et al.*, 2013).

Adaptive radiation has also been proposed to progress in stages in the sense that diversification occurs along different axes at different intervals of a radiation (Streelman & Danley, 2003; Ackerly *et al.*, 2006; Gavrilets & Losos, 2009). Verbal models, as well as a mathematical theory of speciation (Gavrilets, 2004), predict that diversification would (i) be driven by divergence according to macrohabitat, followed by (ii) increasing divergence with respect to microhabitat, (iii) traits that control both for local adaptation and nonrandom mating and (iv) traits that control for survival and reproduction. However, the order of stages seems to depend on diverse factors that differ between adaptive radiations. For example, *Phylloscopus* leaf warblers apparently diverged in the order of body size, foraging morphology/behaviour and then habitat (Richman, 1996), and trophic morphology has been suggested to diversify before macrohabitat adaptations in cichlids from Lake Tanganyika (Muschick *et al.*, 2014). In contrast, Lake Malawi cichlids and marine parrotfish were found to diverge first according to habitat, followed by trophic morphology and sexually selected traits (Streelman & Danley, 2003).

The diversification of Antarctic notothenioid fishes into over 120 extant species represents a prime example of an adaptive radiation in a marine environment. Notothenioids dominate the waters surrounding the Antarctic continent both by species number (47%) and by biomass (90–95%) (Eastman, 2005) and evolved exceptional adaptations in response to an environment that is shaped by subzero water temperatures and the widespread presence of sea ice. A common characteristic of all notothenioids is the lack of a swim bladder. Therefore, most notothenioid species are negatively buoyant. To compensate for this morphological limitation, several notothenioid clades evolved adaptations to regain neutral buoyancy and are able to utilize (in addition to the ancestral benthic habitat) a set of different environments such as semipelagic, epibenthic, cryopelagic or pelagic habitats (Eastman, 2005). Morphological adaptations to enable the exploitation of these habitats include reduced mineralization of the skeleton and deposition of lipids in adipose cells (Balushkin, 2000; Eastman, 2000). These adaptations, probably together with diversification in body and head shape, enabled notothenioids to feed on a diverse diet. Stomach content analyses reveal a diet consisting of fish, krill and mysids for some species as well as polychaetes, ophiuroids and echinoderms for others (Rutschmann *et al.*, 2011).

It is thought that the adaptive radiation of notothenioids followed ecological opportunity after the drop to subzero water temperatures around Antarctica that presumably led to the extinction of most of the previously existing ichthyofauna in the Late Oligocene or Early Miocene (Eastman, 1993; Near, 2004; Matschiner *et al.*, 2011). Due to the emergence of antifreeze glycoproteins (AFGPs) in the ancestor of five predominantly Antarctic notothenioid families (the 'Antarctic clade') (Chen *et al.*, 1997; Cheng *et al.*, 2003), notothenioids of this particularly species-rich group were able to survive in subzero waters and could effectively exploit ecological niches that had become vacant. Thus, AFGPs may have acted as a key innovation, triggering the adaptive radiation of the notothenioid Antarctic clade (Matschiner *et al.*, 2011), possibly facilitated by standing genetic variation (Brawand *et al.*, 2014). However, a recent phylogenetic study (Near *et al.*, 2012) found that major pulses of lineage diversification occurred substantially later than the evolution of AFGPs, which implies that other drivers were more important in driving diversification and acted at later stages. Thus, the timing and trigger of the notothenioid adaptive radiation remains a matter of debate.

Although the diversification of notothenioids has been the subject of a large number of recent investigations (Near & Cheng, 2008; Rutschmann *et al.*, 2011; Near *et al.*, 2012; Dettai *et al.*, 2012), studies dealing with the morphology of notothenioid fishes using modern geometric morphometric approaches remain scarce. This type of analyses has previously been shown to be highly useful for the quantification of shape differences between specimens or species and to display these differences in a way that facilitates their interpretation in an evolutionary context. In a pioneering study,

Klingenberg & Ekau (1996) investigated morphological changes associated with pelagic lifestyle in one of the notothenioid families. More recently, Wilson *et al.* (2013) assessed the shape of the operculum in a range of notothenioid species and correlated it with ecology and phylogenetic relationships. The study revealed a broad diversity of opercle morphologies with clear clustering according to phylogenetic groups as well as a correlation of opercle shape with the position along the benthic–pelagic axis. The authors used a broad taxon sampling including four of five families of the notothenioid Antarctic clade, but found no support for an early burst of opercle variation.

Here, we use a new time-calibrated phylogeny of 49 notothenioid species to test for patterns of taxonomic diversity as well as morphological and ecological disparity over time in the adaptive radiation of Antarctic notothenioids. Although our phylogeny includes less notothenioid taxa than previously published phylogenies (Near *et al.*, 2012), it is based on an extensive comparison of models for Bayesian phylogenetic inference, including models with unlinked gene trees (i.e. the multispecies coalescent approach of *BEAST; Heled & Drummond, 2010), and may thus provide a more accurate picture of notothenioid diversification. We investigate disparity through time (DTT) in multiple ecologically important traits, including body shape, body size, buoyancy adaptations and habitat preferences as approximated by temperature range within species' geographic distributions. We find that notothenioids of the Antarctic clade are characterized both by elevated diversification rates and by an early burst in trophic morphology, thus supporting the adaptive nature of their radiation.

Materials and methods

Sample collection and DNA sequencing

We collected 703 individuals of 42 notothenioid species with bottom and pelagic trawls during two Antarctic expeditions with RV Polarstern in the austral seasons 2010/2011 and 2011/2012 (ANT-XXVII/3 and ANT-XXVIII/4). For 34 species, muscle tissue was extracted from two to three specimens and stored in 95% ethanol until DNA extraction. For *Dissostichus eleginoides*, a freshly caught specimen was obtained at a local fish market in Buenos Aires, Argentina, in November 2009, of which tissue was extracted and stored in the same way.

Genomic DNA was obtained from notothenioid muscle tissue by proteinase *K* digestion followed by sodium chloride extraction and ethanol precipitation. Up to two mitochondrial and four nuclear protein-coding markers (in genes mt-cyb, mt-nd4, enc1, myh6, PTCHD4 and tbr1b) were amplified and Sanger-sequenced on an ABI3130*xl* capillary sequencer (Applied Biosystems, Foster City, CA, USA) with conditions as described in Matschiner *et al.* (2011) and Rutschmann *et al.* (2011). See Table S1 for details including primer sequences and marker references. Sequence base calls were performed with CodonCode Aligner v.4.2.4 (CodonCode Corporation, Centerville, MA, USA) and verified by eye. For each species, we used only sequence data of the individual that provided the best sequencing results. All sequence accession numbers are given in Table S2. Our molecular data set for 35 notothenioid species was complemented with sequences obtained from GenBank and the Barcode of Life Data System (BOLD) (Ratnasingham & Hebert, 2007) to result in a total of four mitochondrial (mt-co1, mt-cyb, mt-nd2 and mt-nd4) and seven nuclear (enc1, myh6, PTCHD4, rps7, snx33, tbr1b, zic1) sequences for 49 notothenioid taxa, with only 19 of 539 (3.5%) sequences missing (see Table S2).

For all 42 species caught during Antarctic field expeditions, up to 61 individuals (see Table S3) were photographed for morphometric analyses using a Nikon D5000 digital camera (Nikon Corporation, Tokyo, Japan) and a tripod. Photographs were always taken of the left side of each specimen with fins spread out, lying on a flat surface while minimizing bending. The camera lens was aligned horizontally to the surface. Overall, the 49 included taxa represent all eight nominal families of notothenioids and 33 of 44 recognized notothenioid genera (Eastman & Eakin, 2000). Species in our data set cover the known notothenioid sizes range, depth and geographic distribution, trophic levels and a variety of different life styles. Our taxon set therefore provides a representative sample of the morphological and ecological diversity found in notothenioids.

Species tree reconstruction

For each marker, sequences were aligned with MAFFT v.7.122b (Katoh & Toh, 2008) using the '—auto' option. Alignments were visualized with Mesquite v.2.75 (Maddison & Maddison, 2009), trimmed to start and end with first and third codon positions, and protein translations of all sequences were checked for stop codons. Finally, we removed phylogenetically uninformative insertions as well as questionable alignment positions adjacent to insertions.

The marker set was partitioned using the programs Concaterpillar (Leigh *et al.*, 2008) and PartitionFinder (Lanfear *et al.*, 2012) as described in Text S1. Bayesian species tree reconstructions were performed with BEAST v.2.1 (Bouckaert *et al.*, 2014) under a wide range of models, including the reversible-jump-based (RB) substitution model implemented in the RB add-on for BEAST 2 (Bouckaert *et al.*, 2013; Drummond & Bouckaert, 2014). Gene trees of individual markers were assumed to be linked or unlinked (using the multispecies coalescent model of *BEAST; Heled & Drummond, 2010) in separate analyses. Clock models were time-calibrated using three secondary divergence age constraints, and support for each model

combination was assessed *a posteriori* using the Akaike information criterion through Markov chain Monte Carlo (AICM) analysis (Raftery *et al.*, 2007). Species reconstruction details are given in Text S2.

After discarding the first 10% of MCMC generations as burn-in, posterior tree samples of replicate analyses were combined and summarized in maximal clade credibility (MCC) trees with 'common ancestor' node heights (Heled & Bouckaert, 2013). All BEAST analyses were repeated with mitochondrial or nuclear markers separately. To account for phylogenetic uncertainty in analyses of diversification rate and DTT (see below), we produced a set of 1000 trees that was sampled at random from the posterior tree distribution obtained with the full data set, combining both mitochondrial and nuclear markers, and with the best supported model combination according to AICM. For analyses that required a manual step for each tree (i.e. summarizing the positions of rate shifts inferred with the MEDUSA method, see below), the set of 1000 posterior trees was subsampled to yield a second set of 100 trees. BEAST XML files for with all model specifications, as well as posterior sets of 100 and 1000 species trees are deposited in Dryad (doi:10.5061/dryad.5jt5j).

As a second tool for species tree inference, we applied maximum pseudolikelihood for estimating species trees (MP-EST; Liu *et al.*, 2010). To use this method, we first produced gene trees for each marker with RAxML v.8.0.26 (Stamatakis, 2006), using partitioning schemes determined by PartitionFinder for the GTR+Gamma model of sequence substitution, which was also used in RAxML. For each marker, 100 bootstrap replicate trees (Felsenstein, 1985) were generated, and these were used to produce 100 species tree replicates with MP-EST. As MP-EST allows only a single outgroup, we removed sequences of *Cottoperca trigloides* from each alignment prior to the RAxML tree inference, leaving *Bovichtus diacanthus* as the only representative of the notothenioid family Bovichtidae. This family was previously shown to be the sister of all other notothenioids (Matschiner *et al.*, 2011; Near *et al.*, 2012) and was therefore used as outgroup for phylogenetic inference. The 100 bootstrap replicate species trees were summarized in a majority-rule consensus tree with a low majority requirement of 10% to obtain the bifurcating tree topology best supported by bootstrap values. To statistically compare this tree topology with posterior tree samples from our BEAST analyses, we reran the BEAST analysis based on the best-supported model according to AICM (which included unlinked gene trees, see Results), but this time constraining the BEAST species tree to match the tree topology of the MP-EST consensus tree.

Diversification rate analyses

To test for diversification rate shifts during the notothenioid radiation, we trimmed all time-calibrated species trees so that nearly the entire extant diversity of the notothenioid suborder could be assigned to the remaining tips, as listed in Table S8. The resulting diversity trees were analysed with the MEDUSA method (Alfaro *et al.*, 2009) implemented in the R package GEIGER (Harmon *et al.*, 2008) to estimate background speciation and extinction rates, and to identify clades with potentially elevated or decreased diversification rates. We expected to observe a single main increase in diversification at or near the base of the AFGP-bearing Antarctic clade of notothenioids, which is usually considered as the 'notothenioid radiation' (Eastman, 2005; Matschiner *et al.*, 2011; Near *et al.*, 2012) as it encompasses nearly the entire notothenioid species richness (122 of 132 species from five of eight families), including the morphologically most specialized groups. In addition, the notothenioid family Artedidraconidae has previously been shown to be exceptionally species rich given its age (Near *et al.*, 2012) and could support a second rate shift in our phylogeny. Diversification rate analyses were conducted with the diversity tree corresponding to the MCC tree resulting from the best-supported model combination, for the tree resulting from rerunning the same model in BEAST with the topological constraint of the MP-EST species tree and with 100 diversity trees based on the set of 100 trees sampled from the posterior distribution of the same BEAST analysis. For effective calculation, we allowed models to contain a maximum of 15 rate shifts, a number that we expected to be much larger than the actual number of shifts. Models assuming different numbers of rate shifts were compared on the basis of their Akaike information criterion corrected for sample size (AICc), and rate shifts were retained whenever they led to improved AICc scores.

Following Near *et al.* (2012; also see Dornburg *et al.*, 2008), we further calculated per-stage floating Kendall–Moran estimates of notothenioid diversification rates. To allow direct comparison with the results of Near *et al.* (2012), we used the same geological time intervals for these analyses: Late Miocene (subdivided into Tortonian, 11.6–7.2 Ma, and Messinian, 7.2–5.3 Ma), Early Pliocene (Zanclean, 5.3–3.6 Ma), Late Pliocene (Piacenzian, 3.6–2.6 Ma) and Pleistocene (2.6–0 Ma). We did not repeat these analyses for the Early and Middle Miocene, as these intervals would have (partially) predated the diversification of Antarctic notothenioids according to our age estimates. Kendall–Moran rate estimates were calculated for the MCC tree, the tree based on the MP-EST topology, and the posterior sample of 1000 trees resulting from the best-supported model combination, and in each case using both the full tree including bovichtid, pseudaphritid and eleginopid outgroups, and a trimmed tree reduced to representatives of the Antarctic clade. To account for missing taxa in our notothenioid phylogeny, Kendell–Moran diversification rates of notothenioids were compared to

rates calculated in the same way for simulated phylogenies that were constrained to be equally old and species rich as Notothenioidei, and were trimmed to the number of species included in our phylogenies. Phylogenetic simulations were performed using Yule and birth–death models of diversification, and tree trimming was performed according to random sampling and a new 'semi-diversified' sampling scheme (see Texts S3 and S4).

Geometric morphometric measurements of body shape

To test for differences in the overall body shape between notothenioid species, we performed geometric morphometric analyses on the basis of digital images. Body shape was quantified in a set of 703 specimens representing 42 ecologically diverse high Antarctic species from the five Antarctic notothenioid families (see Table S3) using 18 homologous landmarks (see Fig. S1).

Body shape variation was digitized using tpsDIG v.2.17 (Rohlf, 2013) and analysed with MorphoJ v.1.06a (Klingenberg, 2011). We performed a canonical variate (CV) analysis, a method that maximizes between-group variance in relation to within-group variance, with species as the grouping criterion to show shape changes associated with shape differences between species. Shape changes were visualized using an outline shape approach as implemented in MorphoJ. Species means for the first two CVs were illustrated in a phylomorphospace plot produced with the R package phytools (Revell, 2011) and used for analyses of DTT following Harmon *et al.* (2003) (see below).

Habitat characterization

To approximate the geographic distribution of individual notothenioid species, georeferenced point occurrence data were downloaded from Fishbase (Froese & Pauly, 2013), which represent a compilation of entries made to the Global Biodiversity Information Facility (GBIF; http://www.gbif.org), the Ocean Biogeographic Information System (OBIS; http://www.iobis.org) and Fishbase itself. To reduce overrepresentation of heavily sampled locations (Ready *et al.*, 2010), point occurrence data were summarized as presence or absence in a grid of 0.5° latitude/longitude cell dimensions. With the exception of bovichtid outgroups ($n = 5$) and *Harpagifer antarcticus* ($n = 8$), each notothenioid species included in our data set was present in at least 24 (*Parachaenichthys georgianus*) and up to 292 (*Pleuragramma antarctica*) grid cells (mean = 79.5; Table S9).

For each of these grid cells, environmental parameters were obtained from the AquaMaps database (http://www.aquamaps.org; Kaschner *et al.*, 2013), a database designed for the prediction of global distributions of marine species. These predictions are made on the basis of a characterization of the environmental preferences of each species, and the database authors selected bottom depth, water temperature, salinity, primary production and sea ice concentration as five parameters that were best suited to quantify these preferences for marine species (Kaschner *et al.*, 2006). As our study aims to investigate ecological niche partitioning during the notothenioid radiation, its incentives differ from those of the AquaMaps database, that is the prediction of species distributions. However, both approaches require a detailed characterization of the ecological niche occupied by a species, and thus, we consider the same parameters that have shown useful for the purpose of the AquaMaps database (Ready *et al.*, 2010) as suitable proxies to study partitioning of ecological niches in marine taxa. For grid cells occupied by notothenioid taxa, we found very little between-species variation in bottom depth, salinity and primary production and, unsurprisingly, a strong correlation between sea ice concentration and water temperature (Fig. S2). Therefore, we here use water temperature as the only environmental parameter to characterize notothenioid habitats. Temperature data stored in the AquaMaps database represent sea surface temperatures extracted from the Optimum Interpolation Sea Surface Temperature atlas (http://www.esrl.noaa.gov/psd/data/gridded/data.noaa.oisst.v2.html) and are averaged over the period 1982–1999 (Ready *et al.*, 2010; Kesner-Reyes *et al.*, 2012). Sea surface temperature may deviate from the actual temperature experienced by notothenioid species in benthic habitats; however, depth-specific temperature data are not available from the AquaMaps database. Thus, we here use sea surface temperature for all notothenioid species, assuming that differences between this measure and the actual temperature in notothenioid habitats are minor compared to those observed between different species. As a result of this approximation, patterns inferred for the evolution of habitat preferences among notothenioids may need to be interpreted with caution.

In addition to sea surface temperature, we use species-specific buoyancy measures (taken from Near *et al.*, 2012) as a second proxy to characterize notothenioid habitats. As notothenioid fishes possess no swim bladder, their position in the water column is directly influenced by adaptations to regain neutral buoyancy such as reduced mineralization of the skeleton and scales or the accumulation of lipid deposits (Eastman, 2000). Thus, buoyancy measures are informative regarding the depth distribution and the lifestyle of notothenioid species.

Disparity through time

Analyses of morphological DTT indicate how the trait space occupied by a clade became partitioned during the diversification of the clade (Foote, 1999; Harmon

et al., 2003). In this type of analyses, the observed DTT trajectory is usually compared to that expected according to pure Brownian motion (BM) (Harmon *et al.*, 2003, 2008), and the difference between these is quantified by the morphological disparity index (MDI). Highly negative MDI values are commonly interpreted as evidence for an early burst in trait evolution in the investigated clade, supporting the adaptive character of the diversification process in this clade (Harmon *et al.*, 2010; Slater *et al.*, 2010; Slater & Pennell, 2014). However, the signature of an early burst, as measured by MDI, might be blurred by other processes that are characteristic of adaptive radiation. If the radiation proceeds in stages, as has been shown for several groups (Richman, 1996; Streelman & Danley, 2003; Gavrilets & Losos, 2009), early bursts would likely only occur along the first axis of diversification. Furthermore, the trait space for many characters may be bounded by hard or soft constraints, so that the evolution of these characters may be poorly approximated by a BM model. Among the parameters here investigated for notothenioid species, hard trait space bounds are obviously present for the temperature of sea water, which usually freezes at −1.86 °C (Eastman, 1993), and similar limits can be assumed for buoyancy values of fishes without swim bladders. In addition, soft bounds have been shown to limit the evolution of body size and shape in a wide range of vertebrate species (Harmon *et al.*, 2010; Gherardi *et al.*, 2013) and may therefore also be present in notothenioids.

To assess the impact of stagewise adaptive radiation and bounded trait spaces on DTT trajectories and their associated MDI values, we conducted simulations of trait evolution according to these more complex models on a large number of simulated phylogenetic trees. Specifically, we generated 2000 replicate trees using a continuous-time pure birth model with speciation rate λ drawn at random from a uniform distribution between 0.1 and 0.4, an extant species richness of exactly 100 taxa and a most recent common ancestor age of 15 million years (trees that did not fulfil these criteria were discarded). We used the Ornstein–Uhlenbeck (OU) model (Hansen, 1997; Butler & King, 2004) for trait evolution, applying a range of values for the constraint parameter α between $\alpha = 0$ (in this case, the OU model is identical to BM) and $\alpha = 0.3$. Positive values of α influence the long-term behaviour of traits and can be interpreted as soft trait space bounds or selection towards an optimum (in our simulations, optimum and starting value were always chosen to be both 0). Different stages of adaptive radiation were simulated by 10-fold elevated rates of trait evolution in the first 5 million years of the radiation (15–10 Ma), the second interval of 5 million years (10–5 Ma) and the period between 5 Ma and the present. The first of these three scenarios is similar to the early burst model of Harmon *et al.* (2010) in having an elevated initial rate of trait evolution, but contrary to the early burst model, the rate does not decline continuously, but with a single, abrupt decrease at 10 Ma. Finally, all simulated data sets were subjected to DTT analyses, and MDI values were calculated on the basis of 100 BM simulations, both using the function dtt() implemented in GEIGER.

We compared DTT plots of simulated trait evolution with those of observed traits characterizing the morphometry and habitat of notothenioid fishes. Here, morphometry of individual species was described by the mean values of the first two canonical variates of body shape variation and by mean body size measured as terminal length. The interspecific variation in habitat use was described by buoyancy measures and by mean sea surface temperature of geographic grid cells in which a species is known to occur (see above). Species means of all five traits are compiled in Table S3. For each trait, we first determined whether a BM model or an OU model of trait evolution provided a better fit to the observed values. Parameters of the two models were optimized for each trait and for each of the 1000 trees drawn from the BEAST posterior tree distribution using the maximum likelihood function fitContinuous() of GEIGER. Per trait and tree, model fit was compared on the basis of AICc scores. The observed DTT curves of the five notothenioid traits were contrasted with DTTs simulated with the best-fitting model of trait evolution, for the same set of trees. Finally, we compared DTT distributions resulting from the extensive set of simulations described above with those based on trait variation observed in notothenioids, both qualitatively by visual inspection and quantitatively by means of the associated MDI values. Note that for comparability between analyses, all MDI values were calculated as the area between a DTT and the median average subclade disparity in 100 simulations of BM trait evolution in the same tree as the DTT.

Results

Species tree reconstruction

Applying gene tree concordance tests with the software Concaterpillar, we found no significant discordance among nuclear markers. However, different evolutionary histories were detected for the concatenated nuclear alignment and the combined mitochondrial marker set (likelihood ratio test based on nonparametric bootstrapping; $P < 0.001$). Maximum likelihood trees resulting from these two alignments differ strongly in their topologies (Fig. S3), and one of the most obvious differences concerns the placement of *Gobionotothen*, which is the first lineage to diverge among Antarctic notothenioids in the mitochondrial tree, but appears nested within this clade based on nuclear data.

Judging from a comparison of parameter traces in Tracer v.1.5 (Rambaut & Drummond, 2007), replicate

BEAST runs always converged to the same solution. After discarding the burn-in, ESS values of likelihood traces (the only traces needed for model comparison by AICM), combined for all replicates, were > 700 for all analyses, and ESS values of model parameters were almost always > 200. According to AICM values, the most parameter-rich model combination, the RB+Gamma substitution model with estimated frequencies and a UCLN clock, outperformed all other models in all analyses, regardless of whether gene trees were linked or unlinked, and with all data sets (combined, mitochondrial, and nuclear). Linking of gene trees led to better AICM values only for the nuclear data set, suggesting that with this data set, the large increase in parameter number outweighs the obtained improvements in the likelihood when gene trees topologies are unlinked. Akaike weights computed from AICM values strongly favoured unlinked gene trees for the combined (Akaike weight = 1.0) and mitochondrial data sets (Akaike weight = 0.997), and supported linking of gene trees for the nuclear data set (Akaike weight = 1.0) (Tables S4–S7).

Both the topology and branch lengths of resulting MCC trees were largely dependent on the assumed models. As a relatively high number of substitutions in nuclear markers separates *P. antarctica* from other Antarctic notothenioids, all MCC trees based on the nuclear marker set and a strict molecular clock inferred *Pleuragramma* to be the earliest diverging lineage among Antarctic notothenioids, with mean separation times of 19.1–14.9 Ma. The same was true for analyses of the combined marker set, but only when gene trees were unlinked (18.7–17.6 Ma). In contrast, almost all MCC trees based on either the combined or nuclear marker set and the UCLN molecular clock identified the earliest divergence among Antarctic notothenioids between two clades, where the first of these clades contains the nototheniid subfamily Trematominae (Lautrédou *et al.*, 2012) and the second clade groups the four more derived families Artedidraconidae, Harpagiferidae, Bathydraconidae and Channichthyidae with other nototheniid lineages. Here, the exception was the MCC tree based on the nuclear marker set, the RB+Gamma substitution model, estimated base frequencies and a UCLN clock, in which *Aethotaxis mitopteryx* diverges first from other Antarctic notothenioids (11.2 Ma), followed by *P. antarctica* (10.4 Ma).

Inferred ages for the onset of the divergence of Antarctic notothenioids (the node marked with * in Fig. 1a) varied strongly between the individual analyses with mean estimates between 10.9 Ma (95% highest posterior density, HPD: 14.6–7.9 Ma) and 28.5 Ma (95% HPD: 33.6–23.5 Ma). As expected, ages inferred with unlinked gene trees were always younger than those based on analyses with linked gene trees. We generally observed lower mean age estimates for more parameter-rich models and found a significant negative correlation between the number of parameters present in the model and the mean age inferred for the first divergence event of Antarctic notothenioids ($b = -0.207$ myr/parameter; $t_{34} = -6.918$, $P < 0.001$, $r^2 = 0.57$) (Fig. 1b).

According to AICM, the best model for analyses of the combined marker set applies the RB+Gamma substitution model with estimated base frequencies and a UCLN molecular clock to unlinked gene trees. This is the most parameter-rich of all used models (76 parameters) and, consequently, required one of the longest MCMC lengths to obtain sufficiently high ESS values (nine replicates with 2 billion MCMC steps each, the first 50% of each replicate were discarded as burn-in). The resulting age estimate for the initial divergence of Antarctic notothenioids is lower than in most other analyses, with a mean of 13.4 Ma and a 95% HPD interval between 17.1 and 10.0 Ma. The corresponding tree topology strongly supports the monophyly of Antarctic notothenioids (Bayesian posterior probability, BPP 1.0), but within this clade, only few groups receive equally strong support. These include Trematominae (Lautrédou *et al.*, 2012), the families Artedidraconidae and Channichthyidae, and the two bathydraconid subfamilies Bathydraconinae and Cygnodraconinae (Derome *et al.*, 2002; see also Near *et al.*, 2012). In agreement with previous studies (Matschiner *et al.*, 2011; Dettai *et al.*, 2012; Near *et al.*, 2012), the same tree further supports a clade combining the four most derived Antarctic families Artedidraconidae, Harpagiferidae, Bathydraconidae and Channichthyidae, as well as a sister-group relationship of Harpagiferidae and Artedidraconidae (both groupings receive BPP 1.0). In contrast to the phylogeny of Near *et al.* (2012), we find no support for Pleuragrammatinae (Balushkin, 2000) as a nototheniid subfamily combining the pelagic genera *Pleuragramma*, *Aethotaxis* and *Dissostichus* (as well as *Gvozdarus*, which is missing from our data set). The monophyly of the family Harpagiferidae and the bathydraconid subfamily Gymnodraconinae (Derome *et al.*, 2002) could not be tested as our data set included only a single representative of both groups.

Despite relatively low bootstrap support, the bootstrap consensus species tree topology obtained with MP-EST agrees well with the MCC tree resulting from the BEAST analysis with the best-supported model combination (Fig. S4). The most noticeable differences include the placement of *Gobionotothen gibberifrons*, which appears as the sister of all other Antarctic notothenioids in the MP-EST species tree, and the placement of Bathydraconinae instead of Cygnodraconinae as the sister group of Channichthyidae. However, both rearrangements receive low support in the MP-EST species tree [bootstrap support (BS) 49 and 54, respectively]. Rerunning the best-supported model combination in BEAST, using the MP-EST species tree topology as a topological constraint, results in very

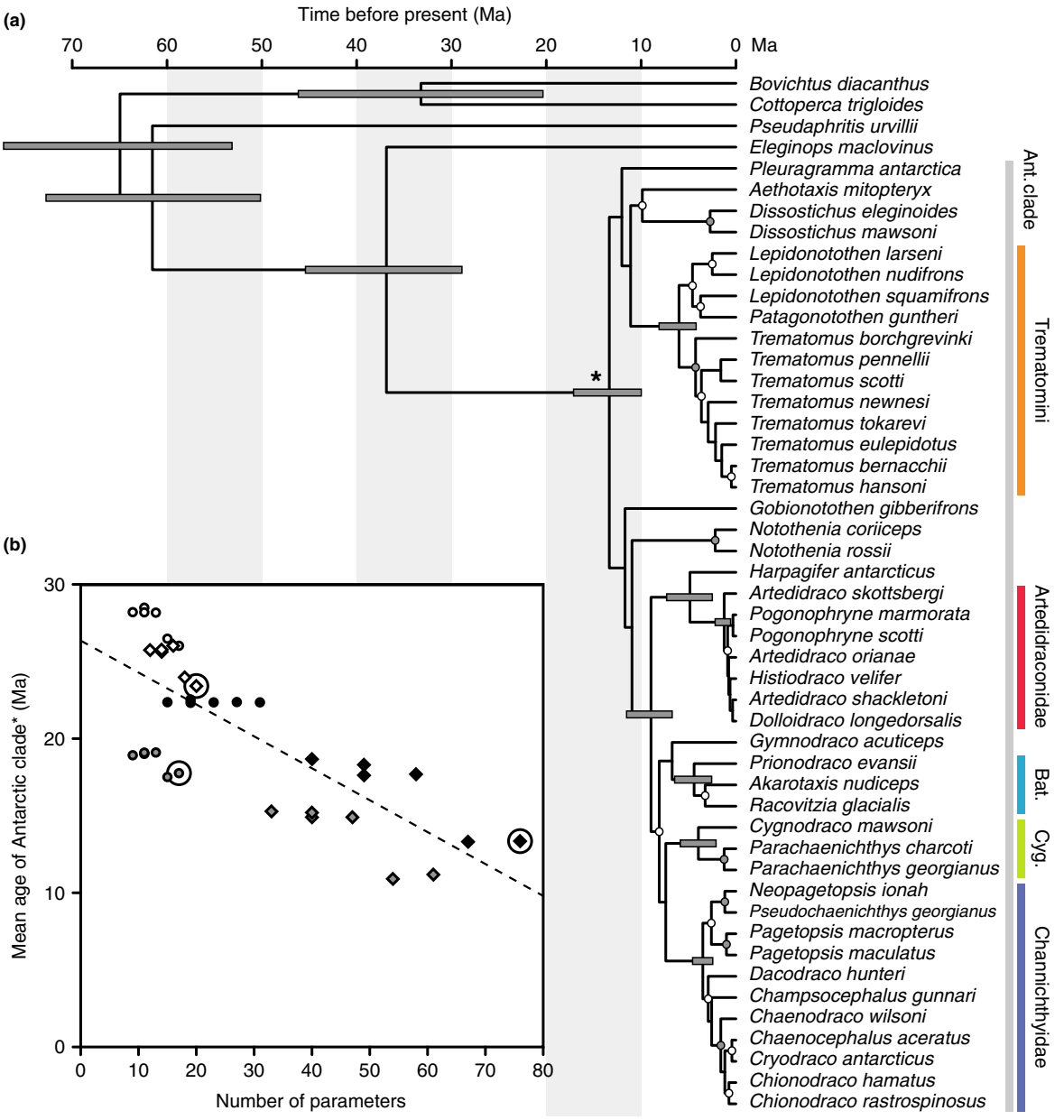

Fig. 1 Time-calibrated species tree of Notothenioidei. (a) The maximal clade credibility (MCC) tree for the BEAST analysis of the combined marker set and the best-supported model combination. Node bars are only shown for clades supported by Bayesian posterior probability (BPP) 1.0 and indicate the divergence date 95% highest posterior density. Gray circles mark nodes supported with BPP > 0.9 and white circles indicate BPP > 0.5. Support values and age estimates for all nodes are listed in Table S10. Vertical colour bars at right indicate monophyletic clades. Bat.: Bathydraconinae; Cyg.: Cygnodraconinae. The vertical gray bar spans the Antarctic clade. A lineage-through-time plot for this MCC tree is shown in Fig. S6. (b) The mean age estimate for the diversification of Antarctic notothenioids (the node marked with *) plotted against the number of parameters used in the respective BEAST analysis. Analyses using unlinked gene trees are represented by diamonds, and those with linked gene trees are marked with circles. Fill colours of circles and diamonds indicate the marker set used for the analysis (white: mitochondrial, gray: nuclear, black: combined). The best-supported model combination for each data set is encircled.

similar age estimates compared to the MCC tree from the unconstrained BEAST run with the same model combination (Fig. S5a). The posterior probability distribution of the topologically constrained analysis was nearly identical to that of the unconstrained runs (Fig. S5b), suggesting that the MP-EST species tree topology was also within the posterior tree distribution of the topologically unconstrained BEAST analysis.

Diversification rate analyses

To identify diversification rate shifts during the evolution of notothenioid fishes, we applied MEDUSA to a diversity tree resulting from the MCC tree based on the BEAST analysis with the best-supported model combination (Fig. 1a), to the tree resulting from a reanalysis of the same model combination, but using the MP-EST species tree as a topological constraint (Fig. S5), and to a set of 100 diversity trees that account for the uncertainty in the phylogenetic estimate resulting from the topologically unconstraint BEAST analysis. In the diversity tree based on the MCC tree, MEDUSA identified a single rate shift at the base of the divergence of all Antarctic notothenioids (the node marked with * in Fig. 1a) that led to an improvement in AICc score of 11.7 units. Maximum likelihood estimates for net diversification (r) and turnover rates (ε) were $r = 0.029$ and $\varepsilon = 0.030$ per myr for non-Antarctic notothenioids, and $r = 0.106$ and $\varepsilon = 0.887$ per myr for Antarctic notothenioids subsequent to the inferred shift. Use of the MP-EST species tree as a topological constraint also resulted in a single rate shift (from the background rates of $r = 0.009$ and $\varepsilon = -0.882$ to $r = 0.251$ and $\varepsilon = 0.614$); however, in this case, the rate shift excludes the genus *Gobionotothen*, which appears as the sister of all other Antarctic notothenioids in the MP-EST topology. In the set of 100 diversity trees, MEDUSA identified a single rate shift in 61 of these trees, two rate shifts in 33 trees and three rate shifts in six trees. One of the shifts always preceded or coincided with the separation of Trematominae from the four families Artedidraconidae, Harpagiferidae, Bathydraconidae and Channichthyidae, and led to elevated diversification rates of $r = 0.215 \pm 0.091$, compared to background rates of $r = 0.020 \pm 0.008$. However, only in 37 of the 100 trees were all Antarctic notothenioids affected by this shift. In the remaining 63 trees, one or several of the nototheniid lineages *Aethotaxis* (in 51 trees), *Dissostichus* (48 trees), *Pleuragramma* (34 trees), *Gobionotothen* (13 trees), *Notothenia* and *Paranotothenia* (both in three trees) diverged before the separation of Trematominae and the four more derived families, and were not included in the same diversification regime. Thus, uncertainty remains whether these lineages should be considered part of the same radiation as Trematominae, Artedidraconidae, Harpagiferidae, Bathydraconidae and Channichthyidae.

As expected, Kendall–Moran estimates of per interval diversification rates were generally lower for trees of all notothenioids included in our taxon set, compared to trees reduced to representatives of the Antarctic clade (Fig. S7). In all time intervals of the Lower Miocene and the Pliocene, trees of the Antarctic clade had comparable diversification rates to simulated phylogenies of the same age and species richness. The exception to this is the Pleistocene, where rate estimates for the Antarctic clade appear high compared to those in simulated phylogenies: when simulations were based on a strict Yule model, the rate estimates for the MCC tree and the tree based on the MP-EST topology, as well as the mean rate in a sample of 1000 trees, were higher than the 99.9% quantile of rates found in simulated phylogenies after application of the semidiversified sampling scheme (Fig. S7e). Compared to phylogenies simulated with a birth–death model, however, these rates appear less exceptional, and only the mean rate in the sample of 1000 trees and the rate of the tree based on the MP-EST topology, but no longer the rate of the MCC tree, were higher than the 95% quantile of rates in simulated phylogenies. This pattern is strikingly different when trees of all notothenioids in our taxon set are compared to simulated trees of the same age and species diversity as Notothenioidei, after trimming these simulated trees to match the number of taxa in our empirical phylogeny, again with a random or semidiversified sampling scheme. In this case, diversification rate estimates in observed trees are higher than the 95% quantiles of rates in simulated trees in almost all tested time intervals, regardless of whether the Yule or birth–death model is used for phylogenetic simulations.

Geometric morphometrics

The first two CVs (Fig. 2a) account for $\sim$55% of the total variance in the body shape data set. CV1 ($\sim$39% of variance) illustrates a shape change towards a shorter, more compressed snout with the mouth facing upward and a deeper body, mainly concerning the abdomen but also the tail and caudal peduncle. The onset of the anal fin is slightly shifted anterior, as is the pelvic fin, whereas the dorsal fin is shifted posterior. Shape change in CV2 ($\sim$16% of variance) is associated with a deeper snout, the eye shifted anterior and both shorter dorsal and anal fins, whereas the caudal peduncle is slightly elongated.

A phylomorphospace plot (Fig. 2b) including the first two CVs shows a clustering according to taxonomy for some families, whereas others show a more diverse body shape distribution. CV1 mainly discriminates between Channichthyidae and Cygnodraconinae characterized by a long, pikelike snout (negative CV1 scores) on one side and an overlapping cluster consisting of Nototheniidae, Artedidraconidae and Trematomini characterized by a shorter, more robust head (positive CV1 scores) on the

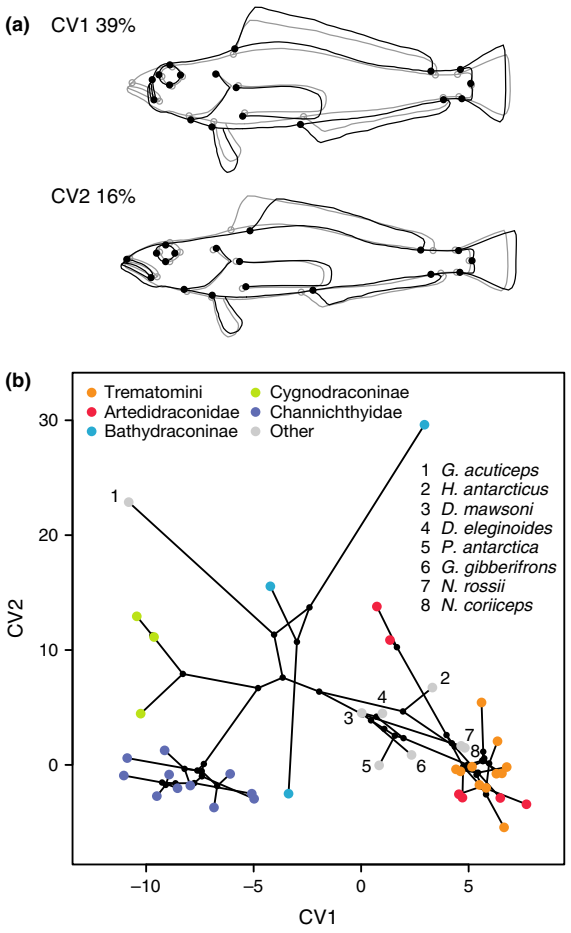

Fig. 2 Body shape variation in notothenioid species. (a) Shape changes along the first two canonical variates. (b) Phylomorphospace plot of the first two canonical variates of body shape variation. Coloured dots show mean values of notothenioid species, whereas dot colour indicates clade membership. Colour code as in Fig. 1a. Species not assigned to clades are represented by gray dots, with labels indicating species names. Black lines show phylogenetic relationships, and black dots represent hypothesized ancestral trait values.

other side. CV2, mainly associated with alterations of the unpaired fins, shows great variation in Bathydraconidae and Artedidraconidae, probably because some family members are characterized by strong reductions or even the complete loss of the first dorsal fin. Other families, such as Channichthyidae, show remarkably constant CV2 values.

Habitat characterization

Sea surface temperature data were extracted from the AquaMaps database for geographical grid cells, in which notothenioid species are known to occur. As expected, sea surface temperature was found to correlate with latitude ($b = -0.40$ °C/degree south; $t_{966} = -56.38$, $P < 0.001$, $r^2 = 0.77$), with a minimum temperature of −1.79 °C found in a total of 126 grid cells between 67.25°S and −78.25°S, in which 28 of the 42 notothenioid species in our trait data set are known to occur. These include *P. antarctica*, *Dissostichus mawsoni*, *Notothenia coriiceps*, seven of eight included members of the genus *Trematomus*, all seven included members of Artedidraconidae, the three included members of Bathydraconinae, *Gymnodraco acuticeps*, *Cygnodraco mawsoni* and seven of 11 included members of Channichthyidae. The maximum temperature of 19.25 °C was found at 34.75°S, 51.75°W, off the Uruguayan coast, which is the northern range limit of *D. eleginoides*. Mean temperatures of grid cells occupied by members of selected notothenioid clades were between −1.62 °C (Bathydraconinae) and −0.51 °C (Trematominae), and temperature ranges of clades varied greatly (Trematominae mean: −0.51 °C, range: −1.79 to 9.11 °C; Artedidraconidae mean: −1.55 °C, range: −1.79 to 0 °C; Bathydraconinae mean: −1.62 °C, range: −1.79 to 0 °C; Cygnodraconinae mean: −0.70 °C, range: −1.79 to 3.23 °C; Channichthyidae mean: −0.89 °C, range: −1.79–3.99 °C). Water temperatures of individual species' ranges are shown in Fig. 3.

Disparity through time

Analyses of DTT were conducted for a wide range of trait evolution simulations and compared to DTTs based on the observed characteristics for the morphology and habitat of notothenioid species. Simulations were performed with either homogeneous or periodically elevated rates of trait evolution that followed an Ornstein–Uhlenbeck (Hansen, 1997) model with a constraint parameter α between α = 0 (in this case, the Ornstein–Uhlenbeck model reduces to BM) and α = 0.3. Traditionally, DTT trajectories are compared to those obtained under a BM null model, and exceptionally low DTT trajectories are taken as evidence for early bursts of trait evolution. Plots in Fig. 4 show mean DTT trajectories (in Fig. 4a–e) and associated MDI values (Fig. 4f–j) when traits evolved with a homogeneous rate or with a rate that is 10-fold higher in the beginning of a clade's diversification, during an intermediate interval, or near the present. As expected, average subclade disparities and the associated MDI values are generally lower when rates are initially elevated, compared to when rates remain constant throughout the clade's history, or are elevated near the present. However, the addition of hard or soft boundaries to trait evolution always leads to a shift to more positive average subclade disparities and MDI values, so that, depending on the position and strength of these boundaries, the signature of initially elevated rates becomes less obvious (Fig. 4b,

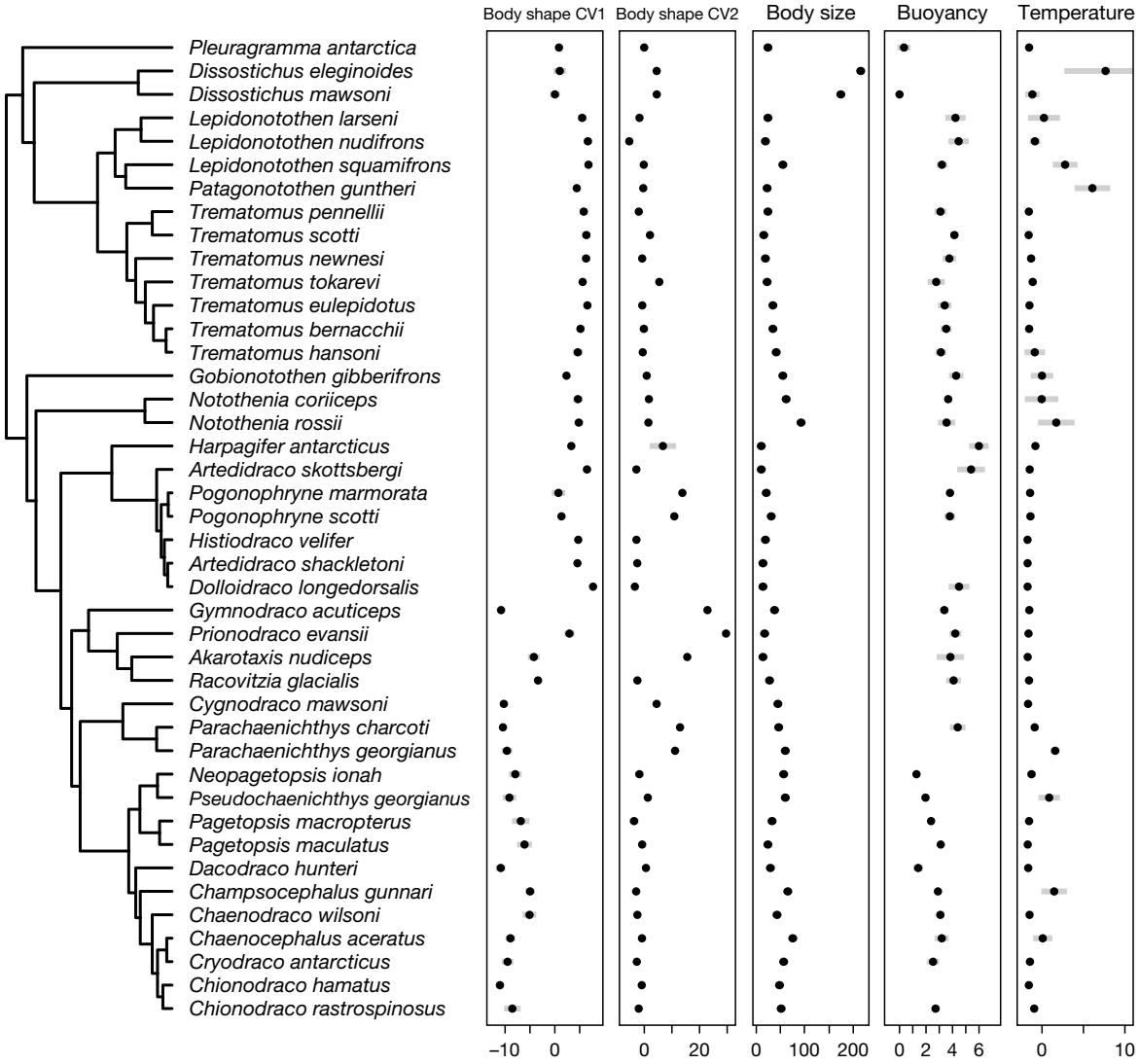

Fig. 3 Variation in morphological and habitat characteristics among notothenioid species. For each species, black dots indicate means of observed trait values, and gray bars represent standard variation. Body size is measured in cm, buoyancy in per cent, and temperature in °C. Buoyancy values are taken from Near *et al.* (2012). The phylogenetic tree is identical to the one shown in Fig. 1a, excluding species with missing trait data.

c) or disappears altogether (Fig. 4d,e). As a result, early bursts may not be detectable when trait space is constrained by hard or soft boundaries. Thus, low observed average subclade disparities and MDI values are likely to indicate elevated rates early in a clade's history, whereas high disparities and MDI values can result from either elevated rates near the present or hard or soft boundaries to trait evolution.

Maximum likelihood model fitting showed that the OU model provided a better fit than BM to trait evolution for body shape CV2, for log body size and for the sea surface temperature of notothenioid habitats (Table 1), with ML estimates of the α parameter between 0.11 (body size) and 0.30 (CV2). DTT curves and MDI densities for notothenioid body shape and size, as well as buoyancy and the sea surface temperature of notothenioid habitats, are shown in Fig. 5. Regardless of clade age, average subclade disparities of CV1 are low compared to those simulated under BM (Fig. 5a,f). Asterisks in Fig. 5f indicate that for CV1, the MDI of the MCC tree (−0.188), the MDI of the MP-EST species tree after branch length optimization with BEAST (−0.177)

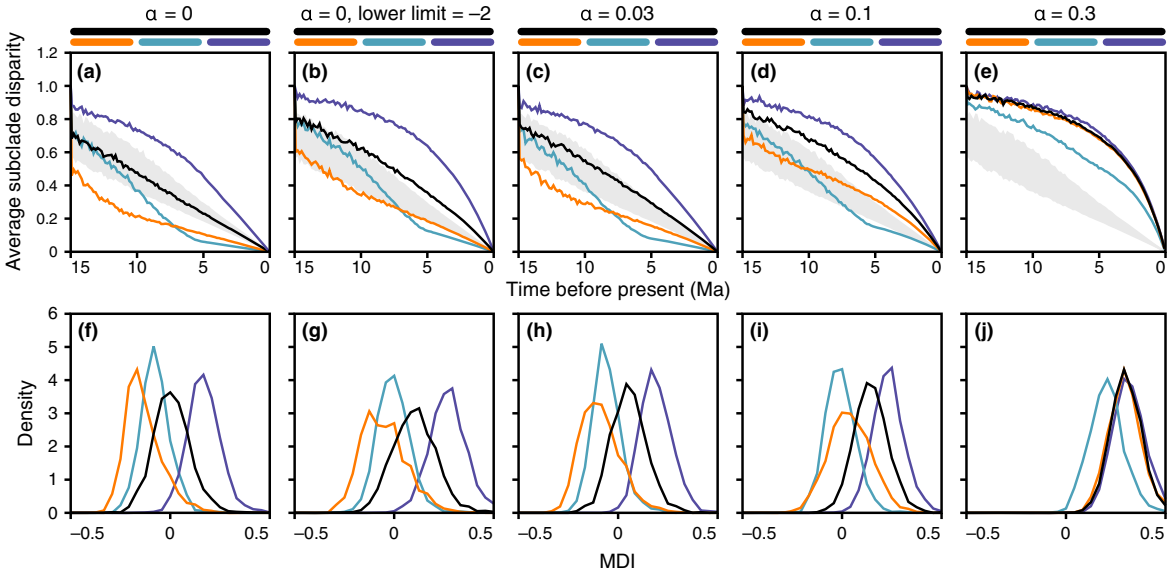

Fig. 4 Disparity through time and associated morphological disparity index (MDI) values for simulated trait evolution. (a–e) Average subclade disparity over time in simulated phylogenies with an age of 15 myr. The horizontal axis represents time. The black line represents the mean value for 2000 replicates of simulated diversification and trait evolution when the rate of trait evolution is homogeneous. Orange, turquoise and blue lines indicate mean values when the rate of trait evolution is 10-fold elevated between 15 and 10 Ma, between 10 and 5 Ma, or between 5 Ma and the present. (f–j) Densities of MDI values in 2000 trait evolution replicates, in the same sequence as (a–e).

Table 1 Maximum likelihood fitting of Brownian motion (BM) and Ornstein–Uhlenbeck (OU) models to trait evolution of body shape, size, buoyancy and habitat temperature.

Trait	Model	σ^2	α	LnL	AICc	#Trees
Body shape CV1	BM	3.47		−112.67	229.65	627
	OU	4.11	0.04	−111.95	230.53	373
Body shape CV2	BM	18.15		−147.53	299.37	40
	OU	39.05	0.30	−140.80	288.24	960
Body size (log)	BM	0.08		−34.02	72.34	335
	OU	0.12	0.11	−31.90	70.43	665
Buoyancy	BM	0.23		−48.94	102.26	723
	OU	0.27	0.03	−48.70	104.17	277
Temperature	BM	1.18		−89.47	183.25	120
	OU	2.37	0.25	−84.75	176.12	880

Parameter values were optimized for the set of 1000 trees drawn from the posterior distribution of the BEAST run with the combined data set and the model combination best supported by AICM. To reduce the impact of outlier estimates, median values are given for σ^2, α, the log likelihood and Akaike information criterion scores, corrected for small sample sizes (AICc). The last column specifies the number of trees for which a model had a lower AICc score than the competing model.

and the mean MDI in a sample of 1000 trees (−0.169) are lower than the 5% quantile (−0.167) of MDI values under a BM expectation, thus suggesting that rates of evolution were high during the early evolution of Antarctic notothenioids. In contrast, MDI values for CV2 (MCC tree: 0.202, MP-EST species tree: 0.209, mean of tree sample: 0.223) are higher than the 95% quantile under BM (0.198), but agree well with an OU model of trait evolution (with $\alpha = 0.30$; see Table 1) (Fig. 5b,g). Both the DTTs of log body size (Fig. 5c,h) and buoyancy (Fig. 5d,i) appear consistent with expectations from a BM null model; however, average subclade disparities and MDI values of log body size (MCC tree: 0.005, MP-EST species tree: 0.006, mean of tree sample: −0.026) are outside of expectations based on the fitted OU model (with $\alpha = 0.11$) for this trait (5% quantile: 0.032),

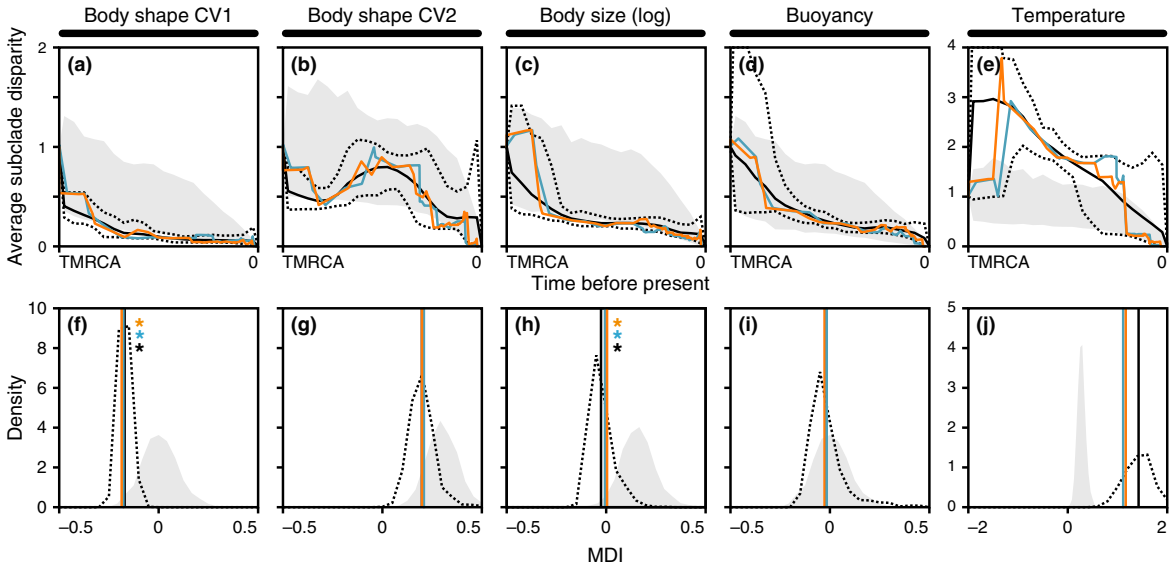

Fig. 5 Disparity through time and associated morphological disparity index (MDI) values for observed notothenioid traits. (a–e) Average subclade disparity over time. The horizontal axis represents time between the time of the recent common ancestor (TMRCA) and the present. Solid and dotted black lines indicate the mean and the 5% and 95% quantiles for average subclade disparity found in a posterior tree sample of 1000 trees. The orange and turquoise lines mark average subclade disparity in the maximal clade credibility (MCC) tree and in the tree based on the MP-EST species tree topology, respectively. The gray area represents the 5% and 95% quantiles for average subclade disparity according to the fitted model of trait variation (see Table 1). (f–j) Solid lines represent MDI values calculated over the first 90% of the chronogram to account for tip overdispersion (Harmon *et al.*, 2003), with colour codes as in (a). The black dotted line shows the density of MDI values in the sample of 1000 trees. The gray shape shows the density of MDI values in 2000 trees simulated with the fitted model of trait evolution (BM for body shape CV1 and buoyancy, OU with $\alpha = 0.30$, 0.11 and 0.25 for body shape CV2, log body size and temperature; see Table 1). Asterisks in (f) and (h) indicate that the tree sample mean MDI, the MDI of the MCC tree and the MDI of the tree based on the MP-EST topology are lower than the 5% quantile of MDI values found with the fitted model. Note the different scales for (e) and (j).

suggesting that despite the improved AICc score of the OU model, BM describes notothenioid body size evolution sufficiently well. Remarkably high average subclade disparities and MDI values were observed for the sea surface temperature of notothenioid habitats (Fig. 5e,j; note the different scale). MDI values for this character (MCC tree: 1.169, MP-EST species tree: 1.114, mean of tree sample: 1.456) were higher than the highest recorded values in 2000 replicate simulations of lineage diversification and trait evolution, regardless of whether these were based on BM (maximum MDI: 0.538) or the fitted OU model (with $\alpha = 0.25$; maximum MDI: 0.952). This pattern seems to be mostly driven by the comparatively late separation (mean age estimate: 2.72 Ma, 95% HPD: 5.47–0 Ma) of *D. mawsoni*, one of the more cold-adapted species (mean temperature of grid cells: −1.15 °C), and *D. eleginoides*, which seems to lack functional AFGP sequences (Cheng & Detrich, 2007) and has the most temperate distribution of all species included in our comparison (mean temperature of grid cells: 7.64 °C). Exclusion of *D. eleginoides* from DTT analyses leads to lower MDI values (MCC tree: 0.421, MP-EST species tree: 0.467, mean of tree sample: 0.408), which are still higher than the 99.5% quantile of MDI values under BM (0.338), but agree with the expectations of the fitted OU model (95% quantile: 0.509).

Discussion

It has previously been shown that Antarctic notothenioids fulfil multiple criteria of adaptive radiation, including common ancestry, rapid diversification, phenotype–environment correlation, trait utility and convergent evolution (Schluter, 2000; Eastman, 2005; Cheng & Detrich, 2007; Bilyk & DeVries, 2010; Rutschmann *et al.*, 2011). However, whether or not other predictions of adaptive radiation theory, such as early bursts in diversity and disparity (Gavrilets & Losos, 2009), are realized in Antarctic notothenioids remains a matter of debate. Here, we thus tested for temporally declining rates in the evolution of notothenioid diversity and disparity on the basis of a novel time-calibrated phylogeny of notothenioid fishes.

The age of the notothenioid radiation

As it has often been hypothesized that the notothenioid radiation in the freezing waters of Antarctica is linked to the evolution of AFGPs (Eastman, 1993), numerous previous studies have attempted to time-calibrate the origin of this radiation to test for possible correlations with cooling events recorded from geological data. Based on fossil occurrences in non-notothenioid outgroup lineages, Matschiner *et al.* (2011) estimated the radiation onset near the Oligocene–Miocene boundary (mean age estimate 23.9 Ma), coincident with the Mi-1 cold event (Naish *et al.*, 2001). The age estimates obtained by Matschiner *et al.* (2011) for the divergence of Bovichtidae, Pseudaphritidae, Eleginopsidae and the Antarctic clade were reused subsequently to time-calibrate the phylogenies of Rutschmann *et al.* (2011) and Near *et al.* (2012), which both used more extensive taxon coverage within Notothenioidei, but did not include non-notothenioid outgroups. As the latter two studies used age constraints on the age of the Antarctic clade, they arrived at mean age estimates very close to that of the applied constraint (24.2 and 22.4 Ma).

The phylogenetic hypotheses presented here (Fig. 1a) are based on inference methods that differ in various aspects from those applied in previous studies of the notothenioid diversification. We produced sets of time-calibrated phylogenies for three different data sets and twelve different model combinations, including – for the first time – the application of the multispecies coalescent model of *BEAST (Heled & Drummond, 2010) to a phylogeny of Notothenioidei. We find that age estimates for the adaptive radiation are strongly dependent on the applied data set and model combination and that for two of three data sets, the most parameter-rich models, which have the drawback of substantially longer convergence times and generally lower node support, provide the best fit according to AICM values (Tables S4–S7). Furthermore, we find over all data sets and model combinations a significant negative correlation between age estimates and model complexity measured in numbers of parameters (Fig. 1b).

Assuming that the BEAST analysis based on the combined marker set and the best-supported model combination (Fig. 1a) provides a realistic time line of notothenioid diversification, the onset of the notothenioid adaptive radiation occurred around 13.4 Ma (95% HPD: 17.1–10.0 Ma), which is substantially younger than a previous estimate by Matschiner *et al.* (2011). As our model comparison shows (Fig 1b), this difference can largely be attributed to different gene tree models, as Matschiner *et al.* (2011) used sequence concatenation and linked gene trees, whereas these remained unlinked in the best-supported model combination of the present study. Nevertheless, the contrasting time estimates of different studies highlight the importance of extensive model testing, including highly parameter-rich model combinations that can account for incomplete lineage sorting (Heled & Drummond, 2010).

If the present age estimates for the notothenioid radiation should be correct, its onset might have coincided with the Middle Miocene climatic transition (MMCT; 14.1–13.9 Ma), during which Southern Ocean sea surface temperatures declined by 6–7 °C (Shevenell *et al.*, 2004) and a full polar climate became established in Antarctica (Lewis *et al.*, 2008). This would support previous speculations that AFGPs evolved between 15 and 10 Ma (Eastman, 1993; Bargelloni *et al.*, 1994) and that the notothenioid radiation was triggered by ecological opportunity following the extinction of less cold-adapted teleost fishes and the availability of new habitats associated with sea ice (Eastman, 1993; Matschiner *et al.*, 2011).

Diversification rates over time in the notothenioid radiation

In agreement with earlier studies (Near *et al.*, 2012), diversification rate analyses with MEDUSA strongly supported a primary rate increase at or near the base of the Antarctic clade. Regardless of whether or not individual lineages, such as *Aethotaxis* and *Pleuragramma* diverged before this event, the observed rate shift supports the view that Antarctic notothenioids represent an adaptive radiation. By comparing time-interval-specific Kendall–Moran diversification rate estimates for an inferred notothenioid phylogeny with those found in simulated phylogenies of the same age and species richness, Near *et al.* (2012) found exceptionally high notothenioid diversification rates only at later stages of the radiation. Based on these results, the authors argued that the bulk of the notothenioid diversity originated long after initial divergences within the Antarctic clade. This disagrees with the notion of Antarctic notothenioids as a case of adaptive radiation, in which diversification is driven by available ecological niche space and speciation rates decrease as more and more niches are occupied. Using the same approach as Near *et al.* (2012), we obtained similar results when phylogenies of notothenioids, including Bovichtidae, Pseudaphritidae and Eleginopsidae, were compared to simulated phylogenies conditioned on the age and extant species richness of Notothenioidei, and resampled to match the number of taxa present in our taxon set. However, at least one positive rate shift event is consistently identified during the notothenioid diversification, at the base of the Antarctic clade (Near *et al.*, 2012; this study). Thus, a comparison with phylogenies simulated under homogeneous rate models is necessarily biased so that empirical rates in early time intervals appear low compared to rates in simulated trees and empirical rates subsequent to the shift appear high in comparison. Consequently, it may be more appropriate to account for the observed rate shift and directly compare empirical

phylogenies that are trimmed to include only taxa descending from the rate shift with phylogenies that are simulated correspondingly. When notothenioid phylogenies are reduced to include only the Antarctic clade, and simulated phylogenies are conditioned on the age and species richness of this clade (and subsequently resampled to match the number of taxa in our data set), a time interval-specific comparison yields no evidence of diversification bursts during the late Miocene (11.6–5.3 Ma) or Pliocene (5.3–2.6 Ma) (Fig. S7). However, notothenioid diversification rates in the Pleistocene still appear high in comparison, which may mostly be driven by the rapid radiation of Artedidraconidae within the Antarctic clade (see Near *et al.*, 2012). Our time calibration indicates a very young age of Artedidraconidae (mean: 1.2 Ma, 95% HPD: 2.2–0.6 Ma), which suggests that repeated habitat fragmentation during glacial cycles of the Pleistocene may have acted as a diversity pump (Clark & Crame, 2010) in this high Antarctic family. However, phylogeographic analyses based on a more extensive taxon sampling of the 30 known artedidraconids will be required to corroborate this hypothesis.

Disparity through time in Antarctic notothenioids

Our trait evolution simulations have shown that early bursts can be difficult to detect, especially when trait space is limited by hard or soft boundaries (Fig. 4). Harmon *et al.* (2010) noted that early bursts are rare in comparative data sets, including classic examples of adaptive radiation. The authors fitted BM, OU and early burst models of body size and shape evolution to phylogenies of 49 animal clades and found that the early burst model received higher support than BM and OU models for only two of these clades. Results from our simulations suggest that if trait evolution in several of these clades was shaped by a combination of early burst and constrained evolution, testing for the two processes separately could easily fail to detect the early burst. With existing methods, trait likelihoods cannot be calculated for a model combining an early burst with soft trait space boundaries; however, such a model could potentially provide a better description of trait evolution in adaptive radiations if these would continue to evolve even after boundaries have been reached. It remains to be tested whether or not this is a commonly occurring process in adaptive radiation.

Even though the pattern of early burst could rapidly be blurred by constrained evolution, we observe a strongly negative MDI value, and therefore a signal for early burst, in CV1 of our geometric morphometric body shape data (Fig. 5). Changes along CV1 affect mostly the shape and size of the snout. Long and pike-like snouts as well as shallower, more elongate bodies are associated with low CV1 values, and compressed and robust bodies and heads with very short snouts are characteristic for species with high CV1 values (Fig. 2). These differences could reflect different feeding behaviours. Additional to the apparent correlation between mouth size and the size of prey that can be taken (i.e. larger mouth gapes allow the consumption of bigger prey items; Boubée & Ward, 1997; Adams & Huntingford, 2002), large and wide snouts and shallower bodies proved to be beneficial when preying on rapidly swimming, elusive target species using ram feeding, whereas short and robust snouts and bodies are better suited for suction feeding on more varied immobile prey (Webb, 1984; Norton & Brainerd, 1993; Huskey & Turingan, 2001). Differences in feeding and foraging modes may help to avoid interspecific competition and might therefore facilitate coexistence of sympatric species (Labropoulou & Eleftheriou, 1997). The highest CV1 values, and thus the most compressed snouts, are found in Trematomini and Artedidraconidae, whereas low CV1 values and elongated snouts and bodies are present in Channichthyidae, Cygnodraconinae and *G. acuticeps*. According to stomach content analyses, the diet of the latter three groups is dominated by swimming prey such as fish, krill and mysids, whereas Trematomini and Artedidraconidae feed on a varied diet that includes slowly moving organisms such as polychaetes, ophiuroids and echinoderms (see Table S3 in Rutschmann *et al.*, 2011). As we observe little variance in CV1 values within individual notothenioid clades, we assume that diversification along CV1 may have driven the notothenioid radiation before the divergence of these clades. According to our time-calibrated phylogeny based on the best-supported model combination, this initial phase of diversification would have lasted from 13.4 Ma to about 9–7 Ma (Fig. 1a). Taken together, these findings point towards a scenario where early diversification along CV1 primarily led to two distinct groups according to (trophic) morphology: (i) one that today comprises Channichthyidae, Cygnodraconinae and *G. acuticeps*, characterized by large, elongated snouts used for ram feeding on elusive prey such as fish, krill and mysids and (ii) one comprising lineages leading to Trematomini and Artedidraconidae, characterized by short, robust snouts and heads used for suction feeding on largely immobile prey such as polychaetes, ophiuroids and echinoderms.

If diversification along CV1 is driven by morphological specializations related to trophic resource acquisition, it could be seen as the second stage of adaptive radiation, as envisioned by Streelman & Danley (2003). Alternatively, morphological changes along this axis could be regarded as α niche diversification that facilitates local-scale coexistence between closely related species in the model of adaptive radiation proposed by Ackerly *et al.* (2006). In their model, α niche specialization occurs primarily in the beginning of an adaptive radiation, whereas differentiation of the β-niche relating to macrohabitat continues throughout the radiation.

In agreement with this model, early diversification in trophic morphology has been suggested also in other prominent examples of adaptive radiation, including Neotropical (López-Fernández *et al.*, 2013) and African cichlid fishes (Muschick *et al.*, 2014). Among the five traits investigated by us, buoyancy and temperature regime could be regarded as β-niches, as diversification in both traits directly affects the habitat of notothenioids in the water column and their distribution range. Observed MDI values for buoyancy and temperature are close to zero (buoyancy; mean of tree sample: −0.016) or clearly positive (temperature; mean of tree sample: 1.456), indicating ongoing diversification along both of these axes. However, given that trait space for buoyancy values is limited by a hard lower boundary at 0 (assuming that obtaining negative buoyancy would require fundamentally different selection pressures that are not present in notothenioids), BM may not be the best model for the evolution of this trait. Similarly, trait space for notothenioid habitat temperatures is obviously limited by the freezing temperature of sea water. As our simulations have shown that similar DTT trajectories can result from both early bursts with bounded trait space and from unconstrained constant trait evolution (Fig. 4d,i), potential early bursts in either buoyancy or temperature regime would be difficult or impossible to detect with DTT trajectories and can therefore not be excluded in notothenioids.

Conclusion

Despite the difficulties associated with sampling in their remote environment, Antarctic notothenioid fishes are rapidly becoming a well-investigated model for an adaptive radiation in the marine realm. They have been shown to fulfil all criteria for adaptive radiations outlined by Schluter (2000), and one of the criteria, the correlation of phenotype and environment, has been demonstrated for at least two phenotypes, freeze protection and buoyancy adaptations. Whether or not other predictions of adaptive radiation theory, such as early bursts in diversity and disparity or evolution in stages, are supported by the notothenioid radiation has so far remained unclear. We here found evidence for a diversification rate increase at or near the origin of Antarctic notothenioids that may have coincided with the evolution of AFGPs. We also identified an early burst in trophic morphology of Antarctic notothenioids, a trait that is known to drive diversification in some of the most prominent adaptive radiations.

Methodologically, our extensive comparison of models for Bayesian phylogenetic inference has demonstrated how divergence time estimates of rapidly diversifying clades depend strongly on the choice of models and that time lines based on any single model should therefore be taken with caution. The fact that more parameter-rich models, and in particular models with unlinked gene trees, were generally better supported than simple models suggests that future phylogenetic investigations of notothenioids should include multiple individuals per species to allow more reliable estimation of coalescent parameters in the multispecies coalescent approach of *BEAST, which could also lead to further improvements in the estimation of the time line of the notothenioid radiation.

Acknowledgments

We thank K. Mintenbeck, L. Rath, N. Koschnick and T. Hirse, as well as R. Knust, L. Magnussen and the crews of RV Polarstern expeditions ANT-XXVII/3 and ANT-XXVIII/4, in 2011 and 2012 for help with sample collection. We are further thankful to K. Unger for help with sequencing, and J. Leigh, R. Bouckaert and G. Slater for guidance on Concaterpillar, BEAST and GEIGER analyses. Feedback from Axios Review and comments of R. Glor, T. Vines, C. Haag and three anonymous reviewers greatly helped to improve the manuscript. This study was supported by the Swiss National Science Foundation (Sinergia Grant CRSII3_136293 to WS and fellowship PBBSP3-138680 to MM) and the German Research Foundation (grant HA 4328/4 to RH).

References

Ackerly, D.D., Schwilk, D.W. & Webb, C.O. 2006. Niche evolution and adaptive radiation: testing the order of trait divergence. *Ecology* **87**: S50–S61.

Adams, C.E. & Huntingford, F.A. 2002. The functional significance of inherited differences in feeding morphology in a sympatric polymorphic population of Arctic charr. *Evol. Ecol.* **16**: 15–25.

Alfaro, M.E., Santini, F., Brock, C.D., Alamillo, H., Dornburg, A., Rabosky, D.L. *et al.* 2009. Nine exceptional radiations plus high turnover explain species diversity in jawed vertebrates. *Proc. Natl. Acad. Sci. USA* **106**: 13410–13414.

Balushkin, A.V. 2000. Morphology, classification, and evolution of Notothenioid fishes of the Southern Ocean (Notothenioidei, Perciformes). *J. Ichthyol.* **40**: S74–S109.

Bargelloni, L., Ritchie, P.A., Patarnello, T., Battaglia, B., Lambert, D.M. & Meyer, A. 1994. Molecular evolution at subzero temperatures: mitochondrial and nuclear phylogenies of fishes from Antarctica (suborder Notothenioidei), and the evolution of antifreeze glycopeptides. *Mol. Biol. Evol.* **11**: 854–863.

Bilyk, K.T. & DeVries, A.L. 2010. Freezing avoidance of the Antarctic icefishes (Channichthyidae) across thermal gradients in the Southern Ocean. *Polar Biol.* **33**: 203–213.

Boubée, J.A.T. & Ward, F.J. 1997. Mouth gape, food size, and diet of the common smelt *Retropinna retropinna* (Richardson) in the Waikato River system, North Island, New Zealand. *New Zeal. J. Mar. Freshwat. Res.* **31**: 147–154.

Bouckaert, R., Alvarado-Mora, M.V. & Rebello Pinho, J.R. 2013. Evolutionary rates and HBV: issues of rate estimation with Bayesian molecular methods. *Antivir. Ther.* **18**: 497–503.

Bouckaert, R., Heled, J., Kühnert, D., Vaughan, T.G., Wu, C.H., Xie, D. *et al.* 2014. BEAST 2: a software platform for Bayesian evolutionary analysis. *PLoS Comput. Biol.* **10**: e1003537.

Brawand, D., Wagner, C.E., Li, Y.I., Malinsky, M., Keller, I., Fan, S. *et al.* 2014. The genomic substrate for adaptive radiation in African cichlid fish. *Nature* **513**: 375–381.

Burbrink, F.T., Chen, X., Myers, E.A., Brandley, M.C. & Pyron, R.A. 2012. Evidence for determinism in species diversification and contingency in phenotypic evolution during adaptive radiation. *Proc. R. Soc. Lond. B Biol. Sci.* **279**: 4817–4826.

Butler, M.A. & King, A.A. 2004. Phylogenetic comparative analysis: a modeling approach for adaptive evolution. *Am. Nat.* **164**: 683–695.

Chen, L., DeVries, A.L. & Cheng, C.-H.C. 1997. Evolution of antifreeze glycoprotein gene from a trypsinogen gene in Antarctic notothenioid fish. *Proc. Natl. Acad. Sci. USA* **94**: 3811–3816.

Cheng, C.-H.C. & Detrich, H.W. III 2007. Molecular ecophysiology of Antarctic notothenioid fishes. *Philos. Trans. R. Soc. Lond. B Biol. Sci.* **362**: 2215–2232.

Cheng, C.-H.C., Chen, L., Near, T.J. & Jin, Y. 2003. Functional antifreeze glycoprotein genes in temperate-water New Zealand nototheniid fish infer an Antarctic evolutionary origin. *Mol. Biol. Evol.* **20**: 1897–1908.

Clark, A. & Crame, J.A. 2010. Evolutionary dynamics at high latitudes: speciation and extinction in polar marine faunas. *Philos. Trans. R. Soc. Lond. B Biol. Sci.* **365**: 3655–3666.

Derome, N., Chen, W.-J., Dettaï, A., Bonillo, C.É. & Lecointre, G. 2002. Phylogeny of Antarctic dragonfishes (Bathydraconidae, Notothenioidei, Teleostei) and related families based on their anatomy and two mitochondrial genes. *Mol. Phylogenet. Evol.* **24**: 139–152.

Dettai, A., Berkani, M., Lautrédou, A.-C., Couloux, A., Lecointre, G., Ozouf-Costaz, C. *et al.* 2012. Tracking the elusive monophyly of nototheniid fishes (Teleostei) with multiple mitochondrial and nuclear markers. *Mar. Genomics* **8**: 49–58.

Dornburg, A., Santini, F. & Alfaro, M. 2008. The influence of model averaging on clade posteriors: an example using the triggerfishes (family Balistidae). *Syst. Biol.* **57**: 905–919.

Drummond, A.J. & Bouckaert, R. 2014. *Bayesian Evolutionary Analysis with BEAST 2*. Cambridge University Press, Cambridge.

Eastman, J.T. 1993. *Antarctic Fish Biology: Evolution in a Unique Environment*. Academic Press Inc, San Diego, CA.

Eastman, J.T. 2000. Antarctic notothenioid fishes as subjects for research in evolutionary biology. *Antarct. Sci.* **12**: 276–287.

Eastman, J.T. 2005. The nature of the diversity of Antarctic fishes. *Polar Biol.* **28**: 93–107.

Eastman, J.T. & Eakin, R.R. 2000. An updated species list for notothenioid fish (Perciformes; Notothenioidei), with comments on Antarctic species. *Arch. Fish. Mar. Res.* **48**: 11–20.

Erwin, D.H. 1994. Early introduction of major morphological innovations. *Acta Palaeontol. Pol.* **38**: 281–294.

Felsenstein, J. 1985. Confidence limits on phylogenies: an approach using the bootstrap. *Evolution* **39**: 783–791.

Foote, M. 1997. The evolution of morphological diversity. *Annu. Rev. Ecol. Syst.* **28**: 129–152.

Foote, M. 1999. Morphological diversity in the evolutionary radiation of Paleozoic and post-Paleozoic crinoids. *Paleobiology* **25**: 1–115.

Froese, R. & Pauly, D. 2013. *FishBase*. World Wide Web electronic publication. www.fishbase.org, version (10/2013).

Gavrilets, S. 2004. *Fitness Landscapes and the Origin of Species*. Princeton University Press, Princeton, NJ.

Gavrilets, S. & Losos, J.B. 2009. Adaptive radiation: contrasting theory with data. *Science* **323**: 732–737.

Gavrilets, S. & Vose, A. 2005. Dynamic patterns of adaptive radiation. *Proc. Natl. Acad. Sci. USA* **102**: 18040–18045.

Gherardi, M., Mandrà, S., Bassetti, B. & Lagomarsino, M.C. 2013. Evidence for soft bounds in Ubuntu package sizes and mammalian body masses. *Proc. Natl. Acad. Sci. USA* **110**: 21054–21058.

Gillespie, R.G. 2004. Community assembly through adaptive radiation in Hawaiian spiders. *Science* **303**: 356–359.

Hansen, T.F. 1997. Stabilizing selection and the comparative analysis of adaptation. *Evolution* **51**: 1341–1351.

Harmon, L.J., Schulte, J.A. II, Larson, A. & Losos, J.B. 2003. Tempo and mode of evolutionary radiation in iguanian lizards. *Science* **301**: 961–964.

Harmon, L.J., Weir, J.T., Brock, C.D., Glor, R.E. & Challenger, W. 2008. GEIGER: investigating evolutionary radiations. *Bioinformatics* **24**: 129–131.

Harmon, L.J., Losos, J.B., Davies, T.J., Gillespie, R.G., Gittleman, J.L., Jennings, W.B. *et al.* 2010. Early bursts of body size and shape evolution are rare in comparative data. *Evolution* **64**: 2385–2396.

Heard, S.B. & Hauser, D.L. 1995. Key evolutionary innovations and their ecological mechanisms. *Hist. Biol.* **10**: 151–173.

Heled, J. & Bouckaert, R. 2013. Looking for trees in the forest: summary tree from posterior samples. *BMC Evol. Biol.* **13**: 221.

Heled, J. & Drummond, A.J. 2010. Bayesian inference of species trees from multilocus data. *Mol. Biol. Evol.* **27**: 570–580.

Huskey, S.H. & Turingan, R.G. 2001. Variation in prey-resource utilization and oral jaw gape between two populations of largemouth bass, *Micropterus salmoides*. *Environ. Biol. Fishes* **61**: 185–194.

Kaschner, K., Watson, R., Trites, A.W. & Pauly, D. 2006. Mapping world-wide distributions of marine mammal species using a relative environmental suitability (RES) model. *Mar. Ecol. Prog. Ser.* **316**: 285–310.

Kaschner, K., Rius-Barile, J., Kesner-Reyes, K., Garilao, C., Kullander, S.O., Rees, T. *et al.* 2013. AquaMaps: predicted range maps for aquatic species. World Wide Web electronic publication. www.aquamaps.org, version 08/2013.

Katoh, K. & Toh, H. 2008. Recent developments in the MAFFT multiple sequence alignment program. *Brief. Bioinform.* **9**: 286–298.

Kesner-Reyes, K., Kaschner, K., Kullander, S., Garilao, C., Barile, J. & Froese, R. 2012. AquaMaps: algorithm and data sources for aquatic organisms. In: *FishBase* (R. Froese & D. Pauly, eds), World Wide Web electronic publication. www.fishbase.org, version (04/2012).

Klingenberg, C.P. 2011. MorphoJ: an integrated software package for geometric morphometrics. *Mol. Ecol. Resour.* **11**: 353–357.

Klingenberg, C.P. & Ekau, W. 1996. A combined morphometric and phylogenetic analysis of an ecomorphological trend: pelagization in Antarctic fishes (Perciformes: Nototheniidae). *Biol. J. Linn. Soc.* **59**: 143–177.

Labropoulou, M. & Eleftheriou, A. 1997. The foraging ecology of two pairs of congeneric demersal fish species: importance of morphological characteristics in prey selection. *J. Fish Biol.* **50**: 324–340.

Lanfear, R., Calcott, B., Ho, S.Y.W. & Guindon, S. 2012. PartitionFinder: combined selection of partitioning schemes and substitution models for phylogenetic analyses. *Mol. Biol. Evol.* **29**: 1695–1701.

Lautrédou, A.-C., Hinsinger, D.D., Gallut, C., Cheng, C.-H.C., Berkani, M., Ozouf-Costaz, C. *et al.* 2012. Phylogenetic footprints of an Antarctic radiation: the Trematominae (Notothenioidei, Teleostei). *Mol. Phylogenet. Evol.* **65**: 87–101.

Leigh, J.W., Susko, E., Baumgartner, M. & Roger, A.J. 2008. Testing congruence in phylogenomic analysis. *Syst. Biol.* **57**: 104–115.

Lewis, A.R., Marchant, D.R., Ashworth, A.C., Hedenäs, L., Hemming, S.R., Johnson, J.V. *et al.* 2008. Mid-Miocene cooling and the extinction of tundra in continental Antarctica. *Proc. Natl. Acad. Sci. USA* **105**: 10676–10680.

Liu, L., Yu, L. & Edwards, S.V. 2010. A maximum pseudo-likelihood approach forestimating species trees under the coalescent. *BMC Evol. Biol.* **10**: 302.

López-Fernández, H., Arbour, J.H., Winemiller, K.O. & Honeycutt, R.L. 2013. Testing for ancient adaptive radiations in neotropical cichlid fishes. *Evolution* **67**: 1321–1337.

Losos, J.B. & Miles, D.B. 2002. Testing the hypothesis that a clade has adaptively radiated: iguanid lizard clades as a case study. *Am. Nat.* **160**: 147–157.

Maddison, W.P. & Maddison, D.W. 2009. Mesquite: a modular system for evolutionary analysis, Version 2.75, http://mesquiteproject.org.

Mahler, D.L., Revell, L.J., Glor, R.E. & Losos, J.B. 2010. Ecological opportunity and the rate of morphological evolution in the diversification of Greater Antillean anoles. *Evolution* **64**: 2731–2745.

Matschiner, M., Hanel, R. & Salzburger, W. 2011. On the origin and trigger of the notothenioid adaptive radiation. *PLoS One* **6**: e18911.

Muschick, M., Nosil, P., Roesti, M., Dittmann, M.T., Harmon, L. & Salzburger, W. 2014. Testing the stages model in the adaptive radiation of cichlid fishes in East African Lake Tanganyika. *Proc. R. Soc. Lond. B Biol. Sci.* **281**: 20140605.

Naish, T.R., Woolfe, K.J., Barrett, P.J., Wilson, G.S., Atkins, C., Bohaty, S.M. *et al.* 2001. Orbitally induced oscillations in the East Antarctic ice sheet at the Oligocene/Miocene boundary. *Nature* **413**: 719–723.

Near, T.J. 2004. Estimating divergence times of notothenioid fishes using a fossil-calibrated molecular clock. *Antarct. Sci.* **16**: 37–44.

Near, T.J. & Cheng, C.-H.C. 2008. Phylogenetics of notothenioid fishes (Teleostei: Acanthomorpha): Inferences from mitochondrial and nuclear gene sequences. *Mol. Phylogenet. Evol.* **47**: 832–840.

Near, T.J., Dornburg, A., Kuhn, K.L., Eastman, J.T., Pennington, J.N. & Patarnello, T. 2012. Ancient climate change, antifreeze, and the evolutionary diversification of Antarctic fishes. *Proc. Natl. Acad. Sci. USA* **109**: 3434–3439.

Norton, S.F. & Brainerd, E.L. 1993. Convergence in the feeding mechanics of ecomorphologically similar species in the Centrarchidae and Cichlidae. *J. Exp. Biol.* **176**: 11–29.

Rabosky, D.L. & Glor, R.E. 2010. Equilibrium speciation dynamics in a model adaptive radiation of island lizards. *Proc. Natl. Acad. Sci. USA* **107**: 22178–22183.

Rabosky, D.L. & Lovette, I.J. 2008. Density-dependent diversification in North American wood warblers. *Proc. R. Soc. Lond. B Biol. Sci.* **275**: 2363–2371.

Raftery, A., Newton, M., Satagopan, J. & Krivitsky, P. 2007. Estimating the integrated likelihood via posterior simulation using the harmonic mean identity. In: *Bayesian Statistics* (J.M. Bernardo, M.J. Bayarri, J.O. Berger, eds), pp. 1–45. Oxford University Press, Oxford.

Rambaut, A. & Drummond, A.J. 2007. Tracer v.1.5. http://beast.bio.ed.ac.uk/Tracer.

Ratnasingham, S. & Hebert, P.D.N. 2007. BOLD: the barcode of life data system (www.barcodinglife.org). *Mol. Ecol. Notes* **7**: 355–364.

Ready, J., Kaschner, K., South, A.B., Eastwood, P.D., Rees, T., Rius, J. *et al.* 2010. Predicting the distributions of marine organisms at the global scale. *Ecol. Model.* **221**: 467–478.

Revell, L.J. 2011. phytools: an R package for phylogenetic comparative biology (and other things). *Methods Ecol. Evol.* **3**: 217–223.

Richman, A.D. 1996. Ecological diversification and community structure in the Old World leaf warblers (genus *Phylloscopus*): a phylogenetic perspective. *Evolution* **50**: 2461–2470.

Rohlf, F.J. 2013. *tpsDig Version 2.17. Department of Ecology and Evolution*. State University of New York at Stony Brook, New York.

Rutschmann, S., Matschiner, M., Damerau, M., Muschick, M., Lehmann, M., Hanel, R. *et al.* 2011. Parallel ecological diversification in Antarctic notothenioid fishes as evidence for adaptive radiation. *Mol. Ecol.* **20**: 4707–4721.

Schluter, D. 2000. *The Ecology of Adaptive Radiation*. Oxford University Press, New York.

Seehausen, O. 2006. African cichlid fish: a model system in adaptive radiation research. *Proc. R. Soc. Lond. B Biol. Sci.* **273**: 1987–1998.

Shevenell, A.E., Kennett, J.P. & Lea, D.W. 2004. Middle Miocene Southern Ocean cooling and Antarctic cryosphere expansion. *Science* **305**: 1766–1770.

Simpson, G.G. 1953. *The Major Features of Evolution*. Columbia University Press, New York.

Slater, G.J. & Pennell, M.W. 2014. Robust regression and posterior predictive simulation increase power to detect early bursts of trait evolution. *Syst. Biol.* **63**: 293–308.

Slater, G.J., Price, S.A., Santini, F. & Alfaro, M.E. 2010. Diversity versus disparity and the radiation of modern cetaceans. *Proc. R. Soc. Lond. B Biol. Sci.* **277**: 3097–3104.

Stamatakis, A. 2006. RAxML-VI-HPC: maximum likelihood-based phylogenetic analyses with thousands of taxa and mixed models. *Bioinformatics* **22**: 2688–2690.

Streelman, J.T. & Danley, P.D. 2003. The stages of vertebrate evolutionary radiation. *Trends Ecol. Evol.* **18**: 126–131.

Webb, P. 1984. Body and fin form and strike tactics of four teleost predators attacking fathead minnow (*Pimephales promelas*) prey. *Can. J. Fish Aquat. Sci.* **41**: 157–165.

Wilson, L.A.B., Colombo, M., Hanel, R., Salzburger, W. & Sánchez-Villagra, R. 2013. Ecomorphological disparity in an adaptive radiation: opercular bone shape and stable isotopes in Antarctic icefishes. *Ecol. Evol.* **3**: 3166–3182.

Yoder, J.B., Clancey, E., Des Roches, S., Eastman, J.M., Gentry, L., Godsoe, W. *et al.* 2010. Ecological opportunity and the origin of adaptive radiations. *J. Evol. Biol.*, **23**: 1581–1596.

Yu, W., Wu, Y. & Yang, G. 2014. Early diversification trend and Asian origin for extent bat lineages. *J. Evol. Biol.* **10**: 2204–2218.

Supporting information

Additional Supporting Information may be found in the online version of this article:

Text S1 Partitioning of molecular markers.
Text S2 Species tree reconstruction.
Text S3 Kendall-Moran estimates of diversication in simulated phylogenies.
Text S4 The semi-diversied sampling scheme.
Figure S1 Landmarks used for geometric morphometric analyses.
Figure S2 Habitat parameters extracted from the AquaMaps database.
Figure S3 Maximum likelihood phylogenies for mitochondrial and nuclear markers.
Figure S4 10% majority-rule consensus tree of MP-EST species trees.
Figure S5 BEAST reanalysis of the MP-EST species tree topology.
Figure S6 Lineages through time.
Figure S7 Kendall-Moran estimates of diversification rates in five time intervals.
Figure S8 MCC tree with node numbers.
Table S1 Gene information for sequence markers.
Table S2 Sequence accession numbers.
Table S3 Mean values for notothenioid characteristics.
Table S4 Model combinations used in BEAST analyses.
Table S5 Model support and tree characteristics for BEAST analyses of the combined marker set.
Table S6 Model support and tree characteristics for BEAST analyses of the mitochondrial marker set.
Table S7 Model support and tree characteristics for BEAST analyses of the nuclear marker set.
Table S8 Species richness used for diversification rate analysis with MEDUSA.
Table S9 Sea surface temperatures of notothenioid habitats.
Table S10 Support values and ages estimates for nodes of the MCC tree.

Data deposited at Dryad: doi:10.5061/dryad.5jt5j/1

Received 23 October 2014; revised 3 December 2014; accepted 8 December 2014

2.2.2
Supporting information

1 Supplementary Text

Supplementary Text 1: Partitioning of molecular markers.
We used the software Concaterpillar v.1.7.2 (Leigh *et al.* 2008) to test for discordant evolutionary histories of the markers included in our data set. Here, and for all other phylogenetic analyses, the four mitochondrial alignments were concatenated and considered as a single marker. The Concaterpillar analysis was performed with default settings and assuming a GTR model of evolution, the only model of nucleotide substitutions available in the software. For tree inference, Concaterpillar was set up to use RAxML v.7.2.8 (Stamatakis 2006).

We found no significant discordance among nuclear markers. However, different evolutionary histories were detected for the concatenated nuclear alignment and the combined mitochondrial marker set (likelihood ratio test based on non-parametric bootstrapping; P ¡ 0.001). For the two sets of concordant markers, and for all individual markers, we conducted separate analyses with the software PartitionFinder v.1.1.1 (Lanfear *et al.* 2012) in order to determine the best-fitting partitioning schemes according to the Bayesian Information Criterion (BIC). In each analysis, primary data blocks were defined within marker sets according to gene and codon position. We used PartitionFinders greedy algorithm and assumed unlinked branch lengths for individual partitions. In separate analyses, we allowed PartitionFinder to test all substitution models available in BEAST, or the HKY+Gamma model only.

Regardless of whether all substitution models available in BEAST, or only the HKY+Gamma model was tested, PartitionFinder always identified two partitions in both the concatenated mitochondrial marker set and the combined nuclear marker set, where the first partition always grouped all first and second codon positions, and the second partition included third codon positions and, for the nuclear marker set, the intronic marker s7. In all analyses of individual nuclear markers, however, PartitionFinder identified only a single partition combining all codon positions.

Thus, all BEAST analyses (see Supplementary Text 2) with linked gene trees were performed with four partitions: mtdna_cp12 for the first two codon positions of mitochondrial markers (2272 bp), mtdna_cp3 for the third codon position of mitochondrial markers (1136 bp), nuclear_cp12 for the first and second codon position of all nuclear markers (2912 bp), and nuclear_cp3 for the third position of nuclear markers as well as s7 (1964 bp). In these analyses, parameters of substitution and clock models were unlinked among partitions. For BEAST analyses with unlinked gene trees (i.e. the *BEAST approach), we allowed individual gene trees for each nuclear marker, and defined a single partition per nuclear marker, as suggested by the results of our PartitionFinder analyses. Thus, we used nine partitions for BEAST analyses with unlinked gene trees: mtdna_cp12 and mtdna_cp3 as above, plus myh6 (705 bp), PTCHD4 (702 bp), enc1 (801 bp), tbr1b (618 bp), rps7 (508 bp), zic1 (837 bp), and snx33 (705 bp).

Supplementary Text 2: Species tree reconstruction.
Bayesian species tree reconstructions were performed with BEAST v.2.1 (Bouckaert *et al.* 2014) under a wide range of models and with both linked and unlinked (i.e. the multi- species coalescent model of *BEAST; Heled & Drummond 2010) gene trees for individual markers. Within each

marker, clock and substitution models remained unlinked for partitions identified by PartitionFinder, a practice that has been shown to improve Bayesian phylogenetic inference (Ho & Lanfear 2010). All analyses used the birth-death tree model (Gernhard 2008) and the same user-specified starting tree based on the phylogeny of Near *et al.* (2012), but we tested both the strict molecular clock and the uncorrelated lognormal (UCLN) relaxed molecular clock (Drummond *et al.* 2006) in separate analyses. Further, two different substitution models were assumed for all partitions: the HKY model (Hasegawa *et al.* 1985), as well as the reversible-jump based (RB) substitution model implemented in the RB add-on for BEAST 2 (Bouckaert *et al.* 2013; Drummond & Bouckaert 2014). Both substitution models were used in combination with a gamma distribution of among-site rate variation. Finally, base frequencies were either empirically determined or estimated in separate analyses.

Due to the lack of a reliable notothenioid fossil record (see Eastman & Grande 1991, Balushkin 1994), clock models were calibrated using three secondary divergence age constraints: Following Rutschmann *et al.* (2011) and Near *et al.* (2012), we applied normal prior distributions to the age of the separation of Bovichtidae (mean: 71.4 million years ago (Ma), standard deviation: 9.0 million years (myr)), Pseudaphritidae (mean: 63.0 Ma, standard deviation: 8.4 myr), and Eleginopsidae (mean: 42.9 Ma, standard deviation: 6.9 myr), based on the higher-level phylogeny of Matschiner *et al.* (2011) that was calibrated with 10 non-notothenioid fossil and biogeographic constraints. Contrary to Rutschmann *et al.* (2011) and Near *et al.* (2012), we chose not to constrain the age of the initial divergence of the Antarctic clade, as we expected that the multi-species coalescent model of *BEAST may detect previously unrecognized incomplete lineage sorting in the early phase of the Antarctic diversification, and may thus support younger species tree divergences compared to the concatenated analyses of Matschiner *et al.* (2011), Rutschmann *et al.* (2011), and Near *et al.* (2012).

Support for each model combination was assessed a posteriori using the Akaike Information Criterion through Markov Chain Monte Carlo (AICM) analysis (Raftery *et al.* 2007) which has been shown to perform favourably compared to marginal likelihoods obtained with the harmonic mean estimator (Baele *et al.* 2012). AICM values were estimated from posterior likelihood distributions with BEAST v.1.8 (Drummond *et al.* 2012), as this option is not implemented in BEAST v.2.1. All model combinations used for the BEAST analyses, together with the resulting AICM values are listed in Supplementary Tables 4-7. For each model combination, between three and nine replicate analyses with a total of 0.3 billion (when gene trees were linked) or 1.5-18 billion (when gene trees were unlinked) MCMC generations were performed, and run convergence was evaluated with effective sample sizes (ESS) and by visual inspection of MCMC traces within and between run replicates, using Tracer v.1.5 (Rambaut & Drummond 2007).

Supplementary Text 3: Kendall-Moran estimates of diversification in simulated phylogenies.
Kendall-Moran estimates (Dornburg *et al.* 2008; Near *et al.* 2012) for five time intervals of the Late Miocene (Tortonian, 11.6-7.2 Ma, and Messinian, 7.2-5.3 Ma), Pliocene (Zanclean, 5.3-3.6 Ma, and Piacenzian, 3.6-2.6 Ma), and Pleistocene (2.6-0 Ma) were calculated for notothenioid phylogenies and compared to null distributions obtained from phylogenies simulated with homogeneous diver-

sification rates. Using a pure-birth (Yule) model, we simulated 1000 phylogenies with the same age, and conditioned on the same extant species richness of (i) the Antarctic clade, or (ii) all Notothenioidei. In both cases, distributions of simulated root ages directly reflected ages of these two groups in the posterior sample of 1000 trees resulting from the BEAST analysis with the combined data set and the best-supported model combination. Simulations were performed with speciation rates λ drawn from wide uniform distribution between (i) 0.1 and 0.45 per myr, or (ii) between 0.02 and 0.2 per myr, and only those trees were retained that resulted in exactly (i) 123 or (ii) 134 extant species. In both cases, simulations were repeated until a total of 1000 phylogenies were found fulfilling these criteria. In order to account for unobserved extinction, we also repreated all simulations with a birth-death model, using a fixed extinction rate μ of 0.2 per myr, and correspondingly higher speciation rates λ between (i) 0.3 and 0.65 per myr, or (ii) 0.22 and 0.4 per myr, to result in the same net diversification rates as in the above Yule models.

All simulated phylogenies were subsequently sampled to match the number of representatives of (i) the Antarctic clade (45 species), or (ii) all Notothenioidei (49 species) included in our data set. For each phylogeny, this was performed according to two different sampling schemes: a random sampling scheme and a previously undescribed sampling scheme that tends to retain more older nodes than strictly random sampling. The incentives behind this sampling scheme are similar to those of the "diversified sampling" scheme of Höhna *et al.* (2011), which choses tips of a phylogeny so that diversity is maximized, and as a result samples all nodes in a phylogeny between its root and the time point at which the number of lineages matches that of sampled tips. Höhna *et al.* (2011) found this sampling scheme to provide a better fit to most phylogenies, as systematists usually attempt to include early-diverging lineages in their taxon sets (Cusimano & Renner 2010). However, at the stage at which systematists compile their taxon sets, the relative ages of lineages may be poorly known, or older lineages may be rare and difficult to sample. Thus, most empirical phylogenies may be more bottom-heavy than randomly sampled phylogenies, but not as bottom-heavy as phylogenies sampled according to the diversified sampling scheme.

Our notothenioid phylogeny is likely to fit this pattern. Like previous authors (Matschiner *et al.* 2011; Rutschmann *et al.* 2011; Near *et al.* 2012), we deliberately departed from a random sampling scheme by including representatives of all major lineages, even if their extant diversity is low, as is the case of Eleginopidae and Pseudaphritidae. However, not all of the oldest lineages could be sampled, as for example samples of *Halaphritis* and *Gvozdarus* could not be obtained. Thus, our empirical taxon sampling is intermediate between random and strictly diversified sampling of Notothenioidei, and as a consequence, an intermediate "semi-diversified" sampling scheme is likely to provide the best fit to our phylogeny. While not exploring the mathematical properties of this semi-diversified sampling scheme in detail (as done by Höhna *et al.*, 2011, for the diversified sampling scheme), we describe an algorithm to apply this scheme in Supplementary Text 4.

For all empirical and simulated phylogenies, we calculated Kendall-Moran estimates of diversification rates in each of the five time intervals using $b = (n - m)/B$, where n and m are the number of species extant at the beginning and end of the time interval, and B is the sum of all branch lengths within this interval (Becerra 2005). Densities of interval-specific diversification rate estimates in empirical and simulated phylogenies, as well as point estimates for the MCC tree and the

tree resulting from rerunning the best-supported model in BEAST with the topological constraint of the MP-EST species tree, are shown in Supplementary Figure 7.

Supplementary Text 4: The semi-diversified sampling scheme.
Let n be the number of extant species, m be the number of sampled extant species, and t_{root} the root age of a reconstructed tree. Then the number of sampled nodes is $m-1$, and if the tree was fully sampled ($m=n$), it would be $n-1$. In the diversified sampling scheme of Höhna *et al.* (2011), m species are sampled to maximize phylogenetic diversity, so that precisely the oldest $m-1$ nodes are present in the sampled tree. Thus, in this model, the probability p that a node is included in the sampled tree is 1 for the $m-1$ oldest nodes, and 0 for the $n-m$ younger nodes. However, for reasons explained in Supplementary Text 3, it is common that in empirical phylogenies, the realized sampling differs from the diversified sampling scheme so that some of the oldest $m-1$ nodes are missing, but some of the youngest $n-m$ nodes are present in the sampled tree. Among the oldest $m-1$ nodes, the younger ones are more likely to be missing, whereas among the youngest $n-m$ nodes, the older ones are more likely to be included. The probability that nodes are included in the sampled tree may thus be assumed to increase continuously with node age. Furthermore, the sampling probability of nodes with age $t_{node}=0$ is 0, and for simplicity, we may assume that nodes with age t_{root} (the root only) are sampled with probability 1.

Thus, we here define the semi-diversified sampling scheme so that nodes are selected at random with uniform probability, and once selected, they are chosen to be sampled with acceptance probability $p_a(t)=\frac{t_{node}}{t_{root}}$. If a node is chosen to be sampled, one extant species is sampled randomly from the extant descendents of both sides of this node, so that the selected node necessarily appears in the sampled tree. This process is repeated until m extant taxa have been sampled. If a selected node is already present in the sampled tree (i.e. both of its descendent lineages are already represented in the list of sampled species), a new node is selected at random. In this model, the root node is sampled with probability $p_a=1$ once it is selected, and it is automatically included in the sampled tree if the next-oldest nodes in both of its descendent lineages are sampled. However, this still leaves a small probability that it is not sampled in the case that it has not been selected before m extant species are sampled and if the next-oldest nodes in at least one of its descendent lineages is not sampled. Thus, for convenience, we may want to ensure that the root is included in the sampled tree. We can do this by sampling at random one extant species from each side of the root as the very first step of this process (if $m>1$).

The effective sampling probability $p_s(t)$ that a node of age t is present in the sampled tree is different from the acceptance probability $p_a(t)$ for several reasons: First, the process is repeated multiple times until m extant species are sampled, so that nodes that were not sampled previously, can be selected again, and are then again sampled with probability $p_a(t)$. Second, even nodes that are not sampled directly can be included in the sampled tree if the next-oldest nodes in both of their descendent lineages are sampled. This will lead to an increase of the effective sampling probability in older nodes (only if $m>2$). The effective sampling probability thus depends on the probability that a node is selected (however, this probability is here assumed uniform), on the acceptance probability $p_a(t)$ that a node is sampled once it is selected, and on the probability that the next-oldest nodes in

both descending lineages are chosen. The effective sampling probability further depends on m and n, because the process is repeated until m extant species are sampled. Thus, the effective sampling probability of a single node is also influenced by the probabilities of all other nodes, because if the other nodes' probabilities are low, the process will have to be repeated more often before m extant species are sampled. This means that a node's effective sampling probability is dependent not only on its own age, but also on the ages of all other nodes, and thus on the node age density. In a reconstructed continuous-rate birth-death process, conditioned on root age t_{root} and extant number of species n, this density is known from Gernhard (2008) and depends on speciation rate λ and extinction rate μ. Thus, calculation of the effective sampling probability may in principle be possible, but is not required in order to apply the semi-diversified sampling scheme, as long as we know that $p_s(t)$ has the desirable properties of, (i) $p_s(t_{root}) = 1$, (ii) $\int_0^{t_{root}} p_s(t) = m$, and (iii) continuous increase with t for $0 \leq t < t_{root}$. Properties i and ii are guaranteed, as (i) descendents from both sides of the root are sampled as a first step, and (ii) nodes can be sampled at most once, but the process is repeated until exactly m extant species are sampled. Without a proof, property iii is also assumed to be fulfilled, as $p_a(t)$ is continuously increasing with t for $0 \leq t < t_{root}$ and older nodes tend to have older descendants, which in turn increases the probability that these are accepted for sampling.

2 Supplementary Figures

Supplementary Figure 1: Landmarks used for geometric morphometric analyses.
Eighteen landmark points were chosen to quantify notothenioid body shape variation. Landmark points 1-17 are homologous to those used in Muschick *et al.* (2012, Figure S5).

Supplementary Figure 2: Habitat parameters extracted from the AquaMaps database.
For each species, black dots indicate means of observed trait values, and gray bars represent parameter range.

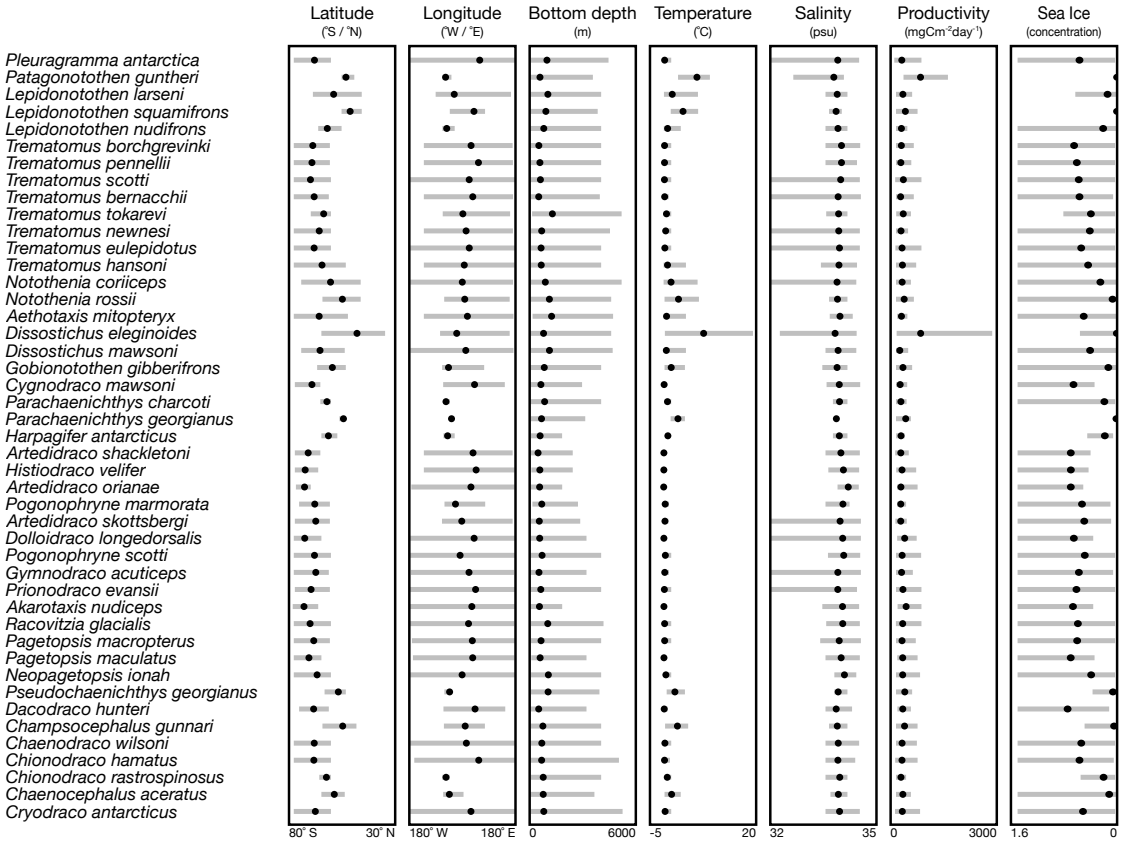

Supplementary Figure 3: Maximum likelihood phylogenies for mitochondrial and nuclear markers.

Phylogenies produced with RAxML for the two sets of concordant markers identified with Concaterpillar. The maximum likelihood tree for the concatenated mitochondrial marker set is shown at left, the tree based on concatenated nuclear markers is at right.

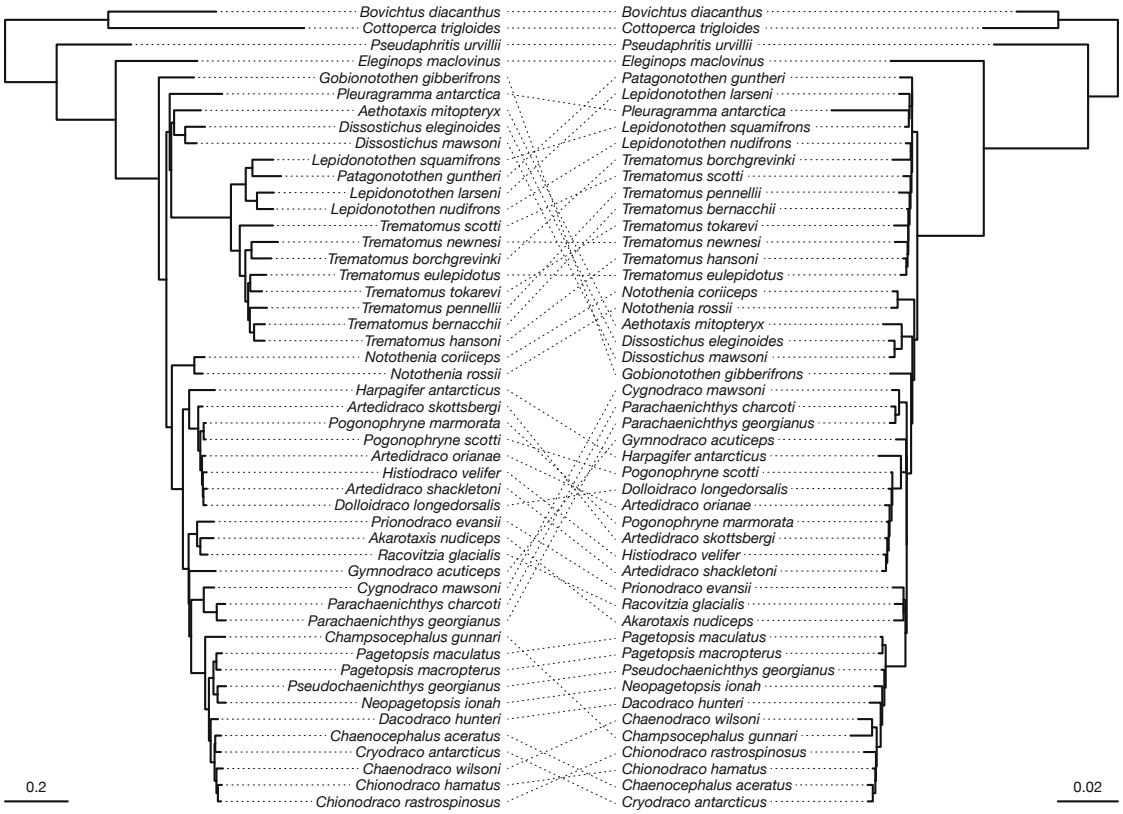

Supplementary Figure 4: 10% majority-rule consensus tree of MP-EST species trees.
Node labels indicate the number of bootstrap replicate MP-EST species trees supporting this node.

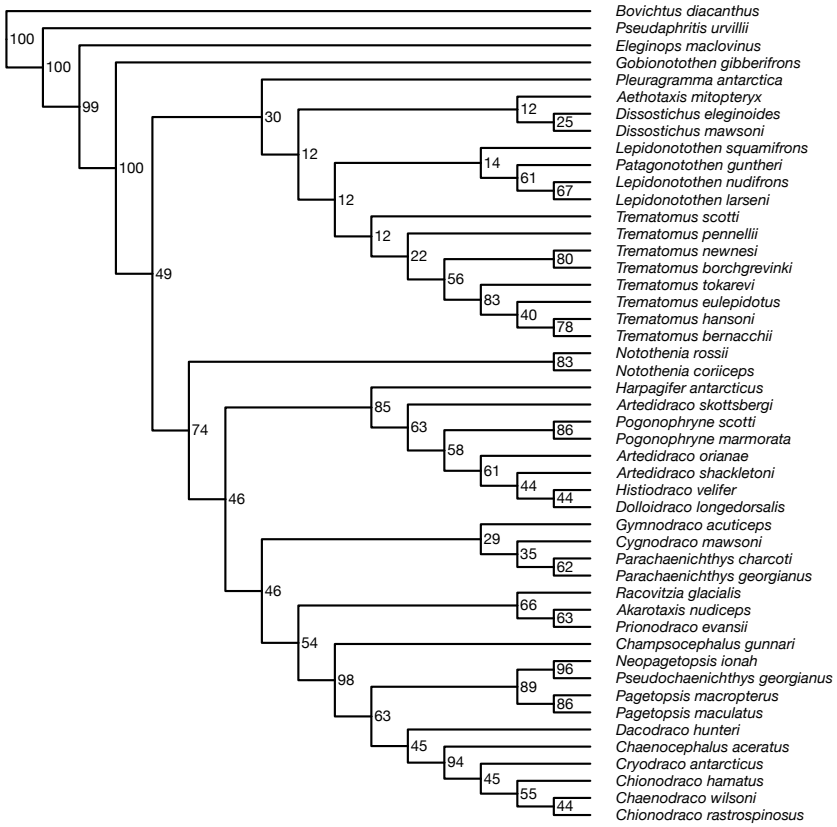

Supplementary Figure 5: BEAST reanalysis of the MP-EST species tree topology.
A) Phylogeny resulting from rerunning the BEAST analysis with the best-supported model combination, constrained to the topology of the MP-EST species tree (see Supplementary Figure 4). B) Comparison of posterior distributions resulting from the topologically unconstrained and constrained BEAST analyses of the combined data set, with the best-supported model combination according to AICM (models 12 and 12* in Supplementary Table 5).

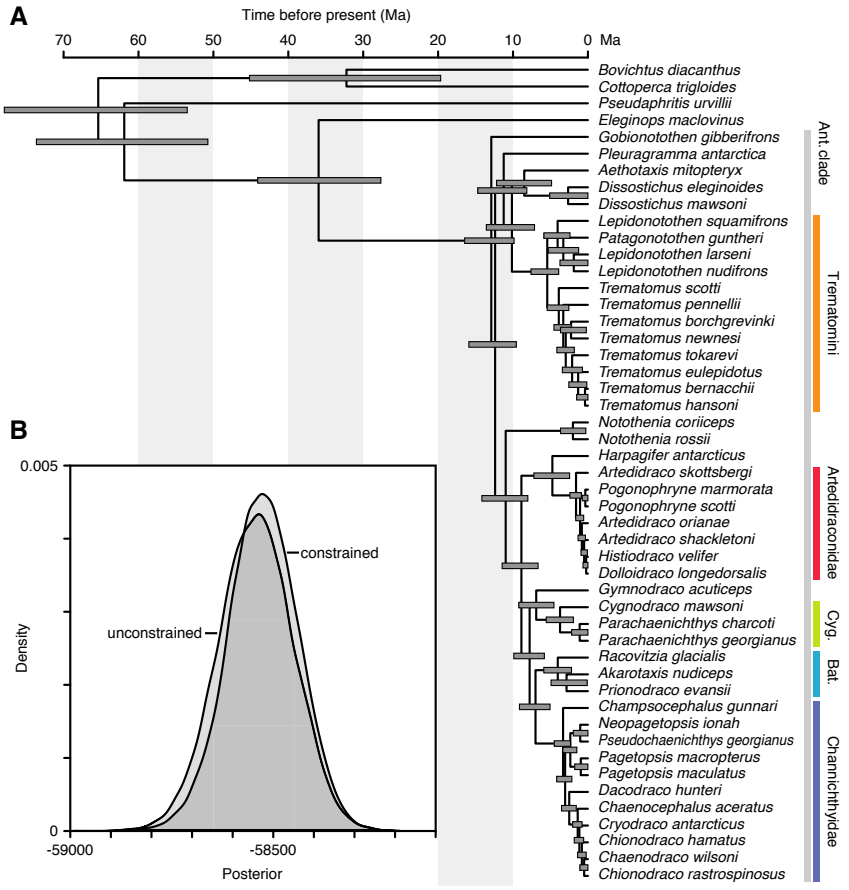

Supplementary Figure 6: Lineages through time.
Accumulation of lineages over time in time-calibrated phylogenies resulting from the BEAST analysis with the best-supported model combination. Gray lines represent number of lineages in 1000 posterior trees, the orange line shows the number of lineages in the MCC tree resulting from the same analysis. The blue line is based on mean age estimates of the BEAST analysis using the topological constraint of the MP-EST species tree.

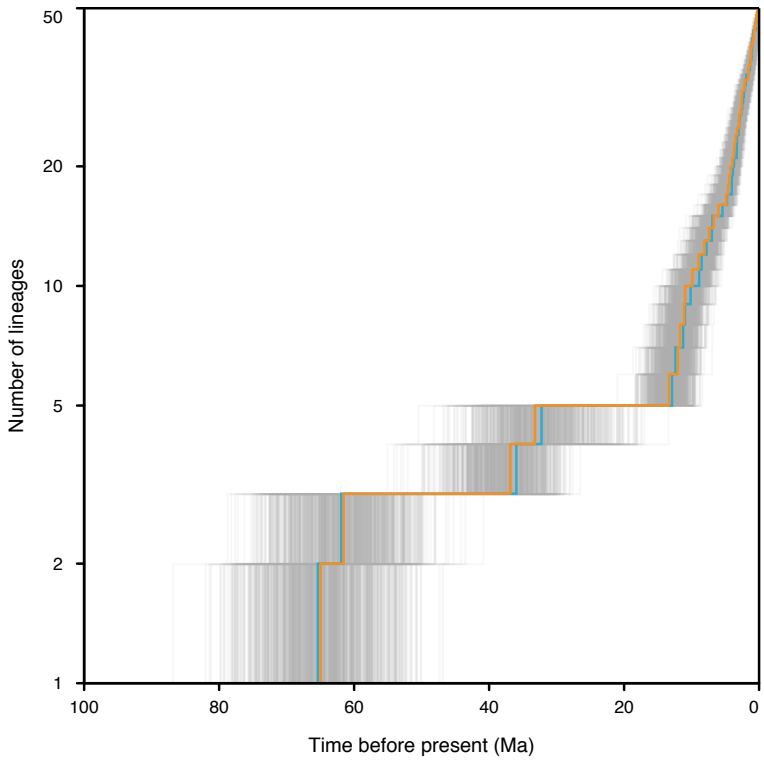

Supplementary Figure 7: Kendall-Moran estimates of diversification rates in five time intervals. Density distributions of Kendall-Moran diversification rate estimates in the posterior sample of 1000 trees resulting from the BEAST analysis of the combined data set and with the best-supported model combination (dashed line), mean values of these distributions (vertical black line), and rate estimates for the MCC tree (orange line) and the reanalysed MP-EST tree (blue line). The density distributions of simulated phylogenies, sampled with random sampling and the semi-diversified sampling scheme (see Supplementary Text 4), are shown as light gray shapes and dark gray lines, respectively. In A)-E) and K)-O), empirical phylogenies were trimmed to include only representatives of the Antarctic clade, and simulated phylogenies were conditioned on the age and species richness of this clade. In F)-J) and P)-T), the full empirical phylogenies were used, and simulated phylogenies were conditioned accordingly. A)-J) and K)-T) differ regarding the model used for simulated phylogenies (Yule or birth-death), but densities of diversification rates of empirical phylogenies are identical between these two sets. Orange, blue, and black asterisks indicate that rate estimates for the MCC tree, the reanalysed MP-EST tree, or mean rate estimates for the sample of 1000 trees, respectively, are larger than the 95% (*), 99% (**), or 99.9% (***) quantile of rates found in simulated phylogenies, after application of semi-diversified sampling.

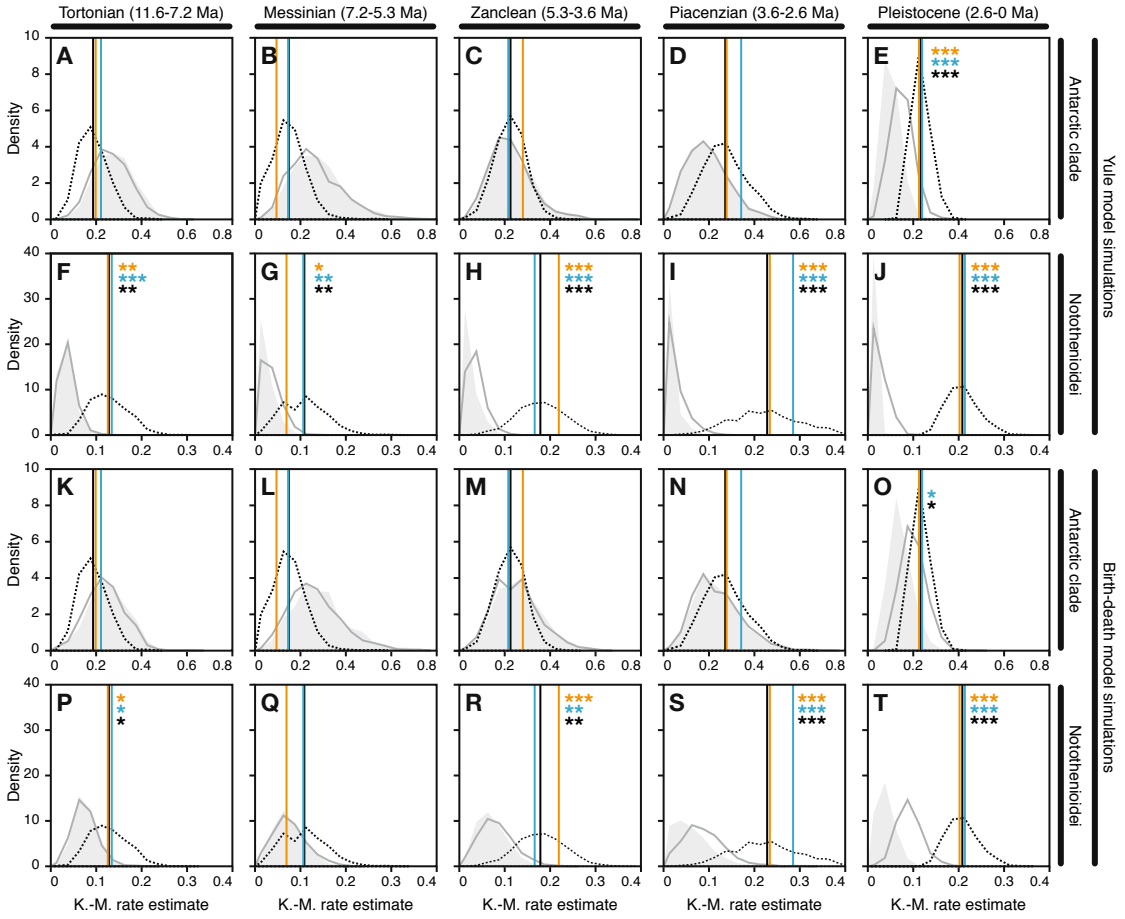

Supplementary Figure 8: MCC tree with node numbers.
The phylogeny is identical to the tree shown in Fig. 1, but with labels indicating node numbers. See Supplementary Table 10 for BPP values and age estimates for each node.

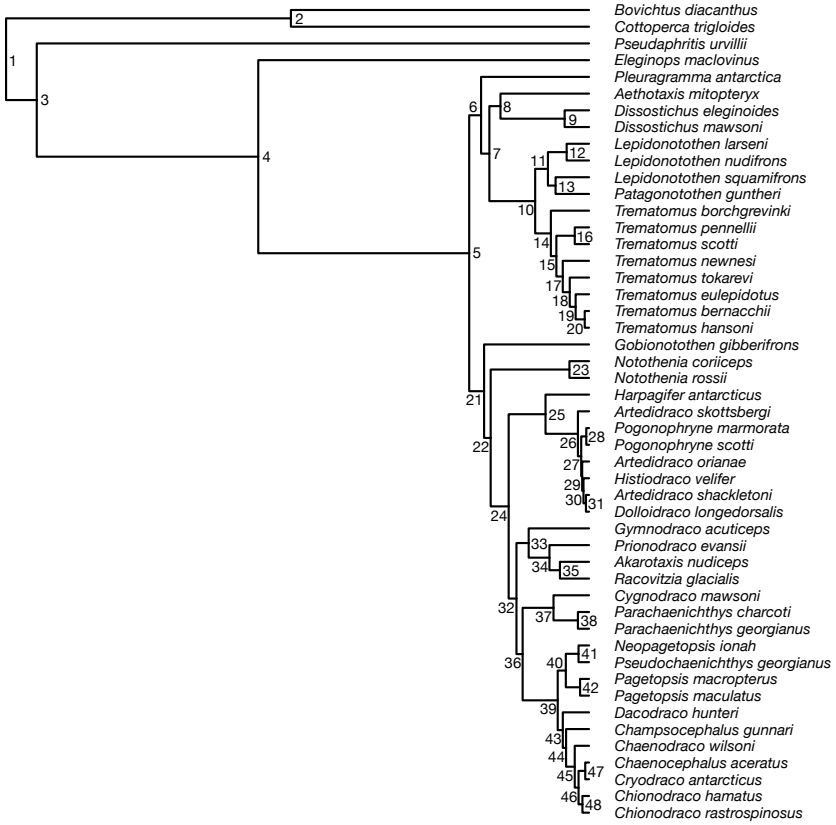

3 Supplementary Tables

Supplementary Table 1: Gene information for sequence markers.
Symbol and name refer to the official gene symbol and name in zebrafish, as listed in the ZFIN database (Sprague *et al.* 2006). Synonyms are given as used in the reference. The location column specifies the location of the marker sequence within this gene, and length refers to the length of each marker's sequence alignment. See references for primer information.

Symbol	Name	Synonym	Location	Length	Reference
mt-co1	cytochrome c oxidase I, mitochondrial	COI	Exon 1	651 bp	Ratnasingham & Hebert (2007)
mt-cyb	cytochrome b, mitochondrial	cyt b	Exon 1	1080 bp	Matschiner *et al.* (2011)
mt-nd2	NADH dehydrogenase 2, mitochondrial	nd2	Exon 1	1044 bp	Near *et al.* (2012)
mt-nd4	NADH dehydrogenase 4, mitochondrial	nd4	Exon 1	633 bp	Matschiner *et al.* (2011)
enc1	ectodermal-neural cortex 1	ENC1	Exon 3	801 bp	Li *et al.* (2007)
myh6	myosin, heavy polypeptide 6, cardiac muscle, alpha	-	Exon 1	705 bp	Li *et al.* (2007)
PTCHD4	patched domain containing 4	Ptr	Exon 3	702 bp	Li *et al.* (2007)
rps7	ribosomal protein S7	S7	Intron 1	508 bp	Chow & Hazama (1998)
snx33	sorting nexin 33	SH3PX3	Exon 1	705 bp	Li *et al.* (2007)
tbr1b	T-box, brain, 1b	tbr1	Exon 6	618 bp	Li *et al.* (2007)
zic1	zic family member 1 (odd-paired homolog, Drosophila)	-	Exon 1	837 bp	Li *et al.* (2007)

Supplementary Table 2: Sequence accession numbers.
Sequences marked with * were produced for this study, those marked with † were taken from BOLD, all other sequences are from Genbank.
See separate file.

Supplementary Table 3 (next page): Mean values for notothenioid characteristics.
Per species, sample size and the mean values for the first two canonical variates of body shape, as well as body size (in cm), buoyancy and sea surface temperature (in °C) are listed. For body size, we used maximum terminal lengths (TL) reported by Gon & Heemstra (1990). For species, for which maximum lengths were given as standard lengths (SL) in Gon & Heemstra (1990), we transformed these values to TL based on per-species mean TL/SL ratios empirically determined from specimens included in our data set.

Supplementary Table 3 (continued)

Species	#	Shape CV1	Shape CV2	Body size	Buoyancy	Temperature
Akarotaxis nudiceps	2	-4.223	15.546	15.0	3.84	-1.71
Artedidraco shackletoni	2	4.547	-2.552	14.6		-1.72
Artedidraco skottsbergi	5	6.472	-2.879	10.6	5.40	-1.47
Chaenocephalus aceratus	39	-8.931	-0.842	75.0	3.19	0.10
Champsocephalus gunnari	41	-4.977	-2.950	66.0	2.90	1.47
Chaenodraco wilsoni	34	-5.087	-2.507	43.0	3.08	-1.49
Chionodraco hamatus	2	-11.039	-0.925	49.0		-1.57
Chionodraco rastrospinosus	28	-8.541	-2.029	52.0	2.72	-0.93
Cryodraco antarcticus	43	-9.503	-2.716	57.0	2.53	-1.44
Cygnodraco mawsoni	4	-10.255	4.462	44.9		-1.67
Dacodraco hunteri	2	-10.881	0.595	29.0	1.41	-1.65
Dissostichus eleginoides	14	0.990	4.483	215.0		7.64
Dissostichus mawsoni	25	0.027	4.518	175.0	0.00	-1.15
Dolloidraco longedorsalis	1	7.689	-3.427	13.7	4.49	-1.72
Gobionotothen gibberifrons	44	2.344	0.867	55.0	4.27	0.00
Gymnodraco acuticeps	2	-10.811	22.875	38.1	3.38	-1.52
Harpagifer antarcticus	2	3.315	6.732	11.4	5.99	-0.79
Histiodraco velifer	1	4.712	-2.850	19.2		-1.73
Lepidonotothen larseni	42	5.501	-1.743	24.0	4.22	0.24
Lepidonotothen nudifrons	31	6.648	-5.438	19.0	4.46	-0.85
Lepidonotothen squamifrons	61	6.771	-0.187	55.0	3.20	2.78
Neopagetopsis ionah	11	-7.946	-1.795	56.0	1.28	-1.26
Notothenia coriiceps	27	4.650	1.658	62.0	3.67	-0.04
Notothenia rossii	30	4.825	1.486	92.0	3.55	1.72
Pagetopsis macropterus	7	-6.845	-3.709	33.0	2.38	-1.55
Pagetopsis maculatus	4	-6.092	-0.784	25.0	3.11	-1.71
Parachaenichthys charcoti	1	-10.436	12.935	46.7	4.39	-0.87
Parachaenichthys georgianus	11	-9.633	11.134	65.1		1.59
Patagonotothen guntheri	11	4.412	-0.384	23.0		6.06
Pleuragramma antarctica	25	0.837	-0.041	25.0	0.34	-1.55
Pogonophryne marmorata	2	0.732	13.787	21.0	3.81	-1.42
Pogonophryne scotti	1	1.341	10.869	31.0	3.80	-1.38
Prionodraco evansii	5	2.946	29.614	17.0	4.21	-1.61
Pseudochaenichthys georgianus	31	-9.140	1.264	60.0	1.96	0.87
Racovitzia glacialis	1	-3.377	-2.505	27.4	4.08	-1.55
Trematomus bernacchii	7	5.159	-0.157	35.0	3.52	-1.54
Trematomus eulepidotus	44	6.549	-0.735	34.0	3.41	-1.50
Trematomus hansoni	19	4.621	-0.561	41.0	3.12	-0.86
Trematomus newnesi	8	6.290	-0.765	20.0	3.76	-1.30
Trematomus pennellii	11	5.817	-2.001	24.0	3.09	-1.57
Trematomus scotti	21	6.343	2.060	16.0	4.14	-1.59
Trematomus tokarevi	1	5.600	5.435	22.4	2.77	-1.11

Supplementary Table 4: Model combinations used in BEAST analyses.
Twelve combinations of gene tree linkage, substitution model, base frequency setting, and clock model are listed. Supplementary Tables 4-6 refer to these model combinations.

Model	Gene trees	Substitution model	Frequencies	Clock model
1	linked	HKY+Gamma	empirical	strict
2	linked	HKY+Gamma	estimated	strict
3	linked	HKY+Gamma	estimated	UCLN
4	linked	RB+Gamma	empirical	strict
5	linked	RB+Gamma	estimated	strict
6	linked	RB+Gamma	estimated	UCLN
7	unlinked	HKY+Gamma	empirical	strict
8	unlinked	HKY+Gamma	estimated	strict
9	unlinked	HKY+Gamma	estimated	UCLN
10	unlinked	RB+Gamma	empirical	strict
11	unlinked	RB+Gamma	estimated	strict
12	unlinked	RB+Gamma	estimated	UCLN

Supplementary Table 5: Model support and tree characteristics for BEAST analyses of the combined marker set.
For each model combination, AICM values, Akaike weights, the number of parameters, the mean BPP, and the mean TMRCA of the diversification of Antarctic notothenioids are listed. Model combination numbers refer to those listed in Supplementary Table 4. Model 12* is identical to model 12, but with the species tree topology constrained to that of the species tree obtained with MP-EST.

Model	AICM	ΔAICM	Akaike weight	Parameters	Mean BPP	TMRCA Antarctic Clade
1	117355.4	1242.0	0.00000	15	0.967	22.36
2	117076.1	962.6	0.00000	19	0.965	22.54
3	116288.8	175.3	0.00000	27	0.964	22.37
4	116952.5	839.1	0.00000	19	0.967	22.32
5	116965.0	851.6	0.00000	23	0.968	22.35
6	116161.9	48.4	0.00000	31	0.971	22.35
7	116963.1	849.7	0.00000	40	0.663	18.67
8	116711.3	597.8	0.00000	49	0.670	18.30
9	116181.2	67.8	0.00000	67	0.684	13.31
10	116575.8	462.3	0.00000	49	0.668	17.62
11	116614.2	500.7	0.00000	58	0.670	17.69
12	116113.4	0.0	0.99956	76	0.684	13.35
12*	116128.9	15.5	0.00044	76	1.000	12.90

Supplementary Table 6: Model support and tree characteristics for BEAST analyses of the mitochondrial marker set.
For each model combination, AICM values, Akaike weights, the number of parameters, the mean BPP, and the mean TMRCA of the diversification of Antarctic notothenioids are listed. Model combination numbers refer to those listed in Supplementary Table 4.

Model	AICM	ΔAICM	Akaike weight	Parameters	Mean BPP	TMRCA Antarctic Clade
1	83604.3	686.5	0.00000	9	0.971	28.20
2	83341.0	423.2	0.00000	11	0.978	28.49
3	83065.2	147.3	0.00000	15	0.957	26.31
4	83243.8	326.0	0.00000	11	0.974	28.19
5	83254.9	337.0	0.00000	13	0.975	28.17
6	82929.3	11.5	0.00321	17	0.964	26.08
7	83607.6	689.8	0.00000	12	0.435	25.54
8	83342.4	424.6	0.00000	14	0.451	25.99
9	83061.7	143.9	0.00000	18	0.397	23.97
10	83243.2	325.4	0.00000	14	0.459	25.81
11	83254.2	336.4	0.00000	16	0.471	25.99
12	82917.8	0.0	0.99679	20	0.443	23.46

Supplementary Table 7: Model support and tree characteristics for BEAST analyses of the nuclear marker set.
For each model combination, AICM values, Akaike weights, the number of parameters, the mean BPP, and the mean TMRCA of the diversification of the Antarctic Clade are listed. Model combination numbers refer to those listed in Supplementary Table 4.

Model	AICM	ΔAICM	Akaike weight	Parameters	Mean BPP	TMRCA Antarctic Clade
1	33313.2	266.6	0.00000	9	0.860	18.92
2	33297.8	251.2	0.00000	11	0.856	19.01
3	33064.7	18.1	0.00012	15	0.808	17.51
4	33273.6	227.0	0.00000	11	0.847	19.09
5	33275.1	228.6	0.00000	13	0.847	19.10
6	33046.6	0.0	0.99988	17	0.794	17.76
7	33270.0	223.4	0.00000	33	0.603	15.28
8	33299.4	252.8	0.00000	40	0.611	15.20
9	33163.5	116.9	0.00000	54	0.570	10.90
10	33242.1	195.5	0.00000	40	0.607	14.92
11	33260.3	213.8	0.00000	47	0.609	14.90
12	33142.5	95.9	0.00000	61	0.582	11.18

Supplementary Table 8: Species richness used for diversification rate analysis with MEDUSA. Number of extant species according to Eastman & Eakin (2000, updated Table 1, version dating from 10 July 2013, available at http://www.oucom.ohiou.edu/dbms-eastman/). Clades were chosen so that the entire extant diversity of the notothenioid suborder could be assigned to them, with two exceptions: we exclude the monotypic genus *Gvozdarus*, which has been provisionally assigned to the non-monophyletic family Nototheniidae (Dettai *et al.* 2012), but is known from only two specimens (Fenaughty *et al.* 2008), of which no molecular sequence data has been produced. Similarly, the monotypic genus *Halaphritis* is known from only three specimens collected off the coast of Tasmania, and attempts to extract DNA from these samples have remained unsuccessful (Last *et al.* 2002). This species has been provisionally assigned to the family Bovichtidae, but shares its biogeographic distribution and morphological characteristics with *Pseudaphritis*, so that its phylogenetic placement remains questionable (Last *et al.* 2002). Thus, we here ignore both *Gvozdarus* and *Halaphritis*.

Family	Clade	Richness
Bovichtidae	*Bovichtus*	7
Bovichtidae	*Cottoperca*	1
Pseudaphritidae	Pseudaphritidae	1
Eleginopidae	Eleginopidae	1
Nototheniidae	*Aethotaxis*	1
Nototheniidae	*Pleuragramma*	1
Nototheniidae	*Dissostichus*	2
Nototheniidae	*Gobionotothen*	4
Nototheniidae	*Notothenia*+*Paranotothenia*	7
Nototheniidae	Trematominae	34
Harpagiferidae	Harpagiferidae	11
Artedidraconidae	Artedidraconidae	30
Bathydraconidae	Bathydraconinae[1]	9
Bathydraconidae	Cygnodraconinae[1]	4
Bathydraconidae	Gymnodraconinae[1]	3
Channichthyidae	*Chaenocephalus*	1
Channichthyidae	*Chaenodraco*	1
Channichthyidae	*Champsocephalus*	2
Channichthyidae	*Chionodraco*	3
Channichthyidae	*Cryodraco*+*Channichthys*+*Chionobathyscus*[2]	4
Channichthyidae	*Dacodraco*	1
Channichthyidae	*Neopagetopsis*	1
Channichthyidae	*Pagetopsis*	2
Channichthyidae	*Pseudochaenichthys*	1
Sum		132

[1]We here follow the subfamilial classification of Derome *et al.* (2002), but also consider *Akarotaxis* and *Vomeridens* to be part of Bathydraconinae, according to the molecular phylogenies of Near *et al.* (2012) and Dettai *et al.* (2012).
[2]Both *Channichthys* and *Chionobathyscus* are missing in our data set, however the phylogenetic analyses of Near *et al.* (2012) suggest that these two genera are most closely related to *Cryodraco*.

Supplementary Table 9: Sea surface temperatures of notothenioid habitats.
For each species, latitude and longitude of geographic grid cell centers are listed, in which this species is known to occur, as well as sea surface temperature extracted for these grid cells from the Optimum Interpolation Sea Surface Temperature atlas.
See separate file.

Supplementary Table 10: Support values and ages estimates for nodes of the MCC tree.
BPP values, mean divergence dates estimates, and 95% HPD intervals for all nodes of the MCC tree resulting from the BEAST analysis of the combined marker set with the best-supported model combination. Bootstrap (BS) values show the number of bootstrapped replicates of the MP-EST species tree analysis that support this node. Node labels refer to those given in Supplementary Figure 8.

Node	BPP	Mean age	95% HPD	BS	Node	BPP	Mean age	95% HPD	BS
1	1.00	64.96	77.24-53.15	100	25	1.00	4.85	7.31-2.49	85
2	1.00	33.22	46.16-20.35	-	26	1.00	1.24	2.19-0.56	63
3	1.00	61.54	72.77-50.15	100	27	0.55	0.87	1.39-0.46	58
4	1.00	36.86	45.40-28.89	99	28	0.46	0.31	0.70-0.00	86
5	1.00	13.35	17.12-9.98	100	29	0.14	0.77	1.28-0.30	61
6	0.26	12.03	16.00-8.66	30	30	0.22	0.62	1.10-0.13	44
7	0.16	11.11	14.89-7.46	12	31	0.18	0.35	0.83-0.00	11
8	0.73	9.87	14.31-5.11	12	32	0.78	8.09	10.35-6.09	46
9	1.00	2.72	5.47-0.00	25	33	0.42	6.73	9.24-4.30	1
10	1.00	6.00	8.11-4.20	12	34	1.00	4.41	6.46-2.56	66
11	0.74	4.58	6.79-2.57	14	35	0.64	3.25	5.38-0.78	15
12	0.80	2.50	4.55-0.00	67	36	0.37	7.40	9.56-5.29	2
13	0.60	3.73	6.12-0.66	10	37	1.00	3.96	5.87-2.10	35
14	0.98	4.26	5.78-2.86	12	38	1.00	1.24	2.41-0.00	62
15	0.50	3.64	5.07-2.28	0	39	1.00	3.49	4.57-2.44	98
16	0.46	1.59	3.44-0.00	4	40	0.81	2.59	3.63-1.60	89
17	0.31	2.93	4.35-1.46	2	41	0.98	1.17	2.19-0.00	96
18	0.49	2.15	3.61-0.55	83	42	1.00	1.00	1.89-0.00	86
19	0.34	1.49	2.97-0.16	40	43	0.73	2.92	3.98-2.00	1
20	0.57	0.48	1.96-0.00	78	44	0.25	2.56	3.56-1.61	17
21	0.48	11.69	15.30-8.64	8	45	0.99	1.59	2.30-0.98	94
22	0.40	10.96	14.30-8.19	74	46	0.40	1.17	1.88-0.51	3
23	1.00	2.18	3.81-0.31	83	47	0.74	0.43	1.20-0.00	2
24	1.00	8.96	11.53-6.72	46	48	0.70	0.74	1.36-0.00	16

References

Baele G, Lemey P, Bedford T *et al.* (2012) Improving the accuracy of demographic and molecular clock model comparison while accommodating phylogenetic uncertainty. *Mol Biol Evol*, **29**, 2157–2167.

Balushkin AV (1994) Fossil notothenioid, and not gadiform, fish *Proeleginops grandeastmanorum* gen. sp. nov. (Perciformes, Notothenioidei, Eleginopidae) from the late Eocene found in Seymour Island (Antarctica). *Voprosy Ikhtiologii*, **34**, 298–307.

Becerra JX (2005) Timing the origin and expansion of the Mexican tropical dry forest. *Proc Natl Acad Sci*, **102**, 10919–10923.

Bouckaert R, Alvarado-Mora MV, Rebello Pinho JR (2013) Evolutionary rates and HBV: issues of rate estimation with Bayesian molecular methods. *Antivir Ther*, **18**, 497–503.

Bouckaert R, Heled J, Kühnert D *et al.* (2014) BEAST 2: a software platform for Bayesian evolutionary analysis. *PLoS Computational Biology*, **10**, e1003537.

Chow S, Hazama K (1998) Universal PCR primers for S7 ribosomal protein gene introns in fish. *Mol Ecol*, **7**, 1255–1256.

Cusimano N, Renner SS (2010) Slowdowns in diversification rates from real phylogenies may not be real. *Syst Biol*, **59**, 458–464.

Derome N, Chen WJ, Dettaï A, Bonillo C, Lecointre G (2002) Phylogeny of Antarctic dragonfishes (Bathydraconidae, Notothenioidei, Teleostei) and related families based on their anatomy and two mitochondrial genes. *Mol Phylogenet Evol*, **24**, 139–152.

Dettai A, Berkani M, Lautrédou AC *et al.* (2012) Tracking the elusive monophyly of nototheniid fishes (Teleostei) with multiple mitochondrial and nuclear markers. *Mar Genomics*, **8**, 49–58.

Dornburg A, Santini F, Alfaro M (2008) The influence of model averaging on clade posteriors: an example using the triggerfishes (family Balistidae). *Syst Biol*, **57**, 905–919.

Drummond AJ, Bouckaert R (2014) *Bayesian Evolutionary Analysis with BEAST 2*. Cambridge University Press.

Drummond AJ, Ho SYW, Philips MJ, Rambaut A (2006) Relaxed phylogenetics and dating with confidence. *PLOS Biology*, **4**, e88.

Drummond AJ, Suchard MA, Xie D, Rambaut A (2012) Bayesian phylogenetics with BEAUti and the BEAST 1.7. *Mol Biol Evol*, **29**, 1969–1973.

Eastman JT, Eakin RR (2000) An updated species list for notothenioid fish (Perciformes; Notothenioidei), with comments on Antarctic species. *Arch Fish Mar Res*, **48**, 11–20.

Eastman JT, Grande L (1991) Late Eocene gadiform (Teleostei) skull from Seymour Island, Antarctic Peninsula. *Antarct Sci*, **3**, 87–95.

Fenaughty JM, Eastman JT, Sidell BD (2008) Biological implications of low condition factor "axe handle" specimens of the Antarctic toothfish, Dissostichus mawsoni, from the Ross Sea. *Antarct Sci*, **20**, 537–551.

Gernhard T (2008) The conditioned reconstructed process. *J Theor Biol*, **253**, 769–778.

Gon O, Heemstra PC (1990) *Fishes of the Southern Ocean*. J.L.B. Smith Institute of Ichthyology, Grahamstown, South Africa.

Hasegawa M, Kishino H, Yano Ta (1985) Dating of the human-ape splitting by a molecular clock of mitochondrial DNA. *Journal of Molecular Evolution*, **22**, 160–174.

Heled J, Drummond AJ (2010) Bayesian inference of species trees from multilocus data. *Mol Biol Evol*, **27**, 570–580.

Ho SYW, Lanfear R (2010) Improved characterisation of among-lineage rate variation in cetacean mitogenomes using codon-partitioned relaxed clocks. *Mitochondrial DNA*, **21**, 138–146.

Höhna S, Stadler T, Ronquist F, Britton T (2011) Inferring speciation and extinction rates under different sampling schemes. *Mol Biol Evol*, **28**, 2577–2589.

Lanfear R, Calcott B, Ho SYW, Guindon S (2012) PartitionFinder: combined selection of partitioning schemes and substitution models for phylogenetic analyses. *Mol Biol Evol*, **29**, 1695–1701.

Last PR, Balushkin AV, Hutchins JB (2002) *Halaphritis platycephala* (Notothenioidei: Bovichtidae): A new genus and species of temperate icefish from Southeastern Australia. *Copeia*, **2002**, 433–440.

Leigh JW, Susko E, Baumgartner M, Roger AJ (2008) Testing congruence in phylogenomic analysis. *Syst Biol*, **57**, 104–115.

Li C, Ortí G, Zhang G, Lu G (2007) A practical approach to phylogenomics: the phylogeny of ray-finned fish (Actinopterygii) as a case study. *BMC Evolutionary Biology*, **7**, 44.

Matschiner M, Hanel R, Salzburger W (2011) On the origin and trigger of the notothenioid adaptive radiation. *PLOS ONE*, **6**, e18911.

Muschick M, Indermaur A, Salzburger W (2012) Convergent evolution within an adaptive radiation of cichlid fishes. *Curr Biol*, **22**, 2362–2368.

Near TJ, Dornburg A, Kuhn KL *et al.* (2012) Ancient climate change, antifreeze, and the evolutionary diversification of Antarctic fishes. *Proc Natl Acad Sci*, **109**, 3434–3439.

Raftery AE, Newton M, Satagopan J, Krivitsky P (2007) Estimating the integrated likelihood via posterior simulation using the harmonic mean identity. In: *Bayesian Statistics* (eds. Bernardo JM, Bayarri MJ, Berger JO). Oxford University Press, Oxford.

Rambaut A, Drummond AJ (2007) Tracer v1.5.

Ratnasingham S, Hebert PDN (2007) BOLD: The Barcode of Life Data System (www.barcodinglife.org). *Molecular Ecology Notes*, **7**, 355–364.

Rutschmann S, Matschiner M, Damerau M *et al.* (2011) Parallel ecological diversification in Antarctic notothenioid fishes as evidence for adaptive radiation. *Mol Ecol*, **20**, 4707–4721.

Sprague J, Bayraktaroglu L, Clements D *et al.* (2006) The Zebrafish Information Network: the zebrafish model organism database. *Nucl Acids Res*, **34**, D581–5.

Stamatakis A (2006) RAxML-VI-HPC: maximum likelihood-based phylogenetic analyses with thousands of taxa and mixed models. *Bioinformatics*, **22**, 2688–2690.

2.3

Ecomorphological disparity in an adaptive radiation: opercular bone shape and stable isotopes in Antarctic icefishes

Ecology and Evolution

I collected the specimens, provided raw data and helped with analyses and interpreting the results. LW conducted the geometric morphometric analyses, did further analyses and wrote the first version of the manuscript. All authors then participated in discussing the manuscript and drafting the final version.

Ecology and Evolution

Open Access

Ecomorphological disparity in an adaptive radiation: opercular bone shape and stable isotopes in Antarctic icefishes

Laura A. B. Wilson[1,2], Marco Colombo[3], Reinhold Hanel[4], Walter Salzburger[3] & Marcelo R. Sánchez-Villagra[1]

[1]Paläontologisches Institute und Museum, Karl-Schmid Strasse 4, CH 8006 Zürich, Switzerland
[2]School of Biological, Earth and Environmental Sciences, University of New South Wales, High Street, Kensington, NSW 2052, Australia
[3]Zoological Institute, University of Basel, Vesalgasse 1, CH 4051 Basel, Switzerland
[4]Institute of Fisheries Ecology, Johann Heinrich von Thünen-Institute, Federal Research Institute for Rural Areas, Forestry and Fisheries, Palmaille 9, 22767 Hamburg, Germany

Keywords
Craniofacial bone, ecology, geometric morphometrics, phylogeny, stable isotopes.

Correspondence
Laura A. B. Wilson, Paläontologisches Institut und Museum, Karl-Schmid Strasse 4, CH 8006 Zürich, Switzerland. Tel: +61(0)-2-9385-3866; Fax: +61(0)-2-9385-1558; E-mail: laura.a.b.wilson@gmail.com

Funding Information
This project is supported by the Swiss National Fund Sinergia project granted to W. S., M. R. S.-V. and Heinz Furrer (CRSII3-136293). L. A. B. W. is currently supported by a fellowship from the Swiss National Science Fund (PBZHP3_141470).

Received: 20 June 2013; Revised: 1 July 2013; Accepted: 3 July 2013

Ecology and Evolution **2013; 3(9): 3166–3182**

doi: 10.1002/ece3.708

Abstract

To assess how ecological and morphological disparity is interrelated in the adaptive radiation of Antarctic notothenioid fish we used patterns of opercle bone evolution as a model to quantify shape disparity, phylogenetic patterns of shape evolution, and ecological correlates in the form of stable isotope values. Using a sample of 25 species including representatives from four major notothenioid clades, we show that opercle shape disparity is higher in the modern fauna than would be expected under the neutral evolution Brownian motion model. Phylogenetic comparative methods indicate that opercle shape data best fit a model of directional selection (Ornstein–Uhlenbeck) and are least supported by the "early burst" model of adaptive radiation. The main evolutionary axis of opercle shape change reflects movement from a broad and more symmetrically tapered opercle to one that narrows along the distal margin, but with only slight shape change on the proximal margin. We find a trend in opercle shape change along the benthic–pelagic axis, underlining the importance of this axis for diversification in the notothenioid radiation. A major impetus for the study of adaptive radiations is to uncover generalized patterns among different groups, and the evolutionary patterns in opercle shape among notothenioids are similar to those found among other adaptive radiations (three-spined sticklebacks) promoting the utility of this approach for assessing ecomorphological interactions on a broad scale.

Introduction

Morphological disparity, a measure of the variability in morphological form, is well recognized to be unequally distributed across vertebrate phylogeny (e.g., Erwin 2007; Pigliucci 2008; Sidlauskas 2008). Evolutionary constraints place viability limits on morphological form, leaving gaps in phenotypic space; for instance, developmental programs begin at selected start points, making the achievement of some forms not possible along a particular ontogenetic pathway (e.g., Arthur 2004; Salazar-Ciudad 2006; Raff 2007; Klingenberg 2010), and the interactions between genetic or phenotypic traits can channel variation in fixed directions (e.g., Marroig and Cheverud 2005, 2010; Brakefield 2006). Understanding why phenotypic spaces possess these properties, and the evolutionary processes underlying their patterning, has long captured the attention of evolutionary biologists (e.g., Wright 1932; Simpson 1953; Gould 1989; Carroll 2005). In this regard, the study of adaptive radiations, groups that have rapidly diversified from a common ancestor to occupy a wide variety of ecological niches, has been of particular interest because these bursts

of speciation have been causally implicated in generating significant portions of biodiversity, or, in other words, filling phenotypic space (e.g., Schluter, 2000; Seehausen 2007).

Classical model examples of adaptive radiation include the *Anolis* lizards of the Caribbean (e.g., Losos 2009), cichlid fishes of East Africa's great lakes (e.g., Kocher 2004; Seehausen 2006; Salzburger 2009; Santos and Salzburger 2012), and Darwin's finches from the Galápagos (e.g., Grant and Grant 2006). These systems have been well studied, and thanks to a host of empirical and theoretical approaches, some commonalities about the process of adaptive radiation have been found. All modern definitions of adaptive radiation feature a multiplication of species and adaptive diversification (Schluter, 2000; Gavrilets and Losos 2009; Glor 2010; Harmon et al. 2010). At the same time, however, the myriad and often lineage-specific interactions that guide evolutionary processes make difficult our understanding of how well these generalities may fit other, less intensively studied adaptive radiations, and much disagreement persists regarding the meaning of adaptive radiation (Harder 2001; Olson and Arroyo-Santos 2009). A main feature of adaptive radiation models is the idea that rapid diversification is possible under conditions of ecological opportunity (Schluter, 2000), and mathematical models predict that speciation rates and major ecological differences are highest at early stages of radiation ("early burst"), but decline as more and more niches become filled over time and ecological opportunity reduces (Gavrilets and Losos 2009). No two environments are the same, and the extent to which ecological conditions may place different demands on the generation and structuring of variation, and therefore impact our understanding of adaptive radiation models, is not well known (Day et al. 2013). To fill these gaps, both a wider sampling of the tempo and mode of adaptive radiations and a focus on probing the diverse boundaries of environments in which radiation has occurred are necessary.

In this study we focus on the Antarctic notothenioids, a suborder of marine perciform fishes that represent an example of adaptive radiation in an extreme environmental setting (Eastman and McCune 2000; Matschiner et al. 2011; Rutschmann et al. 2011; Lau et al. 2012). Antarctic notothenioids are endemic to the Southern Ocean, the world's coldest and iciest marine waters (Dayton et al. 1969; Hunt et al. 2003; Cheng et al. 2006). Together with the purely Antarctic Notothenioidae, Harpagiferidae, Bathydraconidae, Artedidraconidae, and Channichthyidae, the clade also includes the three ancestral families Bovichtidae, Pseudaphritidae, and Eleginopidae, represented by 11 mainly non-Antarctic species. The main radiation of the Antarctic group arose around 23 million years ago, near the Oligocene–Miocene boundary (Matschiner et al. 2011), coincident with the development of Antarctic sea ice and the progressive isolation of the Antarctic shelf. In response to changes in water temperature, Antarctic notothenioids developed adaptive features such as antifreeze glycoproteins (AFGPs) and, in one family, loss of hemoglobin that enabled them to survive and diversify in freezing waters not habitable by other teleosts (Eastman 1993; Chen et al. 1997; Hofmann et al. 2005; Near et al. 2012). Besides their taxonomic diversity, comprising 132 presently recognized species (Eakin et al. 2009), notothenioids occupy a large number of very different ecological roles (Eastman 1993). Several lineages independently evolved toward a pelagic lifestyle, a transition which, because notothenioids do not possess a swim bladder, required extensive morphological and physiological adaptations to achieve neutral buoyancy (Klingenberg and Ekau 1996; Eastman 2005). The purely Antarctic notothenioids include five major groups that differ both in their species richness and extent of morphological and ecological diversification (Eastman 2005), these are as follows: Artedidraconidae, Bathydraconidae, Channichthyidae, Harpagiferidae, and Nototheniidae. The family Nototheniidae has undergone the most ecological and morphological diversification, and includes 33 Antarctic species with life styles that range from purely benthic, epibenthic, semipelagic, and cryopelagic to fully pelagic (Klingenberg and Ekau 1996; Eastman 2005). In contrast, Harpagiferidae represents a monogeneric family of nine ecologically very similar species, and also Artedidraconidae solely comprise benthic species that mainly differ in body size (Eakin et al. 2009). Bathydraconidae are morphologically rather diverse and range from moderately robust to more elongate and delicate species, including the deepest-living notothenioids (DeWitt 1985) as well as shallow-living forms. Channichthyids are fusiform pike-like fishes, and uniquely among vertebrates they lack hemoglobin. Typically living at depths of less than 800 m, channichthyids are quite large fishes (ca. 50 cm length) and most adopt a combined pelagic–benthic lifestyle (Eastman 2005; Kock 2005).

Despite recent attention to the key features of the notothenioid radiation (e.g., Eastman 2005), very few studies have explicitly considered the evolution of morphological and environmental features among notothenioids (Ekau 1991; Klingenberg and Ekau 1996), although there exist a large number of studies of ecomorphology and functional ecology for other fishes (e.g., Lauder 1983; Bemis and Lauder 1986; Wainwright 1996; Westneat et al. 2005; Westneat 2006; Grubich et al. 2008; Mehta and Wainwright 2008; Cooper and Westneat 2009; Holzman et al. 2012). Here, we collect geometric morphometric data to describe shape evolution for a craniofacial bone, the opercle, which articulates with the preopercle and supports the gill cover in bony fish. Use of geometric morphometrics to analyze shape explicitly improves upon previous schemes of simple linear

measurements (Klingenberg and Ekau 1996), which may incur complications due to size-related effects in organisms such as fishes, which are characterized by indeterminate growth. Opercle shape is indirectly related to foraging ecology because besides protecting the gill cover, the opercle plays a primary role in the suction pump phase of the respiration cycle (Hughes, 1960: Anker 1974; Lauder 1979). In a simple distinction, fish feeding on benthic prey typically use a suction-feeding mechanism, whereas those feeding on planktonic prey rely on ram feeding (Gerking 1994; Willacker et al. 2010). The ability to produce strong negative pressure gradients within the oral cavity is recognized as an important evolutionary axis of diversification (Collar and Wainwright 2006; Westneat 2006), and additional factors such as skull kinesis and jaw protrusion interact in a complex way to allow capture of aquatic prey (Holzman and Wainwright 2009). It is likely that differences in opercle size and shape along the trophic axis affect the functionality of the suction pump.

Using the opercle as an example of a functionally important and taxonomically variable craniofacial element, the aim of this study was to assess the interaction between ecology, inferred from stable isotope data, and morphology across the notothenioid clade, and to quantify the tempo and mode of ecomorphological interactions using disparity through time (DTT) and phylogenetic comparative methods. Taking advantage of its relatively well-documented development and growth (e.g., Cubbage and Mabee 1996; Kimmel et al. 2005, 2008), several studies have previously focused on the opercle, using three-spined sticklebacks as a "model" system to investigate the interplay between evolution and development. The three-spined stickleback is an example of a genealogically very recent species complex, repeatedly derived from marine ancestors after the retreat of the Pleistocene ice sheets to colonize freshwaters (Colosimo et al. 2005; Makinen and Merila 2008; Jones et al. 2012a,b). Accompanying these colonizations, opercle shape has been shown to have repeatedly evolved along the same shape trajectory in geographically distinct populations, on a relatively short time scale, following divergence from an oceanic ancestor (Kimmel et al. 2008, 2011; Arif et al. 2009). Variability in opercle shape among freshwater populations was also found to be associated with habitat, differing along the benthic–limnetic axis (Arif et al. 2009). These results demonstrate the utility of geometric morphometrics to quantify opercle shape, and imply that the globally recovered dilation–diminution trajectory of opercle shape change is most likely naturally selected. Fossils are recognized as an important component to the study of adaptive radiation (Gavrilets and Losos 2009), and the opercle model further provides an opportunity to gain insight into the temporal persistence of evolutionary patterns of shape change and their implications for the paleobiology of extinct species flocks (Wilson et al. 2013b).

Material and Methods

Sample and collection

All specimens photographed for this study were collected during RV Polarstern expedition ANT-XXVIII/4 to the Scotia Sea in 2012. Species identification followed Gon and Heemstra (1990) and the FAO species identification sheets for fishery purposes (Fischer and Hureau 1985). The location, date, time, water depth, and station were recorded for each trawl from which fishes were photographed (Table S1).

The study is based on measurements of 89 specimens from 25 notothenioid species (Table 1, Fig. 1), including representatives from each of the families Nototheniidae, Artedidraconidae, Bathydraconidae, and Channichthyidae. Each specimen was photographed in a standardized manner after being fixed in position on a flat surface using large steel needles. A Nikon D5000 camera (Nikon Corporation, Tokyo, Japan) mounted on a tripod, with the camera lens positioned such that it was parallel to the plane of the opercle, was used to capture a close-up image of the left side of the head in lateral orientation. At the initial data collection (photography) stage, each species was represented by

Table 1. Specimens analyzed in this study.

Group	Species	*N*	Lifestyle
Bathydraconidae	*Akarotaxis nudiceps*	1	benthic
Bathydraconidae	*Parachaenichthys charcoti*	1	benthic
Artedidraconidae	*Artedidraco skottsbergi*	1	benthic
Artedidraconidae	*Pogonophryne scotti*	1	benthic
Channichthyidae	*Chaenocephalus aceratus*	3	benthic
Channichthyidae	*Champsocephalus gunnari*	7	pelagic
Channichthyidae	*Chionodraco rastrospinosus*	7	benthic/ benthopelagic
Channichthyidae	*Cryodraco antarcticus*	7	pelagic/benthic
Channichthyidae	*Neopagetopsis ionah*	1	pelagic
Channichthyidae	*Pseudochaenichthys georgianus*	3	pelagic/ semipelagic
Channichthyidae	*Chaenodraco wilsoni*	4	pelagic
Nototheniidae	*Dissostichus mawsoni*	12	pelagic
Nototheniidae	*Gobionotothen gibberifrons*	10	benthic
Nototheniidae	*Lepidonotothen larseni*	1	semipelagic
Nototheniidae	*Lepidonotothen nudifrons*	2	benthic
Nototheniidae	*Lepidonotothen squamifrons*	7	benthic
Nototheniidae	*Notothenia coriiceps*	2	benthic
Nototheniidae	*Notothenia rossii*	9	semipelagic
Nototheniidae	*Pleuragramma antarcticum*	2	pelagic
Nototheniidae	*Trematomus eulepidotus*	1	epibenthic
Nototheniidae	*Trematomus hansoni*	2	benthic
Nototheniidae	*Trematomus newnesi*	2	cryopelagic
Nototheniidae	*Trematomus scotti*	1	benthic
Nototheniidae	*Trematomus tokarevi*	1	benthic
Nototheniidae	*Trematomus bernacchii*	1	benthic

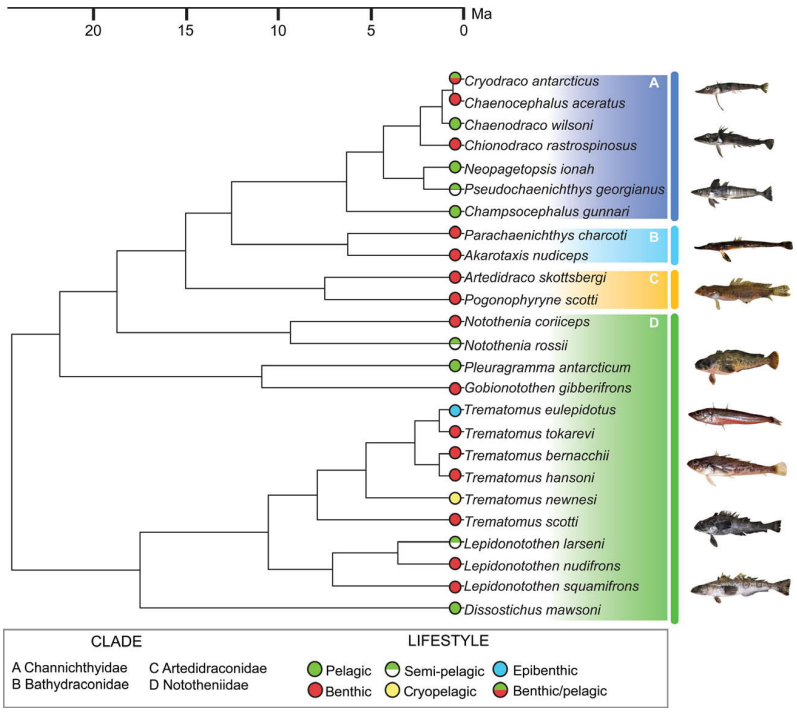

Figure 1. Phylogenetic relationships for the species used in this study. Filled and open circles indicate lifestyle, and major clades are highlighted and labeled. Phylogenetic relationships were based on those reported by Rutschmann et al. (2011) and Matschiner et al. (2011). Photographs of species used in this study (not to scale), from top to bottom, are as follows: *Cryodraco antarcticus*, *Chionodraco rastrospinosus*, *Champsocephalus gunnari*, *Parachaenichthys charcoti*, *Artedidraco skottsbergi*, *Notothenia coriiceps*, *Pleuragramma antarcticum*, *Trematomus eulepidotus, Lepidonotothen squamifroms*, and *Dissostichus mawsoni*. See Table 1 for further details of the study sample.

between two and 30 individuals, as was available on the trawl, and subsequent pruning of the data set for geometric morphometric data collection was conducted to include only undamaged adult specimens, and exclude clear outliers in terms of body length to minimize intraspecific allometric variation.

Morphometric analyses

We used an outline-based geometric morphometric approach to compare opercle shape across the notothenioid species examined. Geometric morphometrics is a useful method to analyze morphological shape, capturing data that are easily visualized in morphospace ordinations and tractable to multivariate statistical methods (e.g., Bookstein, 1991; Adams et al. 2004; Mitteroecker and Gunz, 2009). Here, and similar to a previous study (Wilson et al. 2013b), an outline-based approach was chosen to assess interspecific shape variation because the curved nature of the operculum makes difficult the identification of a sufficient number of biologically meaningful, homologous, landmark points required for an accurate description of its shape across species. Eigenshape (ES) analysis is based on the definition of additional points of reference, or so-called semilandmarks (MacLeod, 1999) that are used to fill landmark-depleted regions, and in doing so enable the shape difference located in-between landmarks to be sampled, and the global aspect of a boundary outline to be evaluated (Wilson et al. 2011). ES analysis has proven to be successful in elucidating subtle shape variation in a wide variety of contexts (e.g., Polly, 2003; Krieger et al. 2007; Wilson et al. 2008; Astrop, 2011; Wilson 2013a) and is particularly suitable for this study as it affords the possibility to examine localized variation in opercular shape.

For each specimen, the outline of the opercle was traced using the software tpsDig (v. 2.16, Rohlf, 2010) (Fig. 2). A type II (Bookstein, 1991) landmark was defined as the starting point for each outline, and is described as the maxima of curvature on the dorsal margin of the bone (Fig. 2). Each outline was resampled to create 100 equidistant landmark points. Cartesian x–y coordinates of these landmark points were converted into the phi Φ form of the Zahn and Roskies (1972) shape function, required for ES analysis (MacLeod, 1999). ES analysis was performed using FORTRAN routines written by Norman MacLeod (NHM London). The method is

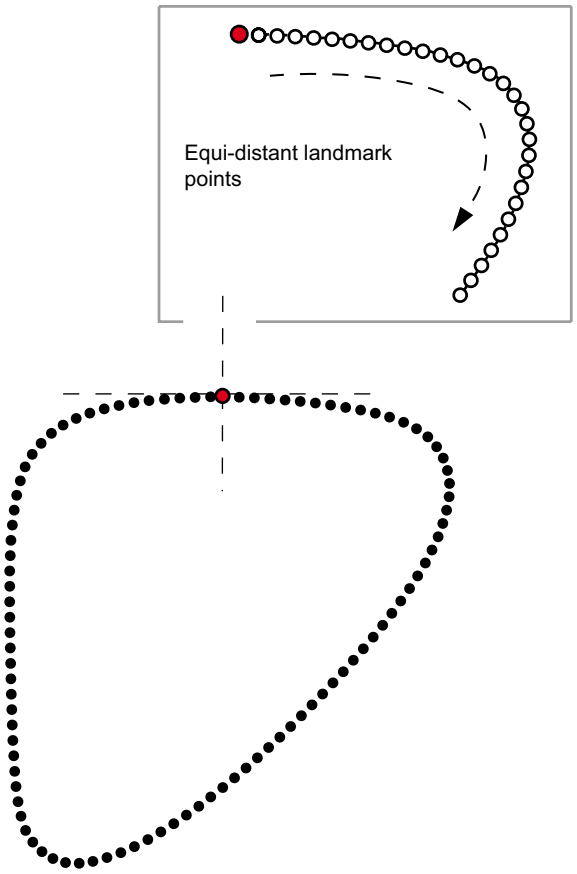

Figure 2. Outline-based geometric morphometric methods were used to capture the entire outline of the bone using 100 equidistant landmarks (open circles). A spatially homologous point (large color filled circle) was defined as starting point for each specimen.

based on a singular value decomposition of pairwise covariances calculated between individual shape functions, and produces a series of mutually orthogonal latent shape vectors which represent successive smaller proportions of overall shape variation such that the greatest amount of shape variation is represented on the fewest independent shape axes. Each specimen has a series of eigenscores, representing its location along each axis, and therefore specimens can be projected into a multidimensional morphospace to visualize shape differences. Interspecific differences in shape were assessed using analysis of variance (ANOVA) coupled with post hoc tests.

Stable isotope data

Stable isotopes of carbon and nitrogen can be used to provide insights into community trophic ecology because they show a stepwise enrichment with trophic level in marine systems (Hobson et al. 1994). The heavier isotope of nitrogen (^{15}N) is enriched by 3–4 per mil per trophic level and can therefore be used to infer trophic position, whereas the heavier isotope of carbon (^{13}C) is typically used to estimate the source of carbon for an organism, and practically applied to distinguish between near-shore (littoral) and open water (pelagic) environments (Post 2002). Isotope data are expressed in delta (δ) notation of per mil (‰) versus atmospheric N_2 (AIR) and carbonate standards (V-PDB), using the equation $\delta = [(R_{sample}/R_{standard})-1] \times 1000$, where R represents the ratio of the heavy to the light isotope (i.e., $^{13}C/^{12}C$ and $^{15}N/^{14}N$) (Rutschmann et al. 2011; p4712). For all species examined, except *Akarotaxis nudiceps*, *Artedidraco skottsbergi*, *Trematomus scotti*, and *Trematomus bernacchii* for which data were not available, stable isotope data ($\delta^{13}C$ and $\delta^{15}N$ isotope) were compiled from Rutschmann et al. (2011) to assess the relation between opercle shape and lifestyle patterns. Rutschmann et al. (2011: File S1) sampled multiple specimens per species and we therefore computed, for each species analyzed here, an average value for $\delta^{13}C$ and for $\delta^{15}N$.

The relation between shape and ecology was assessed using phylogenetic generalized least squares (PGLS) regression of $\delta^{13}C$ with scores for axes ES1–ES8, and separately of $\delta^{15}N$ with scores for axes ES1–ES8. PGLS uses a regression approach to account for phylogenetic relationships and assumes that residual traits are undergoing Brownian motion (BM) evolution (Rohlf 2001; Butler and King 2004; Blomberg et al. 2012). Regressions were conducted in the freely available statistical environment of R (http://r-project.org/) using the packages "geiger" and "nlme" (gls function) on a pruned data set ($N = 21$) comprising all species for which we had stable isotope values.

Disparity analyses

To visualize the relationship between phylogeny and taxon spacing in ES space, phylomorphospaces were constructed using ES scores. For species represented by more than one specimen, average scores along each axis were used for each phylomorphospace ordination. Following Sidlauskas (2008), the plot tree 2D algorithm in the rhetenor module (Dyreson and Maddison 2003) of mesquite (Maddison and Maddison 2011) was used to construct phylomorphospaces for ES1 versus ES2 and ES1 versus ES3, comprising 75.4% of sample shape variance: subsequent axes were not plotted as each contained less than 8.6% of sample variance, and were not deemed significant under the broken-stick model (Jackson 1993). The algorithm in the Rhetenor module reconstructs the ancestral states along ES axes, plots all terminal and internal phylogenetic nodes into the morphospace, and connects

adjacent nodes by drawing branches between them. Phylogenetic relationships were based on those reported by Rutschmann et al. (2011) and Matschiner et al. (2011). Branch lengths were calculated using mean value divergence dates reported by Matschiner et al. (2011).

To assess whether disparity increases rapidly at an early stage in the icefish radiation and then asymptotes, as would be predicted in a scenario of rapid early diversification ("early burst") under conditions of ecological opportunity (Gavrilets and Losos 2009), we used DTT analyses to evaluate how shape disparity changed through time in comparison to trait evolution under a BM model. Analyses were implemented in R using the package "geiger" (Harmon et al. 2008) and the same phylogenetic framework as used for the phylomorphospace visualizations. This method calculates disparity using average pairwise Euclidean distances between species as a measure of variance in multivariate space (e.g., Zelditch et al. 2004). As input we used mean ES scores per species along axes ES1 to ES8, encapsulating 95.8% of shape variance. Following Harmon et al. (2003), relative disparities were calculated by dividing a subclade's disparity by the disparity of the entire clade. Relative subclade disparities were calculated for each node in the phylogeny, progressing up the tree from the root. At each node, the relative disparity value was calculated as the average of the relative disparities of all subclades whose ancestral lineages were present at that time (Harmon et al. 2003: 961). Relative disparity values that are close to 0.0 indicate that subclades contain only a small proportion of the total variation and therefore overlap in morphospace occupation is minimal between the different subclades, whereas, conversely, relative disparity values that are close to 1.0 indicate extensive morphological overlap. To quantify how mean disparity compared to evolution under a BM model, 1000 simulations of morphological diversification were calculated on the phylogeny, and these theoretical subclade disparity values were plotted alongside the observed disparity values for opercle shape data. A morphological disparity index (MDI) metric was obtained, representing the area contained between the line connecting observed relative subclade disparity points versus the line connecting median relative disparity points derived from BM simulations (Harmon et al. 2003). If the observed subclade disparity line plots above the BM line then the clades defined by that time slice have tended to generate higher disparity in the modern fauna than expected under the null and overlap morphospace occupied by the overall clade.

Model fitting

BM, early burst (EB), and Ornstein–Uhlenbeck (OU) evolutionary models were fit to the data set of mean ES1 scores for opercle shape. These models describe different processes of morphological evolution on a chosen phylogeny and offer predictions about measures (e.g., disparity) of morphological trait evolution. The EB model predicts rapid morphological diversity early in the history of a group, followed by limited diversification as ecological niches are filled over time (e.g., Harmon et al. 2010). Under a BM model, trait evolution is simulated as a random walk and after each speciation event, the random walk continues independently of previous changes, and these changes are drawn from a normal distribution of zero and a variance proportional to branch length, hence phenotypic trait variance is predicted to increase with time in an unbounded fashion. The OU model is used to model stabilizing selection for a phenotypic trait value, and is similar to a BM model except traits are being pulled toward an optimal value, measured by a parameter (alpha) (Butler and King 2004; Hansen et al. 2008).

Methods for modeling evolutionary processes are largely implementable only for univariate data and therefore we chose ES1 as representative of opercle shape because it represents the maximum variance in the sample (39.9%). We repeated model fitting also for ES2 (20.6%) to assess the consistency of the best chosen model. Akaike information criterion (AIC) values were used to compare the fit of each model to the data (Akaike 1974; Wagenmakers and Farrel 2004), and specifically we report a modified version, AICc, which performs better when the number of observations per parameter is small (Burnham and Anderson 2010; Hunt and Carrano 2010). The AICc values for each model were transformed into differences from the minimum observed AICc value Δ_i (AICc) = AICc$_i$−min AICc. The differences were then transformed into AICc weights using the calculation:

$$W_i(\mathrm{AICc}) = \frac{\exp[-\frac{1}{2} \times \Delta_i(\mathrm{AICc})]}{\sum_j \exp[-\frac{1}{2} \times \Delta_j(\mathrm{AICc})]}$$

The resulting values sum to one across a set of candidate models, and can be interpreted as the proportional support received by each model (Hunt and Carrano 2010). Model fitting was conducted using the function fitContinuous() in the "geiger" package for R.

Measurement error

Error associated with the shape variables derived from outline data sets was calculated following the methodology of Arnqvist and Martensson (1998). Landmark data collection was replicated five times each for a subset of four specimens (*A. nudiceps*, *A. skottsbergi*, *Chaenocephalus aceratus*, and *Dissostichus mawsoni*), these were selected to include representatives from each of the four

families, and outlines were interpolated for the error repeats and added to the original data set. ES analysis was used to obtain shape variables and a one-way ANOVA was then performed on the outputted shape variables to detect whether the among-individual variance was greater than the within-individual (repeated) variance. The repeatability (R) value scales between 0 and 1. An R value of 0 would represent a sample in which all variance is found within individuals, whereas an R value of 1 would indicate all the variance is due to differences between individuals (see Wilson et al. 2011).

Results

Measurement error

Measurement error was calculated across the first six ES axes (ES1–ES6) accounting for 91.8% of the total sample variance, and each comprising between 3% and 39.9% of variance. One-way ANOVAs conducted on a subsampled data set including all error replicates ($N = 20$) plus original outlines resulted in R values of between 0.90 and 0.99, indicating a high level of replication for outline capture (Table S2).

Patterns of opercle shape change

The first three ES axes accounted for 75.3% of shape variance in the sample. Shape variance along ES1 (39.9%) was localized along two axes of the opercle outline. Negative ES1 scores reflected extension along a diagonal axis from the anterior dorsal margin to the posterior ventral margin of the bone coupled with compression along an axis from the posterior dorsal margin to the ventral tip. Conversely, positive ES1 scores reflected compression along the anterior dorsal margin and posterior ventral margin, in addition to extension along the posterior dorsal margin and ventral tip (Fig. 3A). These differences resulted in separation between species belonging to Notothenioidae, typically having negative scores along ES1, from members of Channichthyidae and Bathydraconidae, mostly characterized by positive ES1 scores (Fig. 3A). Specifically, specimens of *Notothenia rossii* (Fig. 3A, label a) had the most extreme negative scores and specimens of *C. aceratus* the greatest positive scores along the axis (Fig. 3A, label b). As for ES1, mean shape models for shape change along ES2, which represented 20.6% of shape variance in the sample, also indicated two alternating axes of extension and compression along the opercle margin. Negative ES2 scores described extension along the entire dorsal margin of the opercle and lower portion of the ventral margin, alongside compression occurring broadly along the proximal margin and the upper portion

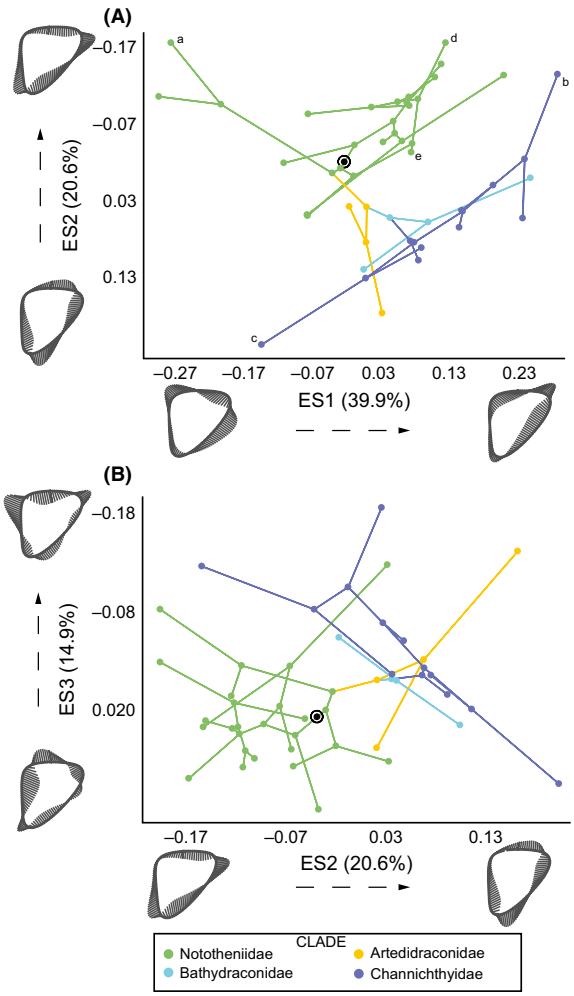

Figure 3. Phylomorphospace projections of notothenioid relationships on eigenshape (ES) axes ES1 and ES2 (A), and ES2 and ES3 (B) axes, describing interspecific differences in opercle shape. Branch lengths are taken from Matschiner et al. (2011), branches are colored by clade, and the root is denoted by concentric circles shaded black. Mean shape models illustrate, using vector displacements, the patterns of outline shape change associated with each axis. Tip labels, see Results for detail: a, *Notothenia rossii;* b, *Chaenocephalus aceratus;* c, *Neopagetopsis ionah;* d, *Trematomus tokarevi*; e, *Trematomus eulepidotus*.

of the distal margin. Positive ES2 scores reflected changes along these axes in the opposite direction (i.e., compression instead of extension, and vice versa). Similar to ES1, *N. rossii* also occupied the most negative portion of ES2, whereas specimens of *Neopagetopsis ionah* (Fig. 3A, label c) had the greatest positive scores, equating to a lateral extension of the distal tip of the operculum, resulting in a right-angled triangle shape appearance of the bone. ES3 accounted for 14.9% of shape variance, and shape

differences included a combination of variance explained by ES1 and ES2, thus resulting in two antagonistic modes of shape change occurring along each margin of the bone (Fig. 3B).

Results from ANOVA tests performed on ES1–ES8 scores, representing 95.8% of the sample variance, using "families" as groups indicated significant differences between Channichthyidae and Nototheniidae along ES1 ($F_{3,89} = 8.525$, $P < 0.001$, Bonferroni corrected), ES2 ($F_{3,89} = 12.387$, $P < 0.001$, Bonferroni corrected), and ES3 ($F_{3,89} = 4.706$, $P < 0.001$, Bonferroni corrected). Canonical variates analysis (CVA) performed on ES1–ES8 scores using all specimens in the sample, resulted in three canonical functions that explained 100% of the sample variance. Only the first canonical function (eigenvalue = 2.73) accounting for 95.6% of the variance was significant using Wilks' Lambda ($\chi^2_{18,\ 89} = 119.46$, $P < 0.001$) (Table S3).

Disparity through time

Phylomorphospace plots of ES1 versus ES2 (Fig. 3A) and of ES2 versus ES3 (Fig. 3B) indicate a phylogenetic structuring of taxon distribution in shape space, particularly the separation of Nototheniidae and Channichthyidae and the distribution of Bathydraconidae and Artedidraconidae typically in-between those other two families. Average clade disparities for each clade were calculated from tip disparity values using the tip disparity function in the geiger package (per Harmon et al. 2003, 2008). These values were summed for each of the four clades and shape disparity was found to be highest for the Nototheniidae (0.96), followed by the Channichthyidae (0.67), the Artedidraconidae (0.16), and lastly the Bathydraconidae (0.11). Because sampling of species was unequal across the families, in part due to underlying differences in species diversity, the disparity values were subject to a simple standardization by number of taxa in each clade to yield an average per species, which was highest for Channichthyidae (0.096), followed by Artedidraconidae (0.081), Nototheniidae (0.074), and, lastly, Bathydraconiidae (0.055).

The DTT method was used to assess how opercle shape and size disparity compared with expected disparity based on simulations using a neutral evolution BM model (Fig. 4). Overall, shape disparity using ES scores reflecting the positioning of taxa in multivariate shape space is greater than expected by BM simulations. A similar result is obtained using only size disparity. MDI values, calculated as the area contained between the solid and dotted lines in Figure 4 or in other words the observed relative disparity points versus the line connecting median relative disparity points from the BM simulations, were similar for shape (0.341) and size data (0.453).

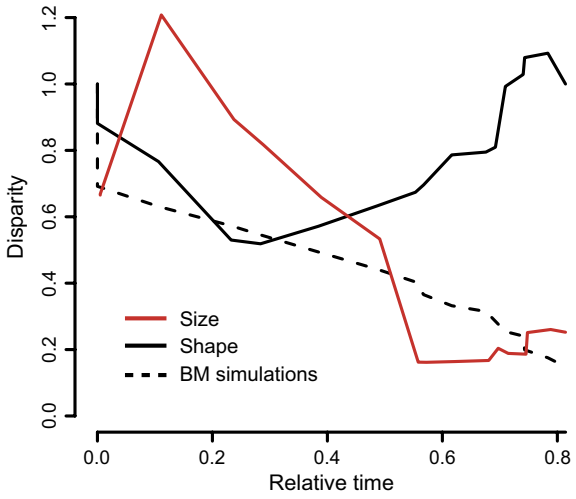

Figure 4. Disparity-through-time plot for opercle shape (solid black line) data, and opercle size from centroid size (solid red line) data. Mean values were used for species with more than one representative specimen. Disparity along the *Y* axis is the average subclade disparity divided by total clade disparity calculated at each internal node. The dotted line represents evolution of the data under Brownian motion (BM) simulations on the same phylogeny. Time values are relative time as per Harmon et al. (2003), whereby 0.0 represents the root and 1.0 represents the tip. The most recent 20% of the plot was omitted to avoid the effect of "tip overdispersion" due to missing terminal taxa (Muschick et al. 2012).

Evolutionary models

The fit of the EB, OU, and BM models was assessed using the Akaike information criterion corrected for small sample size (AICc), which can be used to compare models that have different numbers of parameters (BM has two parameters, OU has three) and therefore have noncomparable log likelihoods. AICc values indicate that the best fit to ES1 shape data was the OU model (AICc = −23.02) followed by the BM model (AICc = −19.21) and lastly the EB model (AICc = −16.59) (Table 2). A similar result was found for ES2, also best supported by OU (AICc = −33.70), followed by BM (AICc = −21.69), and least supported by the EB model (AICc = −19.06). Results of AICc weight calculations indicated a comparatively high probability that the OU model (0.84) was the best model given the data and the set of candidate models (Table 2).

Patterns of shape change in relation to habitat and trophic niche inferred from stable isotope data

A significant relationship was not found for results of PGLS regression analyses using stable isotope values for

Table 2. Comparison of evolutionary models fit to opercle shape data (ES1). Akaike weight was calculated from AICc.

Model	AIC	AICc	Log L	Akaike weight
Early Burst (EB)	−17.79	−16.59	11.89	0.034
Brownian Motion (BM)	−19.79	−19.21	11.90	0.125
Ornstein –Uhlenbeck (OU)	−24.23	−23.02	15.11	0.841

δ^{13}C and δ^{15}N against the matrix of mean scores along ES1–ES8 for all species ($r^2 < 0.15$, $P < 0.60$). Members of the Channichthyidae and the Nototheniidae showed the greatest amount of spread along ES1 and along δ^{15}N values (Fig. 5A) and a general, although not significant ($P = 0.1493$), trend of lower ES1 scores associated with higher δ^{15}N could be observed, indicating that species inferred to occupy higher trophic levels typically had opercles with elongated posterior portions of the dorsal margin and that tapered more sharply along the entire posterior margin (see Fig. 3 top-right mean shape model), although this was not evident for ES2 scores (Fig. 5B). Rutschmann et al. (2011) previously noted that species with lower δ^{13}C values were typically classified as pelagic, whereas benthic species were found to have higher δ^{13}C values. Specific regions of morphospace were not exclusively occupied by benthic or pelagic species (Fig. 6). For instance, bathydraconids and artedidraconids are considered the most benthic families within Notothenioidei (La Mesa et al. 2004), but occupied broadly average scores on ES1 (Fig. 6A) and slightly higher than average scores on ES2 (Fig. 6B), although species with the highest ES2 scores occupied either a pelagic (*N. ionah*, Fig. 6B, label a) or benthopelagic niche (*Cryodraco antarcticus*, Fig. 6B, label b). Of note, *C. aceratus*, an exception among the largely pelagic Channichthyidae, is considered a benthic predator, mainly feeding on *Champsocephalus gunnari* (Reid et al. 2007), and is found to occupy separate regions of ES1 (high positive score, Fig. 6A, label c) and ES2 (high negative score, Fig. 6B, label d) reflecting a slightly different opercle morphology to other members of the group. Labeling of specimens according to their feeding strategy indicates a broad overlap in opercle morphology between benthic and pelagic species, occupying mostly the area of −0.20 to 0.20 along ES1 by −0.10 to 0.10 along ES2 (Fig. 7). Semipelagic species, represented by *Lepidonotothen larseni* and *N. rossii* have low ES1 and ES2 scores, forming a group slightly distinct from the benthic and pelagic species (Fig. 7) and equating to an opercle with an anterior margin tapering along its length in a posterior direction such that its most ventral tip is somewhat shifted posteriorly, compared to species with higher ES scores on these two axes.

Discussion

We investigated the evolution of opercle shape in the adaptive radiation of notothenioids by quantifying shape

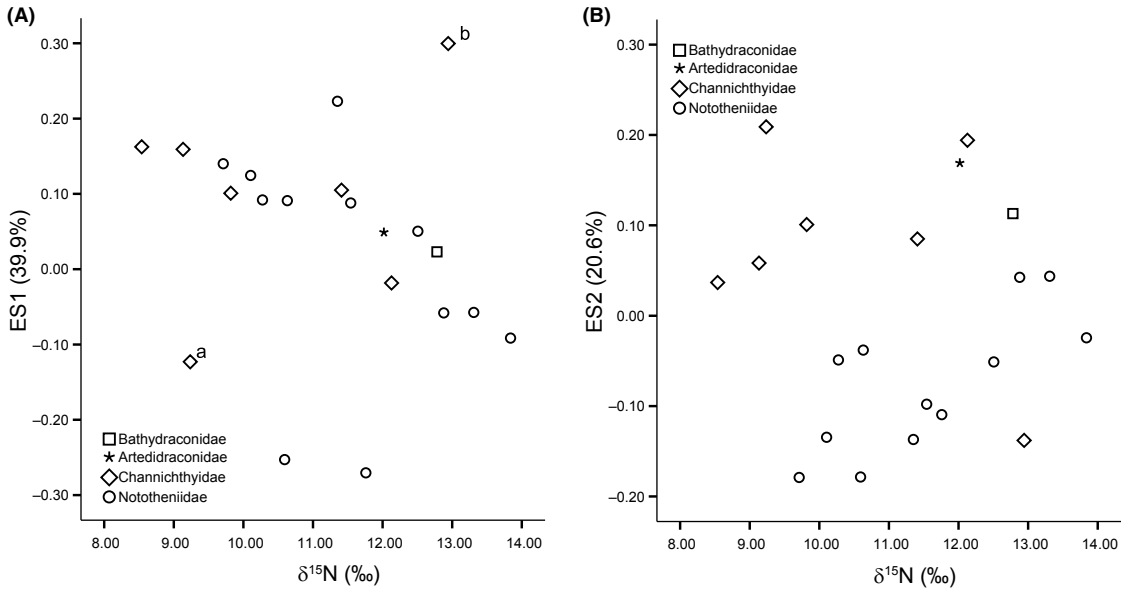

Figure 5. Mean shape scores for each notothenioid species along eigenshape (ES) axes ES1 (A) and E2 (B) plotted against mean δ^{15}N values, denoted per mil (‰), taken from Rutschmann et al. (2011). Tip labels, see Results section for further detail: a, *Neopagetopsis ionah;* b, *Chaenocephalus aceratus*.

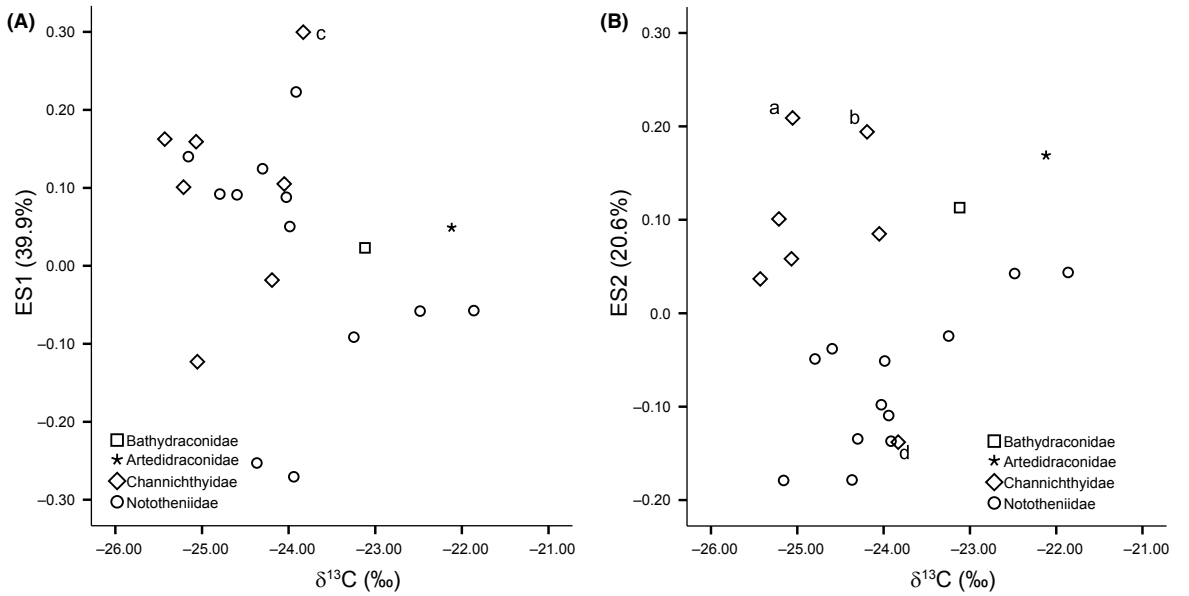

Figure 6. Mean shape scores for each notothenioid species along eigenshape (ES) axes ES1 (A) and E2 (B) plotted against mean δ^{13}C values, denoted per mil (‰), taken from Rutschmann et al. (2011). Tip labels, see Results section for further detail: a, *Neopagetopsis ionah;* b, *Cryodraco antarcticus*, c, d, *Chaenocephalus aceratus*.

disparity, phylogenetic patterns of shape evolution, and ecological correlates in the form of stable isotope values to assess how ecological and morphological (shape) disparity are interrelated. Our focus on the evolutionary morphology of a craniofacial bone addresses how shape disparity data may inform our growing understanding of the features that define the adaptive radiation model or patterns that may be uncovered across different groups.

Our main findings are that (1) DTT results show opercle shape and size disparity for subclades tended to generate higher disparity in the modern fauna than would be expected under the neutral evolution BM model (Fig. 5), and evolutionary model comparisons indicate that the OU model is the best fit to our data and the "early burst" model is the least well supported, (2) the main evolutionary axis of opercle shape change (ES1) reflects movement from a broad and rather more symmetrically tapered opercle to one that narrows along the distal margin, but with only a slight shape change on the proximal margin, (3) the distribution of taxa in shape space ordinations reveals a broad diversity of realizable opercle morphologies (Fig. 3) and phylomorphospace projections show clear phylogenetic groupings for opercle outline shape and a wide distribution of morphospace occupation for members of the family Notothenioidae, particularly extended by species belonging to the genus *Notothenia*, which occupy a portion of morphospace unexplored by other species (Fig. 4), and (4) a significant relationship was not detected between opercle shape and isotope values using PGLS regression.

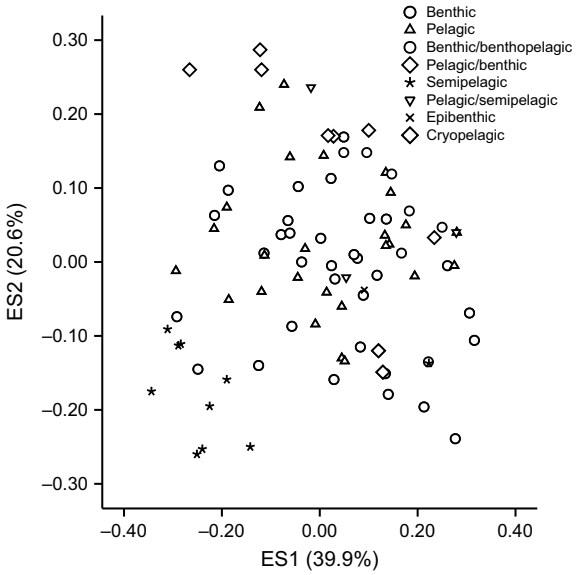

Figure 7. Plot of eigenshape (ES) axes ES1 and ES2 representing 60.5% of the sample variance. Markers indicate feeding strategy taken from literature sources (Gon and Heemstra 1990; Reid et al. 2007; Rutschmann et al. 2011).

Opercle shape and benthic/pelagic trends

In contrast to other morphological features that have been quantified in the classical examples of adaptive radiation such as cichlids and *Anolis* lizards, the study of evolutionary patterns of craniofacial bone shape has received comparatively less attention as previous studies have first focused on traits that are the likely candidates to display ecologically or functionally related variability, such as whole-body shape (Barluenga et al. 2006; Clabaut et al. 2007; Berner et al. 2010; Harrod et al. 2010) or the jaw apparatus (Muschick et al. 2011, 2012). A notable exception are the studies of Kimmel and others that have examined opercle variability (Kimmel et al. 2008; Arif et al. 2009; Kimmel et al. 2010) in different populations of three-spined sticklebacks (but see also Willacker et al. 2010), a well-established subject of study for speciation research (e.g., Schluter and McPhail 1992; Shapiro et al. 2004; Colosimo et al. 2005). The major axis of shape variation found in the opercle of three-spined stickleback populations from Iceland to diverse locations along the western coast of North America reflects a dilution–diminution mode of shape change (Kimmel et al. 2008, 2011), that is, an anterior–posterior stretching coupled with a dorsal–ventral compression of the outline shape. This pattern explains change between freshwater and marine populations, whereas the second axis of shape change (PC2: Kimmel et al. 2011) is attributed to foraging ecology along the benthic–limnetic axis and translates to an overall widening of the opercle. Our mean shape models indicate that for notothenioids the major axis of shape variability (=ES1) in the sample reflects a similar extension and compression, but these axes of shape change are not strictly in the craniocaudal and anterior–posterior direction, instead being slightly offset (Fig. 3). The general trend along ES2 also reflects a widening and narrowing of the opercle margin, as for sticklebacks (Kimmel et al. 2011). A lack of clear phylogenetic segregation in Figure 5A also indicates that along ES1 members of the Channichthyidae and Nototheniidae therefore have evolved broadly similar opercle shapes in relation to their position along the pelagic–benthic axis (Fig. 6A). Besides sticklebacks, differences in feeding mechanism are already known to be reflected in body shape and bone morphology among benthic and limnetic morphotypes in cichlids (e.g., Barluenga et al. 2006; Clabaut et al. 2007; Muschick et al. 2012). The finding that benthic species in this study generally have an extended posterior margin of the opercle compared to pelagic species is consistent with the results of Klingenberg and Ekau (1996) who examined a series of body measurements among several Nototheniidae belonging to the subfamilies Trematominae and Pleuragramminae. Klingenberg and Ekau (1996) found that benthic species had larger values for head width, which we here may consider to be reflected in the opercle by an extension of the posterior margin, and mouth length measures than pelagic species. Those authors speculated that these morphological features may reflect the larger sized prey available for consumption in benthic environments.

Evolutionary model fitting

Our data indicate a strong preference for the OU model, which models selection to a single (global) optimum for all species, and suggests that the here observed disparity patterns may result from an adaptive peak or constraint, as highlighted more broadly in several other fish radiations, such as cichlids (Young et al. 2009; Cooper et al. 2010) and in agreement with a recent broad-scale geometric morphometric study of cranial and postcranial bone shape in actinopterygians (Sallan and Friedman 2012). Assuming that a single global optimum morphology is indeed accurate for notothenioids and given the benthic/limnetic habitat variation in the clade (Rutschmann et al. 2011), one would not expect an association of opercle shape with habitat or diet, which is supported here by a lack of significant relationship between isotope values and opercle shape data. The OU model expects more evolution to be apparent on later branches of phylogeny as selection to the optimum would result in phylogenetic signal generated from evolution at earlier branches being erased. Although the OU model supports the presence of an optimum, this conclusion must be taken cautiously here because the DTT results indicate disparity is concentrated within subclades, that is, to say closely related species differ considerably in morphology. This conflicts with convergence to a single optimum (alpha), and hence we suggest support for the OU model may rather indicate loss of phylogenetic signal due to potentially rapid divergence rather than convergence to an optimum.

At early stages of an adaptive radiation it is predicted under the "early burst" model that measures of disparity are high, followed by a subsequent drop in those values as time passes and available niche space falls to zero (e.g., Seehausen 2006; McPeek 2008). Model comparison results indicate that our data fit least well to this "early burst" model, which had the highest AICc value of all three models tested. Also, although we do find early peaks in opercle shape and size disparity (Fig. 4), which would be indicative of the rapid, early filling of empty niches, our plot does not support an "early burst" scenario (e.g., Gavrilets and Vose 2005) because we find a second peak in disparity occurring later in relative time (before 0.8, Fig. 4), and under an "early burst" scenario there would be little opportunity for subsequent ecological

diversification in subclades (Harmon et al. 2003; Burbrink and Pyron 2010).

The second peak in disparity corresponds to the subclade within the family Nototheniidae including species of *Trematomus*, and the subclade comprising all representative species of the Channichthyidae with the exception of *Champsocephalus gunnari* (Fig. 1). When examining the phylomorphospace plots for ES1 and ES2 (Fig. 3A), morphospace occupation for the Channichthyidae is considerably extended by two taxa: *N. ionah* that displays low ES1 values and high ES2 values (Fig. 3A, label c) and *C. aceratus* that displays high ES1 values and low ES2 values (top right of Fig. 3A, label b). These two species may thus be contributing considerably to high values of disparity later in the DTT plot. Along with species of Notothenia, *N. ionah* also appears as an outlier on plots of δ^{15}N versus ES1 (Fig. 5A, label a), falling well below the majority of taxa in that plot. Similarly, the high score along ES1 for *C. aceratus*, which as a top benthic predator (Kock 2005; Reid et al. 2007) stands out among the other largely pelagic channichthyids, results in that species being located outside (above) the main group in Figure 5A (label b). In the case of *Trematomus*, here represented by six species, Rutschmann et al. (2011) showed that species of this genus were differentiated in isotopic signatures, indicating trophic niche separation within the genus or a large niche space, and reports of stomach contents for different species corroborate this finding (Brenner et al. 2001). Within our sample, the phylomorphospace plot indicates considerable variation particularly in ES2 scores among members of *Trematomus*, especially *T. tokarevi* (benthic, Fig. 3A label d) compared to *T. eulepidotus* (epibenthic/pelagic, Fig. 3A label e), and these differences may have contributed to elevated disparity for that node. Near et al. (2012) conducted a series of DTT analyses on buoyancy measures for 54 species of notothenioids and similarly their plots (Near et al. 2012: Fig. 3A–C) also revealed a second peak in disparity, particularly for Channichthyidae and species of *Trematomus*, which those authors related to the repeated colonization of benthic, epibenthic, semipelagic, and pelagic habitats among closely related lineages. The latter is thought to have happened as a consequence of the repeated creation of open niches following extinctions caused by icebergs and glaciers scouring the continental shelf and decimating near-shore fauna (Tripati et al. 2009; Near et al. 2012).

More broadly, the lack of an "early burst" pattern in our data set fits with the results of Harmon et al. (2010), who performed a broad survey of 49 animal clades and found little evidence of an "early burst" model of morphological change, and recently Ingram et al. (2012) suggested that this may be explained by the ubiquity of omnivory in natural food webs. Ingram et al. (2012) found that the "early burst" scenario was not detected for clades containing many omnivorous species that fed at multiple trophic levels; a feature common also for notothenioids, which include several species that feed opportunistically throughout the water column (e.g., Eastman 2005). Although omnivory was suggested as one possible determinant of the adaptive burst scenario, a general trend hinted by those results is that the persistence of an "early burst" pattern may be related to the relative extent to which niche axes (such as diet, microhabitat, and climate) are distinct and stable over time (Ingram et al. 2012).

Patterns of diversification in notothenioids

The constituent groups of the notothenioid radiation have undergone different amounts of ecological and morphological diversification, with some, such as the artedidraconids that are all sedentary benthic fishes, displaying little (Eastman 2005). Our disparity values and phylomorphospace plots to some extent reflect these patterns, particularly for the notothenioids, which display the highest disparity values and the most expanded occupation of morphospace (Fig. 3). Notothenioids are ecologically diverse and include benthic (around 50% of within-group species diversity, Eastman 1993), epibenthic, semipelagic, cryopelagic, and pelagic forms. They are also the only group containing species that have so far been determined as neutrally buoyant (*Pleuragramma antarcticum* and *D. mawsoni* are examples in our study), a feature that has been achieved, despite not possessing a swim bladder, through reduced skeletal mineralization and lipid deposition (DeVries and Eastman 1978; Eastman and DeVries 1982; Eastman 1993). Most distinct in our morphospace plots is the location of *Notothenia* species that typically have an opercle that widens at the posterior margin (ES1) and has a posteroventrally tapering dorsal margin (see top-left mean shape model, Fig. 3A). Representing the opposite end of the body mass scale compared to the neutrally buoyant members of the Nototheniidae, species of *Notothenia* are large, heavy fishes that are able to move up and down in the water column to feed on both pelagic and benthic prey, and are able to alter their diet in relation to prey availability (e.g., Fanta et al. 2003). *Notothenia coriiceps*, for example, is known to feed on macroalgae, most likely to ingest also the associated amphipods more efficiently (Iken et al. 1997; Fanta et al. 2003), when its preferred food source of krill is unavailable. *Notothenia rossii* also ingests different food during its juvenile stages, switching from a pelagic to largely benthic habit in adulthood, which may have further implications for opercle and craniofacial bone development in general. Burchett (1983) examined this ontogenetic shift

from pelagic to benthic lifestyle and found an associated change in head shape (length and diameter) and a deepening of the body over the course of ontogeny. The main result of the foraging habit versus opercle shape plot, showing broad overlap in opercle morphology among different foraging categories (Fig. 7), is perhaps not unsurprising, given the dietary plasticity of many notothenioids (Eastman 2005), the aforementioned *Notothenia* being an excellent example (e.g., Foster and Montgomery 1993). The most logical reasoning behind the range of morphotypes is that notothenioids inhabit an ecosystem with relatively low species diversity and reduced competition, both of which would not act to accelerate ecomorphological divergence (Eastman 2005) to the degree found among other radiations.

Conclusions

A major impetus for the study of adaptive radiations is to uncover generalized patterns among different groups. In this way, common features may speak for the importance of a given process in the generation of morphological diversity (Gavrilets and Losos 2009). Here, we use outline-based geometric morphometrics to quantify opercle shape across notothenioids. We identify axes of shape change, particularly a widening of the opercle bone, that have been recovered in other adaptive radiations (threespined sticklebacks) and a trend in opercle shape change along the benthic–pelagic axis, underlining the importance of this axis for diversification in notothenioids. We find that opercle shape and size disparity for subclades tended to generate higher disparity in the modern fauna than would be expected under neutral evolution, and that the OU model best fits the evolution of opercle shape. Support for the OU model may reflect loss of phylogenetic signal due to potentially rapid divergence. Opercle shape represents one of few features that can be quantitatively assessed for both extant and extinct species flocks (Wilson et al. 2013b), and therefore provides an especially useful opportunity for integrative study between evolutionary biology and paleontology (e.g., Sánchez-Villagra 2010; Wilson 2013b), an approach that has yet to be fully explored in the context of adaptive radiation, and one that holds potential to yield valuable insights into modes of species diversification in deep time.

Acknowledgments

We thank the Thünen-Institute of Fisheries Ecology for giving M. C. the opportunity to participate in the RV Polarstern expedition ANT-XXVIII/4, and Malte Damerau and the whole Polarstern crew for their excellent work and help during that expedition. We thank Michael Matschiner, Moritz Muschick, Robin Beck, and Steve Heard for helpful comments. This project is supported by the Swiss National Fund Sinergia project granted to W. S., M. R. S.-V., and Heinz Furrer (CRSII3-136293). L. A. B. W. is currently supported by a fellowship from the Swiss National Fund (PBZHP3_141470).

Conflict of Interest

None declared.

References

Adams, D. C., F. J. Rohlf, and D. E. Slice. 2004. Geometric morphometrics: ten years of progress following the 'revolution'. Ital. J. Zool. 71:5–16.

Akaike, H. 1974. A new look at the statistical model identification. IEEE Trans. Automat. Contr. 19:716–723.

Anker, G. Ch.. 1974. Morphology and kinetics of the head of the stickleback, *Gasterosteus aculeatus*. Trans. Zool. Soc. Lond. 32:311–416.

Arif, S., W. E. Aguirre, and M. A. Bell. 2009. Evolutionary diversification of opercle shape in Cook Inlet threespine stickleback. Biol. J. Linn. Soc. 97:832–844.

Arnqvist, G., and T. Martensson. 1998. Measurement error in geometric morphometrics: empirical strategies to assess and reduce its impact on measures of shape. Acta Zool. Academ. Sci. Hung. 44:73–96.

Arthur, W. 2004. The effect of development on the direction of evolution: toward a twenty-first century consensus. Evol. Dev. 6:282–288.

Astrop, T. I. 2011. Phylogeny and evolution of Mecochiridae (Decapoda: Reptantia: Glypheoidea): an integrated morphometric and cladistic approach. J. Crustacean Biol. 31:114–125.

Barluenga, M., K. N. Stölting, W. Salzburger, M. Muschick, and A. Meyer. 2006. Sympatric speciation in Nicaraguan crater lake cichlid fish. Nature 439:719–723.

Bemis, W. E., and G. V. Lauder. 1986. Morphology and function of the feeding apparatus of the lungfish, *Lepidosiren paradoxa* (Dipnoi). J. Morphol. 187:81–108.

Berner, D., M. Roesti, A. P. Hendry, and W. Salzburger. 2010. Constraints on speciation suggested by comparing lake-stream stickleback divergence across two continents. Mol. Ecol. 19:4963–4978.

Blomberg, S. P., J. G. Lefevre, J. A. Wells, and M. Waterhouse. 2012. Independent contrasts and PGLS regression estimators are equivalent. Syst. Biol. 61:382–391.

Bookstein, F. L. 1991. P. 435 *in*Morphometric tools for landmark data. Cambridge Univ. Press, Cambridge 435 pp.

Brakefield, P. M. 2006. Evo-devo and constraints on selection. Trends Ecol. Evol. 21:362–368.

Brenner, M., B. H. Buck, S. Cordes, L. Dietrich, U. Jacob, K. Mintenbeck, et al. 2001. The role of iceberg scours in

niche separation within the Antarctic fish genus *Trematomus*. Polar Biol. 24:502–507.
Burbrink, F. T., and R. A. Pyron. 2010. How does ecological opportunity influence rates of speciation, extinction, and morphological diversification in New World rat snakes (Tribe Lampropeltini)? Evolution 64:934–943.
Burchett, M. S. 1983. Food, feeding and behaviour of Notothenia rossii nearshore at South Georgia. Brit. Antarct. Surv. Bull. 61:45–51.
Burnham, K. P., and D. R. Anderson. 2010. Model selection and multimodel inference. Springer, New York, NY.
Butler, M. A., and A. King. 2004. Phylogenetic comparative analysis: a modelling approach for adaptive evolution. Am. Nat. 164:683–695.
Carroll, S. B. 2005. Endless forms most beautiful: the new science of Evo Devo and the making of the Animal Kingdom. W. W. Norton and Company Inc, New York, NY.
Chen, L., A. L. De Vries, and C.-H. C. Cheng. 1997. Evolution of antifreeze glycoprotein gene from a trypsinogen gene in Antarctic notothenioid fish. Proc. Natl. Acad. Sci. USA 94:3811–3816.
Cheng, C.-H. C., P. A. Cziko, and C. W. Evans. 2006. Nonhepatic origin of notothenioid antifreeze reveals pancreatic synthesis as common mechanism in polar fish freezing avoidance. Proc. Natl Acad. Sci. 103:10491–10496.
Clabaut, C., P. M. E. Bunje, W. Salzburger, and A. Meyer. 2007. Geometric morphometric analyses provide evidence for the adaptive character of the Tanganyikan cichlid fish radiation. Evolution 61:560–578.
Collar, D. C., and P. C. Wainwright. 2006. Discordance between morphological and mechanical diversity in the feeding mechanism of centrarchid fishes. Evolution 60: 2575–2584.
Colosimo, P. F., K. E. Hosemann, S. Balabhadra, G. Villareal, M. Dickson, J. Grimwood, et al. 2005. Widespread parallel evolution in sticklebacks by repeated fixation of ectodysplasin alleles. Science 307:1928–1933.
Cooper, W. J., and M. W. Westneat. 2009. Form and function of damselfish skulls: rapid and repeated evolution into a limited number of tropic niches. BMC Evol. Biol. 9:24.
Cooper, W. J., K. Parsons, A. McIntyre, B. Kern, A. McGee-Moore, R. C. Albertson, et al. 2010. Bentho-pelagic divergence of cichlid feeding architecture was prodigious and consistent during multiple adaptive radiations within African rift lakes. PLoS One 5:e9551.
Cubbage, C. C., and P. M. Mabee. 1996. Development of the cranium and paired fins in the zebrafish *Danio rerio* (Ostariophysi, Cyprinidae). J. Morphol. 229:121–160.
Day, J. J., C. R. Peart, K. J. Brown, J. P. Friel, R. Bills, and T. Moritz. 2013. Continental diversification of an African catfish radiation (Mochokidae: *Synodontis*). Syst. Biol. 62:351–365.
Dayton, P. K., G. A. Robillia, and A. L. Devries. 1969. Anchor ice formation in McMurdo Sound Antarctica and its biological effects. Science 163:273–274.
DeVries, A. L., and J. T. Eastman. 1978. Lipid sacs as a buoyancy adaptation in an Antarctic fish. Nature 271: 352–353.
DeWitt, H. H. 1985. Reports on fishes of the University of Southern California Antarctic Research Program, 1962–1968. I. A review of the genus *Bathydraco* Günther (family Bathydraconidae). Cybium 9:295–314.
Dyreson, E., and W. P. Maddison. 2003. Rhetenor package for morphometrics for the Mesquite system.
Eakin, R. R., J. T. Eastman, and T. J. Near. 2009. A new species and a molecular phylogenetic analysis of the Antarctic fish genus *Pogonophryne* (Notothenioidei: Artedidraconidae). Copeia 4:705–713.
Eastman, J. T. 1993. Antarctic fish biology: evolution in a unique environment. Academic Press, San Diego.
Eastman, J. T. 2005. The nature of the diversity of Antarctic fishes. Polar Biol. 28:93–107.
Eastman, J. T., and A. L. DeVries. 1982. Buoyancy studies of notothenioid fishes in McMurdo Sound, Antarctica. Copeia 2:385–393.
Eastman, J. T., and A. R. McCune. 2000. Fishes on the Antarctic continental shelf: evolution of a marine species flock? J. Fish Biol. 57:84–102.
Ekau, W. 1991. Morphological adaptations and mode of life in high Antarctic fish. Pp. 23–39 *in* G. di Prisco, B. Maresca and B. Tota, eds. Biology and Antarctic fish. Springer, Berlin.
Erwin, D. H. 2007. Disparity: morphological pattern and developmental context. Palaeontology 50:57–73.
Fanta, E., F. S. Rios, L. Donatti, and W. E. Cardoso. 2003. Spatial and temporal variation in krill consumption by the Antarctic fish *Notothenia coriiceps*, in Admiralty Bay, King George Island. Antarct. Sci. 15:458–462.
Fischer, W., and J. C. Hureau. 1985. FAO species identification sheets for fishery purposes. South Ocean: fishing areas 48, 58 and 88 (CCAMLR convention area). Vol. 1. Food and agriculture organization of the United Nations, Rome.
Foster, B. A., and J. C. Montgomery. 1993. Planktivory in benthic nototheniid fish in McMurdo Sound, Antarctica. Environ. Biol. Fishes 35:313–318.
Gavrilets, S., and J. B. Losos. 2009. Adaptive radiation: contrasting theory with data. Science 323:732–737.
Gavrilets, S., and A. Vose. 2005. Dynamic patterns of adaptive radiation. Proc. Natl. Acad. Sci. USA 102:18040–18045.
Gerking, S. D. 1994. Feeding ecology of fish. Academic Press, San Diego.
Glor, R. E. 2010. Phylogenetic insights on adaptive radiation. Annu. Rev. Ecol. Evol. Syst. 41:251–270.
Gon, O., and P. C. Heemstra. 1990. Fishes of the Southern Ocean. JLB Smith Institute of Ichthyology, Grahamstown.

Gould, S. J. 1989. Wonderful life: the burgess shale and the nature of history. W. W. Norton and Co, New York, NY.

Grant, P. R., and B. R. Grant. 2006. Evolution of character displacement in Darwin's finches. Science 313:224–226.

Grubich, J. R., A. N. Rice, and M. W. Westneat. 2008. Functional morphology of bite mechanics in the great barracuda (*Sphyraena barracuda*). Zoology 111:16–29.

Hansen, T. F., J. Pienaar, and S. H. Orzack. 2008. A comparative method for studying adaptation to a randomly evolving environment. Evolution 62:1965–1977.

Harder, L. D. 2001. Mode and tempo of species diversification. Am. J. Bot. 88:1707–1710.

Harmon, L. J., J. A. Schulte, A. Larson, and J. B. Losos. 2003. Tempo and mode of evolutionary radiation in iguanian lizards. Science 301:961–964.

Harmon, L. J., J. T. Weir, C. D. Brock, R. E. Glor, and W. Challenger. 2008. GEIGER: investigating evolutionary radiations. Bioinformatics 24:129–131.

Harmon, L. J., J. B. Losos, T. J. Davies, R. G. Gillespie, J. L. Gittleman, W. B. Jennings, et al. 2010. Early burst of body size and shape evolution are rare in comparative data. Evolution 64:2385–2396.

Harrod, C., J. Mallela, and K. K. Kahilainen. 2010. Phenotype-environment correlations in a putative whitefish adaptive radiation. J. Anim. Ecol. 79:1057–1068.

Hobson, K. A., J. F. Piatt, and J. Pitocchelli. 1994. Using stable isotopes to determine seabird trophic relationships. J. Anim. Ecol. 63:786–798.

Hofmann, G. E., S. G. Lund, S. P. Place, and A. C. Whitmer. 2005. Some like it hot, some like it cold: the heat shock response is found in New Zealand but not Antarctic notothenioid fishes. J. Exp. Mar. Biol. Ecol. 316:79–89.

Holzman, R., and P. C. Wainwright. 2009. How to surprise a copepod: strike kinematics reduce hydrodynamic disturbance and increase stealth of suction-feeding fish. Limnol. Oceanogr. 54:2201–2212.

Holzman, R., D. C. Collar, S. A. Price, C. D. Hulsey, R. C. Thomson, and P. C. Wainwright. 2012. Biomechanical trade-offs bias rates of evolution in the feeding apparatus of fishes. Proc. Biol. Sci. 279:1287–1292.

Hughes, G. M. 1960. A comparative study of gill ventilation in marine teleosts. J. Exp. Biol. 37:28–45.

Hunt, G., and M. T. Carrano. 2010. Models and methods for analysing phenotypical evolution in lineages and clades. Pp. 245–269 *in* J. Alroy and G. Hunt, eds. Quantitative methods in paleobiology. Paleontological Society Short Course, 30 October 2010. Vol. 16. The Paleontological Society Papers, Boulder, CO.

Hunt, B. M., K. Hoefling, and C.-H. Cheng. 2003. Annual warming episodes in seawater temperatures in McMurdo Sound in relationship to endogenous ice in notothenioid fish. Antarct. Sci. 15:333–338.

Iken, K., E. R. Barrera-Oro, M. L. Quartino, R. J. Casaux, and T. Brey. 1997. Grazing by the Antarctic fish Notothenia coriiceps: evidence for selective feeding on macroalgae. Antarcti. Sci. 9:386–391.

Ingram, T., L. J. Harmon, and J. B. Shurin. 2012. When should we expect early bursts of trait evolution in comparative data? Predictions from an evolutionary food web model. J. Evol. Biol. 25:1902–1910.

Jackson, D. A. 1993. Stopping rules in principal components analysis: a comparison of heuristical and statistical approaches. Ecology 74:2204–2214.

Jones, F. C., M. G. Grabherr, Y. F. Chan, P. Russell, E. Mauceli, J. Johnson, et al. 2012a. The genomic basis of adaptive evolution in threespine sticklebacks. Nature 484:55–61.

Jones, F. C., Y. F. Chan, J. Schmutz, J. Grimwood, S. Brady, A. M. Southwick, et al. 2012b. A genome-wide SNP genotyping array reveals patterns of global and repeated species pair divergence in sticklebacks. Curr. Biol. 22:83–90.

Kimmel, C. B., A. DeLaurier, B. Ullmann, J. Dowd, and M. McFadden. 2010. Modes of developmental outgrowth and shaping of a craniofacial bone in zebrafish. PLoS ONE 5: e9475.

Kimmel, C. B., B. Ullmann, C. Walker, C. Wilson, M. Currey, P. C. Phillips, et al. 2005. Evolution and development of facial bone morphology in threespine sticklebacks. Proc. Natl. Acad. Sci. USA 102:5791–5796.

Kimmel, C. B., W. E. Aguirre, B. Ullmann, M. Currey, and W. A. Cresko. 2008. Allometric change accompanies opercular shape evolution in Alaskan threespine sticklebacks. Behaviour 145:669–691.

Kimmel, C. B., W. A. Cresko, P. C. Phillips, B. Ullmann, M. Currey, F. von Hippel, et al. 2011. Independent axes of genetic variation and parallel evolutionary divergence of opercle bone shape in threespine stickleback. Evolution 66:419–434.

Klingenberg, C. P. 2010. Evolution and development of shape: integrating quantitative approaches. Nat. Rev. Genet. 11:623–635.

Klingenberg, C. P., and E. Ekau. 1996. A combined morphometric and phylogenetic analysis of an ecomorphological trend: pelagization in Antarctic fishes (Perciformes: Nototheniidae). Biol. J. Linn. Soc. 59:143–177.

Kocher, T. D. 2004. Adaptive evolution and explosive speciation: the cichlid fish model. Nat. Rev. Genet. 5:288–298.

Kock, K. H. 2005. Antarctic fishes (Channichthyidae): a unique family of fishes. A review, part I. Polar Biol. 28:862–895.

Krieger, J. D., R. P. Guralnick, and D. M. Smith. 2007. Generating empirically determined continuous measures of leaf shape for paleoclimate reconstruction. Palaios 22:212–219.

La Mesa, M., J. T. Eastman, and M. Vacchi. 2004. The role of notothenioid fish in the food web of the Ross Sea shelf waters: a review. Polar Biol. 27:321–338.

Lau, Y.-T., S. K. Parker, T. J. Near, and H. W. III Detrich. 2012. Evolution and function of the globin intergenic regulatory regions of the Antarctic dragonfishes (Notothenioidei: Bathydraconidae). Mol. Biol. Evol. 29:1071–1080.

Lauder, G. 1979. Feeding mechanics in primitive teleosts and in the halecomorph fish *Amia calva*. J. Zool. 187:543–578.

Lauder, G. V. 1983. Functional design and evolution of pharyngeal jaw apparatus in Euteleostean fishes. Zool. J. Linn. Soc. 77:1–38.

Losos, J. B. 2009. Lizards in an evolutionary tree: ecology and adaptive radiation of anoles. Univ. of California Press, Berkley.

MacLeod, N. 1999. Generalizing and extending the eigenshape method of shape space visualization and analysis. Paleobiology 25:107–138.

Maddison, W. P., and D. R. Maddison. 2011. Mesquite: a modular system for evolutionary analysis. Version 2.75. Available at http://mesquiteproject.org.

Makinen, H. S., and J. Merila. 2008. Mitochondrial DNA phylogeography of the three spined stickleback (*Gasterosteus aculeatus*) in Europe – evidence for multiple glacial refugia. Mol. Phylogenet. Evol. 46:167–182.

Marroig, G., and J. M. Cheverud. 2005. Size as a line of least evolutionary resistance: diet and adaptive morphological radiation in new world monkeys. Evolution 59:1128–1142.

Marroig, G., and J. M. Cheverud. 2010. Size as a line of least resistance II: direct selection on size or correlated response due to constraints? Evolution 64:1470–1488.

Matschiner, M., R. Hanel, and W. Salzburger. 2011. On the origin and trigger of the notothenioid adaptive radiation. PLoS One 6:18911.

McPeek, M. A. 2008. The ecological dynamics of clade diversification and community assembly. Am. Nat. 172: E270–E284.

Mehta, R. S., and P. C. Wainwright. 2008. Functional morphology of the pharyngeal jaw apparatus in moray eels. J. Morphol. 269:604–619.

Mitteroecker, P., and P. Gunz. 2009. Advances in geometric morphometrics. Evol. Biol. 36:235–247.

Muschick, M., M. Barluenga, W. Salzburger, and A. Meyer. 2011. Adaptive phenotypic plasticity in the Midas cichlid fish pharyngeal jaw and its relevance in adaptive radiation. BMC Evol. Biol. 11:116.

Muschick, M., A. Indermaur, and W. Salzburger. 2012. Convergent evolution within an adaptive radiation of cichlid fishes. Curr. Biol. 22:1–7.

Near, T. J., A. Dornburg, K. L. Kuhn, J. T. Eastman, J. N. Pennington, T. Patarnello, et al. 2012. Ancient climate change, antifreeze, and the evolutionary diversification of Antarctic fishes. Proc. Natl. Acad. Sci. USA 109:3434–3439.

Olson, M. E., and A. Arroyo-Santos. 2009. Thinking in continua: beyond the "adaptive radiation" metaphor. Bioessays 31:1337–1346.

Pigliucci, M. 2008. Sewall Wright's adaptive landscapes: 1932 vs. 1988. Biol. Philos. 23:591–603.

Polly, P. D. 2003. Paleophylogeography: the tempo of geographic differentiation in marmots (Marmota). J. Mammal. 84:369–384.

Post, D. M. 2002. Using stable isotopes to estimate trophic position: models, methods, and assumptions. Ecology 83:703–718.

Raff, R. A. 2007. Written in stone: fossils, genes and evo-devo. Nat. Rev. Genet. 8:911–920.

Reid, W. D. K., S. Clarke, M. A. Collins, and M. Belchier. 2007. Distribution and ecology of *Chaenocephalus aceratus* (Channichthyidae) around South Georgia and Shag Rocks (Southern Ocean). Polar Biol. 30:1523–1533.

Rohlf, F. J. 2001. Comparative methods for the analysis of continuous variables: geometric interpretations. Evolution 55:2143–2160.

Rohlf, F. J. 2010. tpsDig Version 2.16. Department of Ecology and Evolution, State University of New York at Stony Brook, New York, NY.

Rutschmann, S., M. Matschiner, M. Damerau, M. Muschick, M. F. Lehmann, R. Handel, et al. 2011. Parallel ecological diversification in Antarctic notothenioid fishes as evidence for adaptive radiation. Mol. Ecol. 20:4707–4721.

Salazar-Ciudad, I. 2006. On the origins of morphological disparity and its diverse developmental bases. Bioessays 28:1112–1122.

Sallan, L. C., and M. Friedman. 2012. Heads or tails: staged diversification in vertebrate evolutionary radiations. Proc. Biol. Sci. 279:2025–2032.

Salzburger, W. 2009. The interaction of sexually and naturally selected traits in the adaptive radiations of cichlid fishes. Mol. Ecol. 18:169–185.

Sánchez-Villagra, M. R. 2010. Developmental palaeontology in synapsids: the fossil record of ontogeny in mammals and their closest relatives. Proc. Biol. Sci. 277: 1139–1147.

Santos, M. E., and W. Salzburger. 2012. How cichlids diversify. Science 338:619–621.

Schluter, D. 2000. The ecology of adaptive radiation. Oxford Univ. Press, New York, NY. 296 pp.

Schluter, D., and J. D. McPhail. 1992. Ecological character displacement and speciation in sticklebacks. Am. Nat. 140:85–108.

Seehausen, O. 2006. African cichlid fish: a model system in adaptive radiation research. Proc. Biol. Sci. 273:1987–1998.

Seehausen, O. 2007. Chance, historical contingency and ecological determinism jointly determine the rate of adaptive radiation. Heredity 99:361–363.

Shapiro, M. D., M. E. Marks, C. L. Peichel, B. K. Blackman, K. S. Nereng, B. Jonsson, et al. 2004. Genetic and developmental basis of evolutionary pelvic reduction in threespine sticklebacks. Nature 428:717–723.

Sidlauskas, B. L. 2008. Continuous and arrested morphological diversification in sister clades of characiform fishes: a phylomorphospace approach. Evolution 62:3135–3156.

Simpson, G. G. 1953. The major features of evolution. Columbia Univ. Press, New York, NY.

Tripati, A. K., C. D. Roberts, and R. D. Eagle. 2009. Coupling of CO_2 and ice sheet stability over major climate transitions of the last 20 million years. Science 326: 1394–1397.

Wagenmakers, E., and S. Farrel. 2004. AIC model selection using Akaike weights. Psychon. Bull. Rev. 11:192–196.

Wainwright, P. C. 1996. Ecological explanation through functional morphology: the feeding biology of sunfishes. Ecology 77:1336–1343.

Westneat, M. W. 2006. Skull biomechanics and suction feeding in fishes. Pp. 29–75 *in* G. V. Lauder and R. E. Shadwick, eds. Fish biomechanics. Elsevier Academic Press, San Diego, CA.

Westneat, M. W., M. E. Alfaro, P. C. Wainwright, D. R. Bellwood, J. R. Grubich, J. L. Fessler, et al. 2005. Local phylogenetic divergence and global evolutionary convergence of skull function in reef fishes of the family Labridae. Proc. Biol. Sci. 272:992–1000.

Willacker, J. J., F. A. Von Hippel, P. R. Wilton, and K. M. Walton. 2010. Classification of threespine stickleback along the benthic-limnetic axis. Biol. J. Linn. Soc. 101:595–608.

Wilson, L. A. B. 2013a. Geographic variation in the greater Japanese shrew-mole, Urotrichus talpoides: combining morphological and chromosomal patterns. Mamm. Biol. 78:267–275.

Wilson, L. A. B. 2013b. The contributions of developmental palaeontology to extensions of evolutionary theory. Acta Zool. 94:254–260.

Wilson, L. A., N. MacLeod, and L. T. Humphrey. 2008. Morphometric criteria for sexing juvenile human skeletons using the ilium. J. Forensic Sci. 53:269–278.

Wilson, L. A. B., H. F. V. Cardoso, and L. T. Humphrey. 2011. A blind test of six criteria of the juvenile ilium. Forensic Sci. Int. 206:35–42.

Wilson, L. A. B., H. Furrer, R. Stockar, and M. R. Sánchez-Villagra. 2013. A quantitative evaluation of evolutionary patterns in opercle bone shape in *Saurichthys* (Actinopterygii: Saurichthyidae). Palaeontology 56: 901–915.

Wright, S. 1932. The role of mutation, inbreeding, crossbreeding, and selection in evolution. Proc. 6th Internat. Congr. Genet.1:356–366

Young, K. A., J. Snoeks, and O. Seehausen. 2009. Morphological diversity and the roles of contingency, changes and determinism in African cichlid radiations. PLoS One 4:e4740.

Zahn, C. T., and R. Z. Roskies. 1972. Fourier shape descriptors for closed plane curves. IEEE T. Comput. C-21:269–281.

Zelditch, M. L., D. L. Swiderski, and H. D. Sheets. 2004. Geometric morphometrics for biologists: a primer. Elsevier Academic Press, London.

Supporting Information

Additional Supporting Information may be found in the online version of this article:

Table S1. Specimens analysed in this study.
Table S2. Measurement error results for ES1–ES6 calculated from one-way ANOVAS (df = 1, 39).
Table S3. Results of canonical variates analysis (CVA) on complete sample, using "families" as groups.
Table S4. Information about the trawls from which photographed specimens were collected.

2.3.2
Supporting information

Table S1. Specimens analysed in this study.

Species	Group	Photo Identifier (see Table S4 for trawl information on each specimen)	Stable Isotope (species average)		Habitat	Habitat Reference	Family	Scores on Eigenshape (ES) axes							
			C13	N15				ES1	ES2	ES3	ES4	ES5	ES6	ES7	ES8
Akarotaxis nudiceps		Akarotaxis_nudiceps_1_2			benthic	a	Bathydraconidae	0.261	-0.005	-0.058	-0.075	-0.041	0.032	-0.036	0.016
Chaenocephalus aceratus		Chaenocephalus_aceratus_17_2	-23.831	12.942	benthic		Channichthyidae	0.316	-0.106	-0.183	-0.13	0.094	0.051	-0.016	-0.015
Chaenocephalus aceratus		Chaenocephalus_aceratus_29_2	-23.831	12.942	benthic		Channichthyidae	0.277	-0.239	-0.177	-0.208	0.146	0.032	-0.053	-0.038
Chaenocephalus aceratus		Chaenocephalus_aceratus_9_5	-23.831	12.942	benthic		Channichthyidae	0.306	-0.069	-0.029	-0.053	0.005	0.017	0.046	-0.02
Champsocephalus gunnari		Champsocephalus_gunnari_10_2	-25.2133	9.8181	pelagic		Channichthyidae	0.28	0.04	0.013	0.071	-0.036	0.053	0.056	0.026
Champsocephalus gunnari		Champsocephalus_gunnari_11_2	-25.2133	9.8181	pelagic		Channichthyidae	0.135	0.121	-0.005	0.089	0.025	0.008	0.019	0.055
Champsocephalus gunnari		Champsocephalus_gunnari_15_4	-25.2133	9.8181	pelagic		Channichthyidae	-0.061	0.142	-0.084	-0.062	0.06	-0.04	-0.058	0.025
Champsocephalus gunnari		Champsocephalus_gunnari_21_2	-25.2133	9.8181	pelagic		Channichthyidae	-0.073	0.24	0.033	0.01	0.198	-0.025	-0.005	0.002
Champsocephalus gunnari		Champsocephalus_gunnari_22_2	-25.2133	9.8181	pelagic		Channichthyidae	0.142	0.024	0.095	0.122	0.044	0.016	0.028	-0.01
Champsocephalus gunnari		Champsocephalus_gunnari_2_3	-25.2133	9.8181	pelagic		Channichthyidae	0.275	-0.005	-0.141	0.102	0.005	0.058	0.007	-0.074
Champsocephalus gunnari		Champsocephalus_gunnari_4_2	-25.2133	9.8181	pelagic		Channichthyidae	0.008	0.144	0.086	0.091	0.144	0.061	-0.054	-0.006
Chionodraco rastrospinosus		Chionodraco_rastrospinosus_10_2	-25.068	9.133	benthic/benthopelagic		Channichthyidae	0.183	0.069	0.088	0.014	-0.055	0.064	0.034	0.064
Chionodraco rastrospinosus		Chionodraco_rastrospinosus_14_2	-25.068	9.133	benthic/benthopelagic		Channichthyidae	0.147	0.119	-0.017	0.033	-0.125	0.037	-0.029	0.003
Chionodraco rastrospinosus		Chionodraco_rastrospinosus_26_2	-25.068	9.133	benthic/benthopelagic		Channichthyidae	0.096	0.148	-0.037	0.022	0.028	-0.005	0.018	0.035
Chionodraco rastrospinosus		Chionodraco_rastrospinosus_2_2	-25.068	9.133	benthic/benthopelagic		Channichthyidae	0.167	0.012	-0.238	-0.114	0.028	-0.001	-0.004	0.03
Chionodraco rastrospinosus		Chionodraco_rastrospinosus_3_3	-25.068	9.133	benthic/benthopelagic		Channichthyidae	0.222	-0.135	-0.145	-0.085	0.077	0.029	-0.032	-0.006
Chionodraco rastrospinosus		Chionodraco_rastrospinosus_8_2	-25.068	9.133	benthic/benthopelagic		Channichthyidae	0.049	0.148	-0.013	0.137	0.012	0.059	-0.026	-0.022
Chionodraco rastrospinosus		Chionodraco_rastrospinosus_9_2	-25.068	9.133	benthic/benthopelagic		Channichthyidae	0.25	0.047	-0.021	0.079	-0.039	-0.009	0.082	0.016
Cryodraco antarcticus		Cryodraco_antarcticus_11_2	-24.192	12.128	pel/bent		Channichthyidae	0.234	0.033	0.068	0.086	-0.037	0.049	0.053	-0.001
Cryodraco antarcticus		Cryodraco_antarcticus_12_3	-24.192	12.128	pel/bent		Channichthyidae	0.028	0.17	-0.002	0.057	-0.048	0.017	0.012	0.01
Cryodraco antarcticus		Cryodraco_antarcticus_13_2	-24.192	12.128	pel/bent		Channichthyidae	-0.122	0.287	-0.011	-0.061	0.053	-0.013	-0.001	-0.011
Cryodraco antarcticus		Cryodraco_antarcticus_14_2	-24.192	12.128	pel/bent		Channichthyidae	-0.119	0.26	-0.076	0.006	0.028	0.028	-0.006	0.013
Cryodraco antarcticus		Cryodraco_antarcticus_15_3	-24.192	12.128	pel/bent		Channichthyidae	-0.266	0.26	-0.032	-0.09	0.088	-0.083	0.072	-0.027
Cryodraco antarcticus		Cryodraco_antarcticus_16_2	-24.192	12.128	pel/bent		Channichthyidae	0.017	0.171	0.024	0.007	0.029	0.004	-0.009	0.049
Cryodraco antarcticus		Cryodraco_antarcticus_23_2	-24.192	12.128	pel/bent		Channichthyidae	0.1	0.178	0.037	0.023	-0.073	0.059	-0.026	0.03
Dissostichus mawsoni		Dissostichus_mawsoni_11_2	-23.2471	13.8371	pelagic		Nototheniidae	0.045	-0.13	0.19	-0.083	0.043	0.022	0.012	0.033
Dissostichus mawsoni		Dissostichus_mawsoni_13_2	-23.2471	13.8371	pelagic		Nototheniidae	0.045	-0.06	0.16	-0.001	0.031	0.043	-0.035	0.012
Dissostichus mawsoni		Dissostichus_mawsoni_14_2	-23.2471	13.8371	pelagic		Nototheniidae	0.014	-0.041	0.173	0.009	0.015	-0.023	-0.044	-0.019
Dissostichus mawsoni		Dissostichus_mawsoni_15_2	-23.2471	13.8371	pelagic		Nototheniidae	-0.03	0.018	0.159	-0.004	0.026	0.101	-0.054	0
Dissostichus mawsoni		Dissostichus_mawsoni_17_2	-23.2471	13.8371	pelagic		Nototheniidae	-0.19	0.074	0.077	0.031	0.011	0.047	-0.036	-0.045
Dissostichus mawsoni		Dissostichus_mawsoni_18_3	-23.2471	13.8371	pelagic		Nototheniidae	-0.216	0.045	0.045	-0.064	0	-0.035	0.016	-0.052
Dissostichus mawsoni		Dissostichus_mawsoni_1_3	-23.2471	13.8371	pelagic		Nototheniidae	-0.119	-0.04	0.162	0.043	0.005	0.051	-0.06	-0.052
Dissostichus mawsoni		Dissostichus_mawsoni_20_2	-23.2471	13.8371	pelagic		Nototheniidae	-0.009	-0.084	0.095	-0.072	-0.092	0.013	-0.022	0.036
Dissostichus mawsoni		Dissostichus_mawsoni_24_4	-23.2471	13.8371	pelagic		Nototheniidae	-0.045	-0.021	0.15	-0.008	-0.016	0.036	-0.093	-0.001
Dissostichus mawsoni		Dissostichus_mawsoni_4_2	-23.2471	13.8371	pelagic		Nototheniidae	-0.186	-0.051	0.043	-0.087	-0.041	0.085	-0.015	-0.087
Dissostichus mawsoni		Dissostichus_mawsoni_7_2	-23.2471	13.8371	pelagic		Nototheniidae	-0.294	-0.012	-0.013	-0.052	-0.051	-0.011	0.039	-0.059
Dissostichus mawsoni		Dissostichus_mawsoni_8_5	-23.2471	13.8371	pelagic		Nototheniidae	-0.113	0.009	0.137	0.025	0.003	-0.039	-0.069	-0.023
Gobionotothen gibberifrons		Gobionotothen_gibberifrons_11_2	-21.8615	13.3095	benthic		Notothenidae	0.136	0.058	0.054	-0.067	-0.094	0.005	0.014	0.038
Gobionotothen gibberifrons		Gobionotothen_gibberifrons_13_2	-21.8615	13.3095	benthic		Notothenidae	-0.065	0.056	0.023	-0.015	-0.045	-0.078	-0.012	-0.017
Gobionotothen gibberifrons		Gobionotothen_gibberifrons_15_3	-21.8615	13.3095	benthic		Notothenidae	-0.079	0.037	0.031	0.003	0.02	-0.064	-0.053	-0.019
Trematomus newnesi		Trematomus_newnesi_6_3	-24.3005	10.104	cryopela		Notothenidae	0.129	-0.149	0.012	-0.217	-0.003	0.047	-0.039	0.073
Gobionotothen gibberifrons		Gobionotothen_gibberifrons_16_4	-21.8615	13.3095	benthic		Notothenidae	-0.061	0.039	-0.073	0.027	0.008	-0.096	0.051	0.007
Gobionotothen gibberifrons		Gobionotothen_gibberifrons_21_2	-21.8615	13.3095	benthic		Notothenidae	0.024	-0.005	0.21	-0.069	-0.012	0.024	-0.031	0.043
Gobionotothen gibberifrons		Gobionotothen_gibberifrons_22_2	-21.8615	13.3095	benthic		Notothenidae	-0.114	0.012	0.111	-0.057	-0.014	-0.017	-0.048	0.006
Gobionotothen gibberifrons		Gobionotothen_gibberifrons_2_3	-21.8615	13.3095	benthic		Notothenidae	0.031	-0.023	0.099	-0.025	-0.044	-0.033	-0.024	0.005
Gobionotothen gibberifrons		Gobionotothen_gibberifrons_3_5	-21.8615	13.3095	benthic		Notothenidae	-0.187	0.097	0.079	-0.103	0.04	-0.036	0.02	-0.011
Gobionotothen gibberifrons		Gobionotothen_gibberifrons_5_3	-21.8615	13.3095	benthic		Notothenidae	-0.215	0.063	0.072	-0.155	-0.071	-0.066	0.034	-0.073
Gobionotothen gibberifrons		Gobionotothen_gibberifrons_6_4	-21.8615	13.3095	benthic		Notothenidae	-0.044	0.102	0.063	-0.041	-0.048	-0.091	0.018	-0.016
Lepidonotothen larseni		Lepidonotothen_larseni_24_3	-23.9145	11.3505	semipela		Notothenidae	0.223	-0.137	0.032	-0.062	-0.004	-0.02	0.041	-0.024
Lepidonotothen nudifrons		Lepidonotothen_nudifrons_23_2	-22.482	12.878	benthic		Notothenidae	0.089	-0.045	-0.093	0.102	-0.022	-0.045	-0.014	-0.006
Lepidonotothen nudifrons		Lepidonotothen_nudifrons_27_2	-22.482	12.878	benthic		Notothenidae	-0.205	0.13	-0.169	0.025	0.127	-0.068	0.024	0.072
Lepidonotothen squamifrons		Lepidonotothen_squamifrons_13_2	-23.987	12.506	benthic		Notothenidae	-0.125	-0.14	0.089	0.06	0.017	0.006	0.012	-0.021
Lepidonotothen squamifrons		Lepidonotothen_squamifrons_1_4	-23.987	12.506	benthic		Notothenidae	0.083	-0.115	0.089	-0.02	-0.003	0	0.045	0.011
Lepidonotothen squamifrons		Lepidonotothen_squamifrons_24_2	-23.987	12.506	benthic		Notothenidae	0.029	-0.159	0.086	0.001	0.008	-0.069	0.008	0.036
Lepidonotothen squamifrons		Lepidonotothen_squamifrons_28_2	-23.987	12.506	benthic		Notothenidae	0.117	-0.018	0.057	0.062	-0.036	-0.017	0.012	-0.022
Lepidonotothen squamifrons		Lepidonotothen_squamifrons_31_2	-23.987	12.506	benthic		Notothenidae	0.077	0.005	0.001	0.042	-0.062	-0.036	0.004	-0.007
Lepidonotothen squamifrons		Lepidonotothen_squamifrons_5_3	-23.987	12.506	benthic		Notothenidae	0.07	0.01	0.063	0.014	0.018	0.049	0	0.025
Lepidonotothen squamifrons		Lepidonotothen_squamifrons_6_3	-23.987	12.506	benthic		Notothenidae	0.102	0.059	-0.002	0.035	-0.074	-0.035	0.006	-0.018
Neopagetopsis ionah		Neopagetopsis_ionah_10_2	-25.0542	9.2358	pelagic		Channichthyidae	-0.123	0.209	0.089	-0.069	0.002	-0.051	-0.017	-0.015
Notothenia coriiceps		Notothenia_coriiceps_29_2	-23.9405	11.759	benthic		Notothenidae	-0.292	-0.074	-0.015	-0.049	-0.06	0.011	0.048	-0.041
Notothenia coriiceps		Notothenia_coriiceps_4_4	-23.9405	11.759	benthic		Notothenidae	-0.249	-0.145	0.015	0.04	0	0.048	0.045	-0.022
Notothenia rossii		Notothenia_rossii_12_4	-24.3664	10.5918	semipela		Notothenidae	-0.311	-0.091	-0.093	0.067	-0.076	0.076	-0.011	-0.035
Notothenia rossii		Notothenia_rossii_13_4	-24.3664	10.5918	semipela		Notothenidae	-0.284	-0.111	-0.246	-0.006	-0.096	-0.116	-0.094	0.086
Notothenia rossii		Notothenia_rossii_15_3	-24.3664	10.5918	semipela		Notothenidae	-0.225	-0.195	0.024	0.097	0.027	0.021	0.037	-0.034
Notothenia rossii		Notothenia_rossii_16_4	-24.3664	10.5918	semipela		Notothenidae	-0.251	-0.26	-0.081	0.123	-0.012	0.016	0.011	0.002
Notothenia rossii		Notothenia_rossii_25_2	-24.3664	10.5918	semipela		Notothenidae	-0.19	-0.159	0.012	0.123	0.096	0.015	0.053	0.001
Notothenia rossii		Notothenia_rossii_6_3	-24.3664	10.5918	semipela		Notothenidae	-0.24	-0.253	-0.185	0.109	0.036	0.033	-0.006	0.085
Notothenia rossii		Notothenia_rossii_7_6	-24.3664	10.5918	semipela		Notothenidae	-0.344	-0.175	-0.21	0.104	-0.109	-0.002	-0.08	0.076
Notothenia rossii		Notothenia_rossii_8_4	-24.3664	10.5918	semipela		Notothenidae	-0.289	-0.113	-0.086	-0.034	-0.029	0.059	0.018	0.003
Notothenia rossii		Notothenia_rossii_9_6	-24.3664	10.5918	semipela		Notothenidae	-0.142	-0.25	0.088	0.061	0.066	-0.007	0.067	-0.037

Pleuragramma antarcticum	Pleuragramma_antarcticum_21_2	-24.795	10.2745	pelagic		Nototheniidae	0.051	-0.134	0.137	-0.007	0.074	-0.088	0.009	0.036
Pleuragramma antarcticum	Pleuragramma_antarcticum_8_2	-24.795	10.2745	pelagic		Nototheniidae	0.133	0.036	0.006	0.1	-0.074	-0.034	0.011	-0.035
Pseudochaenichthys georgianus	Pseudochaenichthys_georgianus_1_3	-24.051	11.409	pel/semi		Channichthyidae	0.054	-0.021	-0.017	0.053	0.024	-0.059	0.02	0.023
Pseudochaenichthys georgianus	Pseudochaenichthys_georgianus_3_2	-24.051	11.409	pel/semi		Channichthyidae	-0.018	0.236	0.023	0.031	0.019	0.076	-0.046	0.026
Pseudochaenichthys georgianus	Pseudochaenichthys_georgianus_7_2	-24.051	11.409	pel/semi		Channichthyidae	0.279	0.04	-0.066	0.061	-0.019	0.079	0.063	0.012
Trematomus eulepidotus	Trematomus_eulepidotus_10_4	-24.5965	10.631	epibenth		Nototheniidae	0.091	-0.038	0.024	0.065	-0.044	-0.063	0.024	0.013
Artedidraco skottsbergi	Artedidraco_skottsbergi_4_2			benthic	b	Artedidraconidae	0.002	0.032	0.053	0.067	-0.012	0.004	-0.025	0.009
Chaenodraco wilsoni	Chaenodraco_wilsoni_1_2	-25.43	8.539	pelagic		Channichthyidae	0.135	0.022	-0.298	-0.01	0.01	-0.043	-0.05	-0.049
Chaenodraco wilsoni	Chaenodraco_wilsoni_2_2	-25.43	8.539	pelagic		Channichthyidae	0.145	0.094	-0.125	0.06	-0.028	-0.048	0.008	-0.03
Chaenodraco wilsoni	Chaenodraco_wilsoni_3_2	-25.43	8.539	pelagic		Channichthyidae	0.176	0.05	-0.16	0.012	-0.034	-0.017	-0.025	-0.066
Chaenodraco wilsoni	Chaenodraco_wilsoni_4_2	-25.43	8.539	pelagic		Channichthyidae	0.194	-0.019	-0.173	0.043	-0.016	0.005	-0.057	-0.124
Parachaenichthys charcoti	Parachaenichthys_charcoti_1_4	-23.1191	12.78	benthic		Bathydraconidae	0.023	0.113	0.03	-0.122	-0.089	0.005	0	0.032
Pogonophryne scotti	Pogonophryne_scotti_1_2	-22.118	12.018	benthic		Artedidraconidae	0.049	0.169	-0.145	0.01	-0.052	-0.053	0.032	0.004
Trematomus hansoni	Trematomus_hansoni_5_2	-24.0273	11.5409	benthic		Nototheniidae	0.213	-0.196	0.125	-0.165	-0.035	-0.095	0.002	0.009
Trematomus hansoni	Trematomus_hansoni_8_2	-24.0273	11.5409	benthic		Nototheniidae	-0.037	0	0.02	0.088	0.044	-0.026	-0.014	0.001
Trematomus newnesi	Trematomus_newnesi_6_3	-24.3005	10.104	cryopela		Nototheniidae	0.12	-0.12	0.04	0.068	0.044	-0.067	0.062	0.051
Trematomus scotti	Trematomus_scotti_2_2			benthic	c	Nototheniidae	0.134	-0.151	0.084	-0.056	0.001	-0.011	0.017	0.029
Trematomus tokarevi	Trematomus_tokarevi_1_2	-25.1582	9.71	benthic		Nototheniidae	0.14	-0.179	-0.033	-0.053	0.03	-0.051	0.015	-0.049
Trematomus bernacchii	Trematomus_bernacchii_6_3			benthic	c	Nototheniidae	-0.057	-0.087	0.064	0.093	0.065	-0.013	-0.037	0.02

Reference for stable isotope data:

Rutschmann, S., M. Matschiner, M. Damerau, M. Muschick, M. F. Lehmann, R. Handel, and W. Salzburger. 2011. Parallel ecological diversification in Antarctic notothenioid fishes as evidence for adaptive radiation. Mol. Ecol. 20: 4707-4721.

References for habitat:

non-lettered: Rutschmann, S., M. Matschiner, M. Damerau, M. Muschick, M. F. Lehmann, R. Handel, and W. Salzburger. 2011. Parallel ecological diversification in Antarctic notothenioid fishes as evidence for adaptive radiation. Mol. Ecol. 20: 4707-4721.

a Eastman, J. T. 1993. Antarctic fish biology: evolution in a unique environment. Academic Press, San Diego.

b Lombarte, A., I. Olaso, and A. Bozzano. 2003. Ecomorphological trends in the Artedidraconidae (Pisces: Perciformes: Notothenioidei) of the Weddell Sea. Antarct. Sci. 15(2): 211-218.

c Klingenberg, C. P., and W. Ekau. 1996. A combined morphometric and phylogenetic analysis of an ecomorphological trend: pelagization in Antarctic fishes (Perciformes: Notothenioidae). Biol. J. Linn. Soc. 59: 143-177.

Table S2 - Measurement error results for ES1 - ES6 calculated from one-way ANOVAS (d.f. = 1, 39)

Eigenshape Axis	% Total Variance	% Total Variance Cumulative	Sum of Squares between groups	Sum of Squares within groups	*R*
ES1	39.884	39.884	12.339	0.144	0.988
ES2	20.612	60.495	9.96	1.189	0.892
ES3	14.928	75.423	5.386	0.071	0.986
ES4	8.599	84.022	6.18	0.539	0.919
ES5	4.356	88.378	5.708	0.141	0.976
ES6	3.454	91.833	3.793	0.006	0.998

Table S3. Results of Canonical Variates Analysis (CVA) on complete sample, using 'families' as groups

Eigenvalues

Function	Eigenvalue	% of Variance	Cumulative %	Canonical correlation
1	2.732	95.6	95.6	0.856
2	0.097	3.4	98.9	0.297
3	0.03	1.1	100	0.172

Wilks' Lambda

Test of Function(s)	Wilks' Lambda	Chi-square	df	Sig.
1 through 3	0.237	119.463	18.000	0.000
2 through 3	0.885	10.146	10.000	0.428
3	0.970	2.492	4.000	0.646

Predicted Group Membership

		Bathydraconidae	Artedidraconidae	Channichthyidae	Nototheniidae	TOTAL
Original	Bathydraconidae	2 (100%)	0 (0%)	0 (0%)	0 (0%)	2
		1 (50%)	0 (0%)	1 (50%)	0 (0%)	2
	Artedidraconidae	0 (0%)	2 (100%)	0 (0%)	0 (0%)	2
		0 (0%)	0 (0%)	1 (50%)	1 (50%)	2
	Channichthyidae	2 (6.3%)	5 (15.6%)	24 (75.0%)	1 (3.1%)	32
		5 (15.6%)	6 (18.8%)	20 (62.5%)	1 (3.1%)	32
	Nototheniidae	2 (3.8%)	5 (9.4%)	2 (3.8%)	44 (83.0%)	53
		2 (3.8%)	5 (9.4%)	2 (3.8%)	44 (83.0%)	53

Number of classified cases (% classification)
Number of cross-validated classified cases (% classification)

80.9% of original grouped cases correctly classified
73.0% of cross-validated grouped cases correctly classified

Table S4. Information about the trawls from which photographed specimens were collected. Specimens are grouped according to the the trawl (detailed by two points - profile start and profile end)

Specimens taken from this trawl (Photo IDs)	Date	Time	Station	Gear Abbreviati	Gear	Action	PositionLat	PositionLon	Depth [m]	Speed [kn]	Course [°]	Wind Direction [°/ind Strength [m/	mean Depth
Notothenia_rossii_1 to_16	17/03/08	16:37:00	PS79/0185-1	BT	Bottom trawl	profile start	60° 52,16' S	55° 30,15' W	251.3	4,7	129	271 15	249.55
Lepidonotothen_larseni_1 to _23	17/03/08	17:07:00	PS79/0185-1	BT	Bottom trawl	profile end	60° 53,24' S	55° 26,84' W	247.8	3,7	125	266 16	
Dissostichus_mawsoni_24													
Lepidonotothen_nudifrons_1 to _2													
Cryodraco_antarcticus_1 to _2	17/03/08	10:01:00	PS79/0188-1	BT	Bottom trawl	profile start	61° 11,22' S	54° 35,30' W	277.5	4,0	42	272 18	316.7
Chaenocephalus_aceratus_1 to _8	17/03/08	10:31:00	PS79/0188-1	BT	Bottom trawl	profile end	61° 9,86' S	54° 32,99' W	355.9	3,4	29	263 15	
Pogonophryne_marmorata_1													
Trematomus_newnesi_1 to _2													
Chaenocephalus_aceratus_9 to _14	17/03/08	12:39:00	PS79/0189-1	BT	Bottom trawl	profile start	61° 12,02' S	54° 40,53' W	266.6	3,6	229	275 18	264.95
Trematomus_newnesi_3	17/03/08	13:09:00	PS79/0189-1	BT	Bottom trawl	profile end	61° 13,24' S	54° 42,95' W	263.3	3,3	220	276 17	
Champsocephalus_gunnari_1 to _13													
Pogonophryne_scotti_1													
Champsocephalus_gunnari_14 to _15	17/03/08	15:22:00	PS79/0190-1	BT	Bottom trawl	profile start	61° 12,00' S	54° 52,49' W	71.3	4,9	289	273 14	62.05
Notothenia_coriiceps_1 to _11	17/03/08	15:52:00	PS79/0190-1	BT	Bottom trawl	profile end	61° 12,48' S	54° 56,30' W	52.8	4,2	248	259 16	
Lepidonotothen_nudifrons_3													
Chionodraco_rastrospinosus_1	17/03/08	18:03:00	PS79/0191-1	BT	Bottom trawl	profile start	61° 15,66' S	54° 52,31' W	134.6	3,0	258	261 16	161.8
Notothenia_coriiceps_12 to _13	17/03/08	18:33:00	PS79/0191-1	BT	Bottom trawl	profile end	61° 16,09' S	54° 56,12' W	189	4,1	244	256 14	
Lepidonotothen_nudifrons_4 to _11													
Artedidraco_skottsbergi_1													
Trematomus_newnesi_4													
Trematomus_eulepidotus_5 to _8													
Champsocephalus_gunnari_16 to _20	18/03/08	09:49:00	PS79/0194-1	BT	Bottom trawl	profile start	61° 20,74' S	55° 11,00' W	280.9	4,8	78	261 17	332.3
Trematomus_newnesi_5 to _6	18/03/08	10:19:00	PS79/0194-1	BT	Bottom trawl	profile end	61° 20,12' S	55° 7,38' W	383.7	3,8	69	258 16	
Cryodraco_antarcticus_3 to _6													
Gobionotothen_gibberifrons_1 to _4	18/03/08	13:23:00	PS79/0195-1	BT	Bottom trawl	profile start	61° 20,06' S	55° 31,64' W	148.9	3,1	102	252 16	154.55
Chaenocephalus_aceratus_15 to _18	18/03/08	13:53:00	PS79/0195-1	BT	Bottom trawl	profile end	61° 20,36' S	55° 27,96' W	160.2	2,3	108	261 14	
Notothenia_coriiceps_14 to _17													
Notothenia_rossii_17 to _19	18/03/08	16:16:00	PS79/0196-1	BT	Bottom trawl	profile start	61° 16,43' S	55° 37,38' W	109.2	3,8	173	286 14	119.6
Gobionotothen_gibberifrons_5 to _6	18/03/08	16:46:00	PS79/0196-1	BT	Bottom trawl	profile end	61° 18,36' S	55° 37,86' W	130	3,7	203	272 13	
Lepidonotothen_nudifrons_12 to _19													
Trematomus_newnesi_7 to _9													
Trematomus_hansoni_1	19/03/08	18:53:00	PS79/0197-1	BT	Bottom trawl	profile start	61° 17,04' S	55° 42,73' W	139	3,9	172	290 9	175.6
Dissostichus_mawsoni_1	19/03/08	19:23:00	PS79/0197-1	BT	Bottom trawl	profile end	61° 18,91' S	55° 42,84' W	212.2	3,4	186	287 8	
Trematomus_eulepidotus_1 to _4	19/03/08	09:33:00	PS79/0199-1	BT	Bottom trawl	profile start	61° 4,78' S	56° 1,76' W	244.8	2,7	27	245 4	255.5
Gobionotothen_gibberifrons_7 to _10	19/03/08	09:53:00	PS79/0199-1	BT	Bottom trawl	profile end	61° 4,10' S	55° 59,83' W	266.2	3,0	58	227 5	
Chaenocephalus_aceratus_19 to _23	19/03/08	13:15:00	PS79/0200-1	BT	Bottom trawl	profile start	61° 9,52' S	56° 1,30' W	150.4	3,8	283	165 4	164.65
Gobionotothen_gibberifrons_11 to _13	19/03/08	13:45:00	PS79/0200-1	BT	Bottom trawl	profile end	61° 9,00' S	56° 5,27' W	178.9	2,7	283	161 4	
Pseudochaenichthys_georgianus_1 to _3													
Parachaenichthys_charcoti_1													
Notothenia_coriiceps_18 to _21	19/03/08	15:54:00	PS79/0202-1	BT	Bottom trawl	profile start	61° 10,50' S	55° 55,65' W	124.9	3,1	121	146 6	123
Dissostichus_mawsoni_2	19/03/08	16:24:00	PS79/0202-1	BT	Bottom trawl	profile end	61° 11,29' S	55° 51,94' W	121.1	3,3	112	153 10	
Trematomus_hansoni_2													
Trematomus_eulepidotus_9 to _10	19/03/08	17:24:00	PS79/0203-1	BT	Bottom trawl	profile start	61° 12,98' S	55° 52,64' W	136.7	3,1	210	149 13	147.35
	19/03/08	17:54:00	PS79/0203-1	BT	Bottom trawl	profile end	61° 14,65' S	55° 54,61' W	158	3,7	208	146 11	
Dissostichus_mawsoni_3	20/03/08	09:53:00	PS79/0206-1	BT	Bottom trawl	profile start	60° 49,77' S	55° 37,25' W	479.7	4,1	288	223 6	475.15
Lepidonotothen_squamifrons_1 to _10	20/03/08	10:06:00	PS79/0206-1	BT	Bottom trawl	profile end	60° 49,52' S	55° 38,64' W	470.6	3,5	292	218 6	
Gobionotothen_gibberifrons_14 to _19	20/03/08	12:20:00	PS79/0207-1	BT	Bottom trawl	profile start	60° 53,15' S	55° 36,47' W	174.8	3,0	227	260 5	155.95
Trematomus_bernacchii_1	20/03/08	12:50:00	PS79/0207-1	BT	Bottom trawl	profile end	60° 53,75' S	55° 40,16' W	137.1	4,0	272	269 7	
Chionodraco_rastrospinosus_ 2 to_3													
Gobionotothen_gibberifrons_20 to _23	20/03/08	14:38:00	PS79/0208-1	BT	Bottom trawl	profile start	60° 52,67' S	55° 28,80' W	243.7	2,6	134	283 9	242.25
Lepidonotothen_squamifrons_11	20/03/08	15:08:00	PS79/0208-1	BT	Bottom trawl	profile end	60° 53,60' S	55° 25,68' W	240.8	3,6	122	291 9	
Lepidonotothen_squamifrons_12	20/03/08	16:33:00	PS79/0209-1	BT	Bottom trawl	profile start	60° 51,53' S	55° 30,25' W	290.2	3,8	110	259 10	291

Trematomus_eulepidotus_11 to _12 Cryodraco_antarcticus_7 Lepidonotothen_larseni_24 to _30	20/03/08	17:03:00	PS79/0209-1	BT	Bottom trawl	profile end	60° 52,31' S	55° 26,71' W	291.8	4,4	111	260	10	
Trematomus_eulepidotus_13 to _14 Chionodraco_rastrospinosus Chaenocephalus_aceratus_24 Chionodraco_rastrospinosus_7 to _9 Chaenocephalus_aceratus_25 to _27 Trematomus_bernacchii_2 to _4	21/03/08	16:00:00	PS79/0214-1	BT	Bottom trawl	profile start	61° 2,58' S	55° 45,51' W	111.8	3,6	345	157	12	129.8
	21/03/08	16:30:00	PS79/0214-1	BT	Bottom trawl	profile end	61° 0,70' S	55° 45,00' W	147.8	3,1	16	164	13	
Cryodraco_antarcticus_8 to _10 Lepidonotothen_squamifrons_13 Trematomus_eulepidotus_ 15 to _16	22/03/08	09:46:00	PS79/0218-1	BT	Bottom trawl	profile start	61° 0,53' S	55° 58,39' W	299.2	3,3	23	183	12	299.4
	22/03/08	10:16:00	PS79/0218-1	BT	Bottom trawl	profile end	60° 58,89' S	55° 56,67' W	299.6	3,9	23	195	10	
Trematomus_eulepidotus_17 to _24 Dissostichus_mawsoni_4 to _5 Cryodraco_antarcticus_11 to _15	22/03/08	12:11:00	PS79/0219-1	BT	Bottom trawl	profile start	61° 0,68' S	55° 58,03' W	304.6	3,5	37	181	10	280.45
	22/03/08	12:41:00	PS79/0219-1	BT	Bottom trawl	profile end	60° 59,18' S	55° 55,90' W	256.3	3,1	28	182	10	
Trematomus_eulepidotus_25 to _30	22/03/08	14:12:00	PS79/0220-1	BT	Bottom trawl	profile start	61° 2,59' S	55° 57,03' W	273	3,7	23	187	12	270
	22/03/08	14:42:00	PS79/0220-1	BT	Bottom trawl	profile end	61° 0,80' S	55° 56,10' W	267	3,4	12	197	11	
Pseudochaenichthys_georgianus_4 to _5	22/03/08	17:57:00	PS79/0222-1	BT	Bottom trawl	profile start	61° 7,03' S	55° 54,43' W	126.7	3,8	40	196	9	127.3
	22/03/08	18:27:00	PS79/0222-1	BT	Bottom trawl	profile end	61° 5,29' S	55° 52,84' W	127.9	3,4	28	201	8	
Pseudochaenichthys_georgianus_6 Trematomus_bernacchii_5	23/03/08	09:33:00	PS79/0226-1	BT	Bottom trawl	profile start	60° 58,30' S	55° 55,25' W	212.7	3,3	191	215	5	228.5
	23/03/08	10:03:00	PS79/0226-1	BT	Bottom trawl	profile end	60° 59,95' S	55° 55,46' W	244.3	1,9	179	236	6	
Dissostichus_mawsoni_6	23/03/08	11:32:00	PS79/0227-1	BT	Bottom trawl	profile start	61° 1,09' S	55° 50,69' W	140.2	3,1	13	207	5	146.35
	23/03/08	12:02:00	PS79/0227-1	BT	Bottom trawl	profile end	60° 59,48' S	55° 49,28' W	152.5	3,3	31	220	4	
Harpagifer_antarcticus_1 to _4	23/03/08	16:30:00	PS79/0230-1	BT	Bottom trawl	profile start	61° 7,59' S	55° 42,35' W	64	4,1	137	253	1	73.35
	23/03/08	17:00:00	PS79/0230-1	BT	Bottom trawl	profile end	61° 9,02' S	55° 40,55' W	82.7	2,6	150	280	2	
Trematomus_hansoni_3	unknown													
Lepidonotothen_squamifrons_14 to _19	24/03/08	16:06:00	PS79/0236-1	BT	Bottom trawl	profile start	61° 22,28' S	56° 10,24' W	293.1	3,9	64	249	6	308.3
	24/03/08	16:36:00	PS79/0236-1	BT	Bottom trawl	profile end	61° 21,43' S	56° 7,01' W	323.5	2,3	61	259	7	
Chionodraco_rastrospinosus_10 to _12 Dissostichus_mawsoni_7 Cryodraco_antarcticus_16 to _19	24/03/08	17:32:00	PS79/0237-1	BT	Bottom trawl	profile start	61° 19,92' S	56° 1,97' W	343.1	3,7	69	243	7	334.35
	24/03/08	18:02:00	PS79/0237-1	BT	Bottom trawl	profile end	61° 19,43' S	55° 58,96' W	325.6	3,6	69	256	7	
Cryodraco_antarcticus_20 to _23	24/03/08	20:15:00	PS79/0238-1	BT	Bottom trawl	profile start	61° 25,79' S	56° 7,17' W	297.6	3,1	138	262	8	288.9
	24/03/08	20:45:00	PS79/0238-1	BT	Bottom trawl	profile end	61° 27,24' S	56° 4,65' W	280.2	3,7	139	250	7	
Chionodraco_rastrospinosus_13 to _20	25/03/08	09:37:00	PS79/0239-1	BT	Bottom trawl	profile start	61° 49,50' S	57° 23,61' W	277.5	3,8	122	275	18	274.7
	25/03/08	10:07:00	PS79/0239-1	BT	Bottom trawl	profile end	61° 50,38' S	57° 20,50' W	271.9	3,6	119	272	16	
Lepidonotothen_squamifrons_20 to _31	27/03/12	09:38:00	PS79/0242-1	BT	Bottom trawl	profile start	61° 35,88' S	57° 16,68' W	423	2,4	294	272	18	424.8
	27/03/12	10:08:00	PS79/0242-1	BT	Bottom trawl	profile end	61° 35,55' S	57° 19,73' W	426.6	1,8	284	282	16	
Notothenia_rossii_20 to _22 Dissostichis_mawsoni_8	26/03/08	11:59:00	PS79/0243-1	BT	Bottom trawl	profile start	61° 38,21' S	57° 32,72' W	425.4	3,7	269	294	13	428.5
	26/03/08	12:11:00	PS79/0243-1	BT	Bottom trawl	profile end	61° 38,15' S	57° 34,09' W	431.6	3,2	274	292	13	
Lepidonotothen_nudifrons_20 _23 Notothenia_coriiceps_22 to _30 Notothenia_rossii_23 to _27	26/03/08	13:41:00	PS79/0244-1	BT	Bottom trawl	profile start	61° 38,86' S	57° 47,52' W	322.2	3,2	271	299	13	328.1
	26/03/08	14:11:00	PS79/0244-1	BT	Bottom trawl	profile end	61° 38,80' S	57° 51,31' W	334	3,4	276	303	12	
Pseudochaenichthys_georgianus_7 o _14	26/03/08	18:13:00	PS79/0245-1	BT	Bottom trawl	profile start	61° 45,20' S	58° 31,49' W	282.8	3,2	231	336	11	280.65
	26/03/08	18:43:00	PS79/0245-1	BT	Bottom trawl	profile end	61° 45,94' S	58° 34,57' W	278.5	2,3	242	341	11	
Lepidonotothen_nudifrons_24 to _25 Champsocephalus_gunnari_21 Chaenocephalus_aceratus_28 Cryodraco_antarcticus_24 to _25 Pseudochaenichthys_georgianus_15 to _17	27/03/08	14:24:00	PS79/0247-2	BT	Bottom trawl	profile start	62° 22,19' S	61° 25,78' W	325.4	3,4	158	83	7	339.35
	27/03/08	14:54:00	PS79/0247-2	BT	Bottom trawl	profile end	62° 23,72' S	61° 24,45' W	353.3	3,7	149	71	12	
Dissostichus_mawsoni_9 Chaenocephalus_aceratus_29 to _33 Lepidonotothen_nudifrons_26 to _33	27/03/08	16:51:00	PS79/0248-2	BT	Bottom trawl	profile start	62° 29,18' S	61° 24,57' W	120.3	3,0	38	67	18	130.8
	27/03/08	17:16:00	PS79/0248-2	BT	Bottom trawl	profile end	62° 28,15' S	61° 21,92' W	141.3	3,5	59	68	17	

Champsocephalus_gunnari_22 to _30 Pseudochaenichthys_georgianus_18 to _20														
Pseudochaenichthys_georgianus_21 to _24 Chionodraco_rastrospinosus_21 to _24 Chaenodraco_wilsoni_1	27/03/08 27/03/08	19:47:00 19:56:00	PS79/0249-1 PS79/0249-1	BT BT	Bottom trawl Bottom trawl	profile start profile end	62° 36,42' S 62° 35,97' S	61° 50,45' W 61° 50,33' W	181.1 178.4	4,2 3,3	343 3	59 59	18 18	179.75
Chionodraco_rastrospinosus_25 to _28 Trematomus_hansoni_4 Cryodraco_antarcticus_26 Dissostichus_mawsoni_10	28/03/08 28/03/08	12:18:00 12:48:00	PS79/0251-2 PS79/0251-2	BT BT	Bottom trawl Bottom trawl	profile start profile end	62° 11,23' S 62° 9,78' S	60° 47,24' W 60° 49,44' W	420.1 434.4	3,9 2,8	323 327	86 79	10 9	427.25
Notothenia_rossii_28 to _30 Dissostichus_mawsoni_11 Pseudochaenichthys_georgianus_25	28/03/08 28/03/08	15:21:00 15:51:00	PS79/0252-1 PS79/0252-1	BT BT	Bottom trawl Bottom trawl	profile start profile end	62° 23,80' S 62° 24,28' S	60° 48,81' W 60° 44,91' W	87.7 90.7	3,0 3,1	99 103	76 75	6 5	89.2
Chionodraco_rastrospinosus_29 to _30	28/03/08 28/03/08	17:28:00 17:58:00	PS79/0253-1 PS79/0253-1	BT BT	Bottom trawl Bottom trawl	profile start profile end	62° 19,44' S 62° 20,28' S	60° 27,39' W 60° 31,31' W	110.9 127.8	3,9 3,3	253 244	95 71	3 2	119.35
Dissostichus_mawsoni_12 to _15 Cryodraco_antarcticus_27 to _31 Chaenocephalus_aceratus_34	28/03/08 28/03/08	20:27:00 20:57:00	PS79/0254-1 PS79/0254-1	BT BT	Bottom trawl Bottom trawl	profile start profile end	62° 5,51' S 62° 6,43' S	60° 31,93' W 60° 35,27' W	285.8 363.6	4,1 2,8	229 224	148 0	1 0	324.7
Chionodraco_rastrospinosus_31 Dissostichus_mawsoni_16	29/03/08 29/03/08	14:42:00 15:08:00	PS79/0259-1 PS79/0259-1	BT BT	Bottom trawl Bottom trawl	profile start profile end	61° 59,99' S 61° 59,97' S	59° 14,73' W 59° 11,29' W	129.1 142.8	3,6 3,6	86 90	286 289	11 11	135.95
Dissostichus_mawsoni_17 to _18 Cryodraco_antarcticus_32	29/03/08 29/03/08	16:37:00 17:07:00	PS79/0260-1 PS79/0260-1	BT BT	Bottom trawl Bottom trawl	profile start profile end	61° 51,74' S 61° 50,50' S	59° 15,47' W 59° 12,16' W	259.5 269.1	3,9 3,8	50 58	284 293	5 5	264.3
Gobionotothen_gibberifrons_24 to _26	30/03/08 30/03/08	14:25:00 14:55:00	PS79/0264-1 PS79/0264-1	BT BT	Bottom trawl Bottom trawl	profile start profile end	61° 50,00' S 61° 50,01' S	58° 40,01' W 58° 36,33' W	192.1 189.1	3,6 3,3	87 100	77 83	16 16	190.6
Dissostichus_mawsoni_19 to _21 Gobionotothen_gibberifrons_27 to _31	30/03/08 30/03/08	17:37:00 18:07:00	PS79/0265-1 PS79/0265-1	BT BT	Bottom trawl Bottom trawl	profile start profile end	61° 45,83' S 61° 45,50' S	58° 30,09' W 58° 25,77' W	278.6 279.7	3,8 3,6	87 78	89 88	14 16	279.15
Dissostichus_mawsoni_22 to _23	30/03/08 30/03/08	19:38:00 20:08:00	PS79/0266-1 PS79/0266-1	BT BT	Bottom trawl Bottom trawl	profile start profile end	61° 48,03' S 61° 47,71' S	58° 29,24' W 58° 25,11' W	205.1 209	3,8 3,6	80 80	99 105	17 16	207.05
Trematomus_bernacchii_6 to _7 Trematomus_hansoni_5 to _6 Neopagetopsis_ionah_1 to _3 Chaenodraco_wilsoni_2 to _8	31/03/08 31/03/08	16:18:00 16:43:00	PS79/0269-1 PS79/0269-1	BT BT	Bottom trawl Bottom trawl	profile start profile end	62° 27,59' S 62° 26,14' S	55° 15,62' W 55° 16,16' W	227.3 254.8	3,9 3,5	15 333	105 100	8 9	241.05
Neopagetopsis_ionah_4 to _7 Artedidraco_skottsbergi_2 to _3 Akarotaxis_nudiceps_1 Trematomus_tokarevi_1	01/04/08 01/04/08	13:03:00 13:33:00	PS79/0273-1 PS79/0273-1	BT BT	Bottom trawl Bottom trawl	profile start profile end	62° 22,04' S 62° 23,90' S	55° 57,65' W 55° 58,36' W	336.6 348.5	3,7 3,2	193 190	71 70	12 11	342.55
Pleuragramma_antarcticum_ 1 to _30 Chaenodraco_wilsoni_9 to _30	01/04/08 01/04/08	17:41:00 18:11:00	PS79/0275-1 PS79/0275-1	BT BT	Bottom trawl Bottom trawl	profile start profile end	62° 25,36' S 62° 23,83' S	56° 13,61' W 56° 11,34' W	425.3 450.1	3,6 3,3	34 28	100 85	13 14	437.7
Neopagetopsis_ionah_8	02/04/08 02/04/08	09:45:00 10:15:00	PS79/0278-1 PS79/0278-1	BT BT	Bottom trawl Bottom trawl	profile start profile end	62° 25,80' S 62° 26,34' S	56° 12,58' W 56° 16,46' W	425.9 422.6	3,7 3,2	254 256	102 108	16 16	424.25
Neopagetopsis_ionah_9	unknown													
Neopagetopsis_ionah_10 Trematomus_hansoni_7 to _8	02/04/08 02/04/08	15:37:00 16:02:00	PS79/0279-1 PS79/0279-1	BT BT	Bottom trawl Bottom trawl	profile start profile end	62° 16,69' S 62° 17,23' S	55° 49,96' W 55° 46,64' W	302.3 324.3	3,6 3,9	108 101	114 115	19 19	313.3
Artedidraco_skottsbergi_4 to _5	02/04/08 02/04/08	17:36:00 17:46:00	PS79/0280-1 PS79/0280-1	BT BT	Bottom trawl Bottom trawl	profile start profile end	62° 16,56' S 62° 16,85' S	55° 47,73' W 55° 46,42' W	329.7 337.7	4,0 3,9	115 106	118 117	20 23	333.7
Trematomus_scotti_2	unknown													

Discussion

The work presented in my doctoral thesis focuses on different aspects of adaptive radiations in teleost fish and evolves around different systems, namely Lake Tanganyikan and Central American cichlids and Antarctic notothenioids. I assessed relationships between morphological and physiological characters and the ecology of a diverse sample of teleost fish species and how those are related to the environment a species lives in (i.e. phenotype-environment correlations) (**chapters 1.1, 1.2, 1.3, 1.4, 1.5, 2.4**). In this context I also explored the occurrence of convergence within (**chapters 1.2, 1.5**) and between systems (**chapter 1.1**). Furthermore, I studied the process of morphological and ecological disparity throughout the course of teleost adaptive radiations (**chapters 1.2, 1.3, 1.4, 1.5, 2.2, 2.3**), thereby testing for evidence for 'early bursts' in trait evolution and macro-habitat partition and the generality of the hypothesis that evolution should follow a fixed ordering of temporally discrete stages in adaptive radiations.

Linking morphology with ecology

The study of morphological diversity, disparity and its change through time greatly gains in attractiveness if morphologies or morphological characters can be linked to the ecology of a species. In several studies, I could uncover such correlations, e.g. that the composition of the vertebral column and the number of distinct vertebrae types is connected with a species' position within the food web in Lake Tanganyikan cichlids (**chapter 1.2**). Here, it is particularly the number of abdominal vertebrae that correlates with the trophic niche a species exploits as inferred from the length of the intestinal tract and δ15N stable isotope values. Vertebral numbers, together with the relative length of the vertebrae, are also connected with body elongation as depicted by elongation ratio (ER), whereby the number of caudal vertebrae showed to have greater influence on ER than abdominal vertebral numbers. ER itself, in turn, showed to

be connected to trophic level and macro-habitat choice, ultimately meaning that elongated cichlids tend to be limnetic piscivores (but note that there are prominent deviations from this general pattern, e.g. the *Julidochromis* species). Another morphological feature that can be linked with the trophic niche and the macro-habitat a species forages in is head shape and, tightly connected to that, relative bite force per species (**chapter 1.3**). Head shape showed to be associated with bite force in cichlids in the way that species featuring elongated heads with long snouts showed to be specialized on feeding on elusive prey while exhibiting fast but weak closing of the oral jaws. Species with deeper heads and shorter snouts on the other hand showed to be specialized on feeding on stationary prey items like plants or invertebrates, often attached to the substrate, using a slow but forceful jaw closing mechanism (see also Norton and Brainerd (1993), Webb (1984), Huskey and Turingan (2001)). The latter group consequently showed to predominantly forage in the benthic macrohabitat, while the former group is connected with limnetic foraging behaviour. A similar correlation between bentho-limnetic habitat preference and morphology was revealed concerning the size of pectoral fins and the weight of corresponding pectoral fin muscles in Lake Tanganyikan cichlids: benthically living species tend to feature larger pectoral fins and heavier muscles, probably reflecting increased demands in manoeuvrability connected with the tightly structured benthic macro-habitat (**chapter 1.4**). Similarly, species standing low in the food web tend to exhibit larger pectoral fins and heavier muscles than species occupying higher trophic niches.

Another morphological trait that we examined was the shape of the operculum, a trait that can easily be compared between actinopterygian species flocks, even between extant taxa and extinct flocks like *Saurichthys*. This approach may lead to novel insights and help the understanding of evolutionary processes (see e.g. Wilson (2013)). Opercular bone shape and size was assessed in two systems: Lake Tanganyikan cichlids and Antarctic notothenioids (**chapters 1.5, 2.3**). While in notothenioids opercular shape showed a trend towards extended posterior margins of the opercle in benthic species, Lake Tanganyikan cichlids mainly showed correlations between operculum shape and feeding ecology (see

the last paragraph of this subsection for a further discussion of discrepancies and similarities between the Lake Tanganyikan and Antarctic teleost radiations).
A conspicuous alteration of trophic morphology that is found in various cichlid taxa coming from different radiations is hypertrophied lips (**chapter 1.1**). This thick-lipped phenotype could be linked with a specialization in feeding on hard-shelled food items in two independently evolved species, *Lobochilotes labiatus* from East African Lake Tanganyika and *Amphilophus labiatus* from Central America, thus not only demonstrating a connection between morphology and feeding but also recovering a case of inter-continental convergent evolution.

Convergence

Convergence, i.e. the independent evolution of similar characteristics triggered by similar ecological conditions (see e.g. Schluter (2000) or Losos (2011)), is a widespread phenomenon between (e.g. Blackledge and Gillespie (2004), Schluter (2000), Losos et al. (1998)), but may also occur within adaptive radiations (Muschick, Indermaur and Salzburger 2012, Rueber and Adams 2001). In **chapter 1.1**, we could not only show that the two independently emerged thick-lipped phenotypes are adaptive to a specialised diet but also that the same set of genes is upregulated in both thick-lipped species in comparison to thin-lipped relatives. Convergence in vertebral column compositions can also be found within Lake Tanganyikan cichlids (**chapter 1.2)**, as demonstrated by specific compositions being exhibited by far more (phylogenetically diverse) species than would be expected under neutral evolution. Signs of convergence could also be detected concerning operculum shape in cichlids (**chapter 1.5**), as the morphological distance between species showed to be shorter than phylogenetic distance and also shorter than expected under neutral evolution.

Evolution through time

Convergence is actually not what would be expected for traits that evolved under an 'early burst' scenario as, in theory, an 'early burst' should lead to early divergence between subclades occupying different niches and, as these niches

become filled, further divergence according to those niches (and traits adaptive to those niches) within subclades should be prevented (Schluter 2000, Gavrilets and Losos 2009, Harmon et al. 2003). 'Early bursts', however, showed to be rarely detected in comparative data (Harmon et al. 2010) and that is also true for the data I obtained in the course of this thesis: Most traits that I studied did not show any signs of disparity being initially distributed between subclades but rather showed patterns of recurrent shifts also within subclades. Neither the number of abdominal vertebrae, total number of vertebrae, vertebrae ratio nor elongation ratio showed 'early burst' like patterns although the number of caudal vertebrae and maximal body size depicted patterns that might be interpreted as 'delayed early bursts' with disparity mainly being partitioned between subclades after an initial phase of high within-subclade disparity (**chapter 1.2)**. Our studies of the opercular bone did not reveal an 'early burst'-like pattern in operular shape or size, neither in cichlids (**chapter 1.5**) nor in notothenioids (**chapter 2.3**). Out of the traits studied in notothenioids, neither body size nor buoyancy or temperature preference evolved under an 'early burst'-like pattern (**chapter 2.2**). However, we did reveal an 'early burst' signal in body shape in notothenioids, mainly coinciding with alterations of head morphology (elongated heads with anteriorly oriented mouths *versus* more robust heads with dorsally oriented mouths) and a general elongation of the body (**chapter 2.2**). Interestingly, similar alterations also coincided with an early divergence in body and head shape revealed in Lake Tanganyikan cichlids (**chapter 1.3**), where I furthermore assessed relative bite force that also showed to have evolved in agreement with an 'early burst' scenario.

Comparing two teleost adaptive radiations

The two teleost adaptive radiations that I mainly worked with, Lake Tanganyikan cichlids and Antarctic notothenioids, could, at first glance, not be any more different. Lake Tanganyika is a freshwater lake situated within the continent of Africa near the equator and hence depicts consistently warm temperatures. The seawaters around Antarctica, on the other hand, are characterized by freezing temperatures with the persistent presence of sea ice.

While Lake Tanganyika is geographically separated from the ocean and only connected by a number of rivers and streams to other major water bodies, the Southern ocean encircling Antarctica is not geographically isolated. However, the occurrence of the Antarctic circumpolar current and the Antarctic polar front separates Antarctica from other continental shelves (see **chapter 2.1** and references therein), making Antarctic waters a similarly enclosed environment as many freshwater lakes. While the onset of the Lake Tanganyikan cichlid radiation presumably coincided with the formation of a novel (and hence undercolonized) lake habitat (Salzburger et al. 2002), the Notothenioid radiation is thought to have emerged following ecological opportunity after the extinction of antagonists due to a drop to subzero water temperatures (Eastman, Pratt and Winn 1993, Matschiner, Hanel and Salzburger 2011, Near 2004). There are also apparent differences in diversification rates between the two radiations, as rates seem to be measurably lower in notothenioids when compared to Lake Tanganyikan cichlids (Rutschmann et al. 2011). In spite of these remarkable differences, we found conspicuous similarities concerning the temporal process of diversification between both radiations: We did not recover any 'early burst'-like patterns related to the shape or size of the operculum, instead opercular shape seems to have diversified over a prolonged time span and shows elevated within-subcalde disparity notably late (meaning near-present) in both systems (**chapters 1.5 and 2.3**). Further, I could not reveal patterns of early divergence according to habitat choice and macro-habitat related traits in neither species flock (**chapters 1.2, 1.4, 2.2**), although this is predicted under the radiation in stages hypothesis (Danley and Kocher 2001, Streelman and Danley 2003). Diversification along the bentho-limnetic axis proceeded over a prolonged time span and was not concentrated near the onset of neither radiation as exemplified by habitat choice and ER values in Lake Tanganyikan cichlids and buoyancy measurements in notothenioids. I did, however, find incidences of early divergence with disparity mainly being distributed between subclades in both systems regarding head- and, to a lesser extent, general body shape (**chapters 1.3, 2.2**). Namely trophic morphology pertaining to snout length, gape size and mouth orientation showed to diverge early and showed surprisingly similar axes of shape change in notothenioids as well as in Lake Tanganyikan cichlids. In both

systems, we found these alterations to be attributable to a divergence between morphologies suited for feeding on elusive prey probably using ram feeding and morphologies specialized for efficient suction feeding and/or picking behaviour on stationary prey items (see also Norton and Brainerd (1993), Webb (1984), Huskey and Turingan (2001)). Divergence according to resource use and trophic morphology is generally expected to be stage two in the radiation in stages scenario. Stages one and two thus seem to be reversed or, alternatively, divergence according to habitat use (stage one) could be non-discrete in Lake Tanganyikan cichlids as well as in Antarctic notothenioids. Furthermore, the first axis of divergence that we could find relies on very similar alterations of head- and body shape and trophic morphology in both systems. Lake Tanganyikan cichlids and Antarctic notothenioids thus share, despite all obvious differences, very similar patterns of trait evolution through time.

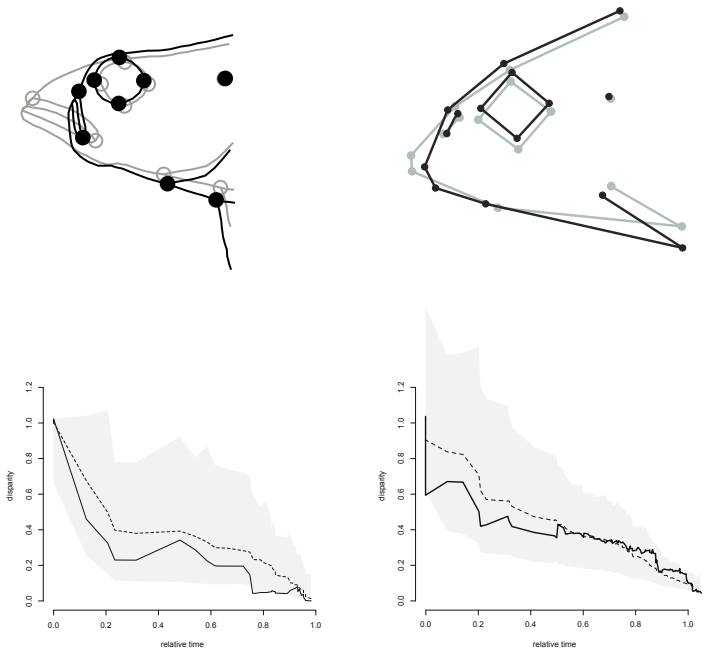

Fig. 1
The first axis of shape change in notothenioids (upper-left) and Lake Tanganyikan cichlids (upper-right). Both axes discriminate between elongated heads and deeper head morphologies and both show an 'early burst'- like pattern of trait evolution (bottom).

References

Blackledge, T. A. & R. G. Gillespie (2004) Convergent evolution of behavior in an adaptive radiation of Hawaiian web-building spiders. *Proc Natl Acad Sci U S A,* 101**,** 16228-33.

Danley, P. D. & T. D. Kocher (2001) Speciation in rapidly diverging systems: lessons from Lake Malawi. *Mol Ecol,* 10**,** 1075-86.

Eastman, J., D. Pratt & W. Winn (1993) Antarctic fish biology: evolution in a unique environment.

Gavrilets, S. & J. B. Losos (2009) Adaptive radiation: contrasting theory with data. *Science,* 323**,** 732-7.

Harmon, L. J., J. B. Losos, T. Jonathan Davies, R. G. Gillespie, J. L. Gittleman, W. Bryan Jennings, K. H. Kozak, M. A. McPeek, F. Moreno-Roark, T. J. Near, A. Purvis, R. E. Ricklefs, D. Schluter, J. A. Schulte Ii, O. Seehausen, B. L. Sidlauskas, O. Torres-Carvajal, J. T. Weir & A. O. Mooers (2010) Early bursts of body size and shape evolution are rare in comparative data. *Evolution,* 64**,** 2385-96.

Harmon, L. J., J. A. Schulte, 2nd, A. Larson & J. B. Losos (2003) Tempo and mode of evolutionary radiation in iguanian lizards. *Science,* 301**,** 961-4.

Huskey, S. H. & R. G. Turingan (2001) Variation in prey-resource utilization and oral jaw gape between two populations of largemouth bass, Micropterus salmoides. *Environmental Biology of Fishes,* 61**,** 185-194.

Losos, J. B. (2011) Convergence, adaptation, and constraint. *Evolution,* 65**,** 1827-40.

Losos, J. B., T. R. Jackman, A. Larson, K. Queiroz & L. Rodriguez-Schettino (1998) Contingency and determinism in replicated adaptive radiations of island lizards. *Science,* 279**,** 2115-8.

Matschiner, M., R. Hanel & W. Salzburger (2011) On the origin and trigger of the notothenioid adaptive radiation. *PLoS One,* 6**,** e18911.

Muschick, M., A. Indermaur & W. Salzburger (2012) Convergent evolution within an adaptive radiation of cichlid fishes. *Curr Biol,* 22**,** 2362-8.

Near, T. J. (2004) Estimating divergence times of notothenioid fishes using a fossil-calibrated molecular clock. *Antarctic Science,* 16**,** 37-44.

Norton, S. F. & E. L. Brainerd (1993) Convergence in the Feeding Mechanics of Ecomorphologically Similar Species in the Centrarchidae and Cichlidae. *Journal of Experimental Biology,* 176**,** 11-29.

Rueber, L. & D. C. Adams (2001) Evolutionary convergence of body shape and trophic morphology in cichlids from Lake Tanganyika. *Journal of Evolutionary Biology,* 14**,** 325-332.

Rutschmann, S., M. Matschiner, M. Damerau, M. Muschick, M. F. Lehmann, R. Hanel & W. Salzburger (2011) Parallel ecological diversification in Antarctic notothenioid fishes as evidence for adaptive radiation. *Mol Ecol,* 20**,** 4707-21.

Salzburger, W., A. Meyer, S. Baric, E. Verheyen & C. Sturmbauer (2002) Phylogeny of the Lake Tanganyika cichlid species flock and its relationship to the Central and East African haplochromine cichlid fish faunas. *Syst Biol,* 51**,** 113-35.

Schluter, D. 2000. *The ecology of adaptive radiation*. Oxford University Press.

Streelman, J. T. & P. D. Danley (2003) The stages of vertebrate evolutionary radiation. *Trends in Ecology & Evolution,* 18**,** 126-131.
Webb, P. W. (1984) Body and Fin Form and Strike Tactics of Four Teleost Predators Attacking Fathead Minnow (Pimephales promelas) Prey. *Canadian Journal of Fisheries and Aquatic Sciences,* 41**,** 157-165.
Wilson, L. A. B. (2013) The contribution of developmental palaeontology to extensions of evolutionary theory. *Acta Zoologica,* 94**,** 254-260.

Acknowledgement

Most importantly, I would like to thank **Walter Salzburger**. Without him, this thesis would have never been possible. I am grateful that he gave me the opportunity to conduct my Ph.D. thesis in his group, took me on several field trips and showed me how interesting but also joyful science can be. He always had an ear for me and my questions and was always a good companion to me, not only as a supervisor but as a friend. Thank you, Walter!

I would also like to thank my family, my parents **Christine** and **Franz** and my brother **Fabio Colombo** and my girlfriend **Sohvi Blatter**. You've always been there for me during my Ph.D. and without your support I probably would not have made it.

I am thankful to **Marcelo Sanchez** for being part of my defence committee and for inviting me several times to present parts of my work at the University of Zürich.

I also would like to thank all my co-authors and collaborators, first of all **Heinz Büscher** and **Florian Meury** who gave me access to their astonishing x-ray archive and greatly helped in collecting data, respectively. Without them, I would probably still be making x-rays, counting vertebrae and calculating ER values. I would also like to thank (in alphabetical order) **Marta Barluenga, Nicolas Boileau, Santiago Ceballos, Malte Damerau, Eveline Diepeveen, Marie Dittmann, Martin Gschwind, Reinhold Hanel, Adrian Indermaur, Isabel Keller, Robin Kovac, Michael Matschiner, Britta Meyer, Moritz Muschick, Marius Rösti, Emilia Santos** and **Laura Wilson** who all greatly helped in my projects and/or gave me the opportunity to participate in theirs.

I am grateful to my friend **Matthias Wyss** for writing the 'FinPix' software and to **Jonas Häfeli** for drawing the wonderful illustration that you can find on the

cover of this thesis. I am also thankful to **Nicolas Boileau** and **Brigitte Aeschbach** for their help in the lab and with organisational issues. A special thank goes to **Bernd Egger**, keep on rockin'!

I am thankful to **Astrid Böhne, Nicolas Boileau, Vasco Campos, Marie Dittmann, Adrian Indermaur, Isabel Keller, Florian Meury, Fabrizia Ronco and Attila Rüegg** for their help in field work and the fun time we had in Africa and **Malte Damerau** and **Nils Koschnick** for introducing me to the live aboard the 'RV Polarstern' and helping me identifying and processing specimens. I would have been lost without you, thanks!

My office mates also deserve a huge 'thank you!': **Nicolas 'Bollo' Boileau, Vasco Campos, Romina Celozzi, Julia de Maddalena, Eveline Diepeveen, Robin Kovac, Dario Moser, Jelena Rajkov, Marius Rösti** and **Sara Stieb**. It was a pleasure sharing an office with you!

Finally, I would like to express my gratitude towards some people that remain close to my heart for various reasons and that I feel were not adequately represented above: **Fabrizia**, **Dario**, **Attila**, thanks for everything!